ALLOSTRATIGRAPHY AND RIVER- AND WAVE-DOMINATED DEPOSITIONAL SYSTEMS OF THE UPPER CRETACEOUS (CENOMANIAN) DUNVEGAN FORMATION, ALBERTA

By

© JANOK BHATTACHARYA, B.Sc.(hons.)

A Thesis

Submitted to the School of Graduate Studies

in Partial Fulfilment of the Requirements

for the Degree

Doctor of Philosophy

McMaster University

May 1989

DOCTOR OF PHILOSOPHY (1989) McMASTER UNIVERSITY

(Geology) Hamilton, Ontario

TITLE: Allostratigraphy and River- and Wave-dominated Depositional Systems of the Upper Cretaceous (Cenomanian) Dunvegan Formation, Alberta

AUTHOR: Janok Bhattacharya, B.Sc. (Memorial University of Nfld.)

SUPERVISOR: Dr.R.G.Walker

NUMBER OF PAGES: xxxiii, 588

ALLOSTRATIGRAPHY AND DEPOSITIONAL SYSTEMS, DUNVEGAN FMTN.

"From the historic aspect the process of sedimentary infilling may be viewed as the record of a contest between land and sea. The strand-line separates the territory of the opposing forces - Poseidon, the god of the ocean, warring against the earth-born Titans. For a time the field may be held by each; the contest oscillates back and forth, recorded by delta conditions. Then, owing to an advantage gained by the sea, the strand-line may be pushed far inland and victory rests with Poseidon. But at other times the strand is driven back to the margin of the continent, the Titans in their turn are temporary victors, and the lord of the ocean is compelled to rule within his proper realm."

Joseph Barrell, December 29th, 1911;

address to the Geological Society of America

ABSTRACT

This study, of 130 cores and about 500 well logs, shows that the Dunvegan Formation (Cenomanian, Cretaceous Western Interior Seaway, Alberta) can be subdivided into seven allomembers, A through G. Each member represents a regression and contains several offlapping shingled sandstones and associated mudstones deposited in about 150,000 to 300,000 years. Members are separated from each other by bounding discontinuities produced by rapid transgressive flooding events.

Isolith maps of sand body geometries, along with facies associations seen in core, show that individual shingles represent various types of prograding shallow marine to non-marine environments ranging from highly river-dominated deltas in the lower members (G, F, and E) to storm- and wave-dominated prograding deltas, barriers, and transgressive sheet sands in the upper members (D, C, B, and A). Shingles are autocyclic in nature and are related to river avulsion and delta switching while members are allocyclic in nature and are probably related to episodic thrusting events in the rising Cordillera to the northwest.

The Dunvegan Formation was deposited during a time of active tectonism (Columbian Orogen), which caused rapid foreland-type subsidence but which did not allow conglomerate phases to be deposited on the shelf. A global third-order eustatic lowstand of sea-level is also associated with deposition of the Dunvegan.

ACKNOWLEDGEMENTS

Tnis thesis took about four and a half years to complete. During that time many people made many important contributions which greatly improved the final manuscript. The project would not have been possible vithout the tireless enthusiasm, editing, and logistical support of Dr.R.G.Walker who acted as supervisor for this project. Whenever difficult problems presented themselves, Roger consistently showed an uncanny ability to immediately propose several ways of arriving at a solution. Financial support was also provided through Natural Sciences and Engineering Research Council operating and strategic grants to Dr.Walker and through NSERC post-graduates scholarships to myself. Access to well logs and base maps was kindly provided by Petro-Canada Resources. Mr.R.Sheppard and all of his staff at the Energy and Resources Control Board Core Laboratory in Calgary (E.R.C.B.) are also thanked for their efficient and friendly service. A large thank-you is also given to the Department Photographer, Mr.Jack Whorwood whose professionalism and efficiency resulted in the high quality of photographs and reproductions included in the final manuscript.

Many undergraduate students worked on various aspects of this project throughout its completion. Kathleen McLaughlin and Liz Barr provided cheery assistance at the E.R.C.B. Core Lab in

Calgary and helped in logging and photographing core. Indraneel Rachaudhuri provided the most entertaining time I ever had at the E.R.C.B. during two weeks in August, 1987. Mark Birchard spent two weeks at the Institute for Sedimentary and Petroleum Geology in Calgary preparing shale samples for micro-paleontological analysis. Access to this lab was made possible through the tremendous help and support of Dr.J.H.Wall and his staff. Despite other heavy demands on his time, Dr.Wall managed to identify all of the collected foram assemblages. Dr.Wall also managed to convince one of his colleagues, Dr.A.Sweet, to process ten of my samples for dinoflagellates. The foram assemblages were hand-picked during one summer as a result of the painstaking effort of Sue Burbidge. Sue also helped throughout the year in drafting some of the original working cross-sections that provided much of the original data used in determining the allostratigraphy of the Dunvegan Formation. Suzanne Nacha and Tim Warmun also helped in drafting some of these original cross sections. During my last summer in Hamilton, Joe Boyce saved me many hours of hard work by drafting most of the isolith and isopach maps and some of the final well log cross sections presented in the thesis.

Many other people helped in more subtle ways through their comments, criticisms and discussions over a cold beer. Dr.D.P.James and Dr.D.A.Leckie are thanked for suggesting the thesis topic. Dr.S.G.Pemberton provided useful comments on the

trace fossils and Mr.Dave Taylor and Dr.Guy Plint provided many thoughtful suggestions which contributed to my understanding of the Dunvegan Formation. A special thank-you is given to Guy for taking several days out of his busy schedule during the summer of 1986 to show me the Dunvegan outcrops that he had been working on.

In addition I would like to thank my many friends and acquaintances at McMaster who made Hamilton such a pleasure, especially Ian Taylor, Bruce Power, Dave McLean, and Simon Pattison. Lastly I would like to thank my wife Lorna, my family here in Ontario and in Newfoundland, and Lorna's family in Calgary, especially her parents Heather and Philip who put up with me during all of my visits to Calgary. The support and love of everybody made it a most merry experience indeed.

Finally, I pay tribute to the writing and ideas of Stephen Jay Gould and the music of Frank Zappa. The prodigious creativity and unique sense of purpose and individuality held by these two men inspired me to undertake this project and continue to be a constant source of personal inspiration.

PREFACE. THE LAYOUT OF THIS THESIS

This thesis has been organized into 13 chapters. Chapter 1 introduces the scientific problem, chapter 2 describes the facies and facies associations, and chapter 3 presents the first allostratigraphic subdivision of the Dunvegan Formation. Chapters 4-10 present detailed descriptions and interpretations of each of the seven newly defined allomembers within the Dunvegan Formation. Because there is considerably more data regarding members E and D, these were presented first. Owing to the length of the chapters 4 and 5, which discuss these members, introductory summary sections are presented for the casual reader. After describing member D, the overlying members are presented sequentially from C to A in shorter chapters (6-8). Chapters 9 and 10 conclude the largely descriptive portion of the thesis with a discussion of members G and F respectively. The final three chapters present the major conclusions of this study. Chapter 11 summarizes the nature of depositional systems observed within sediments of the Dunvegan Formation and compares them with modern and ancient examples of other depositional systems described in the literature, including several examples from the Cretaceous Western Interior Seaway. Chapter 12 goes on to consider the overall evolution of the Dunvegan Formation and accounts for the processes which cause the various levels of cyclicity observed. Chapter 12 also includes a comparison of the Dunvegan with several other Cretaceous clastic units, including the Cardium and Mosby Formations, and discusses the tectonic implications of these comparisons. Chapter 13 summarizes the major conclusions of this thesis.

TABLE OF CONTENTS

CHAPTER 1. THE SCIENTIFIC PROBLEM

CHAPTER 2: FACIES

CHAPTER 3: ALLOSTRATIGRAPHY OF THE DUNVEGAN FORMATION

CHAPTER 4: MEMBER E

CHAPTER 5. MEMBER D

CHAPTER 6. MEMBER C

CHAPTER 7. MEMBER B

CHAPTER 8. MEMBER A

CHAPTER 9. MEMBER G

CHAPTER 10. MEMBER F

CHAPTER 11. DEPOSITIONAL SYSTEMS IN THE DUNVEGAN FORMATION

CHAPTER 12. EVOLUTION OF THE DUNVEGAN FORMATION

CHAPTER 13. CONCLUSIONS AND FUTURE WORK

LIST OF FIGURES

FIGURES (Cntd.)

FIGURES (Cntd.)

FIGURES (Cntd.)

FIGURES (Cntd.)

FIGURES (Cntd.)

FIGURES (Cntd.)

CHAPTER 1. THE SCIENTIFIC PROBLEM

1-1. Background

The background to the scientific problems addressed by a study of the Dunvegan Formation is considered in three parts. The first deals with the more general problems associated with the origin of shelf sandstones in the Cretaceous Western Interior Seaway (C.W.I.S.) of North America. The second part deals more specifically with problems associated with deltaic facies models and especially with the recognition of ancient wave-dominated deltas. The third part deals with the applications of sequence stratigraphic and allostratigraphic concepts developed by Vail et al.(1977) and more recently by Haq et al.(1987) to the Alberta subsurface and to sedimentary rocks of the Dunvegan Formation in particular.

1-1-1. The Origin of Linear Sand Bodies: Shelf Sands vs. Prograding Shorelines

Bergman and Walker (1986) have outlined the problem of the genesis of linear "shelf" sandstones characteristic of the C.W.I.S. One such example is the Mosby Formation in Montana (Fig.1-1, Rice and Gautier, 1983). The Mosby comprises a series of interbedded shales, sandstones and pebbly mudstones. These sandstones form a series of small, thin, linear bodies (less than

2 meters thick and up to a few kilometers long) that show evidence of deposition by storm processes. Sandstone facies are descriptively similar to "tempestites" of Aigner (1982). Rice and Gautier (1983), and Rice (1984) have suggested that the Mosby sandstones were transported up to 1,100 km southward from the time equivalent "Dunvegan Delta" in northwest Alberta, "by geostrophic currents induced by strong winds asociated with winter storms", as is suggested in figure 1-1. It was this diagram that initially prompted a study of the so called "Dunvegan Delta" in order to determine its relation to the Mosby shelf sandstones. Did sand travel from Dunvegan shorefaces all the way to Montana and if so, what effect would such large scale transport mechanisms have on the geometry and facies of Dunvegan shorelines and what kind of sediments would be deposited in between these two systems? Swift and Niedoroda (1985) stress the importance of the shoreface as "the gateway through which all shelf sediment must pass". If Rice and Gautier are correct, an investigation of the depositional edge (i.e., the shoreface) of the Dunvegan Formation should give clues as to how sand may bypass it and be transported onto the shelf.

1-1-2. Recognizing Ancient Wave-Dominated Deltas

Miall (1984a) has pointed out the problems with the recognition of ancient ancient wave-dominated deltas. Ancient examples of deltas are heavily biased toward river-dominated, lobate types. These would include the Tertiary deltas in the Gulf Coast

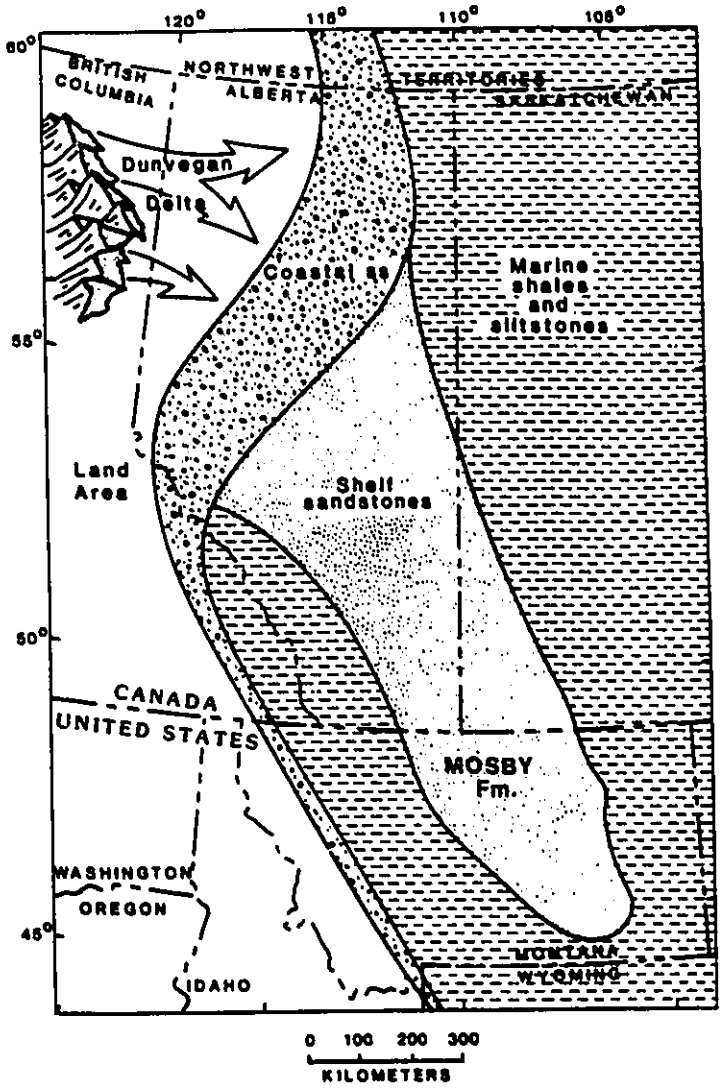

Figure 1-1. Coastal sandstones of the Dunvegan Formation are interpreted to be the source for shelf sandstones of the Mosby Formation, 1,100km to the south in Montana (a few letters indicating structural elements have been deleted from the original; after Rice, 1984).

of Texas(Galloway, 1968) and Carboniferous deltas in the U.K. and U.S.A. (Elliot, 1975; Horne et al., 1978). In the absence of overlying delta plain deposits, or of three dimensional control, wave-dominated deltas may be impossible to distinguish from wave-dominated prograding strandplains because the facies of these two environments are virtually the same. Probably the best subsurface examples of ancient wave-dominated deltas are in the Upper Cretaceous San Miguel Formation, Texas (Weise, 1979)(Fig.1-2). This study documented the three-dimensional geometry of individual deltaic sand bodies but, due to a lack of core control, included very little facies analysis. Many outcrop studies, including the Upper Cretaceous Rock Springs Formation (Kirschbaum, 1986), the Upper Cretaceous Cody-Parkman Delta (Hubert et al., 1972), and the Tertiary Tyee-Coaledo Formation (Chan and Dott, 1986), emphasize vertical facies sequences but lack the good three-dimensional control that subsurface data allows. As Miall (1984a) suggests, therefore, "...very few good examples of ancient wave- and tide-dominated deltas are available..."

A possible candidate for a wave-dominated delta is represented by Upper Cretaceous sandstones of the Dunvegan Formation which occur in the subsurface of Western Alberta. Since this formation has been drilled, logged, and cored extensively, an excellent opportunity for detailed three dimensional analysis of a possible deltaic system exists. In contrast to other ancient examples, this study will combine detailed facies analysis with

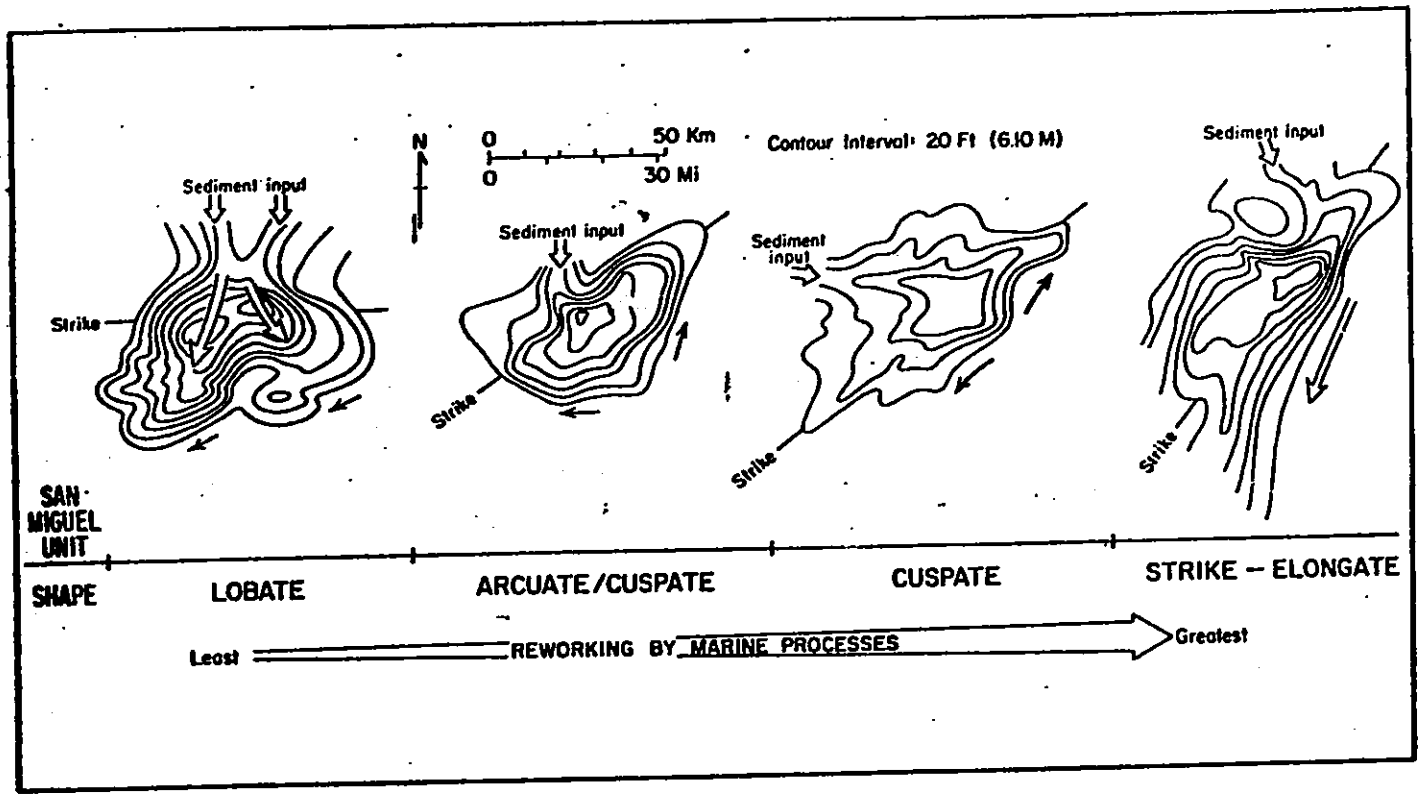

Figure 1-2. Spectrum of sandstone body geometries from largely wave-Dominated deltas in the San Miguel Formation, Texas (after Weise,1979).

three dimensional correlation and mapping. Investigation of the stratigraphic edge of the Dunvegan Formation will also provide an opportunity for analyzing the crucial transition from shoreline (delta margin) to shelf.

1-1-3. The Dunvegan Formation, Delta or Storm-Dominated Shoreface?

Interbedded sandstones and shales of the Upper Cretaceous, Cenomanian Dunvegan Formation in northwest Alberta have been interpreted as deltaic (Stelck and Wall, 1955). Rice and Gautier (1983), and Rice (1984) interpret a storm origin for the Mosby sandstones, and suggest that they originate from this so called "Dunvegan Delta" (Fig.1-1). If storms were powerful enough to transport sands for up to 1,100 km from Dunvegan shorelines, then evidence for these storms should be seen in Dunvegan shorefaces. In a basin characterized by high energy storm processes, wave energy might be expected to smooth out irregularities in existing shorelines (especially deltas) producing shore parallel linear sand bodies. Studies of other sandstones in the C.W.I.S., such as the Cardium Formation (Bergman and Walker, 1986; Duke, 1985a; Plint and Walker, 1987) also suggest that the C.W.I.S. was a relatively high energy basin, and well documented deltas have not been recognized in these studies. It is clear that there may be problems with a deltaic interpretation for the Dunvegan Formation. On one hand a deltaic interpretation has been suggested by previous workers and on the other hand major storms capable of

transporting sand for many hundreds of kilometers are proposed to exist at about the same time. Are these scenarios compatible or is one of the interpretations wrong? Investigation of the depositional edge of the Dunvegan Formation should help to answer this question.

1-1-4. Sequence Stratigraphy

In 1977 the Exxon research group headed up by Peter Vail (Payton,1977) introduced the concepts and models of seismic stratigraphy which have been used to develop the concepts of sequence stratigraphy, event stratigraphy, and allostratigraphy. The data base used to develop this approach comprises seismic data collected from sedimentary basins mostly developed on passive continental margins around the world (Vail et al., 1977, figure 4, p.88). Applications of these ideas to intracontinental sedimentary basins and in particular to the post-Mississippian Alberta foreland basin, are in their infancy. Vail type sequences are recognized on the basis of widespread unconformities, which are defined as erosional surfaces interpreted to result from relative sea-level falls. Swift et al.(1987) point out problems in recognizing unconformities and their associated overlying lowstand deposits in foreland basins.

Sequence stratigraphic ideas can be applied to the Alberta subsurface in at least two ways. Firstly, the overall gross stratigraphic relationships and absolute ages of formations can be compared to the third order global sea-level charts of Haq et

al.(1987). This comparison, shown in figure 1-6, can be used as a basis for interpretation and prediction. Secondly, the sequence stratigraphic approach can be used to subdivide any stratigraphic package. This approach involves;

1. The recognition of vertical cycles in core and on well logs,

2. The lateral correlation of these cycles using core and well log cross sections,

3. Recognition of genetically related packages of sediments based on the relation and extent of strata within observed cycle boundaries and of the surfaces (discontinuities) which separate these cycles.

Interbedded sandstones and shales of the Dunvegan Formation provide a natural subsurface laboratory in which to test the utility of these stratigraphic techniques. Excellent three dimensional well log and core control through the Dunvegan Formation should allow for the recognition and correlation of sequences over a large area. The detailed geologic control available should allow interpretation at all geological scales from individual beds to large allostratigraphic units and should allow interpretation at a far greater level of precision than is currently available to the seismic stratigrapher. The stratigaphy of the Dunvegan Formation will be dealt with in chapters 3 and 12.

1-2. Statement of the Problem

It is now possible to ask a series of questions that may be pertinent to an investigation of the Dunvegan Formation. These are grouped into primary questions about the Dunvegan Formation itself and secondary questions about the relationship between the Dunvegan Formation and other stratigraphic units.

1-2-1. Primary Questions

1. How do individual Dunvegan sandstones die into the basin?

2. Do sandstones in the Dunvegan Formation display deltaic facies patterns and morphologies and, if so, what kinds of deltas do they most resemble?

3. Was the Cretaceous Western Interior Seaway of North America wave and storm dominated during deposition of Dunvegan sediments and, if so, can deltas be preserved or recognized in these sediments?

4. What are the stratigraphic relationships of sandstones within the Dunvegan Formation?

5. What kinds of sequences exist within the Dunvegan Formation and how do they compare with published stratigraphic models?

6. What controls the deposition of individual stratigraphic units within the Dunvegan Formation; delta progradation, storm processes, sea level changes, tides, or perhaps a combination of these and other effects?

7. What other factors control the distribution of the Dunvegan Formation (e.g., tectonics, subsidence, basin structure)?

1-2-2. Secondary Questions

8. What is the actual stratigraphic and paleogeographic relationship between the Mosby and Dunvegan sandstones?

9. Is transport of the Mosby sandstones related to incremental sand transport over a distance of up to 1,100 km or perhaps to a lowering of sea level, and what effect, if any, does this have on the sediments of the Dunvegan Formation?

10. How does the Dunvegan Formation compare to other relatively well understood Upper Cretaceous clastic formations in Western Alberta or in the C.W.I.S.?

1-3. The Dunvegan Formation

1-3-1. Definition, Distribution, and Stratigraphy

The middle Cenomanian (lowermost Upper Cretaceous) Dunvegan Formation comprises a series of interbedded, marine to non-marine, sandstones, siltstones and shales, first described by Selwyn (1877). The Dunvegan Formation was deposited during the *Verneuilinoides perplexus* foraminiferal biozone dated at early Late Cenomanian by Caldwell et al.(1978). Wall (1987) notes an absence of Early Cenomanian foraminifera, especially *Textularia alcasensis*, although he points out that there is a fair amount of uncertainty in dating the Dunvegan at the sub-stage level. Various dates have been assigned for the duration of the Cenomanian. These include 90-94 Ma (Obradovich and Cobban, 1975); 91.5-96Ma (Fouch et al. 1982); 92-96 Ma (Haq et al., 1987), and 91-97.5 Ma (Palmer, 1983)(uncertainty of all dates is about 1

million years). Regardless of the disagreement as to the actual dates, most of these figures indicate that the Cenomanian lasted for about 4 million years except Palmer, who indicates a considerably longer duration of 6.5 my. This latter figure was also used by Vail et al. (1977) who have since revised their estimates to the lower duration of about 4my (Haq et al., 1987). Most other workers in the C.W.I.S. (Obradovich and Cobban, 1975; Weimer, 1984) prefer a duration of about 4 million years and this is the value used in this study. Since the Dunvegan is confined to the mid-Cenomanan, this suggest deposition of the Dunvegan during a time period of about 1 to 2 million years.

The name Dunvegan Group was first used by Dawson (1881) to describe his Cretaceous, "Lower Sandstones" which cropped out along the Peace River Valley. It was named after the Dunvegan Trading Post situated by the Peace River. Sediments of the Dunvegan Formation are exposed on the hills behind the old trading post. Subsequently, McLearn (1919) changed the Dunvegan from group to formational status.

The Dunvegan is underlain by marine shales of the Shaftesbury Formation and is overlain by the marine shales of the Kaskapau Formation (Fig.1-3). It crops out in northeastern B.C., northwestern Alberta and as far north as the Northwest Territories where it is dominantly conglomeratic in nature (Stott, 1982). In the subsurface, it thins dramatically in a southeasterly direction and is thought to pinch out around township 58 (Fig.1-4).

1-3-2.Regional Geology and Tectonic Setting

The Dunvegan Formation forms part of the post-Mississippian clastic sediments deposited into the Alberta foreland basin. This basin was produced as a result of the transformation of the western continental margin of North America from passive to active. The two major periods of tectonic compression and crustal shortening include the Late Jurassic to early Late Cretaceous Columbian Orogeny and the Late Cretaceous to Tertiary Laramide Orogeny (Stott,1984; Price, 1984). Major episodes of uplift should correlate with downwarping of the foreland basin and deposition of sandy clastic wedges into the basin as western highlands are eroded. Within the post-Mississippian clastic wedge Stott (1984, p.86) has recognized three major sandy clastic wedges;

"The first clastic wedge comprises the Jurassic Fernie Formation and the Late Jurassic-earliest Cretaceous Kooteney and Minnes Groups. The second wedge, of Late Neocomian to Early Cenomanian age includes the Blairmore, Bullhead, and Fort St.John Groups and the Dunvegan Formation. The third, and youngest, clastic wedge, late Cencmanian to Maastrichtian, includes the Alberta and Smoky Groups and a thick succession of continental clastic sediments assigned to a large number of formations. Each wedge consists of several large cyclothems and each cyclothem is marked by cycles and subcycles."

Sediments of the Dunvegan Formation are therefore related to late stage tectonism in the Columbian orogen to the north (Stott, 1984). Towards the west, these sediments become increasingly involved in Tertiary deformation due to the Laramide Orogeny and the Western edge of the basin is not preserved.

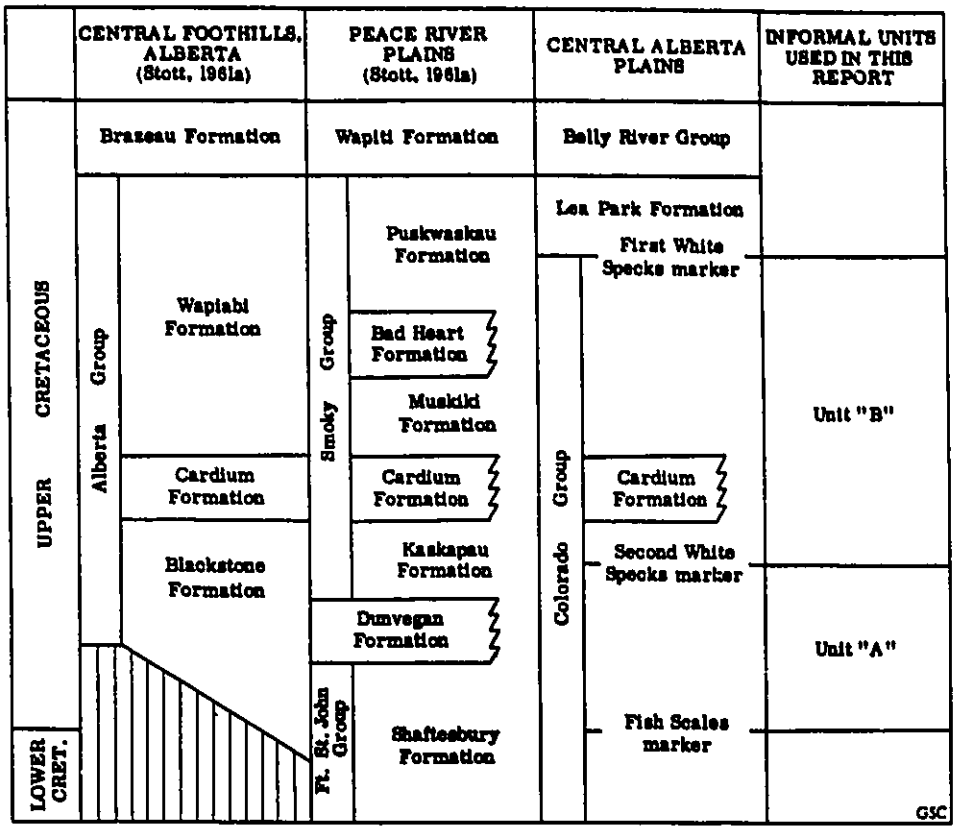

Figure 1-3. Stratigraphy of the Upper Cretaceous of Alberta (from Burk, 1963).

1-3-3.Paleogeography and Correlation

Sediments of the Dunvegan Formation were deposited in the C.W.I.S. of Alberta. The paleogeography (Fig.1-5) during this time has been presented by Williams and Burk (1964) and Stott (1984). They suggest a linear seaway open to the south to the Gulf of Mexico and north to the Arctic Ocean.

Kaufmann (1969), working in the U.S.A., and Stott (1984), working in Canada, have recognized a series of major transgressions and regressions, or cyclothems, in the C.W.I.S. Attempts to correlate Kaufmann's and Stott's cycles across the border have not been completely successful (Jeletsky,1978). Sediments of the Dunvegan Formation were deposited at the beginning of the Greenhorn cycle of Kaufmann (1969) and form part of the shorter Cruiser-Sully cycle of Stott (1984).

Haq et al.(1987) have presented global third order sea-level charts for the entire Cretaceous. Comparison of the Cretaceous clastic wedges shows that they probably correlate in part with global lowstands of sea-level. As shown in figure 1-6, a major drop in sea-level occurred in the mid-Cenomanian at about 94Ma, and lasted for about 500,000 years before the next transgression. This lowstand probably correlates in time with the Dunvegan clastic wedge and will be discussed more fully in chapter 12.

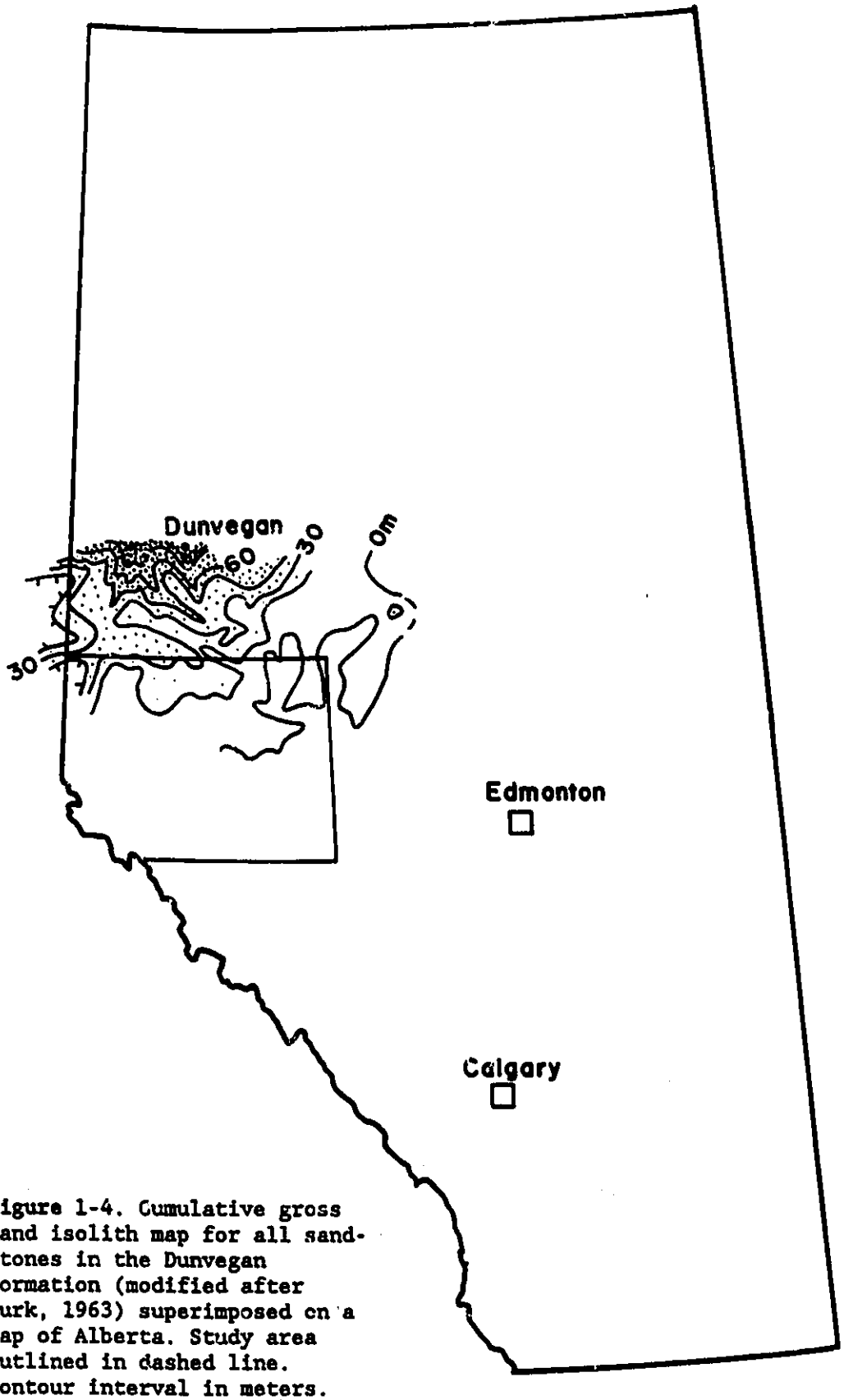

Figure 1-4. Cumulative gross sand isolith map for all sandstones in the Dunvegan Formation (modified after Burk, 1963) superimposed on a map of Alberta. Study area outlined in dashed line. Contour interval in meters.

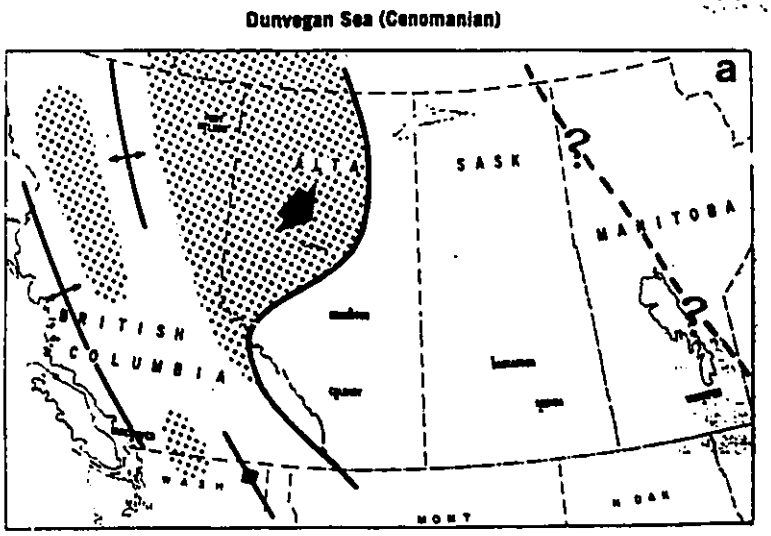

Figure 1-5. Paleogeographic map of Cenomanian Western interior seaway a. from Williams and Burk,1964, b. from Stott,1984. The seaway is interpreted as being connected to the Arctic in the north and to the Gulf of Mexico in the south.

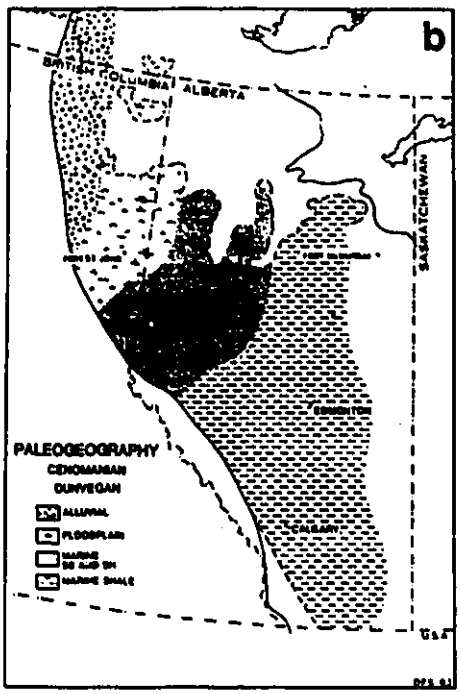

1-3-4. Previous Work

Stott (1982) has written the most up-to-date report describing the sedimentology and paleogeography of the Dunvegan Formation in outcrop. He also presents a concise description of previous work to which the reader is referred for more information regarding the surface geology. This section of the thesis concentrates on the interpretational aspects of previous work but is not a summary of Stott's review.

Selwyn (1877) recognized the presence of marine and non-marine facies within the Dunvegan Formation.

Dawson (1881) consequently suggested deposition under estuarine, fresh water and terrestrial conditions.

McLearn (1919), in a report on the Cretaceous along the lower Smoky River, was the first to evaluate the Dunvegan Formation for its petroleum potential. He was also the first to explicitly propose a deltaic interpretation:

> *"Attention is called to the presence of subaerial delta depcsits (Dunvegan) in the Colorado Group of this section. The Pelican Sandstone may also be so interpreted and, with the Dunvegan, records a delta built out in the Coloradan sea..."*

The Pelican Sandstone, exposed along the Athabaska River, was considered to be the equivalent of the Dunvegan Formation although it now known to be older (Lower Cretaceous, Albian).

In support of his deltaic interpretation, McLearn (1919) noted that;

> *"Thick zones of subaerial, concretionary, massive and crossbedded sandstones, with beds of subaerial shale, alternate with thick zones of thin-bedded sandstone and shale which may in large part be of marine origin"*

Other workers (notably Stott, 1982; Stelck & Wall, 1955; and Stelck et al., 1958) have also interpreted Dunvegan sandstones as deltaic. These interpretations were based largely on vertical facies relationships in outcrop sections. They recognized interstratification of marine and non-marine sandstones and shales in association with channel sandstones as described by McLearn (1919).

The only published subsurface data is that of Burk (1963). In his regional study of the Upper Cretaceous, Burk constructed a structure map for the Fish Scales Marker horizon and compiled a gross, cumulative isolith map of all sandstones within the Dunvegan Formation shown in Figure 1-4. His maps and cross sections show the general northwest to southeast thinning of Dunvegan sandstones, although the broad scope of his study did not permit further stratigraphic subdivision. Since this study was not really an attempt to map environmental lithofacies, no core description or detailed sedimentology was presented.

Tater (1964) conducted a petrographic study of sandstones collected from the type section at Dunvegan, Alberta. This work was done in order to determine provenance of Dunvegan sandstones rather than to make any paleoenvironmental interpretations. Tater

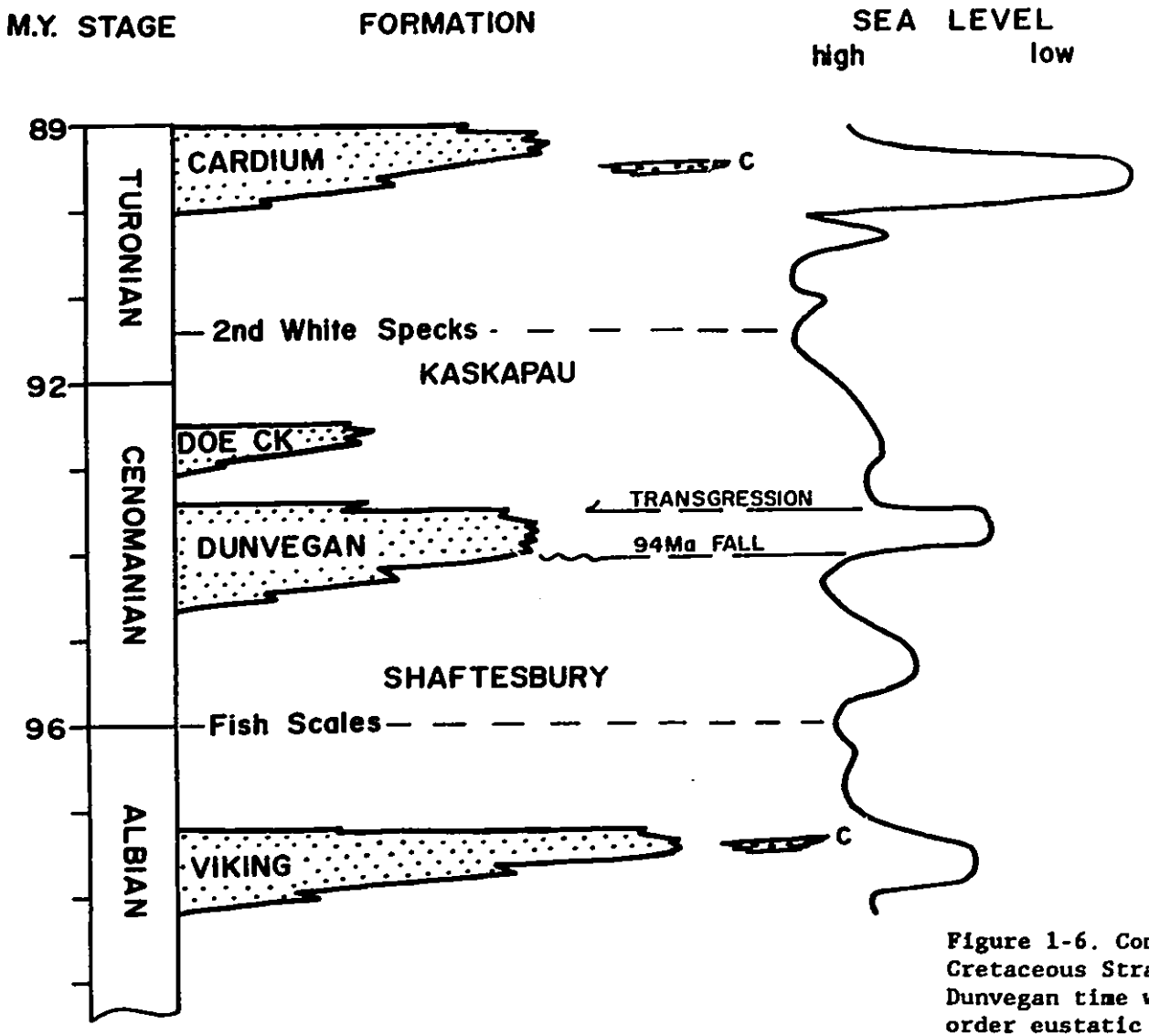

Figure 1-6. Comparison of Cretaceous Stratigraphy around Dunvegan time with the third order eustatic curves of Haq et al. (1987). DOE CK = Doe Creek mbr., C = Conglomerate.

(1964) dated detrital zircons and deduced that they were derived from the progressive unroofing of Jurassic plutonic rocks.

Most of the previous work discussed above is regional in its scope and was designed, primarily, to establish the basic stratigraphy and paleogeography of the Dunvegan Formation with respect to other Cretaceous clastic sequences of Western Alberta rather than to sub-divide the Dunvegan. The facies associations described by previous workers are suggestive of a deltaic setting, but there have been no published attempts at detailed three dimensional facies correlations. As discussed above, these are necessary in order to accurately distinguish deltaic sand bodies and in order to characterize delta types. This study intends to present a more detailed and more accurate interpretation of Dunvegan depositional systems than presently exists and will attempt to present a more detailed and interpretational stratigraphic subdivision based on an allostratigraphic rather than lithostratigraphic approach.

1-4. Solving the Problems

1-4-1. A Hierarchical Approach

A hierarchical approach involving analysis at progressively larger scales has been used in order to address the questions outlined in section 1-2. The study commenced with detailed facies analysis and recognition of vertical sequences (facies successions) in cores through the Dunvegan Formation, followed by construction of detailed core and log cross sections. It was completed by the construction of facies maps incorporating data

from the entire thesis area. This methodology will be briefly explained below in order to give the reader an appreciation of the overall strategy. The details regarding specific aspects will be discussed in relevant chapters throughout the text. After choosing the study area the work was completed in two phases.

1-4-2. Selection of the Study Area

The study area extends from township 50 to township 67 and range 15W5 to range 10W6 and covers a total area of about 30,000 square kilometers (Fig.1-7).

The boundaries of the study area were chosen for the following reasons: the southern (T50) and eastern (R15W5) boundaries were picked on the basis of the gross sand isolith map of Burk (1963) which showed Dunvegan sandstones to pinch out in this area (Fig.1-4). As previously discussed, this represents a key area in which the primary questions listed above may be answered. This area should include sediments deposited in the crucial shoreline to shelf transition zone. South and east of these boundaries Burk (1963) does not indicate any more Dunvegan sands.

As shown in figure 1-8, most of the oil and gas produced from the Dunvegan Formation lies to the south of the northern boundary (T67). The best core data is from these fields.

The western boundary represents the easternmost edge of the deformed belt as shown by Burk (1963). Sub-surface data is sparse in this area and stratigraphic relationships are also complicated by structural deformation and thrusting. Stott (1982) has des-

cribed outcrops of the Dunvegan Formation to the west of the thesis area associated with this deformation.

The available data for this study (Fig.1-7) consists of over one thousand wireline logs (open circles) and about 130 cores (black dots). Most of the core data is concentrated in the major producing pools of the Dunvegan Formation which include Ante Creek, Bigstone, Lator, Jayar, Simonette and Waskahigan (Fig.1-7 and 1-8), although there is scattered core control between these pools.

1-4-3.Phase 1: Facies and Sequence Analysis

The first phase of the study has been detailed in McMaster University Tech. Memo. 85-4 (Bhattacharya, 1985). This phase involved the detailed description and facies analysis of available core in order to erect a general facies scheme and in order to get a preliminary feel for the character of depositional environments as presented in Chapter 2. This also established the degree of cyclicity of depositional cycles within the Dunvegan Formation in vertical sections. Initial regional core and log cross sections were made in order to attempt to correlate these cycles, thereby establishing an overall stratigraphic framework within which later, more detailed correlations could be made.

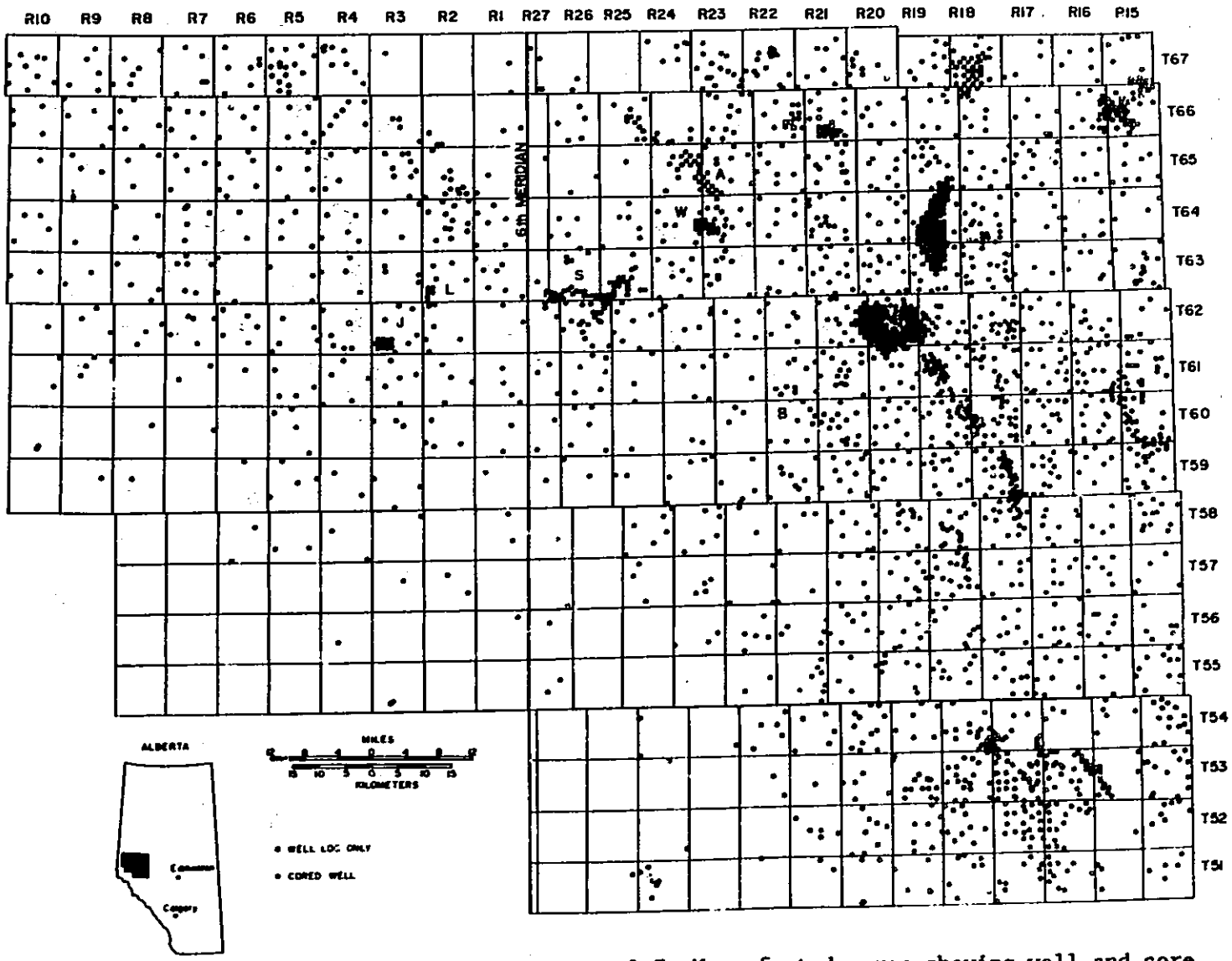

Figure 1-7. Map of study area showing well and core control and important oil and gas pools.

Out of 200 samples collected, 40 were processed for micro-palaeontological analysis.

1-4-4. Phase 2: Correlation and Mapping

The second phase of this study involved detailed three dimensional correlation of facies and sedimentary cycles over the entire thesis area using core and log data. This involved construction of a grid of about 20 cross sections comprising about 450 well logs (Fig. 1-9). Based on these correlations, detailed sandstone thickness maps were made showing the geometry of sandstone bodies and the regional distribution of interpreted depositional environments within individual stratigraphic slices.In some cases, further stratigraphic subdivision was possible. The final result was a series of maps for each stratigraphic slice within the Dunvegan Formation that could be compared with existing deltaic and shallow marine facies models.

1-5. Economic Problems

In addition to the scientific problems that will be addressed by this study, there are important problems of a more economic nature. These problems relate to the controls on the distribution of oil and gas within the Dunvegan Formation. Possible factors that can affect the distribution of oil and gas in a clastic reservoir include;

1. facies control (ie., depositional environment),
2. stratigraphic control or
3. diagenetic control.

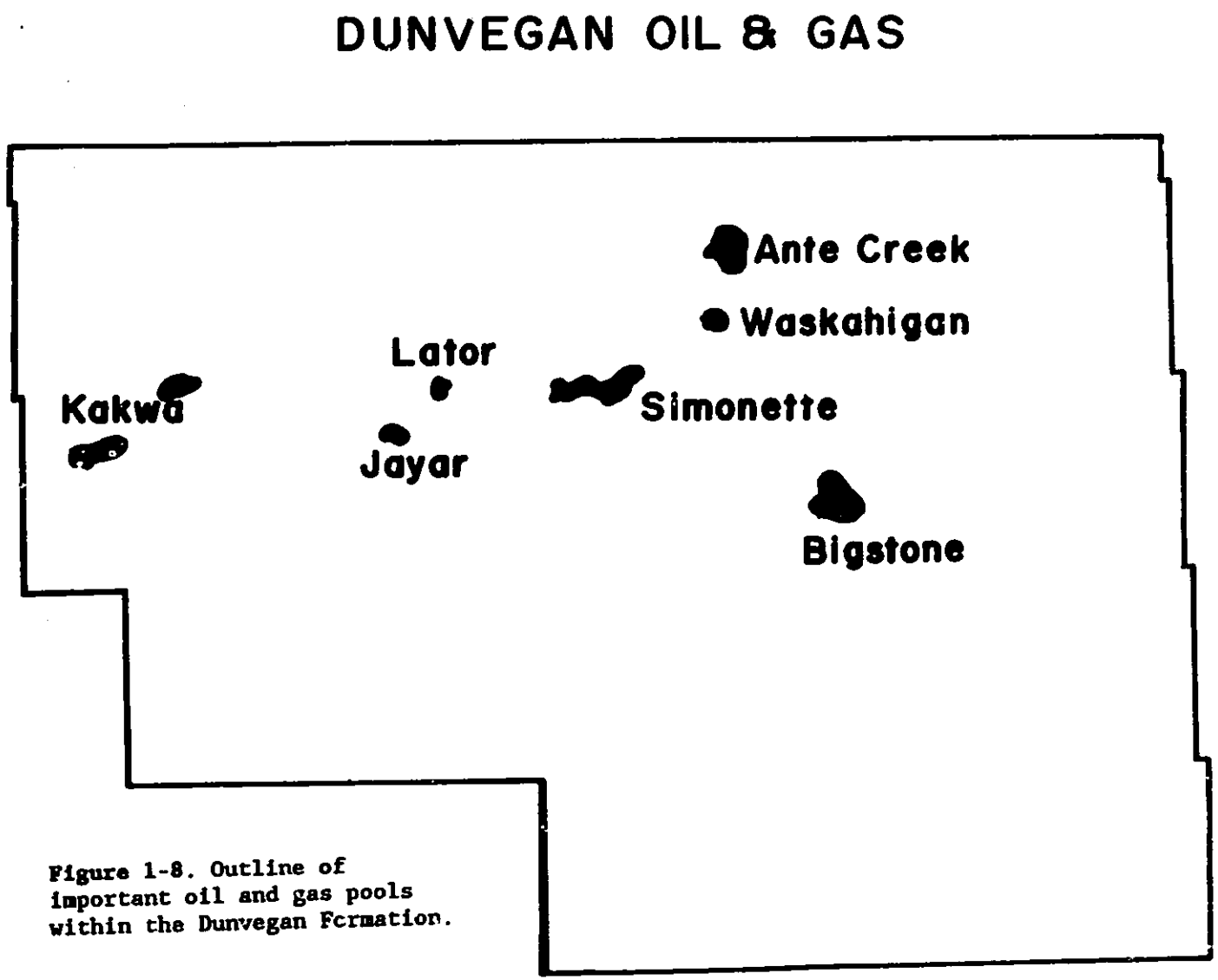

Figure 1-8. Outline of important oil and gas pools within the Dunvegan Formation.

The first two factors may be investigated by comparing known oil production data with cross sections and facies maps produced during phase 2 of this study. The third factor can be investigated primarily by petrographic investigation using thin-sections, cathodoluminescence and S.E.M. Such techniques should establish the species of diagenetic minerals and the relative timing of their growth. Comparison of producing and non-producing sandstones may pinpoint possible compositional or diagenetic controls. Quantification of these controls in a regional and stratigraphic sense may be useful in predicting the occurrence of future petroleum reserves in the Dunvegan Formation. These economic problems will not be addressed in detail in this study. A few preliminary points regarding these questions are outlined in appendix 2.

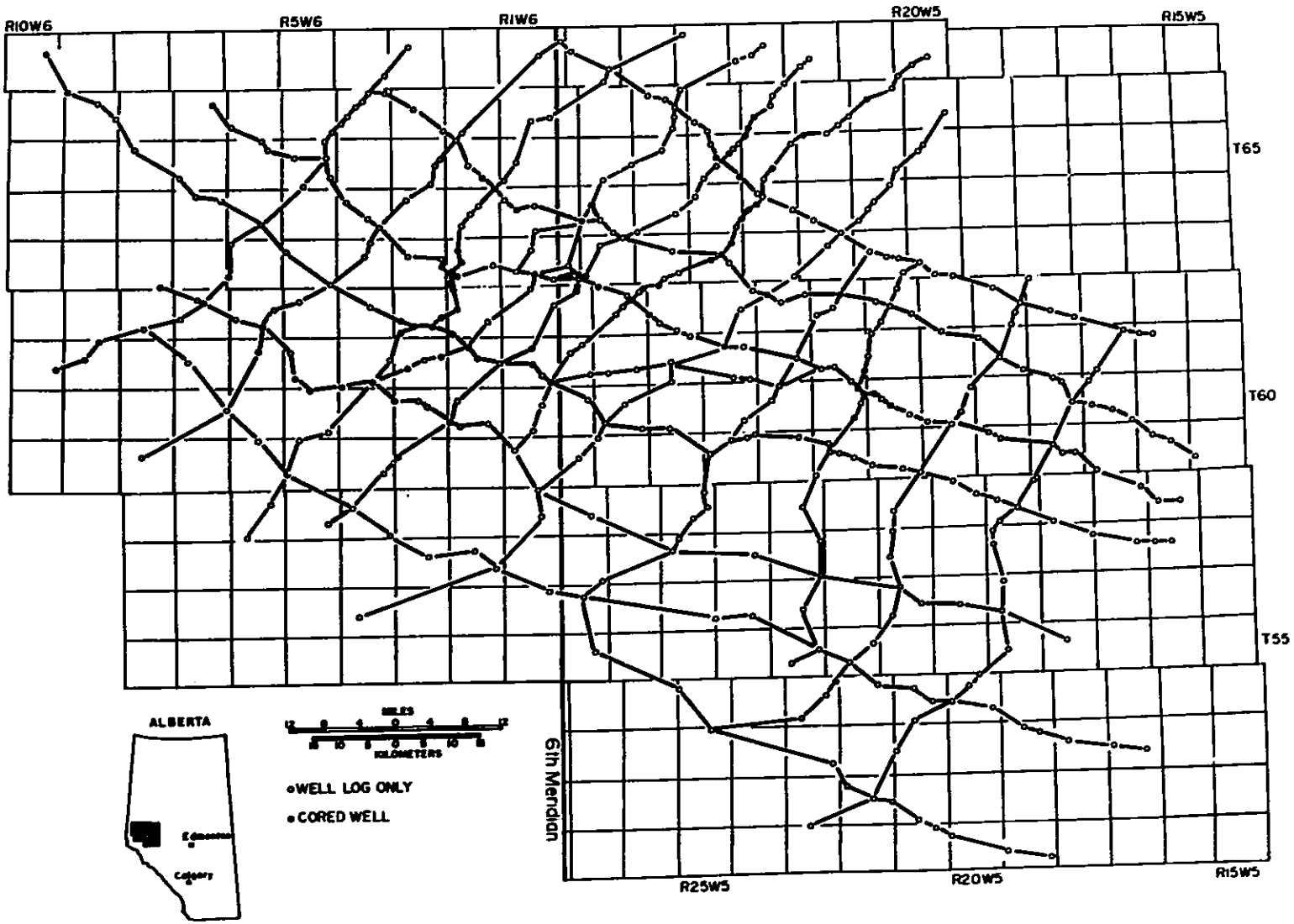

Figure 1-9. Map of study area showing regional cross sections correlated.

CHAPTER 2: FACIES

2-1. Introduction

Designation of facies in core is subjective and will vary according to the nature and scale of problem addressed. The purpose of facies analysis in this study was to erect a general facies scheme useful in broad environmental reconstruction and for the characterization of major sedimentary successions. Detailed, bed by bed facies description on the scale of centimeters or less, was considered impractical and probably unnecessary. Of about 130 cores studied, many exceeded 18 meters and some reached lengths of nearly 70 meters (see core listing in appendix 1). Separate facies units, usually on the scale of a few tens of centimeters or more, were distinguished on the basis of;

1. the nature of interbedding of shale and coarser material (thickness of interbeds and the proportion of shale).

2. primary sedimentary structures (e.g. cross-lamination, cross-bedding and grading).

3. the degree and type of burrowing

4. lithology and grain size, and

5. constituents (e.g. fossils, nodules, plant remains and diagenetic material(especially siderite)).

Seven major facies groups were distinguished in the cores studied. These have been designated as shales, siltstones, pinstriped mudstones, blockstones, banded mudstones, pervasively bioturbated mudstones, and sandstones. In addition there are rarer lag, coal and siderite horizons. Along with the following descriptions, brief interpretations will be given.

2-1-1. Coarse Facies

I did not observe a single cobble, pebble, or granule of primary *extraformational* origin in any of the cores through the sediments of the Dunvegan Formation within the thesis area. The maximum grain size of extraformational clastic material observed was medium-grained sandstone (about 1ϕ). Large *intraformational* clasts within the thesis area included siderite nodules, mudstone clasts, and shell fragments, but no large chert clasts or other large rock fragments.

Throughout the thesis I have expressed grain sizes using written designation (i.e. fine, medium, coarse) rather than the phi scale. I have followed the Udden-Wentworth scheme (Blatt et al., 1980, p.57, figure 3-3) where:

very fine sand: $4 < \phi < 3$

fine sand: $3 < \phi < 2$

medium sand: $2 < \phi < 1$

2-1-2. Thickness estimates

Maximum thicknesses of finer grained facies in core, especially shales and blockstones, will commonly be underestimated since these facies are seldom fully cored due to lower potential reservoir value. Total thicknesses must therefore be estimated from logs. Although log depths are reasonably accurate, to within half a meter, subtle but important differences in facies (e.g. bioturbated versus laminated shale) may not be manifest by an observable change in log character.

2-2. Facies Descriptions

2-2-1. FACIES 1: SHALE

There are three different types of shales. They are distinguished in core on the basis of induration, the degree of bioturbation, the degree of lamination, and the types of organic material (fossilized animal and plant remains).

A. Facies 1A (laminated shale) is characterized by well indurated, blue-black to dark grey, silty laminated shale with relatively little carbonaceous debris (Fig. 2-1, a,c, and d). It occurs relatively frequently and may range in thickness from a few tens of centimeters up about ten meters. Faint silty laminae (Fig.2-1a,c) are usually on the scale of a few centimeters in thickness and usually display well developed colour grading giving a facies which is gradational with the blockstones (Fig. 2-4a). Fauna includes thin-shelled, marine *Inoceramus*, *Corbula* and fish remains (Fig.2-4e, 2-3a). Trace fauna are relatively rare, but in

Figure 2-1. Facies 1, shale; 3cm scale in all photos. A.Facies 1a, totally unburrowed, laminated shale, with centimeter scale silty beds. This facies is gradational with Facies 2. B. Facies 1B, utterly massive, structureless black fissile shale, C.laminated silty shale, sideritic with well developed *Helminthopsis* burrows. D. close-up of c showing millimeter scale *Helminthopsis* burrows.

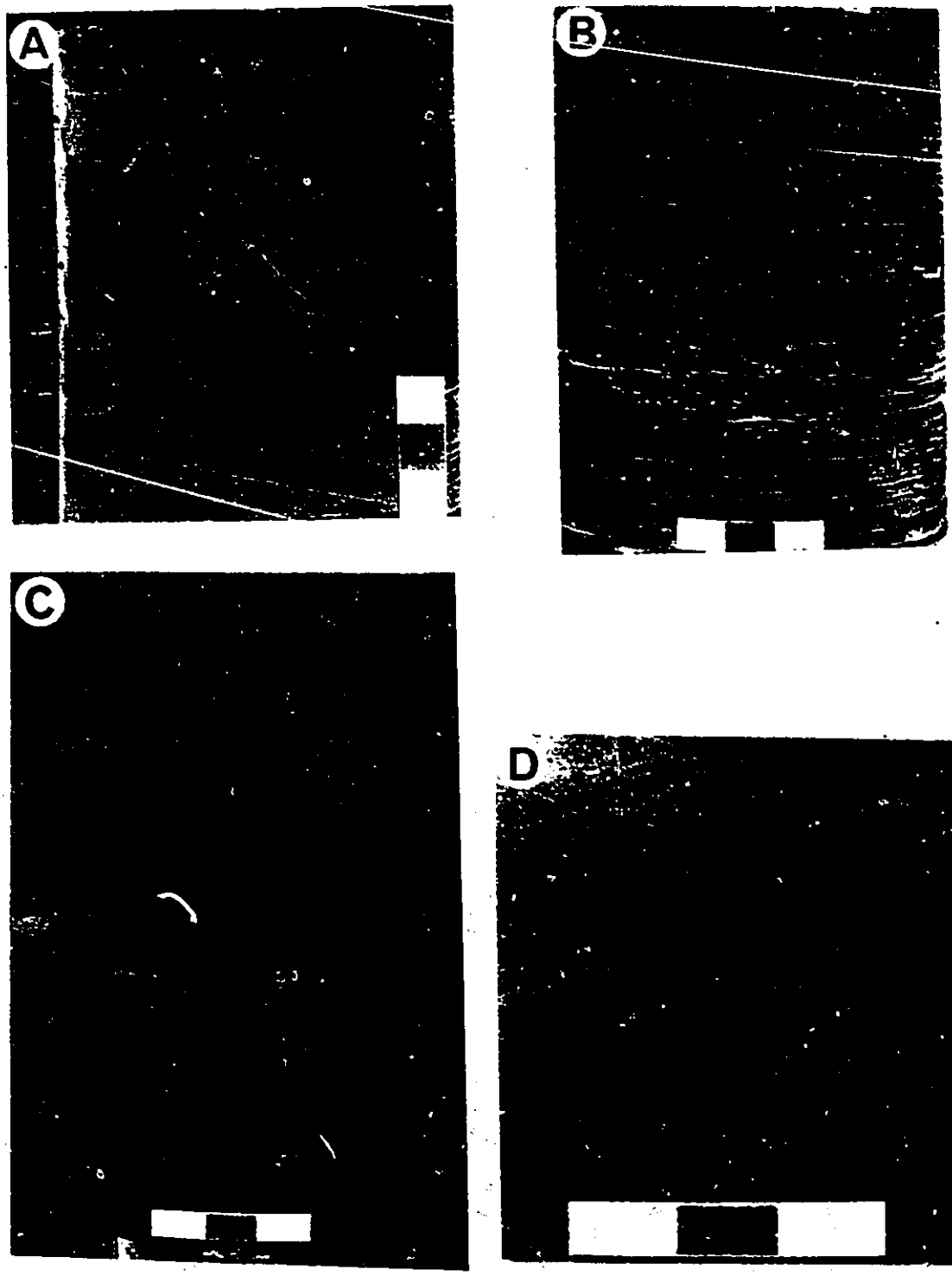
A
B
C
D

places abundant *Helminthopsis* burrows occur (2-1c,d). Marine forams may be present, but are usually relatively low in abundance.

Interpretation

The presence of marine fauna, the thickness (up to ten meters) and the lack of plant debris, suggest that this facies is deposited in a marine environment. The lithology, lack of coarse material, lack of wave-formed sedimentary structures, and presence of occasional graded beds suggests a low energy setting far from a source of coarse clastic material and probably well below storm wave base. The lack of burrowing reflects conditions unsuitable for a large number of organisms. This may reflect anoxic conditions (Ekdale and Mason, 1988) or perhaps high rates of sediment fallout such as in a basinal prodeltaic setting.

B. Facies 1B (bioturbated shale) comprises massive to pervasively bioturbated, poorly indurated, brownish black, crumbly shale usually having a higher proportion of carbonaceous debris than Facies 1A (Fig.2-1b, 2-2c). It is relatively common and ranges in thickness from a few tens of centimeters to a maximum of about ten meters. Its massive nature results from complete reworking by organisms. In places this facies becomes silty and distinct trace fossils, especially *Zoophycos* and *Rhizocorallium* are visible. This facies may grade into Facies 3 (Fig.2-5a). Macrofauna include *Lingula* (usually only a few millimeters in length, Fig. 2-2d) and *Inoceramus*. Unlike Facies 1A, this facies

is usually rich in arenaceous benthic foraminifera and marine dinoflagellates.

Interpretation

The trace fossil assemblage is characteristic of the *Zoophycos* ichnofacies (Frey & Pemberton, 1984) which is thought to be typical of the outer shelf. The presence of marine organisms, including *Inoceramus*, Dinoflagellates and benthic Foraminifera, indicates a marine origin. The lack of coarse sediment, the lack of primary depositional sedimentary structures, and the pervasive bioturbation suggests that this facies was deposited slowly, in a low energy setting far from a coarse clastic source and probably in relatively deep water well below storm wave base (probably in water depths greater than about 15 meters).

C. Facies 1C (carbonaceous shale) comprises dark grey to black, crumbly, highly carbonaceous shale (Fig.2-2a). This is the least common of the three shales, and seldom exceeds a few tens of centimeters in thickness. Coquinas occur in places containing a variety of pelecypods including thin-shelled oysters, *Corbula*, and *Brachydontes sp.* (Fig.2-2b, Fig.2-3a,b,d). Interpretation

These faunal assemblages are similar to brackish water faunas described elsewhere in the Western Interior Cretaceous Seaway (Kauffman,1969). The presence of abundant plant debris and of brackish to restricted marine macrofauna suggests deposition in a transitional marine environment. The shaly lithology suggests a relatively low energy environment while the relative thinness of

Figure 2-2. Facies 1, shale, scale is in centimeters in all photos. A. Facies 1C, carbonaceous shale. Note rather crumbly appearance in core. B. surface photo of shale in a. showing typical fossil assemblage. Oy - Oyster (two valves), Br - *Brachydontes* (one valve shown) C. Facies 1B, bioturbated shale. A few disseminated sandy particles are visible. D. Overlapping valves from the inarticulate brachiopod, *Lingula*. Presence of two valves suggest no physical transport.

Figure 2-3. Fossils, scales are in centimeters. A. *Corbula*, valves are about 1 cm in length. B. Pelecypod, probably a type of *Corbiculid.*, C. Oyster rich mudstone. Oysters are interpreted as being *in situ*. (From well 4-11-65-2W6, 15m, Fig.3-8A).
D. Pelecypods, probably *Corbiculids*.

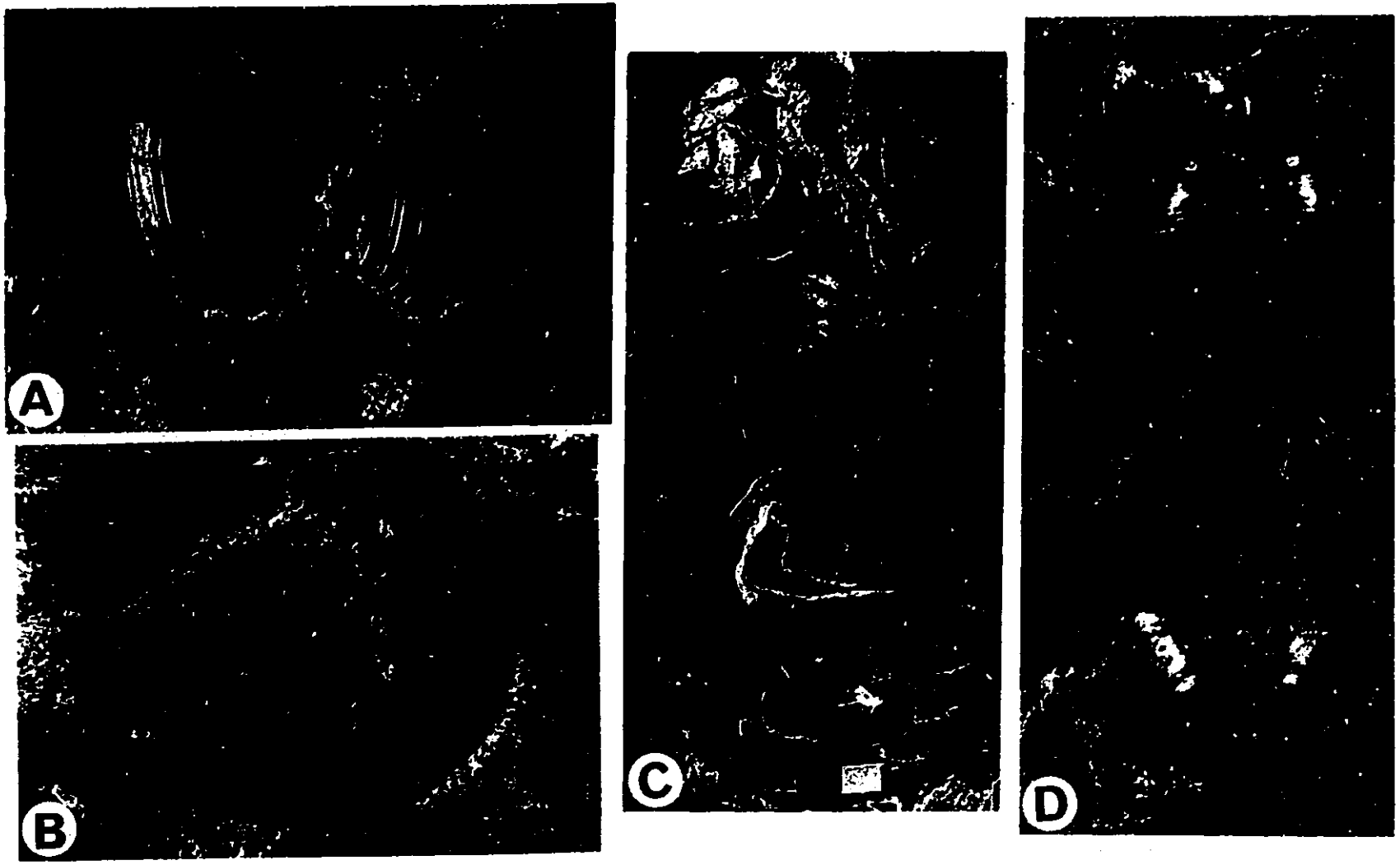
A
B
C
D

occurrences of this facies suggests that conditions of shale deposition were less persistent than in thicker occurrences of facies 1A or 1B. Such conditions of deposition could exist in a variety of low-energy, shallow-water environments including; protected lagoons, estuaries, interdistributary bays or other delta or coastal plain environments.

2-2-2. FACIES 2: BLOCKSTONE (laminated mudstones)

Blockstones (Fig.2-4a,b,c, and d) are generally dark to medium grey in colour and are characterized by interbedded shales, siltstones and very fine-grained sandstones. Interbeds occur on the scale of a few centimeters and exhibit well developed colour grading, which gives a "hockey puck" or blocky appearance to the core (Fig. 2-4 a,b,c,d). This facies is common and ranges in thickness from a few tens of centimeters up to a maximum of about 7 meters. The proportion of shale may vary from as little as 25 to as much as 70 percent. Coarser-grained interbeds nearly always have sharp to scoured bases and may be associated with synæresis cracks (Fig. 2-4 d). Within individual occurrences of this facies, bed thickness may vary from a few millimeters to 4 cm but usually averages about 1 to 2 cm. This facies is characterized by abundant graded bedding, although vague cross lamination (usually wave ripples) may be present in thicker sandy interbeds (Fig. 2-4 c). In general, the sandier the coarser beds, the greater is the amount of cross-lamination. Small scale scour and fill structures (Fig.2-4b) also increase in abundance as the

proportion of shale decreases and blockstones are sometimes cut by spectacular gutter casts, up to 30 cm deep and filled with very fine-grained hummocky cross-stratified or wave rippled sandstones (Fig. 2-4 d). The blockstones are gradational with Facies 1A (laminated, silty shale, Fig. 2-1a, 2-4a). Nodular siderite is fairly common (about 5%) while nodular pyrite is rarer.

Flora and Fauna

Facies 2 tends to show a low degree of bioturbation. Rare marine trace fossils, including *Rhizocorallium*, *Zoophycos*, and *Planolites* occur in places (Fig.2-4a). Macrofauna include large, relatively thin-shelled, marine *Inoceramus*,(Fig.2-4c, and e) *Corbula* and fish remains (scales, bony fragments and teeth). In places, *Inoceramus* may be fairly abundant sometimes occurring in pods or coquina-like beds (Fig. 2-4c).

Interpretation

The presence of marine body fossils and trace fossils, the relatively thick nature of occurrences of Facies 2, and the lack of wave features, in siltier occurrences, suggests that this facies was deposited below storm wave base on an open shelf. Where sandy gutter casts and wave rippled sands are present, deposition above storm wave base is indicated (Duke, 1985b, Whitaker,1973). The presence of synæresis cracks may indicate either dewatering of rapidly deposited sediments during compaction or contraction of shales due to salinity changes (Plummer and Gostin, 1983).

Figure 2-4. Facies 2, Blockstones, scale in photos is 3 centimeters. A. silty blockstone grading up into laminated mudstone (Facies 1A). Arrow points to burrowed layer. Silty beds show good colour grading and scoured bases. B. sandy blockstone. Several of the upper beds are cut by shale-filled micro-scours. Uppermost sand bed shows is laminated. Arrow points to small *Planolites* burrows. C. Sandy blockstone containing *Inoceramus* coquina in upper half. D. Large sand-rich gutter undercuts into Facies 2. Wavy lamination occurs in sandy gutter fill. Arrow points to a syæresis crack. E. Surface view of *Inoceramus* shell showing characteristic ribbing.

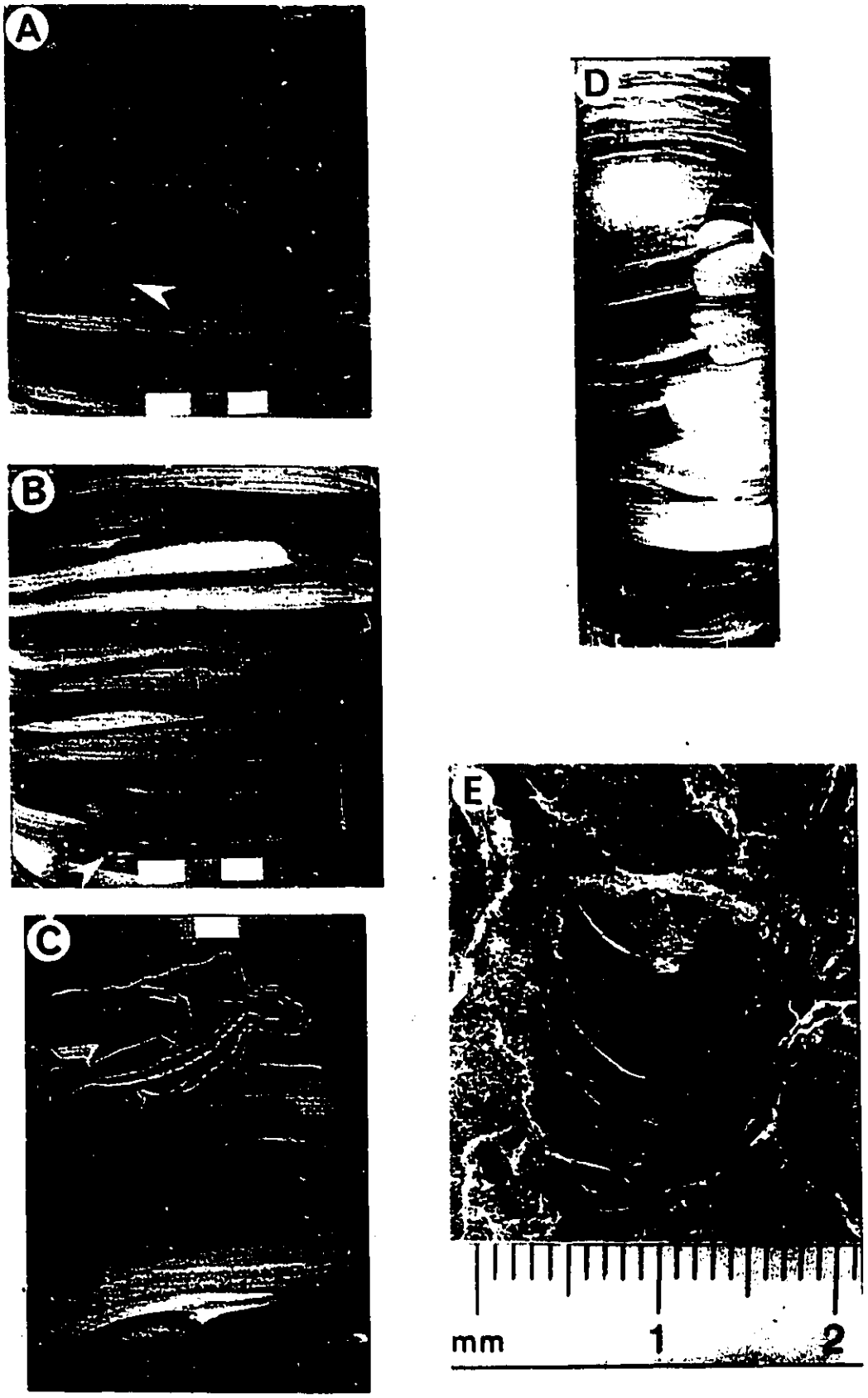
A
B
C
D
E
mm
1
2

The lack of burrowing, the presence of abundant silty graded beds with erosional bases, as well as the relatively high thickness of occurrences of this facies may indicate fairly high sedimentation rates. This may also favour production of synæresis cracks by dewatering during compaction.

The abundance of silt and very fine-grained sandstone may indicate greater proximity to a sandy clastic source than facies 1A or 1B. Proximity to a fresh water source may point to a broadly prodeltaic setting.

2-2-3. FACIES 3: BIOTURBATED MUDSTONE

Two types of bioturbated mudstone facies (Fig.2-5a,b,c, and 2-6a,b) are distinguished on the presence or absence of distinctive burrow forms, the average grain size of coarser material, and on the amount of shale. These are not meant to represent ichnofacies.

A. Facies 3A (Pervasively bioturbated mudstone) (Fig.2-5a,b,c), is the most distinctive and by far the most common of the bioturbated facies. This facies may range from a few centimeters to a maximum of about 3 meters in thickness. Facies 3A is usually dark to medium grey in colour and comprises a bioturbated mixture of very fine to fine-grained sandstone, siltstone, and shale. Proportions of shale vary from about 25% (Fig.2-5c) to 70% (Fig.2-5a) but usually average about 50%. Thicker occurrences of Facies 3A may coarsen upward. Bioturbation is usually total, and laminations are rarely present. Burrow

forms are distinctive and include *Zoophycos*, *Rhizocorallium*, *Planolites*, and *Terebellina* (Fig.2-5 a, b). In thicker occurrences, especially where the facies coarsens upwards, mud lined *Skolithos* burrows, up to a meter in length, clearly post-date earlier *Zoophycos* burrows (Fig.2-5 c). This facies is often gradational with sandier facies which contain abundant *Ophiomorpha* and *Asterosoma* burrows (Fig.2-19d).

Interpretation

Zoophycos, *Rhizocorallium* and *Terebellina* are typical of the *Zoophycos* ichnofacies, while *Skolithos*, *Ophiomorpha*, and *Asterosoma* are distinctive of the *Skolithos* ichnofacies (Frey & Pemberton, 1984). The high abundance and variety of burrowing (i.e. high diversity) in these ichnofacies suggests a fully marine environment. The pervasive bioturbation suggests low sedimentation rates but the occasional preserved wavy lamination may suggest deposition in more agitated water than facies 1 or 2, perhaps above storm wave base but below fair weather wave base. In thicker occurrences, a shallow water *Skolithos* ichnofacies appears to replace a deeper water *Zoophycos* ichnofacies. The replacement of a deeper water ichnofacies with a shallower water ichnofacies within the same lithofacies unit suggests environmental shallowing without a corresponding change in sedimentation rate. This change in trace fossil assemblage may also be due to increasing oxygenation through time although the

Figure 2-5. Facies 3A, Pervasively Bioturbated Mudstones,
A. Bioturbated silty mudstone, mostly *Zoophycos* burrows.
B. bioturbated sandy mudstone, large *Zoophycos* burrow in middle of photo shows characteristic side-filled spreite. Sandy doughnut shaped burrows are *Terebellina*. C. Bioturbated muddy sandstone cut by large *Skolithos* burrow in centre.

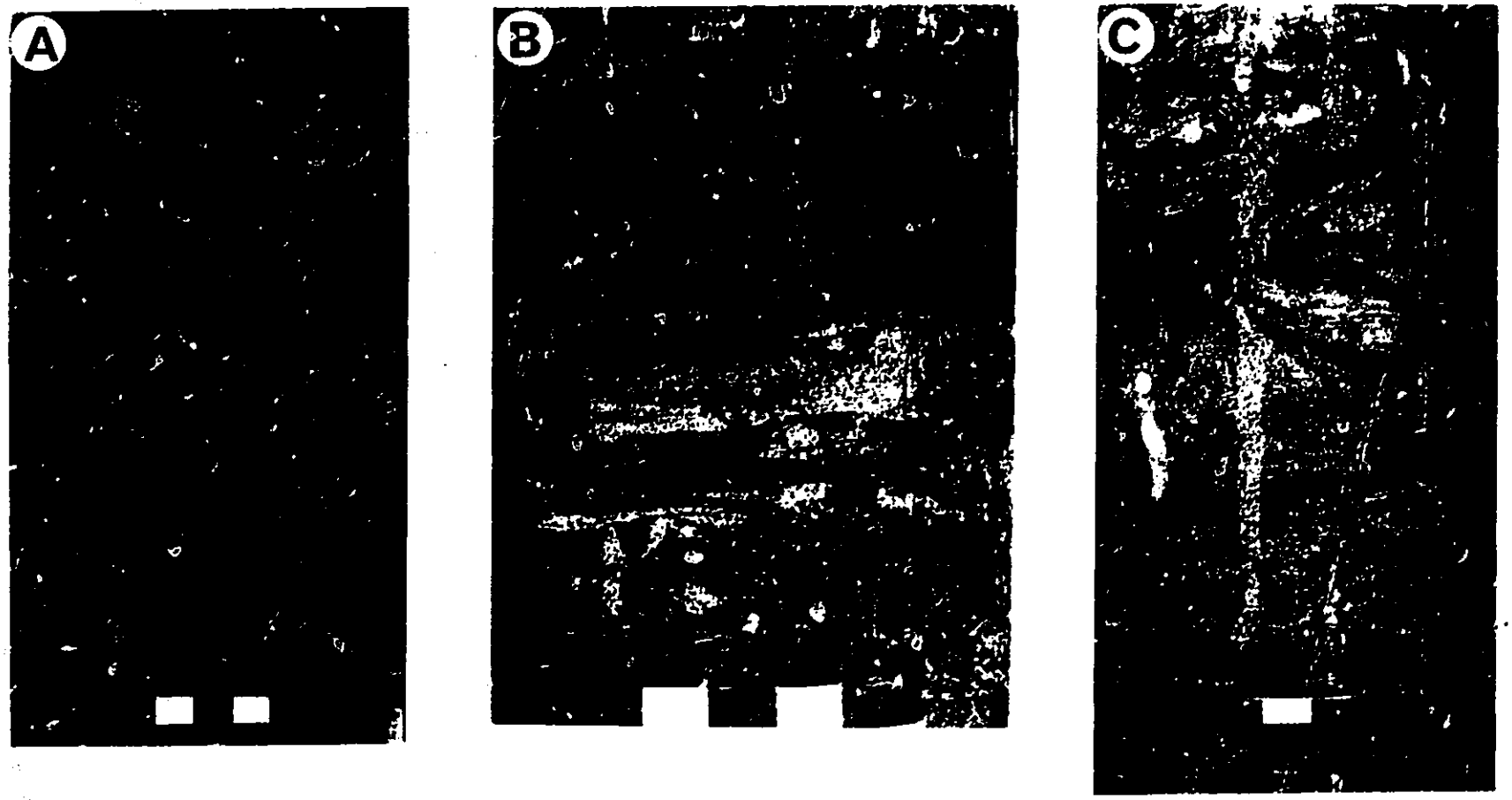
A
B
C

Figure 2-6. Facies 3B, laminated to bioturbated mudstones. A. thin cross-laminated mudstones alternate with bioturbated mudstones. Trace fossils include sandy, tubular burrows near bottom of photo (*Planolites*), *Terebellina* (arrow), and *Teichichnus*. B. Laminated sandy mudstone with syneresis cracks in basal few centimeters penetrated by large *Teichichnus* burrow in centre of photo.

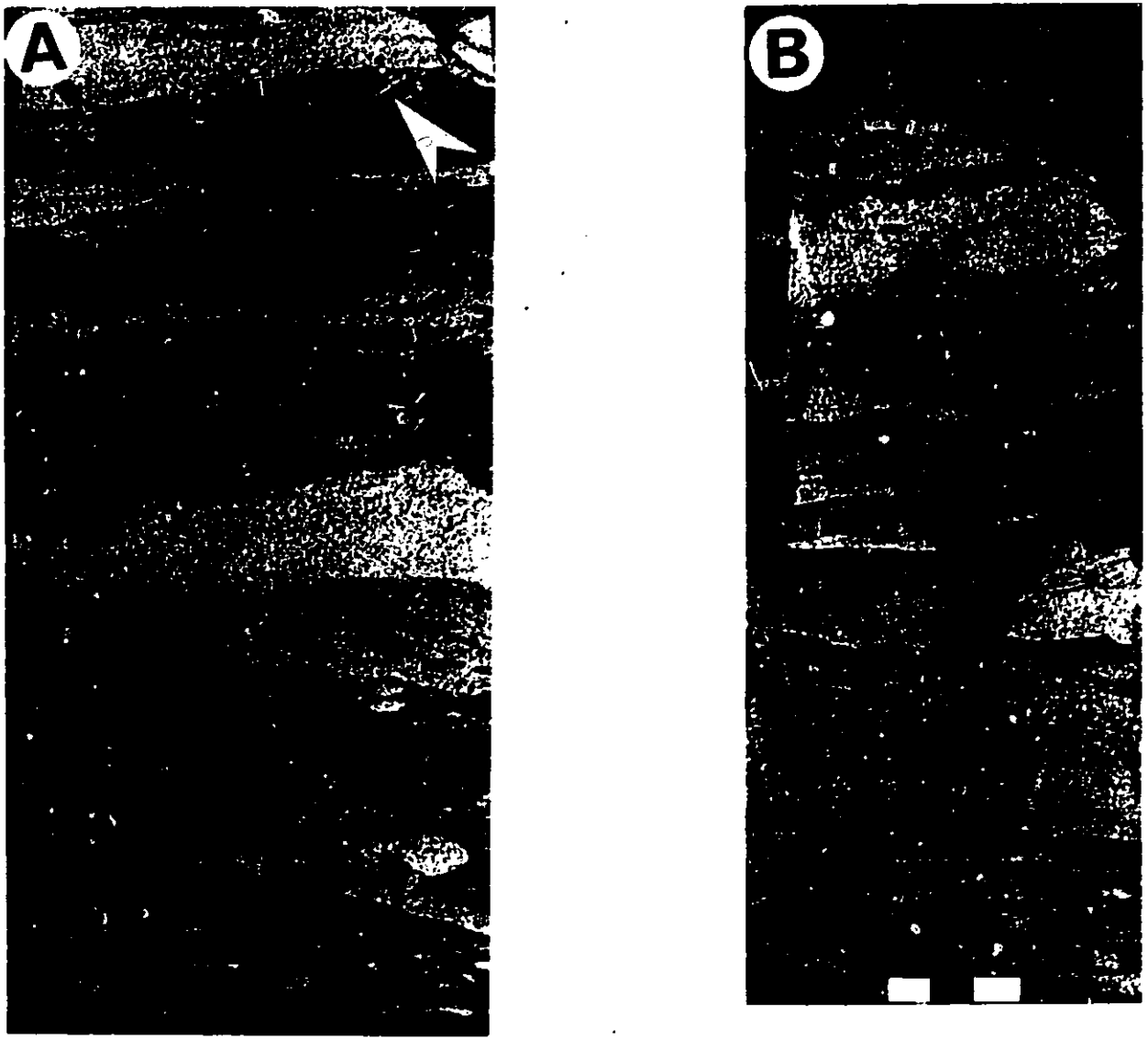
A
B

degree of oxygenation may also be a function of water depth (Ekdale and Mason, 1988).

B. Facies 3B (laminated-bioturbated mudstone) is is common and is often gradational with Facies 5 (banded mudstone). Occurrences range in thickness from a few centimeters up to about a meter. This facies is characterized by burrowed to laminated, relatively coarse-grained sandstone (fine to medium grained) interbedded with black carbonaceous shale (Fig. 2-6a,b). Interbeds are commonly on the scale of centimeters. Siderite is common and in places synæresis cracks may be abundant.

In contrast to Facies 3A, this facies is seldom totally bioturbated. Burrowing may reach 70% and common burrow forms include *Planolites*, *Teichichnus*, *Rhizocorallium*, and *Terebellina (Fig. 2-6a,b,)*. As figure 2-6a,b shows, bedding is usually visible and laminations are preserved in some of the sandier interbeds. The trace fauna indicate a lower overall abundance, and perhaps a slightly lower diversity.

Interpretation

The trace fossil assemblage resembles the *Cruziana* ichnofacies of Frey & Pemberton (1984) interpreted as a sublittoral assemblage. Beynon et al. (1988) document similar inchnofacies as being typical of brackish water environments. The variety and degree of burrowing is less than that seen in facies 3A (i.e. lower diversity), suggesting a more highly stressed environment. The presence of coarser sandstone than seen in facies 3A and the

presence of carbonaceous material suggests proximity to a course clastic source (e.g., shoreline). The degree of burrowing and relative thinness of occurrences of this facies suggests relatively low sedimentation rates. Synæresis cracks may result from salinity changes which may be responsible for producing a more highly stressed environment than interpreted for facies 3A. Possible environments of deposition could include shallow water lagoons, estuaries, or interdistributary bay environments.

2-2-4. FACIES 4: PINSTRIPED MUDSTONES

Facies 4 is characterized by fine scale (<1/2cm), delicate interbedding of sandstones, siltstones and shales which gives it a pinstriped appearance (Fig.2-7a,b,c,d). The proportion of shale may vary from 30 to 70 percent. This facies is common and ranges from a few tens of centimeters to a maximum of about 3 meters in thickness.

The sandstone (mostly very fine-grained although rare fine-grained beds do occur) and siltstone beds may range from a few millimeters to 2 cm in thickness but average about half a centimetre. These beds are almost always sharp based and commonly comprise a single train of starved symmetrical ripples (2-3cm wavelengths) which gives them a characteristic "biscuit" shape. Cross-laminae within individual sandstone beds or within single ripples often dip in the same direction but have a symmetrical profile (Fig.2-7a). These are typical of combined-flow ripples. Synæresis cracks may occur in places at the base of sandstone

Figure 2-7. Facies 4, pinstriped mudstones, A. typical pinstriped mudstone with thin, millimeter scale cross-laminated sandy beds draped by shale. Ripples are symmetrical but laminae tend to dip in the same direction, perhaps indicating combined flow. B. similar facies with rather peculiar sub-vertical burrows. Some of these in the left of the core are black, carbonaceous, and pyritized and may be root casts. C. pinstriped mudstone, similar to a, but containing a rather massive silt bed in the middle which contains silty load casts. D. deformed pinstriped mudstone, gradational with facies 6.

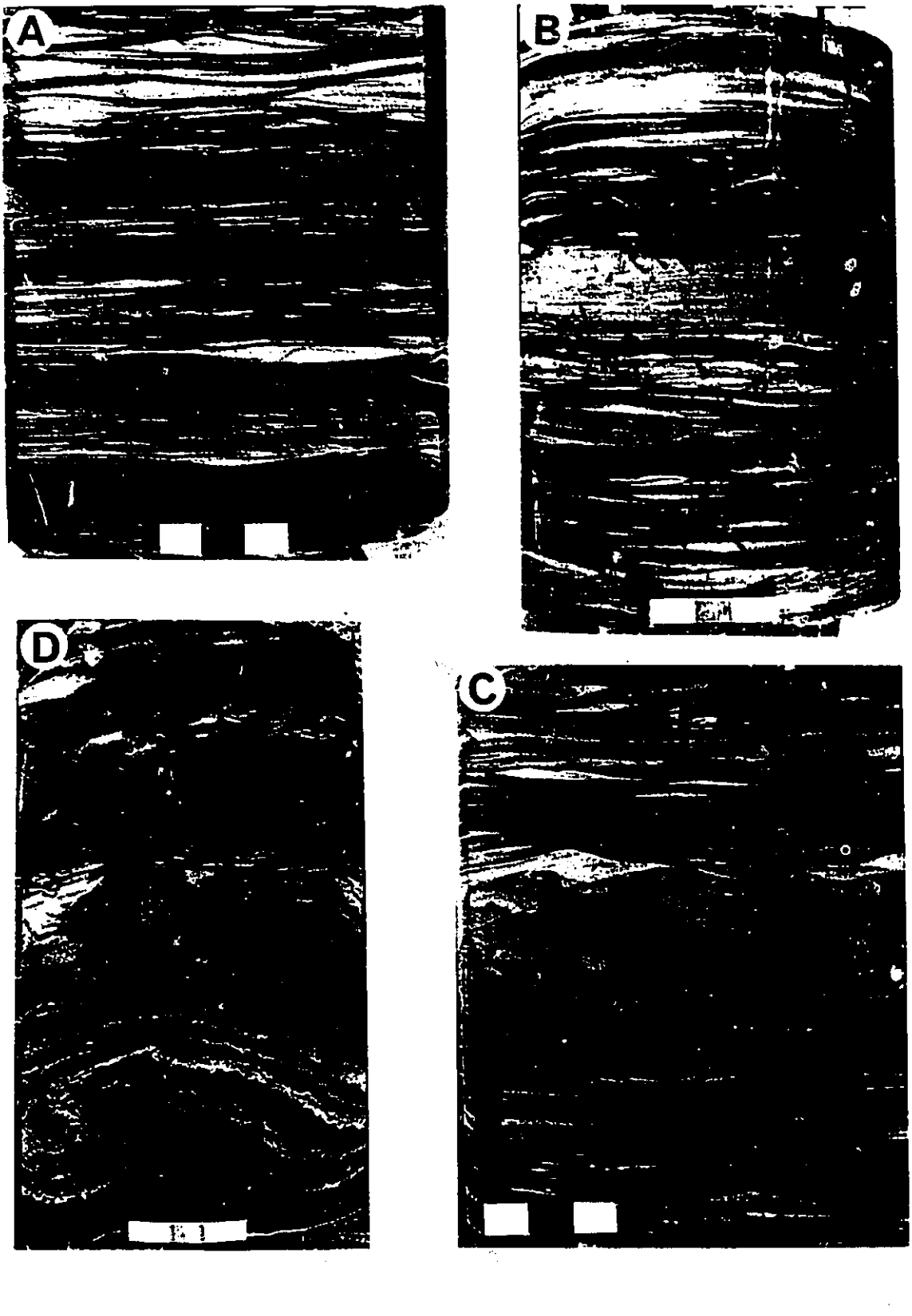
A
B
D
C

beds, but are rare. Siderite is common in this facies, occurring as distinct nodules or as more diffuse beds 1/2 to 2 cm in thickness and which impart a characteristic reddish-brownish colour to this facies (unfortunately this is not obvious in the black and white photos).

Soft sediment deformation features are fairly common in this facies (Fig.2-7c,d) and usually consist of units, a few tens of centimeters or less in thickness, showing folding, convolute bedding and micro faulting, often bounded by horizontally bedded units.

Flora and Fauna

Facies 4 usually shows a low degree of burrowing, the most common burrow forms being *Planolites* (less than 1/2 cm in diameter) and *Skolithos*. Pinstriped mudstones are characterized by relatively abundant carbonaceous debris often with perfectly preserved leaves on bedding plane surfaces. In places, this facies contains pyritized to carbonaceous *in situ* root casts up to half a centimeter in diameter (Fig.2-7b).

Macrofossils include *Corbula sp.* (Fig.2-3a,b,d) and possible *Unio dowlingi* (a non-marine pelycypod (McLearn 1945)). Microfauna are very sparse, and forams were not observed.

Interpretation

Facies 4 has similar characteristics to tidally produced flaser and linsen bedding, defined by Reineck and Wunderlich (1968), and may indicate tidally influenced deposits.

The lack of marine fossils, high proportion of carbonaceous debris, and occasional presence of *in situ* root casts suggest a non-marine to transitional-marine environment of deposition. The fine-grained nature of this facies indicates a relatively low energy environment. The ubiquitous siderite may be indicative of a brackish or marshy environment similar to those forming in similar environments at the present (Pye,1981; Postma,1981). Deposition was probably in a shallow standing body of water that was frequently washed by waves and that was vegetated locally. Possible environments of deposition could include any number of shallow water restricted marine to non-marine environments. These could include delta plain, lagoonal, tidal flat, inter-distributary bay, lacustrine, floodplain or levee environments.

2-2-5. FACIES 5: BANDED MUDSTONES

Facies 5 comprises interbedded sandstone and shale with very little siltstone. The sharp nature of upper and lower bedding contacts within this facies gives it a "black and white" banded appearance in core (Fig.2-8 a,c). This facies is fairly common and may range from a few tens of centimeters up to a few meters in thickness. Thickness of interbeds is usually highly variable from a few millimeters to a few centimeters even within the same unit (Fig.2-8c). Sandstone may vary from very fine to medium-grained. Sandy interbeds usually have razor-sharp bases and tops and show various types of cross-lamination (wave and current). Abundant synæresis cracks are characteristic features

Figure 2-8. Facies 5, banded mudstone, A. interbedded fine sandstone and black shale with abundant compacted synæresis cracks showing typical V-shape. B. oblique view of synæresis cracks showing typical spindle-shape on surface. C. heterolithic mixture of sandstone, pinstriped mudstone, and banded mudstone. Circular, sandy features in upper third may be *Planolites* burrows.

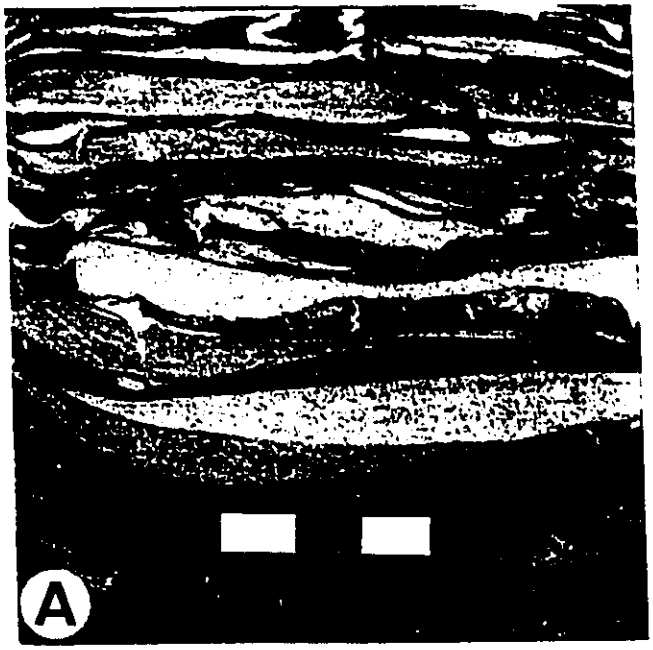
A

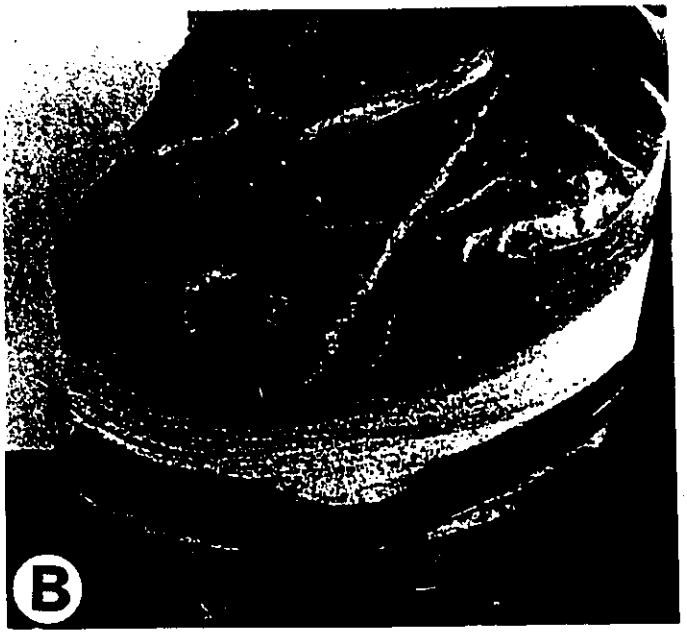
B

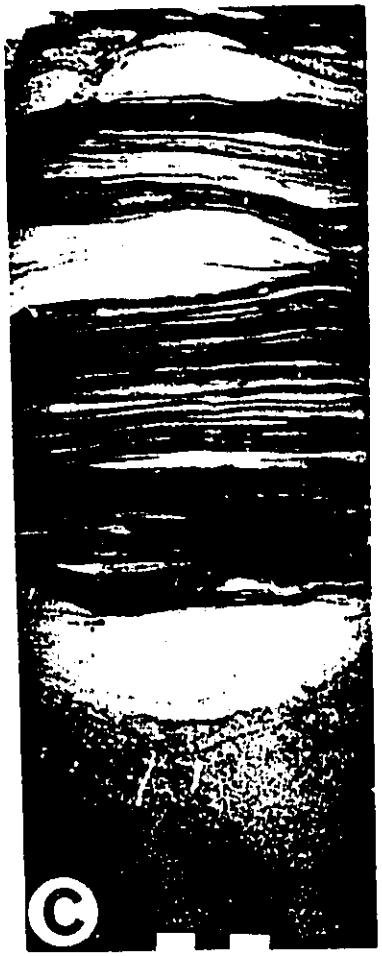
C

at the base of sandstone beds (Fig.2-8a,b,c). They are V-shaped in cross-sectional views and thin downwards although compaction often deforms the cracks imparting a wiggly appearance. Synæresis cracks on bedding plane surfaces show characteristic spindle-shapes (Plummer and Gostin, 1983). Sandstone beds are draped with black, carbonaceous shaly interbeds. Shale may vary in proportion from 30% to a maximum of about 50%. Siderite is relatively common and may occur as discrete nodules or bands. In places burrowing may be moderately well developed, *Planolites*, *Chondrites*, and *Teichichnus* were the most commonly recognized burrow forms. This facies is gradational with Facies 3B.

Interpretation

The trace fossils are similar to those observed in Facies 3B suggesting a similar stressed, brackish to transitional marine environment (see previous discussion in section 2-2-3B). The occurrence of sharply bounded, relatively coarse, laminated to wave-rippled sandstone beds suggests sudden, episodic deposition from a sandy source, possibly in fairly shallow water. The abundant synæresis cracks probably result from salinity changes and perhaps indicate a periodic fresh water influence. Descriptively this facies is very similar to linsen bedding which has been interpreted as characteristic of tidal flats environments (Reineck and Wunderlich, 1968).

2-2-6. FACIES 6: DEFORMED MUDSTONES

Facies 6 (deformed mudstones) comprises massive to deformed silty mudstones with rare bedding (Fig.2-9a,b,c,d). This facies is fairly common and usually averages about 1 to 3 meters thick. Soft sediment deformation features are commonly visible and may include sandy load casts, and ball and pillow structures (Fig.2-9a,b,c); as well as highly deformed beds, a few tens of centimeters thick with sharp (sometimes irregular) upper and lower contacts (Fig.2-9d). Pyritized roots are sometimes observed. This facies is commonly gradational with blockstones (Facies 2) and pinstriped mudstones (Facies 4, Fig.2-7d).

Interpretation

The associations with roots and lack of marine fossils may indicate deposition in a non-marine to transitional marine setting. Soft sediment deformation features may be produced in a number of ways (Blatt et al., 1980, p.188-193; Allen,1984 vol.II, p.343-393) but usually indicate sediment instability. Load structures suggest that coarser sandy units were deposited onto a rather soupy, water rich substrate into which they sank. These are interpreted to indicate high sedimentation rates. In units with a lot of disseminated organic material, disruption may be caused by gas produced during decomposition of organic material. More massive units may indicate slumping. Distinction of these different mechanisms may be difficult, especially in core.

Figure 2-9. Facies 6, deformed mudstones, A. laminated sandy load casts in a silty mudstone, B. sandy ball loading into laminated silty mudstone, another possible muddy load structure above scale, C. large sandy ball encased in silty, sideritic mudstone. Mudstones are laminated at the base and show greater compaction underneath the ball. D. Massive, totally deformed sandy mudstone. Laminations at right are vertical. Shiny surface indicates slickenside. Unit interpreted as possible slump structure.

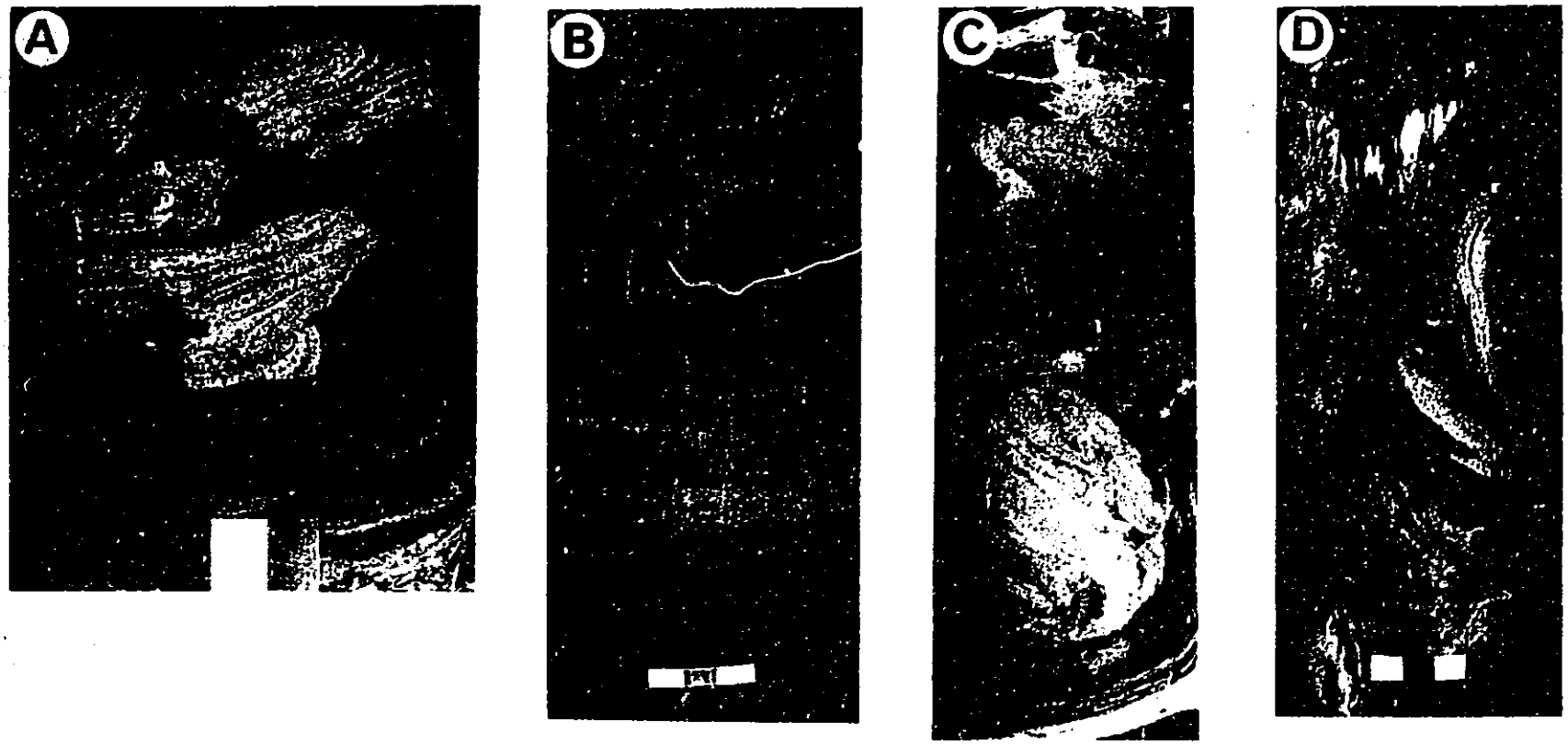
A
B
C
D

2-2-7. FACIES 7: SANDSTONE

Eight sandstone facies were recognized. They were distinguished on the basis of sedimentary structures, grain size, and the degree and type of burrowing although these facies are often gradational with each other. Several textbooks and special publications have documented the interpretation of depositional processes and environment based on the stratification of sandstones and a knowledge of sedimentary bedforms (e.g., Allen, 1984; Blatt et al., 1980; Harms et al., 1975)

A. Facies 7A (HCS Sandstone)

Facies 7A (Fig.2-10a,b,c,d and 2-11a,b,c) is common and ranges from 10cm to a maximum of about 3 meters in thickness. Facies 7A comprises very fine-grained sandstone with thin shaly laminae in places. Sandstones exhibit low-angle inclined to low-angle intersecting lamination (less than about 12°) showing no preferred orientation in core and commonly showing convex upward curvature. Sandstone beds may range from a few centimeters to a few meters in thickness, are commonly sharp-based and may have shaly bioturbated tops.

Thicker beds often show evidence of amalgamation, such as shale drapes and scours, erosively cutting the bioturbated tops of previously deposited beds (Fig.2-22b). This may produce alternating beds of laminated to bioturbated sandstone. Common burrow forms include *Asterosoma*, *Paleophycos*, *Conichnus*, *Skolithos* and occasional escape burrows (Fig.2-22b,c,d).

In places, isolated beds of Facies 7A, 10 to 30 cm thick and sometimes interbedded with shale, erosively cut into blockstones to produce spectacular gutter casts as shown in figure 2-11a,b, and c.

Interpretation

This characteristic low-angle, curved lamination in these sandstones is interpreted as representing hummocky cross-stratified beds, deposited below fair-weather wave base but above storm wave-base on a shelf or in the lower shoreface. HCS has been described and interpreted by Harms et al., 1975 and Duke,1985b. Occasionally, these beds have highly scoured bases which are interpreted as gutter casts (Whitaker, 1973; Duke,1985a,b).

B. Facies 7B (wave rippled sandstone, Fig.2-12)

Facies 7B is fairly common ranging from a few centimeters up to a few tens of centimeters thick. It comprises very fine-grained to lower fine-grained sandstone characterized by symmetrical wave ripples. Cross laminae may show evidence of a preferred direction of dip. Rare burrows may include *Asterosoma*, *Skolithos* and *Ophiomorpha*,. In some places, this facies is gradational with Facies 7A.

Interpretation

Wave ripples are produced by oscillatory flow although where a preferred orientation of cross-laminae is observed combined-flows are possible (Harms et al., 1982; Clifton and Dingler, 1984). Possible environments of deposition are highly variable

Figure 2-10. Facies 7A, HCS sandstone, A and C. Very fine-grained sandstones containing low angle intersecting laminae interpreted as hummocky cross stratification, B.HCS sandstone with inter-stratified wave ripples, D. HCS sandstone with thin shaly interbeds. Underlying bed is burrowed.

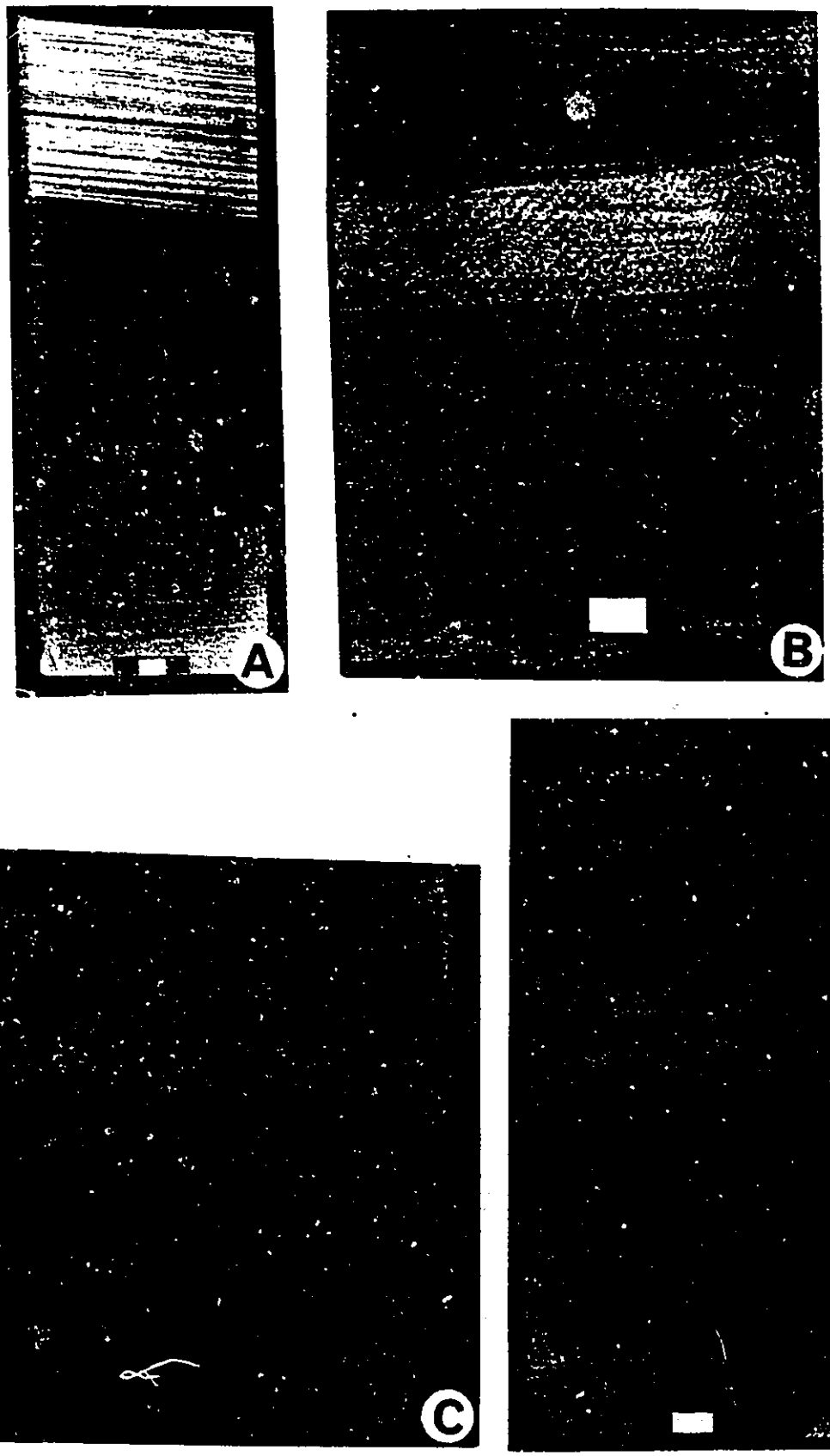
A
B
C
D

Figure 2-11. Facies 7A, sand-filled gutter casts, A. Laminations are seen abruptly terminating against sides of gutter cast, B. Back view of same gutter as shown in a, showing low-angle curved lamination interpreted as HCS. Truncations visible in middle of core, C. Gutter cast cutting into laminated shales (Facies 1A). Gutter undercuts semi-consolidated siderite nodule. Gutter is filled with wave-rippled to HCS sandstone.

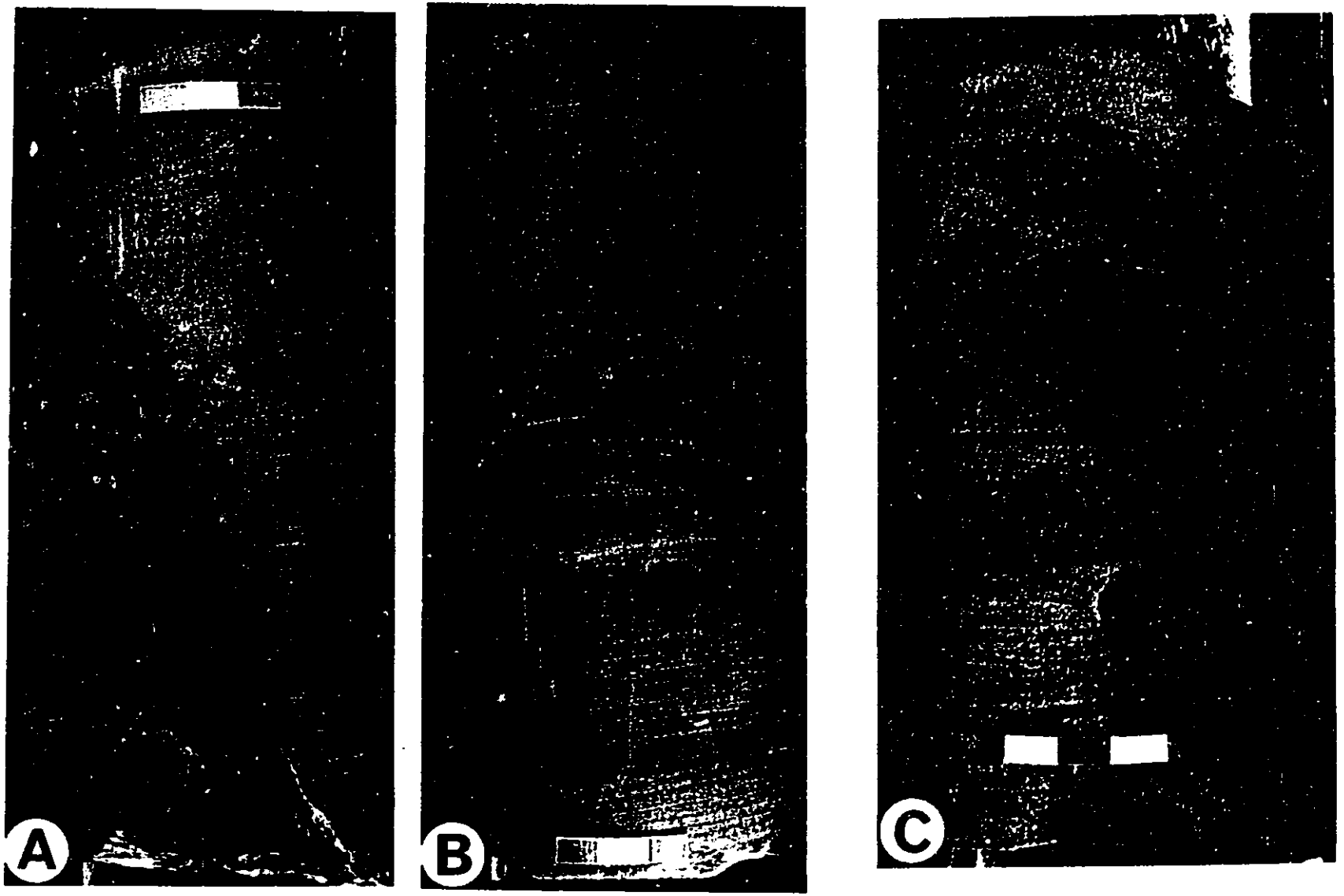
A
B
C

Figure 2-12. Facies 7B, wave-rippled sandstone, A. Low angle inclined laminated sandstone passing up into wave rippled sandstone, interpreted as resulting from a waning storm flow, B. Wave rippled sandstone with thin shaly drapes, C. Wave rippled sandstone bed in blockstones. Gradational with HCS sandstone below. Scale in all photos is 3cm.

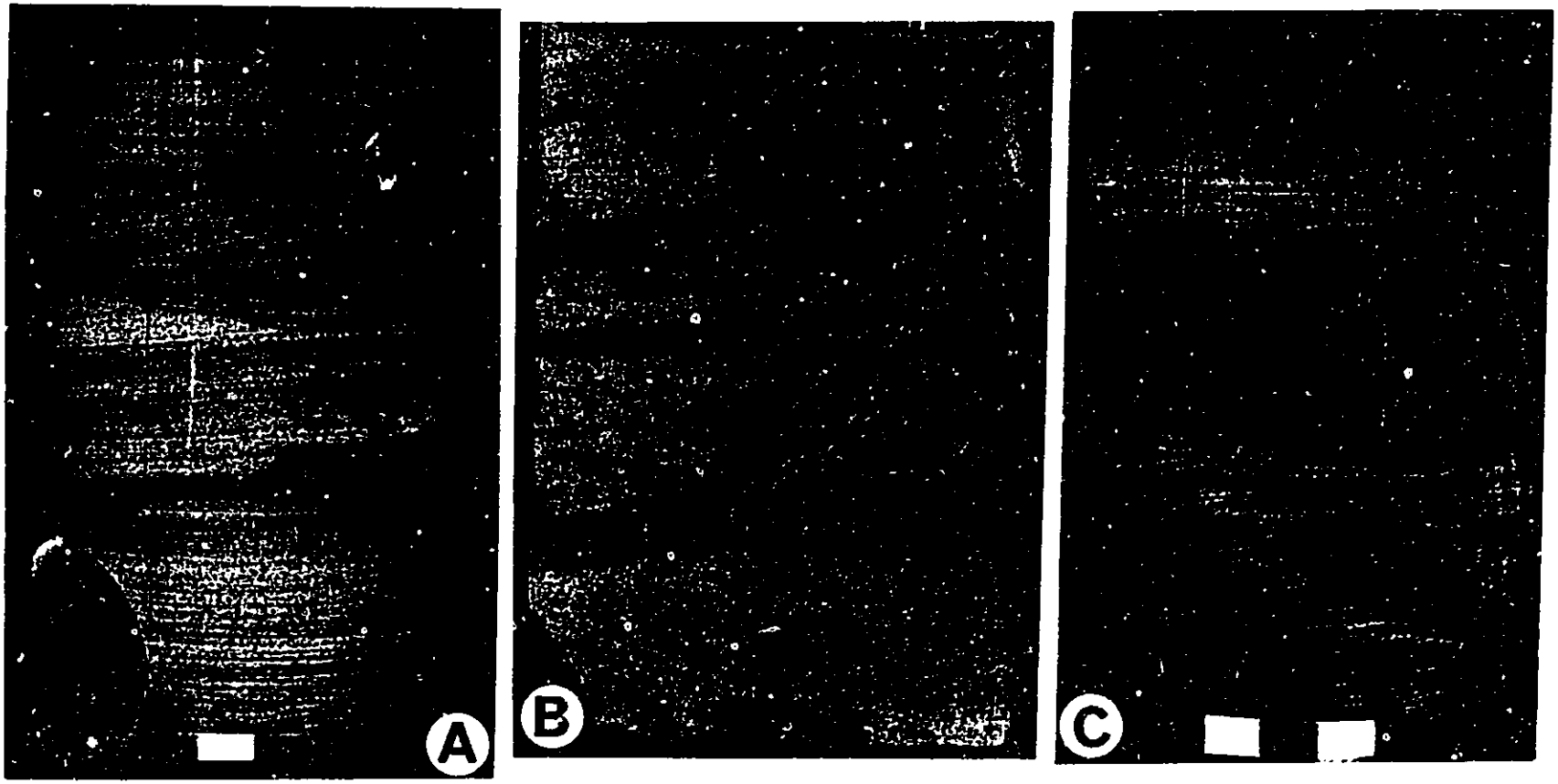
A
B
C

and interpretation will often depend on the associated facies. Where marine trace fossils are associated a marine origin is indicated.

C. Facies 7C (current rippled sandstone, Fig.2-13)

Facies 7C is fairly common and ranges from a few centimeters up to about 2 meters in thickness. It comprises very fine to fine-grained sandstone characterized by asymmetrical ripples which may occur in climbing sets (Fig.2-13a,b). Cross-laminae always show a preferred orientation and are often defined by very thin shaly laminae, which sometimes thicken toward the ripple toeset (Fig. 2-13a). Beds are commonly sharp based and may contain mud chips and siderite clasts (Fig.2-13 d). Sandy beds may begin with plane parallel lamination capped by ripples (Fig. 2-13e) which may become shaly upwards. Burrowing is usually rare to absent, although *in situ* root traces (Fig. 2-13c) and *Skolithos* traces sometimes occur near bed tops. Occurrences greater than a few tens of centimeters in thickness, may contain thin shaly partings.

Interpretation

The presence of asymmetrical ripples and climbing ripples suggests deposition by unidirectional currents (Blatt et al., 1980, p.146-154). Where root traces are present, a non-marine environment is indicated. Thicker occurrences with erosive bases may be associated with channels. Parallel laminated to current rippled sandstone are descriptively similar to Bouma Sequences (Bouma,1962) and represent deposition from waning unidirectional

flows. Possible environments are variable but indicate a lack of marine re-working. The associated facies will be important in determining the environment of deposition. Possible environments in a shallow marine setting could include crevasse splays or channels, or major distributary channels; on a non-marine flood plain, on a delta plain, or feeding into an interdistributary bay.

D. Facies 7D (cross bedded sandstone, Fig.2-14)

Facies 7D is relatively common and ranges in thickness from about 10 centimeters up to a maximum of about 15 meters. It comprises fine to medium-grained sandstone characterized by large scale, but usually vaguely defined, planar tabular and trough, cross bedding in sets ranging from 10 cm to half a meter in thickness, with foreset dips of up to 23° (Fig.2-14a,b,c). The large scale cross laminae are distinct from Facies 7A in showing a preferred orientation. Shale rip-ups (commonly sideritized) and shaly partings up to 1.5 cm thick occur in places.

Flora and Fauna

Burrows are rare to absent in this facies but may include occasional *Skolithos*, *Asterosoma*, escape burrows and occasionally root traces. Rare body fossils may include *Inoceramus* (Fig.2-14a), and oyster fragments but they are usually restricted to basal portions of beds. Large woody coal fragments are observed in places, especially at the base of thick sandstones.

Figure. 2-13. Facies 7C, trough cross-laminated sandstone, A. climbing ripple sets. Cross laminae defined by thin shaly partings, B. Climbing ripple sets. Cross laminae are defined by sideritization of shaly laminae. Proportion of shale increases upward. C. current rippled sandstone containing well developed root trace in middle, probably causing physical disruption at the base of the sand bed above the scale, D. current ripples associated with sideritized mud-rip up clasts, E. Bouma-like unit from parallel sandstone up into cross-laminated sandstone.

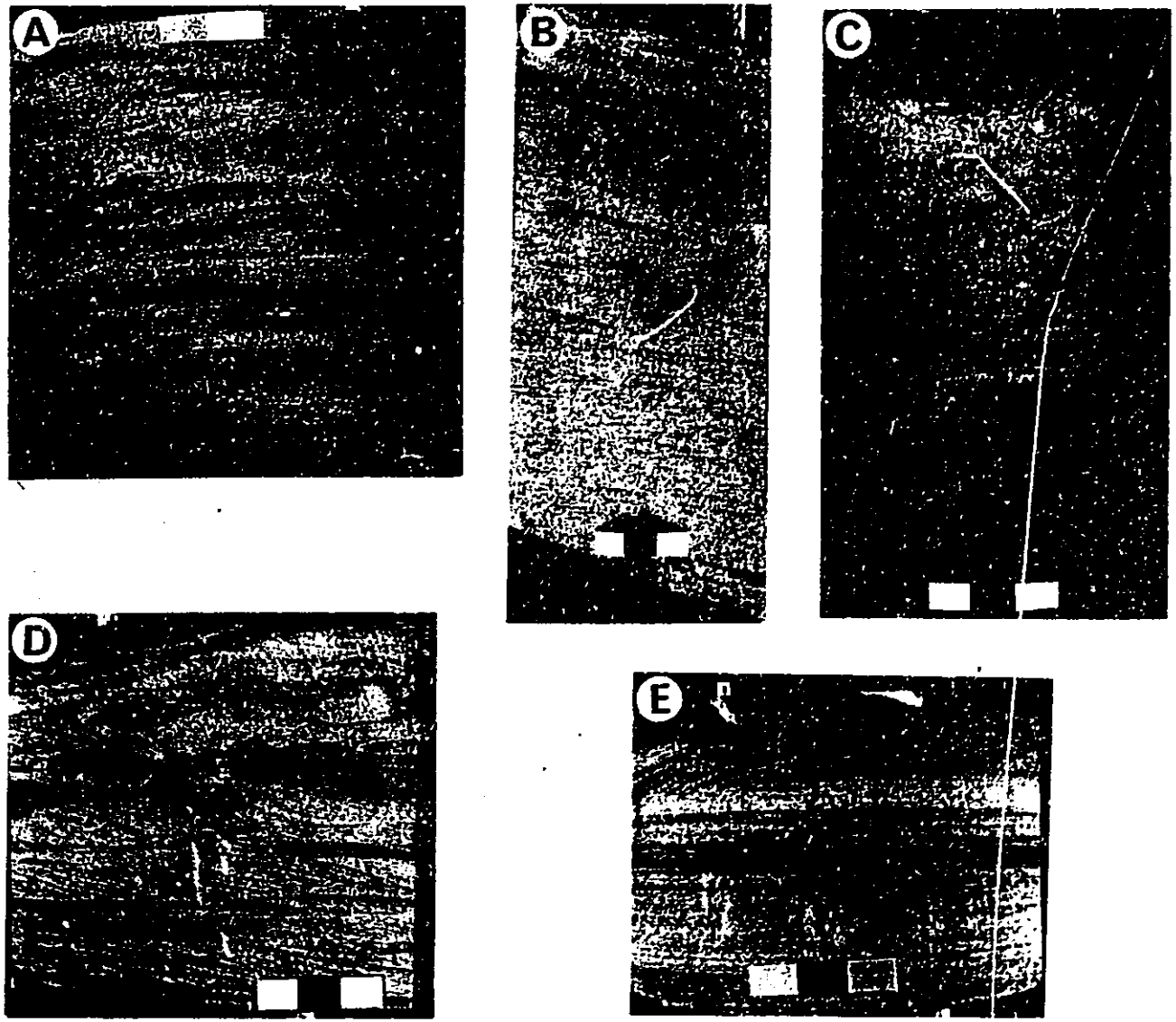
A
B
C
D
E

Figure 2-14. Facies 7D, cross-bedded sandstone, A.cross-bedded sandstone containing *Inoceramus* shells in the base, B.cross-bedded sandstone with wafer-thin shaly parting in upper third, C.Massive to cross-bedded sandstone.

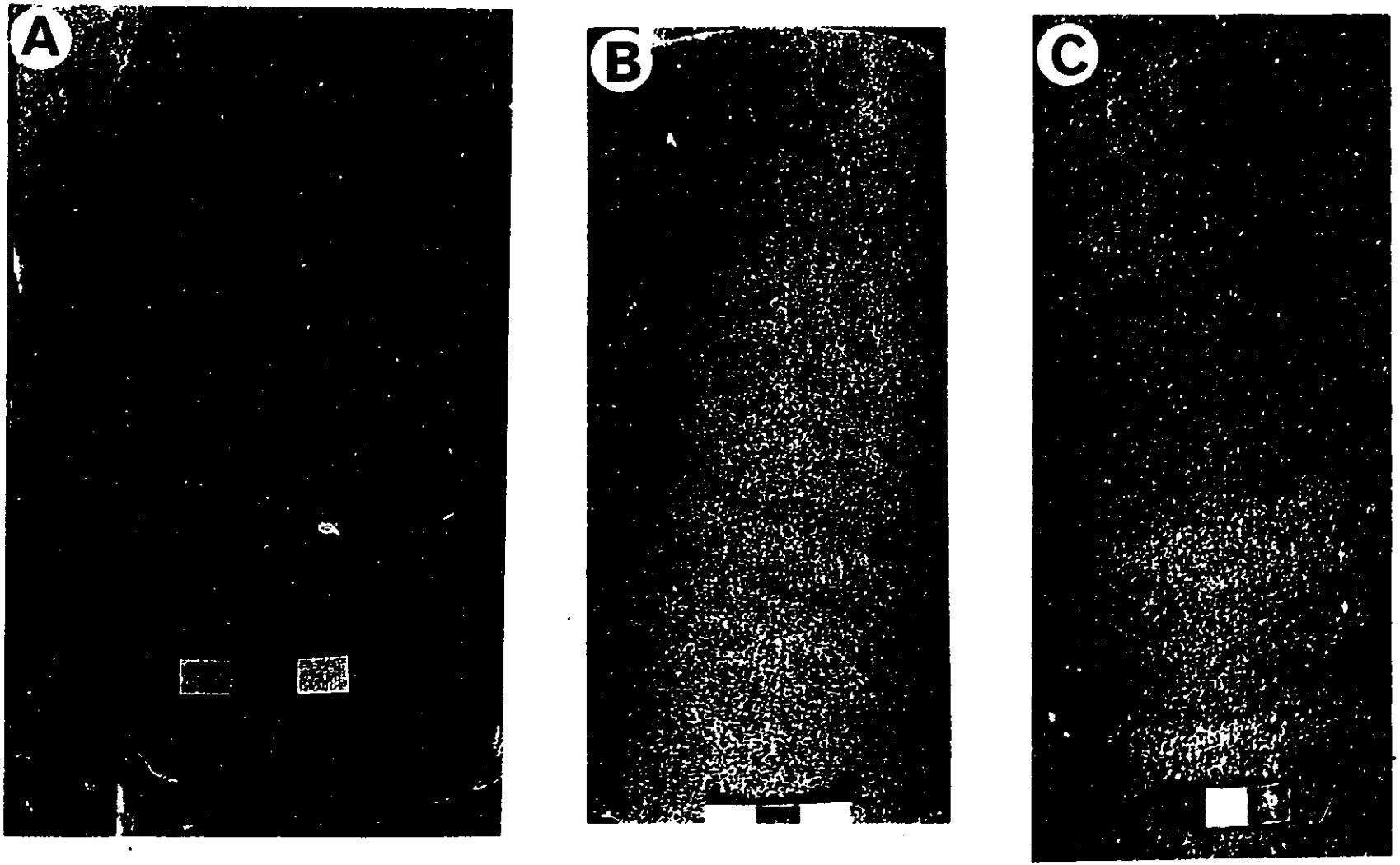
A
B
C

Interpretation

Medium to large scale cross bedding is produced by the migration of large bed forms; dunes (megaripples) or sandwaves (Blatt et al., 1980; Harms et al., 1975). The grain size (greater than fine sand), thickness, and occasional association with root casts in this facies suggest a shallow water origin. Cross bedding is not restricted to a particular water depth or depositional environment and may be produced by open channel unidirectional flow (e.g., channel sands) and in the zone of longshore drift (e.g., shoreface sands). The specific environmental interpretation will depend on the associated facies.

E. Facies 7E (sigmoidally cross-bedded sandstone)

Facies 7E (Fig.2-15) is usually found at the base of fining upwards facies successions. It may reach 3 meters in thickness and usually comprises cross-bedded, fine-grained sandstone often containing siderite clasts, mudstone clasts and shell debris. The cross bedding is defined by millimeter thick, carbonaceous shaly laminae which vary in thickness and number upwards. These laminae comprise poorly to well defined mud couplets (2-15a,b,c, Fig.2-22a). In places, the angle of cross bedding flattens rather than steepens upwards (Fig.2-15a,c) and the shaly laminae also disappear upwards as the sandstone becomes more structureless. Over a thickness of a few meters, this alternation of laminated to more massive sandstone may appear to be cyclic.

Cross-bedding is on a similar scale to sigmoid cross-bedding described by Kriesa and Moiola (1986) occurring in sets that average a few tens of centimeters in thickness.

Interpretation

The presence of ripped-up mudstone and siderite clasts suggests erosion. The cross bedding, presence of mud couplets, and regular alternation of laminated to massive sandstone is characteristic of tidally influenced sand bodies (Kriesa and Moiola, 1986; Visser,1980). The association of this facies, occurring in the lower portion of an erosionally based, fining upwards facies succession, suggests deposition in a tidally influenced channel.

F. Facies 7F (structureless sandstone, Fig.2-16)

Facies 7F is common, and may occur in massive beds reaching a maximum thickness of about 10 meters. It comprises massive to structureless, fine to medium-grained sandstone but is commonly gradational with other sandstone facies, especially Facies 7C and 7D (Fig.2-16a,b). Shale rip-ups, siderite clasts, and shale partings may define crude bedding and occasional vague lamination. Sedimentary structures in some oil producing sandstones are often not discernable and sandstones therefore appear structureless. Burrowing in this facies is rare, although root casts, up to a few tens of centimeters long and a few millimeters in width, are sometimes seen (Fig.2-21a).

Figure 2-15. Facies 7E, sigmoidally cross-bedded sandstone, A. regularly oriented cross-beds are defined in the lower half by thin mud-couplets. These are lost upwards as the cross-laminae flatten. B. close-up of mud couplets (arrows) from a, C. cross-bedded sand with flattening-upward laminae. Thin muddy drapes define lower-most laminae. Siderite pebble is also visible. D. cross-bedded sandstone with possible reversing current ripples climbing up toeset (arrow). Interpreted as of possible tidal origin.

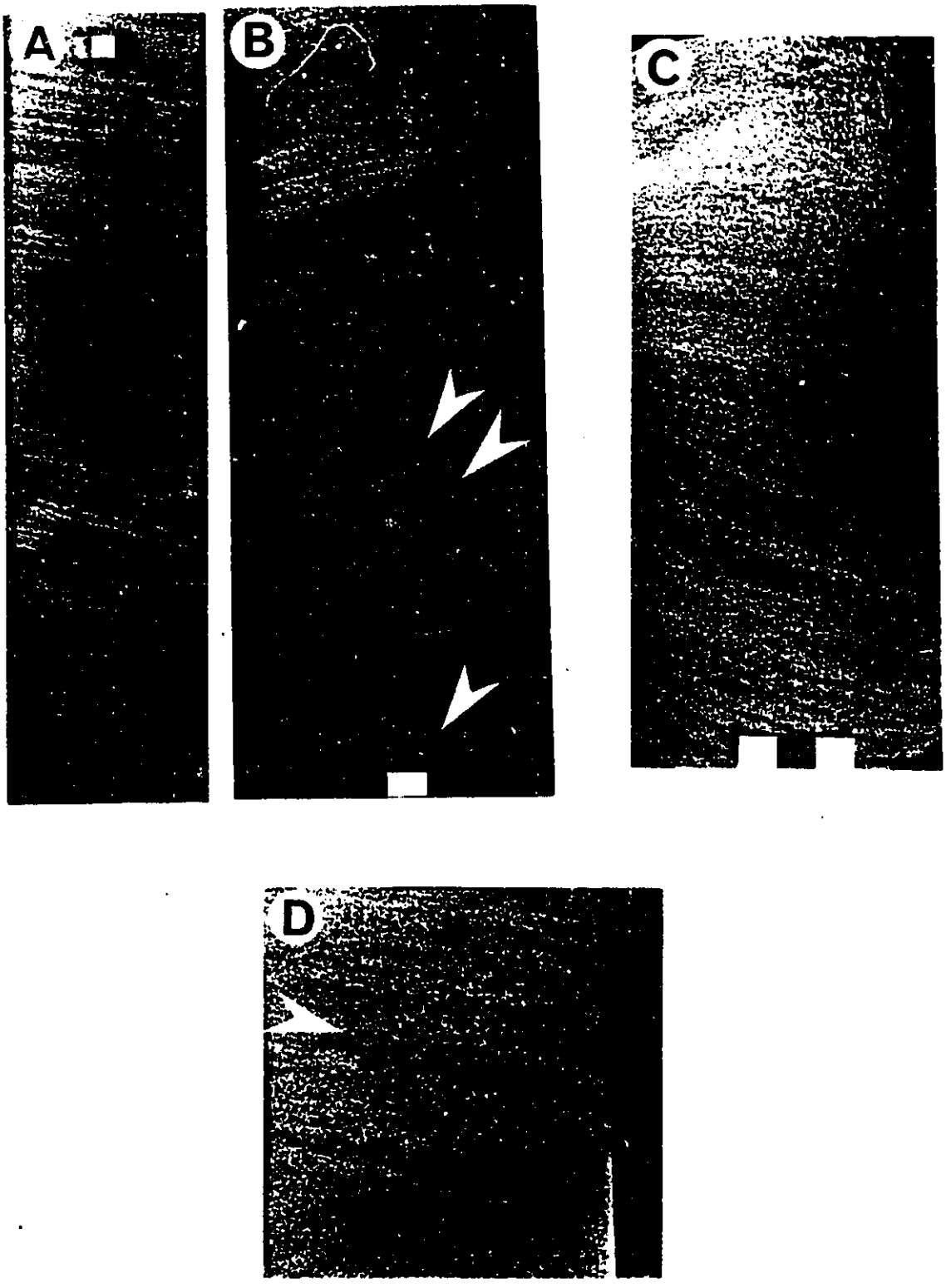
A
B
C
D

Figure 2-16. Facies 7F, structureless sandstone, A. totally featureless sandstone, B.massive sandstone with thin zone of current-rippled sandstone (Facies 7C) at top. Possible crude parallel lamination is visible near the base.

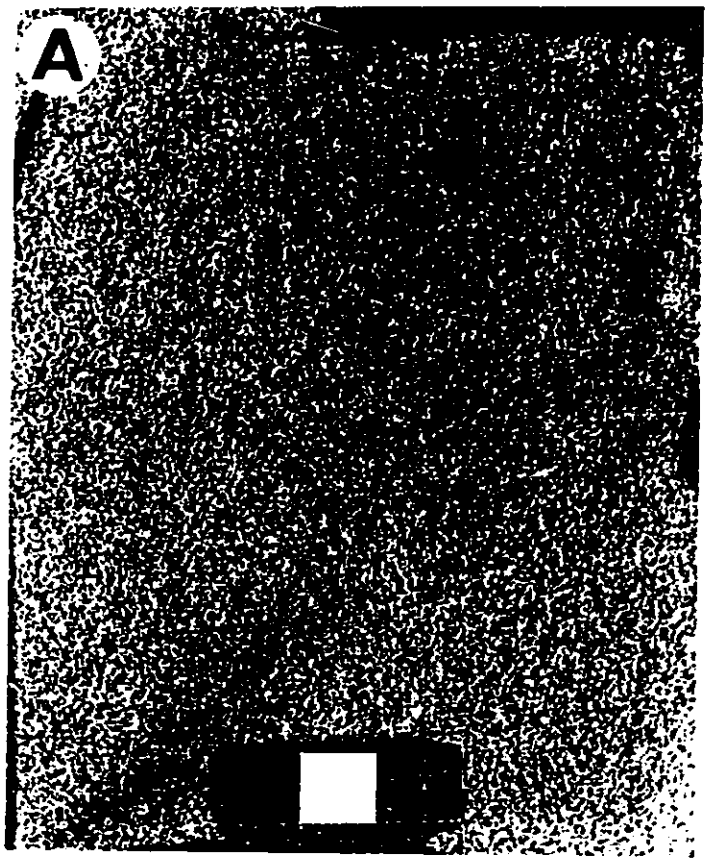
A

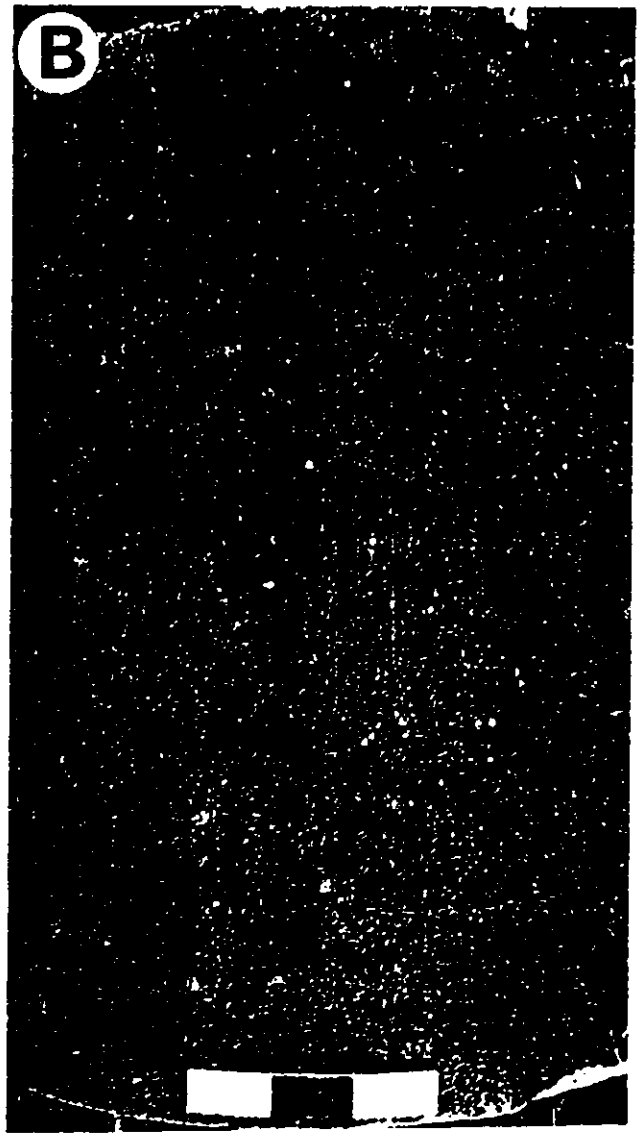
B

Interpretation

Structureless sandstones may form by a variety of processes including; bioturbation (by animals or by plants), homogeneity of sand size and composition (inability to produce lamination), and very rapid deposition. Rapid deposition by powerful currents may be indicated when sandstones contain large siderite clasts and mudstone rip-up horizons, and especially at the base of fining-upward facies successions.

G. Facies 7G (flat laminated sandstone, Fig.2-17)

Facies 7G is relatively uncommon and does not usually exceed about 2 meters in thickness. It comprises fine-grained sandstones usually showing flat, planar lamination sometimes distinguished by subtle differences in calcite cement (Fig.2-17a,b) and sometimes by wafer thin interlaminae comprising macerated coalified plant debris and siderite which resemble "coffee grounds".

Interpretation

Flat laminated sandstone can be produced by a variety of processes including deposition in the upper flat bed field (upper flow regime) by unidirectional currents or by oscillatory flows (Harms et al., 1982). In core, planar, very low angle bedding, less than about 5°, may appear as flat laminated sandstone. This type of lamination is typical of that produced by swash and backwash on a beach.

H. Facies 7H (convoluted sandstone, Fig.2-18)

Facies 7H is relatively uncommon, and usually comprises very-fine grained sandstone. This facies may reach thicknesses of up to about a meter and is characterized by high angle over-steepened to vertical, large scale cross lamination (Fig.2-18a,b). Occasionally this facies may show total disruption of laminae and may be associated with distorted shaly or silty interbeds and with slickensides. Body fossils and bioturbation structures were not noted.

Interpretation

Convoluted sandstones can be produced by a variety of processes (Allen,1984). Rapid rates of deposition may produce high pore fluid pressures. This may result in convolution during de-watering. Where sandstones de-water, dish structures may be expected. Over-steepening of laminae may also result as a result of shear stresses due to deposition of overlying beds. Convolution may also result from loading of sandstone into a thixotropic substrate or as a result of slumping.

I. Facies 7I (pervasively bioturbated sandstone)

Facies 7I (Fig.2-19) is relatively uncommon and comprises pervasively bioturbated, very fine-grained sandstone but may get quite silty. It ranges from a few tens of centimeters up to about 2 meters thick. The original bed boundaries are usually destroyed by burrowing. The burrow forms are absolutely distinctive and comprise marine trace fossils *Ophiomorpha* (Fig.2-19a)

Figure 2-17. Facies 7F, parallel laminated sandstone, A.alternating light and dark layers represent calcitic and non-calcitic cement. Thin black streaks in the middle of the core are carbonaceous debris, B.parallel-laminated sandstone.

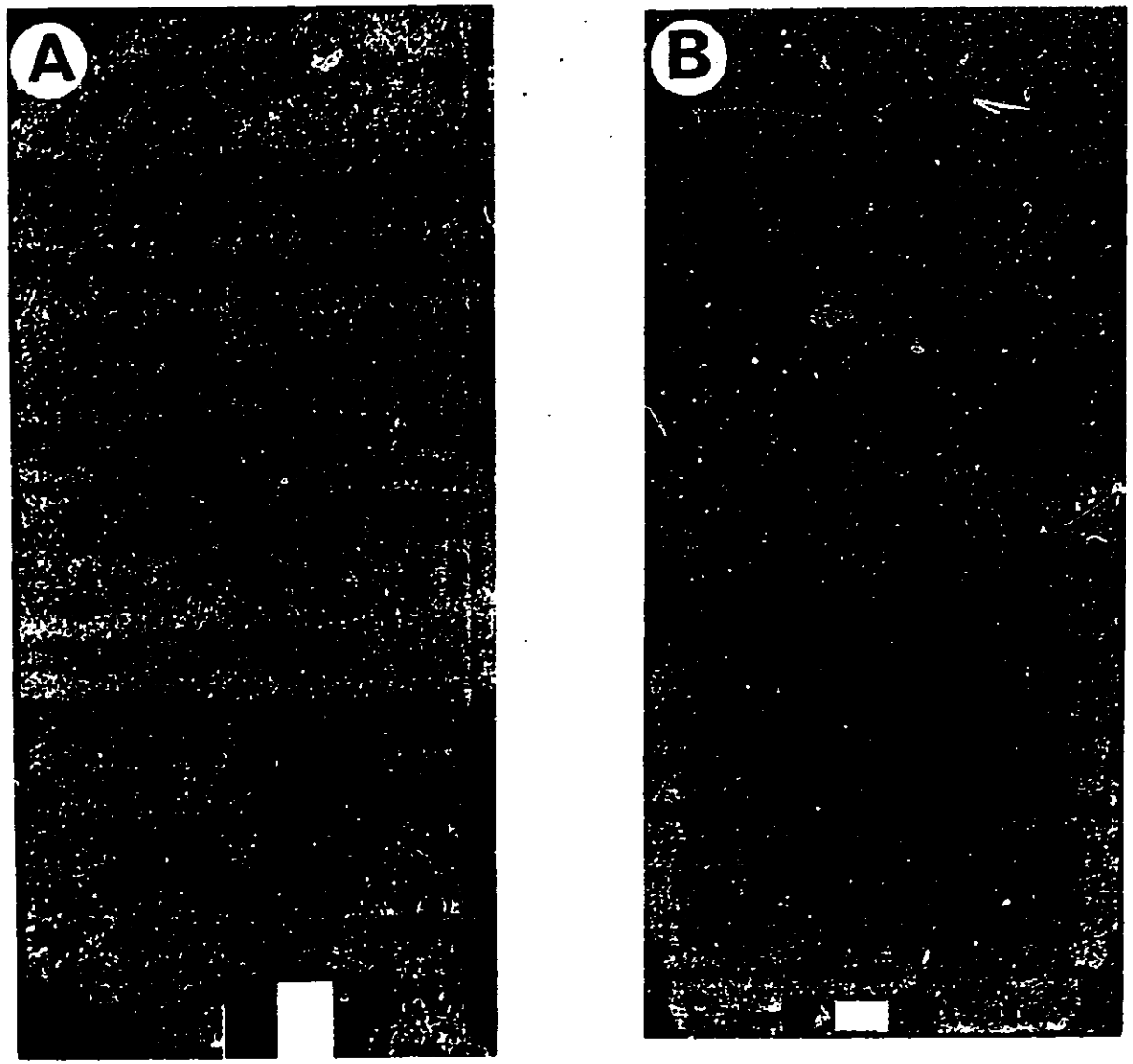
A
B

Figure 2-18. Facies 7G, convolute laminated sandstone, A. oversteepened laminae in very-fine grained sandstone. Highlightes laminae indicate low-angle truncations suggesting that sand bed originated as HCS, B. oversteepened to vertical lamination in very-fine grained sandstone, C. sandy load cast originally deposited as a current rippled bed. Current ripples are still clearly visible. Deformation increases toward the centre of the sandy load.

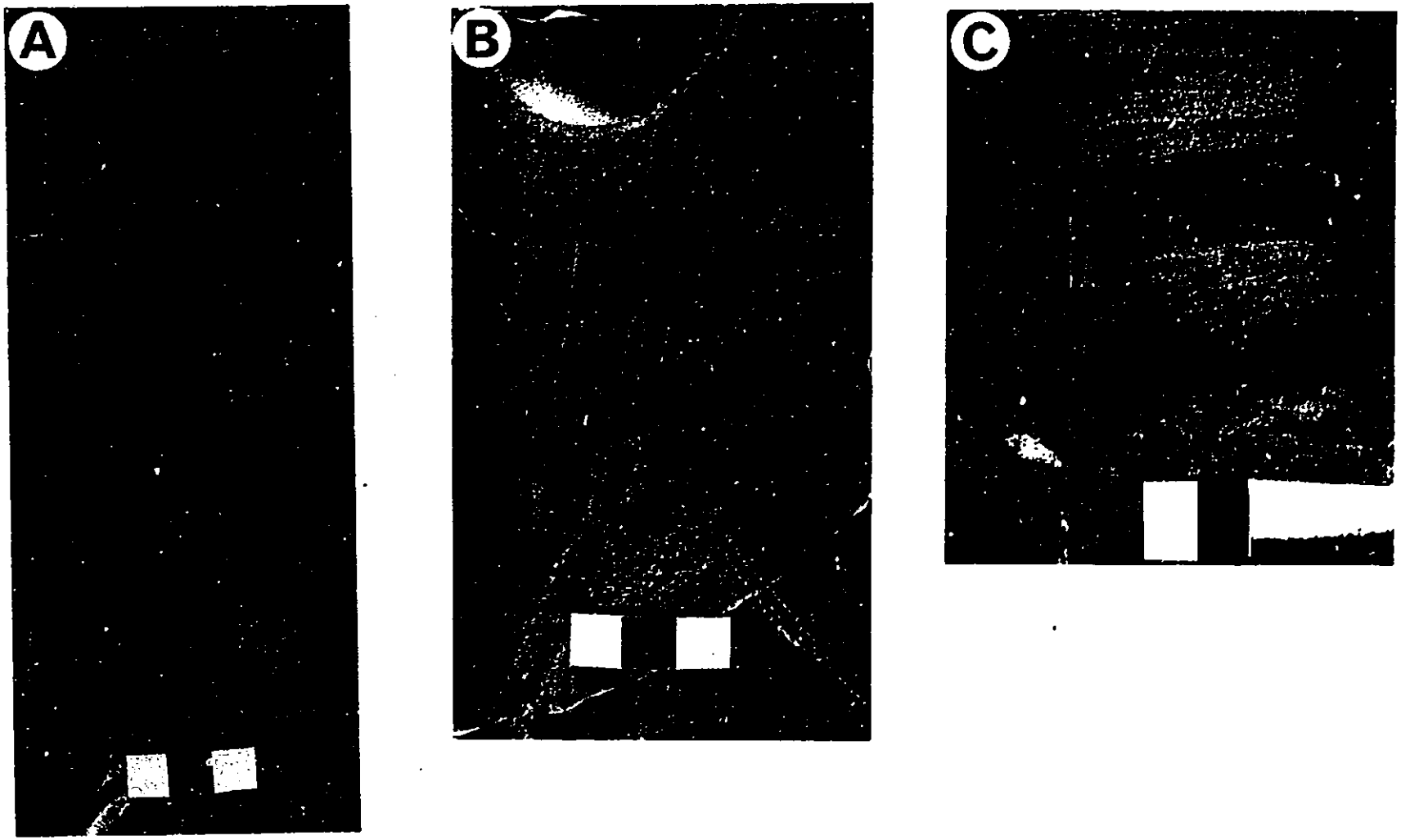
A
B
C

Figure 2-19. Facies 7I, pervasively bioturbated sandstone, A. Pervasively bioturbated sandstone with well developed *Ophiomorpha* burrows showing characteristic knobby wall, B. Sand filled *Thalassinoides* in mudstone overlain by sandstone shown in figure 2-19a, C. Pervasively bioturbated sandstone, with *Ophiomorpha*, *Palæophycus*, and *Asterosoma* burrows.


A

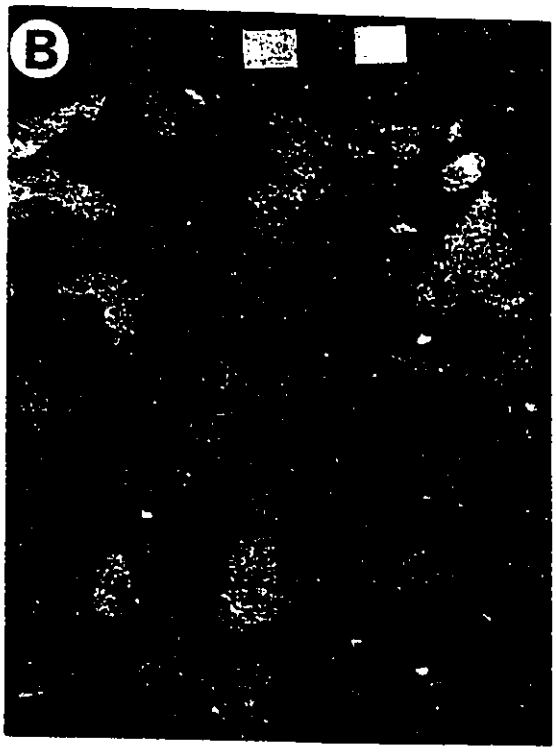
B


C

and *Thalassinoides* (Fig.2-19b) almost exclusively, although *Asterosoma* and *Paleophycos* (Fig.2-19c) are also sometimes present.

Interpretation

The trace fossil assemblage is characteristic of the *Skolithos* ichnofacies (Frey and Pemberton, 1984), and is thought to be indicative of relatively high energy, shallow marine settings in shifting substrates.

2-2-8. FACIES 8-LAG

There are two types of lags, those associated at the bases of channels and those associated at the tops of coarsening upward facies successions and usually produced during marine transgression. This facies is relatively uncommon (but important) and usually ranges from a few centimeters up to 20 cm thick. Lags associated with channels are usually thicker and may consist of clast or matrix supported conglomerate. Clasts usually consist of pebble- to cobble- sized, rounded siderite clasts (Fig.2-20d) and various shell fragments including *Inoceramus* and oyster fragments (2-20c). Shell lags are not always present, and in places lags consist of mud chip conglomerate (Fig.2-20a,b). The matrix nearly always comprises fine to medium grained sandstone. Imbrication and stratification were not noted in any of the lag deposits.

Interpretation

A lag is usually indicative of erosion. The thickness of a lag is usually proportional to the amount of material eroded. Lags are often present at the bases of channels but may occur also

at more widespread erosion surfaces. The significance of lags and erosional surfaces will be discussed in chapter 3.

2-2-9. FACIES 9; PALEOSOL

This facies is relatively rare but consists of greenish-grey, waxy looking, carbonaceous, crumbly shales often with coalified root casts, less than 1 cm thick but showing bifurcation downward (2-21c). The facies reaches a maximum thickness of about 50 cm. Paleosols are interpreted as representing periods of prolonged subaerial exposure.

2-2-10. FACIES 10. COAL

Thin coals, usually less than 20 centimeters, sometimes lie above rooted horizons (2-21a,b). Coals are relatively poorly developed in sediments of the Dunvegan Formation and are frequently gradational with Facies 1C (carbonaceous mudstone). In places, sharp deflections on gamma and sonic logs indicate the presence of coals up to 1 meter thick, however these were not cored.

Interpretation

Coals (especially overlying rooted horizons) indicate emergence. Preservation of coals usually indicate wet environments (swamp and marsh). They can occur in a variety of settings including swamps and marshes, along levees exposed beaches and barrier islands, and in lacustrine environments.

Figure 2-20. Facies 8, Conglomerate lags, A and B. Mud-chip conglomerates within channel fill associations (member D), C.Channel lag comprising shell fragments (mostly oysters), plant debris (arrow) and siderite clasts. Note large siderite clast in the lower middle part of the core. Lag is mixed with fine-grained sandstone. D.Siderite lag with broken shell debris just above the scale.

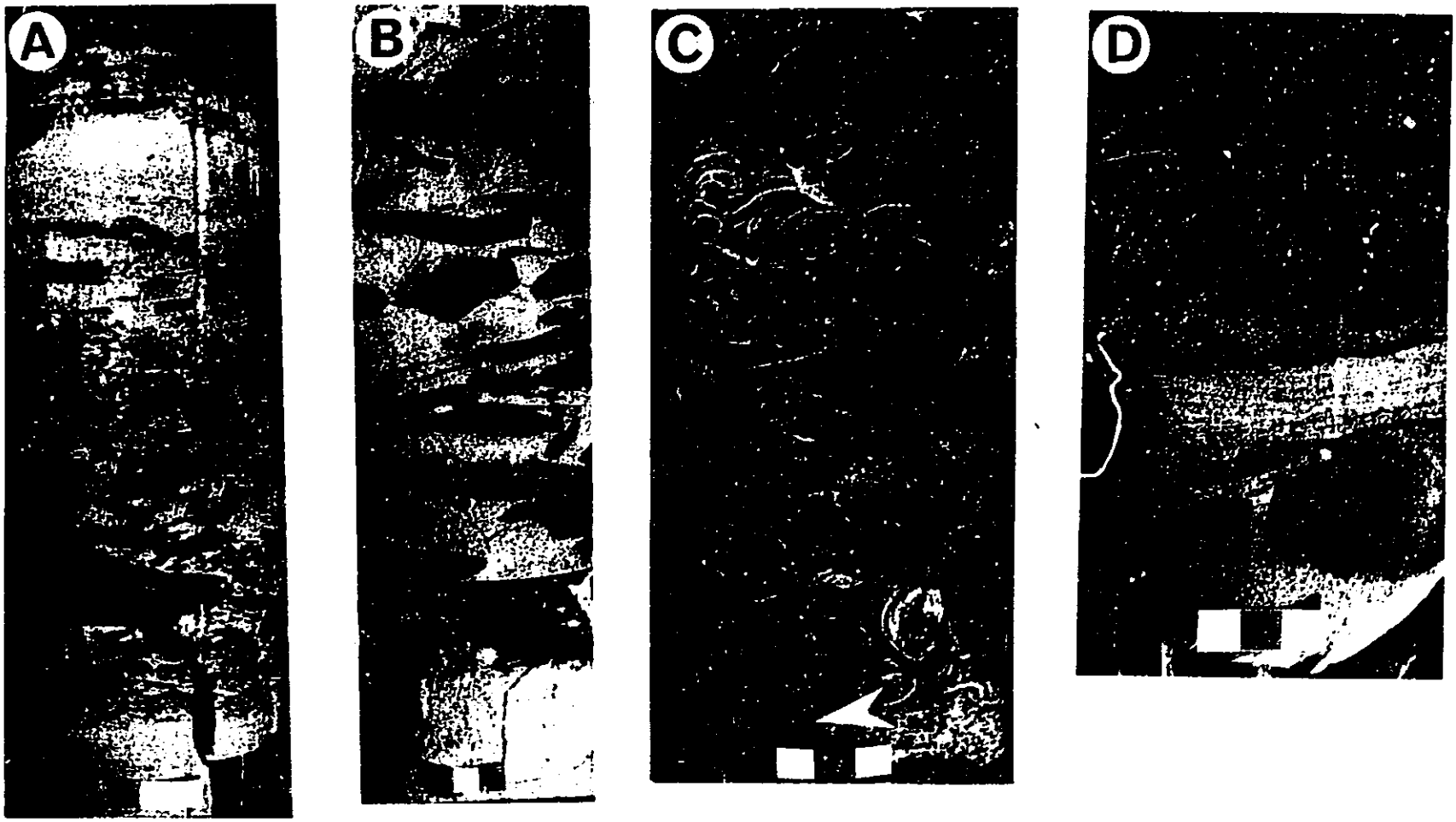
A
B
C
D

Figure 2-21. Facies 9 and 10, Paleosol and coals, A. Black coal overlying structureless sandstone containing abundant root traces B. surface photograph of carbonaceous material of woody origin, C. Grey, crumbly, waxy looking paleosol with well developed root traces.

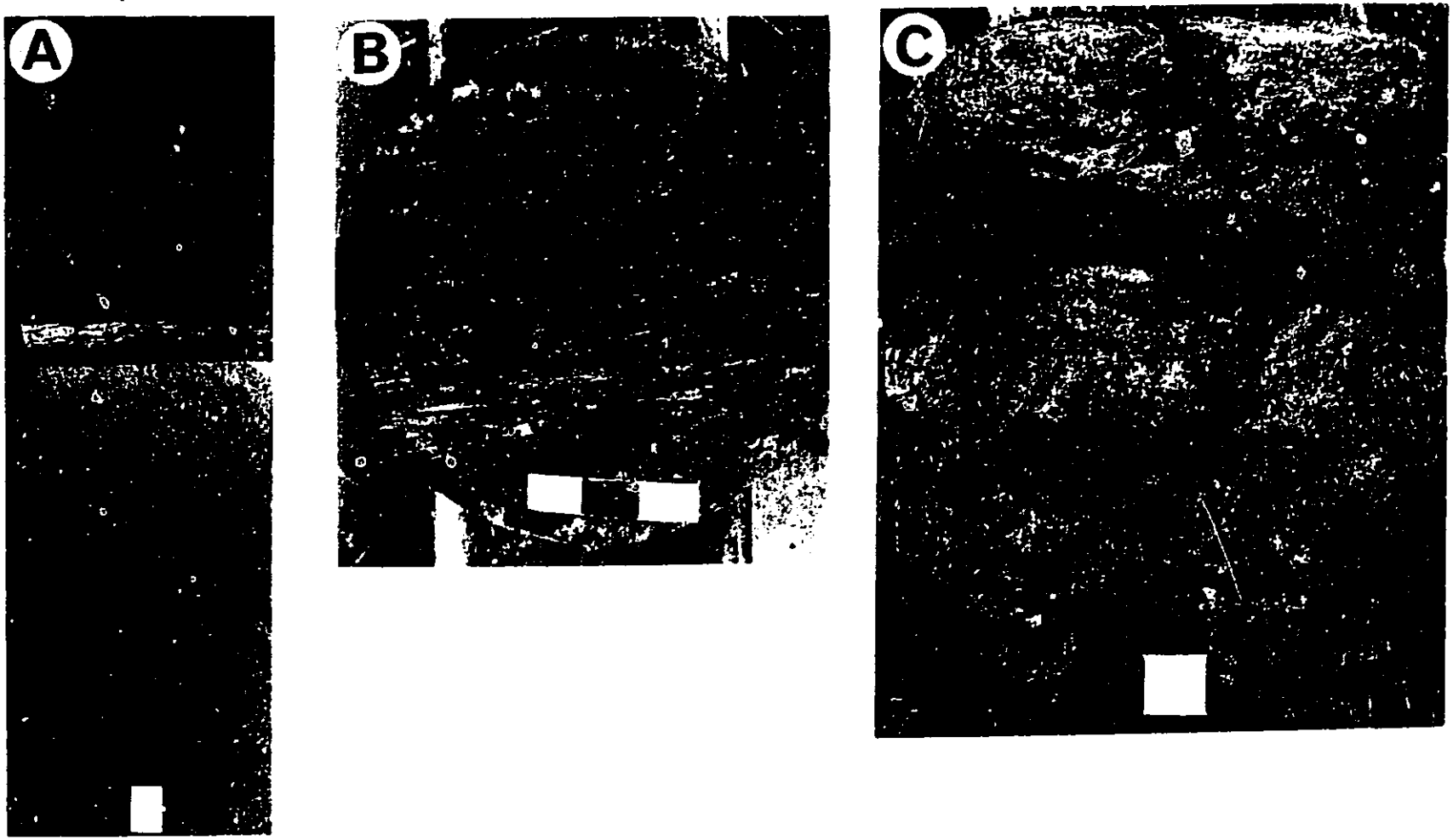
A
B
C

Figure 2-22. Facies 7, various sub-facies, A. Cross bedded sandstone, possibly showing vague mud-couplets, erosively cutting into underlying bioturbated muddy sandstone, B. Bioturbated top of underlying bed is erosively overlain by next, vaguely laminated sandstone bed. This type of stratification is typical of intermittent storms, C. Low angle laminated sandstone containing burrow interpreted as an anemone resting trace., D. Laminated sandstone disrupted by escape burrow. Sand bed is capped by *Palæophycus* burrows.

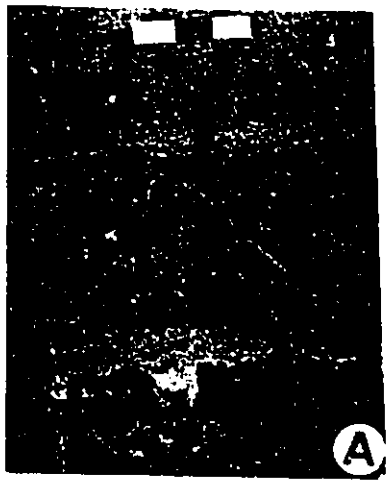
A

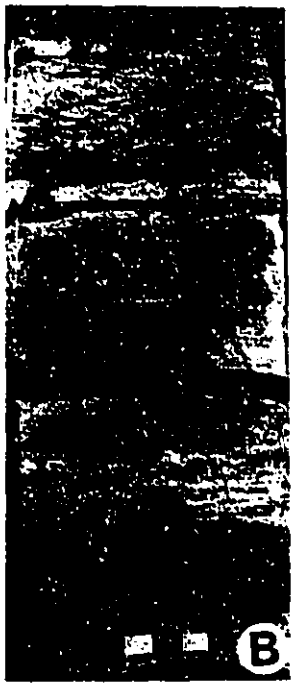
B

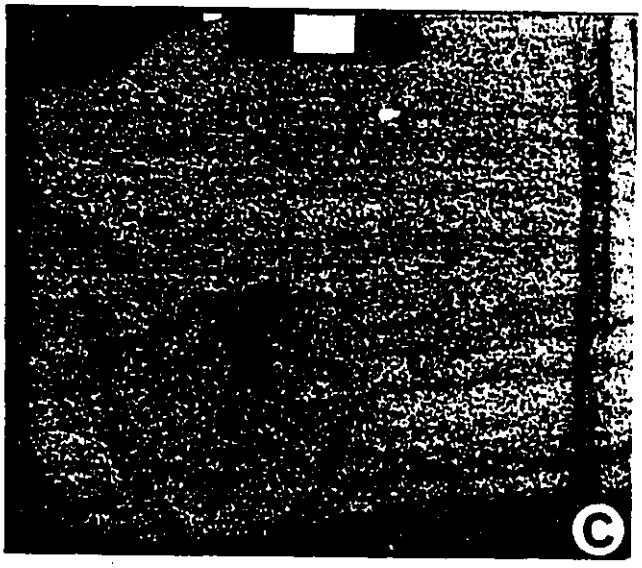
C

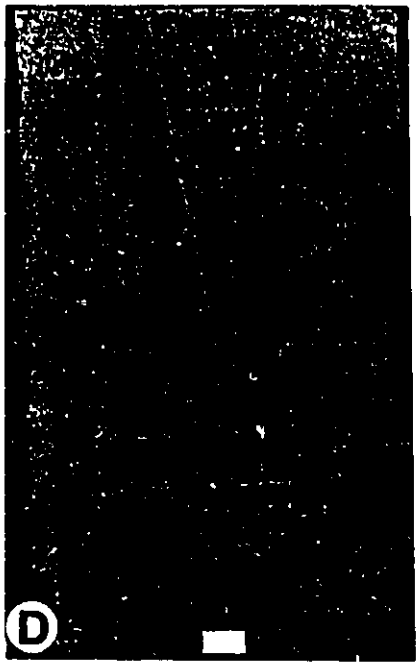
D

2-3. FACIES ASSOCIATIONS

In order to avoid confusion with the term sequence, as used by sequence stratigraphers (Posamentier et al., in press), I have used the term facies succession rather than facies sequence to refer to a specific package or example of vertically stacked facies units. The term Facies Association is used to refer to frequently observed facies successions which usually show a regular pattern, such as fining or coarsening upward. Most of the facies associations described below display gradational contacts between successive facies units and are commonly capped by by discontinuities. Facies associations therefore usually represent a genetically related package of sediment. Facies associations form the basis for the recognition of cyclicity within sediments of the Dunvegan Formation. Although specific vertical facies associations are defined below, lateral facies associations are also recognized and discussed in relation to the various cross sections presented throughout the thesis.

Three groups of vertical facies associations were recognized in core;

1. coarsening upward facies associations,
2. erosionally based, fining upward facies associations, and
3. non-sequential associations often associated with roots.

These three groups were further subdivided into six distinct facies associations described below. Recognition of these six Facies Associations was based on observations made on data from

about 130 cores. Confirmation of the existance of these Facies Associations using rigorous statistical facies analysis techniques (e.g., Markov Chain analysis), was not deemed necessary and was not attempted. Most of the facies successions described in core sections throughout the thesis can be classed as being typical of one of the six end-member facies associations described below, although some facies successions show similarities to more than one facies association.

Presentation of facies associations follows the format of the previous section; description followed by a brief interpretation. Descriptions are first presented in schematic form, followed by a written description. The Facies in brackets indicate that this group of facies units occurs but that individual facies units within the group may be missing or, if all units are present, may not show a regular ordering. As an example, in Facies Association 1A below, HCS and/or wave-rippled sandstone is always followed by cross-bedded, structureless, and/or parallel laminated sandstone.

2-3-1. Coarsening Upward Facies Associations

A. Facies Association 1A

The idealized, complete facies association, in sequence is:

1B - 3A - (7A,7B) - (7D,7F,7G) - 10

This Facies Association is illustrated in figure 2-23. Most of the facies contacts are gradational although individual sand beds within a facies unit may have an erosive base. Facies 10 also

Figure 2-23. Graphic representation of Facies Association 1A interpreted as being typical of wave-dominated prograding shoreface. Coarsening upward Facies Association begins with bioturbated mudstones. It coarsens upward through HCS sandstones (Facies 7A) and into sandy, cross-bedded sandstones (Facies 7D) to parallel-laminated sandstones (Facies 7G) deposited in the shoreface and beach. Upper meter comprises massive root mottled sandstone capped by coal. Figure based on core through shingle D2 in well 7-10-63-1W6, shown in detail in figure 5-7A,B. See text for details and figure 2-29 for facies legend.

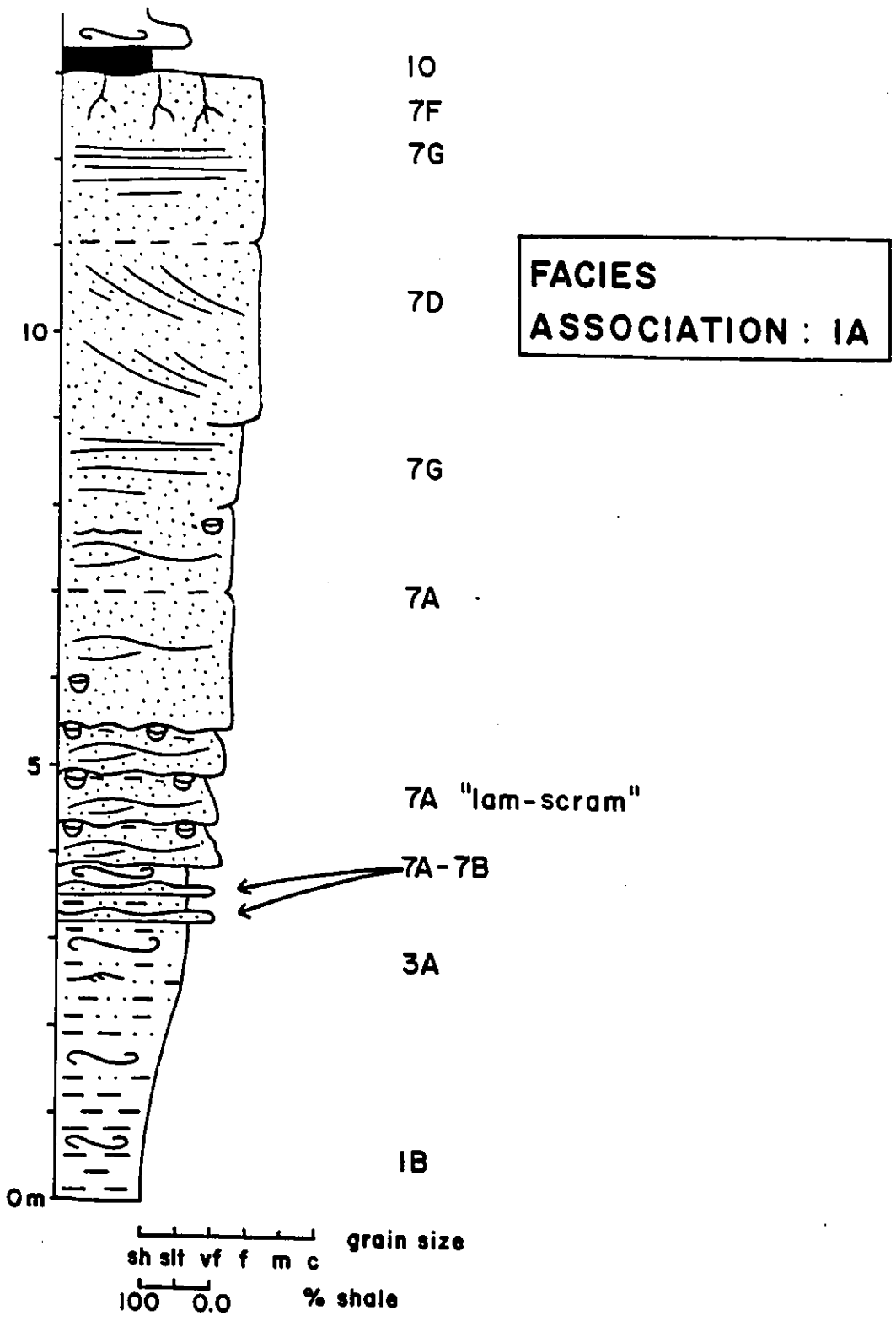
FACIES
10
7F
7G
7D
7G
7A
7A "lam-scram"
7A-7B
3A
1B
10
5
0m
FACIES ASSOCIATION : 1A
grain size
sh slt vf f m c
100 0.0 % shale

usually has a sharp contact with underlying facies. Facies Association 1A shows a regular coarsening upward and repetition of facies units upward (e.g. interbedded shales) is not common. This association is common and, when complete, reaches a maximum thickness of about 15 meters.

Facies Association 1A always begins with 1-3 meters of pervasively bioturbated shales (Facies 1B) or mudstones (Facies 3A) which become sandier upwards (Fig.2-23). As the amount of sandstone increases, lamination may be preserved. The bioturbated mudstones are gradually replaced upwards by very fine-grained HCS sandstones (Facies 7A) to wave rippled sandstones (Facies 7B) commonly exhibiting bioturbated tops and containing shaly interbeds. Successive HCS sandstone beds erode into the underlying bioturbated tops of previously deposited sandy beds producing alternation of laminated to bioturbated beds. Upwards, shaly interbeds are lost and the HCS sandstones amalgamate. Bioturbation decreases and the association grades into massive sandstone showing low-angle intersecting laminae, interpreted as swaley cross stratification (SCS), and sometimes containing anemone burrows (Fig.2-22c). The association grades upwards into fine-grained, cross bedded sandstone (Facies 7D) to massive, structureless sandstones (Facies 7F) and may be capped by a couple of meters or so of parallel, flat laminated fine-grained sandstone (Facies 7G). The top of the association may contain *Skolithos*

burrows and *in situ* root casts, sometimes sharply capped by a thin coal (Facies 10).

This Facies Association may not always contain the upper facies units forming incomplete, top-absent associations.

Interpretation

Facies Association 1A is readily interpreted as a shallowing upward facies succession produced by the progradation of a storm- and wave-dominated sandy marine shoreline. It is similar to other high energy shoreface deposits described elsewhere (Reinson, 1984; Moslow and Pemberton, 1988). Shelf deposits, represented by pervasively bioturbated mudstones (Facies 3A), grade up through sandier facies and culminate in rooted sandstones which indicate sub-aerial exposure and emergence. The base of the shoreface is defined at the transition from interbedded HCS sandstones and bioturbated mudstones to amalgamated HCS with no preserved mudstone. Cross bedded sandstones are interpreted as being deposited in the surf and breaker zones in the upper shoreface. Parallel laminated sandstones, in the context of Facies Association 1A, are interpreted as representing deposition by swash and back-wash on a beach.

Overally, the facies in Association 1A are characterized by an abundance of storm- and wave-formed sedimentary structures (HCS, SCS and wave ripples) which suggests that storm and wave processes dominate.

Top absent facies associations may also be readily interpreted on the basis of a proximal/distal relationship to the final position of the prograding shoreline, upper units of the association being lost with increasing distance away from the shoreline. Caution must be exercised however. Top absent associations may also be produced by the subsequent erosion of upper facies units (e.g., channel cutting, erosional shoreface retreat). The overlying facies and especially the presence of an erosional lag (Facies 8) will be crucial in determining whether erosion has occurred.

B. Facies Association 1B

The idealized, complete association, in its normal sequence is:

1A - (2,4B) - 6 - (7H,7C,7F,7D,7G,7B) - 10

Facies Association 1B is illustrated in figure 2-24. It usually begins with several meters of laminated, marine shales (Facies 1A) and blockstones (Facies 2), often with abundant siderite. In contrast to Facies Association 1A (Fig.2-23), the basal mudstones show very little burrowing except for rare zones of *Helminthopsis*. Features characteristic of soft sediment deformation, especially load casts, are ubiquitous. Massive to deformed siltstones (Facies 6) are also common. Upwards, these siltstone beds are interbedded with ripple cross-laminated sandstone (Facies 7C) to convolute, very fine-grained sandstone (Facies 7H). The proportion of mudstone beds decreases upward as

the association becomes sandier. These grade upward into very fine to fine-grained, structureless (Facies 7F) to cross bedded (Facies 7D), and often contain shaly partings and shale rip-up horizons. Current rippled sandstone (Facies 7C) and parallel laminated sandstone (Facies 7G) are common, while wave rippled sandstone (Facies 7B) and HCS (Facies 7A) is relatively rare. Burrowing is relatively rare throughout the association. Trace fauna usually comprises the *Skolithos* ichnofacies (Frey and Pemberton, 1984). *In situ* root traces followed by a thin coal may cap the association.

Facies contacts may be sharp to gradational. Facies units and transitions are often repeated, although a general coarsening upward trend is always observed. This facies association is considerably more shaly than Facies Association 1A and the nature of upward coarsening is much less regular (Fig. 2-23, 2-24). Facies Association 1B is common and may reach thicknesses of up to 20 meters. Top and bottom absent associations are sometimes observed.

Interpretation

Facies Association 1B is interpreted to represent a shallowing upward facies succession beginning with marine shales and siltstones (Blockstones) and grading up into the deposits of an emergent sandy, probably deltaic shoreline. The shoreline was probably considerably different from that interpreted for Facies Association 1A. In contrast to Facies Association 1A, mudstones

Figure 2-24. Facies Association 1B interpreted as being typical of prograding river-dominated deltaic shorelines. Compare with figure 2-23. Note the absence of bioturbated mudstones, HCS sandstone, and the abundance of soft-sediment deformation features. Based on core from shingle E1 in well 7-11-69-22W5, shown in figure 4-11B, and shingle E2 in well 15-31-62-26W6, figure 4-7A,B. Detailed logged section and core photos are presented in chapter 4 for well 15-31. See text for further explanation and figure 2-29 for legend.

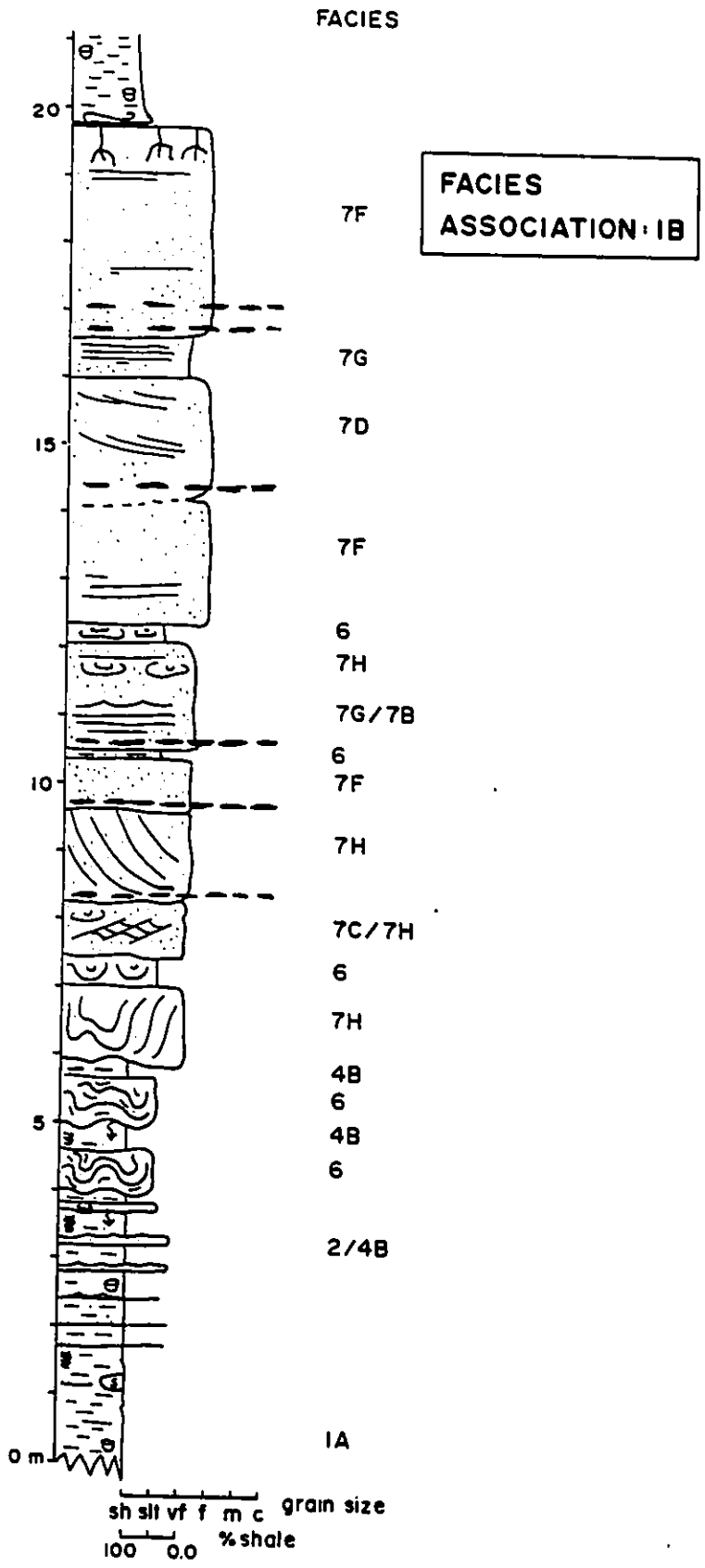
FACIES
20
15
10
5
0 m
FACIES ASSOCIATION: 1B
7F
7G
7D
7F
6
7H
7G/7B
6
7F
7H
7C/7H
6
7H
4B
6
4B
6
2/4B
1A
sh slt vf f m c grain size
100 0.0 % shale

in Facies Association 1B are laminated and show a low degree of bioturbation and show features characteristic of soft sedimentary deformation. Sandstones are characterized by facies indicative of unidirectional current flows and lack wave-formed sedimentary structures. These features suggest that sediment was supplied rapidly and that wave and biologic processes in the basin of deposition were insufficient to cause significant reworking. The coarsening upward is more erratic than in Facies Association 1A and contains a greater proportion of interbedded mudstones throughout.

The environment of deposition is typical of prograding river-dominated sandy deltas, characterized by high sedimentation rates (Elliot, 1986). The abundant shaly interbeds may relate to times of lower fluvial discharge.

In order to prove that these facies associations are related to deposition in river-dominated deltas, it will be shown in later chapters that the sandstones exhibit a plan-view deltaic morphology and that they are associated with distributary channels.

Top absent associations may have the same implications as interpreted for Facies Association 1A and may represent facies succession deposited seaward of the final shoreline position.

C. Facies Association 1C

This association comprises the following facies units in sequence:

1A - 2 - (7A,7B) - (7D, 7G) - ?10

Facies Association 1C displays characteristics of both Facies Association 1A and Facies Association 1B, although it is less common and is therefore not cored as often. Facies Association 1C is illustrated in figure 2-25 and displays a fairly smooth and regular coarsening upward, similar to Facies Association 1A. Contacts between facies units are usually gradational. Facies Association 1C usually begins with several meters of laminated to burrowed shales and mudstone (Facies 1A to Facies 2), similar to basal mudstones in Facies Association 1B. In contrast to Facies Association 1B, however, soft sediment deformation features are rare and the Facies Association grades upward into very fine-grained HCS sandstones (Facies 7A) which commonly occur as gutter casts but become more massively bedded upwards. As the Facies association coarsens, it is replaced by cross-bedded sandstones sometimes containing ripped-up shale clasts.

Figure 2-25 is based on core from well 2-21-61-9W6 (Fig.4-8), which did not penetrate the top of the succession. Most of the occurrences of Facies Association 1C are confined to the northwest where there is little core data. Log data indicate indicate that this Association may reach 15 to 20 m in thickness. Where this association is more commonly cored (in the southeast) the upper facies units are missing (top-absent).

Figure 2-25. Facies Association 1C is interpreted as being typical of wave-influenced prograding deltas. Compare facies with those in figures 2-23 and 2-24. The lack of burrowing in the basal mudstones indicates higher sedimentation rates than basal mudstones in Facies Association 1A (Fig.2-23). Storm wave influence is suggested by the predominance of HCS sandstone in the lower shoreface (5-8m). The lack of shaly interbeds above about 5m suggests higher energy conditions than in Facies Association 1B. Cross bedded sandstones at 8m may indicate a distributary channel associated with prograing deltaic lobe or, perhaps deposition in a high energy upper-shoreface. This figure is based on core from well 12-21-61-9W6, member E, shingle E4 (Fig.4-8). See text for explanation and figure 2-29 for legend.

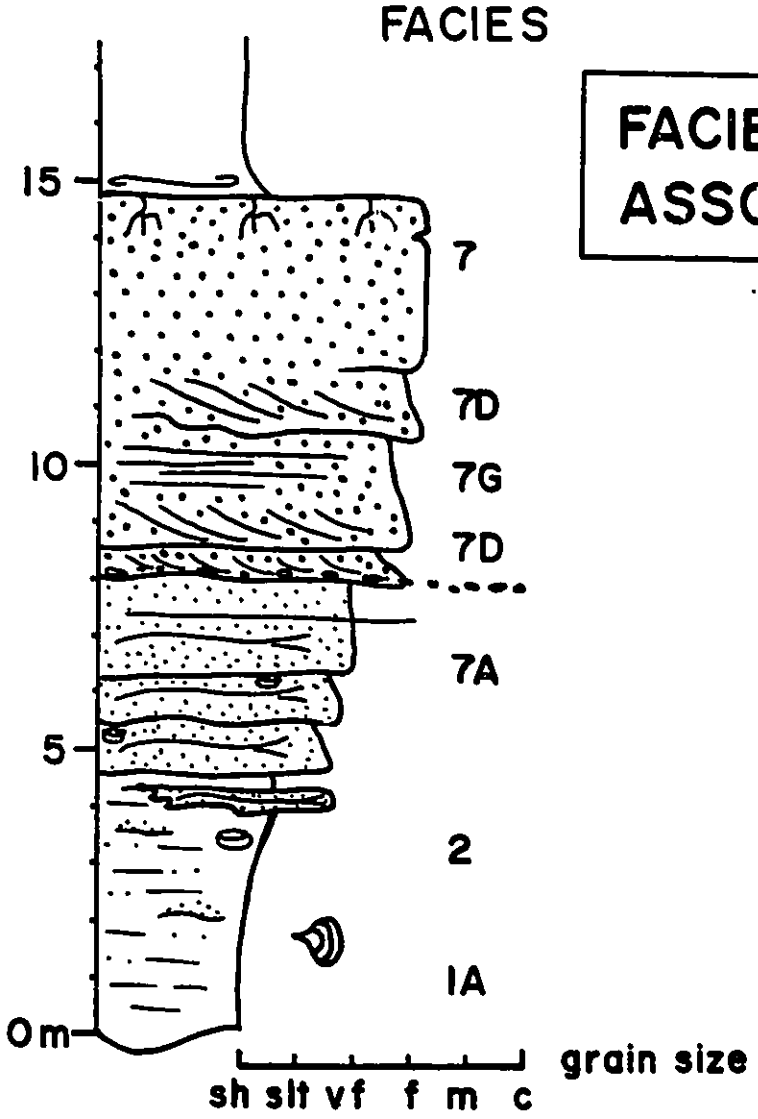

FACIES ASSOCIATION IC

Interpretation

Facies Association 1C is interpreted as being environmentally in between Facies Association 1A and 1B. The coarsening upward and the inferred presence of non-marine facies at the top indicate that this Association is also the result of a prograding shoreline. The lack of bioturbation in the basal mudstones may indicate higher sedimentation rates than interpreted for Facies Association 1A, but the lack of soft sediment deformation features and the smooth nature of the coarsening upward may indicate lower sedimentation rates than interpreted for Facies Association 1B. The abundance of HCS sandstone and the lack of shale interbeds upward indicates frequent storm wave reworking.

2-3-2. Erosionally Based, Fining Upward Facies Associations

A. Facies Association 2A

This association in its idealized, complete form is:

8 - (7D,7F,7G) - 7C

Facies Association 2A is illustrated in figure 2-26 and always has an erosive relationship with underlying facies which often comprise marine blockstones (Facies 2). A siderite clast and shell rich lag (Facies 8), up to a few tens of centimeters thick, often lies immediately above the lower erosional contact. This is followed by several meters of cross bedded sandstone (Facies 7D) to structureless sandstone (Facies 7F). Sandy facies may alternate, although structureless to cross bedded sandstone is often gradually replaced upward by current rippled sandstone

(Facies 7C). The Association may contain several fining upward sub-cycles or graded beds comprising medium- to fine-grained sandstone containing shale rip-up horizons at the base, and grading up into fine- to very fine-grained sandstone sometimes capped by a thin mudstone. Burrows are rare to absent although occasional *Asterosoma* may be found in the upper portions of this facies association. In places the association may be associated with overlying non-marine facies (e.g. roots and coals).

This association is relatively common and may reach thicknesses of up to 25 meters, although usually it usually average 15 meters or less.

Interpretation

The basal lag consists of material derived from the underlying facies. Broadly, the facies associations represents a decrease of energy upwards. A coarse lag grades up into sandstones exhibiting primary sedimentary structures characteristic of waning channel flow (Blatt et al., 1980; Harms et al., 1975; Walker and Cant, 1984). The lack of marine trace fossils and in-situ body fossils suggests a broadly non-marine setting, especially where vertically or laterally associated with other non-marine facies. These associations possibly represent sand filled distributary channels and are typical of sandy channel fills (Walker and Cant, 1984).

Figure 2-26. Facies Association 2A interpreted as being typical of sandy channel fills. Figure based on core through shingle E1 from well 11-5-63-26W5, shown in figure 4-12B, and well 14-6-63-26W5, shown in figure 4-9A,B. Box photos of well Well 14-6 are shown in detail in figure 4-9B. See text for details and figure 2-29 for legend.

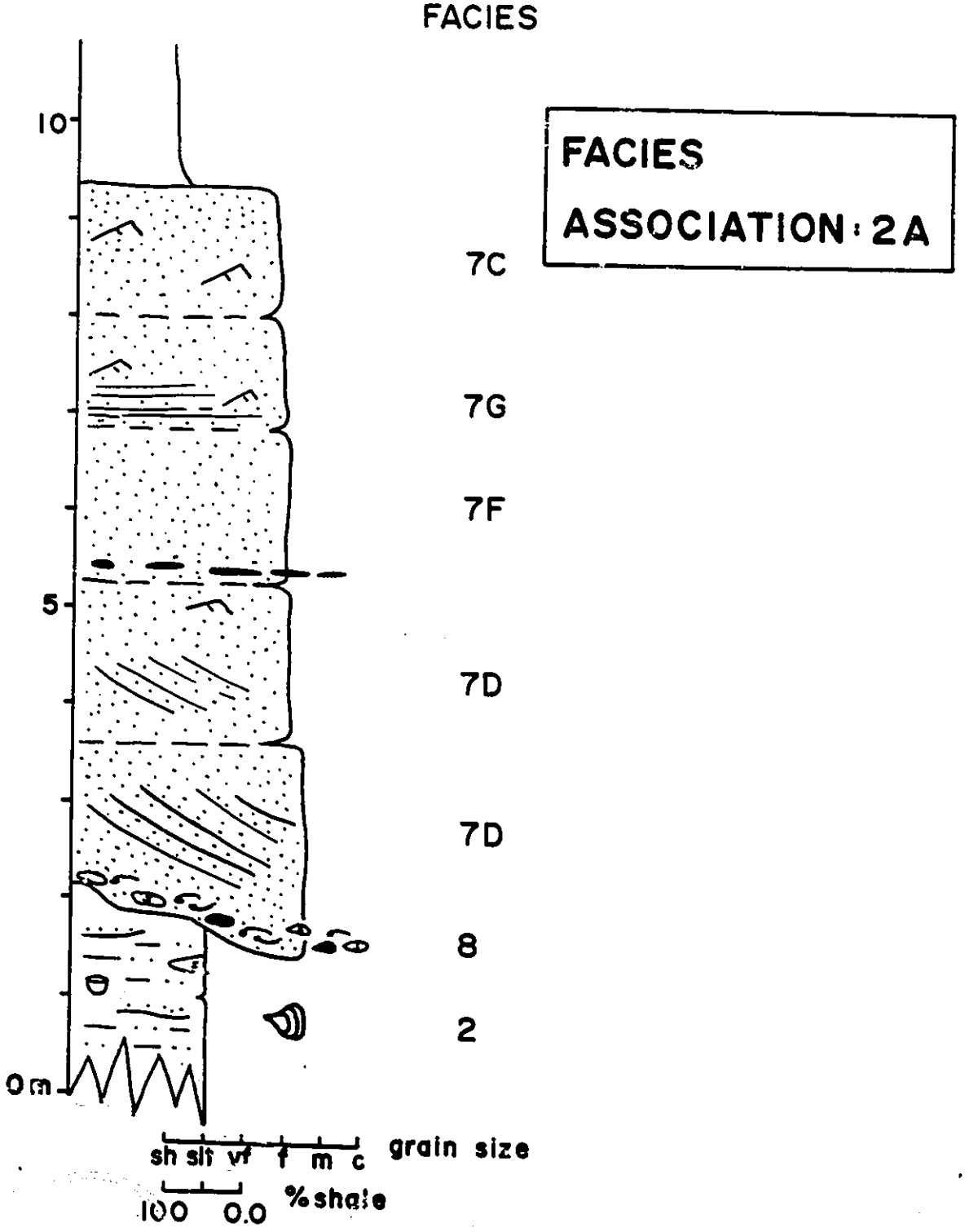
FACIES
FACIES ASSOCIATION: 2A
10
5
0m
7C
7G
7F
7D
7D
8
2
sh slt vf f m c grain size
100 0.0 %shale

Caution must be exercised in making such an interpretation at this stage. Channels are morphological features and can only be properly recognised when three dimensional control indicates that such a facies association fills a channel shaped erosional feature.

B. Facies Association 2B

This facies association is less common, but may be laterally equivalent to Association 2A. It comprises;

(7E,7F,7C,7G) - (3A,3B) - 5

A typical example of this Facies Association is illustrated in figure 2-27. The association always has an erosive relationship with underlying facies which usually comprise marine blockstones (Facies 2). Basal lags seem to be more rare in Facies Association 2A. The sandy basal portion of the association usually begins with sigmoidally cross bedded sandstone (Facies 7E, Fig.2-15) and may grade up into rippled (Facies 7C) to parallel laminated sandstone (Facies 7G). These sandstones usually grade into interstratified burrowed mudstones (Facies 3A/3B) to banded mudstones (Facies 5) sometimes with interbedded wave- to combined-flow rippled sandstones. Marine trace fauna include *Teichichnus*, *Planolites*, *Rhizocorallium* and *Terebellina*. *Inoceramus* occur in places. While this represents a fairly diverse assemblage, the degree of burrowing seldom exceeds about 70%. As previously stated, this facies association is less common than Association

2A, but is often associated with it. Its thickness usually does not exceed about 15 meters.

Interpretation

Facies Association 2B defines an overall fining upwards facies succession suggestive of waning energy conditions. The sigmoidal cross bedding may suggest a tidal influence and the increase of shale and marine trace fauna upwards suggests an increasing marine influence. The erosively based nature of this association may indicate channelling. The association may therefore represent channel fill. The presence of abundant marine trace fauna in marine mudstones suggests a probable estuarine setting.

2-3-3. Non-Sequential Facies Associations

A. Facies Association 3

This facies association may include the following facies: 1C , 3B , 4A , 5 , 6 , 7B, 7C, 9, and 10.

A typical example of Facies Association 3 is illustrated in Figure 2-28. The order of the succession of facies may be variable, although local fining and coarsening trends may occur. Pinstriped and banded mudstones containing synæresis cracks (Facies 4 and 5) associated with non-marine rooted horizons (Facies 9 and 10) are common. These may be cut by occasional current rippled sandstone beds (7C) a meter or so thick. Burrowing in this facies association is usually fairly low. Carbonaceous mudstones (Facies 1C) containing brackish water fauna

Figure 2-27. Facies Association 2B interpreted as being typical of tidally influenced, estuarine channel fills. Figure based on core through shingle D1 in well 2-18-64-23W5, shown in figure 5-5A,B. Box photos of core through well 2-18 are shown in figure 5-6. Compare with figure 2-26, and note that upper half of channel is filled with burrowed mudstones (Facies 3B). See text for further discussion and figure 2-29 for legend.

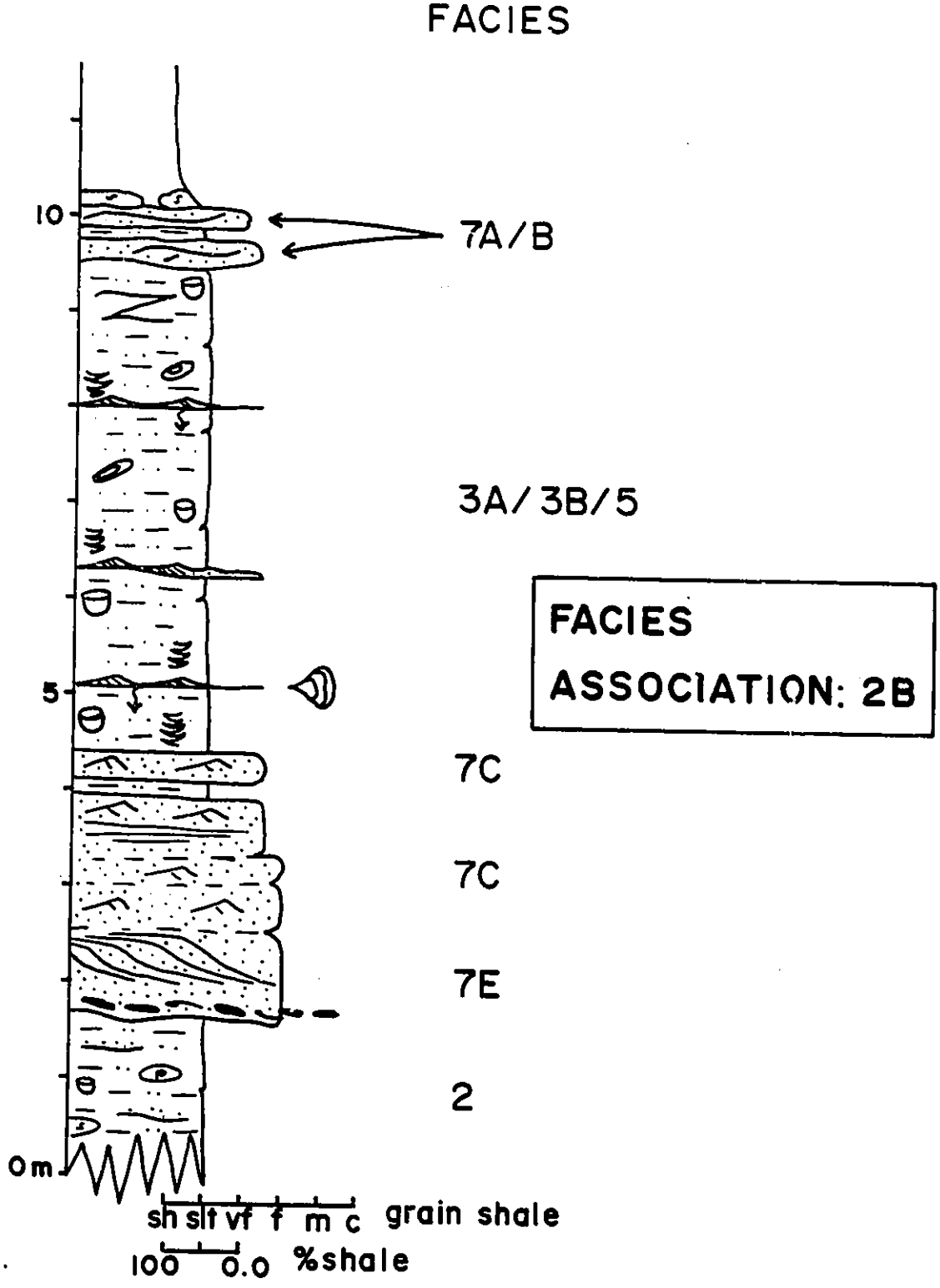
FACIES
10
7A/B
3A/3B/5
FACIES
ASSOCIATION: 2B
5
7C
7C
7E
2
0m
sh slt vf f m c grain shale
100 0.0 %shale

Figure 2-28. Facies Association 3, interpreted as representing depositrs of a restricted marine to non-marine environment. Well developed coarsening and fining upward facies successions are not present. The facies succession is interpreted as representing a broadly shallowing depositional environment, such as might be developed in an interlobe area of a major delta system. Vertical section based on facies succession in core from well 8-8-62-3W6 through shingle E3 (shown in figure 4-41B (9.0 - 23.0 m) photos not available). Detailed core section through a similar facies succession from well 6-11-62-3W6 is shown in figure 3-7B. Box photos of core are shown in figure 3-7C. See text for further details and see figure 2-29 for legend.

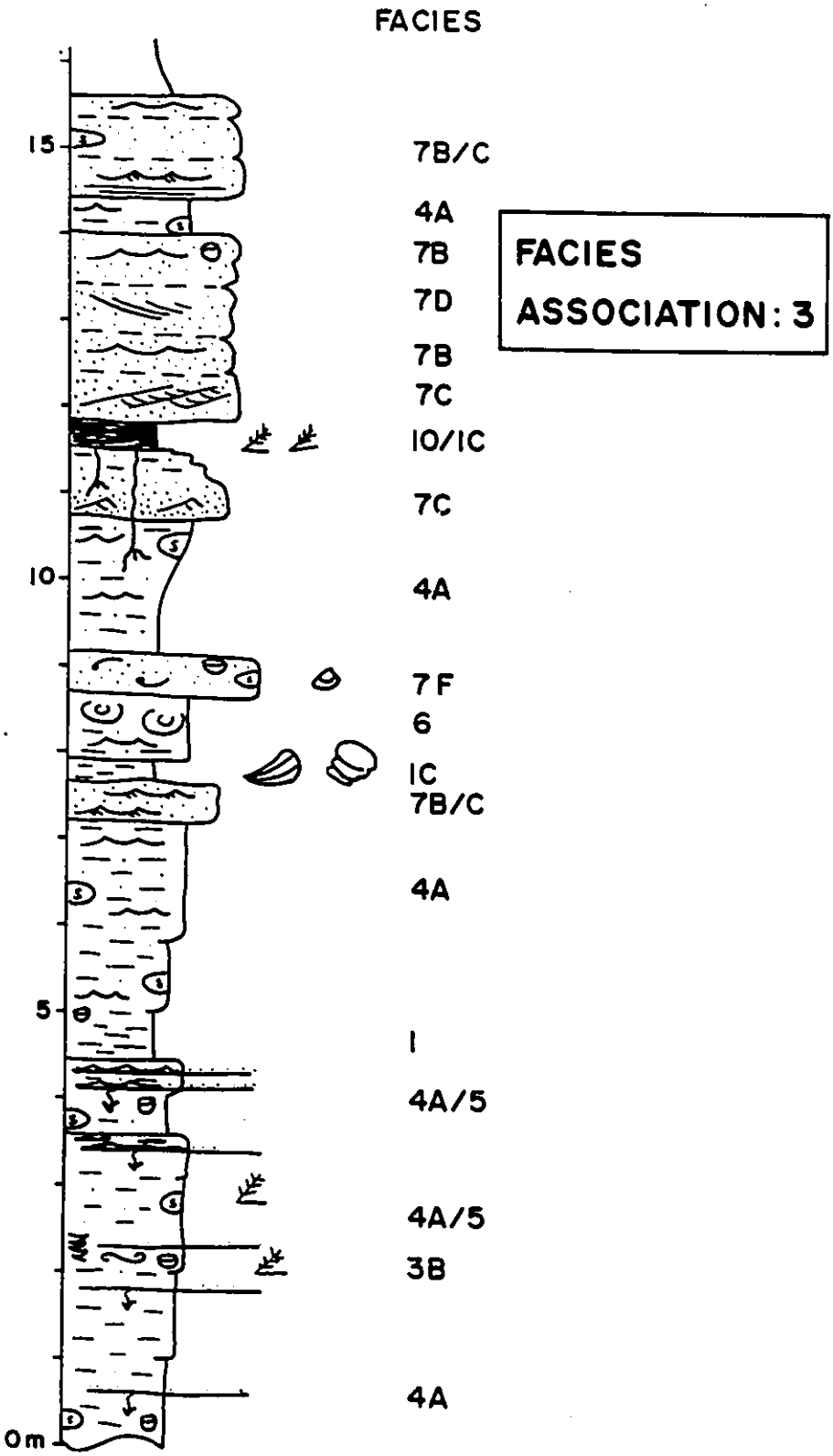
FACIES
15
10
5
0m
7B/C
4A
7B
7D
7B
7C
10/1C
7C
4A
7F
6
1C
7B/C
4A
1
4A/5
4A/5
3B
4A
FACIES
ASSOCIATION: 3

Figure 2-29. Facies Legend for all vertical core sections and core-cross sections.

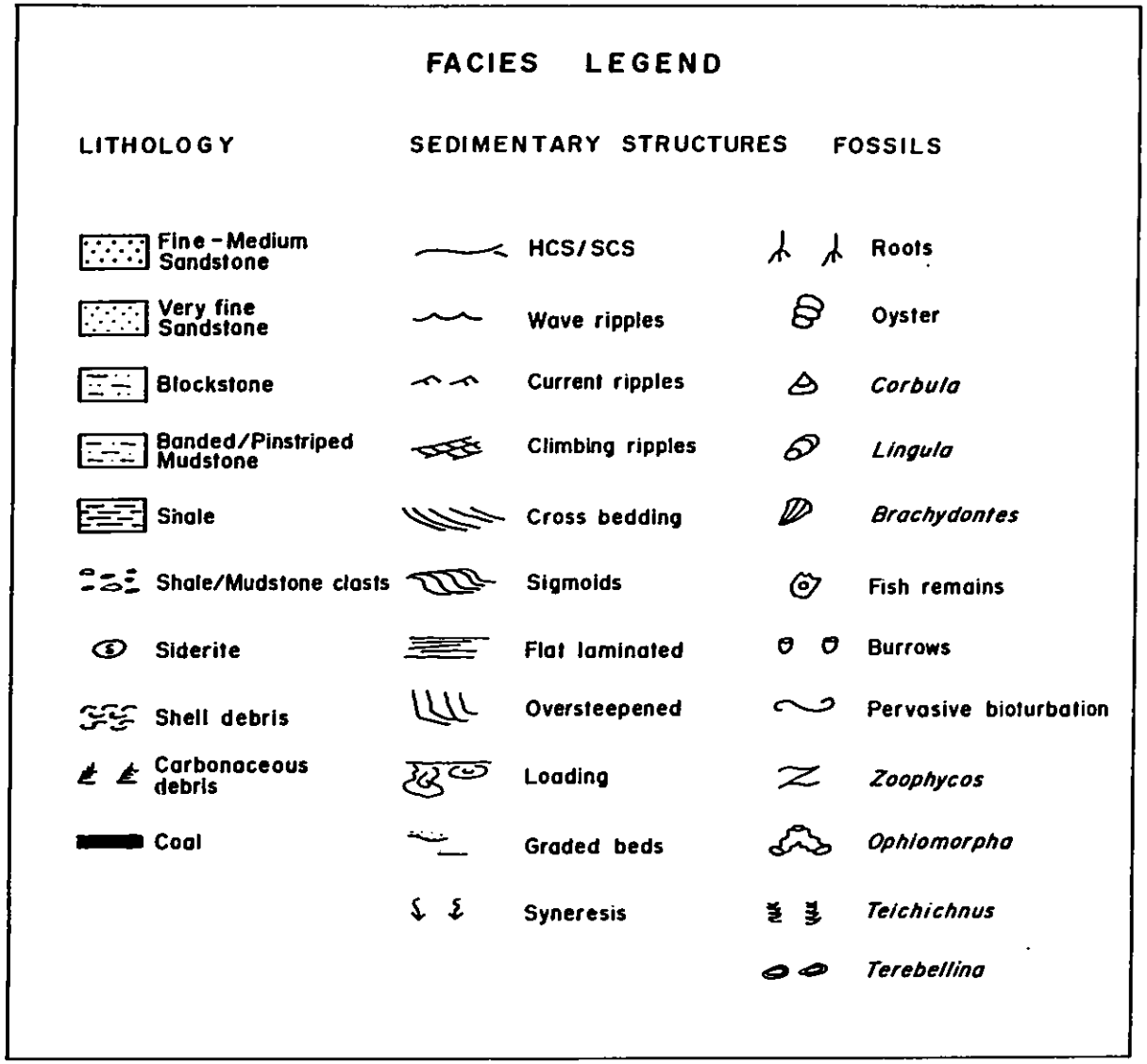
FACIES LEGEND
LITHOLOGY
SEDIMENTARY STRUCTURES
FOSSILS
Fine - Medium Sandstone
Very fine Sandstone
Blockstone
Banded/Pinstriped Mudstone
Shale
Shale/Mudstone clasts
Siderite
Shell debris
Carbonaceous debris
Coal
HCS/SCS
Wave ripples
Current ripples
Climbing ripples
Cross bedding
Sigmoids
Flat laminated
Oversteepened
Loading
Graded beds
Syneresis
Roots
Oyster
Corbula
Lingula
Brachydontes
Fish remains
Burrows
Pervasive bioturbation
Zoophycos
Ophiomorpha
Teichichnus
Terebellina

(e.g. oyster beds, *Brachydontes sp.*) are also common. This association is fairly common but seldom exceeds about 10 meters thick.

Non-marine facies may become more predominant upwards.

Interpretation

Facies Association 3 is interpreted as representing the deposits of low energy, shallow marine to non-marine environments. These could include low energy inter-distributary bay fills, lagoons or delta plain environments including flood plain and lacustrine deposits. Occasional thicker sandstone beds may represent deposits of crevasse channels and splays. Where non-marine facies become more predominant upwards, a shallowing upward of environments is indicated.

CHAPTER 3: ALLOSTRATIGRAPHY OF THE DUNVEGAN FORMATION

3-1. Internal Subdivision of the Dunvegan Formation

Until this study, there have been no published attempts at stratigraphic subdivision of the Dunvegan Formation in the Alberta subsurface. In addition, no formal stratigraphic subdivisions have been proposed for Dunvegan outcrop. This thesis represents the first attempt to formally subdivide the Dunvegan Formation. Previous isopach and isolith maps have been based on 100 meters or more of undifferentiated Dunvegan Formation (Burk, 1963) but could not be sensibly interpreted in terms of depositional systems. The allostratigraphic scheme presented in this chapter forms the basis for the detailed maps and more realistic interpretations of depositional systems presented in chapters 4 to 10. It is emphasized that these interpretations would not have been possible without the benefit of this allostratigraphic scheme.

This chapter will show that the Dunvegan Formation can be subdivided into seven formally defined allomembers (North American Commission on Stratigraphic Nomenclature, 1983). Each allomember represents a genetically related package of interstratified sandstones and shales separated from other allomembers by a widespread bounding discontinuity. Allomembers are highly variable in thickness. They range from 0 to 80m in thickness and

average about 30m. Many of the members were further subdivided into lens-shaped sedimentary sub-units of more limited extent. These sub-units are termed shingles and average about 20m in thickness. The remainder of this introduction will present a brief history of the way in which this allostratigraphic subdivision of the Dunvegan Formation was achieved.

3-1-1. History and Summary of This Study

This study began with the detailed logging and description of the longest cores (up to 70m) available through the Dunvegan Formation (Bhattacharya, 1985). During this early phase of the study, commonly occurring vertical facies successions were used to define the Facies Associations described in chapter 2. These Facies Associations were used to recognize the major sedimentary cycles within the Dunvegan Formation.

The most obvious sedimentary cycles within the Dunvegan Formation comprise coarsening upward facies successions sharply capped by a thin pervasively bioturbated sandy mudstone (Facies 3) which is in turn sharply overlain by several meters of bioturbated to laminated marine shales. This transition into marine shales is interpreted as indicating marine transgression. These transgressive shales are easy to identify in well logs and initial correlations showed that seven of these relatively thick marine shales were regionally widespread. At first, seven sandy members were defined, each separated from each other by one of these marine shales. Later it was realized that these sandy members

comprised several offlapping or shingling sand bodies which interfingered and passed gradationally southeastwards into marine shales. Furthermore the "underlying" shales were actually the time equivalents of shingled sandstones to the northwest and were observed tp pass gradationally upwards and laterally into the "overlying" sandstones members. No physically continuous surface separated the "overlying" sandstones from the "underlying" marine shales.

Soon afterwards it was realized that the contact between the underlying coarsening upward cycles and their overlying marine shales represented widespread physically continuous surfaces, or bounding discontinuities, which probably related to a time of maximum transgression or flooding (T-surface). The recurrence of these widespread transgressive flooding surfaces (rather than the shales) led to the reconstruction of a large scale event stratigraphy or allostratigraphy for the Dunvegan Formation. This allostratigraphic scheme is summarized in figure 3-9B. Within the members defined, it was observed that sandstones are composite and comprise several overlapping, or shingled, sand bodies which prograded into the basin to the southeast. Each member is therefore interpreted to represent an overall progradational or regressive event (this produces the overall coarsening upward) punctuated by a widespread transgression (the cycle boundary). The thick marine shales were seen to be genetically related to the progradational phase of sand deposition as they built over the

underlying T-surface. The marine shales and their equivalent sandstones were therefore combined into single allomembers. Each allomember therefore comprises a heterogeneous package of interbedded sandstones and shales, and represents a genetically related package of sedimentary rock, separated from other members by widespread bounding discontinuities (T-surfaces) as defined by the North American Commission on Stratigraphic Nomenclature (1983) (see discussion in section 3-1-2).

The term allomember is rather clumsy and, for the sake of simplicity, the term member rather than allomember has been used throughout the thesis. Unless otherwise indicated, all members mentioned in this thesis are allostratigraphic and not lithostratigraphic units. All of the members within the Dunvegan Formation are formally defined as allomembers following the definition of the North American Commission on Stratigraphic Nomenclature (1983).

The framework and details of the allostratigraphic scheme outlined above, are presented in the rest of this chapter.

3-1-2. Criteria of Stratigraphic Subdivision, an Allostratigraphic Approach

A good stratigraphic scheme should satisfy two criteria. First, it should be practical and capable of being easily used and understood by other workers. Second, it should act as a basis for understanding the relationship of geological events within the unit of interest. In regard to the second criteria, I have used an

approach based on the ideas of Wheeler (1958), Busch (1974, p.24-30), Haq et al.(1987), and Swift et al. (1987). These workers favour use of a time-stratigraphic or allostratigraphic approach rather than stratigraphic schemes solely based on lithostratigraphic correlation. Their stratigraphic schemes involve the recognition of genetically related packages, increments, or sequences of strata. An allostratigraphic unit is defined by the North American Commission on Stratigraphic Nomenclature (1983 p.865) as "a mappable stratiform body of sedimentary rock that is defined and identified on the basis of its bounding discontinuities". Allostratigraphic units contain laterally heterogenous facies. A bounding discontinuity represents a physically continuous surface that represents a hiatus or break in deposition which may or may not be accompanied by erosion. Sedimentary cycles (coarsening upward cycles, fining upward cycles) are usually bounded by physical surfaces which can be used in correlation and stratigraphic subdivision. The nature and definitions of these different types of surface are defined in section 3-2-1.

Stratigraphic subdivision of a complex unit, such as the Dunvegan Formation, involves three major steps;

1. recognition of vertical sedimentary cycles using core,

2. correlation of these cycles within the basin using core and well log cross sections and,

3. subdivision of gross stratigraphic units on the basis of regionally persistent cycle boundaries and on the basis of changes in stratal configurations.

After the following section (3-1-3), which defines some terms used in this thesis, the subsequent sections will outline this method of stratigraphic analysis as applied to this study and will introduce the various stratigraphic components that make up the Dunvegan Formation. Stratigraphic marker horizons and time-synchronous surfaces used to constrain correlations within the Dunvegan Formation will also be described.

3-1-3. Definitions

Several purely descriptive terms have been used throughout this thesis in order to describe the physical relationships of strata. These terms are derived from Mitchum et al. (1977) and are defined below. They are illustrated in figure 3-1.

ONLAP - This is defined where initially horizontal sedimentary strata terminate against a lower, inclined surface (Fig.3-1, B1).

DOWNLAP - This is defined where initially inclined strata terminates against a lower surface (Fig.3-1, B2).

TOPLAP - This is defined where initially inclined strata terminate against a usually horizontal upper boundary but where this termination is due to non-deposition rather than erosion (Fig.3-1, A2). Strata tend to approach the upper boundary asymptotically.

EROSIONAL TRUNCATION - This is defined where inclined or horizontal strata terminate against an upper boundary as a result of

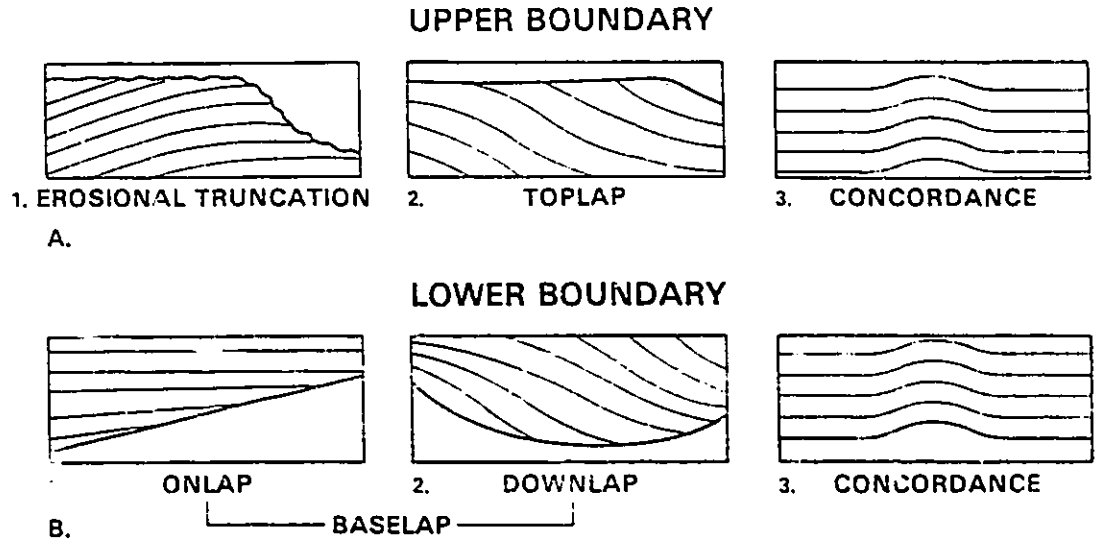

Figure 3-1. Stratigraphic terminology showing relationships of strata to boundaries of depositional sequences (from Mitchum et al., 1977 p.58). A. shows termination of strata against an upper boundary and B. shows termination of strata against a lower boundary. Box 3, in both A and B, represent conformable relationships. See text for further discussion.

erosion (Fig.3-1, A1). Strata do not approach the upper surface asymptotically. Where horizontal strata are truncated it usually implies an undulating erosion surface (e.g. channel). Depositional toplap may be very difficult to distinguish from erosional truncation, especially at large scales.

3-2. Setting Up The Framework For Allostratigraphic Subdivision

3-2-1. Recognition and Definition of Surfaces

This thesis defines three important types of surfaces observed within sediments of the Dunvegan Formation. These surfaces are;

1. Ec Surfaces; Erosional surfaces associated with channels,
2. Em Surfaces; Marine erosional surfaces and,
3. T-Surface; Transgressive surfaces.

These surfaces are illustrated in figures 3-2, 3-3, and 3-4. Examples of what these surfaces look like in core are indicated by the circles (3-2, circles A,B,C,D, and E). In core these surfaces can be recognized by the anomalous juxtaposition of facies and of facies associations and are shown in figures 3-3 and 3-4. Ec surfaces are defined as erosional surfaces associated with channels. They commonly lie at the base of fining-upward cycles. Non-marine facies containing a basal lag sit erosively on marine facies at these surfaces. An example would be a sandy channel lag (Facies 8) sharply overlying marine blockstones (Fig.3-2, circle B). Two examples of erosional surfaces overlain by

coarsesiderite pebble lags are shown in figure 3-3A and B. Em surfaces are defined as surfaces which are demonstrably erosional in nature. These surfaces, however, are not usually associated with channels and are usually sharply overlain by marine rather than non-marine facies. They are not specifically associated with any particular type of sedimentary cycle. Immediately overlying marine facies are usually coarser than underlying facies but may pass rapidly upward into marine shales. In core, Em surfaces are characterized by a sharp or demonstrably erosive contact between pervasively bioturbated sandstone or mudstone with the underlying facies (Fig.3-2, circles A,D, and E, Fig.3-3C). In places, a lag may lie immediately above the contact. This type of surface is thought to be associated with transgressions. Underlying facies may vary. One example is pervasively bioturbated sandstones (Facies 7G) abruptly overlying shallow water, rooted pinstriped mudstones (Fig.3-2, circle A; Fig.3-3C). T-surfaces are characterized by a sharp transition upwards into marine shales and nearly always cap coarsening upward sedimentary cycles. These surfaces usually separate underlying shallow water deposits from overlying bioturbated or laminated marine shales deposited in deeper water (Facies 1A or 1B). These surfaces may be represented by marine on non-marine or marine on marine facies transitions. One example is bioturbated marine shales (Facies 1B) sharply overlying a rooted non-marine sandstones (Fig.3-2, circle C, Fig.3-4C). Another example is bioturbated marine mudstones

Figure 3-2. Surfaces in the Dunvegan Formation. Where significant erosion is absent and when the sediment preserved between T and Em surfaces is less than about 10 cm, the Em surface is not separated for the purposes of correlation and on cross sections they are collectively correlated as a T-surface. The error is less than the thickness of the lines used for correlation. This figure is based on member E but is applicable to all members within the Dunvegan Formation. See text for further explanation.

SURFACES IN THE DUNVEGAN FORMATION

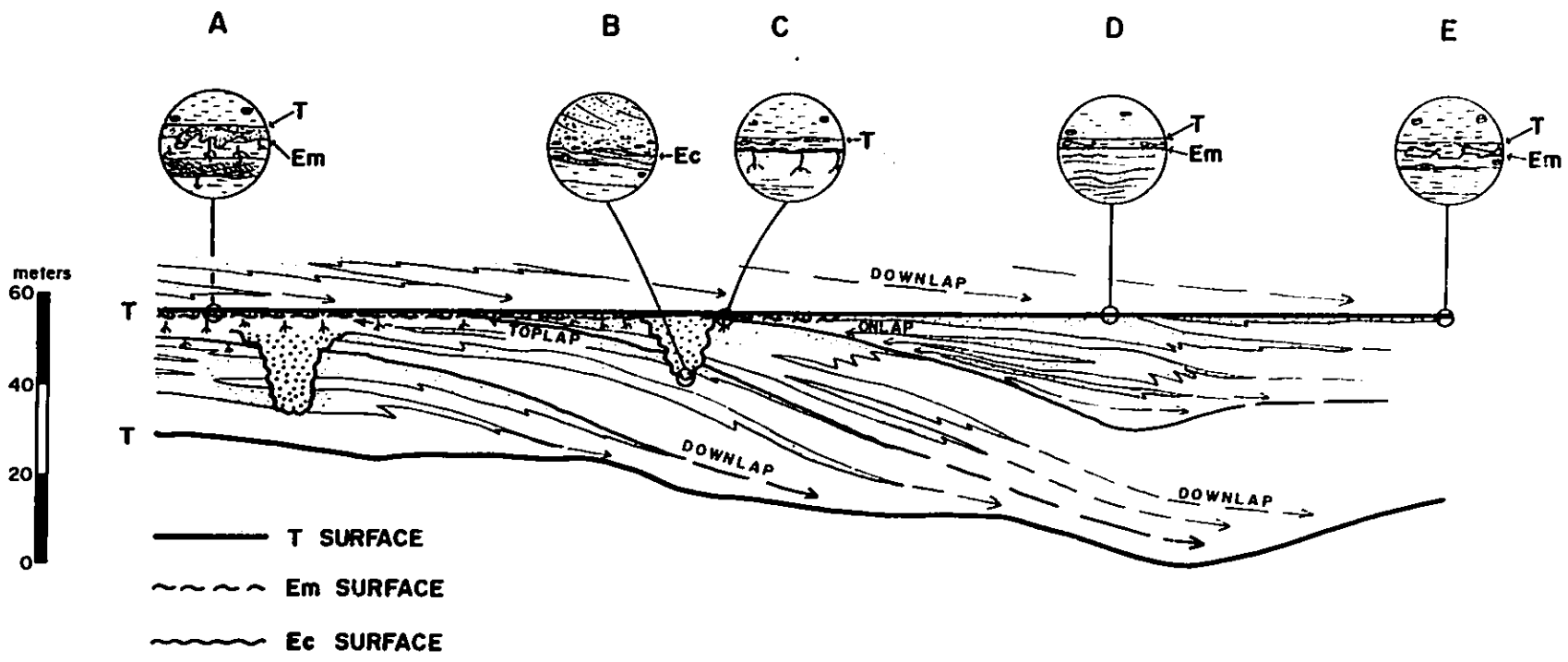

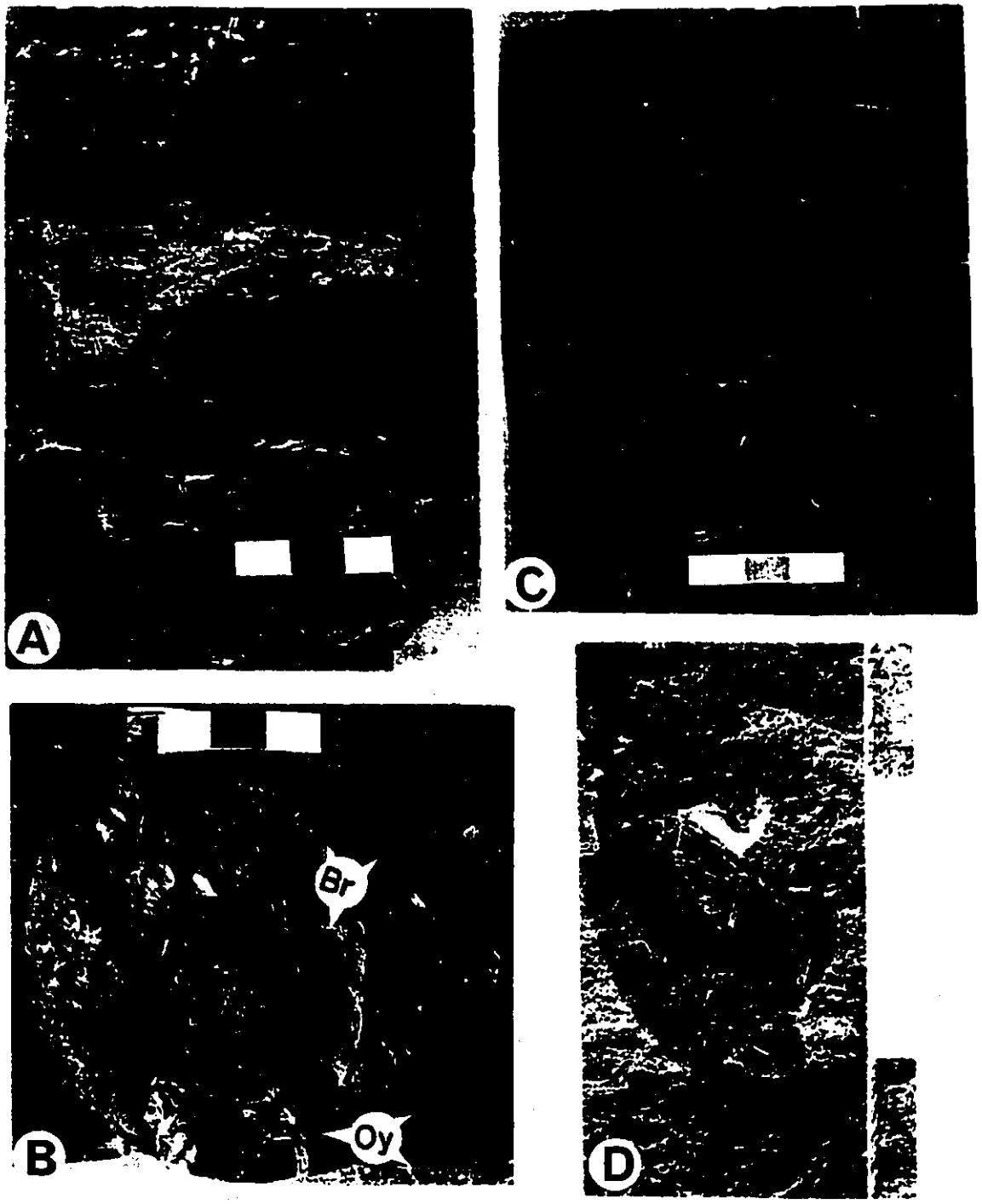
A
B
Br
Oy
C
D

Figure 3-3. E-surfaces; A. Coarse siderite pebble lag with a sharp angular erosional contact with underlying sandstone (Ec surface). Overlying sandstone is coarser grained. B. Sand-rich, siderite lag cuts into marine silts and shales and passes upwards into bioturbated marine mudstones (Facies 3A). This surface is associated with channeling at the base of shingle D1 and is interpreted as an Ec surface. C. Pervasively bioturbated muddy sandstone (Facies 7H) sits sharply on laminated sideritic, pinstriped mudstone (Facies 4, member C). Sand filled *Ophiomorpha* burrows penetrate down into underlying mudstones. The contact is interpreted as an Em surface. Scale in all photos is 3cm.

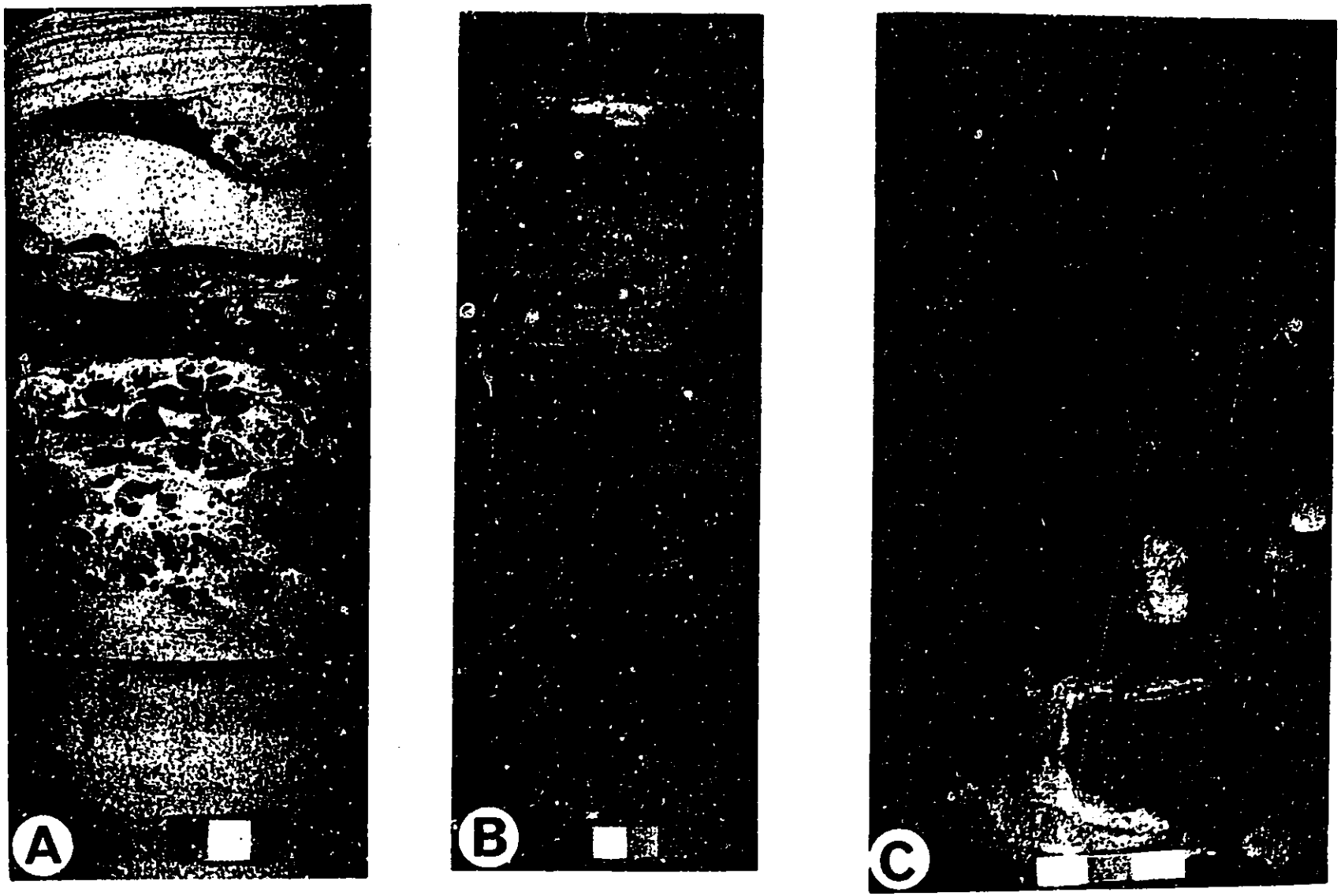
A
B
C

Figure 3-4. T surfaces, A. laminated sandstones at base of core, sharply overlain by about 5 cm of bioturbated mudstone (Facies 3A) and passing up into laminated silty shales (Facies 1A). Contact between sandstone and mudstone is obscured by burrowing, B. Laminated sandstone at base of core sharply overlain by pervasively bioturbated sandy mudstone (Facies 3A). Contact is bioturbated. Siderite nodule visible in upper right side of core, C. Pervasively bioturbated sandy mudstone sharply overlying rooted, non-marine sandstone. Scale in all photos is 3 centimeters.

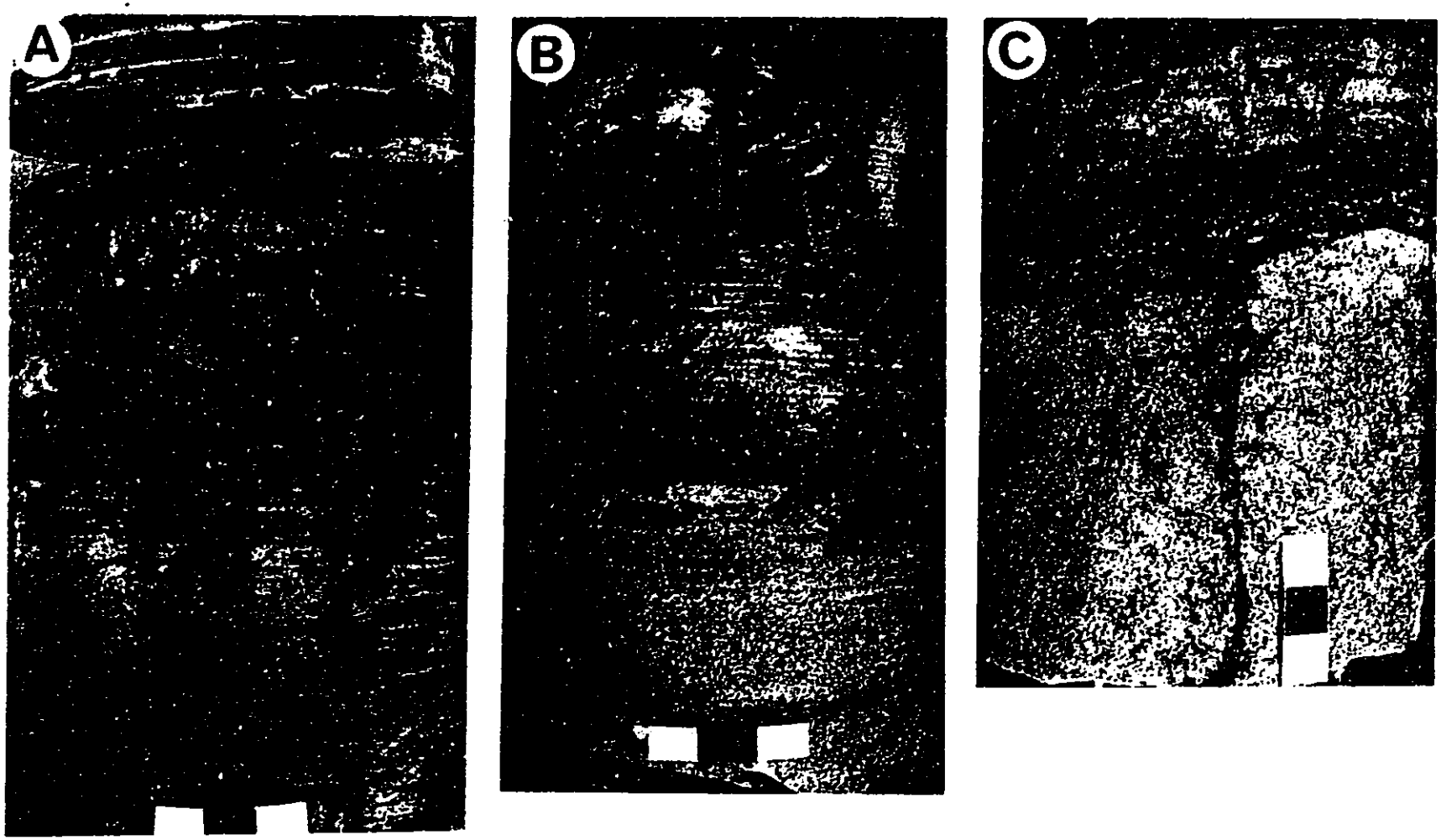
A
B
C

abruptly overlying fine-grained marine sandstone (Fig. 3-2, circle D, Fig.3-4A,B). These surfaces are interpreted to indicate abrupt deepening related to marine transgressions (flooding surface). On well logs, these surfaces are usually the easiest to distinguish because of the lithologic contrast between underlying coarser grained material and overlying finer grained marine shales and mudstones. For this reason they have been used as the basis for subdivision of sediments within the Dunvegan Formation (i.e. they are easy of recognize and use).

Another type of surface, defined by Haq et al.(1987), occurs where overlying units prograde or downlap onto a lower surface. These downlap surfaces are most easily recognized on cross sections rather than in individual core. In the Dunvegan Formation, these downlap surfaces nearly always coincide with T-surfaces and are therefore not usually separated.

Within most of the cores examined, a large number of coarsening upward sedimentary cycles capped by T-surfaces were recognized. The regional importance of any particular surface recognized in core, however, can only be determined by detailed correlation and mapping over the entire area under study. It is the regional persistance of a surface rather than its appearance in any individual core that determines its importance as a stratigraphic marker. This point will be returned to throughout the thesis in defining and mapping stratigraphic units and depositional systems.

3-2-2. Datums and Log Markers

The first step in correlating a complex stratigraphic unit, such as the Dunvegan Formation, is to choose stratigraphic datums. Ideally, these should be regionally persistent stratigraphic horizons or surfaces that are practically synchronous over the entire area of interest. It is preferable to have reliable datums both above and below the stratigraphic unit of interest. This will provide stratigraphic constraints within which to correlate units between these datums

Figure 3-5 shows a typical gamma and resistivity (Dual Induction) log through the Dunvegan Formation. Shales of the Kaskapau and Shaftesbury Formations (respectively, above and below the Dunvegan Formation) contain important marker horizons which are useful as datums within which to constrain correlations. The upper datum used in this study is the base of the Second White Speckled Shale. This is a relatively highly radioactive, fossiliferous shale that probably represents maximum transgression of the Kaskapau sea. Its base is clearly marked on the gamma ray log by a sharp deflection to the right at about 2320m (Fig.3-5). Resistivity logs show an increase (deflection to the right) over this unit. Approximately 40 meters below the base of the Second White Specks, at about 2360m (Fig.3-5), is the K1 marker (20 - 60m over the entire thesis area). In core, this is a thin pervasively bioturbated, silty mudstone (Facies 3A) that may be sideritized (Fig.3-7B at about 67m; and box 2, interval 67.3-71.9 in Fig. 3-

Figure 3-5. Well log from Dome Lator 3-20-62-2W5, depths are in meters, root symbols at top of members E and D indicate non-marine facies. See text for details and explanation.

DOME LATOR
3·20·62·2W5

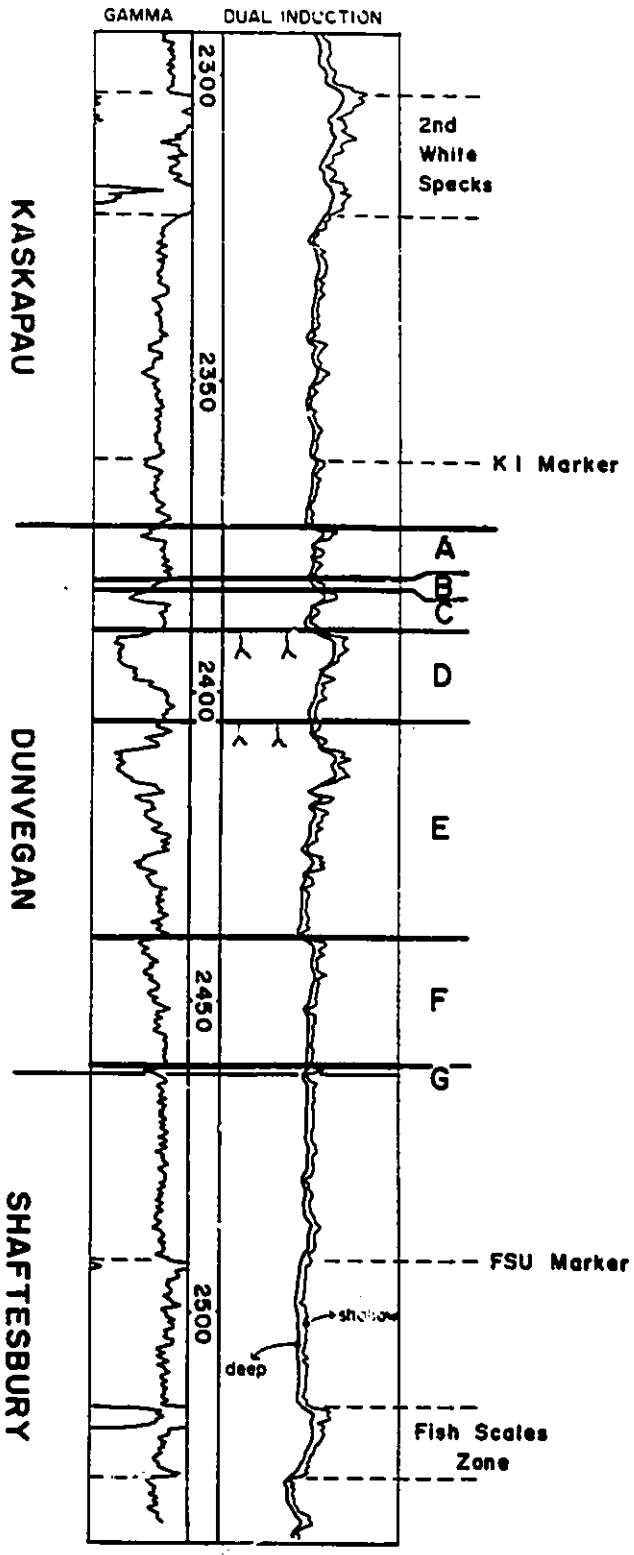

7C). In the box phoros, the reader will notice that the mudstones in boxes 1 and 2 (interval 67.3-71.9), below the K1 marker, are a lighter grey than the black, pervasively bioturbated mudstones to the right in boxes 3 and 4, but the contrast is more easily seen in colour photos. On logs it shows up as a slight increase in resistivity and as a decrease in gamma radiation (deflection to the left)(Figs.3-5 and 3-7A). In core it coarsens (or becomes sandier) upwards(Fig.3-7B,C). In cross sections (Figure 3-9A,B) the K1 and base of the Second White Specks markers are seen to converge towards the southeast. This is possibly a result of depositional thinning into the Dunvegan basin.

The first of the lower datums is picked at the top of the Fish Scales Zone within the underlying Shaftesbury Formation (Fig.3-5). This horizon is a widespread, relatively highly radioactive shale, rich in fish remains. It is interpreted to represent maximum transgression of the Shaftesbury sea and probably represents a condensed horizon (Leckie, 1987). It is marked by a sharp deflection to the right on gamma ray logs and by an increase in resistivity (Fig.3-5). A similar, but less intense deflection on the gamma ray logs lies at about 25 meters above the top of the Fish Scales (ranges from 10-40m over thesis area). The shales above this deflection are less radioactive than the shales below, as suggested by a slight overall decrease in gamma log intensity, and may indicate an increase in siltiness upwards. This marker is informally designated as the FSU (Fish Scale Upper)

marker due to its resemblance to the Fish Scales (Fig.3-5). In cross section (Fig. 3-8B and 3-9A), it roughly parallels the Fish Scales marker, although they both converge towards the east and southeast probably as a result of depositional thinning into the basin.

These four marker horizons are all assumed to represent geologically instantaneous events and are therefore considered to be time lines. Correlations of the Dunvegan Formation will be constrained between these markers. Erosion surfaces and unconformities will be defined where log markers terminate or are truncated.

All log cross sections presented in this study were first hung on the base of the Second White Specks. The K1, top of Fish Scales and FSU markers were then correlated. The wedge shaped geometry defined between these markers was used to constrain correlations within the Dunvegan Formation.

3-2-3. Establishing Depositional Strike and Dip

It is useful to first establish the approximate overall depositional strike and dip before constructing a cross sectional grid. For sediments of the Dunvegan Formation, the regional strike can be seen on the gross sandstone isolith map of Burk (1963). His map (Fig.1-4) shows that sandstones within the Dunvegan thin towards the southeast as described in Chapter 1.

In order to check Burk's results, I constructed a total isopach map from the base of the K-1 marker to the top of the FSU

Figure 3-6. Total isopach map of the K-1 marker to the FSU marker. Arrow shows direction of depositional dip. Depositional strike is at right angles to this and trends approximately southwest/northeast. Bullseye in T57 R3W6 is due to tectonic thickening. The positions of the two major regional cross sections (Figs. 3-8 and 3-9) are shown. Large black dots represent wells cored on cross sections. See text for further discussion.

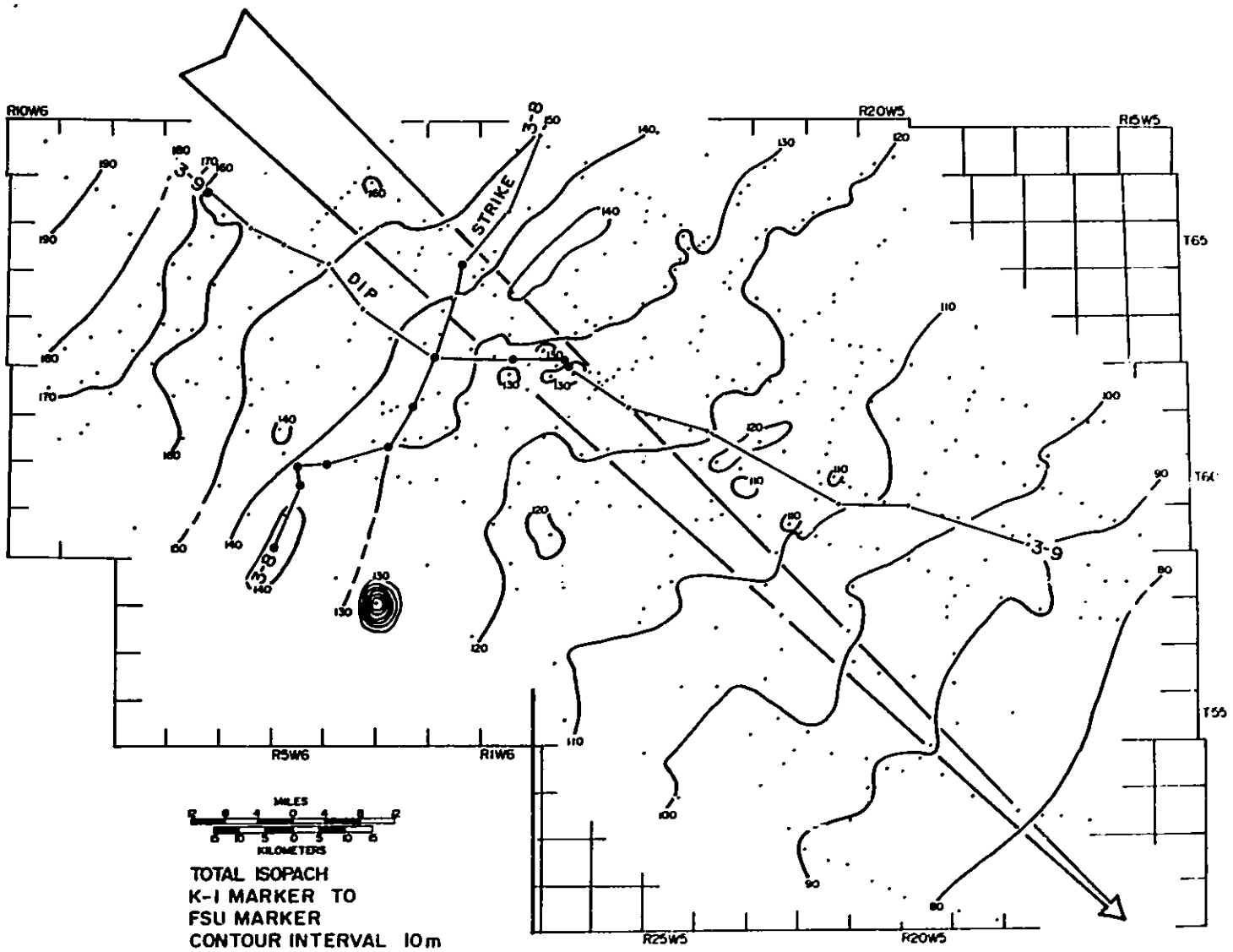
R10W5
R20W5
R5W5
STRIKE
DIP
3-8
3-9
T65
T64
T55
R5W6
R1W6
R25W5
R20W5
MILES
KILOMETERS
TOTAL ISOPACH
K-I MARKER TO
FSU MARKER
CONTOUR INTERVAL 10m

marker horizon. This map is shown in figure 3-6. The sediments between these horizons thin from a maximum of about 190 meters in the northwest corner of the map area down to about 80 meters in the southeast corner. The anomalous bullseye in the south-central portion of the map (around Township 57 R3W6) represents an unusual thickness of Dunvegan sediments due to tectonic overthickening. Examination of the well log in this area shows repeated section and indicates the presence of thrusting (see section 5-3-8, Fig.5-9A). The contours show that the Dunvegan Formation gradually thins at about half a meter per kilometer towards the southeast (about 134 degrees). I have assumed that this represents the general depositional dip direction for sediments of the Dunvegan Formation which is consistent with the gross sandstone isolith map presented by Burk (1963). Nineteen regional cross sections were put together. Seven of these were oriented parallel to dip while the remaining 12 were oriented parallel to strike. This resulted in a northeast\southwest, northwest\southeast interlocking cross sectional grid which was used as the basis for correlation and mapping (Fig.1-9).

3-2-4. Vertical Cycles

Before correlation, it was considered crucial to establish the degree of vertical cyclicity within the Dunvegan Formation. This involved the recognition of coarsening upwards and fining upwards facies successions using core and well logs. The study

was begun in the Lator area since there were extremely good complete cores through most of the Dunvegan Formation there.

One of the best examples is shown in well 6-11-62-3W5 (Fig.3-7A,B, and C, FSU and Fish Scales markers not penetrated). Cycles are immediately apparent from the well logs alone (Fig.3-7A). "Funnel"-shaped profiles are generally thought to be characteristic of coarsening upward cycles while "bell"-shaped profiles are characteristic of fining upward cycles (Cant,1984). On the well log (Fig.3-7A) 14 cycles are identified. Most of these, especially cycles 2,3,4,9, and 14, show well developed funnel-shaped profiles on both the gamma and the dual induction logs. Poorly developed bell-shaped profiles are present in cycles 8 and 11. The last 10 of these cycles (cycles 4 to 14) have been cored and are shown in figure 3-7B and C.

Figure 3-7B shows the sedimentary cycles, surfaces of erosion and transgression, facies associations, and members within the Dunvegan Formation. Photographs of this entire core are shown in figure 3-7C. Many of the cycles show fairly well developed coarsening upward facies successions. This is evident in cycles 4, 9b, 9a, 13 and 14 which exhibit type 1 Facies Associations. Several of the other coarsening upwards cycles are rather poorly developed and some are truncated by Em surfaces. Em surfaces are especially prominent in cycles 10 and 11 (box 1 and 3, interval 44.2-49.0, Fig.3-5C) and are marked by a razor sharp transition from laminated mudstones into pervasively bioturbated facies. In

Figure 3-7A. Well logs from Dome Lator 6-11-62-3W5. Vertical bar indicates cored interval illustrated in figure 3-7B and C. Depths are in meters. See text for eplanation.

DOME LATOR
6-11-62-3W5

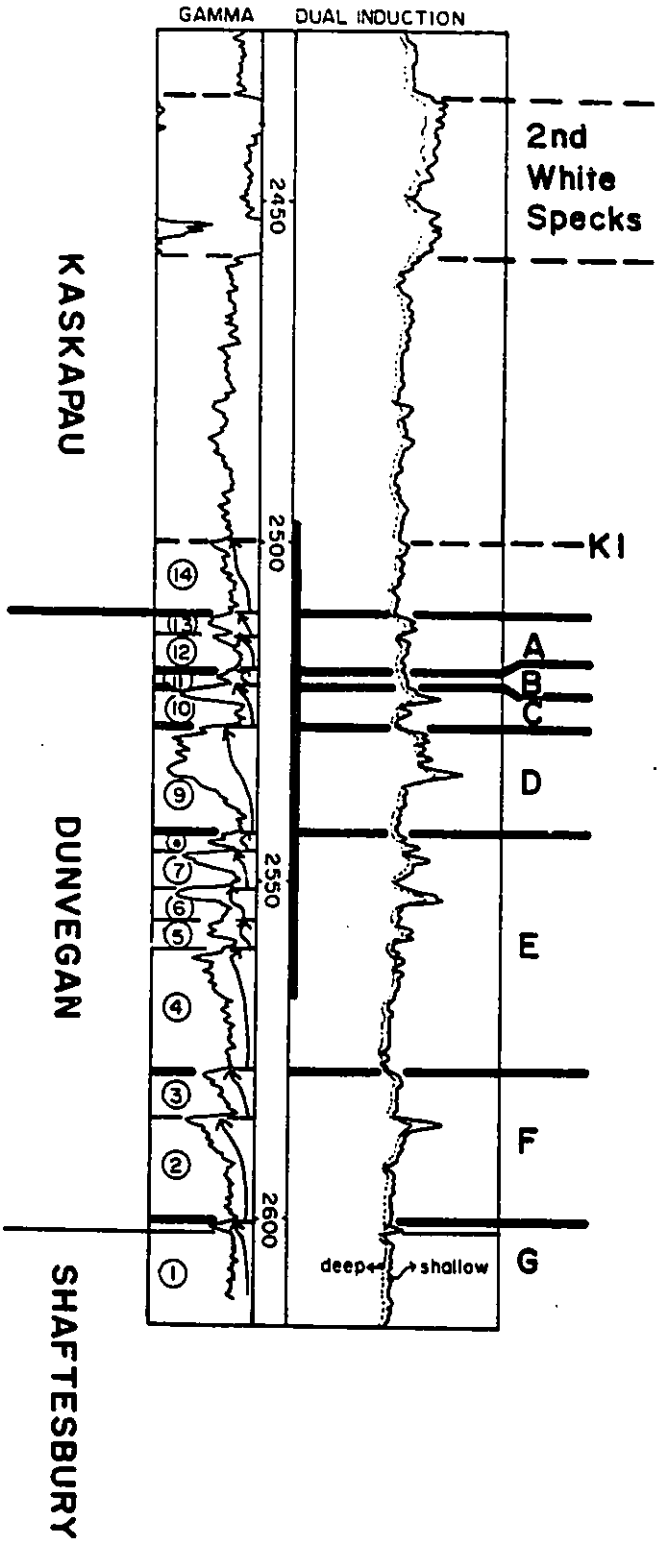

Figure 3-7B. Logged Core section from Dome Lator 6-11-62-3W6. Sedimentary Cycles and positions and types of cycle contacts shown. See text for explanation and figure 2-29 for legend.

DOME LATOR
6-11-62-3W5

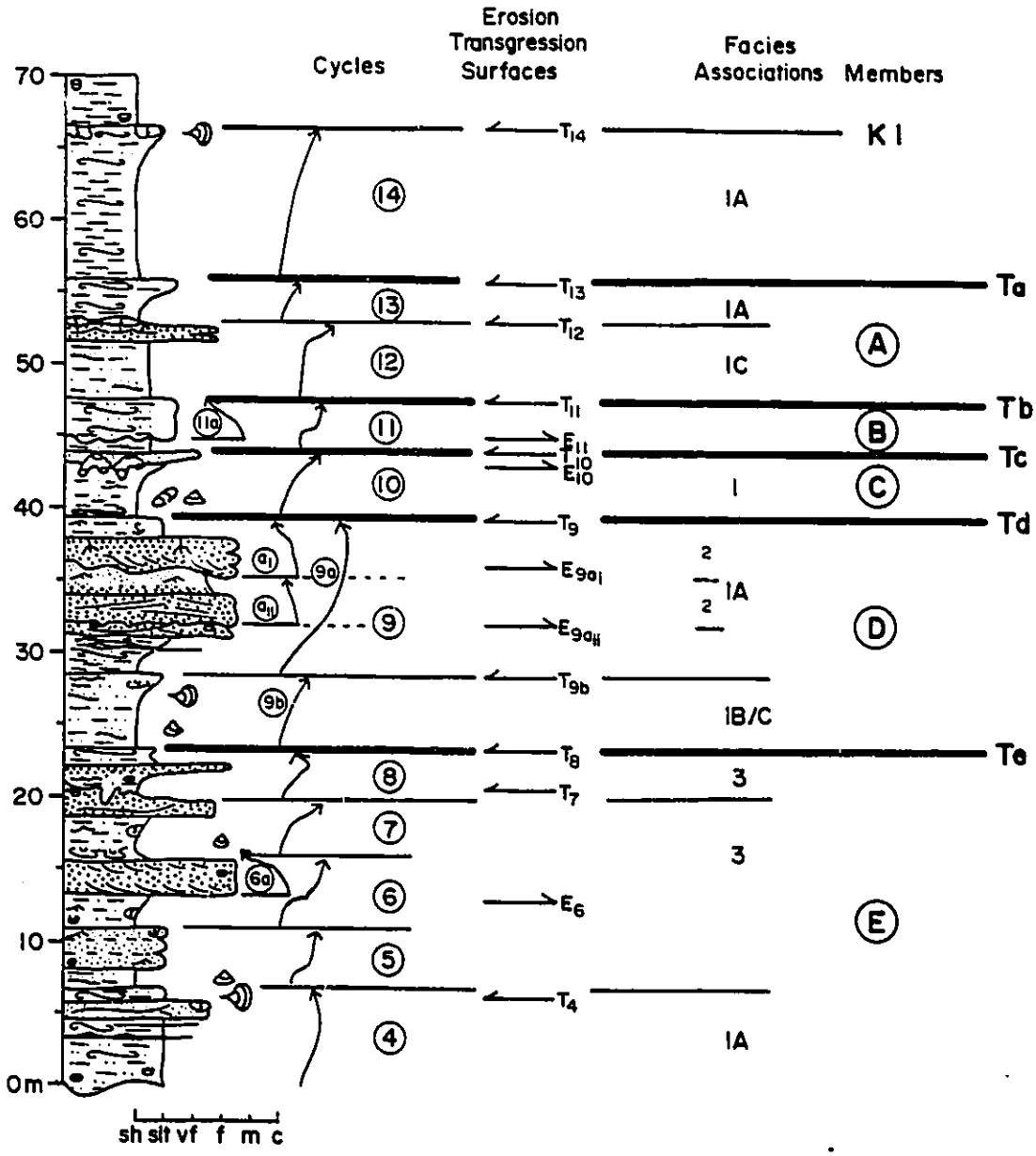

Figure 3-7C. Core Box Photos from well 6-11-62-3W6. In all photos, bottom of core is in lower left and top of core is at the upper right, in the position of the title card. Depths on the title cards are measured from the base of the core upwards. Depths in core of member boundaries are as follows: member E, 0.0 to 24.3m; member D 24.3 to 40.3m; member C, 40.3 to 47.0m; member B, 47.0 to 49.6m; member A, 49.6 to 57.3m; Kaskapau, 57.3 to 71.9m. Box numbers for each 4.5 meter interval are written at the bottom. See text for further discussion.

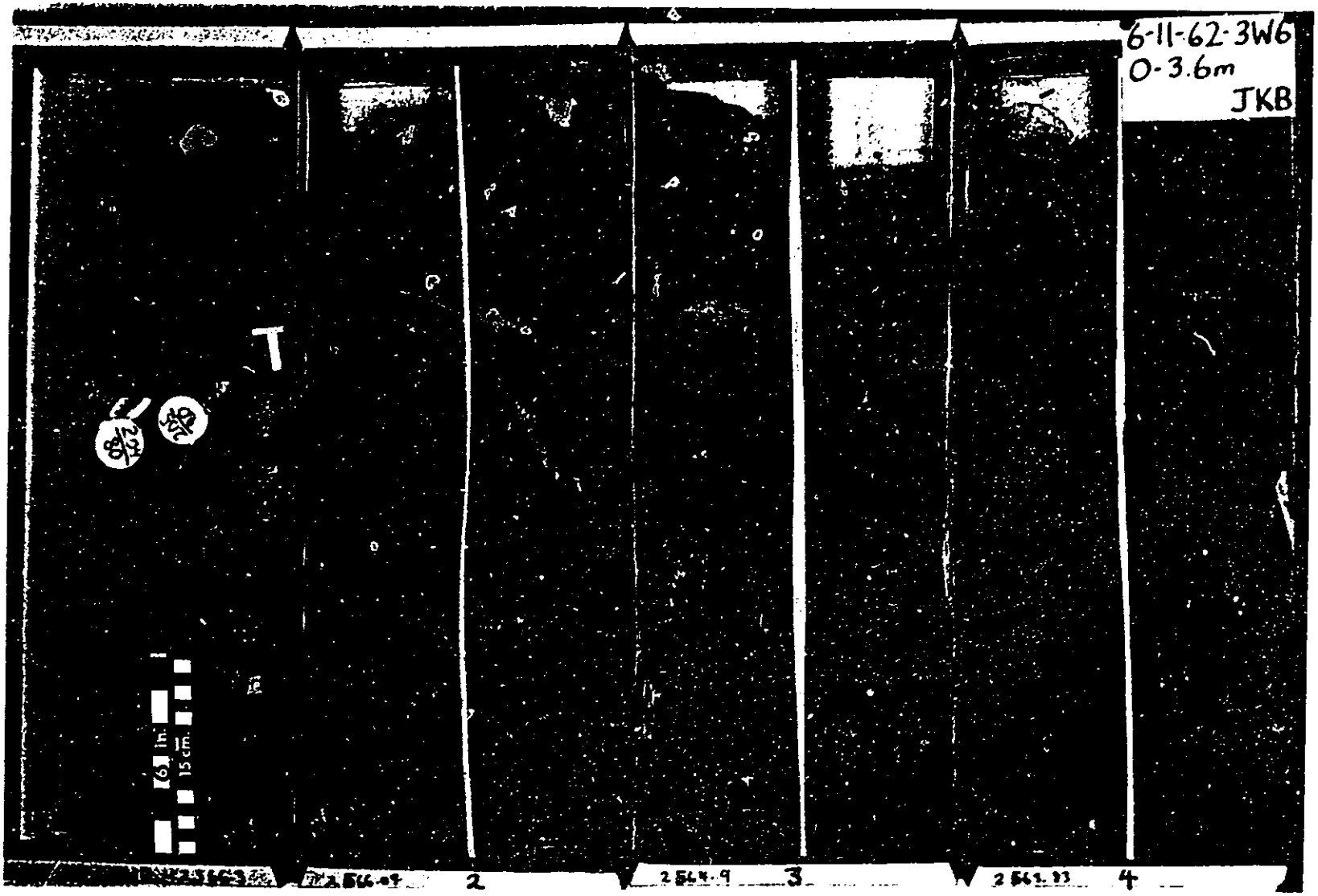
6-11-62-3W6
0-3.6m
JKB
6 in.
15 cm.
2541.9
2
2541.9
3
2541.33
4

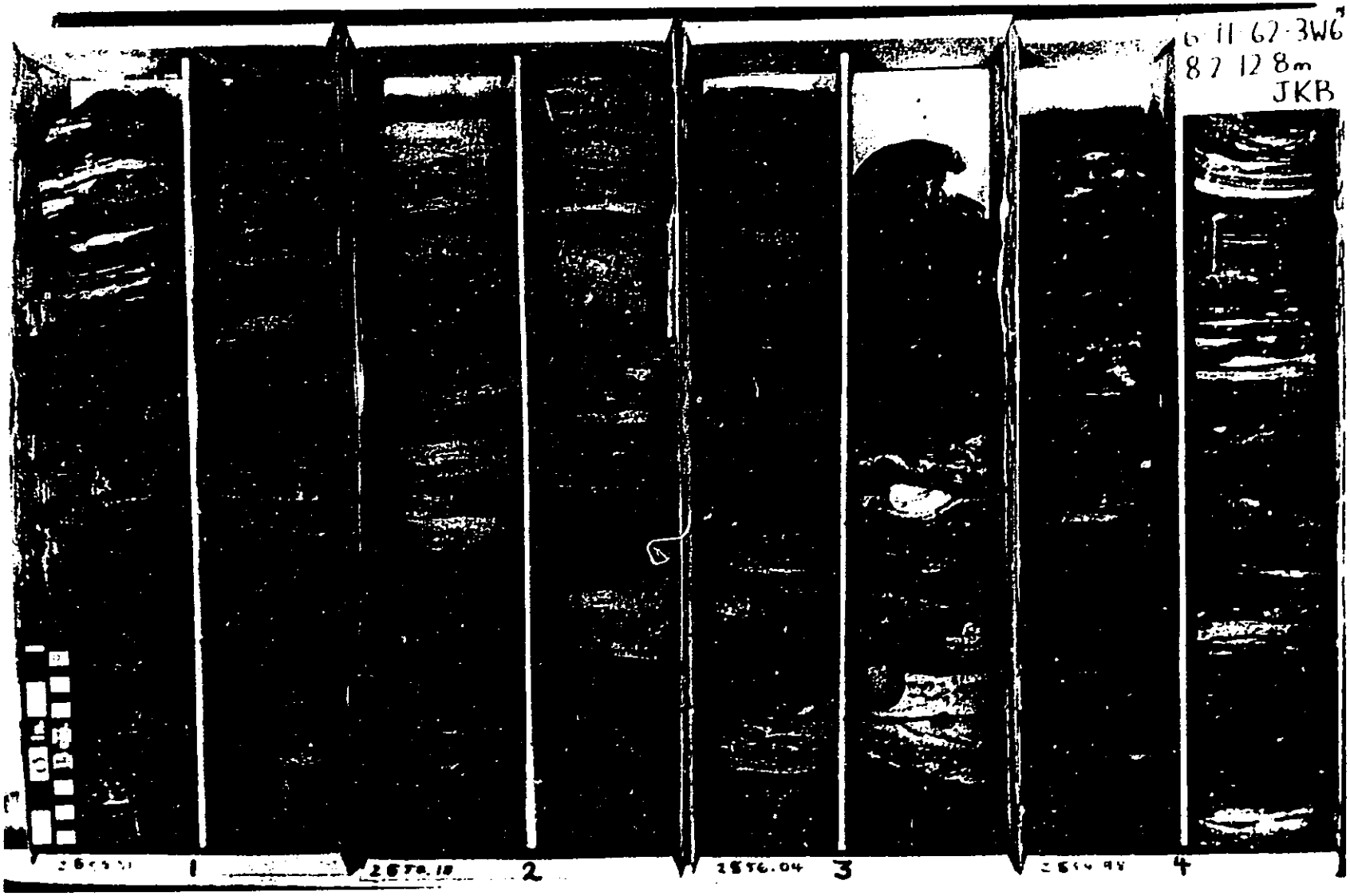
6 11 62-3W6
87 12 8m
JKB
1
2
3
4


6-11 62 3W6
36 82 m
JKB
E4
1
2
3
4


6-11 62 3W6
12 8 16.6m
JKB
6 in.
15 cm.


6-11-62-3WE
16.6-21.3m
JKB

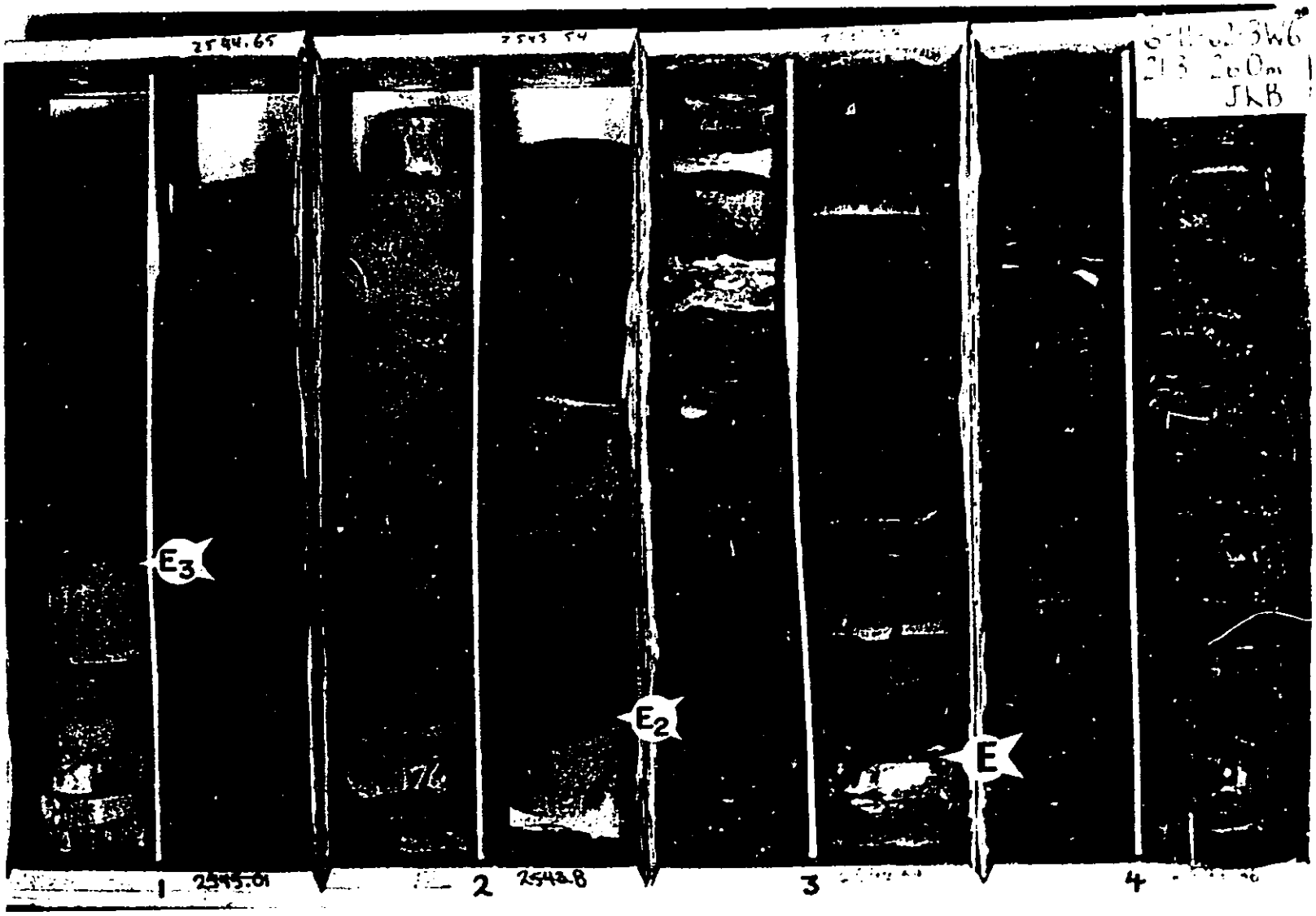
E3
E2
E
1
2
3
4

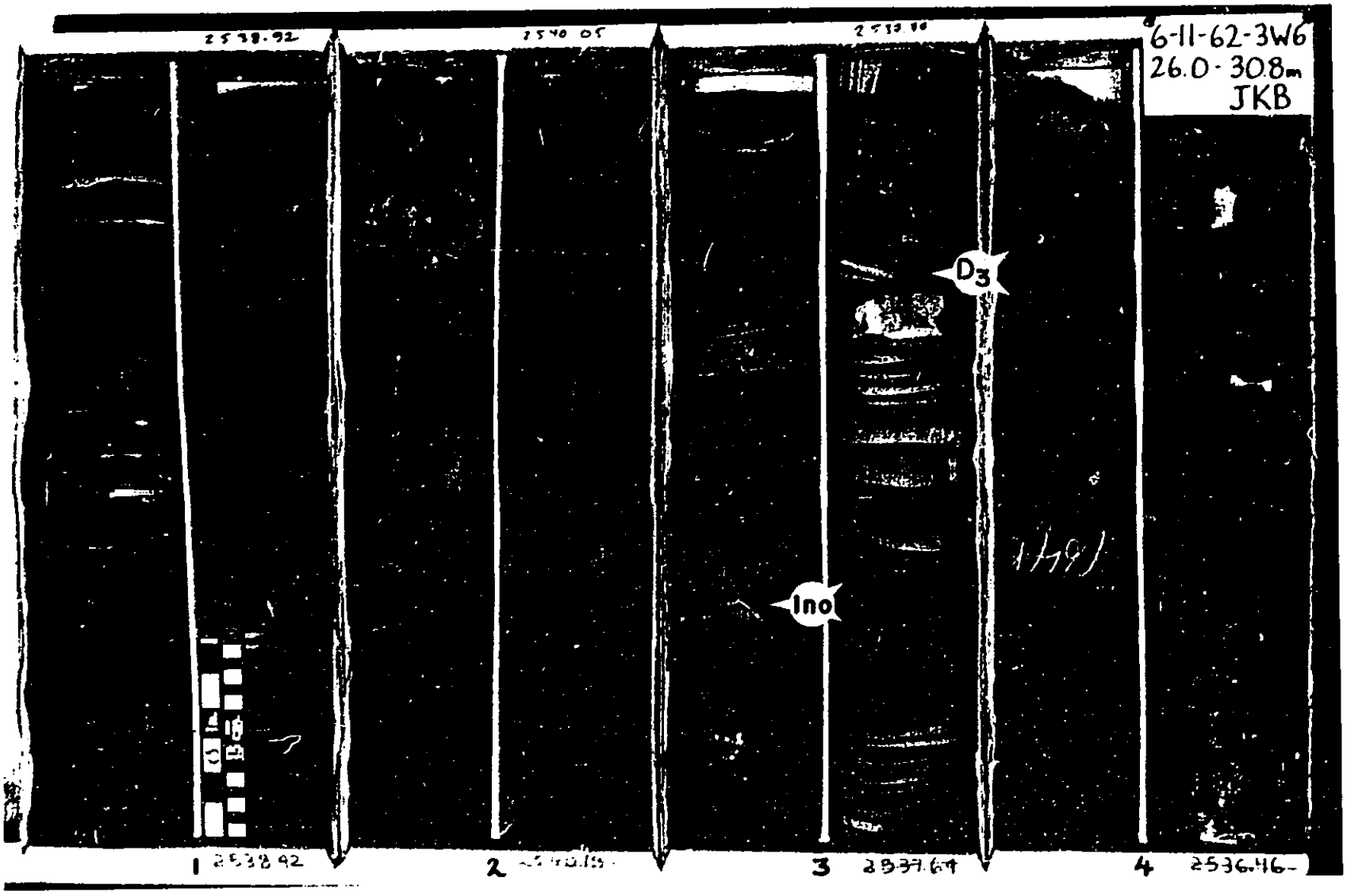
6-11-62-3W6
26.0 - 30.8m
JKB
D3
Ino
1
2538.92
2
3
2537.69
4
2536.46

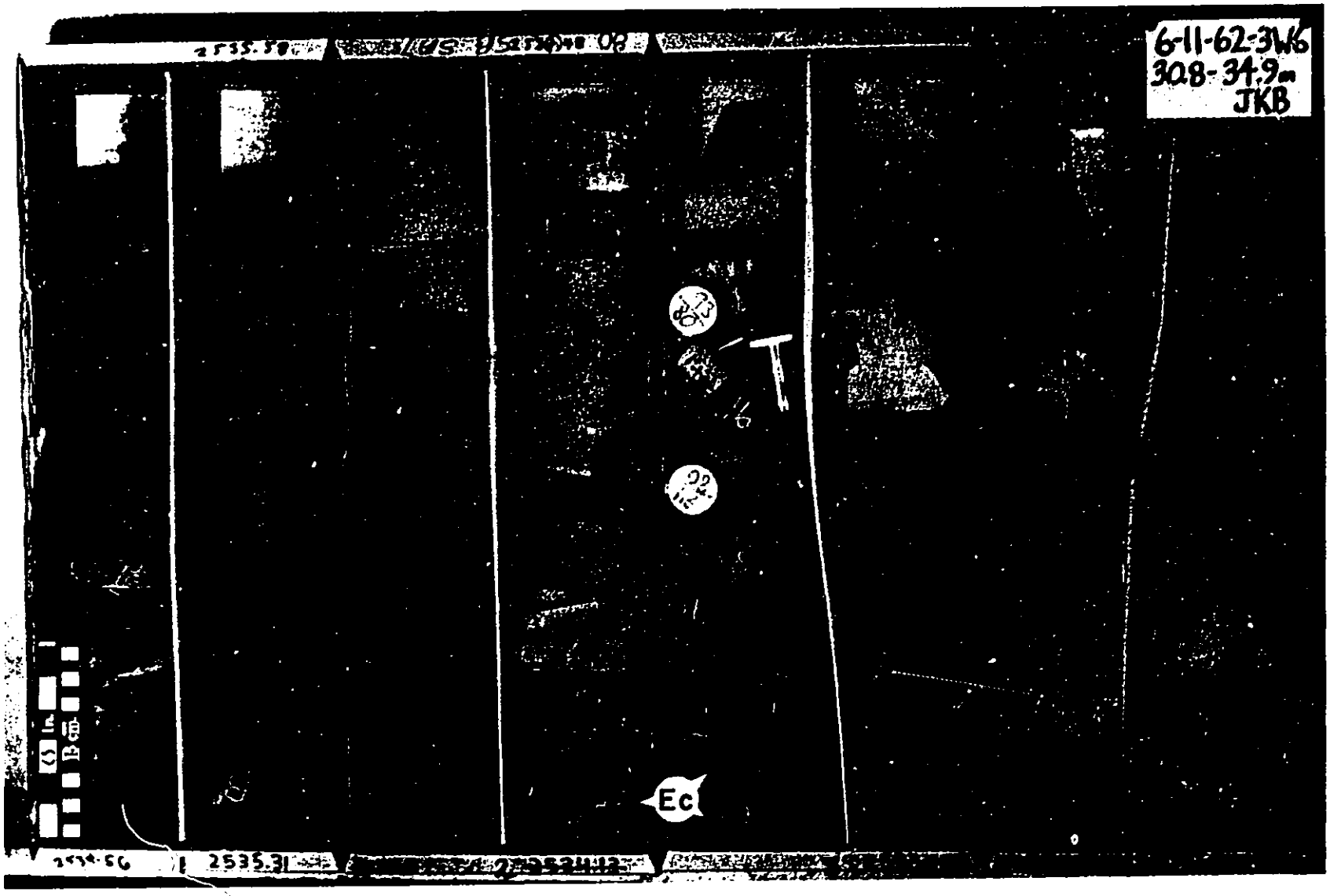
6-11-62-3W6
308-34.9m
JKB
Ec
2535.3

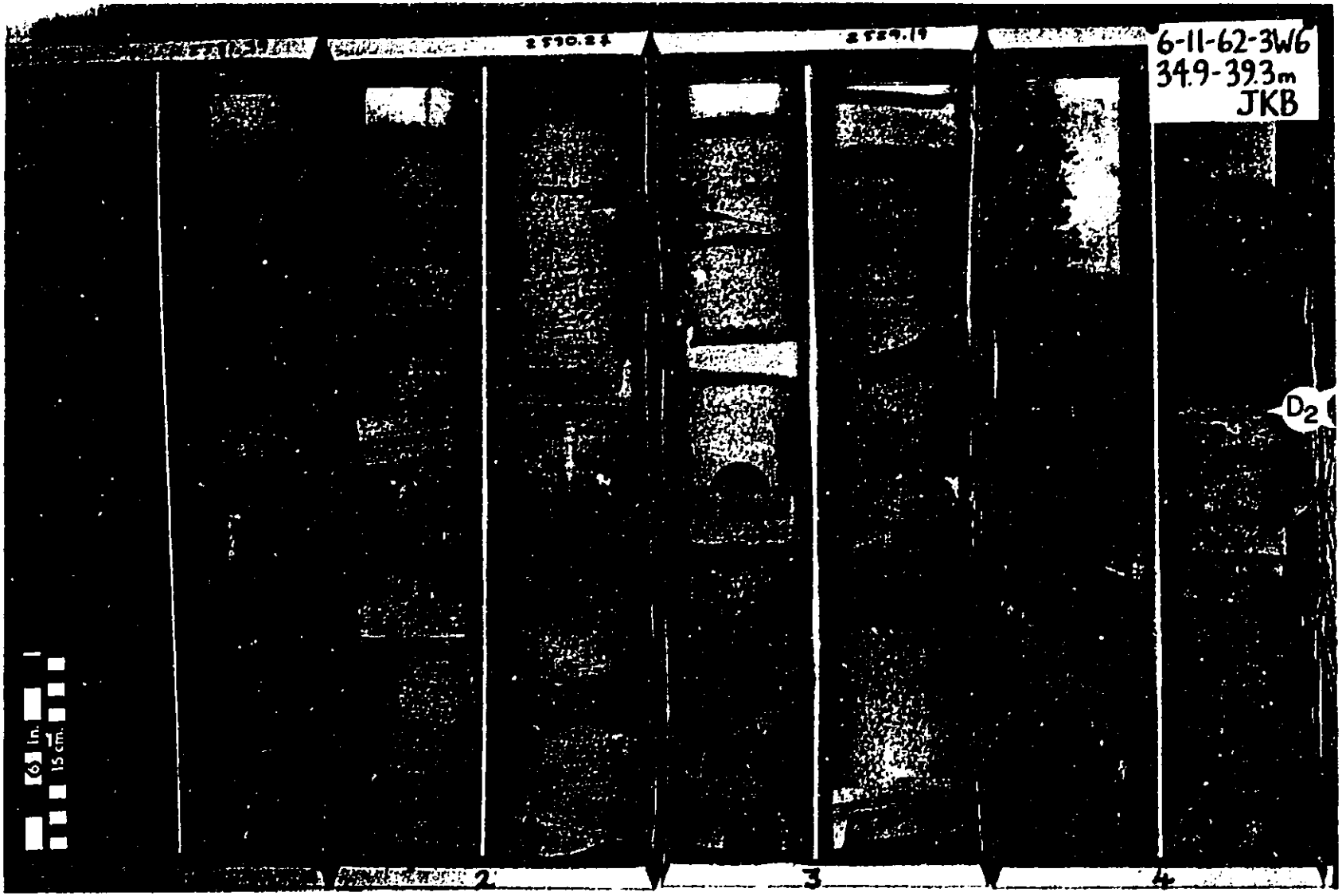
6-11-62-3W6
34.9-39.3m
JKB
D2
2
3
4

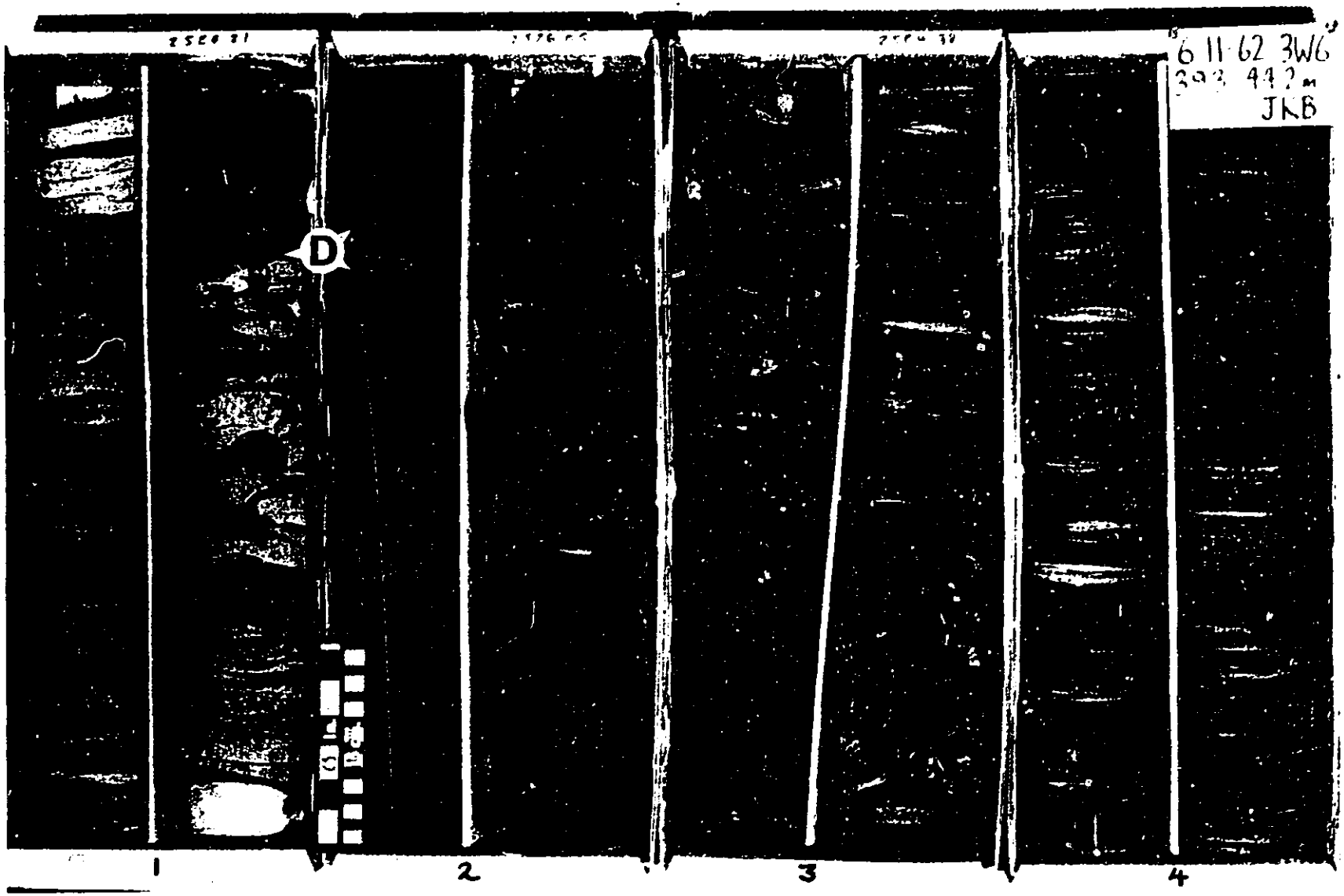
6 11 62 3W6
JKB
D
1
2
3
4

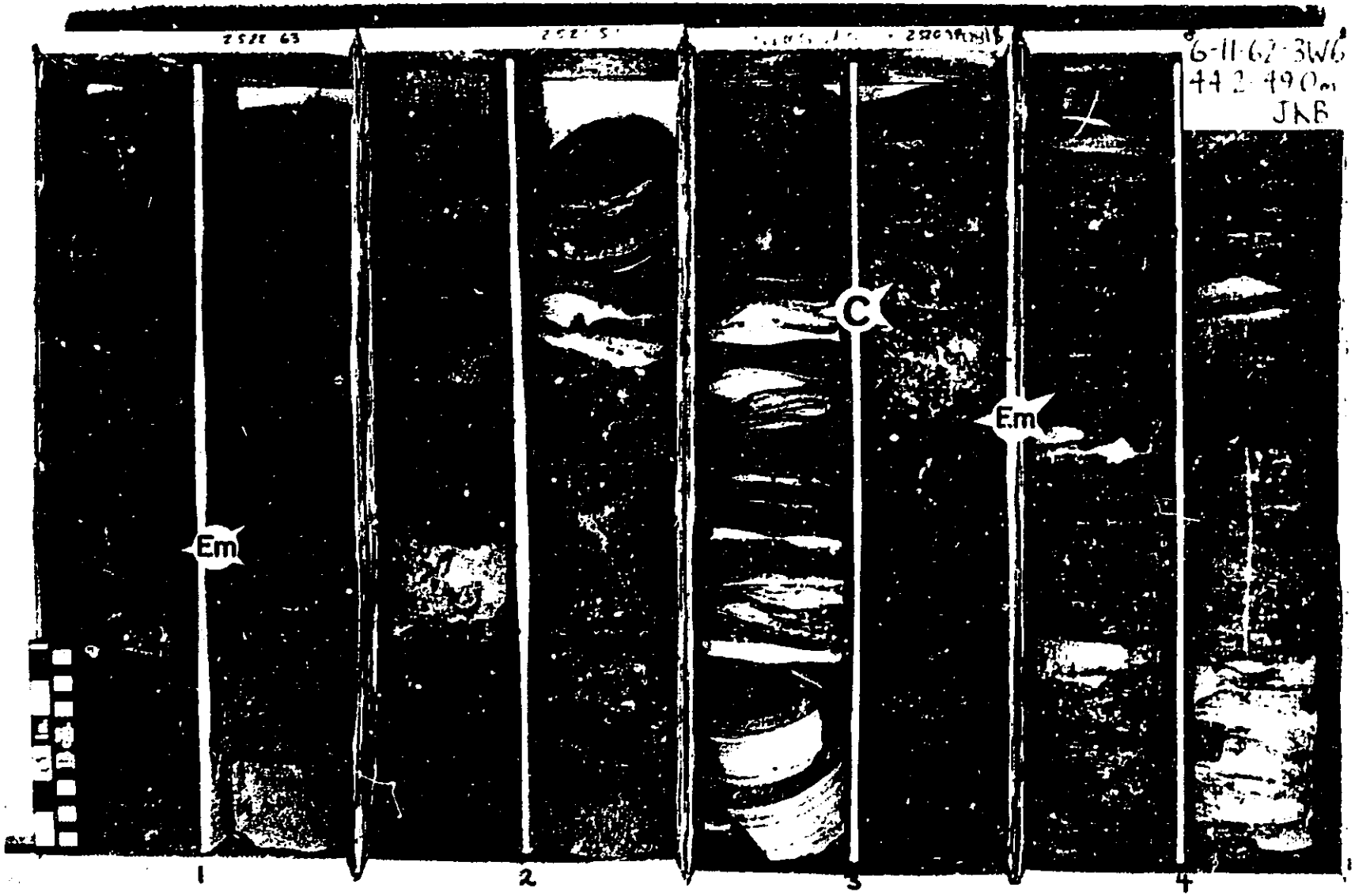
6-11-62-3W6
4422-4900m
JAB
Em
C
Em
1
2
3
4

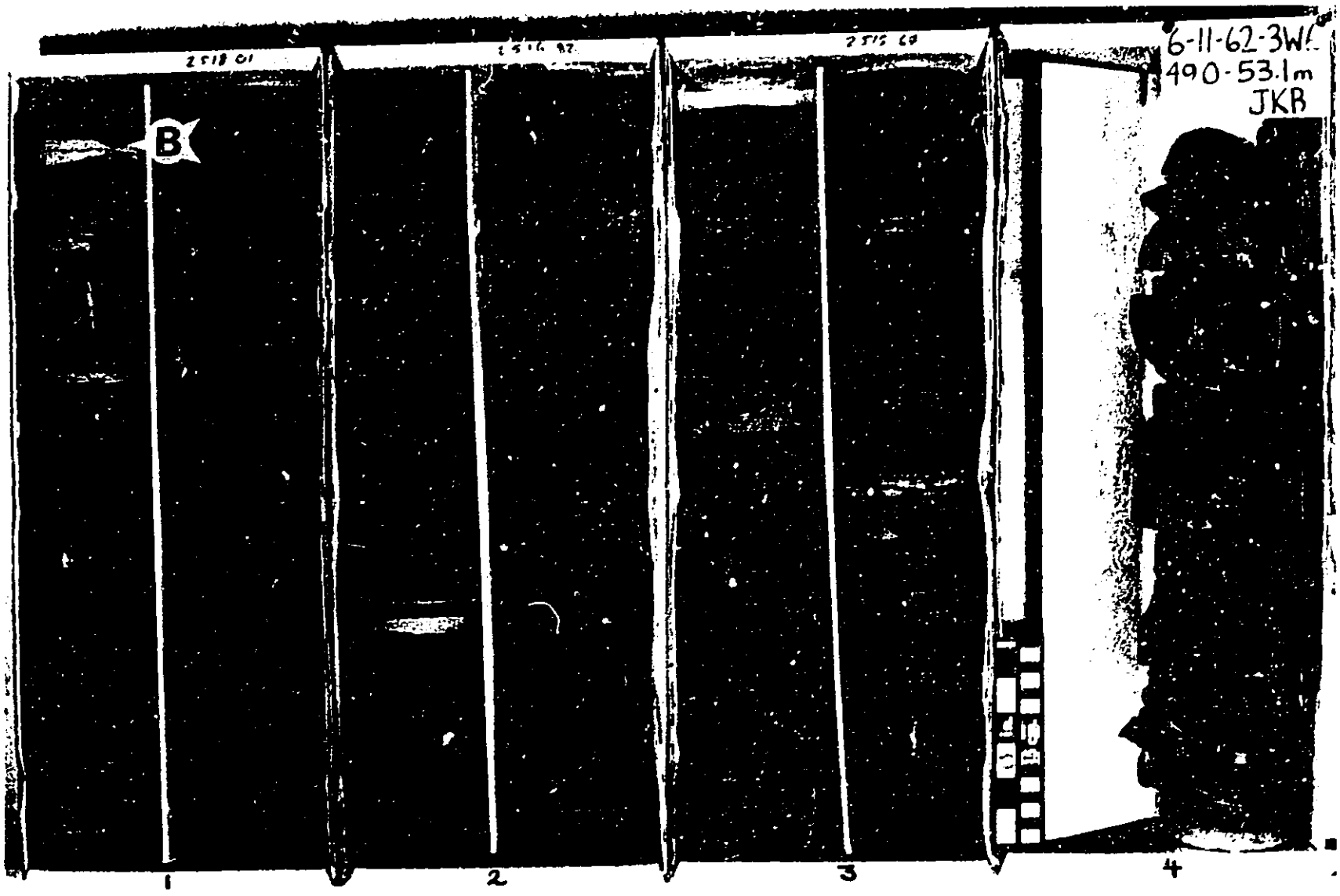
6-11-62-3W
490-53.1m
JKB
B
1
2
3
4


2514.13
2512.93
2511.94
6-11-62-3W6
531-579m
JKB
A1
A2
A
1
2
3
4

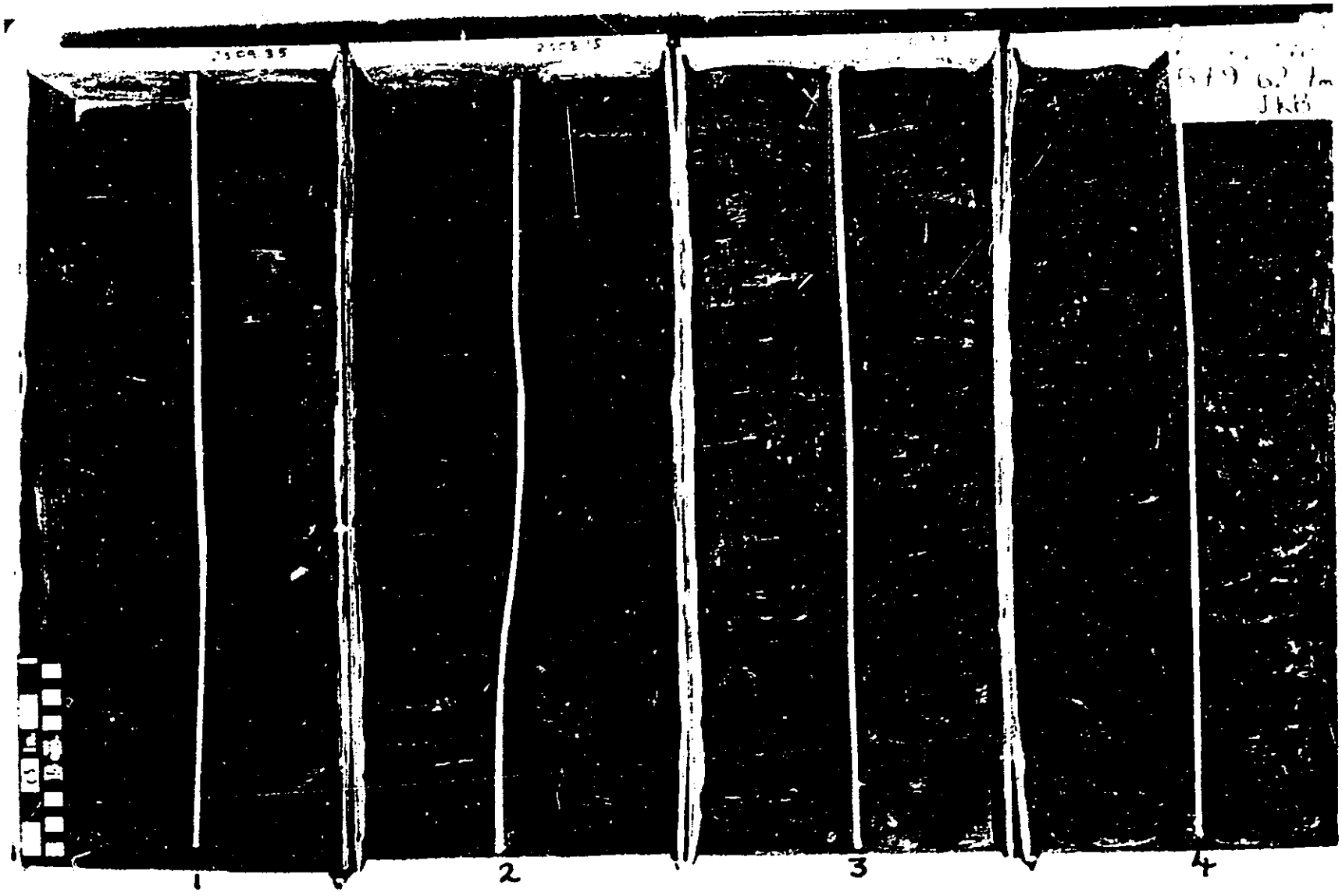
1
2
3
4

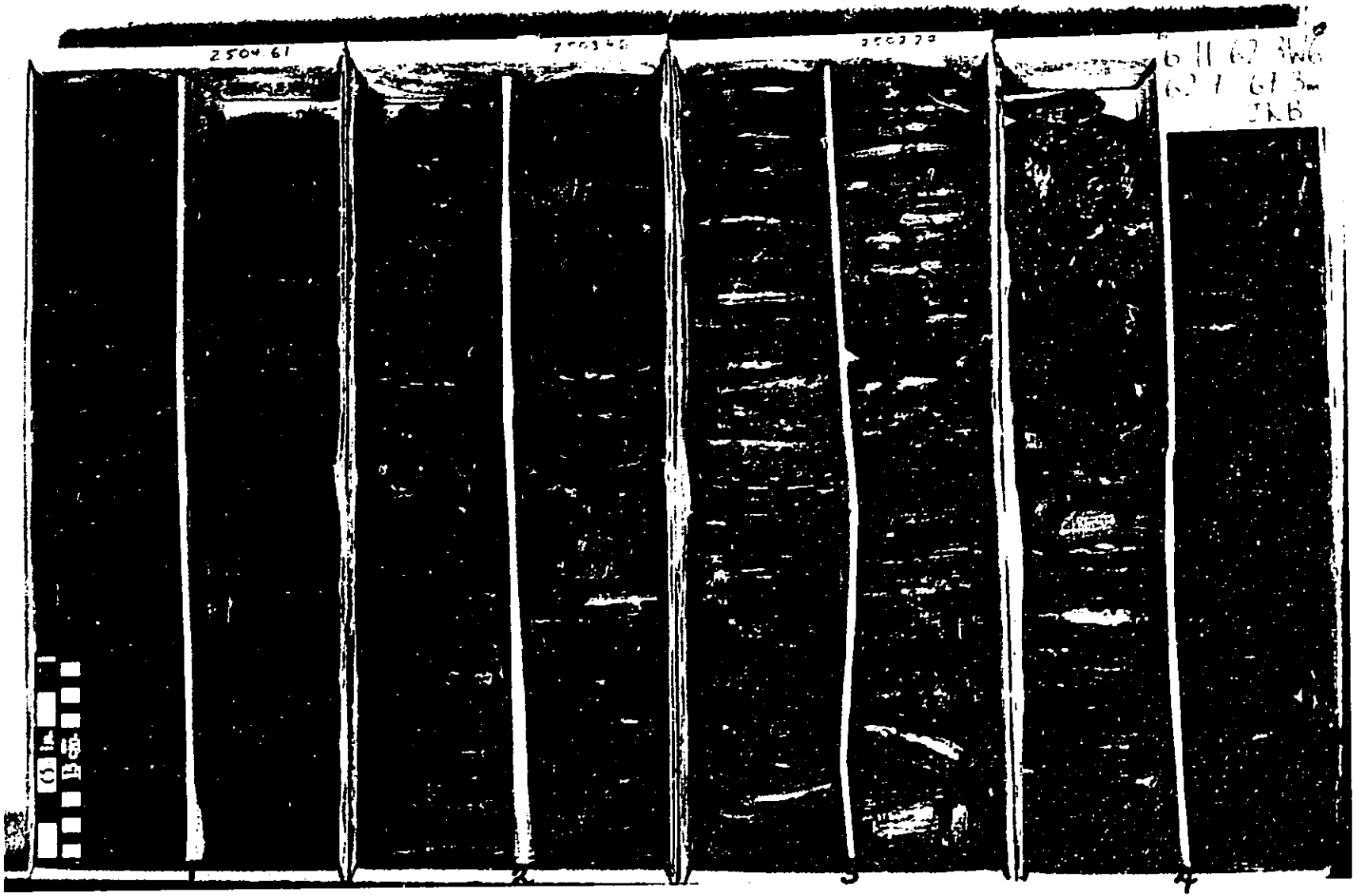
2504 61
6 11 62 3W6
6 7 61 3m
JKB


6-11-62-3W6
673 - 71.9m
JKB
K1
1
2
3
4

cycle 10 (box 1), laminated silty marine shales and pinstriped mudstones (Facies 1A to Facies 4) are erosively truncated by a thin pervasively bioturbated sandstone containing *Ophiomorpha* (Facies 7I). In cycle 11 (box 3) blockstones (Facies 2) are sharply overlain by a few meters of pervasively bioturbated sandy mudstones (Facies 3A).

At least three, poorly developed, nested fining-upwards cycles occur, one in cycle 6, and two in cycle 9a (Fig.3-7B). Erosion is associated at the base of all of these fining upwards cycles. *In situ* root traces at the top of 9ai (top of D2 in box 4, interval 34.9-39.3, Fig.3-7C) indicate non-marine conditionsand may indicate that the underlying E surface is an Ec surface (Ec in Box 2, interval 30.8-34.9, Fig.3-7C). The most easily recognized surfaces are those T-surfaces which cap coarsening upwards facies successions and which are overlain by several meters of marine shales or blockstones. In well 6-11 (Fig.3-7A,B, and C) these surfaces are all marked by a few centimeters of intense bioturbation and include T8 (top of E, box 3, interval 21.3-26.0, Fig 3-7C), T9 (top D, box 1, interval 39.3-44.2m, Fig.3-7C), T11 (top B, box 1, interval 49.0-53.1), T13 (top A, box 4, interval 53.1-57.9) and T14 (K-1 in box 2, interval 67.3-71.9). T4, T7, T9b, T10 and T12 are overlain by thinner shales.

As suggested above in section 3-2-1, only by lateral correlation is it possible to determine which of these T or E surfaces are regionally significant. Lateral correlation of these

cycle 10 (box 1), laminated silty marine shales and pinstriped mudstones (Facies 1A to Facies 4) are erosively truncated by a thin pervasively bioturbated sandstone containing *Ophiomorpha* (Facies 7I). In cycle 11 (box 3) blockstones (Facies 2) are sharply overlain by a few meters of pervasively bioturbated sandy mudstones (Facies 3A).

At least three, poorly developed, nested fining-upwards cycles occur, one in cycle 6, and two in cycle 9a (Fig.3-7B). Erosion is associated at the base of all of these fining upwards cycles. *In situ* root traces at the top of 9ai (top of D2 in box 4, interval 34.9-39.3, Fig.3-7C) indicate non-marine conditionsand may indicate that the underlying E surface is an Ec surface (Ec in Box 2, interval 30.8-34.9, Fig.3-7C). The most easily recognized surfaces are those T-surfaces which cap coarsening upwards facies successions and which are overlain by several meters of marine shales or blockstones. In well 6-11 (Fig.3-7A,B, and C) these surfaces are all marked by a few centimeters of intense bioturbation and include T8 (top of E, box 3, interval 21.3-26.0, Fig 3-7C), T9 (top D, box 1, interval 39.3-44.2m, Fig.3-7C), T11 (top B, box 1, interval 49.0-53.1), T13 (top A, box 4, interval 53.1-57.9) and T14 (K-1 in box 2, interval 67.3-71.9). T4, T7, T9b, T10 and T12 are overlain by thinner shales.

As suggested above in section 3-2-1, only by lateral correlation is it possible to determine which of these T or E surfaces are regionally significant. Lateral correlation of these

surfaces and cycles will be documented in the following section.

3-2-5. Lateral Correlation of Sedimentary Cycles and T-surfaces Within the Dunvegan Formation

After picking and correlating datums on regional cross sections and recognizing vertical sedimentary cycles in core and well logs, the next step in unravelling the stratigraphy of the Dunvegan Formation was to correlate T-surfaces and their accompanying overlying shales initially identified in core. This involved the use of cross sections and fence diagrams in conjunction with facies relationships observed in core.

Figure 3-8A represents the major, regional, strike-oriented core cross-section through the Dunvegan Formation. It penetrates cycles 3 to 14 (defined in well 6-11, Fig.3-7A,B,C) and extends for a length of about 70 kilometers. Relevant well logs, which accompany the cores presented, are shown on the accompanying well-log cross-section (Fig.3-8B). The core cross-section is hung on the K-1 marker (T14). Core from wells 3-6-61-4W6, 10-33-60-5W6 and 12-22-60-5W6 have been combined into a single, composite stratigraphic column for illustrative purposes.

Six of the T-surfaces defined in figure 3-7 can be traced laterally along the entire cross section. These include T-surfaces T8, T9, T10, T11, T13 and T14 and have been designated on the cross section (right hand side) Te, Td, Tc, Tb, Ta and K-1 respectively. Two other surfaces, Tf and Tg, are correlated only on the well-log cross-section (Fig.3-8B); Tf is cored only in well

12-22-60-5W6 at about 6 meters, and Tg is not present in any of the wells on the cross section. Shales and blockstones (Facies 1 and 2), containing marine fauna (including fossils, microfossils, and trace fossils), occur above each of these six surfaces. The other T-surfaces, first described in well 6-11 (Fig.3-7A,B,C), either change their character or do not correlate along the entire cross section. T9b, for example (indicated with a dashed wiggly line at the top of unit D3 in Fig.3-8A), turns out to be an Em surface in adjacent wells (e.g. at 13 meters in well 7-17). The greatest discrepancy between the number of cycles described in core 6-11 and the number of cycles correlatable across the core cross section is in the sediments bounded by Tf and Te. Cursory examination of the upper sediments bounded by these transgressive surfaces shows a high degree of variability. The lower half, cored in well 12-22-60-5W6 (E4, Fig.3-8A), and shown in well 6-11 (interval 0.0-8.2m, Fig.3-7C), shows a well developed coarsening upwards facies succession (similar to Facies Association 1A). In the upper half, in contrast, abrupt facies changes occur between wells making correlation difficult. These facies successions include coaly horizons containing *in situ* root traces, present at both ends of the core cross section (Fig.3-8A) in wells 12-7-59-5W6 (below 5m) and 4-11-65-2W6 (below 15m). These facies successions are similar to sediments of Facies Association 3, described in chapter 2. Transgressive surfaces within this upper half could not be correlated with any confidence over the entire length

Figure 3-8A. Regional strike-oriented core cross-section. Three wells, 3-6, 10-33, and 12-22, have been combined into one composite vertical section. See Fig.3-8B for position of cores on well logs and see text for discussion. Location of cross section is shown in figure 3-6. Facies legend is shown in figure 2-29.

Figure 3-8B. Regional strike-oriented well log cross section. All logs are gamma logs. Vertical bars indicate position of cored intervals shown in Fig.3-8A. The interpretation of this cross section is shown in Fig.3-8C, without the well log traces. See text for further discussion.

Figure 3-8C.Schematic regional strike-oriented cross section. Root symbols indicate predominantly non-marine facies, fine stipple indicates marine sand and coarse stipple indicates channels fills (thickest in member E). Thick horizontal black lines indicate member bounding T-surfaces, wiggly correlation lines indicate erosion. Note truncation in the middle of the cross section at the top of member F. See text for further details and discussion. Cross section based on figure 3-8B.

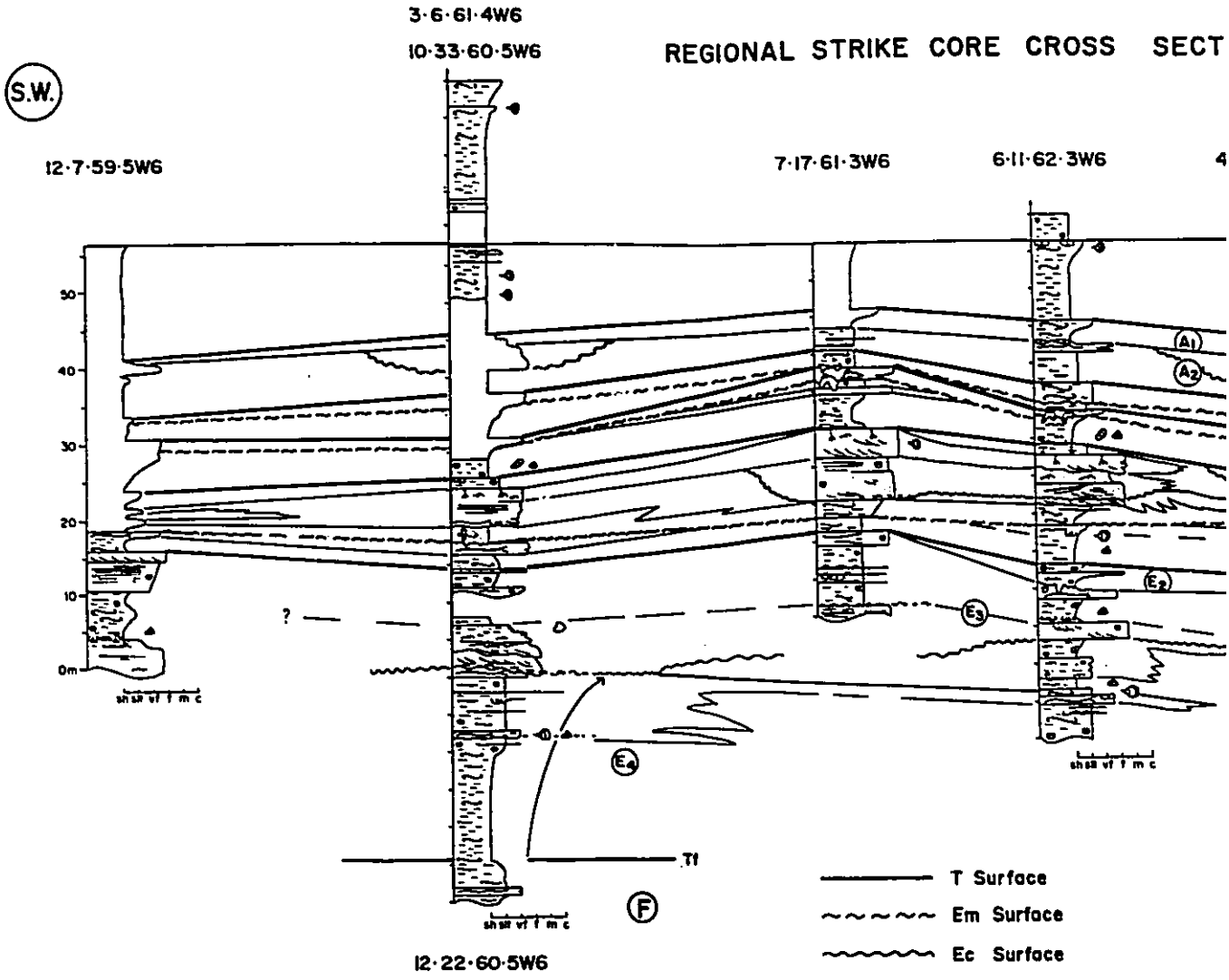
3·6·61·4W6
10·33·60·5W6
REGIONAL STRIKE CORE CROSS SECT
S.W.
12·7·59·5W6
7·17·61·3W6
6·11·62·3W6
4
50
40
30
20
10
0m
A1
A2
E2
E3
E4
T1
F
?
sh sil vf f m c
T Surface
Em Surface
Ec Surface
12·22·60·5W6

;TRIKE CORE CROSS SECTION

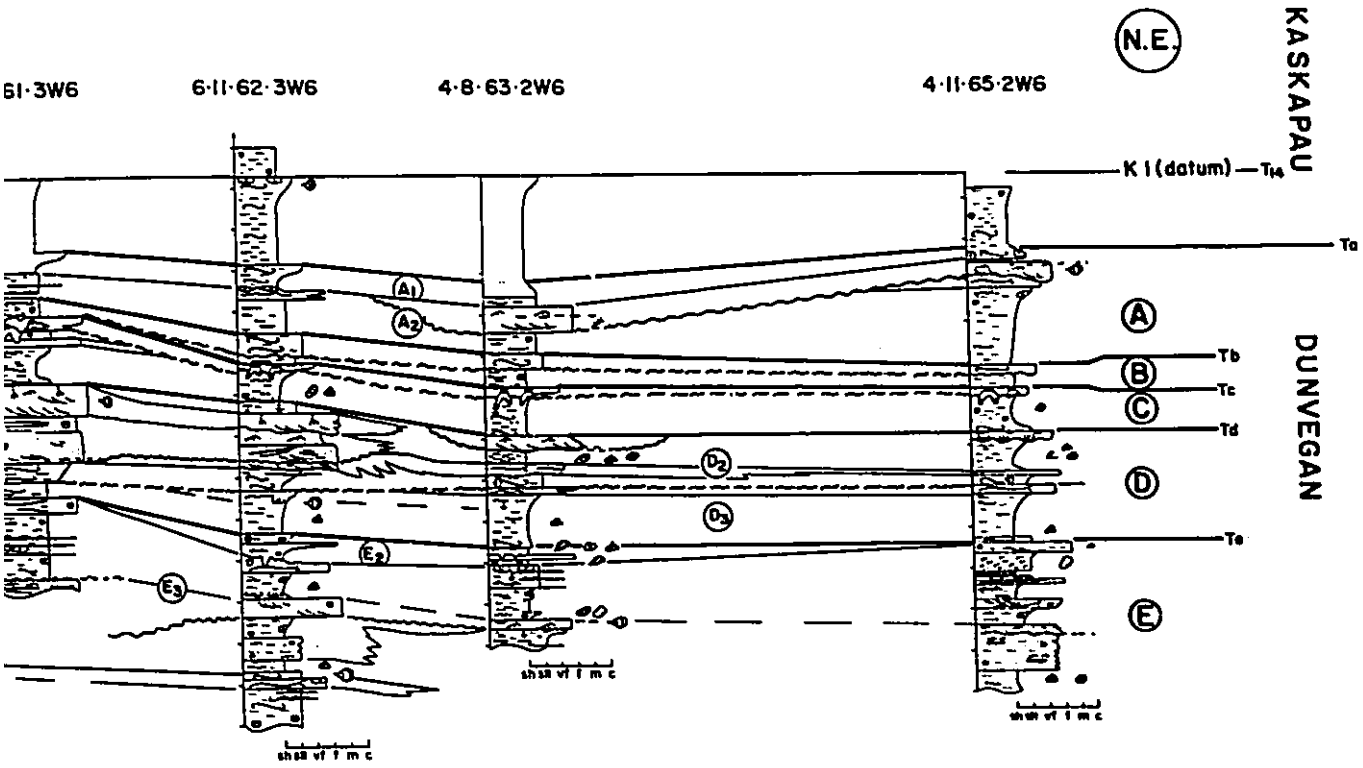

T Surface

Em Surface

Ec Surface

TOTAL LENGTH ≃ 70km

REGIONAL STRIKE WELL LOG CROSS

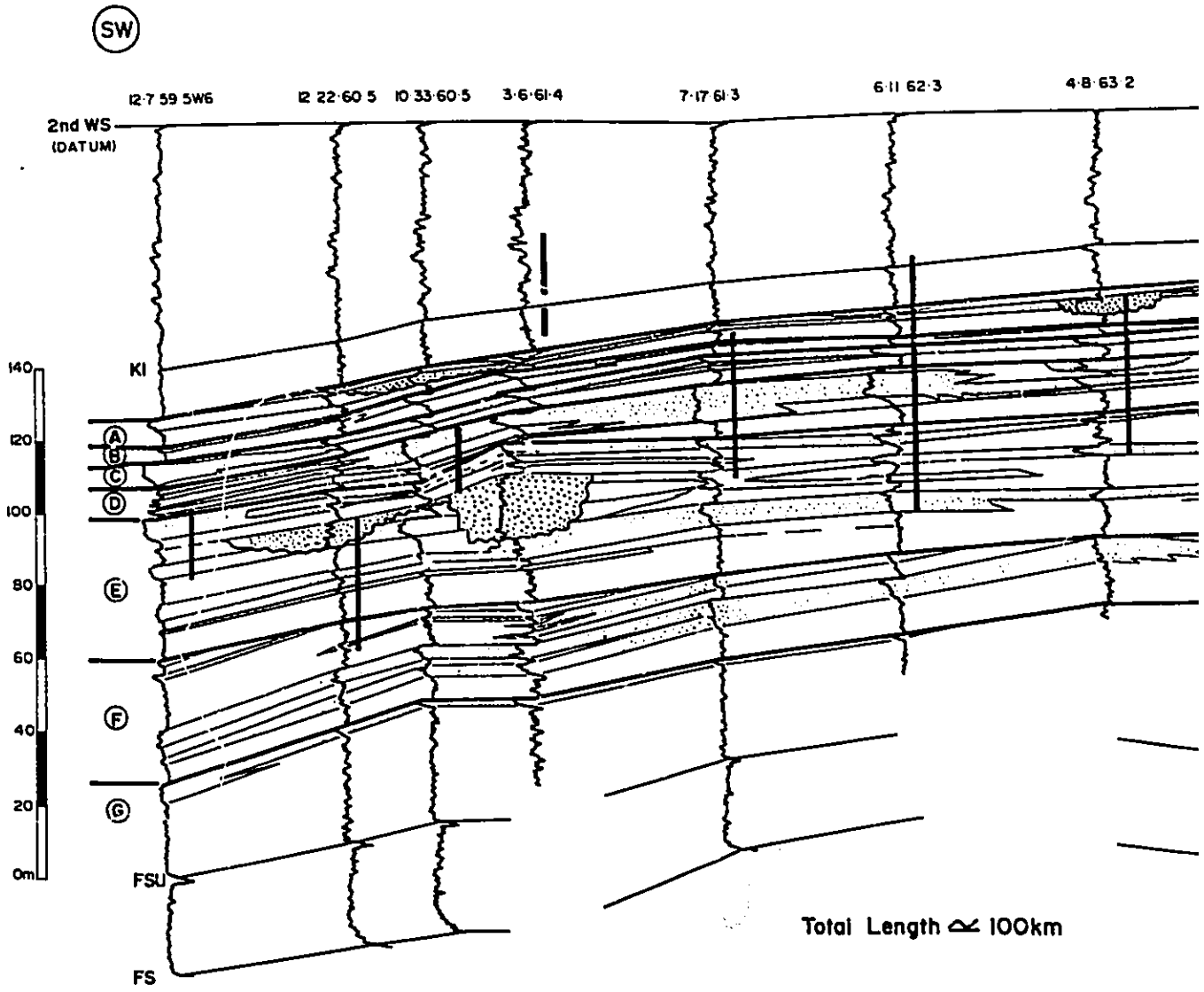

IKE WELL LOG CROSS SECTION

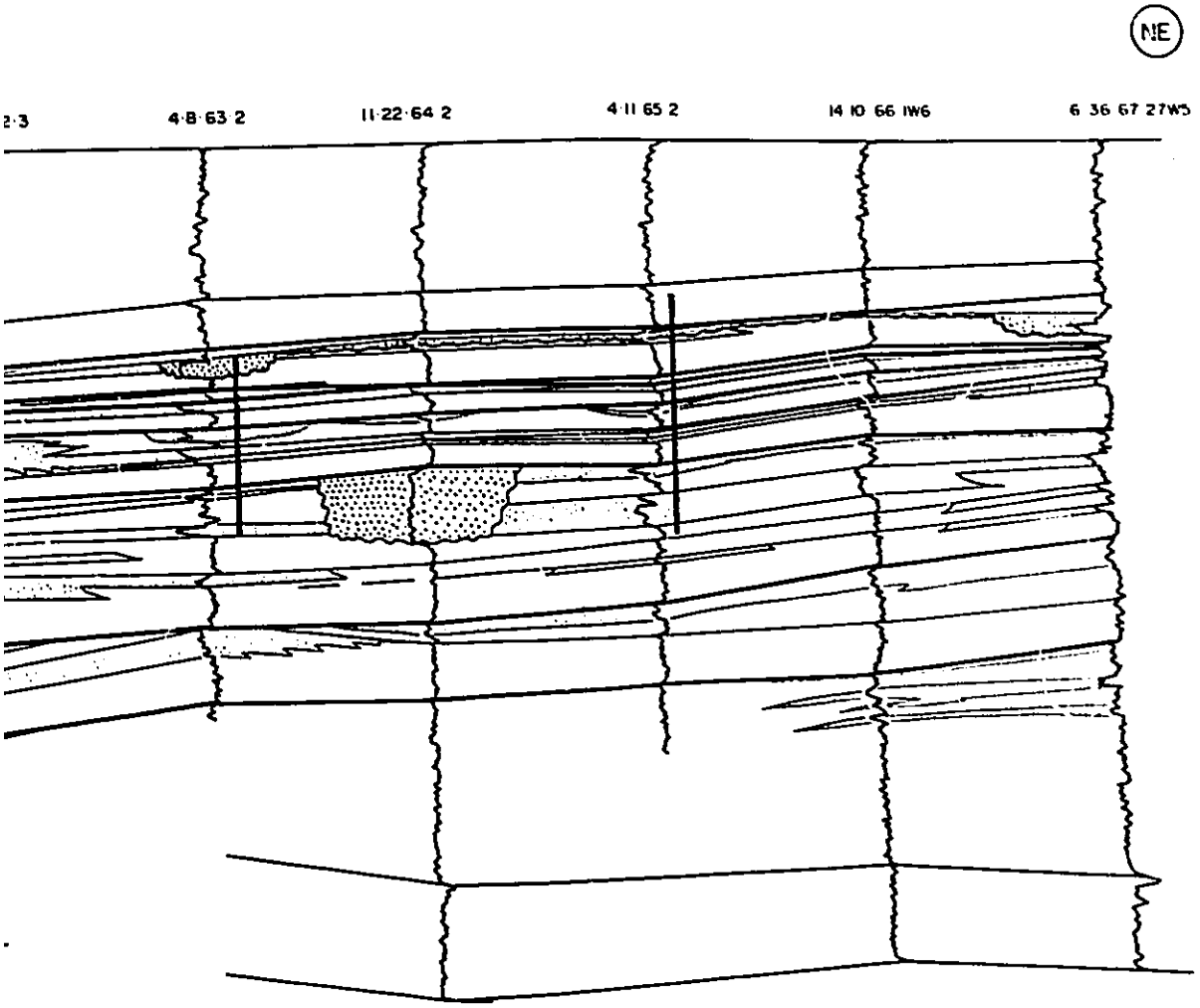

th ≃ 100km

S.W.

SCHEMATIC REGIONAL CROSS SECTION

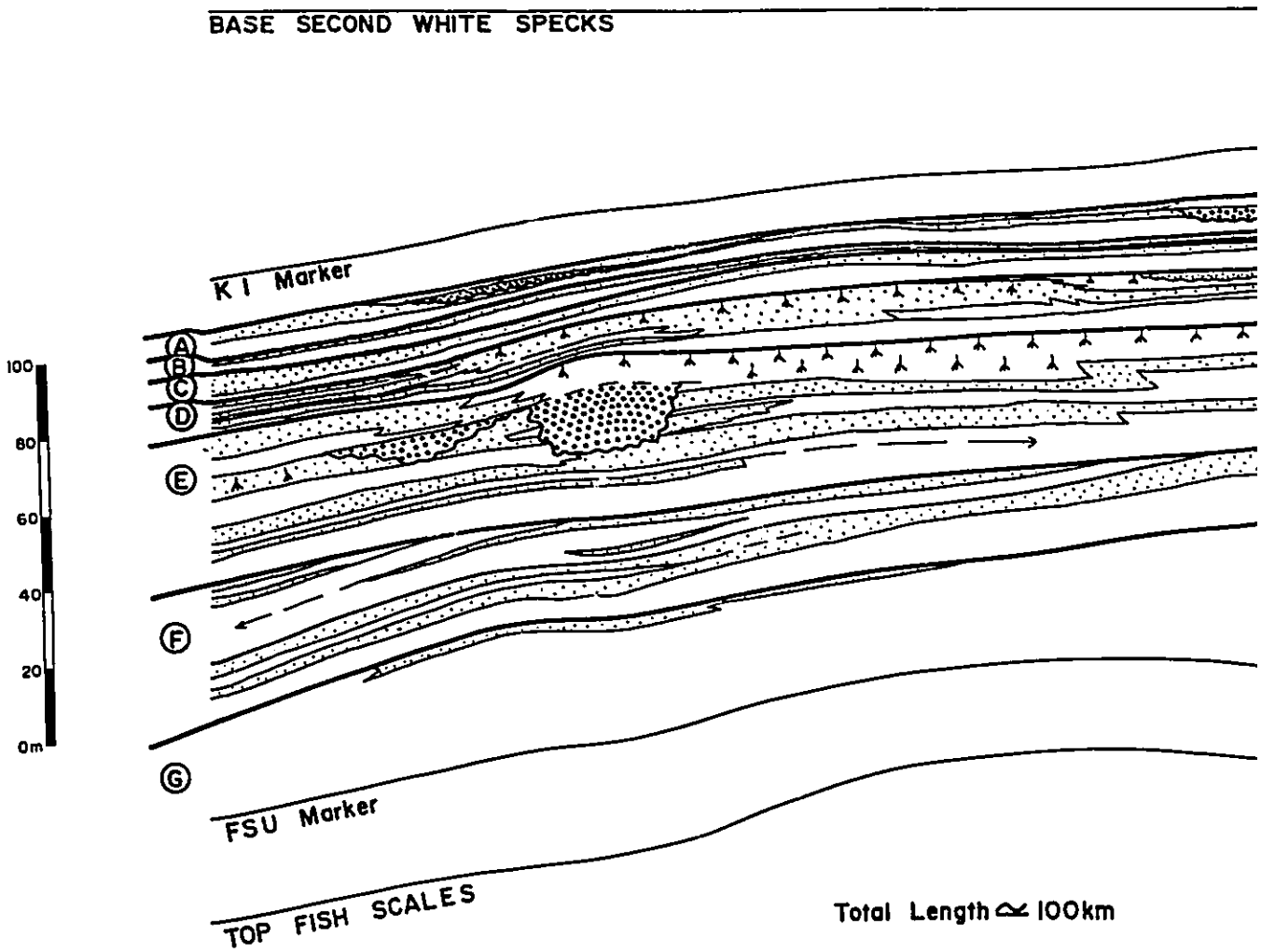

CHEMATIC REGIONAL STRIKE

CROSS SECTION

N.E.

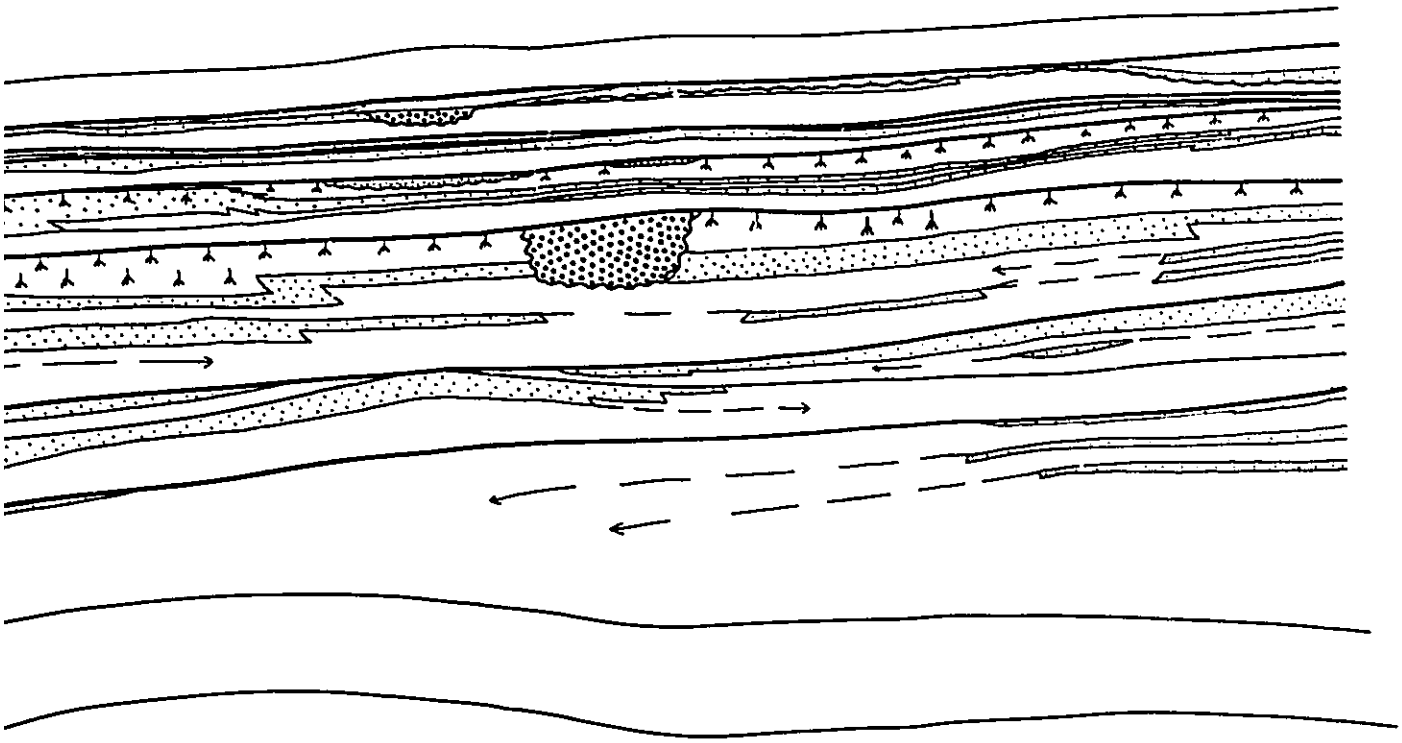

Total Length ≃ 100km

of the well log cross section (100 kilometers)(Fig.3-8B). The sediments between Tf and Te (member E) will be discussed fully in chapter 4.

In the core cross section (Fig.3-8A) the shales above Te in unit D3 thin towards the southwest while the shales above Tc (which were described above as being thin in well 6-11) become thicker towards the southwest. In well 7-17-61-3W6, two sandstones are present between Tc and Td while only one is present in the adjacent wells. Associated with these anomalous thickness changes and loss of sandstones are sharply to erosively based bioturbated zones which sometimes contain lags.

The shales above Ta are lacking in interbedded sandstone and contain Foram assemblages that are typical of those described from the Kaskapau Formation (Wall, 1987).

Interpretation

The anomalous changes in shale thicknesses above Te and Td and the loss of sandstones below Tc are interpreted as being the result of erosion. Since sharply bioturbated horizons erosively overly these units (e.g. well 7-17 at 13m and again at 33m), and sometimes contain associated lags, it is inferred that erosion probably occurred during marine transgression. The base of the bioturbated units therefore represents the actual surface of initial transgression while the bioturbated units represent thin preserved transgressive deposits. At Tc the upper contact between transgressive sandy siltstone and overlying marine mudstone may be

interpreted as the surface of maximum transgression, produced when rate of relative sea-level rise was at its highest, although this may not necessarily coincide with the actual maximum depth of the sea.

The sediments between Tf and Te showed facies successions similar to Facies Association 3 and are interpreted as being deposited in complex, transitional-marine to non-marine environments. Transgressive surfaces within this unit are laterally impersistent and do not correlate along the entire length of the cross section. They were therefore lumped together for the purposes of stratigraphic subdivision.

The shales above Ta have been included with the Kaskapau Formation due to the similarity of their microfauna with Kaskapau assemblages (Wall,1987) and because of the lack of interbedded sandstone.

3-3. Allostratigraphy

3-3-1. Members

It is now possible to define members within the Dunvegan Formation on the basis of the recognition of the seven regionally persistent T-surfaces defined above. These seven surfaces are designated as Ta, Tb, Tc, Td, Te, Tf and Tg. The Dunvegan Formation has been correspondingly divided into seven informally named members designated A, B, C, D, E, F, and G from top to bottom (Fig.3-9B). Each member is made up of several shingled sandstones which exhibit a regular arrangement as they more or less progres-

sively offlap in a southeastward direction. The progressive southeasterly offlap of sandy shingles (defined below) suggests more or less continuous progradation of shallow marine environments (largely comprising Facies Association 1). Members therefore represent relatively gradual regressive episodes, marked by the progressive seaward shift of depositional environments, punctuated by transgressive surfaces. Each member can be interpreted as a genetically related sedimentary package exhibiting marked lithic heterogeneity and separated by regionally persistent bounding discontinuities (T-surfaces). They are therefore allomembers (North American Commission on Stratigraphic Nomenclature, 1983). Sandstones within each of the seven members die out toward the east and southeast (Fig.3-9B). Sandstones within lower members disappear before those in the upper members. Conventional lithostratigraphic nomenclature defines the base of the Dunvegan Formation as the first thick sandstone encountered above the Shaftesbury shale. Using this approach, the base of the Dunvegan Formation is therefore highly diachronous, with the shales at the base of members E, F, and G eventually merging with and becoming indistinguishable from the shales of the Shaftesbury Formation to the southeast (Fig.3-9B). In the chronostratigraphic sense, however, the Shaftesbury is seen to be the southeastward basinal equivalent of Dunvegan sandstones to the northwest. This point is discussed below in section 3-5.

Figure 3-9A. Regional dip-oriented well log cross section. All well traces are gamma ray logs. Thick black vertical lines represent cored intervals. Root traces indicate non-marine facies. The interpretation of this cross section is shown in Fig.3-9B minus the well log traces. See text for explanation.

Figure 3-9B. Schematic regional dip-oriented cross section, based on figure 3-9A. Root symbols indicate non-marine facies, light stipple indicates marine sandstone, heavy stipple indicates channel fills. Note that shingles in overlying members downlap onto underlying T-surfaces, and are especially well developed in member E. See text for further discussion.

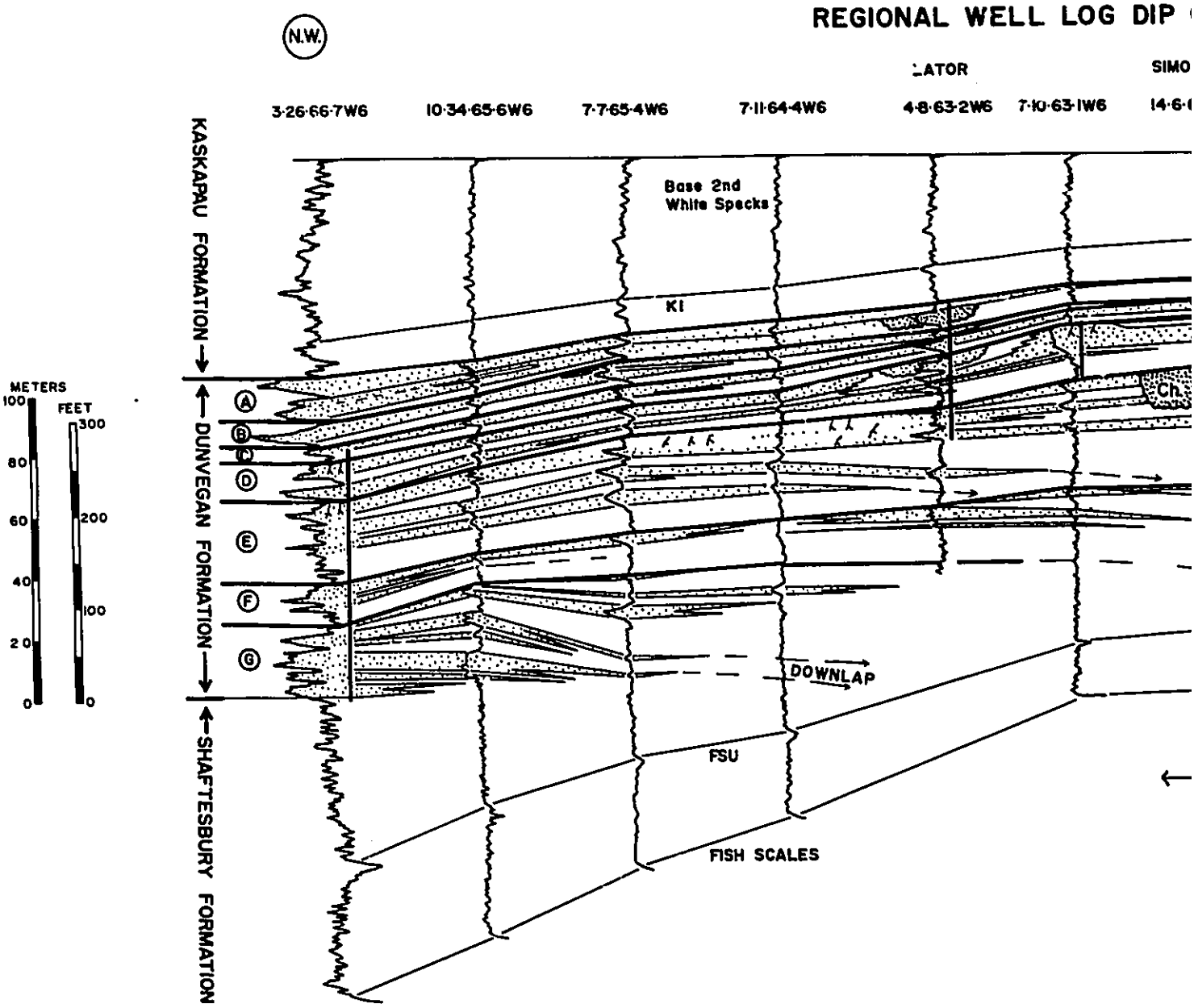
REGIONAL WELL LOG DIP
N.W.
3-26-66-7W6
10-34-65-6W6
7-7-65-4W6
7-11-64-4W6
4-8-63-2W6
7-10-63-1W6
KASKAPAU FORMATION
DUNVEGAN FORMATION
SHAFTESBURY FORMATION
Base 2nd White Specks
KI
A
B
C
D
E
F
G
DOWNLAP
FSU
FISH SCALES
METERS
FEET
100
80
60
40
20
0
300
200
100
0

.L LOG DIP CROSS SECTION

S.E.

SIMONETTE

BIGSTONE

7-10-63-1W6 14-6-63-26W5 3-8-62-25W5 2-26-61-24W5 11-14-31-23W5 11-5-60-21W5 11-3-60-20W5 6-13-59-18W5

15-31-62-26W5

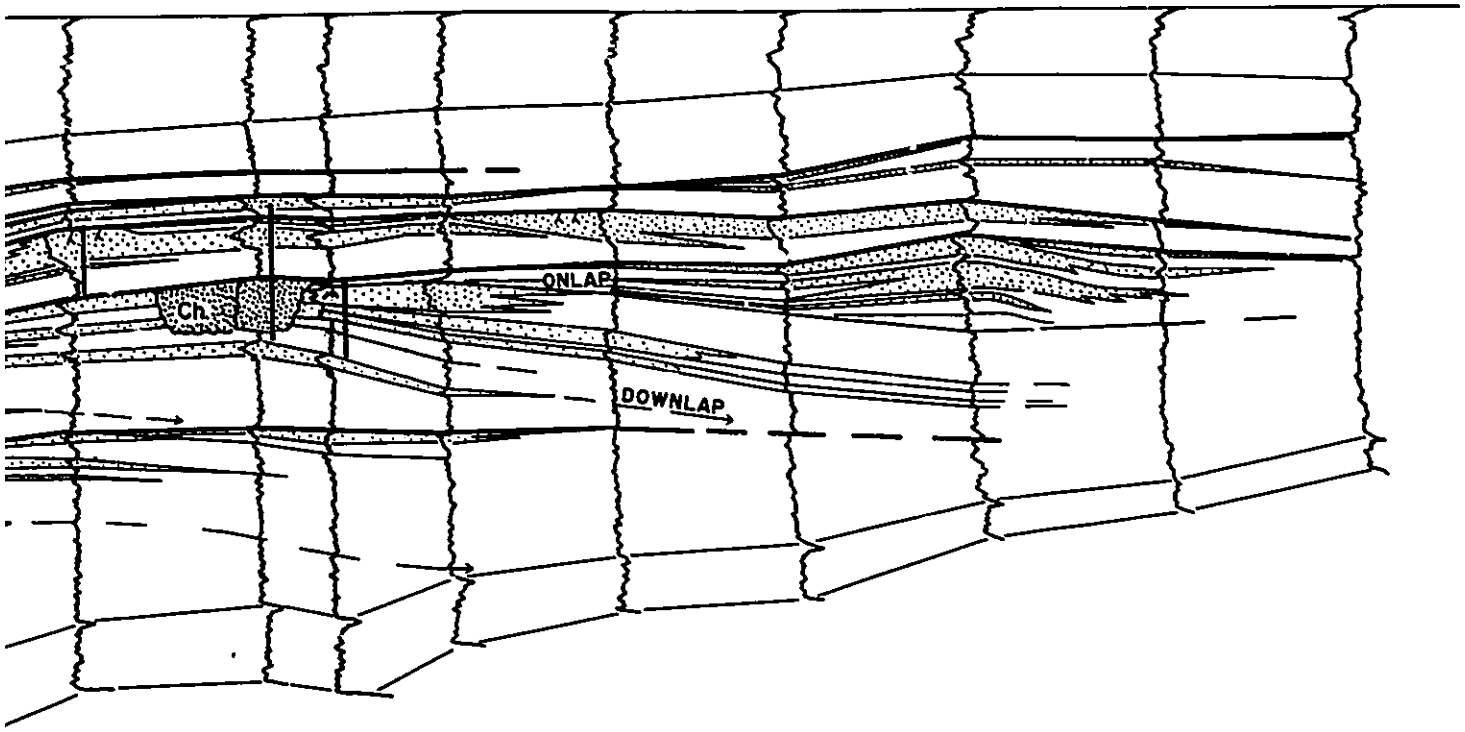

TOTAL WIDTH ≃ 170 km

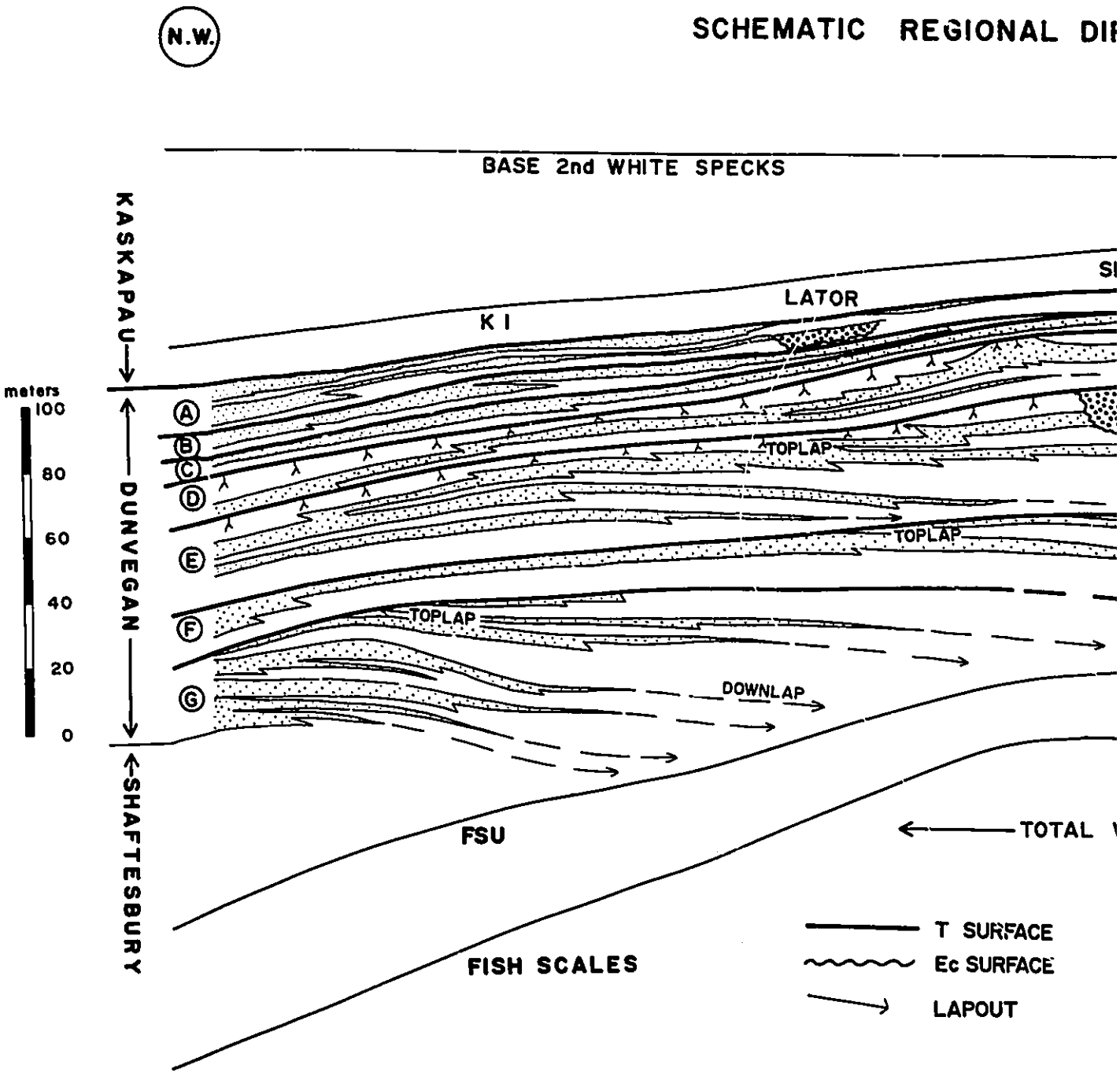
N.W.
SCHEMATIC REGIONAL DI
BASE 2nd WHITE SPECKS
KASKAPAU
DUNVEGAN
SHAFTESBURY
meters
100
80
60
40
20
0
K I
LATOR
A
B
C
D
E
F
G
TOPLAP
TOPLAP
TOPLAP
DOWNLAP
FSU
FISH SCALES
TOTAL
T SURFACE
Ec SURFACE
LAPOUT

AL DIP CROSS SECTION

S.E.

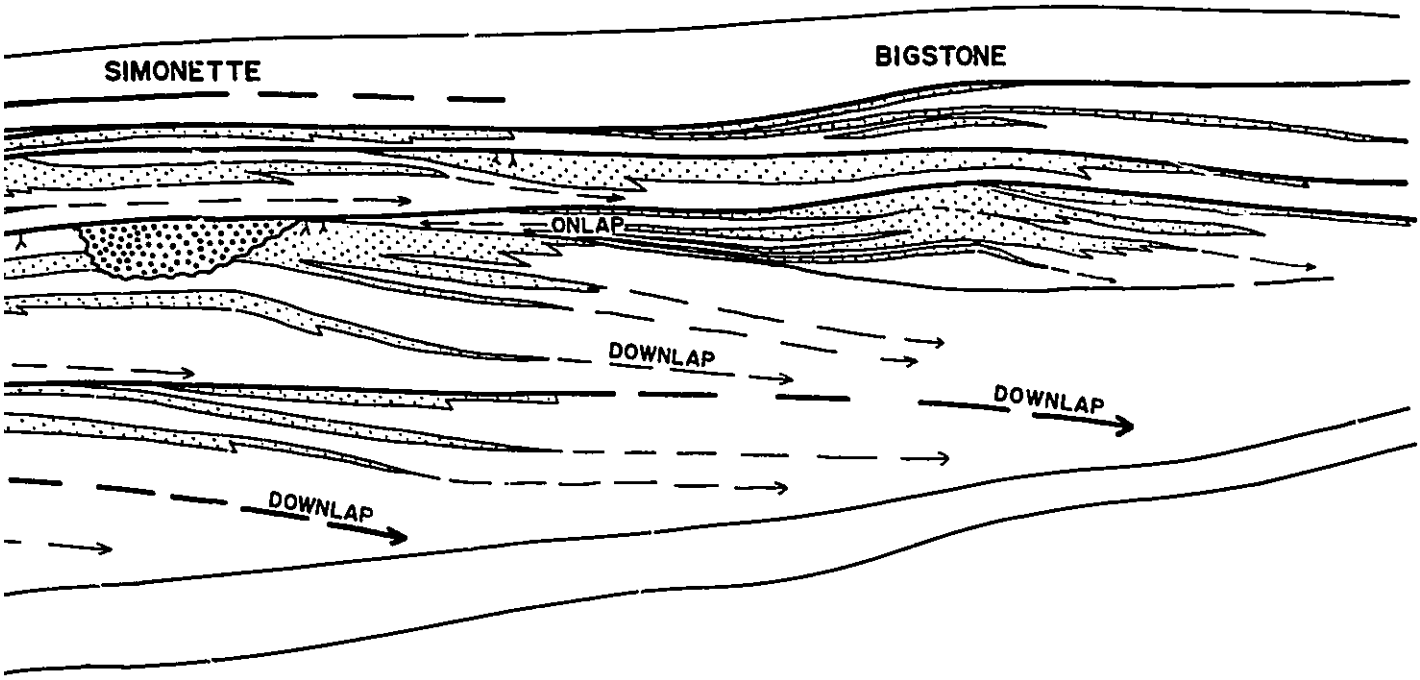

TOTAL WIDTH ≃ 170 km ⟶

ACE

ACE

Members D and E have been studied in detail and will therefore comprise the bulk of descriptions, interpretations and discussions presented in this thesis. In general (Fig.3-8C, 3-9B) they display a relatively tabular, pod-shaped geometry. Non-marine facies, containing *in situ* root traces and including carbonaceous shales and other coastal plain facies associations (e.g. Facies Association 3) become more predominant to the northwest. The shale, which comprises the basal portion of member D, thins toward the northwest. Differentiation of members D and E may therefore be difficult outside the thesis area. In turn, correlation of any of these informal members may also be difficult outside of the thesis area, especially to the west and northwest where the Dunvegan Formation becomes more non-marine in character and in which T-surfaces may be more difficult to recognize and correlate. The farthest southeasterly (basinward) position of thick sandstone was observed in Member E in the Bigstone area, as shown in figure 9-3B.

3-3-2. Shingles

Shingles are defined as regionally impersistent, lens-shaped sedimentary units arranged in an *en-echelon* pattern within the same member. Lateral overlap may also occur along strike. Typically, a shingle will comprise a single coarsening upward facies succession (Facies Association 1) usually culminating in a shallow marine sandstone or non-marine facies. Shingles, as defined in this study, are descriptively similar to parasequences of Van

Wagoner (1988). Shingles may be separated from each other in a seaward direction (southeast) by T-surfaces and by Em or Ec surfaces in a landward direction (northwest). They may be overlain by impersistent shales, mudstones and bioturbated facies of various environmental affinity (marine or non-marine) or they may erode into each other in an updip direction. In a southeasterly direction (i.e. seaward), shingles dip toward underlying transgressive surfaces as the sandy portion shales out, suggesting downlap. Erosional surfaces to the northwest are usually associated with channels (Ec surfaces) but usually become conformable with underlying units towards the southeast (basinward). Upper surfaces of successive shingles, within the same member, merge in a northwesterly direction and terminate updip against the overlying member-bounding T-surface producing a toplap surface. The contact with overlying thick marine shales defines this toplap surface. In some cases, significant erosion may be associated with these transgressive surfaces producing a truncational rather than toplapping surface as seen at the top of member F in figure 3-8C. In some cases it may be difficult to distinguish erosional truncation from toplap.

Erosional truncation associated with transgression should produce an Em surface (see section 3-2-1). If erosion were due to subaerial exposure, fluvial downcutting should be expected.

It was not always possible to distinguish shingles over a large enough area to be able to map them separately, especially

where the stratigraphic relationships are complex such as in member G. It was also sometimes difficult to distinguish multiple sandstones within shingles (such as in member E and C) from shingles. Shingles are therefore largely defined on the basis of the ease with which they can be recognized and correlated. Shingles are therefore less rigorously defined than members within this study.

Two regional cross sections will be discussed below in order to illustrate the various aspects of this allostratigraphic scheme. The main purpose of the following discussions is to establish the degree to which members can be correlated and subdivided and to preview some of the themes of the later chapters dealing with individual members. I will return to a more detailed discussion and interpretation of Dunvegan allostratigraphy in chapter 12.

3-3-3. Dip Oriented Well Log Cross Section

The major regional northwest-southeast cross section illustrates some of the stratigraphic relationships within the Dunvegan Formation (Fig.3-9A and B) . Figure 3-9B was produced by tracing the correlation lines and lithologies interpreted in figure 3-9A but without the actual well log traces. The heavy black horizontal lines (Figs. 3-9A and B) represent T-surfaces which separate the seven members designated with letters A to G at the left hand side of figures 3-9 A and B. The vertical black

lines in figure 3-9A indicate cored intervals. The cross section is hung on the base of the Second White Specks.

Overall the Dunvegan Formation has a pronounced wedge-shaped cross sectional geometry. It comprises a series of stacked sandy units which, in general, dip and thin towards the southeast. The base of the Dunvegan is highly diachronous and sandstones are seen to shale out to the southeast into the Shaftesbury Formation. The member bounding transgressive surfaces (T-surfaces) at the top of members F and G, as well as sandstones within member G, dip in a southeast direction toward the FSU marker. Shingles within overlying members also downlap onto underlying T-surfaces. This is clearly seen in sandstones at the base of member E which dip towards the transgressive surface at the top of member F (Fig.3-9B). Other shingles are especially prominent in members D and F and also dip towards underlying transgressive surfaces.

Ec surfaces (channelized erosion surfaces) have been recognized in members A, C, D, and E. Two are traversed by this cross section in the Simonette and Lator areas (Fig.3-9B). The most prominent Ec surface cuts into member E while a less obvious Ec surface lies in member A. The Ec surface in member E lies in the Simonette area (well 14-6-63-26W5) at the top of the member. This surface has been correlated towards the southeast where its correlative conformity underlies a sedimentary wedge which reaches a maximum thickness (about 20m) in the Bigstone area. The unit bounded above by the T-surface at the top of member E and below by

this Ec surface and its correlative conformable surface underlying the Bigstone wedge (marked by a medium black line), represents the last shingle in member E. Sandstones within the Bigstone wedge onlap the lower surface towards the northwest (Fig.3-9B).

Possible toplap, towards the northwest, occurs at the upper boundaries of members D, E, F and G. Shingles within these members terminate upwards against overlying T-surfaces (Fig.3-9B). It is not clear from this cross section whether this termination is due to erosional truncation or non-deposition. The character of upper surfaces will be discussed more fully when individual members are described.

Members A, B, and G are restricted to the northwestern half of the cross section and are wedge-shaped. They are thickest in the northwest and thin towards the southeast. Members C, D, E, and F are pod-shaped and are present over the entire length of the cross section. More detailed descriptions and discussions of the internal stratigraphy of specific members will be saved for the succeeding relevant chapters and will be summarized in chapter 12.

3-3-4. Strike Oriented Well Log Cross Section

Figure 3-8C represents a schematic interpretation of the major strike-oriented well log cross section previously discussed. The interpreted correlation lines from figure 3-8B have been traced onto figure 3-8C minus the well log traces. The Fish Scales and FSU markers appear to be domed upwards in the middle of the cross section (this may be an artefact of the datum).

Sandstones towards the northeast, within member G, are seen to dip towards this "dome". Member F shows rather anomalous thickness changes, thickening towards the southwest and northeast. Upper shingles within member F are clearly truncated in the centre-right of the cross section where they are overlain by marine shales of member E. Stratigraphic relationships within member E are complex and indicate several overlapping shingles and at least two major channels. The northeast channel occurs at the top of member E while the southwest channel occurs about 10 meters below the top. The rest of the members are relatively uniform in thickness over the cross section. Member D shows a slight thickening towards the northeast. Interpretation and discussion of these relationships will be presented in chapters 4 to 10.

3-4. Duration and Timing of deposition of Members and Shingles

It is now possible to make a simplistic analysis in order to determine the time scales involved in deposition of members and shingles. Based on the available biostratigraphic and chronostratigraphic information, as outlined in chapter 1 and shown in figure 1-6, the Dunvegan is interpreted as being deposited over a time period of between 1 and 2 million years. Dividing these times by the total number of members (seven) suggests that each member was deposited in an average time period of between about 143,000 to 286,000 years. There are a total of

19 shingles which suggests that shingles may represent deposition in a time period of between 53,000 to 105,000 years.

It has been stressed in this chapter that member-bounding discontinuities (T-surfaces) are regionally widespread and can be correlated over hundreds of kilometers. This indicates that these discontinuities are regional in nature and in turn suggests that they are controlled by processes on a regional scale.

Shingles, in contrast, are regionally impersistent and may be produced by more localized processes. This point will be returned to and discussed fully in chapter 12.

3-5. Preliminary Discussion and Summary of the Allostratigraphy of the Dunvegan Formation

3-5-1. Discussion

The Dunvegan Formation comprises a thick wedge of stacked sandstones and mudstones which thins to the southeast (Fig.3-9B). The Dunvegan Formation has been formally defined as a lithostratigraphic unit which conformably overlies the Shaftesbury Formation and which is conformably overlain by shales of the Kaskapau Formation (Alberta Society of Petroleum Geologists, 1960 p.105). As a lithostratigraphic unit, the base of the Dunvegan Formation is highly diachronous produced as sandstones dip and thin towards the southeast as seen in figure 3-9B. There is no single physically continuous surface that separates the Dunvegan Formation from the Shaftesbury Formation. In the allostratigraphic sense, however, sandstones of the Dunvegan Formation do not

actually overlie shales within the upper portion of the Shaftesbury Formation. Rather, shales of the Shaftesbury Formation are seen to be the lateral seaward equivalent of Dunvegan sandstones to the northwest (Fig.3-9A,B). The Shaftesbury and Dunvegan Formations, at least the portion above the FSU marker, are therefore genetically related in time and can be thought of as different facies related to the same event(s).

The top of the Dunvegan Formation is defined in this study on the basis of a regionally persistent T-surface at the top of member A, which is interpreted as a time line. The shales of most of the overlying Kaskapau Formation are therefore genetically unrelated to the sandstones of the underlying Dunvegan Formation. In the Bigstone area, member A was difficult to distinguish from the Kaskapau Formation indicating that the top of the Dunvegan is also diachronous although to a lesser degree than the base. Previous workers have described the Dunvegan as interfingering with shales of the Kaskapau (ASPG, 1960 p.187), although these relations were described mostly from outcrop studies. Plint et al. (1988) have pointed out the problems in mixing lithostratigraphically defined units (e.g. Dunvegan Formation) with allostratigraphically defined units (e.g. members A to G).

It is hoped that the reader will clearly understand what type of units are being referred to in this thesis. The allomembers defined above, cross formational boundaries and can not be strictly defined solely as members of the Dunvegan

Formation. Rather, they represent allomembers of both the Dunvegan and portions of the Shaftesbury and Kaskapau Formations.

3-5-2. Summary

Within sediments of the Dunvegan Formation, seven regionally persistent transgressive flooding surfaces (T-surfaces), each overlain by several meters of marine mudstones and shales, were correlated over distances of hundreds of kilometers. The Dunvegan Formation has been sub-divided into seven informal members (allomembers) on the basis of the recognition and correlation of these seven widespread T-surfaces. These members are designated A, B, C, D, E, F, and G from top to bottom. Each member consists of one or more overlapping lens-shaped shingled sand bodies. The sand body and its associated shales are termed shingles. Successive shingles within the same member show progressive offlap towards the southeast and downlap onto underlying, member-bounding T-surfaces. Some shingles erode into underlying shingles towards the northwest. This type of erosion is usually associated with fluvial downcutting associated with channels (Ec surface).

Each member is interpreted to represent the relatively gradual regression of sandy shallow marine environments. These regressive episodes may sometimes involve subaerial erosion. Each member is punctuated by a relatively rapid and widespread transgression which produces a member bounding discontinuity (T-surface). Em surfaces (due to marine erosion) may occur where these transgressions are associated with some erosion, especially

in an updip (northwest) direction. The broad implications of this stratigraphic framework will be dealt with in later chapters, especially regarding the application of sequence stratigraphic concepts and models. The following 7 chapters (4-10) will treat each of these seven members in varying detail.

CHAPTER 4: MEMBER E

4-1. Introduction

This chapter has been organized into six parts beginning with this brief introduction (section 4-1). The second section (4-2) highlights the salient descriptive and interpretational aspects of member E, and includes a geological history. The third, fourth, and fifth parts (sections 4-3,4-4, and 4-5) present detailed descriptions of all of the aspects of member E and include preliminary interpretation where appropriate. Readers who do not wish to delve into the details of member E may skip sections 4-3, 4-4, and 4-5. The sixth and final section (4-6) presents detailed interpretations of each shingle within member E.

The third, fourth, fifth and sixth parts of this chapter may be treated as an appendix of detailed information and interpretations regarding member E. If any aspect of member E particularly intrigues the reader or if the reader is unclear as to any aspect of the interpretation presented in the first two sections, he or she may wish to probe further by reading the relevant aspects in the more lengthy descriptive portions of this chapter.

4-2. General Description and Interpretation

4-2-1. Thickness, Extent and Stratigraphy

A total isopach map of member E (Fig.4-1) shows that it is roughly pod-shaped. It extends over the entire thesis area, and ranges in thickness from about 20m, in the far southeast of the map area, to a maximum of about 65 meters east of the middle of the map area. Stratigraphic relationships between shingles within member E are complex and are illustrated in figure 4-2. This regional dip cross section is a schematic representation of the stratigraphy presented on the major regional dip-oriented cross section through the Dunvegan shown in chapter 3 (Fig.3-9A). Figure 4-2 shows four shingled sedimentary units labelled E1 to E4 which offlap from northwest to southeast. The lower three shingles downlap onto the T-surface at the top of member F, and their upper surfaces terminate up-dip against the T-surface at the top of member E producing a toplap surface. Some of this toplap may be due to erosional truncation of the upper shingles towards the northwest. Non-marine facies in the upper part of member E thicken toward the northwest.

A major erosion surface at the top of member E, associated with the Simonette channel (shingle E1), truncates portions of shingles E2 and E3 in well 14-6-63-26W5 (Fig.4-2). This Ec surface is correlated with the top of E2 where it dips towards the southeast. Sandstones of shingle E1, in the Bigstone area, onlap this surface towards the northwest (i.e. landward). Major

channelized sand bodies also occur in shingle E3 as shown between wells 10-34 and 7-7 on figure 4-2 forming another Ec surface.

Member E is sharply overlain by widespread marine shales and blockstones comprising the base of the overlying member D. This contact is usually marked by a thin, sharply-based sandy bioturbated horizon, although in a few places (e.g. Fig.4-14B, well 13-28) this horizon reaches a few meters in thickness.

4-2-2. Sand Body Geometries and Facies

Mapping of sandstones within member E reveals a series of stacked and overlapping, lobate to highly digitate sand bodies in each of the four shingles (Figs. 4-3A,B, 4-4A,B, 4-5A,B and 4-6A,B). These sand bodies are outlined and collectively shown together in figure 4-16. This figure indicates that there is a relatively small degree of overlap, especially between shingles E1 and E2 and particularly between the more lobate portions of the sand bodies. In shingles E1, E2 and E3 (Figs. 4-3A, 4-4A, and 4-5A respectively) these lobate sand bodies narrow towards the northwest in an updip direction, producing a prominent bottleneck. This bottleneck usually culminates in a prominent narrow linear "shoestring" sand. Cores through the lobate portions of these sand bodies show coarsening upwards facies successions. In the upper shingles (E1 and E2) these facies successions coarsen upward and are typical of Facies Association 1B (Fig.4-7A, Fig.2-24). Facies successions through lobes in shingles E3 and E4 are more similar to Facies Association 1C (Fig.4-8, Fig.2-25). Shoestring

Figure 4-1. Total isopach map of member E. See text for discussion. Data points indicated with dots, isopach values in meters.

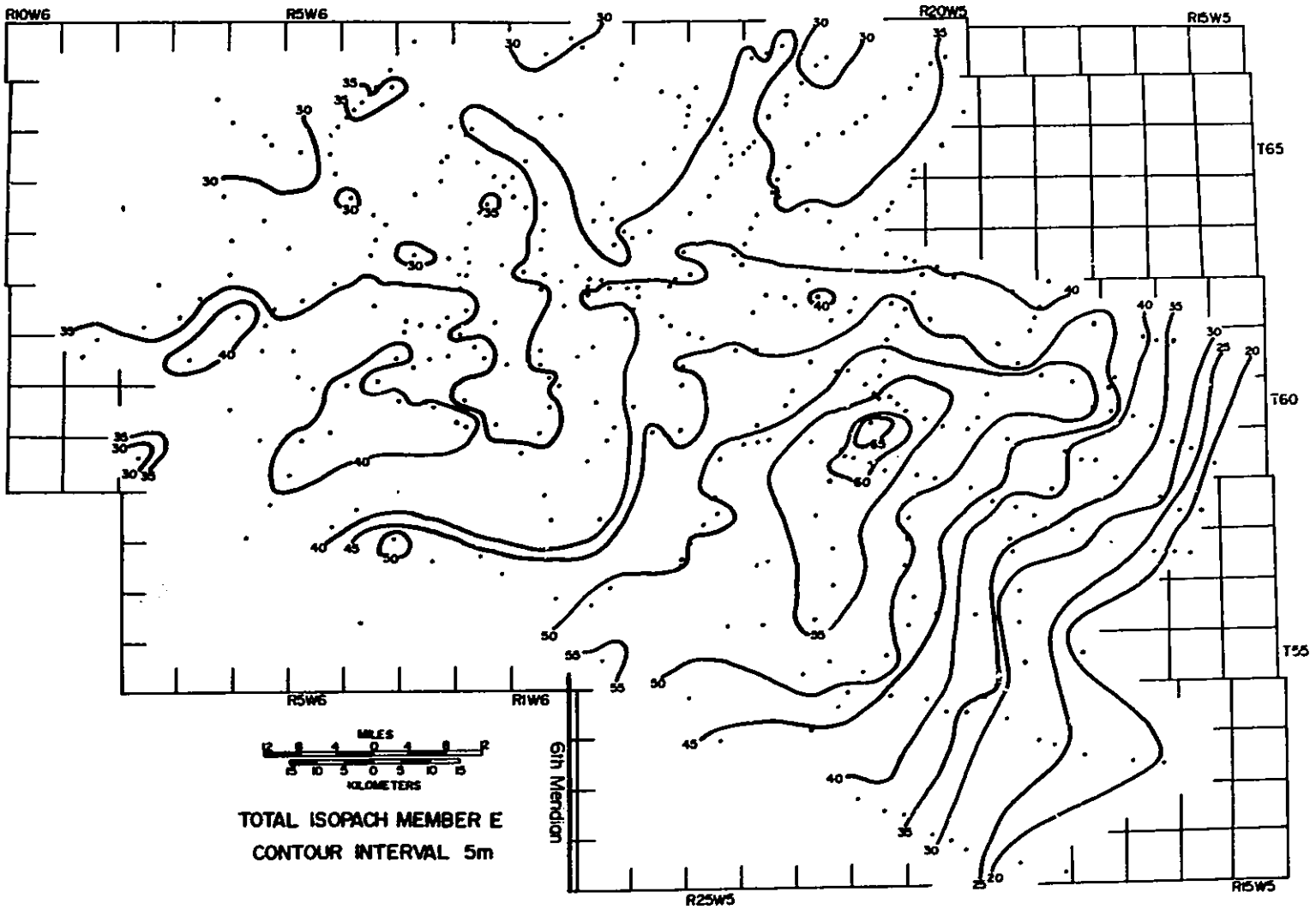
R10W6
R5W6
R20W5
R15W5
T65
T60
T55
R5W6
R1W6
R25W5
R15W5
6th Meridian
MILES
KILOMETERS
TOTAL ISOPACH MEMBER E
CONTOUR INTERVAL 5m

Figure 4-2. Regional schematic dip oriented cross section through member E based on the regional dip cross section (Fig.3-9A). Sandstones are stippled. Root symbols indicate non-marine facies. Shingles E4, E3, and E2 downlap onto lower T-surface towards the southeast. Shingle E1 onlaps the upper surface of shingle E2 to the northwest. Channels in shingles E1 and E3 erode into underlying shingles. See text for further explanation.

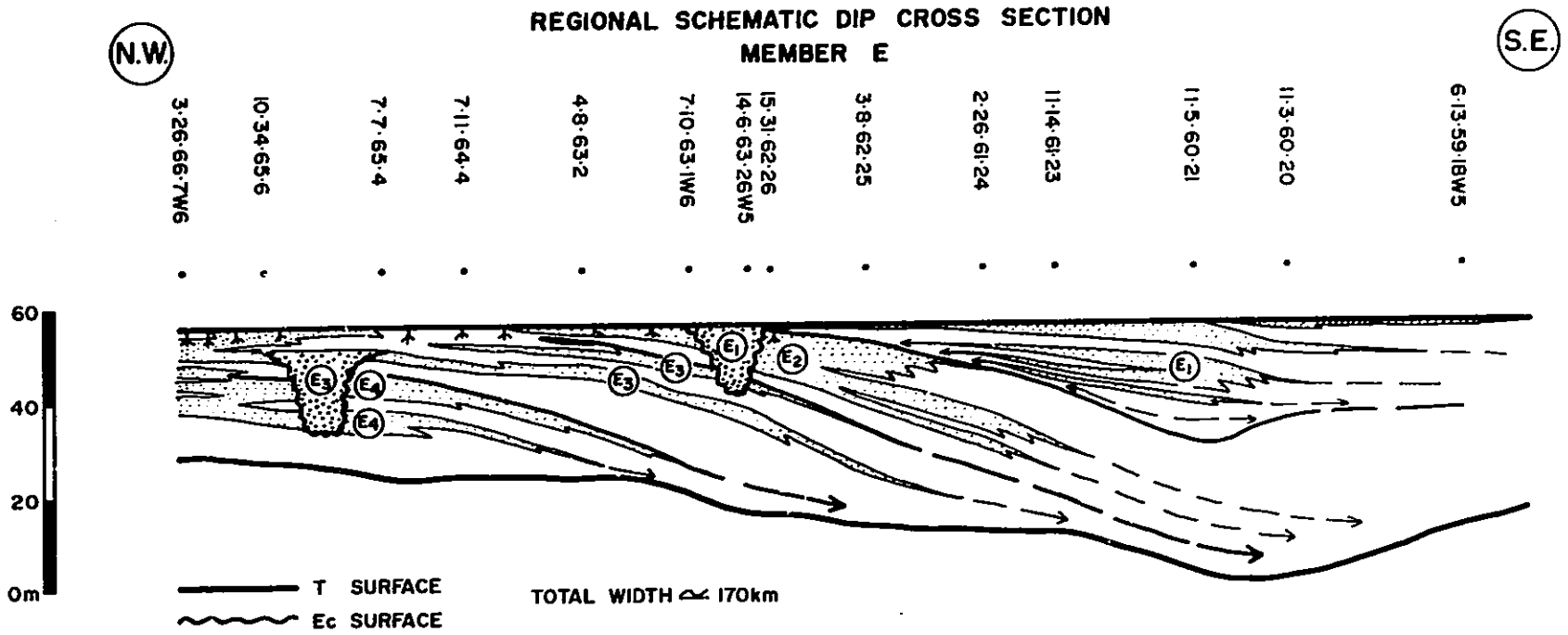
REGIONAL SCHEMATIC DIP CROSS SECTION
MEMBER E
N.W.
S.E.
3-26-66-7W6
10-34-65-6
7-7-65-4
7-11-64-4
4-8-63-2
7-10-63-1W6
15-31-62-26
14-6-63-26W5
3-8-62-25
2-26-61-24
11-14-61-23
11-5-60-21
11-3-60-20
6-13-59-18W5
60
40
20
0m
E1
E2
E3
E4
T SURFACE
Ec SURFACE
TOTAL WIDTH ≃ 170km

sandstones are characterized by fining-upwards facies successionstypical of Facies Association 2A (Fig.4-9A, Fig.2-26). Brief descriptions of each shingle follow.

Shingle E4

A map of sandstones within shingle E4 (Fig.4-6A and B) indicates two distinct sandy lobes confined to the northwestern half of the map area and reaching 12 meters in thickness. Each sandstone becomes narrower toward the north and northwest, although shoestring sandstones were not detected. Core cross sections through the distal portion of shingle E4 (Fig.4-14B and 3-8A) indicate coarsening upwards facies successions, similar to Facies Association 1A. Core through the thicker sandy portions of shingle E4, toward the northwest, indicate type 1A and 1C Facies Associations (Fig.4-8, Fig.9-5A). In places, sandstones at the top of shingle E4 are overlain by a thin bioturbated sandy horizon followed by marine blockstones containing *Inoceramus* (e.g. Fig.4-14B, wells 3-9 and 6-11, also shown in core photos, box 3, interval 3.6-8.2m, Fig 3-7C). Elsewhere, shingle E4 is erosively truncated by channelized sandstones associated with shingle E3 (e.g.Fig.3-8B, wells 3-6 and 12-22 and Fig.3-8A, well 12-22 at 31m).

Shingle E3

A map of sandstones within shingle E3 (Fig.4-5A) indicates several finger-like, lobate sand bodies which narrow towards the northwest into two major shoestring sand bodies. These are

outlined in figure 4-5B. The bottleneck in the more southerly sand body is associated with a prominent shoestring sand up to 20 meters in thickness and having a maximum width of about 5 kilometers. The maximum sandstone thickness in the lobes is about 9 meters. A core cross section, oriented obliquely through the northern edge of the southern lobe (Fig.4-14 A and B), shows the sedimentary facies within the lobe and in the inter-lobe areas. On the core cross-section (Fig.4-14B), shingle E3 shows a transition from dominantly marine facies to non-marine facies. This transition occurs both upwards and towards the northwest. Northwest of well 2-6-62-2W6, in the inter-lobe area, the facies successions indicate a shallowing upwards typical of Facies Association 3. Well developed coarsening and fining upward facies successions are not developed. In each of wells 7-7, 8-8, 3-9, and 6-11, the succession begins with several meters of laminated marine blockstones (Facies 2), containing *Inoceramus*. These blockstones pass upwards into laminated sideritic pinstriped mudstones (Facies 4) cut by thin channelized sandstones. In wells 7-7, 8-8, and 3-9 the facies succession passes upward into rooted coaly horizons (Facies 10) associated with carbonaceous mudstones and shales (Facies 1C) containing oysters and *Brachydontes* sp. Another example of this facies association in core is shown in figure 3-8A, well 4-11. In figure 4-14B, well developed coarsening upwards facies successions, typical of Facies Association 1C, occur towards the southeast (basinward).

A cross section through the sandy shoestring sandstone in the south (Fig.3-8A and B) indicates the presence of a thick channelized sand body in well 3-6-61-4W6 (3-8B). Core through this sand body (well 12-22-60-5W6 in Fig.3-8A) shows the development of a coarse, basal lag followed by a well developed fining upwards facies succession, typical of Facies Association 2A. In places, the contact between shingles E2 and E3 is conformable, with marine blockstones sharply overlying HCS sandstones (e.g. Fig. 4-14B, well 6-22-61-2W6, 7.0m). In other wells, the contact is erosively cut into by channelized sandstones associated with upper shingles (e.g. Fig.4-14B, well 11-15).

Shingle E2

Mapping of sandstones in shingle E2 indicates at least three overlapping lobate sand bodies, including the Simonette lobe (Fig.4-4A and B). These lobes show highly irregular digitate seaward margins comprising several sub-lobes. Sand body #2, in the middle of the map area, narrows towards the northwest producing a bottleneck. This bottleneck coincides with the position of the Simonette channel shown with the dashed lines (Fig.4-4B). A similar shoestring sandstone is associated with lobate sand bodies in the south.

A well log cross section through the Simonette lobe (Fig.4-13A) indicates that it is made up of several offlapping sand bodies separated by thin shaly interbeds. These sandstones thin towards the southeast and are overlain by the E1 erosion surface.

The accompanying core cross section (Fig.4-13B) shows well developed irregular coarsening upwards facies successions typical of Facies Association 1B. A typical core example of this Facies Association is shown in figure 4-7A and B. These associations are characterized by laminated marine mudstones (Facies 1A, 2 and 4) at the base which coarsen upwards into convolute laminated siltstones and sandstones (Facies 6). These grade upwards into current rippled to cross-bedded sandstones (Facies 7C to 7D). Wave and storm produced structures, such as wave ripples and HCS are uncommon. The cross bedded sandstones at the top of the main coarsening upward succession in well 15-31 (Fig.4-7A and 4-7B, 4-13B) contain *in situ* root traces and are overlain by a coaly mudstone (Facies 1C). In places (e.g. well 15-31, Fig.4-13B), these carbonaceous mudstones at the top of shingle E2 are overlain by a thin sandy bioturbated horizon which is sharply followed by marine shales or blockstones (Facies 1 or Facies 2) of member D, while elsewhere (well 11-15, Fig.4-14A,B and Fig.4-12) channelized sandstones of shingle E1 erode into shingle E2.

A core cross section perpendicular to the northern (Simonette) channel also includes core through the inter-lobe areas of the Simonette lobe (wells 14-35 and 6-35, Fig.4-12B). Although shingle E2 in well 6-36 exhibits a shallowing upwards facies succession, similar to Facies Association 3, neither well contains thick sandstones.

Shingle E1

Two major sand bodies lie within shingle E1 (Fig. 4-3A and B). These include a large lobate sand body in the southeastern half of the map area and a major shoestring sandstone, which extends to the northwest. The seaward margin of the southeastern sand body (Bigstone Lobe, Fig.4-3B) is highly irregular and comprises several birdfoot-shaped sub-lobes including producing sandstones in the Bigstone pool. The shoestring sand (Simonette channel, Fig.4-3B) includes producing sandstones in the Simonette area. It has an average width of about 4 kilometers and reaches 17 meters in thickness.

A well log cross-section, oriented approximately along depositional strike, through the Bigstone Lobe (Fig.4-11A) shows that the lobe occupies a shallow valley-shaped depression defined by the top of shingle E2. Shingle E1 comprises several overlapping sand bodies, separated by thin mudstone interbeds, which onlap onto the sides of this "valley" (Fig.4-11A). In a dip oriented cross section (Fig.4-10A) these sandstones are seen to dip towards the top of shingle E2 towards the southeast. They onlap shingle E2 in a landward direction toward the northwest (Fig. 4-2). Accompanying core cross sections (Figs. 4-10B and 4-11B) show well developed coarsening upwards facies successions typical of Facies Association 1B. In a few places (e.g. well 14-16-60-21W5, Fig. 4-10B) vaguely laminated possible HCS sandstones are present.

A strike oriented well log cross section through the Simonette area (Fig.4-12A) shows the Simonette channel (E1). The accompanying core cross section (Fig.4-12B) shows well developed, fining-upwards type 2A Facies Associations through the channelized sandstone in wells 7-6-63-26W5 and 11-5-63-26W5. A typical core through the Simonette channel is illustrated in figure 4-9A and B. In the box photos (Fig.4-9B) note the razor sharp basal contact of the channel (E1), the thick cross-bedded to massive sandstones upward, which are highlighted with black marker, and the occasional *Asterosoma* burrows in the upper half of the channel. The channel is sharply overlain by laminated marine mudstones (Facies 1A) which comprise the base of member D.

4-2-3. General Interpretation and Discussion of Deltaic Depositional Systems in Member E

Mapping of sandstones within member E indicates a series of lobate sand bodies, each of which has a highly irregular seaward margin. Most of these sand bodies narrow towards the northwest (updip) and many are associated with prominent shoestring sand bodies. Cores through the lobes indicate facies successions typical of prograding, river-dominated, emergent shorelines (Facies Association 1B), while cores through the shoestring sandstones show well developed fining upwards facies successions typical of sandy channel fills (Facies Association 2A). The geology therefore indicates irregular prograding lobate shorelines associated with major shoestring channel sands which apparently

feed these shorelines. By definition (Elliot, 1986), these depositional systems are therefore deltaic. Deltas in member E are mostly river-dominated. This is indicated by several lines of evidence. The highly lobate to digitate shape of the sand bodies indicates that basinal processes were insufficient to significantly re-distribute delta front sands. In addition, the sand body geometries are similar to other ancient and modern river-dominated deltas (e.g. Coleman and Wright,1975). The facies also indicate a predominance of fluvial processes. Burrowing of shelf mudstones (i.e. prodelta facies) is relatively minimal in most of the shingles. HCS and wave-rippled sandstones are relatively uncommon, suggesting that storms and waves did not significantly affect sediments in member E. Sandstones are characterized by sedimentary structures typical of unidirectional flows, including current-ripples and cross-bedding. The abundance of soft sediment deformation features (mostly load casts) and climbing current-ripples, especially in the sandy lobes, indicates high sedimentation rates probably produced by high fluvial discharge.

A more detailed discussion of depositional systems in the Dunvegan Formation, including comparison with modern and ancient examples, will be saved until chapter 11. Next I will outline the geological history of member E.

4-2-4. Geological History of Member E

Member E consists of a series of at least four shingled shallow marine, composite sand bodies which progressively offlap from northwest to southeast into the basin (Fig.4-2). These sand bodies consist mostly of highly river-dominated deltaic lobes which are fed by northwest trending distributary channels as shown in the schematic paleogeographic reconstructions in figure 4-15. The paleogeographic position of each succeeding lobe is strongly controlled by the position of underlying, older lobes as indicated in figure 4-16. Younger lobes tend to occupy the inter-lobe areas of older deltas. Member E is sharply overlain by a widespread, transgressive marine shale which comprises the base of the next overlying member D. Member E therefore represents an overall regression of environments punctuated by a widespread transgression.

The following is a point by point summary of the depositional history of member E. This geological history is also illustrated in figure 4-15.

1. Deposition of member E began with the progradation of sandstones and shales of shingle E4 into the northwestern half of the map area towards the southeast (Fig.4-15a). The sandstone geometries (Fig.4-6A and B) indicate fairly irregular shorelines to the southeast and suggest progradation of two sandy delta lobes. Coarsening upwards facies successions through these shoreline deposits reflect a relatively high degree of reworking

by basinal processes (mostly HCS sandstone) and suggest that these shorelines were influenced by storm waves.

2. As the locus of deposition changed, portions of the E4 deltas were transgressed and a bioturbated "abandonment" facies was produced. Shingle E4 was followed by the progradation of shingle E3 (Fig.4-15b). Shingle E3 comprises two overlapping river-dominated deltas, forming two elongate birdfoot-shaped sandy lobes (Fig.4-5A,B). These lobes were fed by major distributary channels which cut into shingle E4 producing a local Ec surface (Fig.3-8A and B). These channels are filled with fining-upward facies successions, typical of Facies Association 2A, and comprising non-marine sandstone and shale (Fig.3-8A, well 12-33). These sandy distributary channel fills map out as extensive linear shoestring sand bodies. Between these channels lie extensive interdistributary bays. Facies successions through these bay fills (Facies Association 3) indicate a gradual shallowing upwards. These facies successions begin with open marine blockstones and culminate in the deposits of rooted crevasse splay and wave-washed levee environments. Thick shoreface sandstones are not present. Associated delta plain environments towards the west are similar and are characterized by swampy muddy salt marshes containing oyster beds and *Brachydontes* sp.

3. The next phase of sedimentation involved another basinward shift in the locus of deposition as sediments of shingle E2 prograded over shingle E3 (Fig.4-15c). Locally, portions of

shingle E3 were transgressed and an abandonment facies, comprising bioturbated marine mudstones (Facies 3A), was deposited. Gross sandstone isolith maps (Fig.4-3A) indicate that shingle E2 comprises a series of at least three, discrete to partly overlapping, river-dominated, sandy deltaic lobes exhibiting highly irregular basinward margins, and fed by major distributary channels to the northwest. These sandy lobes are composite in nature and comprise several overlapping sand bodies (sub-deltas, Fig.4-4A).

Facies successions through these lobes (Fig.4-7A,B, and 4-13A,B) are typical of river-dominated prograding sandy shorelines, and exhibit very little influence of basinal processes. Inter-lobe areas show an overall shallowing upwards but do not contain thick shoreface or delta front sands (Fig.4-12B and 4-14B).

4. Shingle E2 culminates in a widespread erosional event accompanied by subaerial exposure and erosion in the northwest. This erosion is associated with channels and produces an Ec surface. Locally, especially in the Simonette area, a channel, up to 4 kilometers wide, erodes up to 18 meters into the underlying shingles E3 and E2 (Fig.4-12A,B). The Simonette channel is interpreted as re-occupying the former position of the older channels which fed the E2 deltas. Erosion at the end of E2 culminates in a major basinward shift in the position of Dunvegan shorelines with the deposition of the Bigstone deltaic complex (Figs.4-15d). It occupies a major valley-shaped depression in the

lower southeastern half of the map area (Fig.4-11A). The Bigstone delta comprises a highly lobate, to digitate sand body (Fig.4-3A), which contains several overlapping sub-deltas. Cross sections through the sand body indicates a composite nature with many shaly interbeds (Fig. 4-10A and 4-11A). Coarsening upwards facies successions through these lobes indicate that Bigstone shorelines were highly river-dominated (Fig.4-10B and 4-11B), although rare HCS sandstone indicate some storm influence. The lack of *in situ* root traces or coaly horizons may suggest that the Bigstone delta was probably not emergent and suggests that it was deposited mostly subaqueously. It is also possible that evidence of emergence may have been removed by marine erosion during subsequent transgression. Sandstones of the Bigstone delta onlap the upper surface of shingle E2 in a landward direction. Towards the end of deposition of member E, the Simonette channel was gradually back-filled with sandstone, although it never became demonstrably estuarine.

5. Locally, the initial phases of transgression, at the end of member E, produce a marine erosion surface (Em Surface, Fig.4-14B) which cuts into shingles E1 and E2 in the northwest. This transgression culminates in the deposition of widespread marine shales and blockstones which comprise the base of the overlying member D and which produces a T-surface which defines the top of member E.

The next three sections, 4-3, 4-4, and 4-5, present the full details of the sand body geometries, facies successions, and interpretations of member E and its component shingles. Some of the readers may wish to skip this rather lengthy middle section and go directly to the final interpretations presented in section 4-6.

4-3. Gross Sandstone Isolith Maps

4-3-1. Shingle E1

Figure 4-3A shows a gross sandstone isolith map for sandstones within shingle E1. Two major sand bodies are represented and include a major lobate sand body in the southeastern half of the map area and a major shoestring sandstone which extends towards the northwest. These are schematically outlined in figure 4-3B. The southeasterly sand body includes several areas of thicker sandstone and it has been subdivided into at least two sub-lobes. The most easterly of these sub-lobes has the shape of a cloverleaf. It covers an area of about 1500 square kilometers and reaches a maximum thickness of about 20 meters. The stalk of the cloverleaf, on figure 4-3B, lies at about township 60 range 20W5. A second and more widespread sub-lobe lies to the south. It covers an area of about 2500 square kilometers but reaches only about 8 meters in thickness. It shows

Figure 4-3A. Gross sandstone isolith map, shingle E1. Data points shown with dots. Mapping not extended to the southwest. See text for explanation.

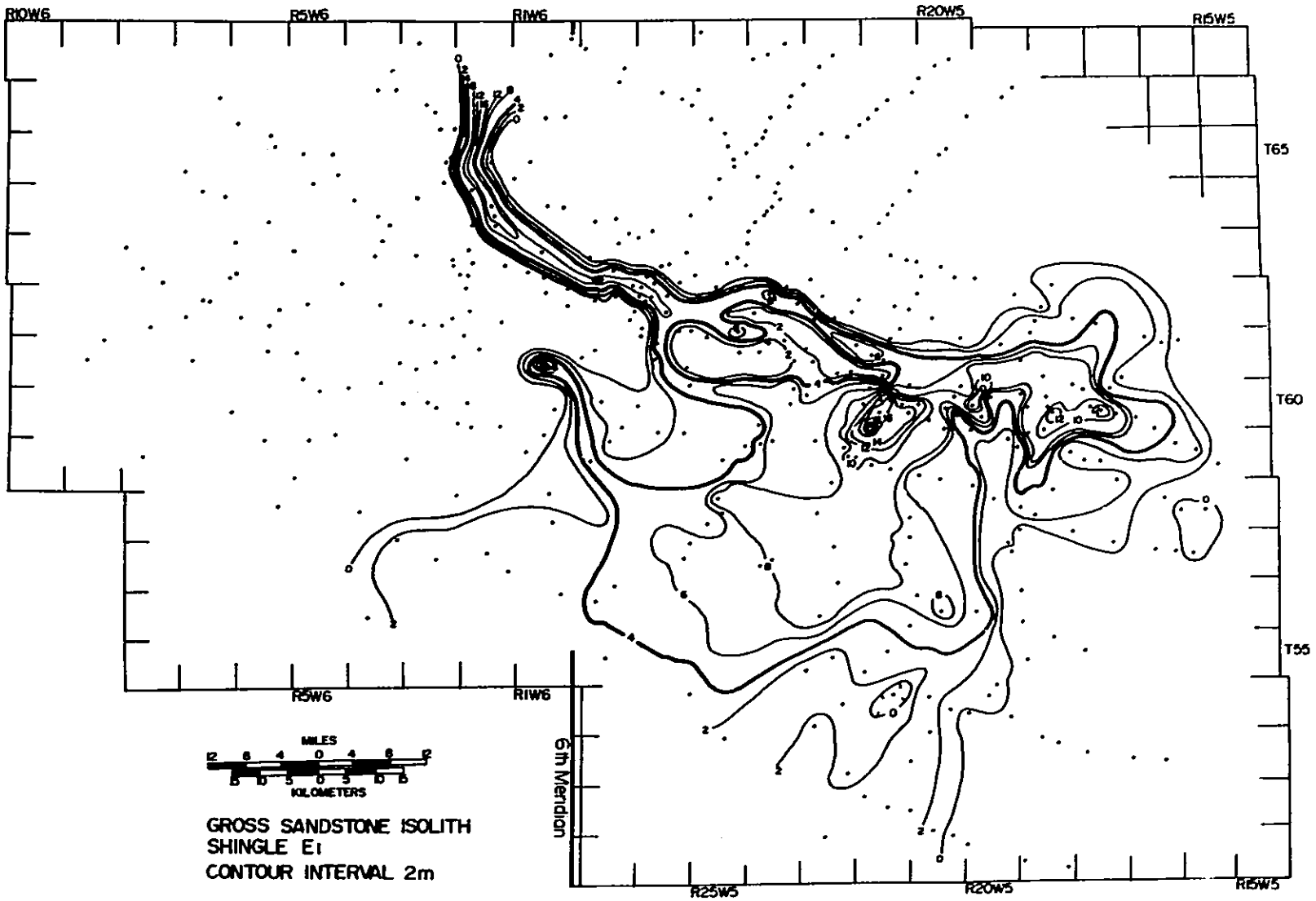
R10W6
R5W6
R1W6
R20W5
R15W5
T65
T60
T55
R5W6
R1W6
6th Meridian
R25W5
R20W5
R15W5
MILES
KILOMETERS
GROSS SANDSTONE ISOLITH
SHINGLE E1
CONTOUR INTERVAL 2m

Figure 4-3B. Outline of sandstone in shingle E1 with locations of cross sections shown and sandstone bodies numbered and named. 0m and 4m contours from figure 4-3A are outlined. Positions of cross sections discussed are designated with the relevant figure number. Open circles represent uncored wells while black dots represent wells on core cross sections. See text for discussion.

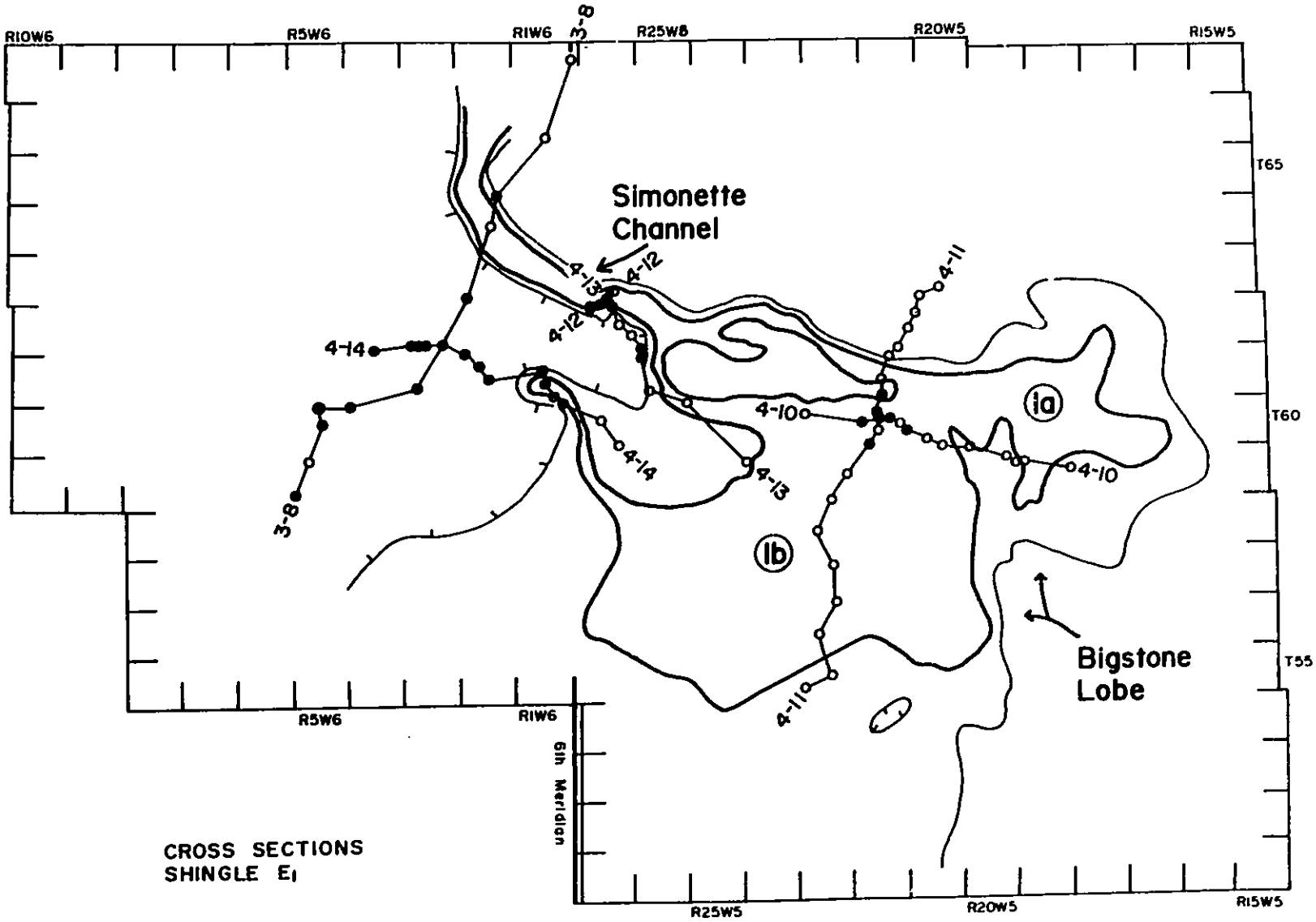

CROSS SECTIONS
SHINGLE E1

a distinct bottleneck towards the northwest and culminates in a thick sandstone at about township 61 range 1W6, which produces a prominent bullseye (Fig.4-3A). This bullseye-shaped sandstonebody was not detected in any other adjacent wells. A third, areally restricted but thick, blob shaped sub-lobe lies within townships 59 and 60, ranges 21W5 to 22W5 between the two other sub-lobes. This sub-lobe includes producing reservoirs within the Bigstone pool (Fig.4-3B).

The seaward margin of the entire southeastern sand body (including all three of its sub-lobes) is highly irregular. It appears to narrow in at least two places towards the northwest. The northernmost bottleneck culminates in a northwest-southeast oriented shoestring sandstone which has been traced updip for at least 50 kilometers and which reaches up to 17 meters in thickness. It includes producing reservoirs in the Simonette area. Isolith values drop rapidly over a distance of about 5 kilometers to 0 meters on the northeastern and southwestern sides of this sand body. Southeast of Township 62 Range 26W5, this sand body trifurcates and feeds the southeastern sand body.

4-3-2. Shingle E2

Figure 4-4A shows a map of sandstones within shingle E2. The eastern (seaward) margin of sandstones within E2 is highly irregular. Shingle E2 comprises at least three distinct lobate sand bodies which are schematically outlined in figure 4-4B. Each of these sandy lobes has a highly irregular, digitate geometry. For reasons which will become apparent later, the position of the E1 shoestring has also been plotted on figure 4-4B.

The northernmost sand body (#1, Fig.4-4B) comprises an irregular, tri-digitate sand body which shows a mild narrowing toward the north and which flares out to the south. It covers an area of about 1700 square kilometers and reaches a maximum thickness of about 6 meters. It thins gradually in a peripheral direction, except towards the far north.

Sand body #2 comprises two distinct sub-lobes. The eastern-most sub-lobe (#2A) covers an area of about 750 square kilometers but does not exceed about 6 meters in thickness. It flares out in a seaward direction (eastward) and narrows towards the west, coinciding with the eastern extension of the Simonette shoestring sandstone. Sub-lobe #2B covers an area of about 2000 square kilometers and is slightly thicker (up to 9 meters) than sand body #2A. The outline of the 4 meter contour indicates that it too flares towards the southeast and narrows towards the northwest where it coincides with the position of the Simonette shoestring.

Figure 4-4A. Gross Sandstone Isolith map, Shingle E2. Data points shown with dots. See text for explanation.

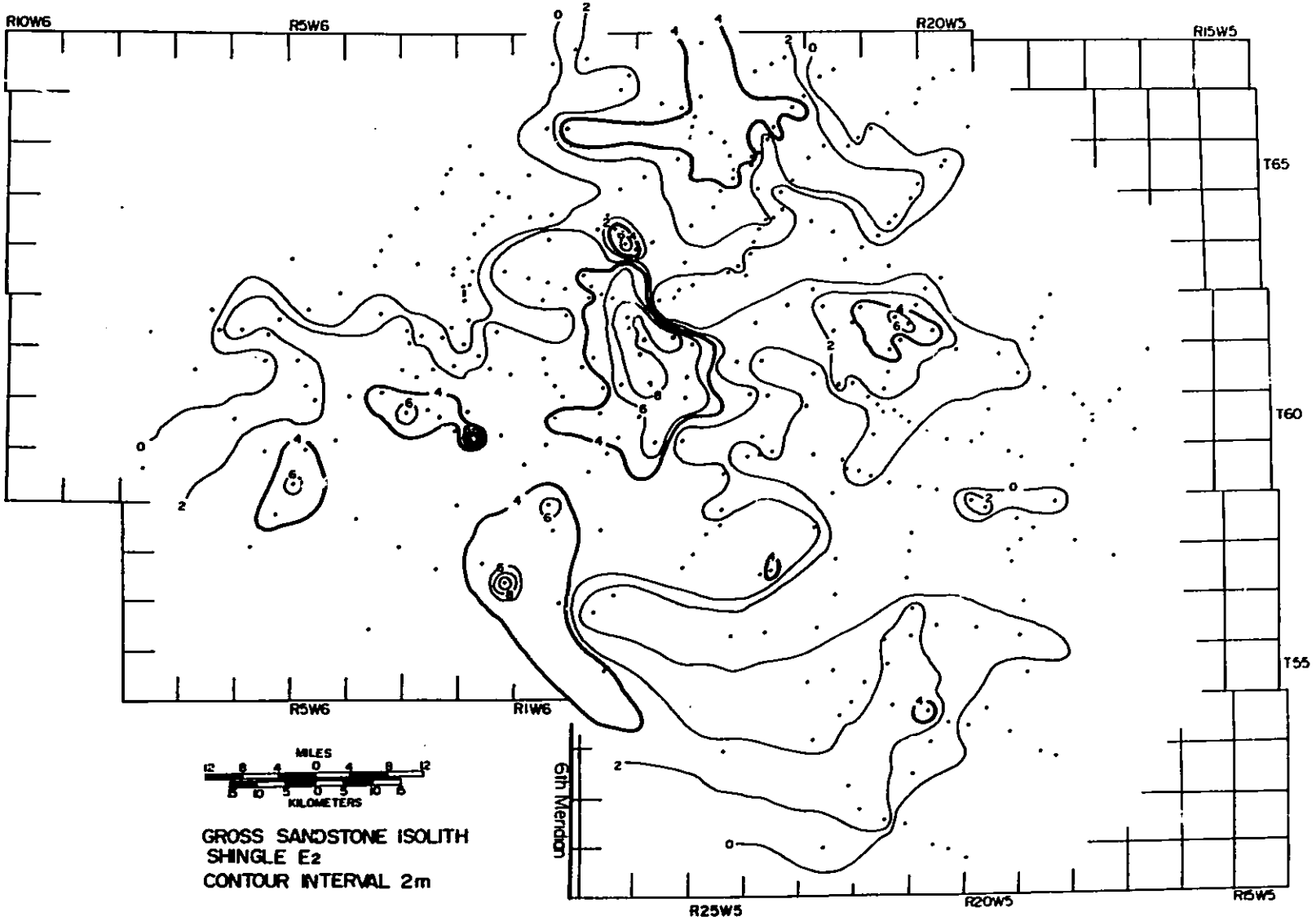
R10W6
R5W6
R20W5
R15W5
T65
T60
T55
R5W6
R1W6
R25W5
R20W5
R15W5
6th Meridian
MILES
KILOMETERS
GROSS SANDSTONE ISOLITH
SHINGLE E2
CONTOUR INTERVAL 2m

Figure 4-4B. Outline of Sand Bodies in shingle E2, based on figure 4-4A with location of pertinent cross sections shown. 0m and 4m contour lines are shown. Dashed lines represent interpreted positions of distributary channels. Open circles represent uncored wells, black circles represent cored wells shown on the core cross sections. See text for discussion.

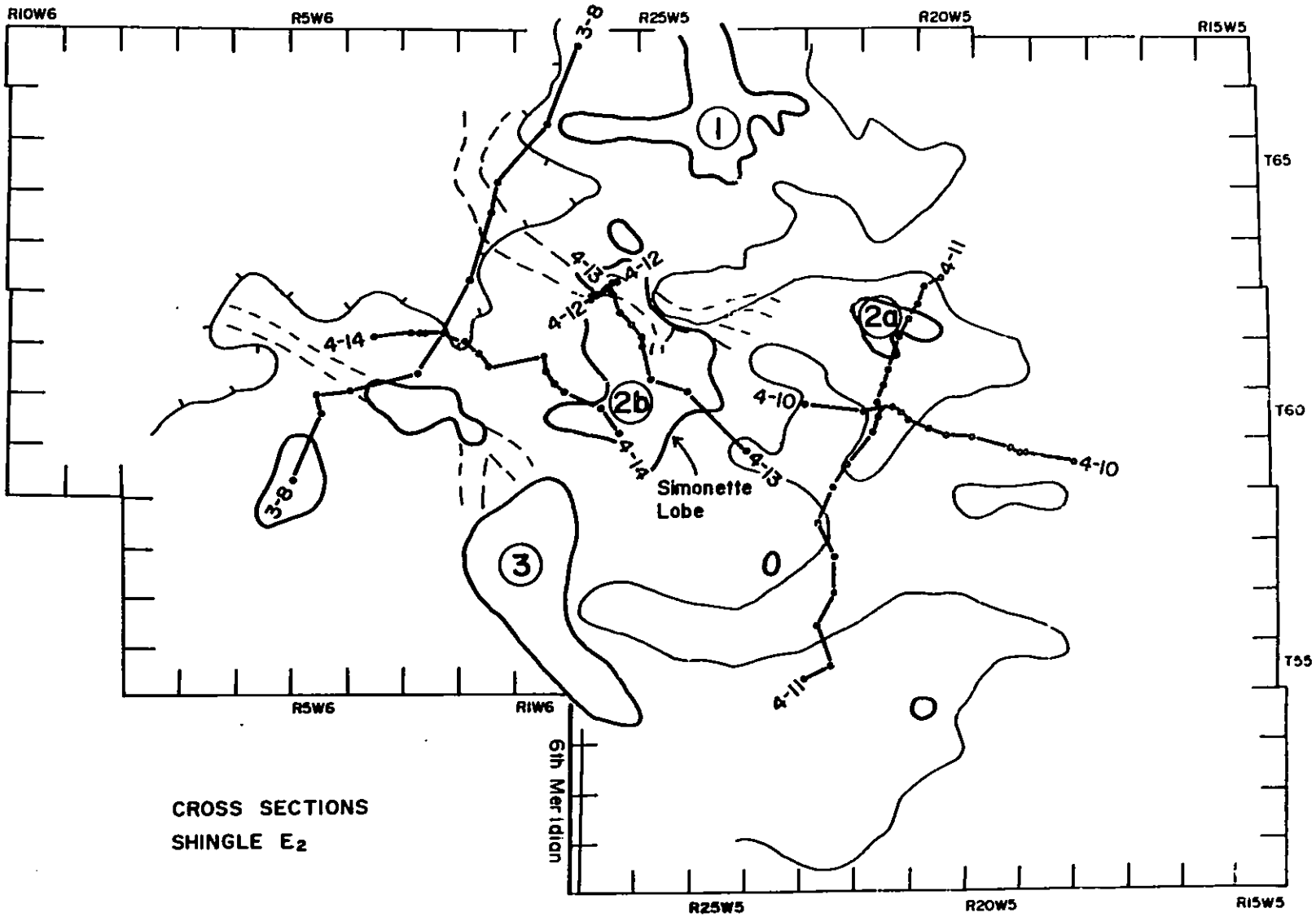

CROSS SECTIONS
SHINGLE E_2

Delineation of sand bodies to the south is less clear. The geometry of the main area of accumulation (delineated by the 4 meter contour) is unclear and has not been mapped to the south. Sand body #3 covers an area of at least 2800 square kilometers but does not show a pronounced bottleneck. It is associated with a series of bullseye sandstones towards the northwest. The eastern portion of sand body #3 comprises a large but thin sandy lobe (2000 square kilometers in area but less than 4 meters thick).

4-3-3. Shingle E3

Figure 4-5A shows a gross isolith map of sandstones within shingle E3. The map indicates several finger-like, lobate sand bodies which narrow towards the northwest into two major shoestring sand bodies. These lobate and shoestring sand bodies are schematically outlined in figure 4-5B. The southern shoestring is well defined and fairly narrow (<5km) while the northern sand body is more of a swath than a true shoestring, and is about 10km wide. A westward shift in the eastern edges of the sandstone bodies, as compared with sandstones mapped in shingles E1 and E2, is at once apparent. The outline of the 4 meter contour indicates two main sand bodies, although they merge at around township 62 range 2 and 3W5 (Fig,4-5A and B).

The northern lobe (sand body #1) lies in the northern part of the map. It covers an area of about 2000 square kilometers and reaches a maximum thickness of about 13 meters. The southeastern margin of the sand body is distinctly tri-lobate in nature (sub-

lobes #1a, #1b and #1c, Fig.4-5B) and includes a rather prominent east-facing sub-lobe (#1a). To the south of this sub-lobe lies a small irregular sandy blob (#1d). A fairly prominent bottleneck lies to the northwest which flares towards the southeast but westward of sub-lobe #1a.

Sand body 2 (southern lobe) lies to the south of sand body 1 and comprises an elongate finger-like lobe which covers an area of about 1500 square kilometers, although it does not exceed about 7 meters in thickness. The sand body narrows at township 60 range 4W6. A narrow shoestring sand body, which reaches a maximum thickness of about 20 meters, lies to the west of this bottleneck. Two lobate sand bodies, about 6m thick are seen attached to the northern side of this shoestring sandstone. The eastern margin of sand body 2, delineated by the 4 meter contour, (fig.4-5A and B), is highly irregular and comprises at least three major finger-like sub-lobes (#2a, #2b and #2c). Sub-lobe #2c overlaps sub-lobe #1c.

In the far southwest lies a third sand body. The map suggests a finger-like shape although poor well control does not allow accurate delineation of its true shape.

4-3-4. Shingle E4

Figure 4-6A shows a gross sandstone isolith map for the lowermost shingle in member E. Sandstones thin towards the southeast and there is once again a westward shift in the sandstone depositional edge relative to the overlying sandstones in shingle E3. This depositional edge is relatively irregular,

Figure 4-5A. Gross Sandstone Isolith Map, Shingle E3. Dots indicate data points. Hatched 0m contour to the northwest, represents area of non-deposition. See text for details.

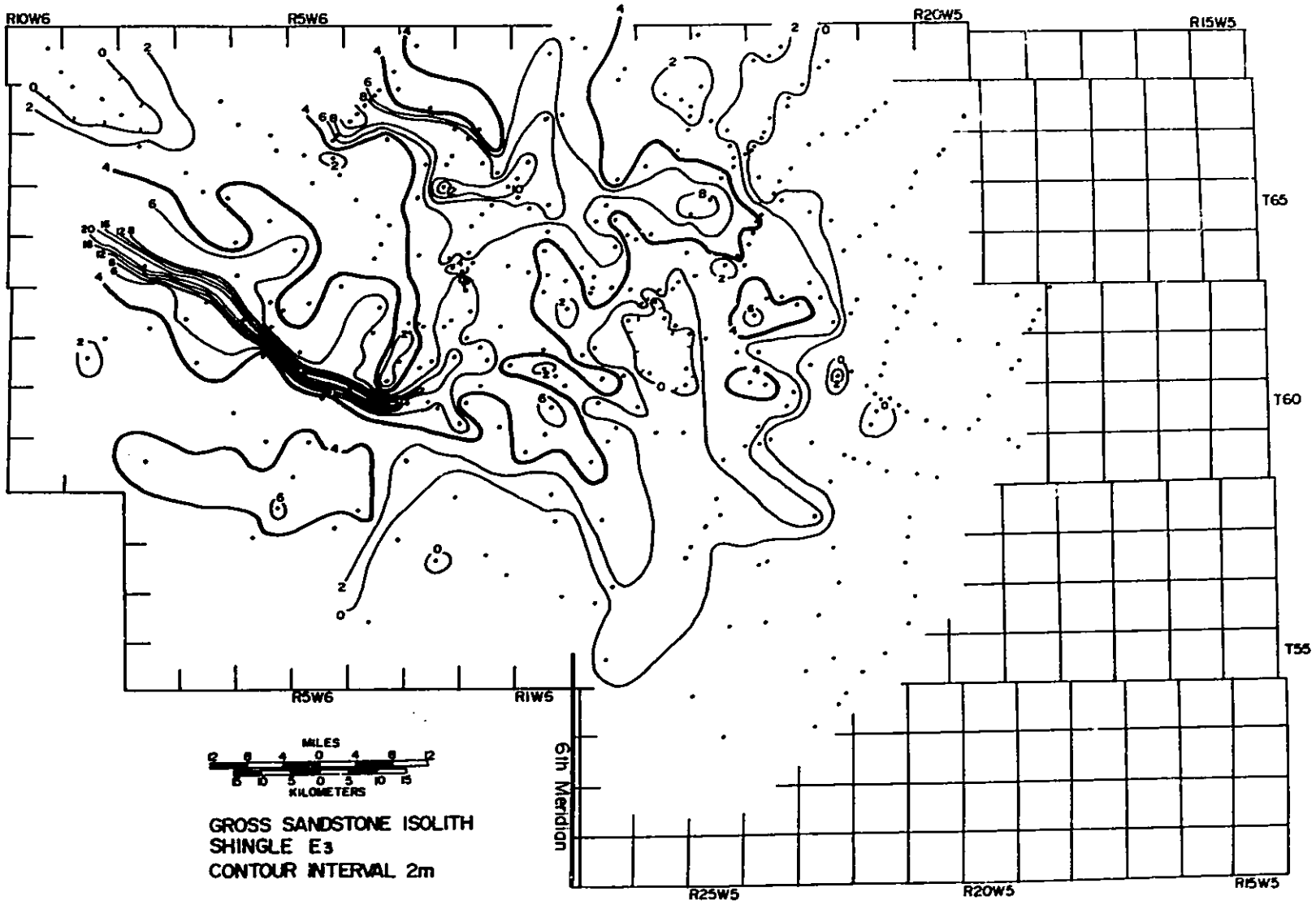
R10W6
R5W6
R20W5
R15W5
T65
T60
T55
R5W6
R1W5
MILES
KILOMETERS
6th Meridian
R25W5
R20W5
R15W5
GROSS SANDSTONE ISOLITH
SHINGLE E3
CONTOUR INTERVAL 2m

Figure 4-5B. Outline of E3 sandstones from figure 4-5A with location of pertinent cross sections shown. 0m and 4m contour lines are shown. The dashed lines represent the positions of interpreted distributary channels. Sub-lobes attached to the northern margin of channel 2 are interpreted as crevasse splay sandstones. See text for discussion and explanation.

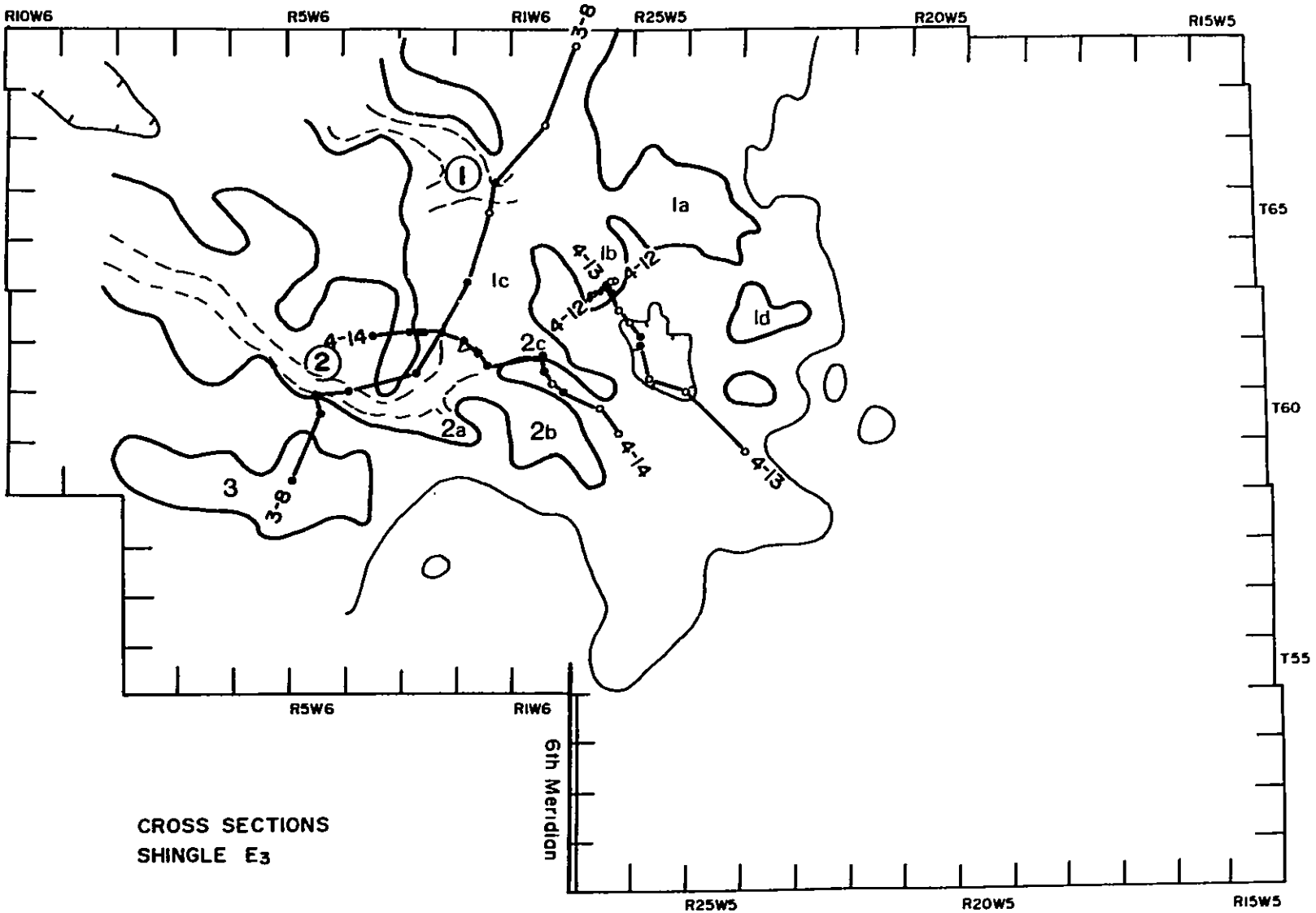

CROSS SECTIONS
SHINGLE E_3

Figure 4-6A. Gross Sandstone Isolith Map, Shingle E4. See text for details and explanation.

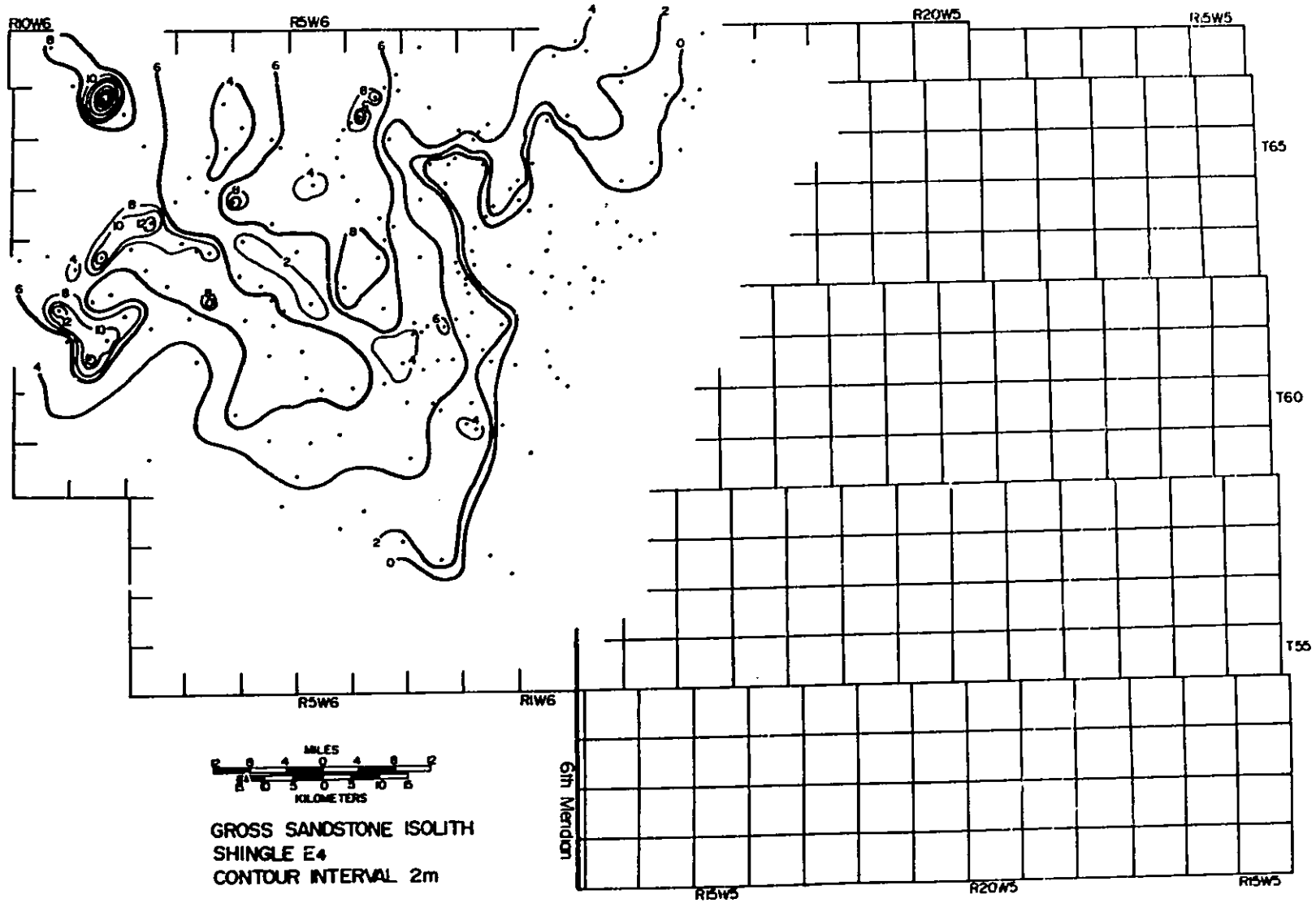

GROSS SANDSTONE ISOLITH
SHINGLE E4
CONTOUR INTERVAL 2m

Figure 4-6B. Outline of sandstones in shingle E3, based on figure 4-6A. 0m and 6m contours are shown. The dashed lines represent the positions of interpreted distributary feeder channels. The location of relevant cross sections are shown. Open circles on cross sections represent uncored wells. See text for explanation.

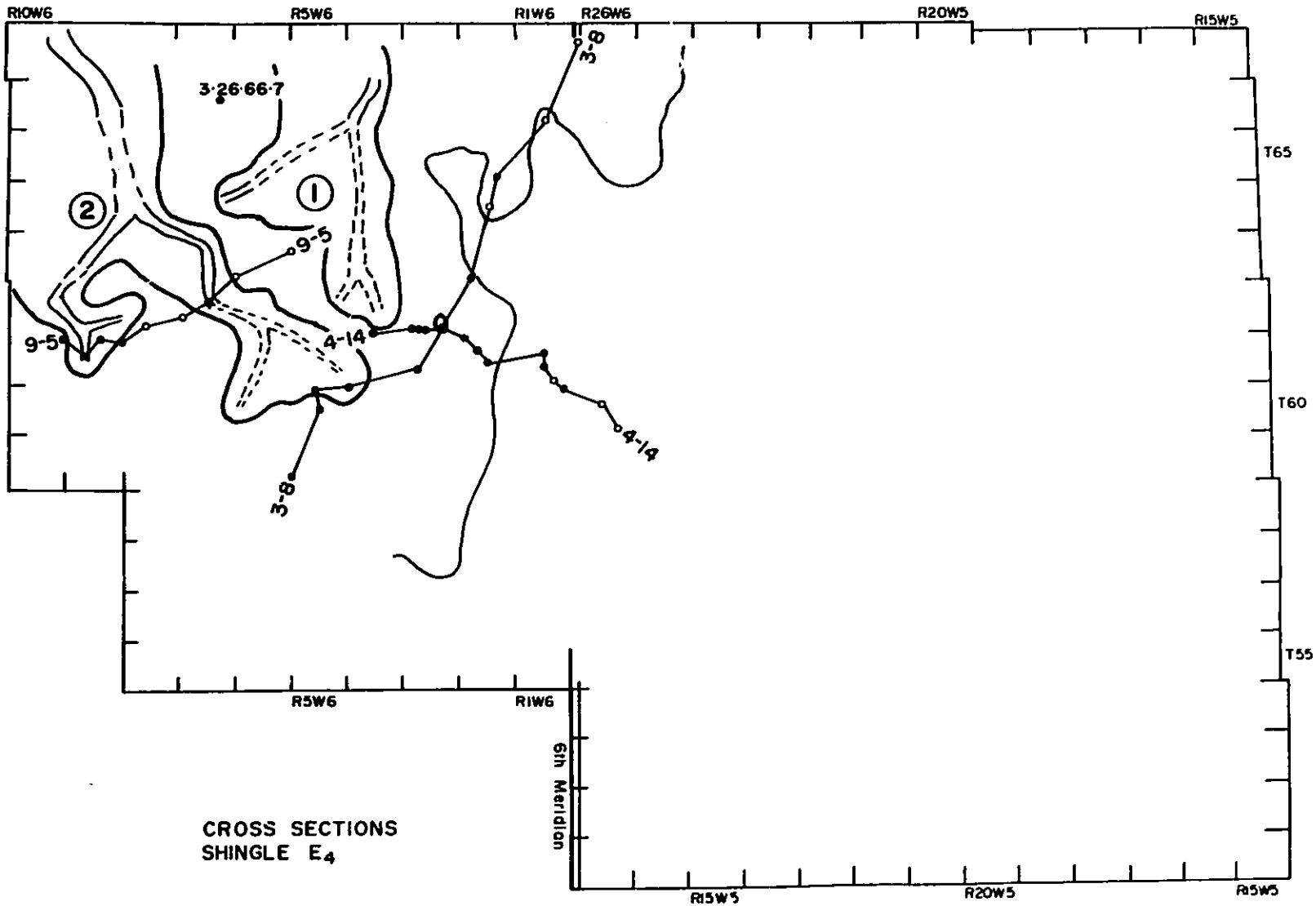

CROSS SECTIONS
SHINGLE E_4

although it is smoother than those in the overlying shingles. The outline of the 6 meter contour indicates two distinct, digitate sand bodies, each covering an area of about 830 square kilometers. Each lobe reaches a maximum thickness of about 12 meters. The distal end of the southern lobe consists of two sub-lobes which are elongated in a southeastward direction and each exhibits a cuspate geometry. The northern lobe is oriented roughly north\south.

4-4. Typical Facies Associations

4-4-1. Facies Association 1B, Lobes

As shown in figures 4-3 to 4-6, lobate to birdfoot shaped sand bodies typify member E. Cores through these lobes show characteristic coarsening upward facies successions. In shingles E1 and E2 these are usually typical of Facies Association 1B. These successions coarsen upwards in a rather irregular fashion and sandstones and mudstones are interbedded throughout. The proportion of mudstone decreases upwards. Core 15-31-62-26W5 (Fig.4-7A and B) is typical and penetrates sandstones of shingle E2 at the top of member E in the Simonette area. Three coarsening upwards facies successions are penetrated, although only the top 50 cm of the basal succession is observed. The middle succession is about 6 meters thick and resembles an incomplete Facies Association 1B. It begins in laminated marine mudstones which quickly grade upward into convolute laminated mudstone and sandstone overlain by about 30cm of cross laminated sandstone.

The middle and lower successions are correlated with shingle E3. The uppermost succession (correlated with shingle E2) is about 11 metres thick and is also typical of Facies Association 1B. It begins with 3 5 metres of laminated offshore marine mudstones containing sparse forams and exhibiting very little bioturbation (Facies 1A). Isolated sandy load casts are seen in box 9 of figure 4-9B. The succession grades upwards into interbedded mudstones and sandstones most of which show spectacular loading features (Facies 6) between boxes 5 and 8 (Close-up photo in figure 2-18c) . About 13 metres from the base, the facies become dominantly sandy. Climbing, ripple-cross-laminated sandstone (Facies 7C) are seen at the base of the final sleeve in box 5 (Close-up photo of the same unit is shown in figure 2-13a). These sandstones alternate with and pass upward into about 3.5 metres of parallel laminated to cross-bedded sandstone (Facies 7G and Facies 7C). The cross bedded sandstones at the top of the succession contain *in situ* root traces. A thin black coaly shale (Facies 1C) lies sharply above the rooted zone and is immediately overlain by a thin sandy bioturbated horizon. This bioturbated sandy horizon marks the top of member E and in turn quickly grades into a dark bioturbated marine shale (Facies 1B) at the base of member D.

Interpretation

The facies successions shown in Figure 4-7A and B are characteristic of prograding, river-dominated deltaic environments (Elliot, 1986) as outlined in chapter 2 (secrion 2-3-1B). The

Figure 4-7A. Logged core section through well 15-31-62-26W5. Gamma log illustrated on left. E3 and E2 represented by coarsening upward facies associations typical of prograding river-dominated deltas. Box photos of core shown in figure 4-7B. See text for further explanation. Legend in figure 2-29.

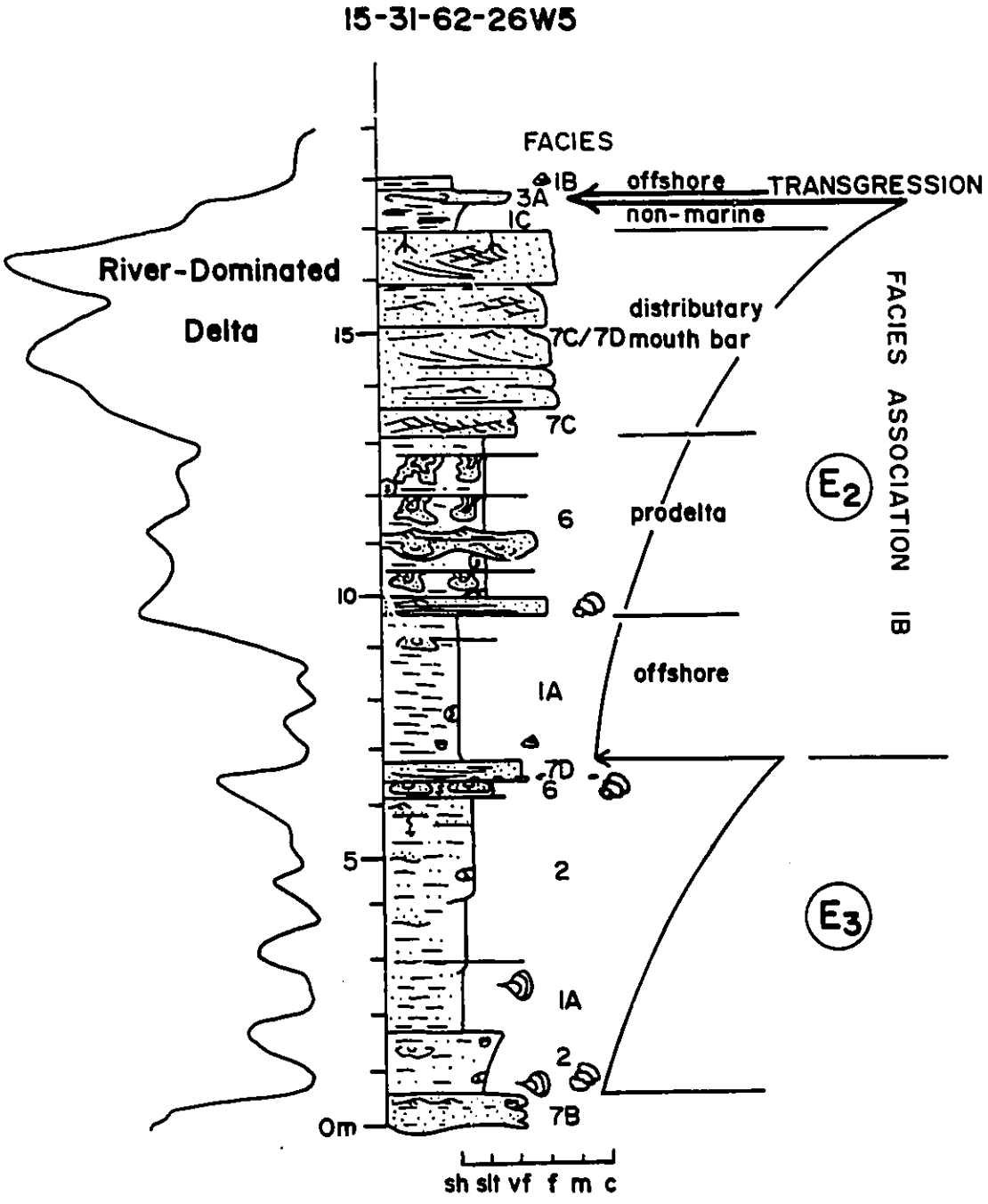
15-31-62-26W5
FACIES
1B
3A
1C
offshore
non-marine
TRANSGRESSION
River-Dominated
Delta
15
7C/7D
distributary
mouth bar
7C
6
prodelta
10
offshore
1A
7D
6
5
2
1A
2
7B
0m
sh slt vf f m c
FACIES ASSOCIATION 1B
E2
E3

Figure 4-7B. Core photos of well 15-31-62-26W5. Bottom of core is at the lower left in box 16 (interval 0.0-4.8m). Top of core is at the upper right of box 1 (interval 14.0-18.5m). Top of member E is indicated by a T-surface comprising about 10cm of bioturbated mudstone (Facies 3A) and marked with an E arrow. Note well developed root traces in cross bedded sandstones in box 2. Scale is 15cm in length. See text for further explanation.

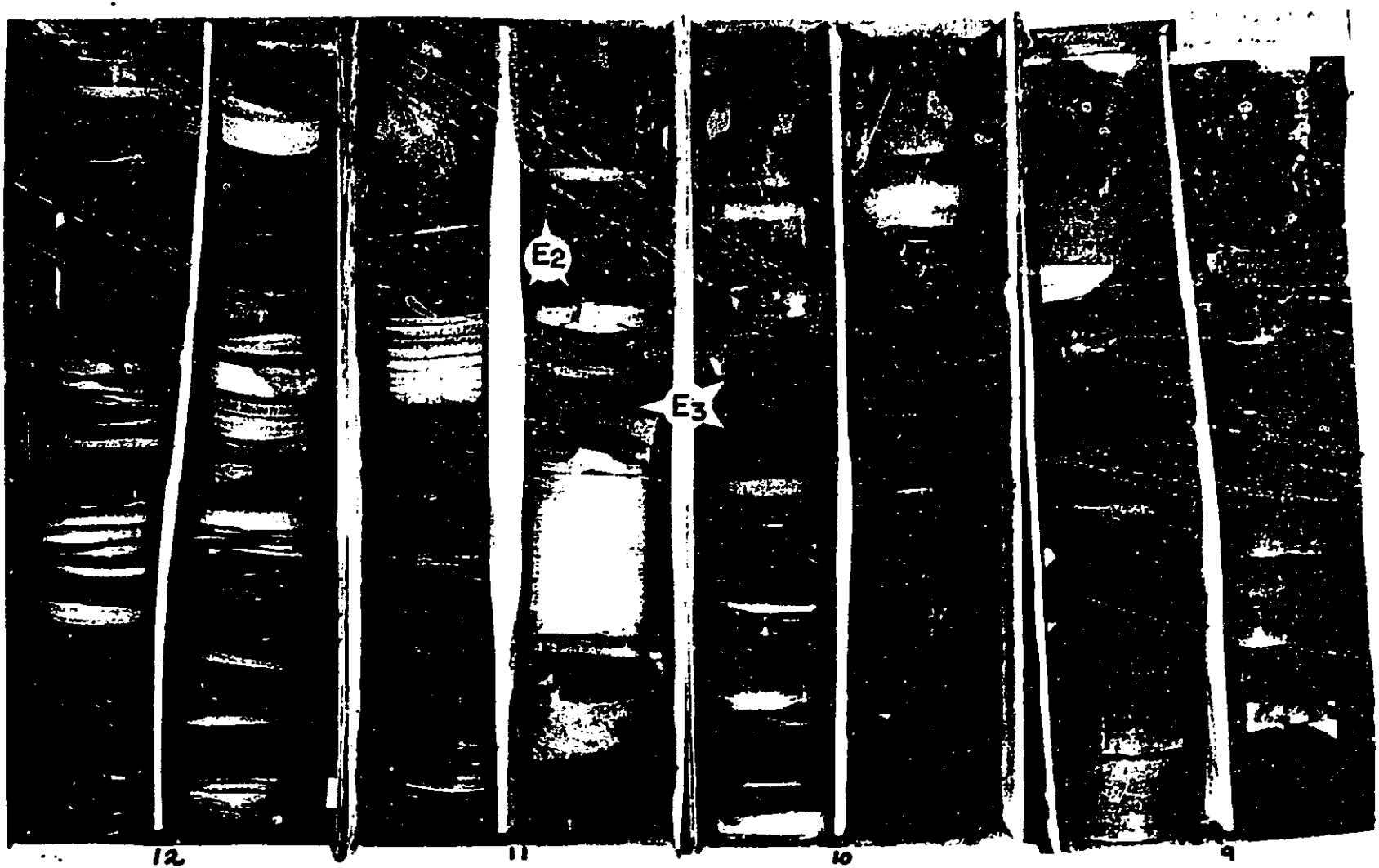
E2
E3
12
11
10
9

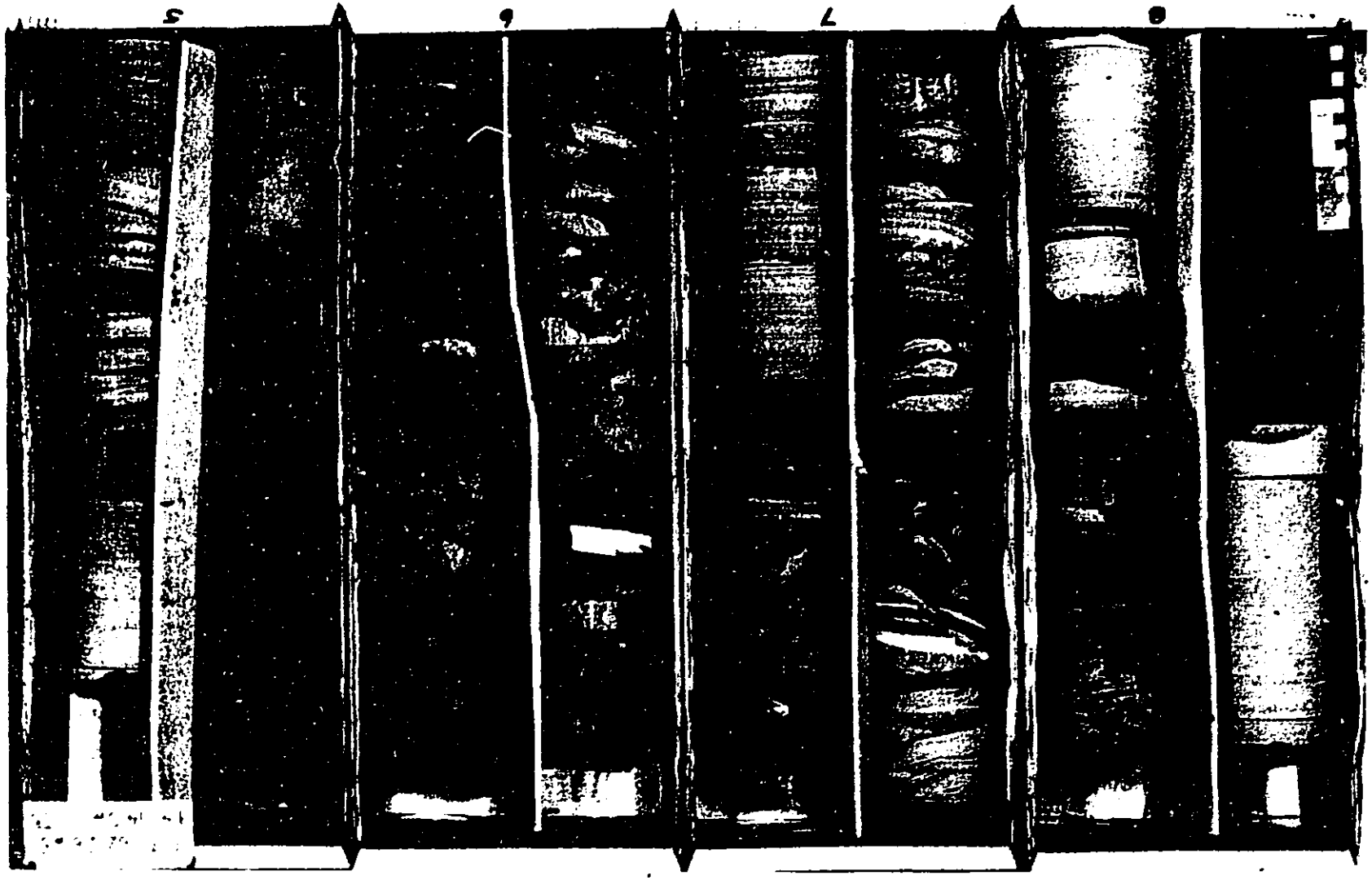
5
6
7
8

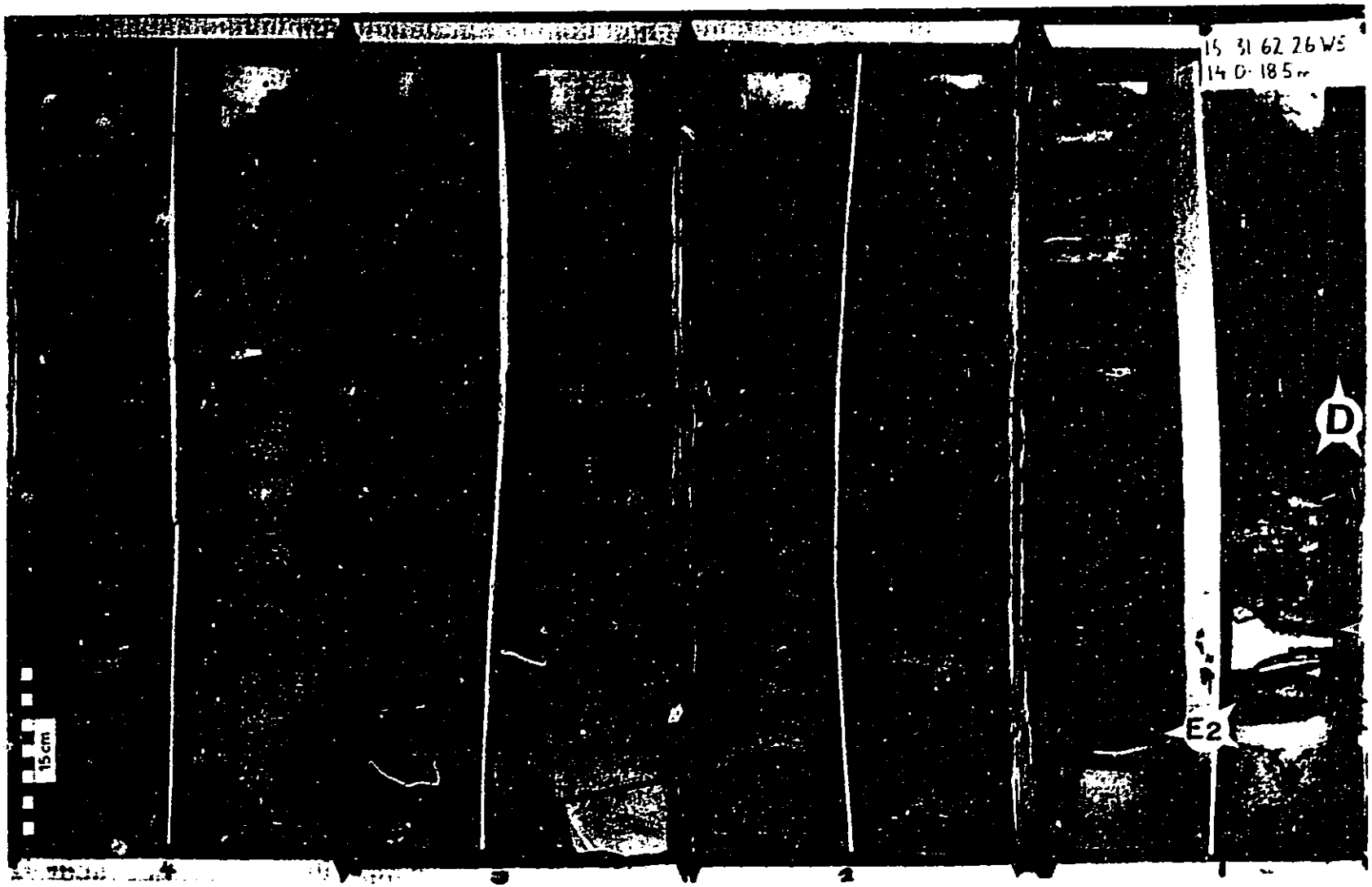
15 31 62 26 WS
14 0 18 5 m
D
E
E2
15cm

lack of bioturbation in the laminated offshore mudstones suggests that they are deposited too rapidly for organisms to rework the substrate. The loading features result from density contrasts as higher density sandstones are episodically deposited onto a water laden, muddy substrate. The introduction of coarser-grained sandstones suggests proximity to a prograding delta front (prodelta). Where present, the upper sandy portion of the successions suggest relatively continuous deposition of sediment. High sedimentation rates are also suggested by the presence of climbing ripple-cross-laminated sandstones. The lack of wave-formed structures and the lobate geometry of the associated sand body suggests deposition as a river-dominated delta front sandstone (i.e. distributary mouth bar). The abundance of shaly interbeds throughout the facies succession suggests episodic sedimentation, perhaps related to fluctuating discharge in the associated updip distributary feeder channel. The sandy bioturbated horizon, immediately overlying the coaly shale at the top of the third succession, represents a relatively rapid transgression (T-surface) that correlates with the top of member E.

4-4-2. Facies Association 1C. Lobes

Facies successions through some lobes, especially in shingle E4, also coarsen upward but show some differences from the coarsening upward facies successions described above. Core through shingle E4 in well 12-21-61-9W6 is typical (Fig.4-8

Figure 4-8. Logged core section from well 12-21-61-9W6. The coarsening upward facies succession is interpreted as representing deposition in a prograding, storm-influenced delta front environment, and is typical of Facies Association 1C. Note the abundance of HCS sandstones and the lack of soft sediment deformation features in the lower portion of the core. The well is shown on the stratigraphic cross section through member G (Fig.9-5A). Gamma log trace at left. See text for further details. Core photos not presented. Legend in figure 2-29.

12·21·61·9W6

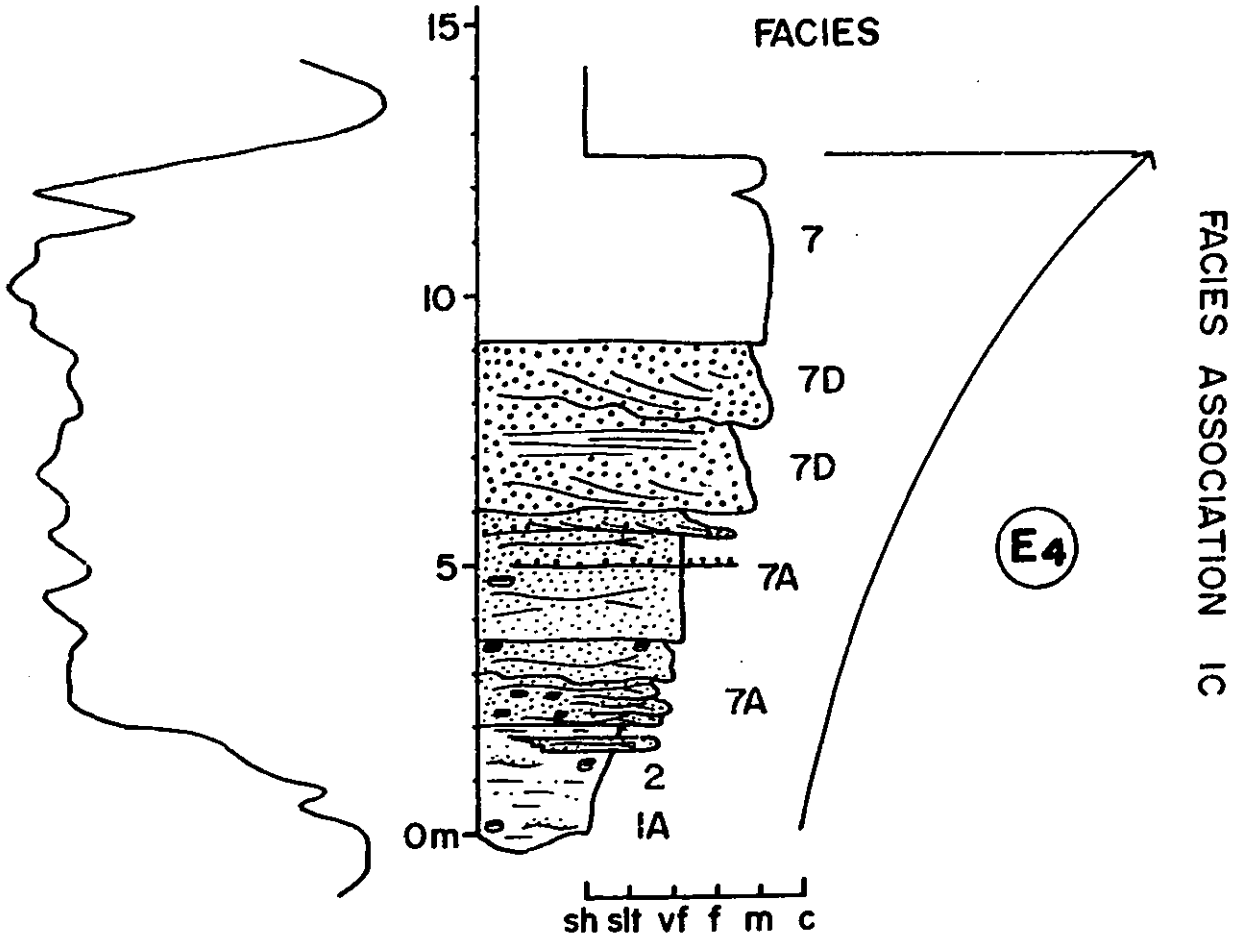
15
10
5
0m
FACIES
7
7D
7D
7A
7A
2
1A
E4
sh slt vf f m c
FACIES ASSOCIATION IC

located on Fig.9-5A). It penetrates thick sandstones of the southern lobe of shingle E4 (Fig.4-6B). It shows a relatively smooth, coarsening upwards facies succession typical of Facies Association 1C. The lowermost two meters comprise laminated marine shales and blockstones (Facies 1A to Facies 2). Upwards, the mudstones are cut by gutter casts filled with HCS sandstone (Facies 7A) to wave rippled, very fine-grained sandstone (Facies 7B). These HCS sandstones amalgamate upwards and pass into fine- to medium-grained cross bedded sandstone (Facies 7D). Unfortunately, the uppermost portions of this succession were not cored however the gamma log indicates continuous sandstone up to about 13 meters. There are fewer interbedded mudstones in these types of facies associations and the coarsening upward tends to be more regular. Thick convolute laminated sandstones and siltstones (Facies 7H and 6) are also less common in type 1C Facies Associations.

Interpretation

This facies succession is typical of Facies Association 1C and probably represents progradation of a sandy, storm- and wave-influenced deltaic shoreline (as outlined in chapter 2, section 2-3-1C). The lack of abundant shaly interbeds suggests that sedimentation was less episodic than interpreted for type 1B Facies Associations. The abundance of HCS sandstones in the lower half suggest frequent storm events. The lowermost mudstones, however, were relatively inhospitable to organisms, as indicated

by the relatively low degree of burrowing. This may result from sedimentation rates higher than interpreted for type 1A Facies Associations.

4-4-3. Facies Association 2A. Channels

Several of the shingles are associated with prominent shoestring shaped sand bodies. A typical example of a core through one of these shoestring sand bodies is shown in figure 4-9A and B. This core penetrates the Simonette channel in shingle E1. The sandstone lies with a razor sharp erosional contact on laminated offshore marine mudstones (Facies 2) containing sandy gutter casts (Facies 7A) (Gtr fig.4-9B). The erosion surface is marked by a thin basal lag containing scattered siderite clasts and shelly debris (Facies 8). The facies succession above this erosion surface is about 13 metres thick and fines upwards. It is typical of Facies Association 2A. The facies succession begins with fine-grained, vaguely cross-bedded sandstones (Facies 7D), highlighted in the box photos with black marker (Fig.4-7B, interval 1971.8-1976.0m). Finer grained, current-rippled sandstones (Facies 7C) occur upwards, although these are hard to distinguish in the box photos. A few *Asterosoma* burrows are observed in the uppermost parts of the sandstone (Ast Fig.4-9B, interval 1963.3-1967.5m).

The sandstone is sharply overlain by laminated marine mudstones that comprise the lower portion of member D.

Figure 4-9A. Logged core section from well 14-6-63-26W5. Core interpreted as a typical fining-upward, sandy channel fill facies succession, typical of Facies Association 2A. Gamma log trace at left. Legend in figure 2-29. Box photos of core are shown in figure 4-9B. See text for further details and explanation.

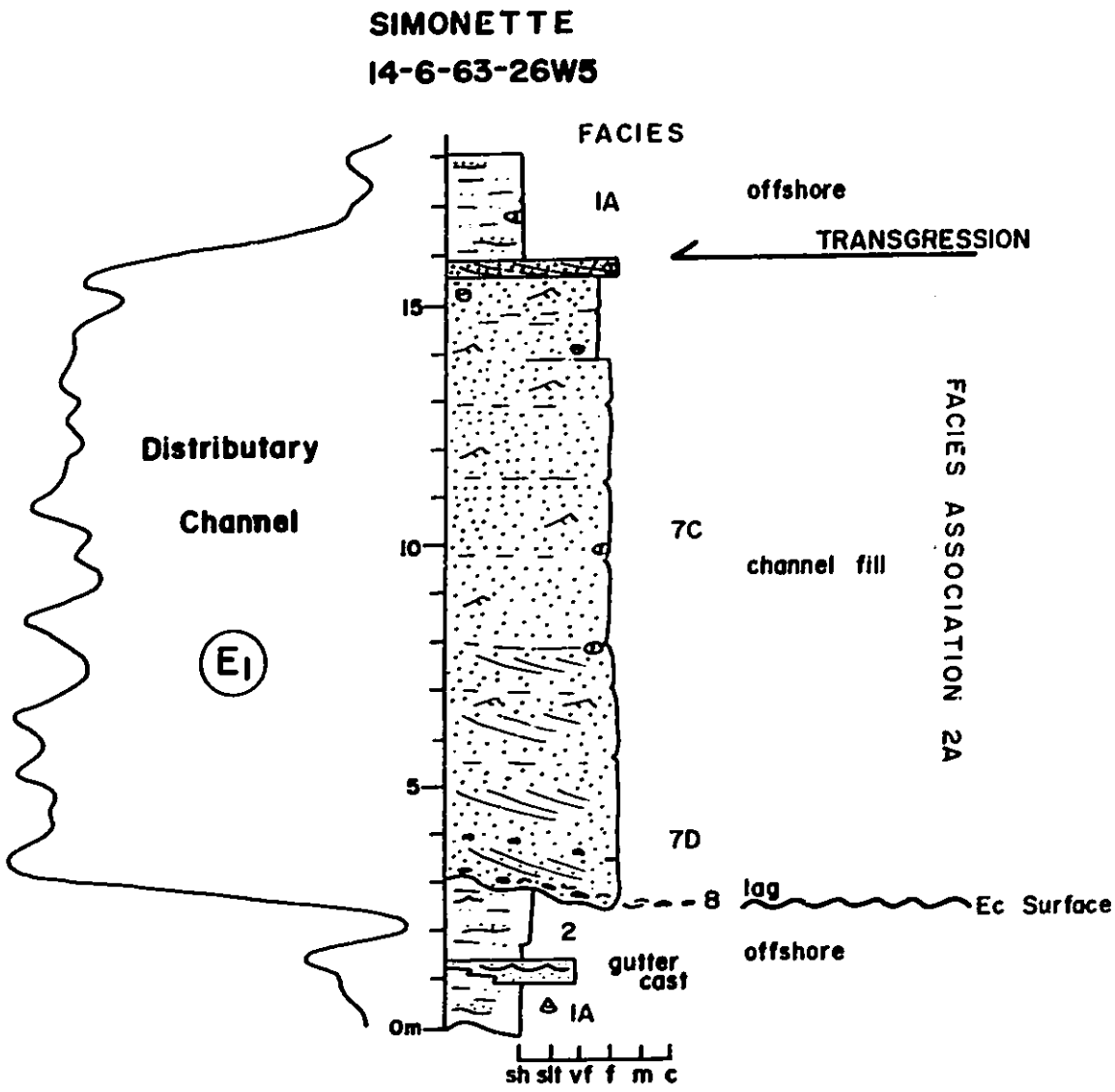
SIMONETTE
14-6-63-26W5
FACIES
IA
offshore
TRANSGRESSION
15
Distributary
Channel
E1
7C
channel fill
FACIES ASSOCIATION 2A
10
5
7D
lag
8
Ec Surface
2
offshore
gutter cast
IA
0m
sh slt vf f m c

Figure 4-9B. Box photos from core of well 14-6-63-26W5. Bottom of core is at lower left (1980m), top is upper right. Gtr = gutter cast, Ast = *Asterosoma* burrow. Bar scale in tags is 5cm in length. Logged core in figure 4-9A. Close-up shots of gutter cast are shown in figure 2-11a and b. Sandy channel fill is sharply overlain by T-surface marking the base of member D. See text for further details.

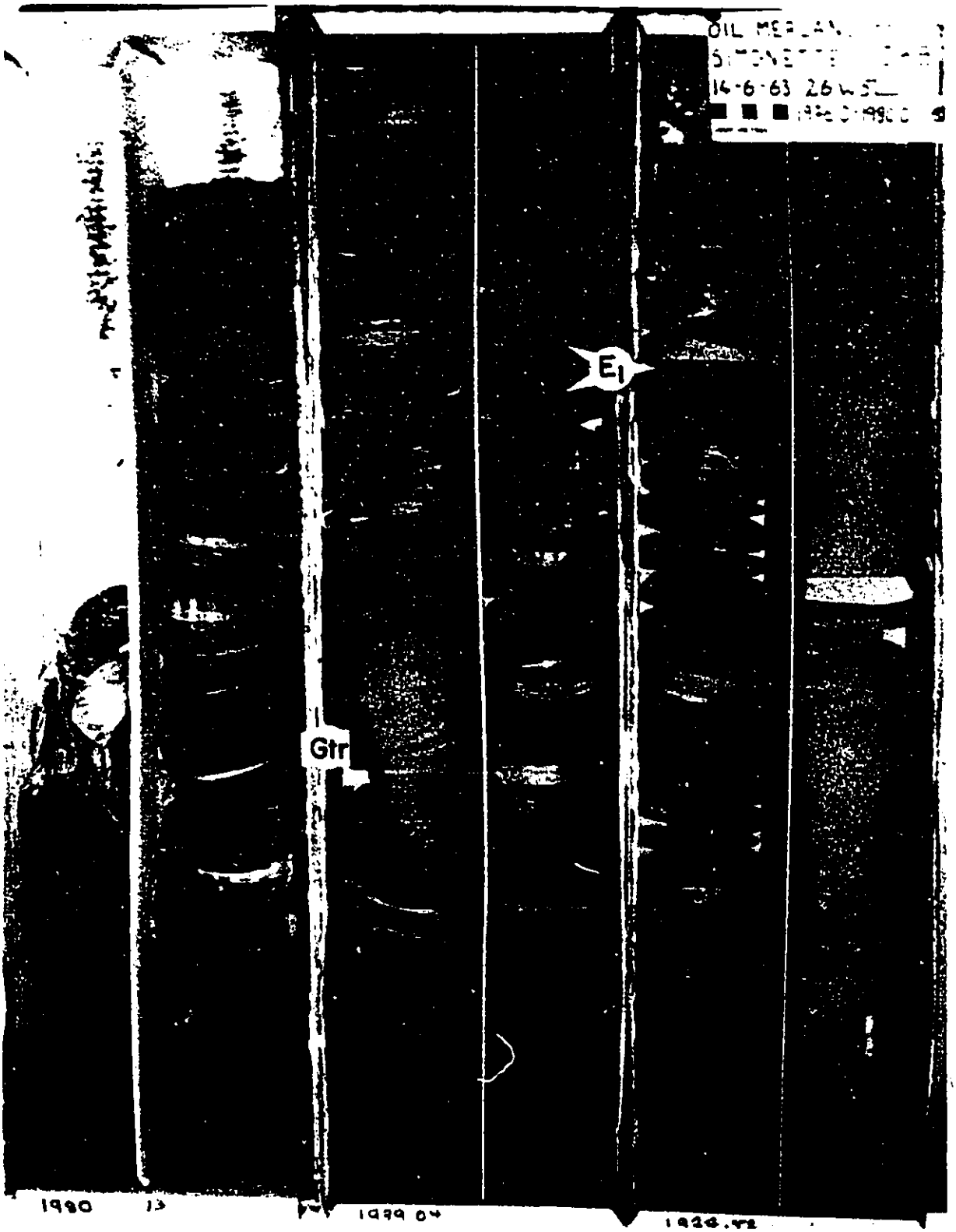
E1
Gtr
1990
1999 04
1924.42

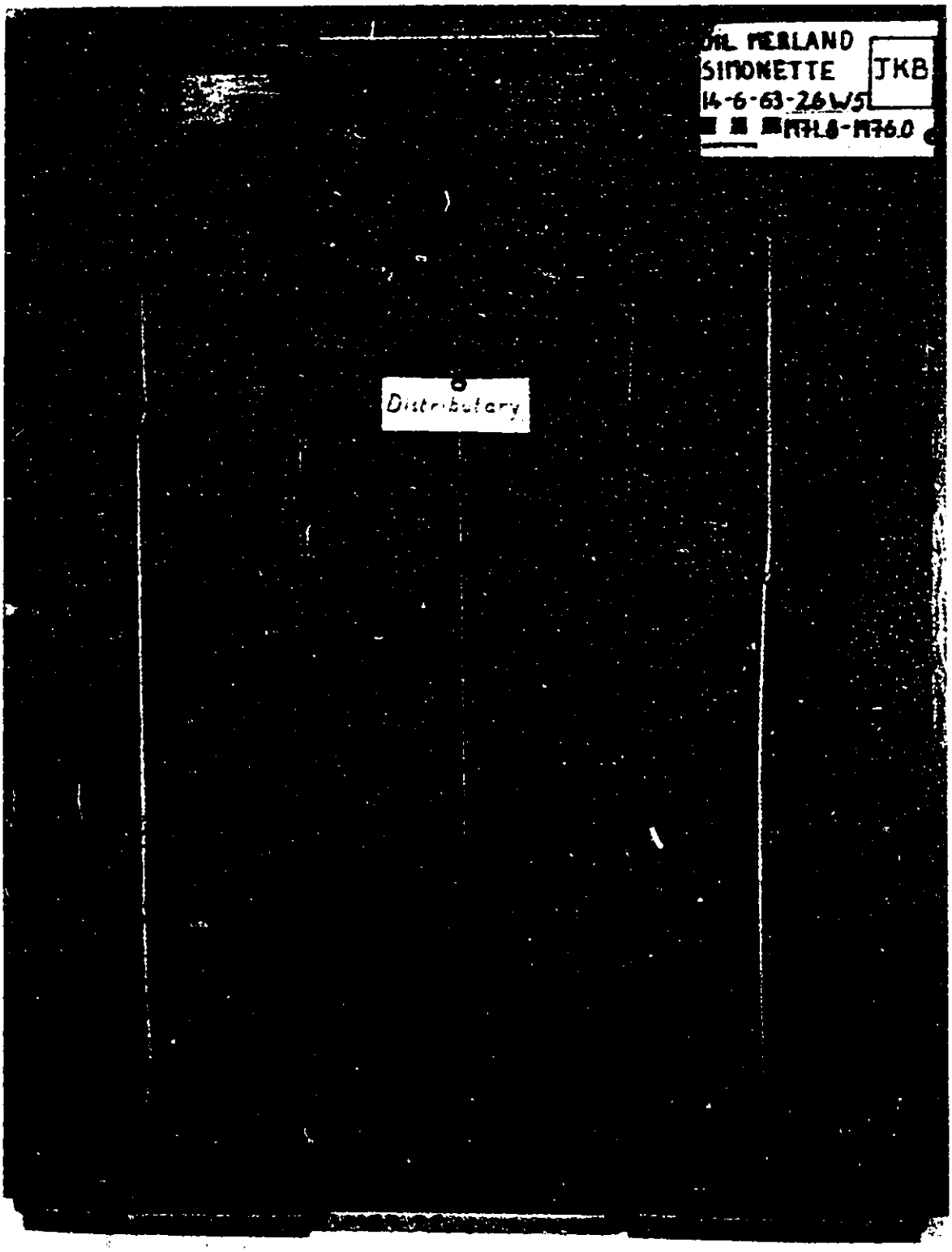
SIMONETTE
14-6-63-26W5
Distributary

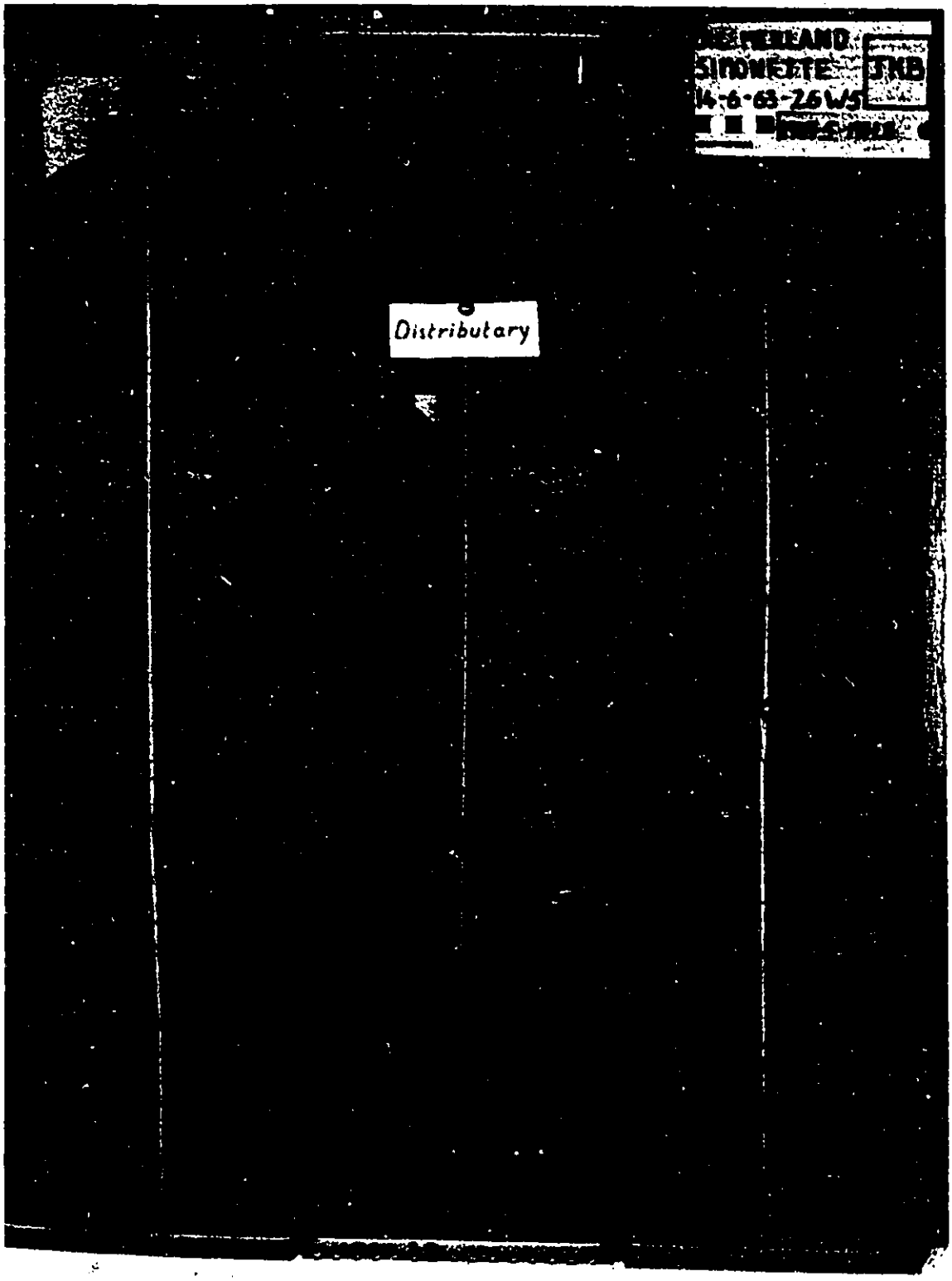
Distributary

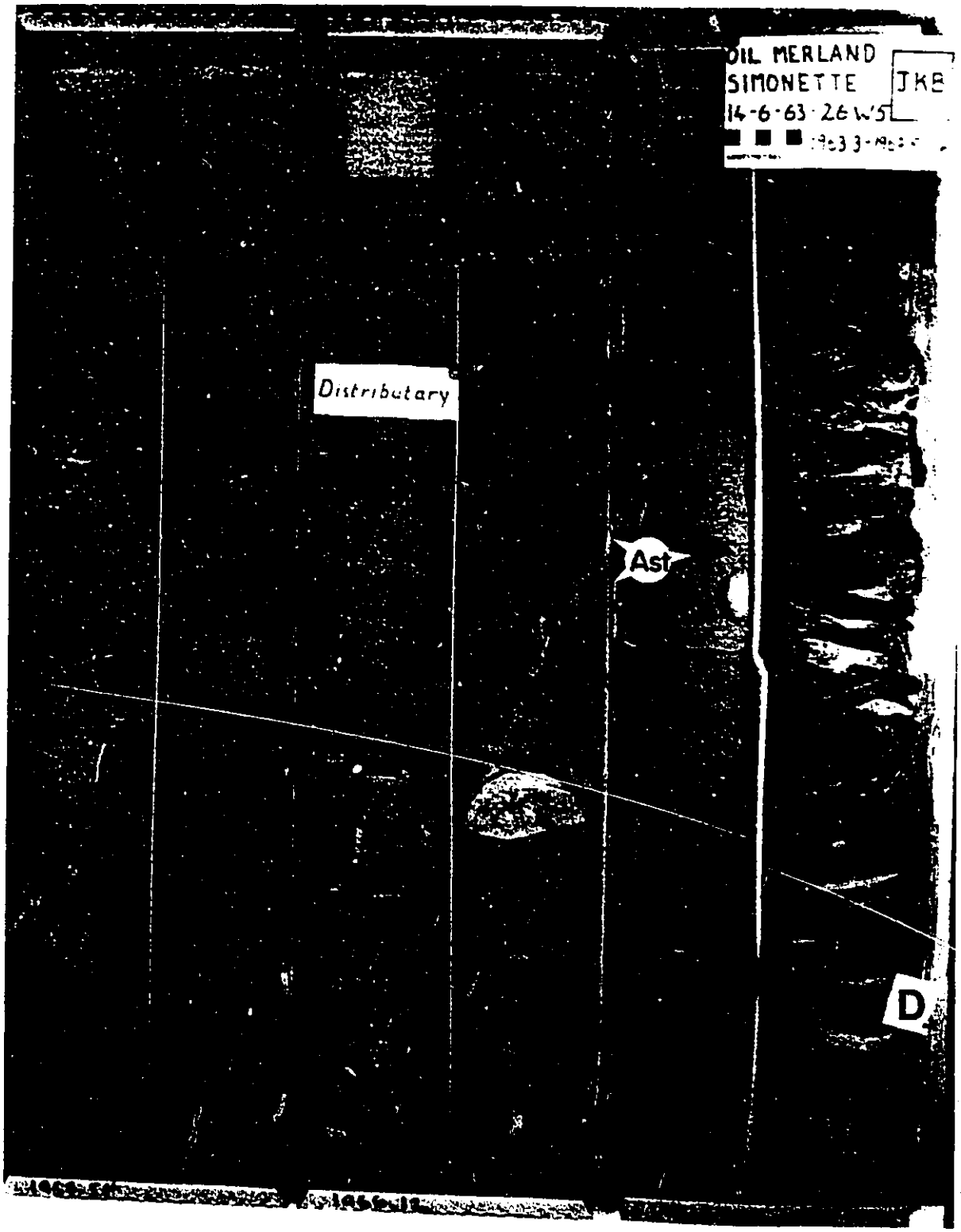
OIL MERLAND
SIMONETTE
14-6-63-26 W5
JKB
Distributary
Ast
D

Interpretation

The basal lag is derived from the underlying sediments during erosion. The facies succession above this erosion surface fines upward, indicating a progressive decrease in energy upwards. The sedimentary structures indicate a predominance of unidirectional flows. The lack of wave-formed features suggests a lack of marine influence, although the presence of occasional *Asterosoma* burrows may herald the beginning of marine influence at the top of the facies succession. The facies succession is similar to sandy channel fills (Walker and Cant, 1984) although non-marine mudstones were not observed at the top.

The contact between the top of the sand body and the overlying laminated marine shales represents the transgressive surface that separates member D from member E.

4-5. Well Log and Core Cross Sections through member E

4-5-1. Dip Cross Section, Bigstone Lobe, Shingle E1

Figure 4-10A,B represents a roughly East\West cross section oriented approximately down-dip through the E1 shingle in the Bigstone area (Fig.4-3B). The well log cross section (Fig.4-10A) is hung on the base of the Second White Specks and extends for a length of about 40 kilometers. All of the well traces are gamma logs except for wells 10-22-60-22W5 and 2-25-60-22W5 which represent resistivity logs traced backwards so that the sense of deflection corresponds to the other gamma logs. The internal stratigraphy of shingle E1 is complex and comprises at least four

Figure 4-10A. Dip Oriented Well Log Cross Section, Bigstone Lobe, Shingle E1. All wells represent gamma ray log traces except for wells 10-22-60-22 and 2-25, which are resistivity logs traced backwards. Stipple represents sandstone. Vertical bars represent cored intervals presented in figure 4-10B. See figure 4-3B for location of cross section. Note that shingle E1 comprises several overlapping sand bodies which downlap onto the top of shingle E2. See text for further details.

DIP WELL LOG CROSS SECTION

BIGSTONE LOBE, MEMBER E

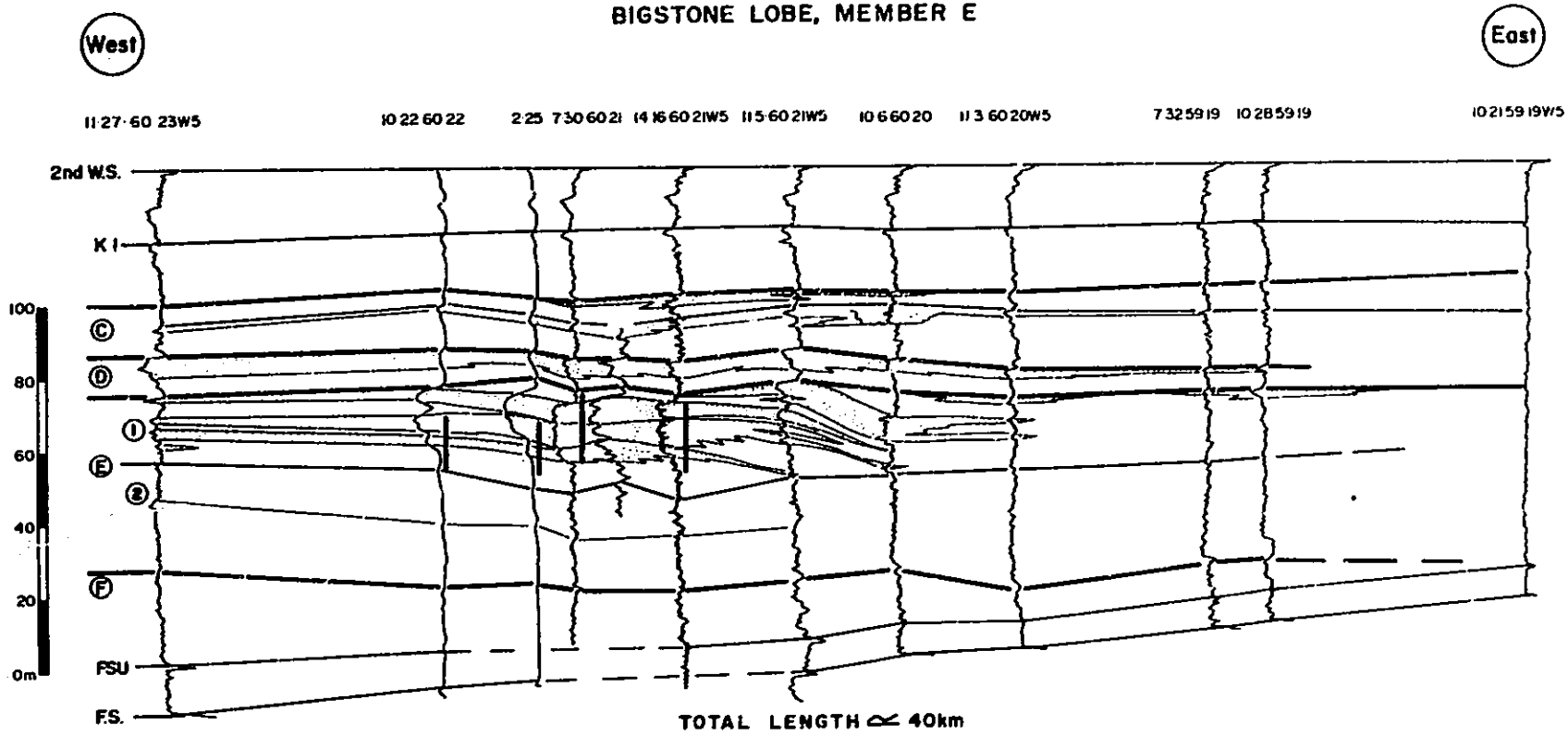

Figure 4-10B. Dip oriented core cross section through Bigstone lobe, shingle E1. Cross section hung on the top of member E. Arrow indicates coarsening upward. See figure 4-3B for location of cross section and figure 2-29 for legend. Well 2-25 ties with figure 4-11A,B. The basal mudstones are un-bioturbated and the sandier facies indicate an abundance of soft sediment deformation structures and a lack of storm and wave produced structures. See text for further details and discussion.

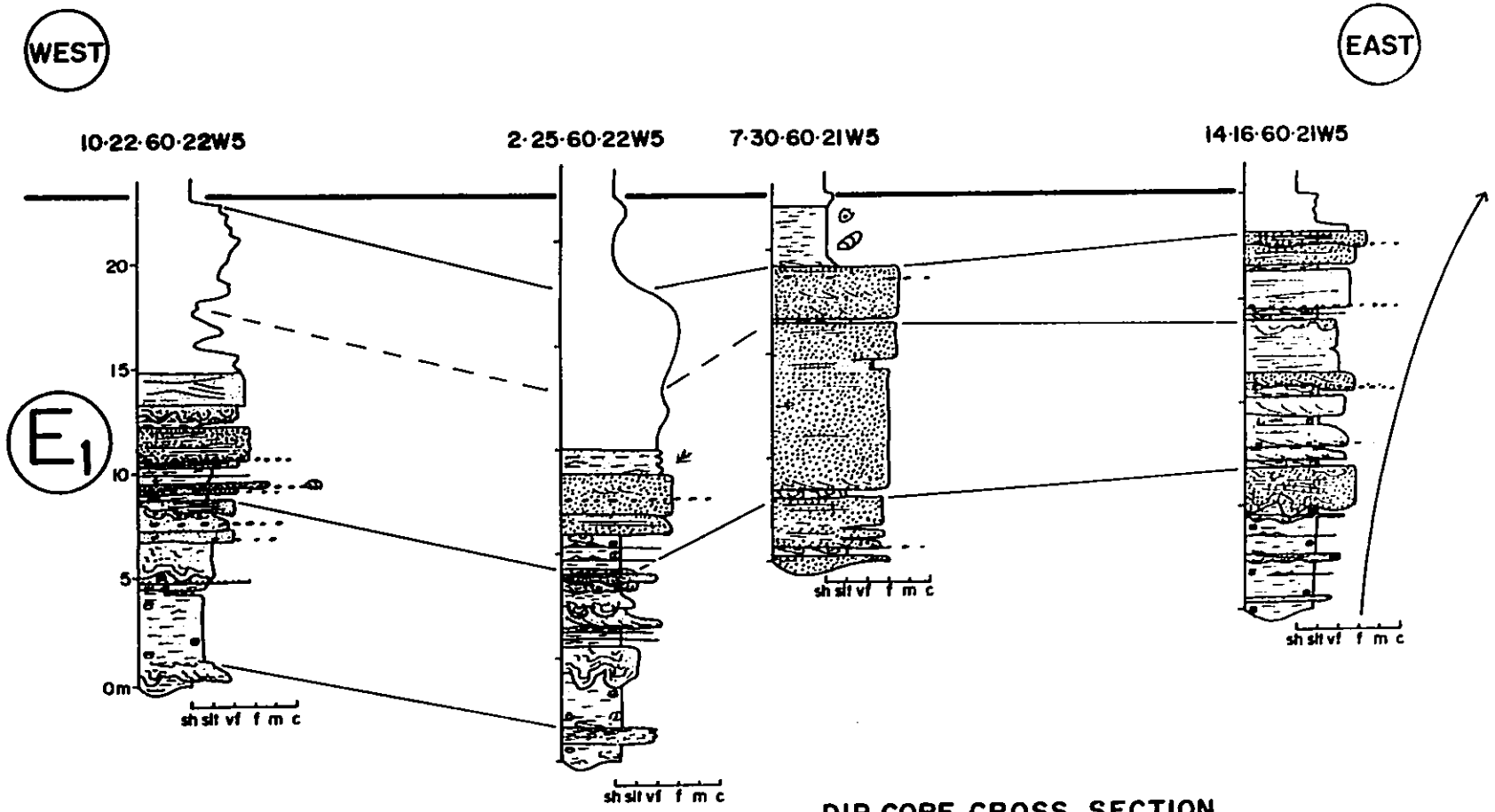

TOTAL LENGTH ≃ 10km

DIP CORE CROSS SECTION
BIGSTONE LOBE, SHINGLE E_1

relatively thick overlapping sands. These sands are separated by thin shaly interbeds which dip eastward, towards the upper surface of shingle E2. This cross sectional geometry is similar to that through the Simonette lobe (Fig.4-13A). Log traces through member E are funnel-shaped, although the funnels are quite ratty, indicating irregular sanding or coarsening upward cycles containing numerous shaly interbeds. These funnel shapes are well developed in wells 7-30-60-21W5 and 14-16-60-21W5. The sands become thinner and less numerous as they dip towards the east and pinch-out into laterally equivalent shales.

The accompanying core cross-section (Fig.4-10B) is hung on the top of member E and extends for about 10 kilometers. All of the wells show well developed coarsening upwards facies successions which are typical of Facies Association 1B, although *in situ* root traces were not noted. Sedimentary structures in the sandstones tend to be vague, and massive sandstones, such as in well 7-30-60-21W5, are dominantly structureless, although faint parallel lamination occurs in places. Flat laminated to possible HCS sandstones occur in well 10-22-60-22W5 below 15 meters and throughout core from well 14-16-60-21W5. Cross-bedded sandstones, containing mud rip-ups, are common in well 14-16 and in the upper sandy portion of well 7-30. A thin silty bioturbated horizon lies above these sandstones in well 7-30 at about 14 meters. This bioturbated horizon quickly grades upwards into several meters of laminated shales (Facies 1A).

4-5-2. Strike Cross Section, Bigstone Lobe, E1

Figure 4-11A,B represents a north of northeast/south of southwest, roughly strike-oriented cross section through the Bigstone lobe. All of the wells traces are gamma log traces except wells 2-25-60-22W6 and 10-27-62-21W5 which are resistivity logs traces backwards (Fig.4-11A). The well log cross section is hung on the base of the Second White Specks and extends for a length of about 75 kilometers. The internal stratigraphy of shingle E1, like in figure 4-10A, is complex. The sandy portion consists of a series of overlapping sandy lenses separated by numerous mudstone interbeds. Sandstones within shingle E1 show an overall thinning towards either end of the cross section. These sandstones dip towards, and pinch out against, the upper surface of shingle E2 which rises towards the northeast and towards the southwest. This surface produces a wide, shallow, valley-shaped depression within which sediments of shingle E1 lie. Shingle E1 pinches out completely towards the northeast, between wells 11-18-61-21W5 and 7-31-61-21W5, at the edge of this "valley". Irregular, funnel-shaped gamma logs characterize shingle E1 in most of the wells between 6-24-55-23W5 and 16-1-61-22W5. These shapes suggest irregular sanding- or coarsening-upwards.

The core cross section (Fig.4-11B) is hung on the top of member E. Coarsening upwards facies successions occur in all of the wells on the cross section, as indicated by the arrows, and are typical of Facies Association 1B. In general there is a

Figure 4-11A. Strike Oriented Well Log Cross Section, Bigstone Lobe, Shingle E1. The top of shingle E2 defines a broad valley between wells 7-31-61-21W5 and the SSW side of the cross section (well 11-9-55-23W5) into which the sediments of the Bigstone lobe (shingle E1) are deposited. This is not an erosional valley and shingle E1 is essentially conformable except towards the side of the 'valley' where the sediments onlap. Note the composite nature of sandstones in shingle E1. See text for further explanation. Vertical black bars represent cored intervals shown in figure 4-11B. All wells are gamma logs except for wells 2-25-60-22W5 and 10-27-62-21W5 which represent resistivity logs traced backwards. Well 2-25 ties with figure 4-10A,B.

Figure 4-11B. Strike-oriented core cross section through Bigstone lobe, Shingle E1. Delta front sandstones are interpreted as thinning to the north. Arrows indicate coarsening upward facies successions, typical of Facies Association 1B. Note abundance of soft sediment deformation features and lack of HCS or wave rippled sandstones in all of the wells. Basal mudstones in all of the wells are laminated. Cross section hung on the top of member E. See text for further details and explanations. See figure 2-29 for legend.

S.S.W.

STRIKE WELL LOG CROSS SECTION
BIGSTONE LOBE, SHINGLE E_1

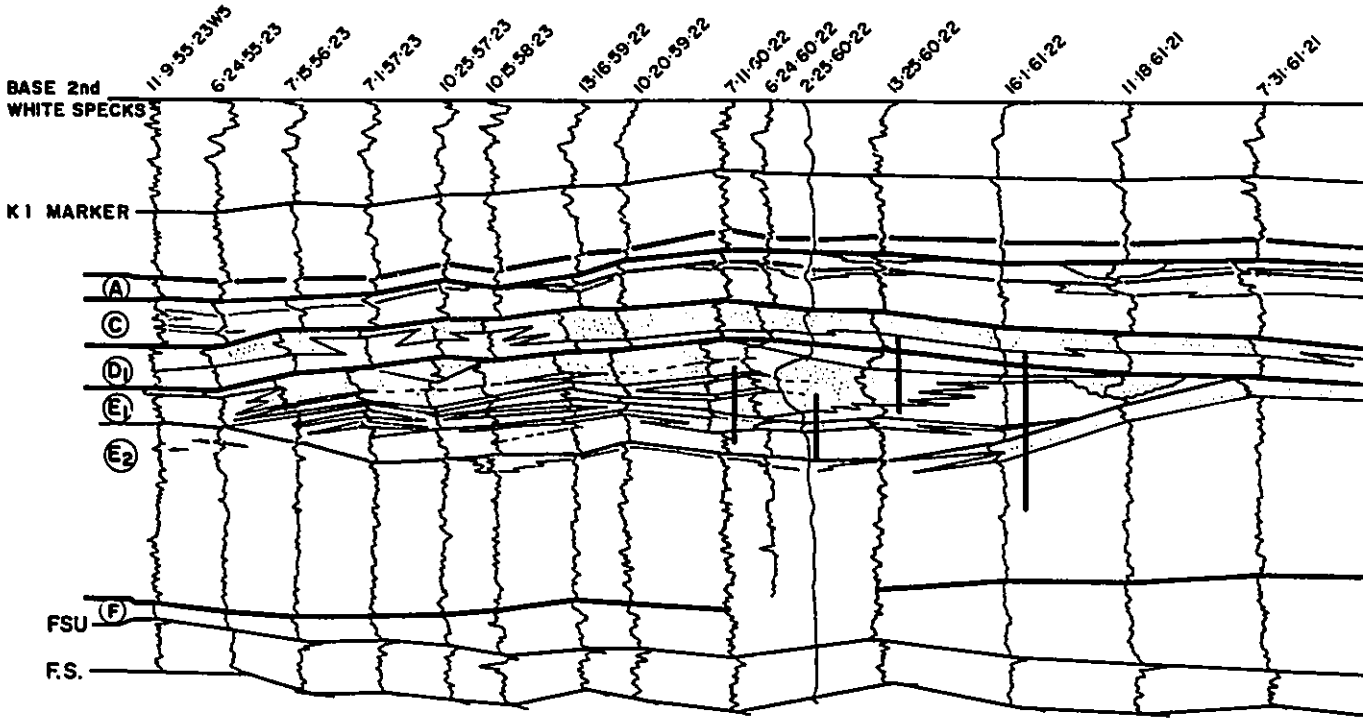

TOTAL LENGTH ≃75km

N.N.W.

ELL LOG CROSS SECTION
ONE LOBE, SHINGLE E_1

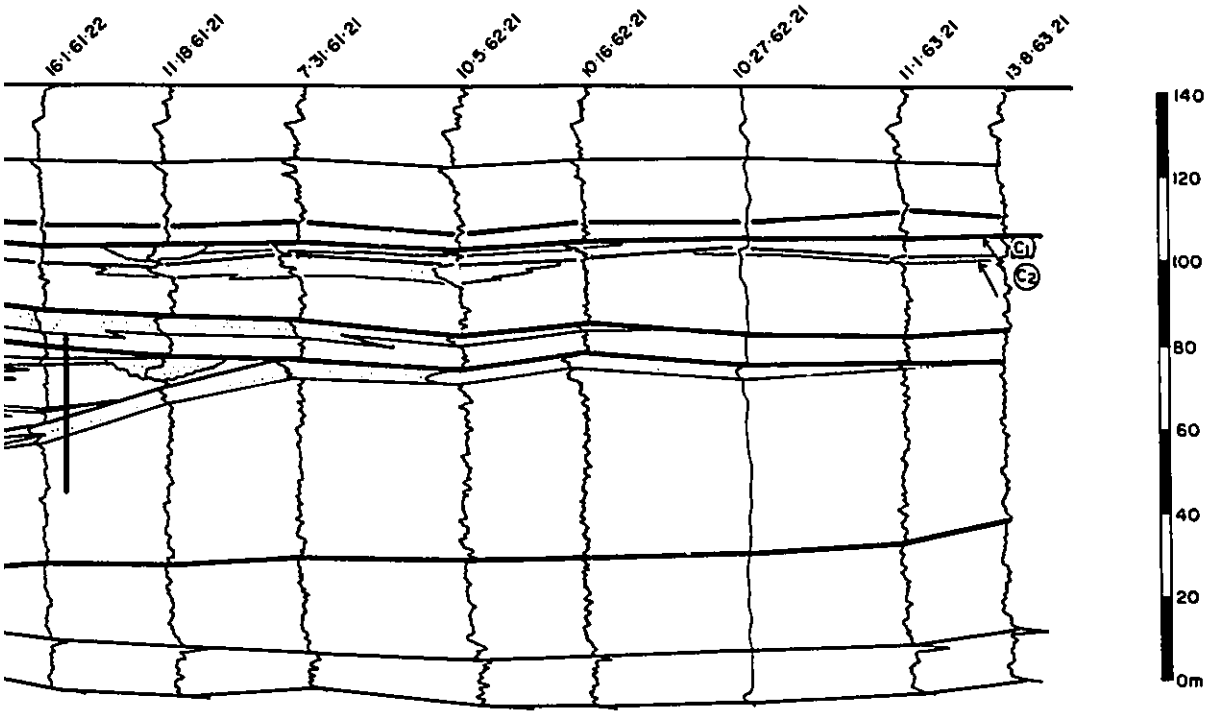

≃75km

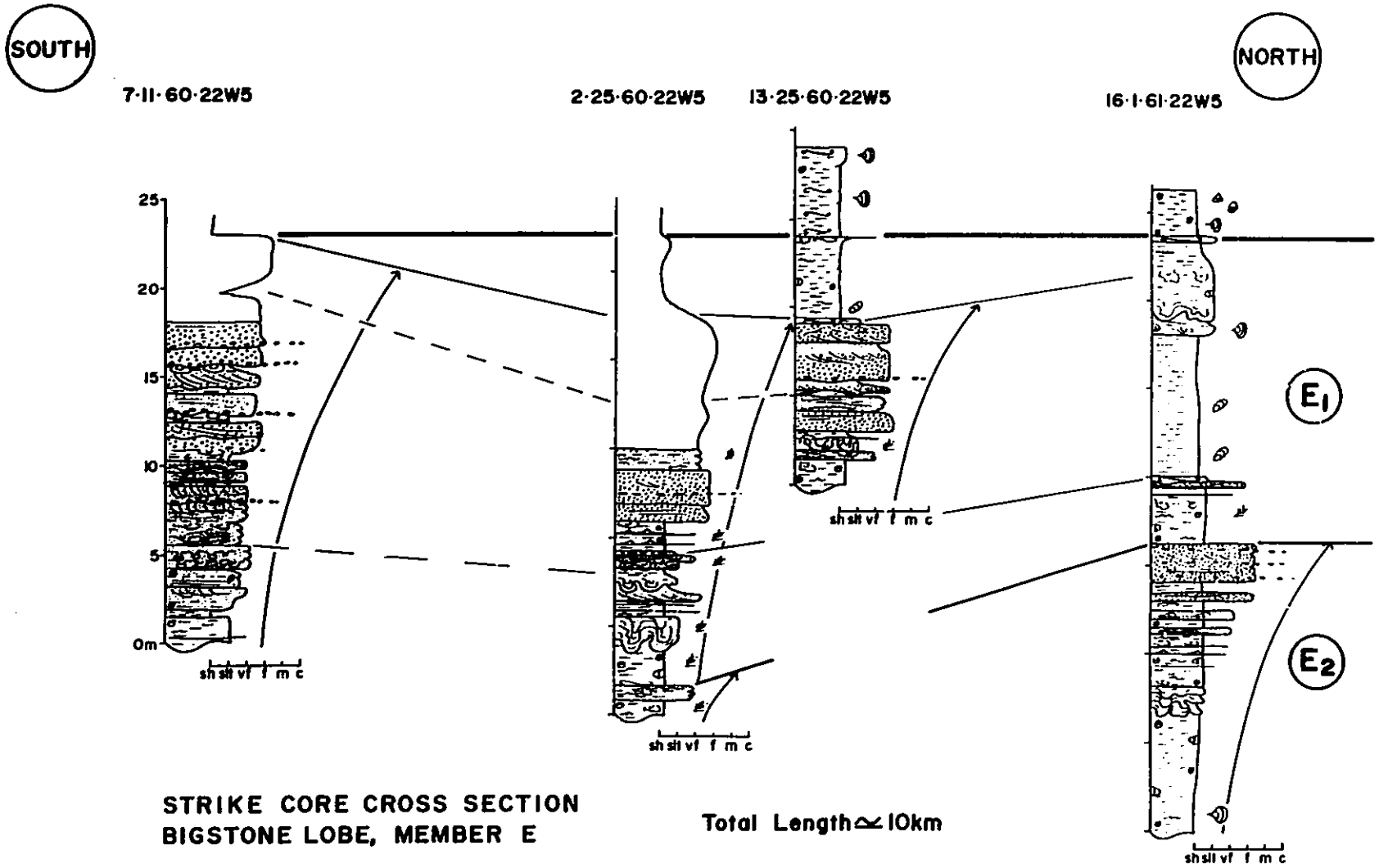

STRIKE CORE CROSS SECTION
BIGSTONE LOBE, MEMBER E

Total Length ≃ 10km

thinning of sandstone towards the northeast; the thickest sands occurring in well 7-11-60-22W5. In well 16-1-61-22W5, shingle E1 comprises laminated blockstones and massive, deformed to laminated, siltstones. Thick sandstones are not present. The underlying shingle (E2) is characterized by a well developed coarsening-upwards facies succession, also typical of Facies Association 1B.

The sandstones within shingle E1 in the other wells are characterized by convolute lamination (Facies 7H), cross-bedding (Facies 7D) and current ripple lamination (Facies 7C), and are interbedded with numerous shales. Some of the sandstone beds contain a basal zone of intraformational sideritized, mud-chip conglomerate and fine or grade upwards, such as at 16 meters in well 7-11 and above 5 meters in well 13-25. Wells 7-11 and 13-25 contain several of these graded beds, nested within the overall coarsening upwards. HCS sandstone is uncommon and occurs only in well 13-25-60-22W5 below 5 meters from the base.

A thin sandy bioturbated horizon lies sharply above the main sand in shingle E1, in well 13-25, at about 9 meters. This bioturbated horizon quickly grades upwards into about 5 meters of laminated silty blockstone and laminated shale (Facies 2 and Facies 1A). These blockstones culminate with a thin pervasively bioturbated sideritic sandy mudstone (Facies 3A) which is sharply overlain (at about 14m) by several meters of bioturbated marine shale bearing *Inoceramus* (Facies 1B).

Interpretation, Bigstone Lobe

The facies associations are typical of prograding river-dominated delta fronts, as described above for well 15-31-62-26W5 (Fig.4-7A,B) and in chap[ter 2 (section 2-3-1B). The presence of rare HCS sandstones may suggest occasional storm reworking of the Bigstone delta front sandstones. The lack of *in situ* root traces or coals suggests predominantly subaqueous deposition. Deposition occurred in pulses, as indicated by the abundant shaly interbeds and rapid lateral facies changes, perhaps produced as a result of fluctuating discharge in the Simonette feeder channel. The presence of several meters of laminated mudstones in well 13-25, may represent local switching and abandonment of sub-deltas of the Bigstone lobe. The major transgression, which marks the end of E deposition, is marked by the sandy bioturbated horizon (T-surface) which is in turn overlain by the *Inoceramus* bearing bioturbated transgressive marine shales of the overlying member D.

4-5-3. Strike Cross section, Simonette Channel, shingle E1, E2 and E3

Figure 4-12A,B represents a core and well log cross section perpendicular to the shoestring sand in the Simonette area. The well log cross section (Fig.4-12A) is hung on the base of the Second White Specks. The cross section extends for about 5.5 kilometers and along the line of the cross section, member E is about 40 meters thick. In well log 1-8-63-26W5, the gamma profile suggests three stacked coarsening upward cycles, as indicated by

the arrows. Irregular coarsening upwards is suggested by the rather ratty nature of the funnel-shaped gamma log profiles. All three of these cycles are present over the whole cross section, although the gamma log through the upper cycle is even more ratty in the other wells and does not show a well developed pattern of any kind. The lower two cycles correlate with shingle E3 while the upper cycle correlates with shingle E2.

In the middle of the cross section, between wells 14-35-62-27W5 and 1-8-63-26W5, the gamma logs through the upper portion of member E have distinctly blocky to bell-shaped profiles indicating thick sandstone. As shown in figure 4-12A, this sandstone clearly truncates markers within shingle E2 indicating erosion. This erosion surface undulates and is overlain by sandstones with a maximum thickness of about 13 meters in well 3-6.

The accompanying core cross section (Fig.4-12B) is hung on the top of member E. About 15 meters of shingle E3 is cored in well 1-8-63-26W5. The core, and the rather ratty nature of the gamma log, indicates that shingle E3 contains one relatively well developed coarsening upwards cycle from about 3 to 9 meters. Core through the bottom portion of the lower cycle indicates about two meters of burrowed blockstone and very fine-grained current rippled sandstone which passes into several meters of laminated to bioturbated marine shales containing oysters and *Lingula*. This coarsens upwards into bioturbated mudstones and ends with about 2 meters of very fine-grained, wave-rippled, burrowed sandstone at

Figure 4-12A. Strike Oriented Well Log Cross Section through Simonette Channel, Shingle E1. Sandy channel of shingle E1 erodes into shingle E2 between wells 14-35 and 1-8. Channel is less than 5 km wide but up to 13 meters deep in well 3-6. Channel sands (e.g. well 10-6) exhibit bell-shaped to blocky profiles on gamma logs while delta front sands show funnel-shaped, coarsening upward profiles, highlighted with the arrows in well 1-8. All well traces are from gamma ray logs. Stipple represents sandstone. Vertical black bars represent cored intervals shown in figure 4-12B. See text for further details and explanation.

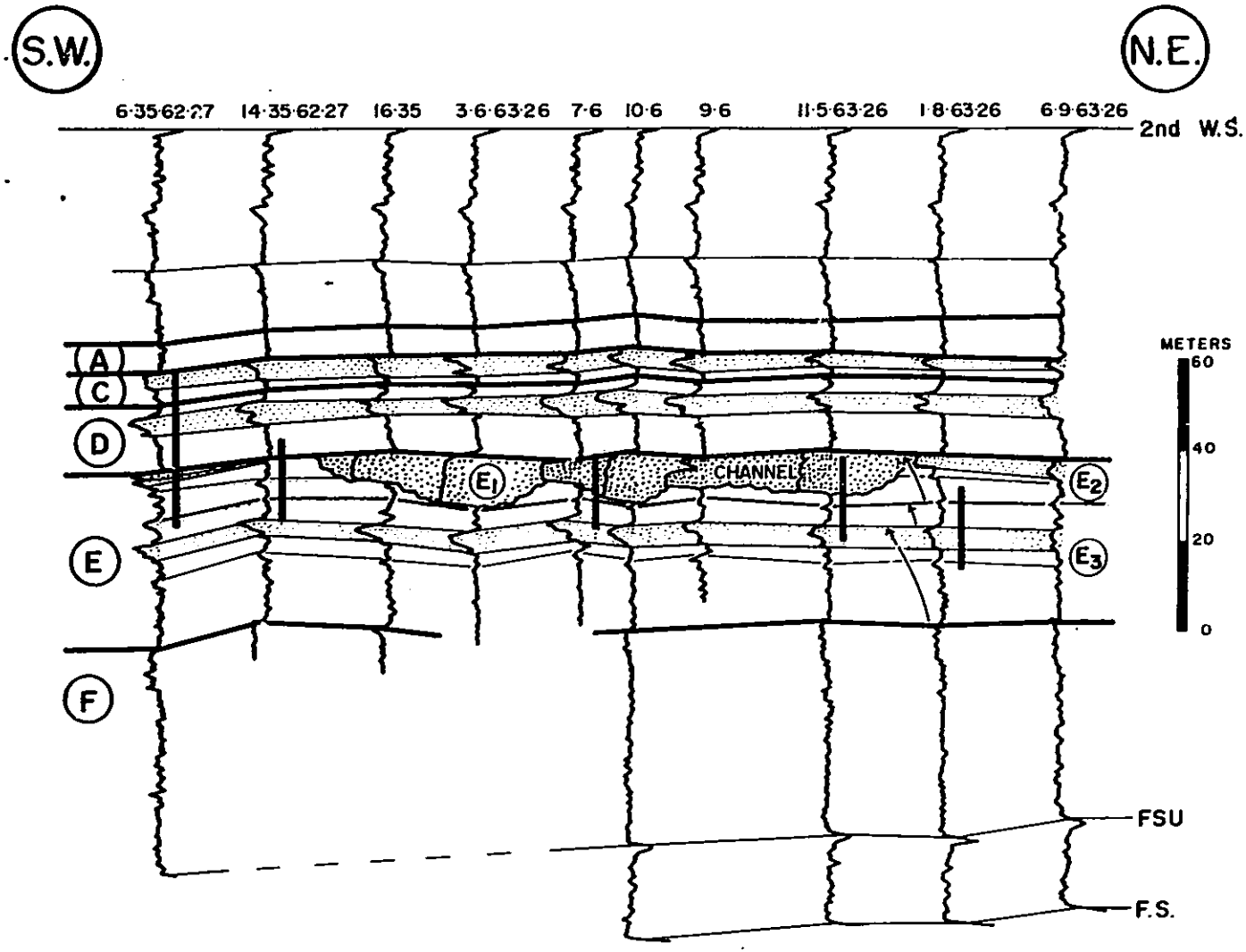

TOTAL LENGTH ≃ 5.5km

STRIKE WELL LOG CROSS SECTION
SIMONETTE CHANNEL, MEMBER E

Figure 4-12B. Strike Oriented Core Cross Section through Simonette Channel, Shingle El. Cores through channel in wells 7-6 and 11-5 show typical type 2A Facies Associations. Non-sequential facies succession in well 14-35 is typical of interdistributary and interlobe areas. Coarsening upward and fining upward facies successions are indicated with arrows. Cross section hung on the top of member E. See text for further explanation and see figure 2-29 for facies legend.

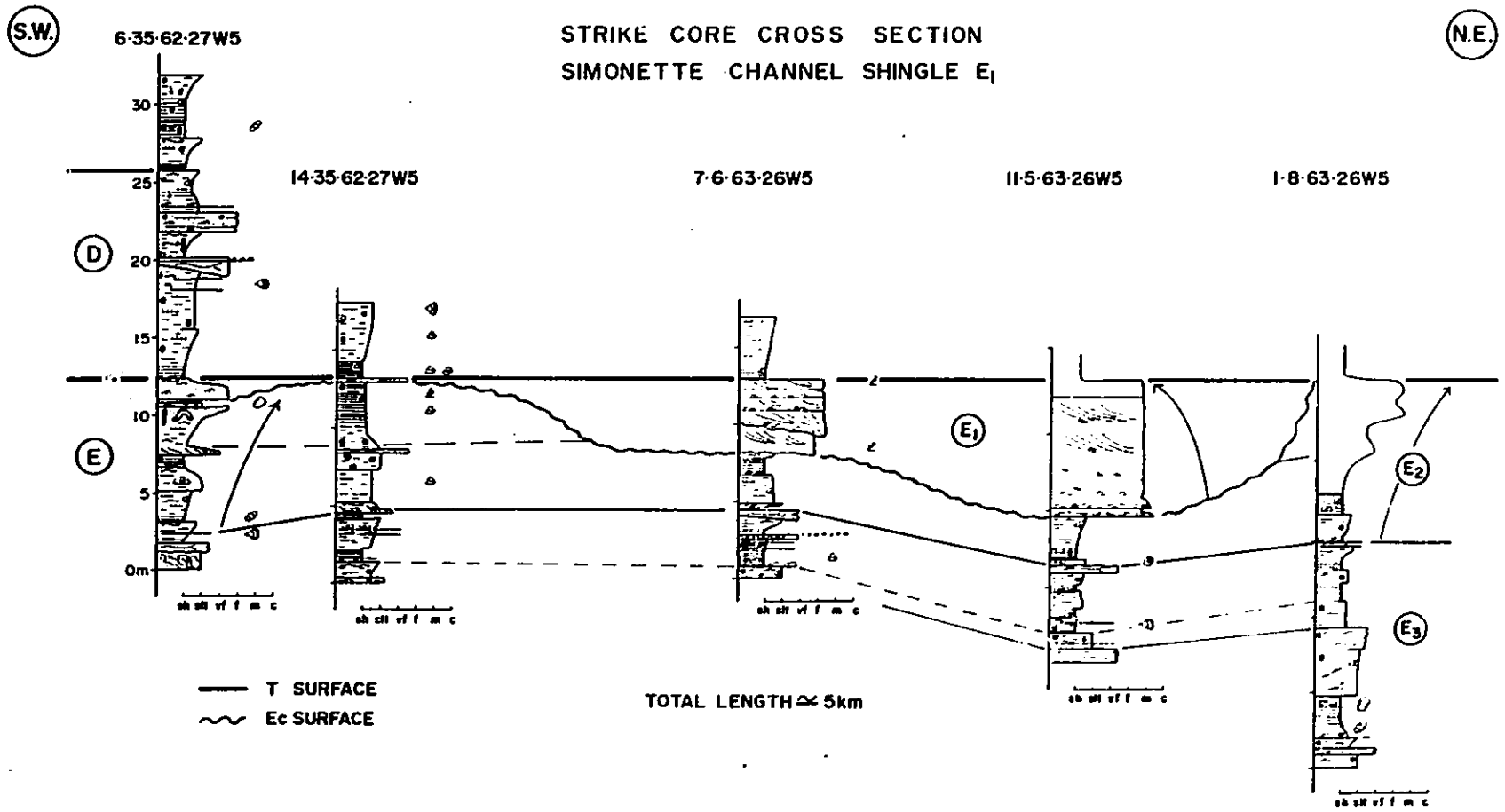
S.W.
N.E.
STRIKE CORE CROSS SECTION
SIMONETTE CHANNEL SHINGLE E1
6-35-62-27W5
14-35-62-27W5
7-6-63-26W5
11-5-63-26W5
1-8-63-26W5
30
25
20
15
10
5
0m
D
E
E1
E2
E3
T SURFACE
Ec SURFACE
TOTAL LENGTH ≃ 5km

about 9 meters. This marks the top of the first subcycle in shingle E3 and the succession passes sharply back into about 6 meters of laminated blockstones and shales (Facies 2A and 1A). In the adjacent wells (11-5, 7-6, and 14-35) the upper sub-cycle in shingle E3 shows a crude coarsening upward but is essentially non-sequential. The facies successions in these wells is typical of Facies Association 3. *Inoceramus* were noted in the upper sub-cycle of shingle E3 in wells 6-35 and 22-5-63-26W5. The top of shingle E3 is marked by a thin pervasively bioturbated sandy mudstone (Facies 3A) in all of the wells.

Facies successions in shingle E2 are irregular (especially well 14-35) and are similar to Facies Association 3. The only coarsening upward facies succession completely cored on this cross section is in well 6-35-62-27W5. This succession shows some similarities to Facies Association 1B, but is not complete. It comprises about 9 meters of interbedded blockstones, deformed sandy siltstone, pinstripes and a few very fine-grained wave rippled to HCS sandstones. The succession coarsens upwards rather crudely and is capped at 11 meters by about 2 meters of fine-grained bioturbated sandstones. Thick current-rippled to cross-bedded sandstones (Facies 7C to Facies 7D), as in well 15-31-62-26W5 (Fig.4-7), are not present, although current-rippled sandstone associated with shingle E1 is seen in the last 2 meters of member E.

The facies succession through shingle E2 in well 14-35-62-7W5 is dominated by laminated shales and blockstones (Facies 1A and 2) interbedded with occasional thin, very fine-grained, current-rippled sandstones (Facies 7C) and convolute laminated sandy siltstone (Facies 6). No regularity was noted in the succession of facies which is similar to Facies Association 3.

Wells 7-6-63-26W5 and 11-5 penetrate the thick sandstone at the top of member E which clearly erodes into shingle E2. The facies successions in these wells are similar to Facies Association 2A. Shingle E1, in well 11-5, begins with a coarse lag (Facies 8) and fines into thickly bedded, medium to fine-grained, cross-bedded sandstones (Facies 7D) containing ripped-up sideritized mud chips and shell fragments. Well 7-6 begins with about 2 meters of fine-grained cross bedded sandstone which is erosively cut by medium-grained, cross-bedded sandstone containing siderite clasts and shell fragments. Sandstones within both wells contain several thin mudstone beds.

Interpretation

The shoestring geometry of the sand body suggests a major distributary channel. This interpretation is supported by the presence of a major erosional surface, underlying this sand body, which truncates adjacent marine facies successions. The facies succession above the erosion surface fines upwards and suggests a progressive decrease in energy, typical of sandy channel fills, as discussed in chapter 2 (section 2-3-2A). Because the erosion

surface cuts into the Simonette lobe, the Simonette channel must be younger than the Simonette lobe. The largely non-sequential facies successions in adjacent wells (e.g. well 14-35, Fig.4-12B) suggest laterally equivalent, shallow marine, interdistributary bay environments occasionally affected by storms, producing wave-rippled, pinstriped mudstones cut by rare HCS sandstones. Crevasse splays occasionally flooded these shallow water interdistributary bay environments producing thin, very fine-grained, convolute laminated to current-rippled sandstone beds. Coarsening upwards facies successions (e.g.in well 6-35, Fig.4-12B) resemble incomplete type 1B Facies Associations, and are interpreted to represent the lateral edges of the sandy deltaic Simonette lobe described below (Section 4-5-4).

The facies succession through shingle E3 crudely coarsens upwards and is similar to Facies Association 1C. The presence of typical brackish water fossils (oysters and *Lingula*) and laminated to burrowed mudstones containing wave-rippled and current-rippled sandstone beds suggests a distal lobe or interdistributary bay environment. Basinal processes are more important in these environments than in proximal lobe positions.

4-5-4. Dip cross section, Simonette lobe, E2

Figure 4-13A,B is a northwest/southeast, dip-oriented cross section through the Simonette lobe (sand body #2B in Fig.4-4B). The well log cross section (Fig.4-13A) is hung on the base of the second white specks and extends for a length of about 40

kilometers. All well traces are gamma logs except for well 10-3-62-26, which represents a resistivity log traces backwards. Gamma and resistivity log profiles through member E on figure 4-13A exhibit an overall funnel shape suggesting a decrease in shale upwards (sanding-or coarsening-upwards). Two major coarsening upward cycles are present corresponding to shingles E2 and E3, although the lower cycle may be further subdivided into an upper and lower cycle. The tops of both of these cycles dip toward the southeast. This southeastward dip is also indicated on the regional schematic cross section (Fig.4-2). The coarsening upward cycle at the top of member E, in well 4-34-59-24W5, corresponds to shingle E1. Sandstone thicknesses within shingle E2, range from 0 to 10 meters becoming thinner, in general, towards the southeast. Sandstones of the Simonette lobe are seen to thin and die out between wells 2-4-61-25W5 and 4-34-59-24W5. These sandstones contain several shaly streaks which also dip towards the southeast and which emphasize overlapping relationships between sandy layers within shingle E2.

The accompanying core cross section (Fig.4-13B) extends over a length of about 12 km through the northern half of the Simonette lobe and is hung on the top of member E. The cross section includes well 15-31-62-26W5, which has been presented above (section 4-4-1). All of the wells penetrate the topmost coarsening upwards facies succession, but the lower successions are not penetrated in wells 10-3-62-26W5 and 10-34-61-26W5. The

Figure 4-13A. Dip Oriented Well Log Cross Section through the Simonette Lobe, Shingle E2. Note that sandstone are complex and contain numerous shaly interbeds. Correlations suggest that sandstones downlap to the southeast. All well traces are from gamma ray logs except well 10-3 which represents a resistivity log traced backwards. Vertical black bars represent cored intervals shown in figure 4-13B. Stipple represents sandstone. See text for further details and explanation.

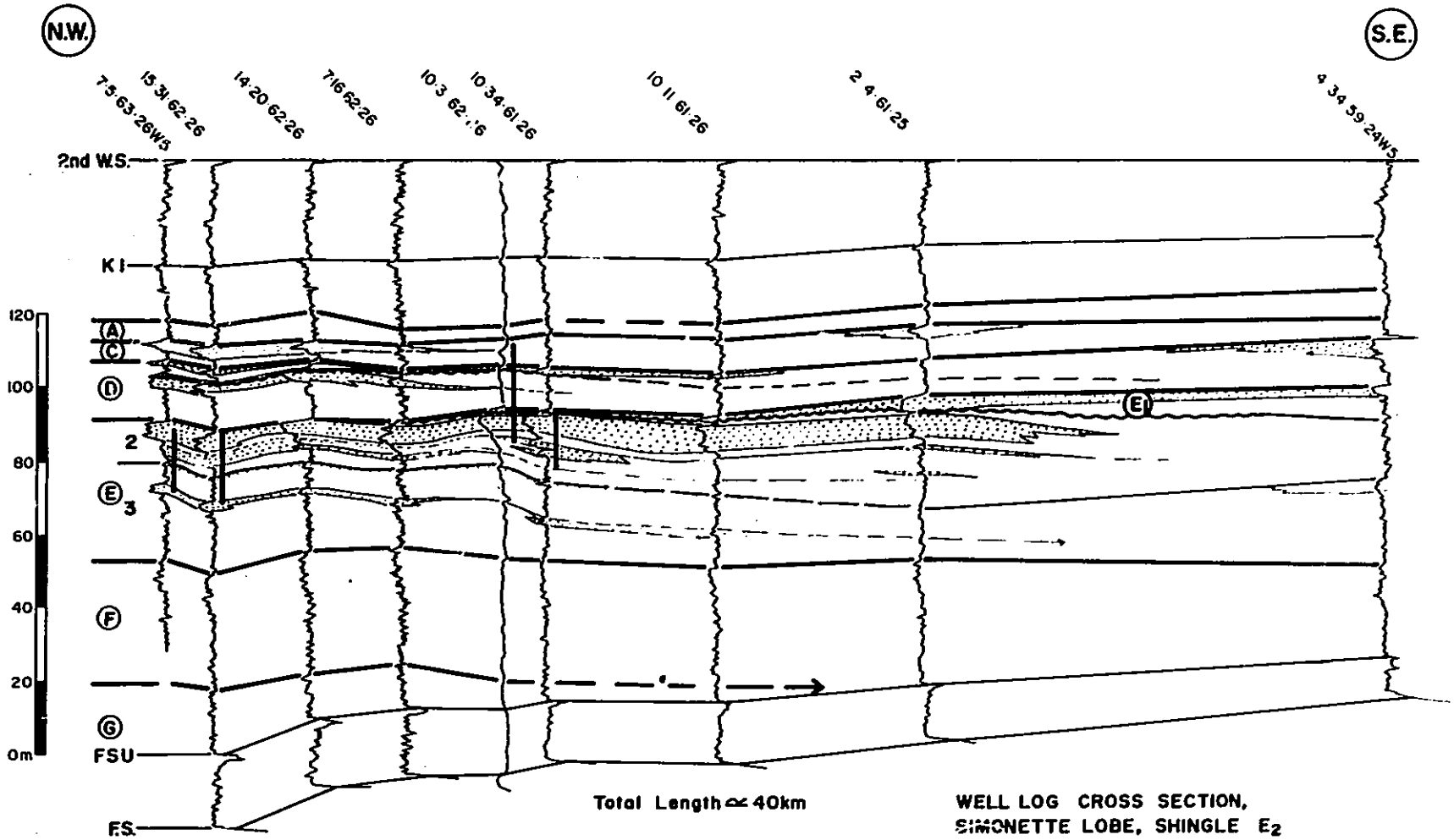
N.W.
S.E.
7-5-63-26W5
13-31-62-26
14-20-62-26
7-16-62-26
10-3-62-16
10-34-61-26
10-11-61-26
2-4-61-25
4-34-59-24W5
2nd W.S.
K I
A
C
D
2
E3
F
G
FSU
FS
E1
120
100
80
60
40
20
0m
Total Length ≈ 40km
WELL LOG CROSS SECTION,
SIMONETTE LOBE, SHINGLE E2

Figure 4-13B. Dip Oriented Core Cross Section through Simonette Lobe, Shingle E2. Well developed coarsening upward facies successions, typical of Facies Association 1B, are present in all of the wells. These are indicated by the arrows and are interpreted as being typical of prograding river-dominated delta front environments. Note the laminated, non-bioturbated nature of basal mudstones; the lack of HCS or wave-rippled sandstone; and the abundance of soft sediment deformation features in shingle E2 in all of the wells. Emergence at the end of shingle E2 coincides with channel downcutting associated with shingle E1. Cross section is hung on the top of member E. See text for further details and explanations, and figure 2-29 for facies legend.

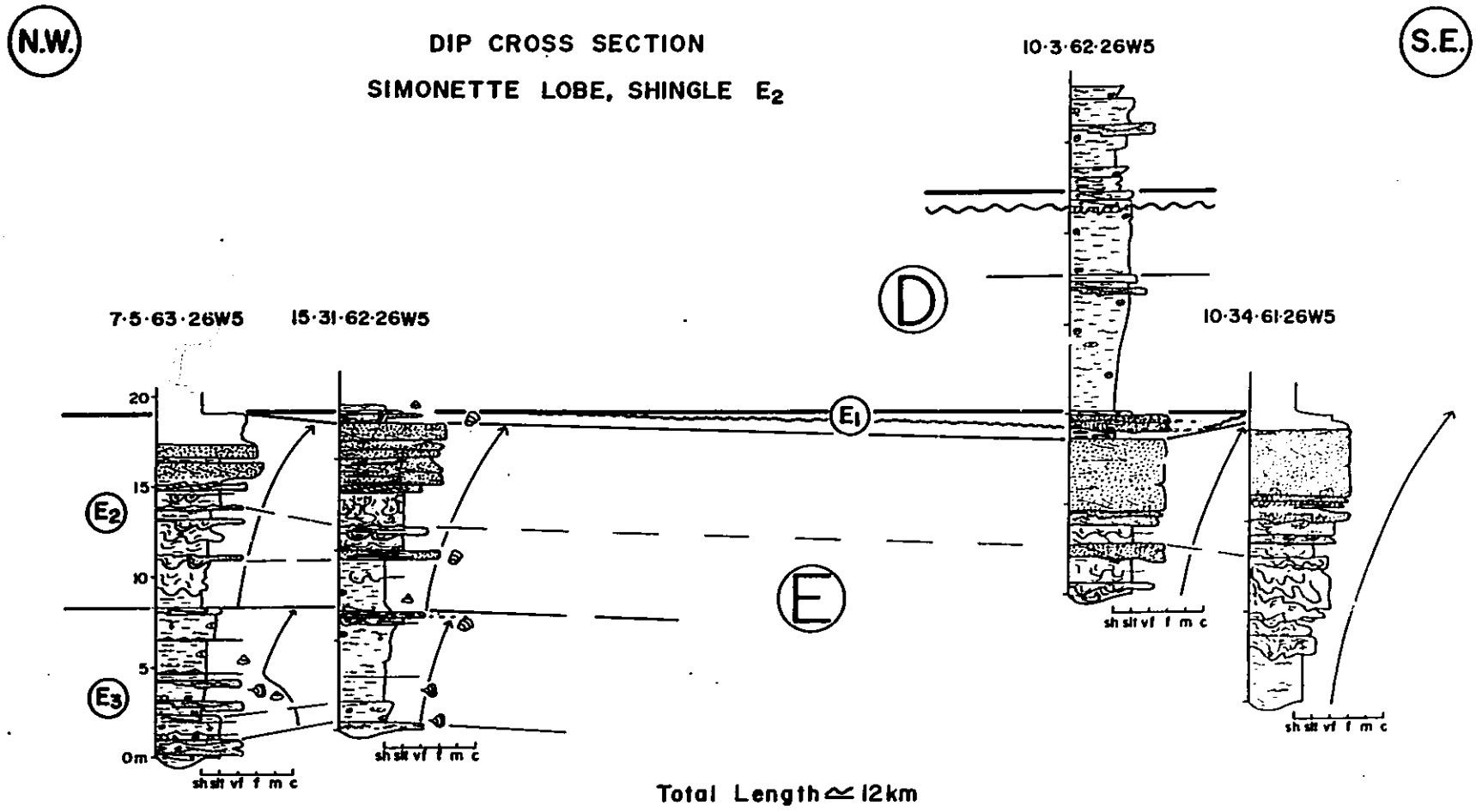
N.W.
DIP CROSS SECTION
SIMONETTE LOBE, SHINGLE E2
S.E.
10-3-62-26W5
7-5-63-26W5
15-31-62-26W5
10-34-61-26W5
D
E1
E2
E3
E
20
15
10
5
0m
sh slt vf f m c
Total Length ≃ 12km

main coarsening upwards facies succession in each of the wells (indicated with the arrows) is similar and is typical of Facies Association 1B. Large scale soft sediment deformation features are ubiquitous in all of the cored wells. Wave rippled and HCS sandstones (Facies 7B and 7A) are not observed and current-rippled to cross-bedded sandstones (Facies 7C and 7D) predominate. Sandstones are mostly fine-grained and are more massively bedded in wells 10-3 and 10-34 than in wells 7-5 and 15-31. In wells 15-31 and 10-3, thin carbonaceous shales (Facies 1C) cap the main succession, although root traces were not observed to the southeast in well 10-3. Below the top of member E, in well 10-3, about one meter of coarser-grained cross-bedded sandstone containing numerous mud-chips sharply lies above the carbonaceous shale.

Interpretation

The coarsening upwards facies successions are typical of the deposits of prograding, river-dominated deltas, as outlined in section 4-4-1 and in chapter 2 (section 2-3-1B). The lobate geometry of the sandstone body and the presence of an updip bottleneck is similar to the sand body geometries of river-dominated deltas (Coleman and Wright, 1975; Elliot,1986). The facies and sand body geometries suggest that sand body 2 represents a sandy deltaic lobe fed by a distributary channel towards the northwest. The well log cross section suggests that the surface of this lobe dips towards the southeast.

4-5-5. Cross Section Through E3 Lobe and E3 Inter-lobe

Figure 4-14A and 4-14B represent well log and core cross sections respectively through the southern lobe of shingle E3. The well log cross section is hung on the base of the Second White Specks and extends for about 50 kilometers. It passes through the northern side of the western half of the southern lobe (Fig.4-5B, #2c). The internal stratigraphic relationships of shingles within member E, as shown on the well log cross section (Fig.4-14A), are similar to those shown on the regional schematic cross section (Fig. 4-2). Three shingled sand bodies (E2, E3 and E4) are evident, each dipping towards the southeast. Sandstones belonging to shingle E4 pinch out between wells 6-22-61-2W6 and 5-27-61-1W6, as indicated with the dashed correlation line. Gamma logs through E4 show fairly well developed funnel-shaped profiles, indicating sanding or coarsening upwards. Shingle E3 is relatively uniform in thickness (about 15 meters) over the length of the cross section. On the southeastern half of the cross section (Fig.4-14A) gamma logs through E3 show fairly well developed funnel-shaped profiles, especially in wells 2-6-62-2W6 and 6-22-61-2W6. The response becomes more irregular to the northwest and southeast.

Shingle E2 thins towards the northwest. Southeast of well 3-9-62-3W6, gamma logs through shingle E2 indicate coarsening upwards. A major "blocky" channelized sand body erodes into shingles E2 and E3 in well 11-15-61-1W6. This sandstone is

Figure 4-14A. Dip Oriented Cross Section, Southern Lobe, Shingle E3. All well traces are gamma logs. Vertical bars represent cored intervals shown in figure 4-14B. Heavy stipple indicates channelized sandstone. Light stipple indicates sandstone. Shingles E4, E3, E2, and E1 are shown with the medium black correlation lines within member E. The lowest is shingle E4 which pinches out between wells 6-22 and 3-11. The only portion of shingle E1 that is present is the channel sandstone in well 11-15. These shingles dip to the southeast. See text for further discussion.

Figure 4-14B. Dip Oriented Core Cross Section through southern lobe of Shingle E3. Cross section is hung on the K1 marker. Arrows represent coarsening upward facies successions. Well 6-11 ties with the regional strike oriented cross section (Fig.3-8A). See text for explanation and figure 2-29 for facies legend. Members D, C, B, and A are discussed in relevant chapters.

DIP WELL LOG
E_3 LOBE & INTE

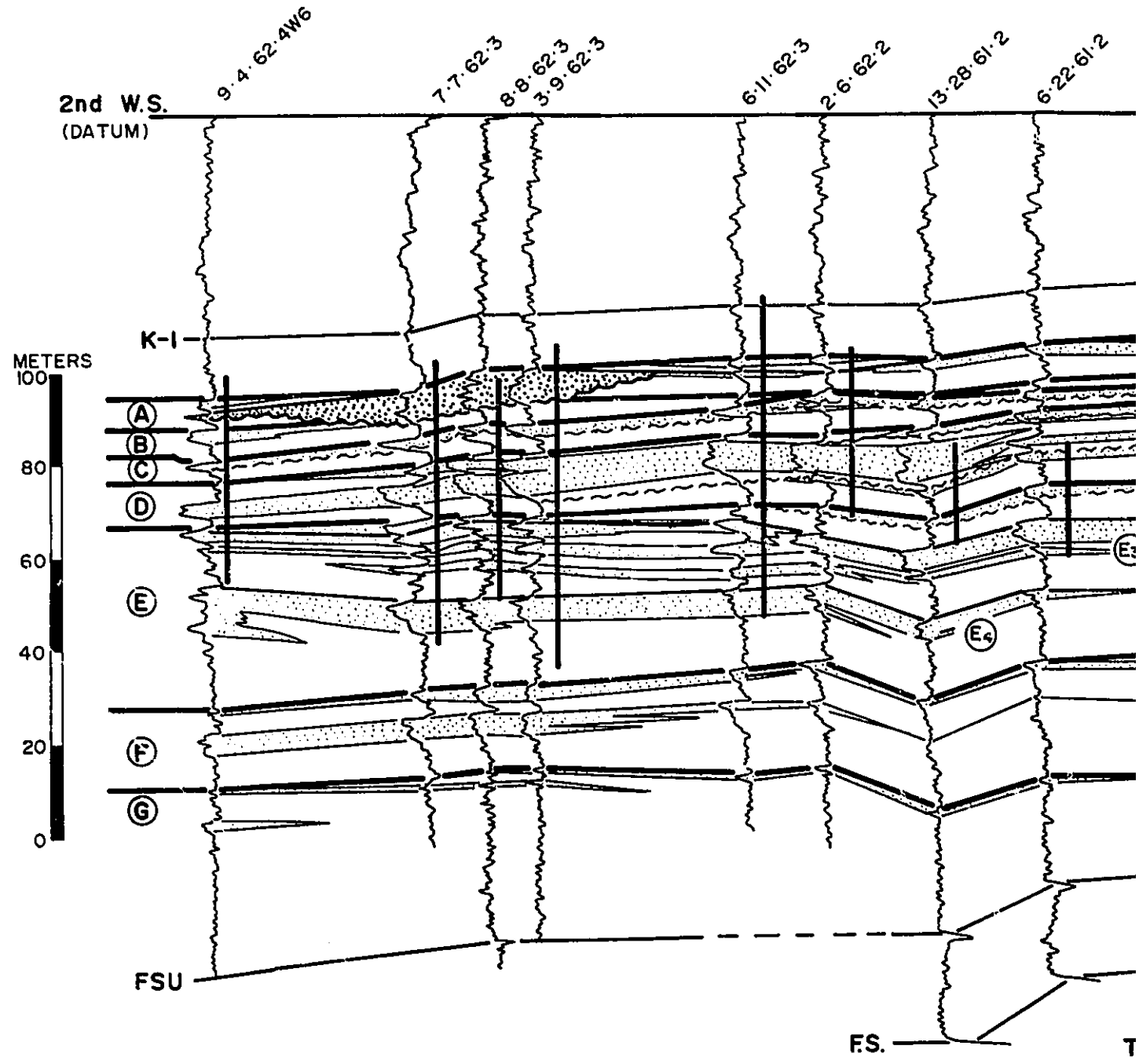

. LOG CROSS SECTION
3 INTERLOBE

S.E.

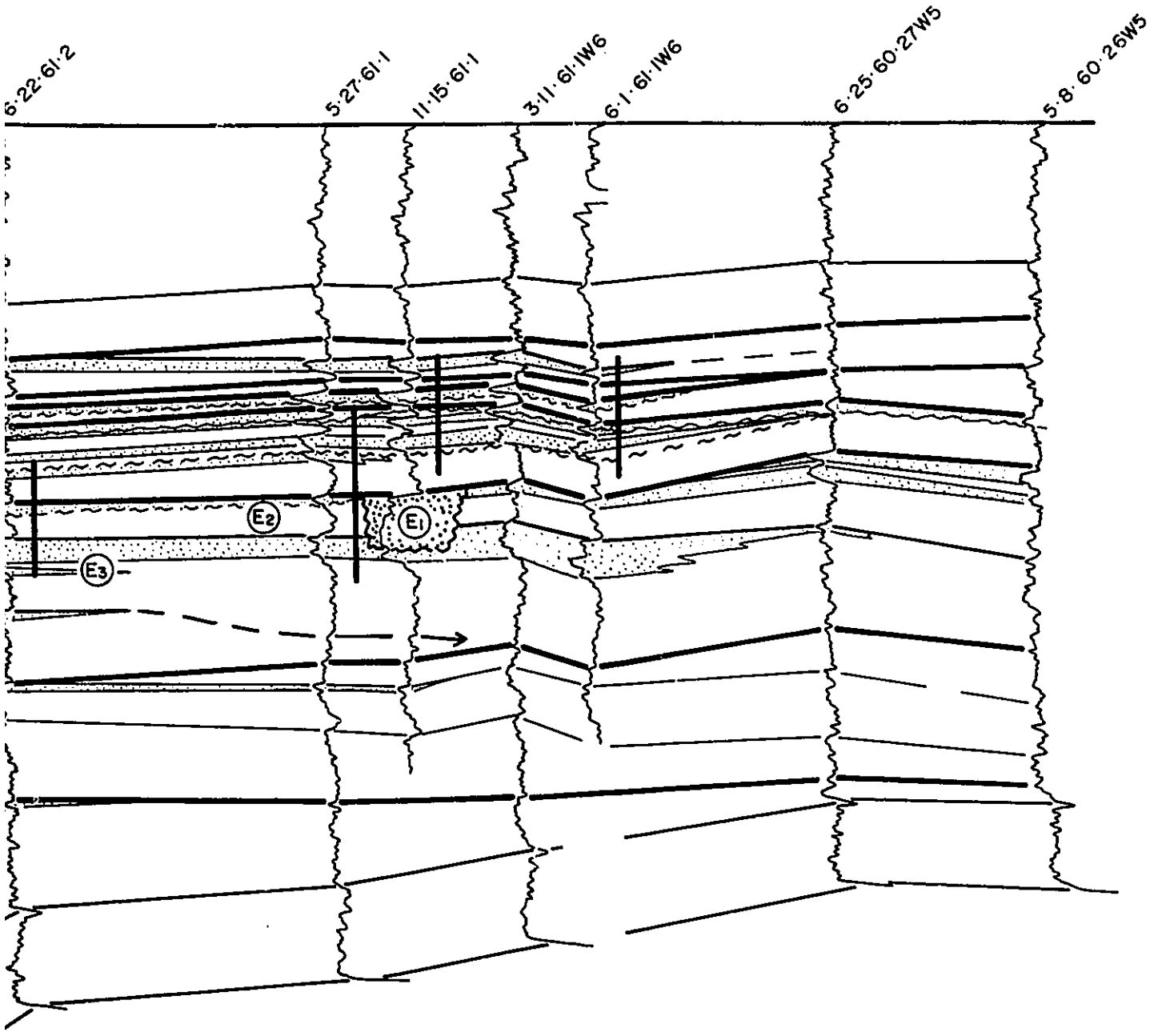

TOTAL LENGTH ≃ 50km

DIP CORE CROS
E_3 LOBE & IN

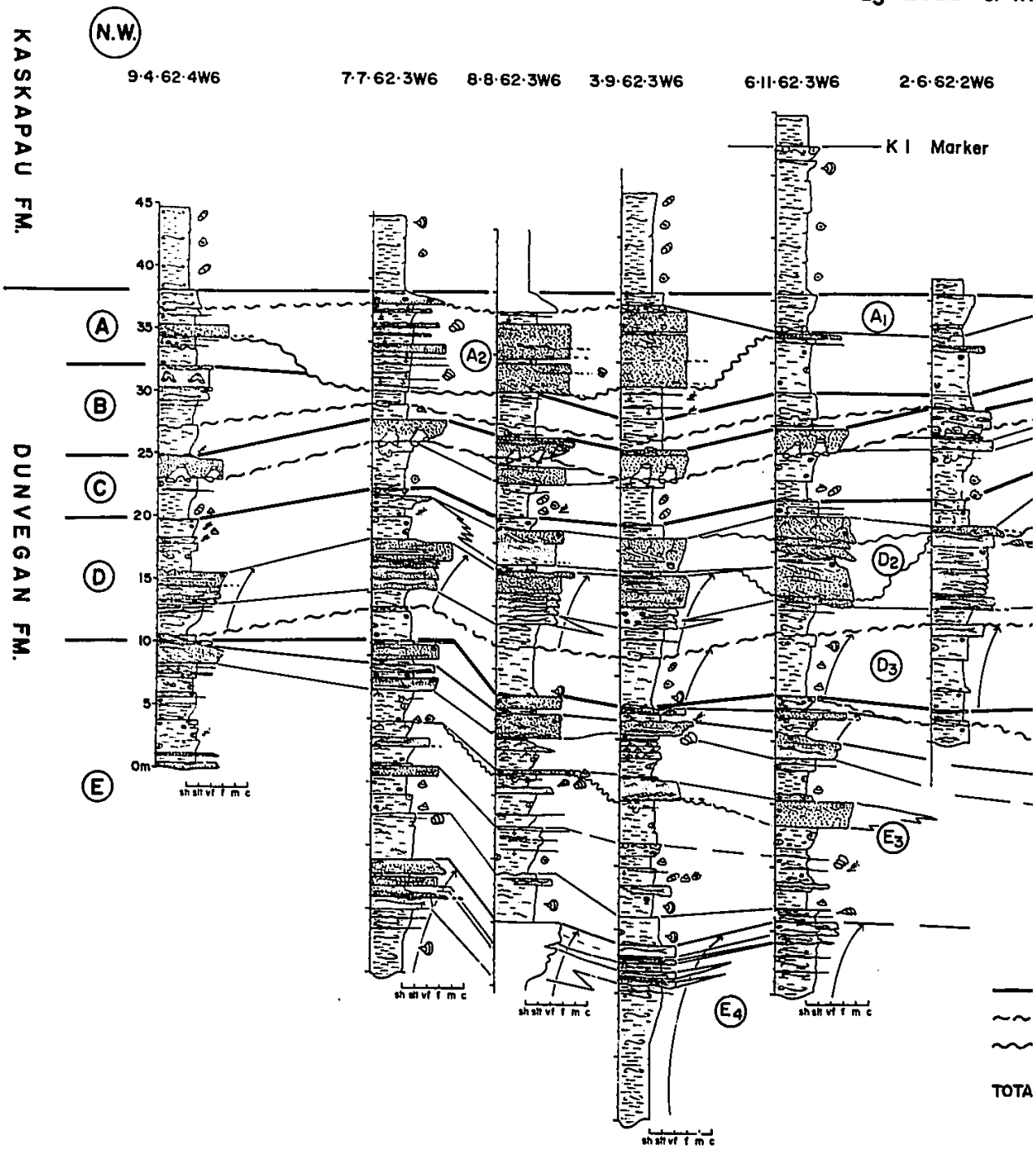

CORE CROSS SECTION
LOBE & INTERLOBE

S.E.

2-6-62-2W6 13-28-61-2W6 6-22-61-2W6 5-27-61-1W6 11-15-61-1W6 6-1-61-1W6

C1 Marker

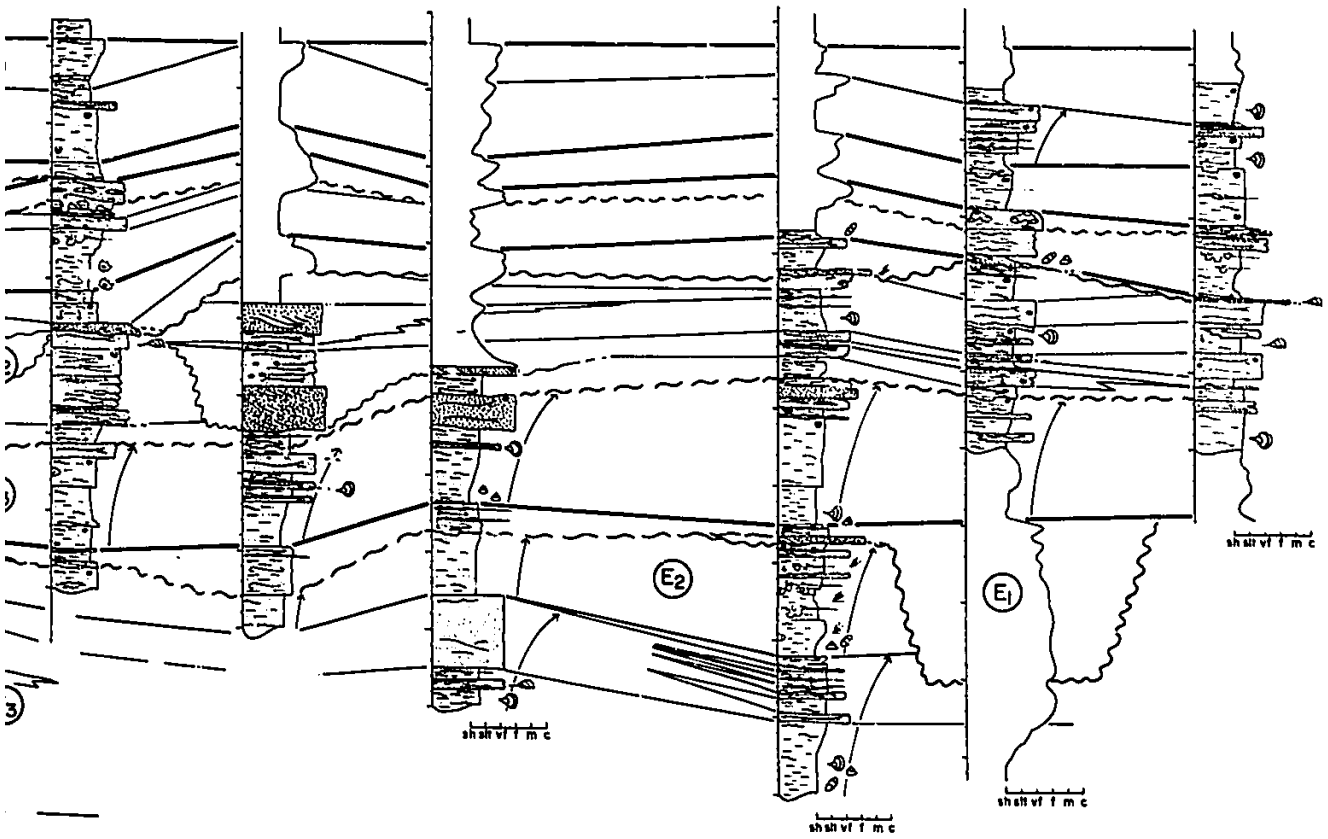

T SURFACE
Em SURFACE
Ec SURFACE

TOTAL LENGTH ≈ 35km

associated with shingle E1 and produces the southern "bullseye" in the map of E1 sandstones (Fig.4-3A).

The accompanying core cross section (Fig. 4-14B) extends for about 35 kilometers and is hung on the contact between the Dunvegan and Kaskapau Formations (top of member A). Shingle E4 is cored in wells 7-7-62-3W6, 3-9-62-3W6 and 6-11-62-3W6. All three cores show a well developed coarsening upwards facies succession typical of an incomplete (top missing) Facies Association 1A. Core photos of shingle E4 in well 6-11-62-3W6 are also shown in figure 3-7C (lower 0.0-6.2m). Pervasively bioturbated mudstones (Facies 3A) coarsen upwards into HCS sandstones (Facies 7A). These sandstones thin towards the southeast, especially between wells 3-9 and 6-11. These sandstones are sharply overlain by several meters of bioturbated to laminated marine mudstones containing *Inoceramus* which comprise the base of the next overlying shingle (E3).

Shingle E3 shows a rather drastic down-dip change in the types of facies successions it contains. Northwest of well 2-6-62-2W6 the facies successions are relatively non-sequential and are typical of Facies Association 3. In well 9-4, the facies alternate between current rippled sandstone (Facies 7C) and laminated to burrowed pinstriped mudstones and blockstones (Facies 4 and 2) and culminates in about a meter of fine-grained, cross bedded sandstone (Facies 7D) at about 9 meters. In wells 7-7, 8-8-62-3W6, 3-9, and 6-11 shingle E3 is completely cored. Broadly, the

facies show a shallowing upwards beginning with marine blockstones and culminating in sandstones and mudstones containing *in situ* root traces and coaly horizons. In well 3-9 (a typical well) the facies succession begins with about 5 meters of Inoceramus bearing marine blockstones (at about 15 meters) containing one sandy gutter cast and many synæresis cracks. These blockstones pass upward into about 6 meters of burrowed, sideritic pinstriped mudstones (Facies 4) which contain two nested coarsening upwards cycles in the lower half. Convolute lamination occurs towards the top in the upper half. Equivalent mudstones in well 8-8 (at about 16 meters) contain *Brachydontes* sp. and oysters, but no forams: These pinstriped mudstones in both wells are erosively overlain by a sandstone which is dominated by climbing current-ripple cross laminated sandstone (Facies 7C) in well 3-9. The basal erosion surface is marked by a thin siderite and fossil rich lag. This sandstone is not present in well 7-7, but its equivalent is a surface containing *in situ* root traces. In well 6-11, this sandstone also has a sharp base and is characterized by high angle cross bedding (Box 3, 14-16m, Fig.3-7C). In Figure 3-7C, a few large burrows are visible towards the top of this sand body. In the adjacent wells (Fig.4-14B) this sandstone grades up into more pinstriped mudstones containing *in situ* root traces which are in turn overlain by a thin coal (Facies 10). A thin bioturbated sandstone lies above this coaly horizon, in well 3-9, and quickly coarsens upwards into wave-rippled sandstone (Facies

7B) also containing *in situ* root traces at about 47 meters. Core through E3, in well 6-11-62-3W6 (Fig.3-7A,B,C), shows a similar facies succession, but in contrast the coaly and rooted horizons are absent and the uppermost sandstone (at about 20 meters) is burrowed and shows HCS and wave-rippling. Core photos of this well are shown in figure 3-7C. A close-up photo of the wave rippled sandstones from box 4, at about 20m, is shown in figure 2-12a. Shingle E3 begins with about a meter of bioturbated mudstone which passes abruptly upward into laminated blockstones in box 4 (3.6-8.2m). These are overlain by about 6 meters of burrowed banded mudstones (Facies 5) and pinstriped mudstones (Facies 4) (boxes 1-4, interval 8.2 to 12.8m, and boxes 1 and 2, interval 12.8 to 16.6m). These mudstones are sharply overlain by about 2 meters of cross bedded sandstone with a few burrows towards the top (boxes 2,3, and 4, interval 12.8-16.6m). This sandstone passes back into several meters of mostly pinstriped mudstones. These mudstones grade upward into about 2 meters of cross bedded to HCS sandstone which in turn is sharply overlain by black mudstone which marks the upper contact of shingle E3 in box 1, interval 21.3-26.0. Shingle E3 is followed by about 1.5 meters of laminated to bioturbated muddy sandstones. These are sharply overlain by the laminated mudstones comprising the base of member D in box 3, interval 21.3-26.0m.

Towards the southeast, in wells 6-22-61-2W6 and 11-15-61-1W6, shingle E3 shows a well-developed coarsening upwards facies

succession, typical of Facies Association 1C as indicated with the arrows. Laminated shales and blockstones (Facies 1A and 2) containing *Inoceramus* grade up into structureless to HCS sandstones (Facies 7F and 7A). In well 6-22, HCS is poorly defined in the uppermost sandstone. These sandstones thin towards the southeast between the two wells and are sharply overlain by mudstones comprising the base of shingle E2. The upper contact of shingle E3 is variable in nature. In some of the wells, such as 6-11 and 5-27, the contact is burrowed to angular and sharply overlain by laminated to burrowed shales and mudstones. In other wells, the contact is sharp but flat and overlain by blockstones (e.g. well 6-22) while in other wells, notably 11-15, the contact is erosively cut into by channelized sandstones associated with upper shingles.

Shingle E2 thins dramatically towards the northwest. The greatest preserved thickness of E2 sediments cored on this cross section (Fig.4-14B) is in well 5-27-61-1W6. The facies succession in this well coarsens upwards and is typical of Facies Association 1B. Thick sands are not present and the succession is truncated at about 16 meters by fine-grained cross-bedded sandstones (Facies 7D) of shingle E1. In the wells to the northwest, bioturbated marine mudstones sit sharply on laminated mudstones of shingle E2. These bioturbated sediments are thickest in well 13-28-61-2W6 (3 meters). Sharply overlying these sediments are the laminated marine shales and blockstones which comprise the base of

overlying member D. This contact is marked by a bioturbated sandy mudstone in every well except 9-4 and 7-7.

Interpretation

A few specific aspects of the geology of shingle E3 will be discussed here as well as some comments on the nature of the upper contact of shingle E2. In general E3 shows a transition from relatively deep marine mudstones (Facies 2) to dominantly brackish to non-marine facies (characterized by the coaly rooted horizons) both upwards and from southeast to northwest (i.e. landward). In wells 7-7, 8-8, 3-9 and 6-11, there are no thick sandstones which mark this vertical transition from marine to non-marine facies. The facies succession produced is typical of Facies Association 3 and is interpreted as representing the deposits of prograding delta-plain and interdistributary bay environments. A relatively open marine environment is represented by the *Inoceramus* bearing blockstones containing sandy gutter casts. This environment gradually becomes more restricted in character as represented by the overlying wave-rippled, pinstriped mudstones. Channels and crevasse splays occasionally spilled into this environment as indicated by the presence of thin, erosively-based, current-rippled sandstones. Laterally equivalent shallow, vegetated, marshy environments also existed at this time as indicated by the presence of typical brackish water fauna (e.g. *Brachydontes* sp. and oysters) and rooted highly carbonaceous mudstones. A subtle transgression is indicated by the presence of a thin bioturbated

to wave-rippled sandstone in well 3-9 which also contains *in situ* root traces.

Towards the southeast, shingle E3 becomes dominantly more marine in character. The mudstones, which are equivalent to the non-marine pinstriped mudstones towards the northwest, are primarily blockstones. These blockstones contain abundant *Inoceramus* which probably indicate a more open-marine environment (Kaufmann, 1969). About 5 meters of HCS sandstones, probably deposited in a lower shoreface environment, lie above these blockstones.

The upper contact of shingle E2 is variable. Locally, such as in well 11-15, it is erosively truncated by shingle E1 producing an Ec surface (equivalent in time to the Simonette channel). In other wells (e.g. 6-22 and 13-28) bioturbated marine mudstones (Facies 3A) erosively truncate E2 producing an Em surface. These bioturbated sediments resemble bounding sediments and may be related to transgression. This Em surface, however, is interpreted as being later in time than the Ec surface related to erosion by the Simonette channel.

4-5-6. Regional Strike Cross Section and Core Through E3 Shoestring

Figure 3-8A and 3-8B, introduced in chapter 3, include cores through member E. The well log cross section (Fig.3-8B) penetrates two shoestring sandstones. The youngest is indicated at the top of member E in well 11-22-64-2W6. It shows a blocky

log response indicating about 17 meters of sandstone, although it was not cored in this well. This sandstone cuts into adjacent shingles (E2 and E3) and is correlated with the Simonette channel (E1). The shoestring sandstone indicated on the gross sandstone isolith map of shingle E3 (Fig.4-5A) is penetrated in well 3-6-61-4W6 and is indicated by a similar blocky log response indicating about 18 meters of sandstone. Correlation with adjacent wells indicates significant erosion of shingle E4 and the lower portions of shingle E3. This erosion surface is penetrated in well 12-22-60-5W6, where it is seen cutting into shingle E4. The facies succession above the surface fines upwards and is typical of Facies Association 2A. It begins with a fossil rich basal lag (Facies 8) erosively overlying very fine-grained HCS sandstones (Facies 7A). This lag is followed by about 5 meters of fine-grained, cross bedded sandstones (Facies 7D) comprising two erosively based graded beds which pass upward into very fine-grained, current-rippled sandstones (Facies 7C) interbedded with shales. Similar sandstones are seen at about the same stratigraphic level in all of the adjacent wells. The facies successions through member E, in wells 4-11-65-2W6, 4-8-63-2W6, 7-17-61-3W6 and 12-7-59-5W6, are similar and are broadly typical of Facies Association 3. In well 4-11, the cross bedded sandstones in shingle E3 pass upwards into pinstriped mudstones containing one HCS to cross-bedded sandstone at about 10 meters. These pinstriped mudstones pass upwards into thin sandstones and

deformed siltstones capped by carbonaceous, coaly shales (Facies 1C) containing *in situ* root traces. Overlying this is about 3 meters of oyster-rich bioturbated mudstones which are in turn overlain by cross bedded sandstone (Facies 7D). A close-up photo of this oyster bed is shown in figure 2-3c.

The facies succession through E3 in well 4-8 is shalier and contains abundant oyster and *Brachydontes* rich horizons, but not as thick as in well 4-11. Shingle E2 is thin to non-existent over most of the cross section. In most of the wells, member E is capped by a thin sandy bioturbated horizon which quickly grades into laminated blockstones (Facies 2) comprising the base of member D.

In well 12-22-60-5W6 (Fig.3-8A), shingle E4 shows a coarsening upwards facies succession typical of an incomplete type 1A Facies Association. It begins with about 15 meters of pervasively bioturbated shales (Facies 1B) and mudstones (Facies 3A). The upper portion is truncated by sandstones in shingle E3.

Interpretation

The E3 shoestring sandstone is interpreted is a major distributary channel. The sandstone is erosively based and exhibits a fining-upwards facies succession typical of sandy channel fills (Facies Association 2A). The laterally equivalent sandstones in most of the other wells (e.g. well 4-8) are thinner and may represent time-equivalent crevasse channel or crevasse splay deposits. Some of the associated pinstriped mudstones,

containing *in situ* root traces, may represent laterally equivalent marshy levee deposits.

4-6. General Interpretations

For each of the shingles discussed below I have presented a paleogeographic reconstruction shown in figure 4-15 a, b, c, and d. These reconstructions combine data from isolith maps and cross sections. These paleogeographies are combined in figure 4-15 in order to illustrate the evolution through time of shorelines and deltas within member E.

4-6-1. Shingle E4

Shingle E4 is interpreted as representing the deposits of prograding lobate deltas which show a relatively high degree of reworking by basinal processes (Fig.4-15a). The sandstone body geometry of shingle E4 (Fig.4-6A) indicates an irregular, but fairly smooth, depositional edge and the presence of at least two distinct deltaic lobes, although channelized shoestring sandstones were not detected. Coarsening upward facies successions through the thicker portions of these lobes are typical of Facies Association 1C (Fig.4-8), and 1A (Fig.3-8A) and support an interpretation as resulting from the progradation of storm- and wave influenced shorelines. The distal, basinward equivalents of these coarsening upwards facies successions are more similar to the lower portion of Facies Association 1A (e.g. well 12-22, Fig.3-8A). These facies associations are interpreted as resulting

Figure 4-15. Paleogeographic reconstructions based on gross sandstone isolith maps and facies, a. Shingle E4, b. Shingle E3, c. Shingle E2, d. Shingle E1. Note that sandstones within successive shingles lie progressively farther seaward into the basin. Heavy stipple indicates subaerial portion of deltas. Light stipple indicates marine sandstones associated with each deltaic system. Channels are indicated by bifurcating lines. Areas of non-deposition are indicated to the northwest of the barbed line. Plant symbol indicates the approximate area of vegetated exposed regions. This becomes larger with each succeeding shingle. The actual probable shoreline configuration is interpreted to correspond approximately to the contact between the heavy and light stipple. The dashed region indicates areas dominated by marine mud deposition (prodelta to shelf). See text for further explanation and discussion.

DUNVEGAN PALEOGEOGRAPHY
MEMBER E

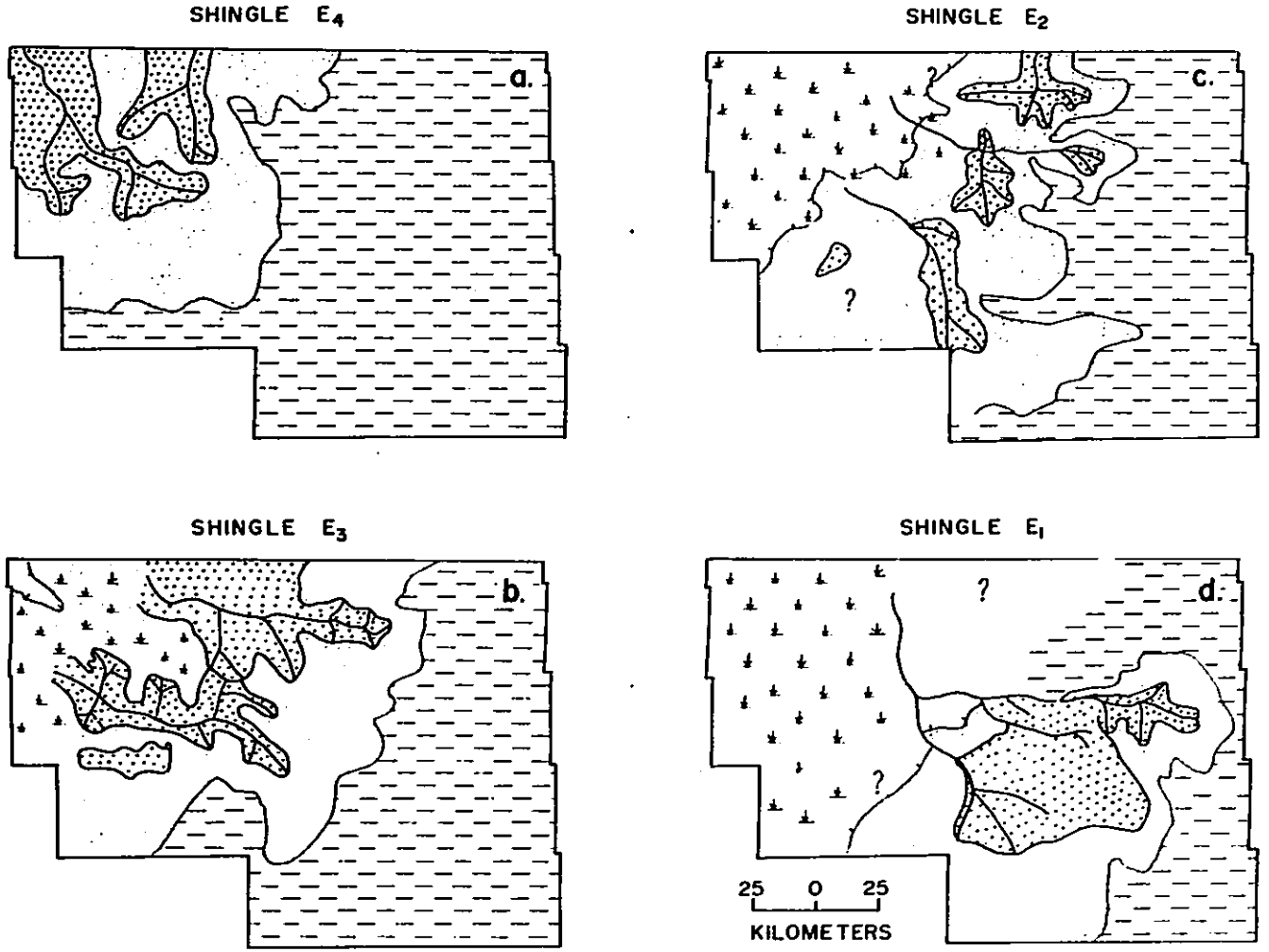

from lower sedimentation rates and a relatively greater degree of wave and storm reworking in the deeper parts of the basin. This is probably a function of decreasing river influence farther into the basin rather than an absolute increase in the energy of basinal processes.

4-6-2. Shingle E3

Shingle E3 is interpreted as representing the deposits of at least two overlapping river-dominated deltas with some reworking, mostly by storm processes (Fig.4-15b). The sand body geometries (Fig.4-5A,B) suggest the presence of two discrete sandy deltaic lobes associated with shoestring sands interpreted as sandy distributary channels. Each lobe is composite in nature and exhibits an elongate digitate geometry comprising three finger-shaped sub-lobes. These geometries are typical of river-dominated deltas (Coleman and Wright, 1975). Additional sub-lobes attached to the northern side of the southern distributary probably represent crevasse splays produced during over-spilling of the distributary.

Towards the northwest (as shown on cross section 4-14B) the facies indicate that shingle E3 is dominantly non-marine in character. The facies successions are typical of Facies Association 3 and are interpreted to indicate typical interdistributary bay and delta-plain environments with associated *in situ* roots and coaly horizons and oyster-rich beds. These delta plain environments are cut by major distributary channels

(Fig.3-8B) up to 18 meters thick, which also erode into underlying shingle E4. These channels lie in a southeast/northwest direction and suggest a paleoslope toward the southeast. This orientation is consistent with the direction of depositional dip determined in chapter 3. Some of the associated rooted horizons and thinner current-rippled sandstones may represent laterally equivalent levee and crevasse splay deposits. These crevasse splays produce small sub-lobes attached to the north side of the southern channel (Fig.4-5A,B). Towards the basin (southeast), delta front sands are fairly thin (less than about 6 meters) and the facies indicate some reworking by storm and wave processes (Facies Association 1C). The absence of thick shoreface sands in the northwestern half of figure 4-14B suggests that this storm and wave reworking was not enough to redistribute delta front sandstones over large areas, and shore parallel sand bodies were not observed. In areas in which there was no encroachment of delta fronts (e.g. interdistributary bays), shallowing-upwards facies successions are produced without a well developed coarsening upwards, and without the deposition of thick sands. This results from the gradual restriction of open-marine environments produced as the E3 deltas prograded on either side of the position of cross section 4-14A,B. As the locus of deposition changed to shingle E2, local transgression occurred over shingle E3 in the southwest. In the Simonette area, shingle E3 was erosively cut by a major channel associated with shingles E2 and E1.

4-6-3. Shingle E2

Shingle E2 is interpreted as representing a series of overlapping, lobate, emergent, river-dominated deltas fed by major distributary channels (Fig.4-15c). Sand bodies 2 and 4 on figure 4-4B exhibit lobate to digitate geometries similar to river-dominated deltas described by Coleman and Wright (1975). The basinal margins of these sand bodies are highly irregular in shape. The cross sectional geometry through E2 (Fig.4-13A) suggests that each lobe comprises a series of offlapping sand bodies (or sub-deltas) separated by thin interbedded shales and mudstones. The coarsening upwards facies successions through these lobes (capped by *in situ* root traces and carbonaceous, coaly shales) are typical of Facies Association 1B and are characteristic of prograding, emergent, river-dominated deltas (Elliot, 1986). In core, the sub-deltas are characterized by nested, often poorly developed, coarsening upwards sub-cycles within the overall coarsening upwards facies succession. These facies successions are characterized by an abundance of features indicative of high sedimentation rates. These include soft sediment deformation features (mostly load casts) and climbing current-rippled sandstone. The effects of basinal processes are minimal, as suggested by the lack of HCS and wave-rippled sandstones. As well, there is a lack of sedimentary reworking by marine organisms. Facies successions in inter-lobe areas are

essentially non-sequential (Facies Association 3) and are typical of low-energy interdistributary bay environments.

The sandy deltas of sand body 2 narrow updip into a major shoestring sandstone, which produces oil and gas in the Simonette area. This shoestring sandstone is interpreted as the feeder channel for these sandy deltas. Actually, the Simonette channel also cuts into E2, as shown on cross section 4-12, and is therefore interpreted to be younger (E1). The coincidence of the E2 bottleneck with the Simonette channel suggests, however, that the distributary channel which fed E2 occupied the same position as later occupied by the Simonette channel.

A drop in relative base level is indicated by evidence of emergence and erosion at the end of E2 deposition. As demonstrated on cross section 4-14B, E2 is truncated in a landward direction. It is not clear how much sediment has been eroded, although locally, erosion due to the Simonette channel reaches up to 18 meters. Portions of E2 are also eroded during marine transgression of member E producing an Em surface.

4-6-4. Shingle E1: The Bigstone Lobe

The Bigstone lobe is interpreted as a major, southeasterly oriented, river-dominated delta fed by the Simonette channel (Fig.4-15d). The Bigstone delta occupies a large shallow valley-shaped depression in the southeastern half of the map area (Fig.4-11A). The multi-lobate shape of the E1 sandstone compares with other river-dominated deltas described by Coleman and Wright

(1975) and suggests that it comprises a series of overlapping sub-deltas. The multi-component nature of the sand body also supports this interpretation. The basinal margin of E1 is highly irregular, suggesting that delta front sandstones were not significantly re-worked or re-distributed by basinal processes.

The Bigstone delta was built as a series of offlapping lobes separated by thin shaly beds. These sub-lobes produce nested coarsening upwards cycles within the overall coarsening upwards facies succession. Facies successions through the Bigstone lobe are typical of Facies Association 1B and indicate progradation of river-dominated shorelines into a relatively low-energy basin. Rare HCS sandstones in some of the delta front sandstones, may indicate some storm influence. The lack of *in situ* root traces and coals suggests that the Bigstone delta may have been deposited mostly subaqueously.

The Simonette channel is oriented towards the northwest and suggests a paleoslope towards the southeast. This direction is in agreement with the orientation of depositional dip determined in chapter 3. The isolith values (Fig.4-3A) and cross sectional geometry (Fig.4-12A and B) suggest that the channel is about 2 kilometers in width. The channel is mostly sand filled and burrows are rare suggesting that marine influence was negligible during back-filling of the channel, probably as a result of high sedimentation rates.

Sediments of the Bigstone lobe onlap shingle E2 as shown on the regional schematic dip cross section (Fig.4-2) and on the north\south cross section through the Bigstone lobe (Fig.4-11A). This represents an abrupt basinward shift in the position of coastal onlap and may represent a major drop in base level. The widespread erosion of shingle E2, especially landward (northwest) may also be associated with this drop in base level. Although the Bigstone delta occupies a broad valley, shown on figure 4-11A, there is no evidence that suggests that this is an erosional valley. Also, while the Simonette channel shows significant erosion, it is no deeper than channels in shingle E3.

4-7. Relationship of Deltaic Systems

Figure 4-16 superimposes the outlines of the delta lobes shown in the preceding diagrams. It shows that there is not a great degree of overlap between succeeding delta lobes and indicates that the position of overlying deltaic sand bodies is controlled by the position of underlying deltas. It shows that the Bigstone delta lies about 30km seaward of sandy lobes in shingle E2 and also indicates a seaward shift of about 30km between shingles E4 and E3. In chapter 3 it was suggested that it is difficult to distinguish depositional toplap from erosional truncation. Member E records the progressive seaward progradation of sandy deltaic depositional systems accomplished in a series of seaward steps of about 30 km and culminating with the Bigstone delta. The nature of contacts between shingles is variable, as

Figure 4-16. Superimposition of Deltaic Lobes in Shingles of Member E. Based on gross sandstone isolith maps (Figs. 4-3, 4-4, 4-5, and 4-6). See text for explanation.

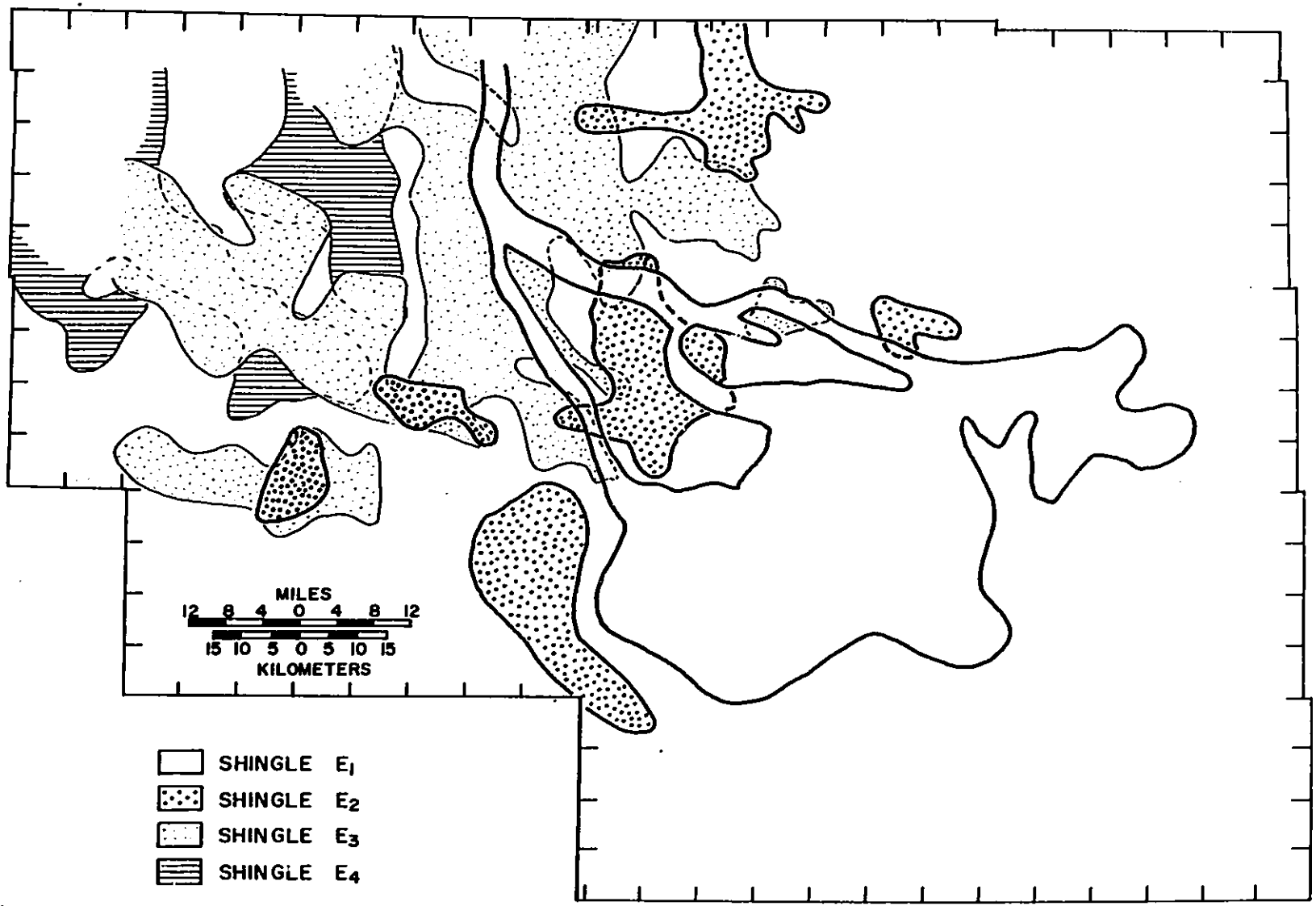
MILES
12 8 4 0 4 8 12
15 10 5 0 5 10 15
KILOMETERS
SHINGLE E1
SHINGLE E2
SHINGLE E3
SHINGLE E4

has been stressed in this chapter. While transgressive shales are being deposited on one part of an older delta system (or shingle) another part will be undergoing erosion as the next system progrades over the older one. As an example, in places, shingle E2 is directly overlain by marine shales of member D (e.g. in the northeast) while in the Simonette area, shingle E2 is eroded by the younger Simonette channel which is related to progradation ofthe Bigstone delta (shingle E1). This suggests that transitions between shingles relate to autocyclic process related to river avulsion and delta switching. This point will be returned to in the discussion of the overall evolution of the Dunvegan Formation in chapters 11 and 12.

CHAPTER 5. MEMBER D

5-1. Introduction

Like the previous chapter, this chapter has been organized into four parts beginning with this brief introduction. The second section (5-2) presents a general description of the salient aspects of member D and is followed by a general interpretation and summary of the geological history of member D. The third part presents detailed descriptions of all components of member D, along with preliminary interpretations of some of these components, and the fourth section presents general interpretations of each shingle within member D.

The casual reader may also wish to read only parts 5-1, 5-2, and 5-4. If the reader is intrigued by any particular aspect of member D or if any portion of the general description and summary is unclear, he or she may wish to probe further by reading the relevant aspects in the more lengthy descriptive portion of this chapter (section 5-3).

5-2: General Description and Summary

5-2-1. General Description

Member D produces in the Waskahigan pool (T64 R23W5 and 24W5) and in Ante Creek (T65 R23W5)(Fig. 1-8). It extends throughout the thesis area and is pod shaped ranging from about 8

to 22 meters in thickness, as shown in the total isopach map of member D (Fig 5-1). A schematic dip-oriented cross section through member D (Fig 5-2) shows that it comprises three shingled sand bodies (D3, D2 and D1) which offlap progressively towards the southeast. Towards the northwest, shingle D1 sits erosively on D2 and shingle D2 sits erosively on D3, although these relationships become conformable into the basin (southeastward) as indicated by the medium dashed lines. Erosion at the base of shingle D1 is associated with major channels (Ec Surface) while erosion at the base of D2 is not (Em Surface). The upper surfaces of these shingles dip towards the T-surface that defines the top of member E (indicated by arrows on figure 5-2).

A gross sandstone isolith map of all sandstones within member D (Fig 5-3A) shows three distinct sand bodies, also outlined in figure 5-3B. The most easterly of these sand bodies (D1 Lobe in figure 5-3B) correlates with shingle D1 and comprises a large irregular lobe which narrows towards the northwest producing a pronounced "bottleneck" in the Waskahigan area (T64 R23W5 and 24W5). The second sand body (D1 Finger in figure 5-3B) lies in the southwest portion of the map area and comprises a roughly northeast oriented finger-like sand body which reaches a thickness of over 30 meters. The third sand body (D2 Barrier in figure 5-3B) lies in the northwest half of the map and comprises a linear, northeast\southwest oriented sand body which thins towards the southwest. Its northeastern end coincides with the Waskahigan

bottleneck. This sand body is correlated with shingle D2 of figure 5-2. Sandstones within shingle D3 are not well developed and are not expressed as a distinct sand body on the gross sandstone isolith map (Fig.5-3A). The regional dip cross section (Fig.5-2) indicates that D3 sandstones are confined to the northwest.

Facies successions within shingle D3 coarsen upward and are typical of Facies Association 1C. Thick sandstones were not noted and the top of shingle D3 is truncated by a marine erosion surface as indicated in the core cross section parallel to the D2 sandstone (Fig.5-8B). A thin coarse siderite lag occurs at this surface at about 6.6m in well 7-10 (also see Fig.5-7A and 5-7B, box 10, D3 arrow). Overlying this erosion surface are the bioturbated marine sediments that comprise the base of shingle D2.

Cores through the main portion of the linear northwestern D2 sand body (Fig.5-7B; 5-8B) and the D1 lobe (Fig.5-4) show well developed, coarsening upwards facies successions typical of Facies Association 1A. Core photos of well 7-10-63-1W6 (including the D2 shingle) are shown in figure 5-7B. The succession begins with pervasively bioturbated marine mudstones (Facies 3A) and culminates in a rooted sandy shoreface overlain by a thin *in situ* coal (Facies 10) (Fig.5-7A,B). Cross section 5-8A,B (Located in Fig.5-3B) parallels the crest of the D2 linear sand body. Within D2, facies successions broadly coarsen upward (Facies Association 1A) although some of the wells on the core cross section (Fig.5-

8B), including 7-17-61-3W6 and 13-28-61-2W6, indicate nested fining-upwards facies successions, shown with arrows, similar to Facies Association 2. On the core cross section perpendicular to D2 (Fig.5-8B), the sediments behind the D2 sandstone (e.g. well 10-13-63-3W6, 14-19m) show facies successions typical of Facies Association 3. These include mudstones, which contain fauna of a brackish tc restricted marine affinity (Kaufmann,1969), including *Brachydontes* sp. and *Corbula* sp., cut by thin channelized sandstones.

A core and well log cross section through the Waskahigan bottleneck (Fig.5-5A,B) shows a well-developed asymmetric erosional channel, associated with shingle D1, which cuts into shingles D2 and D3 producing an Ec surface. The sediments which fill this channel comprise a fining upwards facies succession which begins with a coarse lag. These fining upward successions are similar to Facies Association 2B and in places the upper parts comprise mudstones containing abundant marine trace fossils. Photographs from a typical core from well 2-18-64-24W5 through this channel are shown in figure 5-6. This same D1 channel is also seen cutting into the northern end of the cross section parallel to D2 (wells 16-2 and 2-23 in Fig.5-8A) although it is not cored here. The sense of asymmetry is reversed.

The Ec surface underlying this channel is seen to extend southwestward and is picked up on the cross section parallel to the D1 finger (Fig.5-10A and B) where it erodes into the underly-

ing member E forming another major channel-like feature. The sediments which fill this southern channel (Fig.5-10B) are not burrowed and do not contain marine fossils.

Sediments of member D are blanketed by widespread bioturbated marine shales comprising the base of member C. This contact (T-surface) is always sharp, as indicated on the core and well log cross sections.

5-2-2. Summary: Geological History of Member D

Member D comprises a series of three shingled, shallow marine sand bodies and associated shales which progressively step out (offlap) into the basin from northwest to southeast (Fig.5-2). Member D is blanketed by marine shales of the overlying member C. Member D therefore represents an overall regression and is followed by a rapid basin-wide transgression.

The following is a point by point summary of the interpretations and geological history of member D.

1. Deposition of member D begins with progradation of shales and sandstones of shingle D3 onto the top of member E producing a coarsening upwards facies succession typical of Facies Association 1C. Thick shoreface sandstones were not detected in shingle D3, although they may have been removed by subsequent erosion. The incomplete facies successions present (Fig.5-8A,B) suggest that D3 represents distal, shelf equivalents of a prograding shoreline to the west. The laminated nature of the

basal mudstones may indicate relatively rapid sedimentation rates.

2. Shingle D3 is overlain by a marine erosion surface to the northwest (Em surface), which becomes conformable to the southeast. Major transgressions are usually followed by widespread deposition of thick marine shales producing T-surfaces. The absence of thick shales above this Em surfaces suggests perhaps a minor transgressive episode or stillstand.

3. Progradation of shingle D2 begins with the deposition of typical bioturbated "bounding sediments" (Fig.5-7A,B). A major, strike-oriented, linear sand body (Fig.5-3A,B) is interpreted as an extensive sandy barrier island which grew from northeast to southwest. A paleogeographic reconstruction of shingle D2 is shown in figure 5-11. Along the axis of this barrier sand, the facies comprise coarsening-upwards, wave-dominated shorefaces containing nested, fining-upwards facies successions interpreted as tidal inlet fills (Fig.5-8B; Fig.5-11, A-A'). The barrier sands dip and thin towards the southeast into shelf mudstones and, towards the northwest, they are interfingered with facies exhibiting a lagoonal affinity (Fig.5-9B; Fig.5-11, B-B').

4. Progradation of shingle D2 is followed by a major erosional event. Erosion is fluvial in nature as indicated by the presence of major channels. This erosion resulted in truncation of the northeastern end of the D2 barrier island sandstone by the

meandering Waskahigan channel (Fig.5-5A,B; Fig.5-12) and erosion of a major valley in front of the D2 barrier in the southwest (Fig.5-10A,B: Fig.5-12). Some erosion of the seaward margin of the D2 barrier is also indicated (Fig.5-2). The Waskahigan channel feeds a major cuspate to elongate sandy lobe to the southeast (D1 Lobe in Fig.5-3B; Fig.5-12, X-X') whose shape is typical of sandy wave-dominated deltas (Coleman and Wright, 1975; Weise,1979; Elliot, 1986). A paleogeographic reconstruction of shingle D2 is shown in figure 5-12. The facies within this lobe indicate significant storm and wave reworking of the sediments (Facies Association 1A). Sand is transported up to 100 km southward by longshore drift (large arrow, Fig.5-12). The preserved portions of the older D2 barrier island are overlain by non-marine swamp and marsh environments, as indicated by the presence of thin *in situ* coals. As deposition ceased in member D, the Waskahigan channel became an estuary and during the initial phases of transgression of member D it was backfilled with marine deposits producing a fining upwards facies succession typical of Facies Association 2B (Fig.5-5B; Fig.5-12, X-X'). As this transgression progressed it reached a critical point at which the entire basin was dominated by the deposition of marine shales which blanketed member D.

The reader may wish to skip the remainder of this chapter unless interested in the details of the facies successions and interpretations presented above. If the reader wishes merely to

read the interpretation of each shingle he or she may skip to section 5-6.

5-3. Detailed Descriptions with Preliminary Interpretations

5-3-1. Thickness, Extent

Member D extends throughout the thesis area and ranges from about 8 to 22 meters in thickness (Fig 5-1). A total isopach map from the top of member D to the top of member E has the shape of an undulating sheet with a rather prominent northeast-southwest oriented bump which straddles the sixth meridian. Anomalous thicknesses in the southwestern portion of the isopach map are likely the result of tectonic overthickening (Fig.5-10A).

5-3-2. Regional Dip Cross Section

Figure 5-2 is a schematic version of log correlations shown within member D on Figure 3-2. The cross section is hung on the top of member D and lithologies were traced and correlated based on interpretations made from core and well logs. The cross section is oriented northwest-southeast and is roughly parallel to the direction of depositional thinning. Figure 5-2 shows that member D comprises at least three shingled sand bodies designated D1, D2 and D3 with D1 being the youngest and D3 the oldest. The shingles progressively offlap in an east to southeasterly direction (seaward). The top surface of each shingle is interpreted as dipping into the basin and towards the transgressive surface at the top of member E. In a landward direction (northwestward)

Shingle D1 erodes into D2 and is associated with channelling (Ec Surface). Erosion also occurs at the top of shingle D3, although it is not immediately obvious from well log cross sections alone (see following detailed descriptions). This surface therefore represents a downlap surface. The shingles comprising member D are collectively overlain by a transgressive surface.

5-3-3. Gross Sandstone Isolith Map

Figure 5-3A shows a gross sandstone isolith for all sandstones within member D. Three major sand bodies are indicated and are schematically outlined and named on figure 5-3B. The most easterly sand body (D1 Lobe) covers an area of about 6500 square kilometers (2500 sq.miles) and reaches a maximum thickness of about 10 meters. It correlates with shingle D1 on figure 5-2. It shows a rather irregular north-south oriented lobate geometry which narrows towards the northwest producing a prominent bottleneck. The bottleneck lies in the Waskahigan area (T64 R23W5 and 24W5) and comprises a sandstone of much more limited extent than the southeasterly lobe, but up to 16 meters thick. The 6 meter outline of the eastern lobe defines a sand body having a distinctly cuspate geometry.

The second sand body (D2 Barrier) occupies the northwestern portion of the map area and lies westward of the eastern lobe. It comprises a northeast-southwest oriented linear sand body which ranges from 10 to 15 kilometers in width and has a length of about 100 kilometers. It pinches out in the southwest while its nor-

Figure 5-1. Total Isopach map of member D. Map indicates that member D is pod-shaped with the greatest accumulation in the northwest half of the map area. See text for discussion.

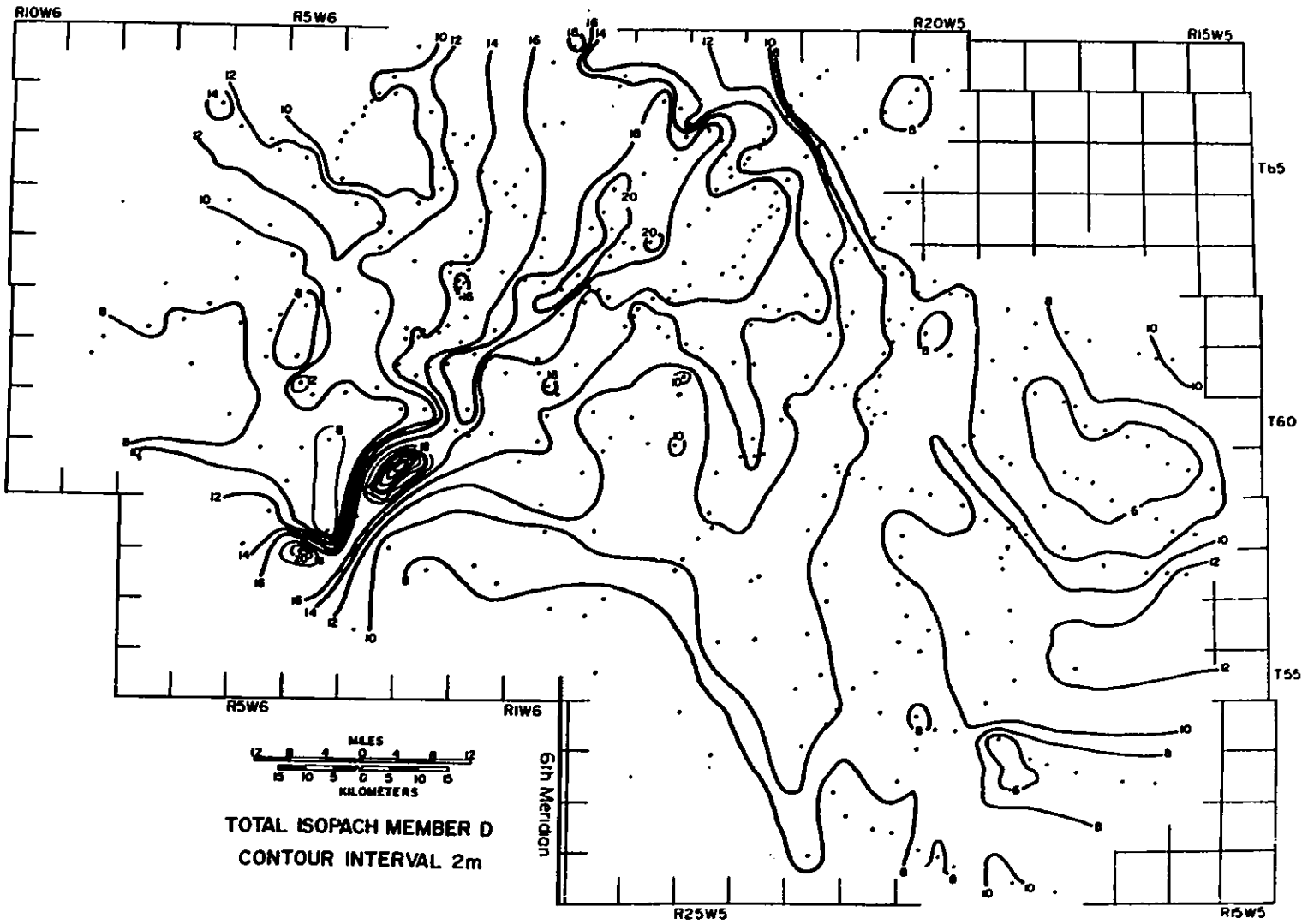
R10W6
R5W6
R20W5
R15W5
T65
T60
T55
R5W6
R1W6
6th Meridian
R25W5
R15W5
MILES
KILOMETERS
TOTAL ISOPACH MEMBER D
CONTOUR INTERVAL 2m

Figure 5-2. Schematic dip oriented cross section through member D. Root symbols indicate lagoonal and non-marine facies. Light stipple indicates sandstone. The contact between D3 and D2 is an Em surface towards the northwest which becomes conformable southeast of well 14-6-63-26W5. Shingle D1 erodes into D2 towards the northwest but becomes conformable southeast of well 3-8-62-25W5. Shingles downlap underlying T-surface. This figure is based on the regional dip cross section (Fig.3-9A). See text for further explanation.

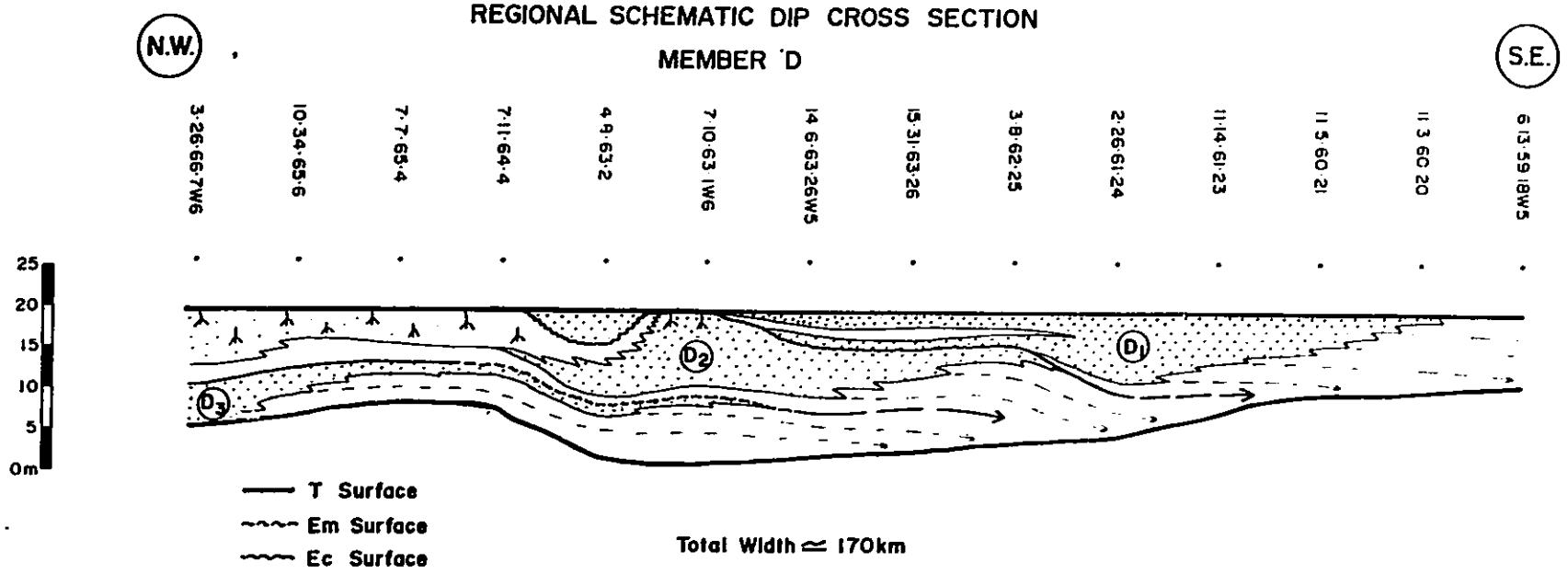
REGIONAL SCHEMATIC DIP CROSS SECTION
MEMBER 'D
N.W.
S.E.
3-26-66-7W6
10-34-65-6
7-7-65-4
7-11-64-4
4-9-63-2
7-10-63 1W6
14-6-63-26W5
15-31-63-26
3-8-62-25
2-26-61-24
11-14-61-23
11-5-60-21
11-3-60-20
6-13-59-18W5
25
20
15
10
5
0m
D3
D2
D1
T Surface
Em Surface
Ec Surface
Total Width ≃ 170km

Figure 5-3A. Gross sandstone isolith map, data points indicated by black dots, see text for discussion,

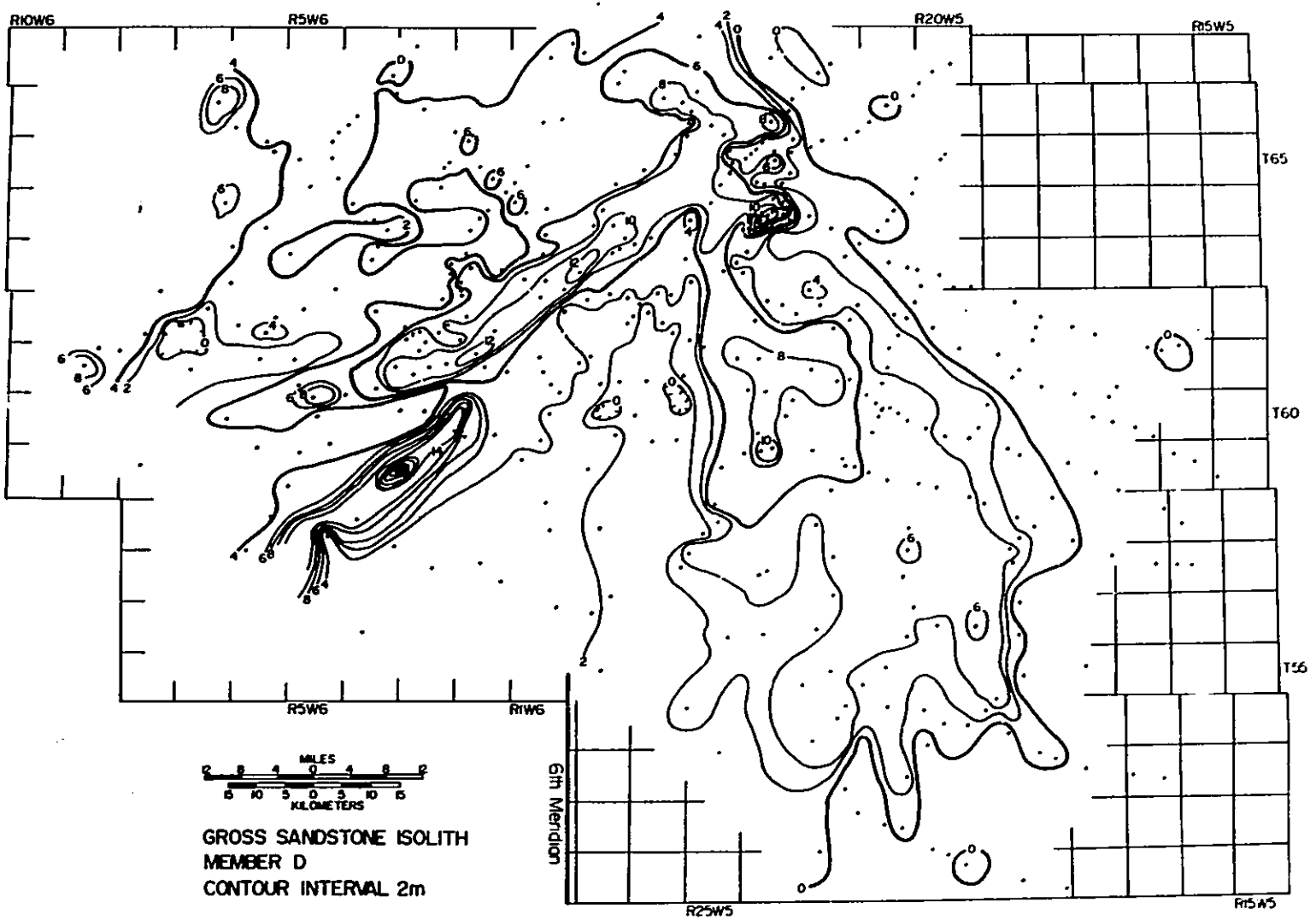
R10W6
R5W6
R20W5
R15W5
T65
T60
T55
R5W6
R1W6
R25W5
R15W5
6th Meridian
MILES
KILOMETERS
GROSS SANDSTONE ISOLITH
MEMBER D
CONTOUR INTERVAL 2m

Figure 5-3B. Outline of sandstones in member D with positions of pertinent cross sections superimposed. Open circles represent uncored wells, filled circles represent cored wells shown on core cross sections. Outlines based on Fig.5-3A. Dashed line represents 4m contour, other line represents 6m contour. See text for discussion.

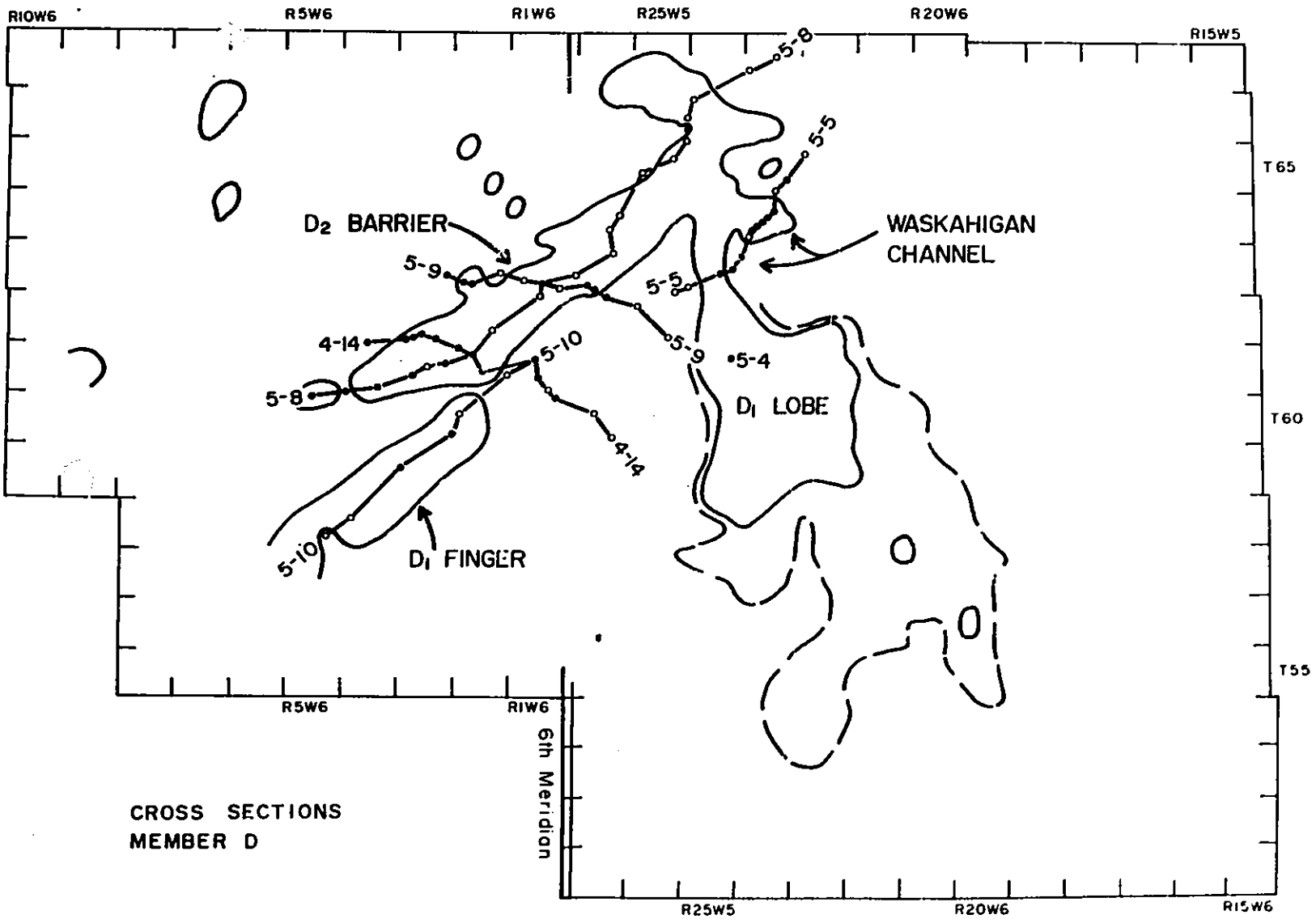
R10W6
R5W6
R1W6
R25W5
R20W6
R15W5
T65
T60
T55
R5W6
R1W6
R25W5
R20W6
R15W6
6th Meridian
D2 BARRIER
WASKAHIGAN CHANNEL
D1 LOBE
D1 FINGER
5-8
5-5
5-9
5-5
4-14
5-10
5-9
5-4
5-8
4-14
5-10
CROSS SECTIONS
MEMBER D

theast margin ends in a rather thick accumulation of sand which coincides with the Waskahigan bottleneck. Its northwest and southeast margins are relatively smooth as the sandstone thins in both directions. This sandstone correlates with D2 on the schematic cross section (Fig.5-2). A third sand body (D1 Finger) also shows a northeast-southwest orientation and lies to the southeast, between the other two sand bodies. This sand body is finger-shaped and covers an area of around 300 square km, reaching a maximum thickness of about 30 meters. Unfortunately, well control is poor in the southwest due to structural deformation of the section and it is not possible to precisely determine the geometry of this sand. It is correlated in time with shingle D1. The following will present and discuss various aspects and components of member D. Some of the cross sections presented penetrate other members. Discussion of details about members other than member D will be reserved for other more relevant chapters.

5-3-4. Facies, D1 Lobe

Only one core is available through the eastern lobe of shingle D1 (3-28-61-24W5, Fig.5-4). It penetrates two coarsening upward facies successions. The lowest succession (D2) is typical of Association 1C. It comprises about 3.7 meters of laminated marine shales (Facies 1A) and blockstones (Facies 2) and is capped with 30cm of fine-grained HCS sandstone (Facies 7A). The second succession correlates with shingle D1 and is typical of Facies

Association 1A. It begins with about half a meter of pervasively bioturbated marine mudstones (Facies 3A). It coarsens upward into very fine-grained HCS sandstone beds with bioturbated tops (Facies 7A). These sandstones amalgamate upwards into massive SCS sandstones (Facies 7A) with a few thin mudstone stringers. Unfortunately, the top of this succession is not cored, but the well logs show a large kick at the top (high gamma, high resistivity and low sonic response) which may indicate a coal (Facies 10) about one meter in thickness. This coal is fairly extensive and covers about 3 townships along the western-central margin of D1.

Interpretation

The lower succession does not contain thick sandstones. The lack of wave formed structures and the lack of abundant bioturbation suggests deposition below storm wave-base. The D2 succession probably represents the distal shelfward equivalents of a prograding shoreface. The thick hummocky to swaley sandstones of the upper succession are typical of storm and wave dominated shorefaces. The overall coarsening upward succession capped by a coal suggests progradation of a wave- and storm-dominated shoreface which eventually became emergent.

5-3-5. Cross Section Through Waskahigan Bottleneck, Shingle D1

The core and log cross section through the Waskahigan area crosses the bottleneck in a northeast-southwest orientation and is shown in figure 5-5A and B. The well log cross section

Figure 5-4. Logged core section from well 3-28-61-24W5. This facies succession is similar to Facies Association 1A and is interpreted as resulting from deposition of a wave- and storm-dominated prograding sandy shoreface. See text for discussion. Gamma ray log on left. Top of D1 not penetrated. See Fig. 2-29 for facies legend.

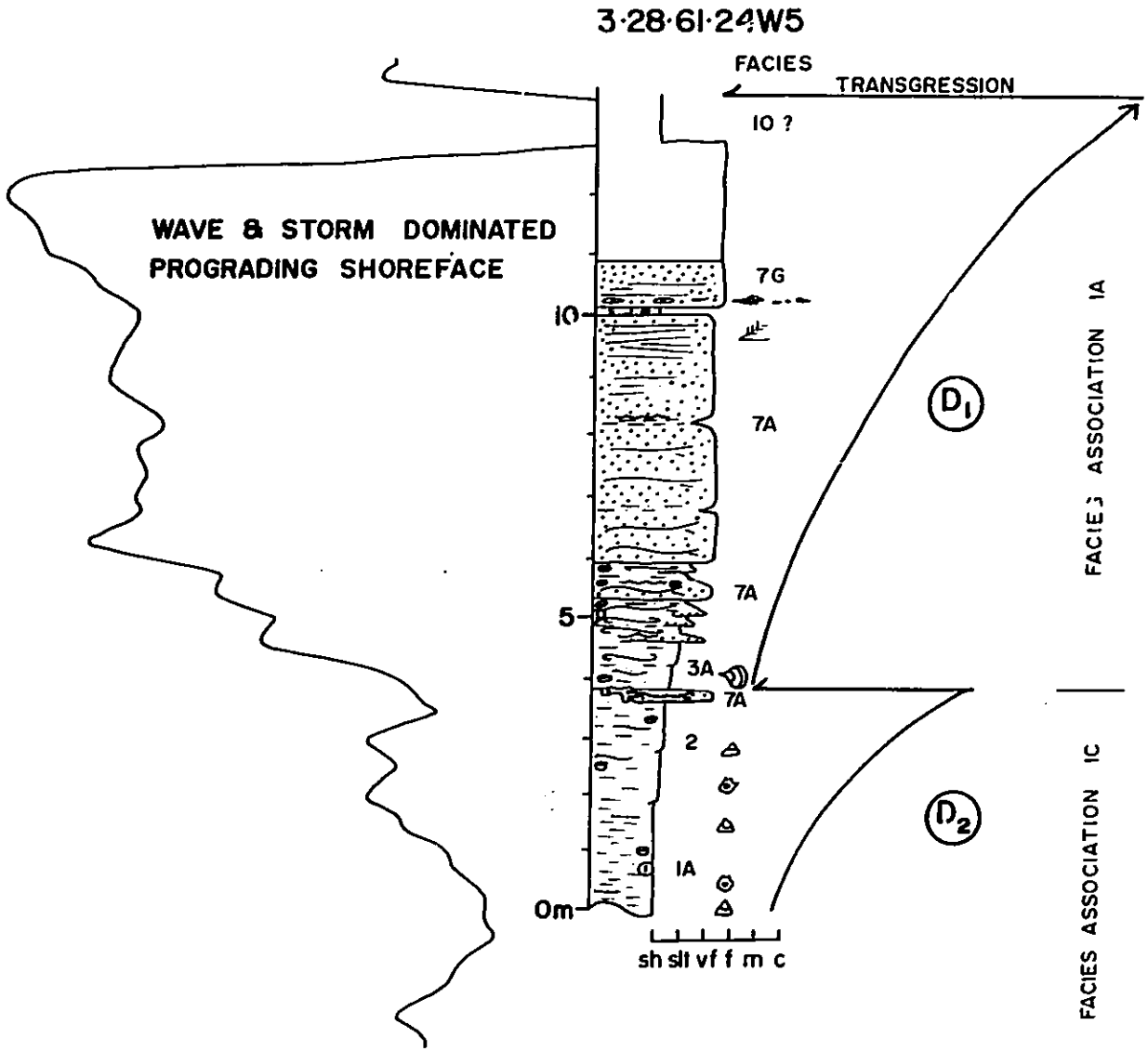
3-28-61-24W5
FACIES
TRANSGRESSION
10 ?
WAVE & STORM DOMINATED
PROGRADING SHOREFACE
7G
10
7A
7A
5
3A
7A
2
1A
0m
sh sll vf f m c
D1
D2
FACIES ASSOCIATION 1A
FACIES ASSOCIATION 1C

(Fig.5-5A) extends for about 35 km and is hung on the base of the Second White Specks. In well 15-12-6..-24W5 and 12-3-63-25W5, the gamma response through member D has a funnel shape, suggesting a decrease in the amount of shale upwards (sanding- or coarsening-upward). Sandstones in adjacent wells (especially 11-16-63-24W5, 6-18-64-24W5, 2-18-64-24W5, 10-18-64-24W5, 6-20-64-23W5 and 4-28-64-23W5) show characteristic blocky to bell shaped profiles suggesting an increase in shale upwards (fining-upwards). The core cross section (Fig.5-5B) is hung on the top of member D and extends for about 15 km. Well 15-12-64-24W5 exhibits a coarsening-upward facies succession typical of Facies Association 1A and similar to that described above for well 3-28-61-24W5 (section 5-3-4). The succession is incomplete, however, and culminates in very fine-grained sandstones containing no evidence of emergence. Adjacent wells (10-26-63-24W5 and 6-18-64-23W5) contain radically different, and considerably coarser, facies successions which fine upwards and are typical of Facies Association 2. A coarse lag, comprising siderite clasts and shelly debris (Facies 8), is well developed at the base of the main sandstone in wells 10-26, 10-18, 6-20 and 11-10 (Fig.5-5B). This lag is probably derived from marine sediments below and suggests the presence of a major erosional surface indicated on the cross section with a wiggly correlation line (Ec Surface). Northeast of well 15-12, the erosion surface has a markedly asymmetrical shape, steepest on its southwest margin (where it erodes

up to 17 meters deep), and shallowing more gradually towards the northeast (Fig.5-5A and 5-5B). To the southwest, the erosion surface also has an asymmetrical shape, deepest (maximum about 5 meters) towards the southwest in well 2-11-63-24W5 and shallowing to the northeast towards 15-12 (Fig.5-5A). The erosion surface does not cut as deeply in the southwestern half of the cross section (Fig.5-5A). Facies successions above this erosional surface are typical of Facies Association 2. Well 2-18-64-23W5 (Fig.5-5B) contains a facies succession typical of Facies Association 2B. Box photos of cores from this well are shown in figure 5-6. The basal erosion surface (marked by the D1 arrow) is indicated by the presence of sandstone clasts and a rather sharp transition from laminated shales and blockstones below (interval 0.0 -2.6m, Fig.5-6) into banded mudstones above. This is followed rather sherply by massively bedded, structureless to cross bedded, fine-grained sandstones containing ripped-up mud clasts. The sandstones (interval 2.6-5.6) contain mud couplets, highlighted with the small black circles, and may indicate tidal sigmoids (Facies 7E). The facies succession fines upward into about 8 meters of burrowed sandy mudstone (Facies 3B) in the interval from 5.6 to 14.1 m, containing marine trace fossils including *Teichichnus*, *Planolites* and *Rhizocorallium*. The last core sleeve, in the interval 11.3-11.4m, indicates a transition back into sandstone displaying low angle lamination interpreted as possible HCS. The material; showing the reverse colour grading at the top of D

Figure 5-5A. Well log cross section through Waskahigan bottleneck, shingle D1. Thick black vertical lines represent cored intervals shown on core cross section (5-5B),see text for discussion. All well traces are gamma logs, light stipple represents marine sand, heavy stipple represents channel fill, note channels in members D and C.

Figure 5-5B. Core cross section through the Waskahigan bottleneck, shingle D1. The major portion of the channel is transected in wells 6-18 to 11-10. Thickest portion to the southwest, in well 6-18, is interpreted as representing the deepest part of the channel (cutbank). This channel is asymmetric and shallows more slowly to the northeast. Thick marine mudstone in well 2-18 indicates estuarine conditions. See text for details and figure 2-29 for facies legend.

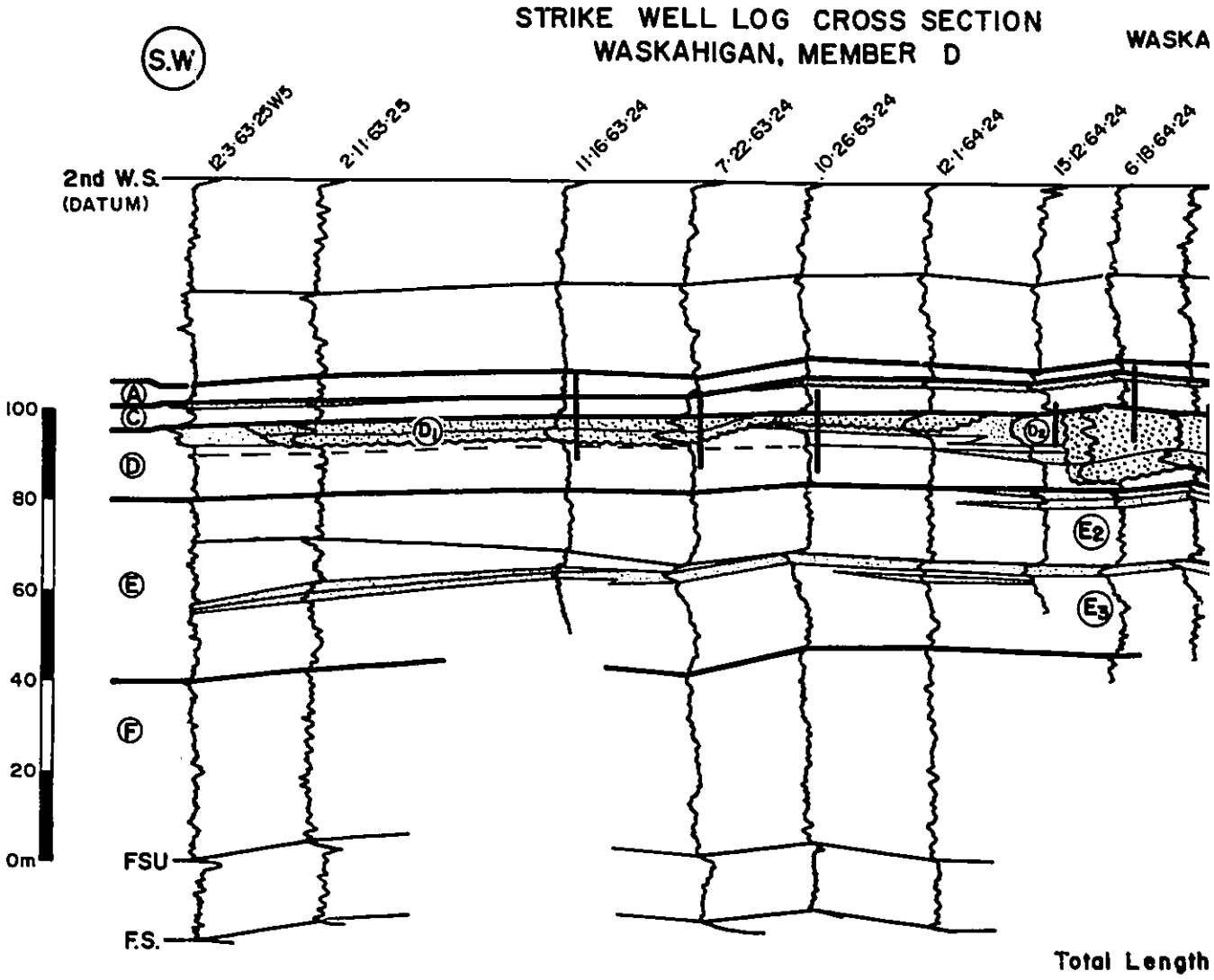
STRIKE WELL LOG CROSS SECTION
WASKAHIGAN, MEMBER D
WASKA
S.W
12-3-63-25W5
2-11-63-25
11-16-63-24
7-22-63-24
10-26-63-24
12-1-64-24
15-12-64-24
6-18-64-24
2nd W.S.
(DATUM)
A
C
D
E
F
D1
D2
E2
E3
100
80
60
40
20
0m
FSU
F.S.
Total Length

CROSS SECTION
MEMBER D

WASKAHIGAN

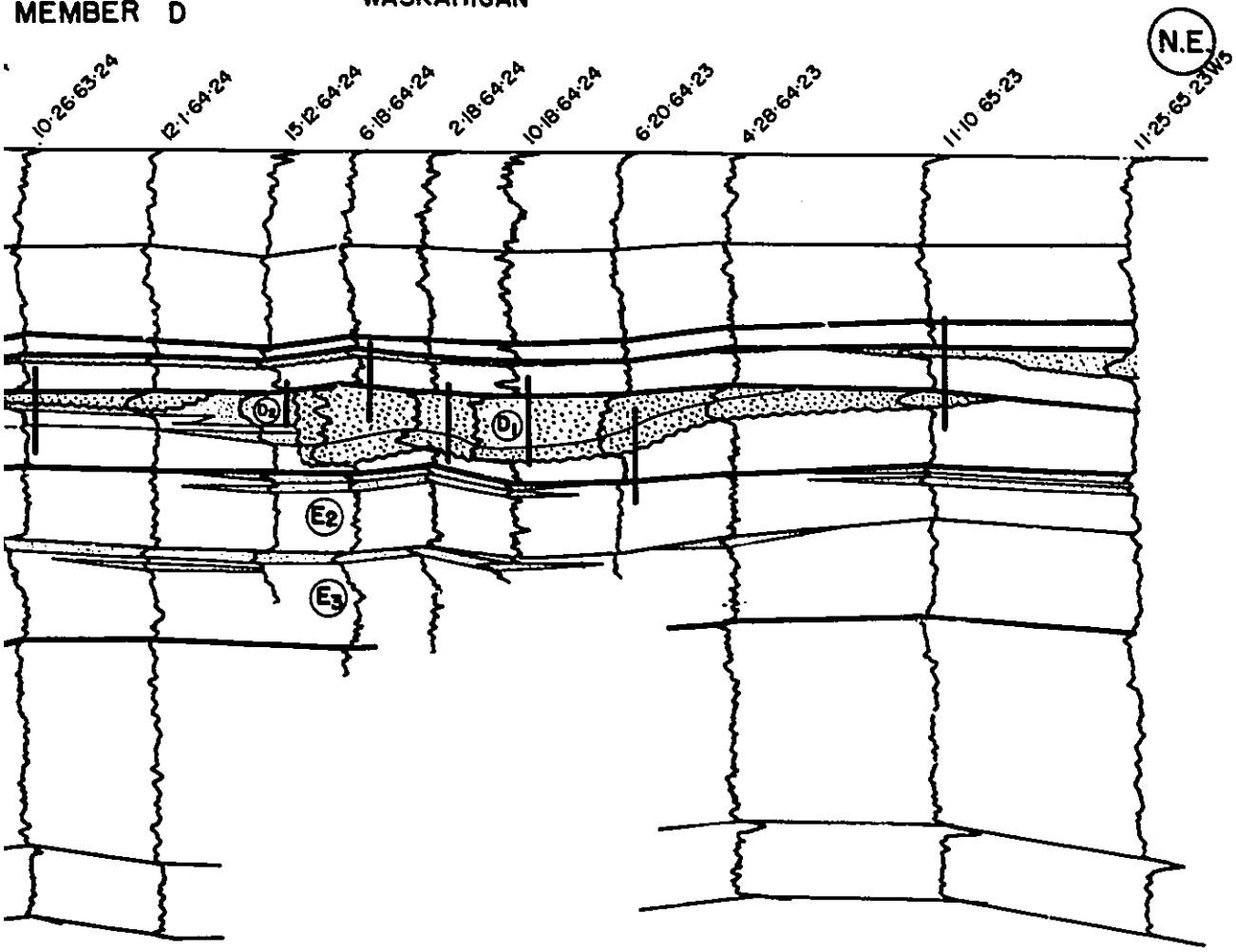

Total Length ≃ 35km

SW

CORE CROSS SECTION, WAS

MEMBER D

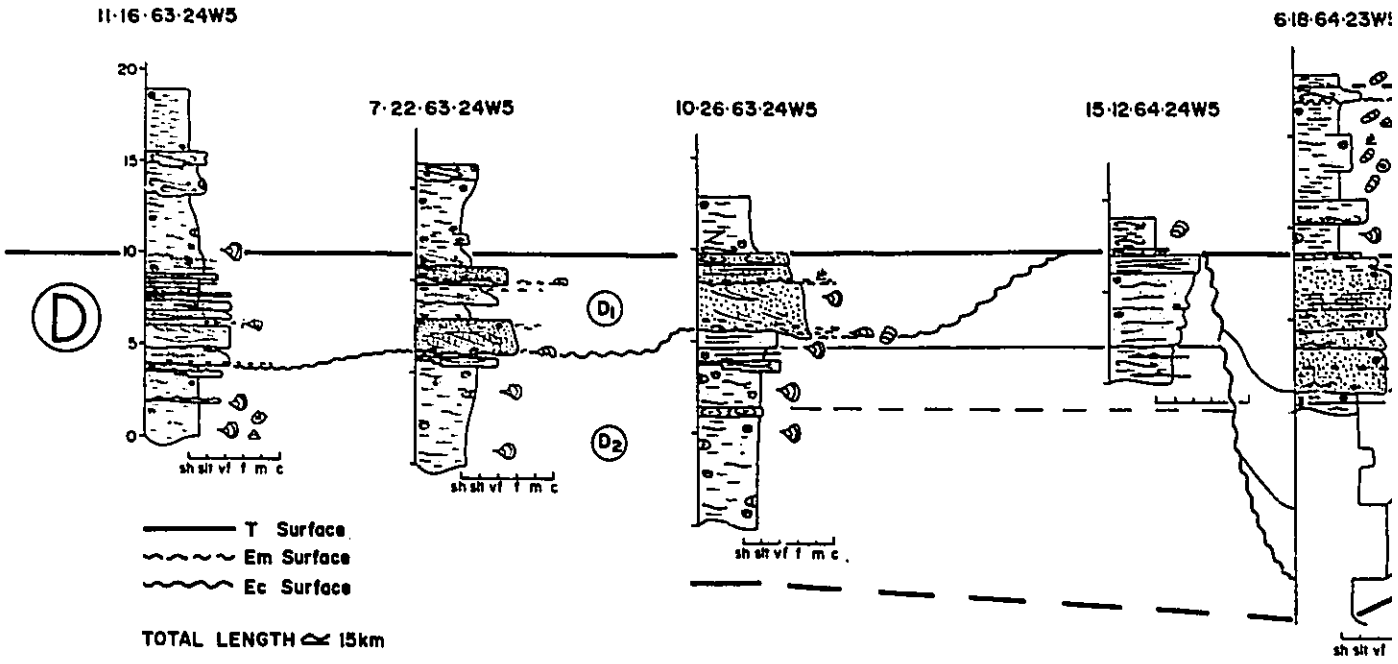

ION, WASKAHIGAN CHANNEL

MEMBER D

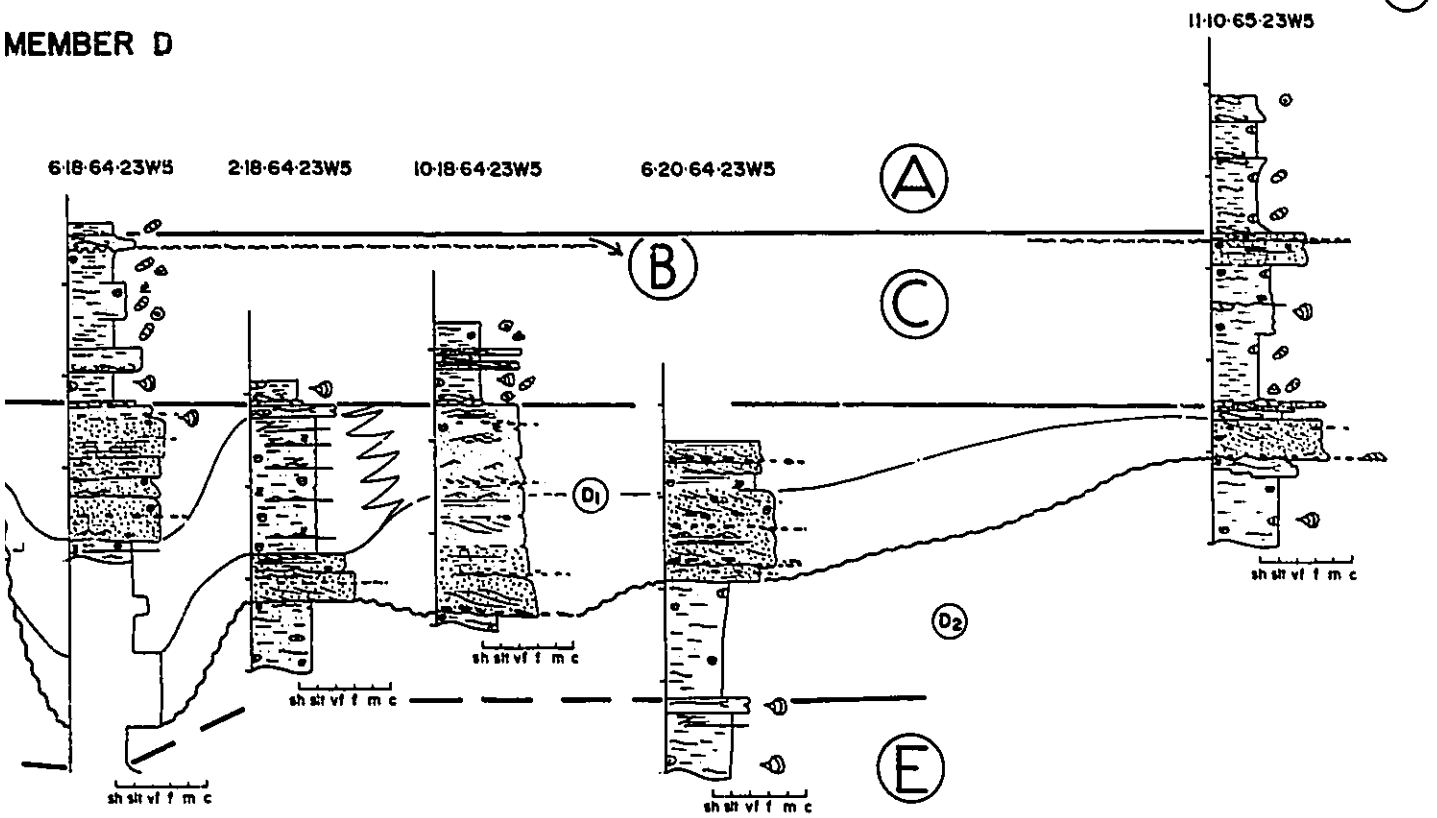

(interval 14.1-15.5m) is large siderite nodule (S) and the top of D is marked by a sharp transition into bioturbated to laminated marine shales comprising the base of member C.

A similar facies succession is exhibited in well 11-16-63-24W5 (Fig.5-5B). Fining upward facies successions in other wells (10-26, 10-18, 6-20, and 11-10) are dominantly sandy (Facies Association 2A). The base of member D is not cored in well 6-18, but the ratty nature of the gamma log suggests interbedded sandstone and mudstone, probably similar to the upper half of well 2-18. Correlation of mudstone beds above the erosion surface suggests that they dip towards the southwest.

Member D is capped by a thin silty bioturbated horizon (T Surface) overlain by transgressive shales of member C.

Interpretation

The Waskahigan bottleneck is interpreted as a major distributary channel. The southwest dip of mudstone beds above the erosional base and the asymmetrical shape in cross section suggest lateral migration of the channel towards the southwest. The deepest parts of the channel are partially filled with marine mudstones suggesting that the channel may have been partly filled as an estuary. The channel erodes into older coarsening upward facies successions representing lower shoreface deposits belonging to shingle D2, a remnant of which is preserved in well 15-12. The re-occurrence of the channel west of 15-12 suggests either that

Figure 5-6. Photos of well 2-18-64-24W5 (see figure 5-5A and B for well log and logged core section respectively). Bottom of cores at lower left, top of cores marked by label. Box photos are presented sequentially from base to top. Scale is 15cm. Erosional base, marked by D1 arrow, cuts into underlying laminated shales and blockstones (interval 0.0-2.6m). Mud couplets, probably representing tidal influence, highlighted in circles in incerval 2.6-5.6m. Upper half of channel fill (interval 5.0 to 13.5m) comprises burrowed mudstones (Facies 3B) indicating brackish water (estuarine) conditions. Last meter of channel is filled with sandstone. Channel fill culminates with large siderite nodule (indicated with S) and is capped by a T-surface indicated by a thin pervasively bioturbated mudstone and marked with the D arrow. T-surface overlain by laminated shales (Facies 1A) at the base of member C. See text for further discussion.


2-18-64-23W5
0.0-2.6m JKB


2·18·64·23W5
2.6 - 5.6m JKB
D1

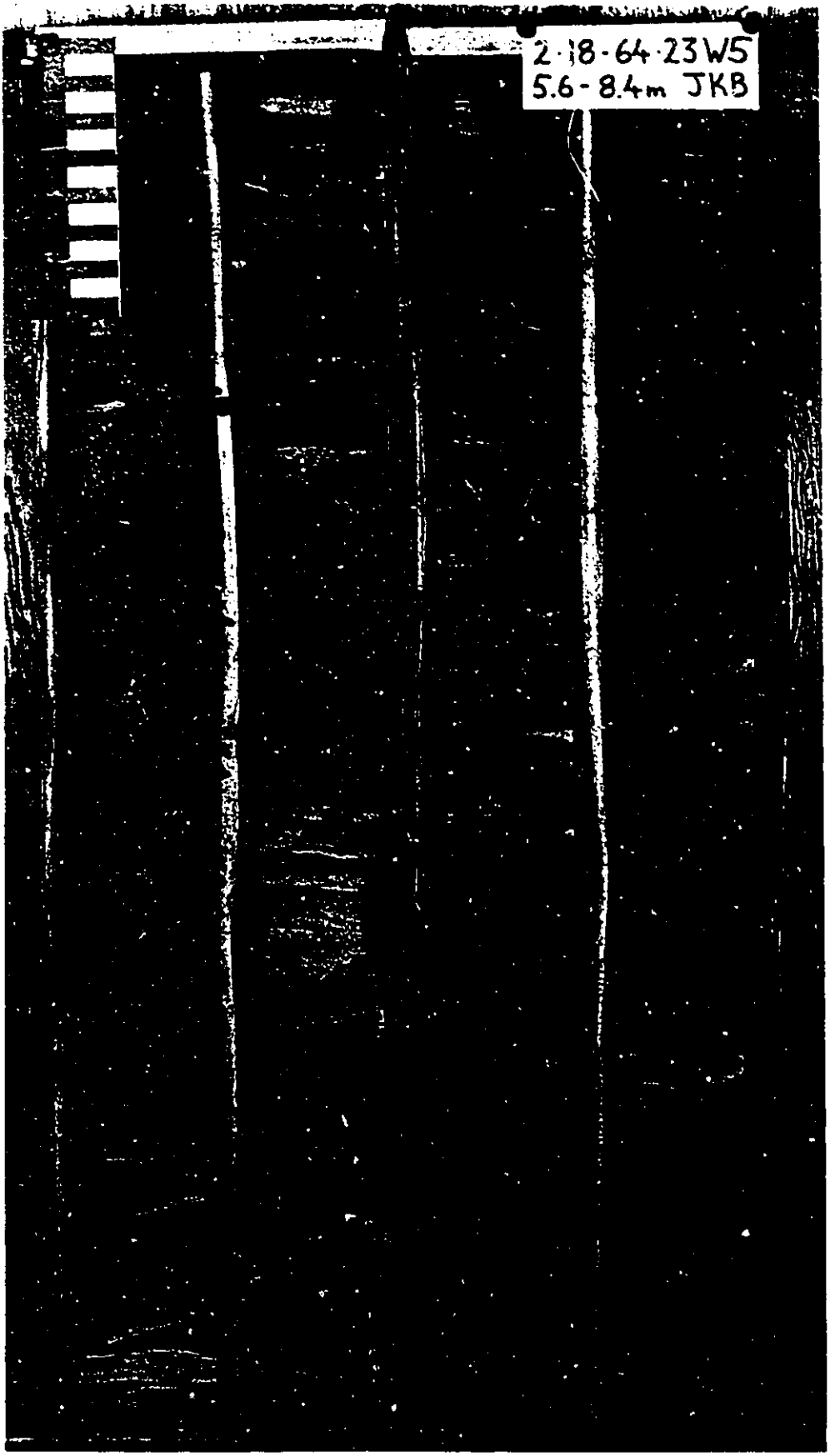
2-18-64-23W5
5.6-8.4m JKB

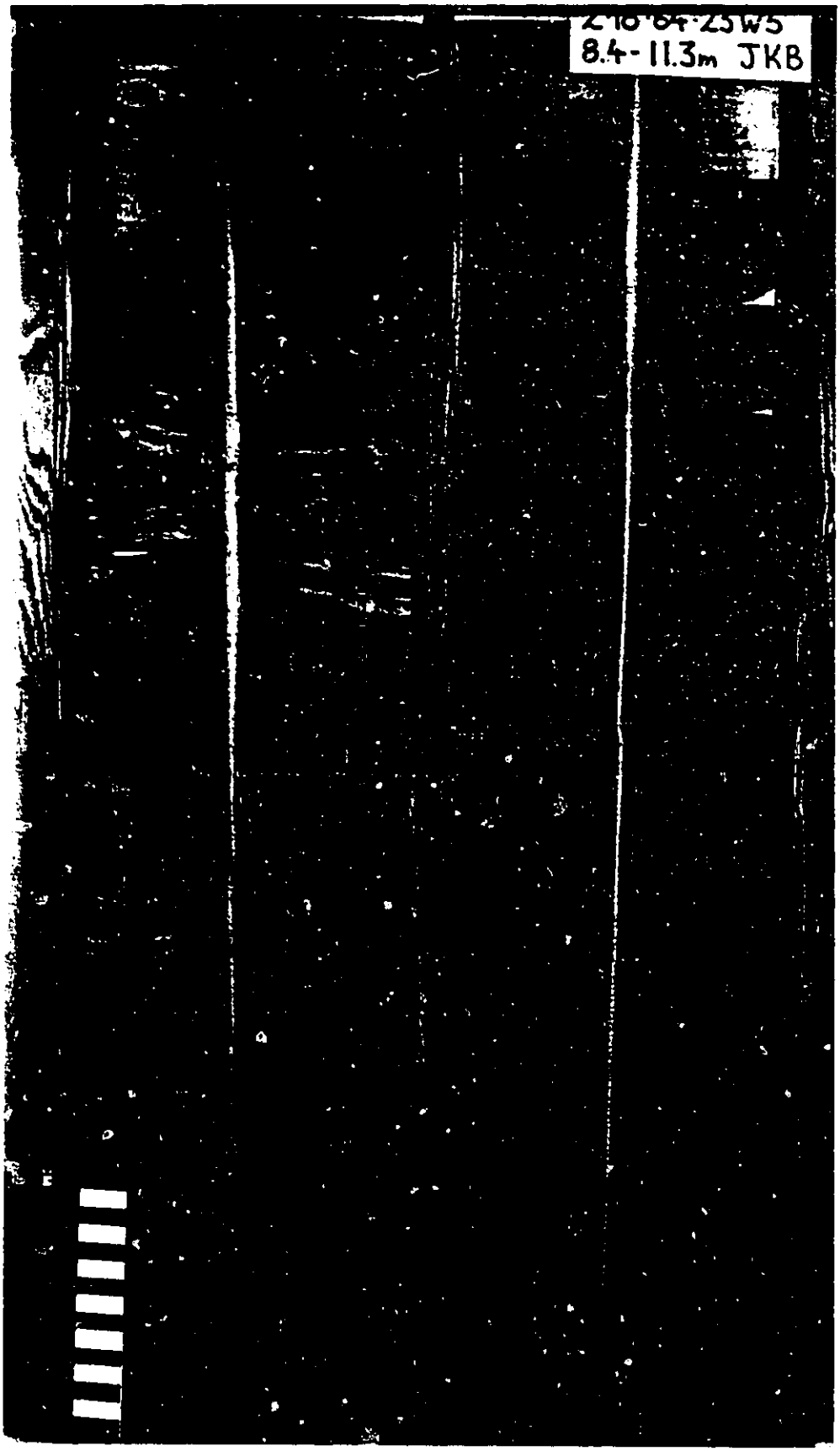
216-64-25W5
8.4-11.3m JKB

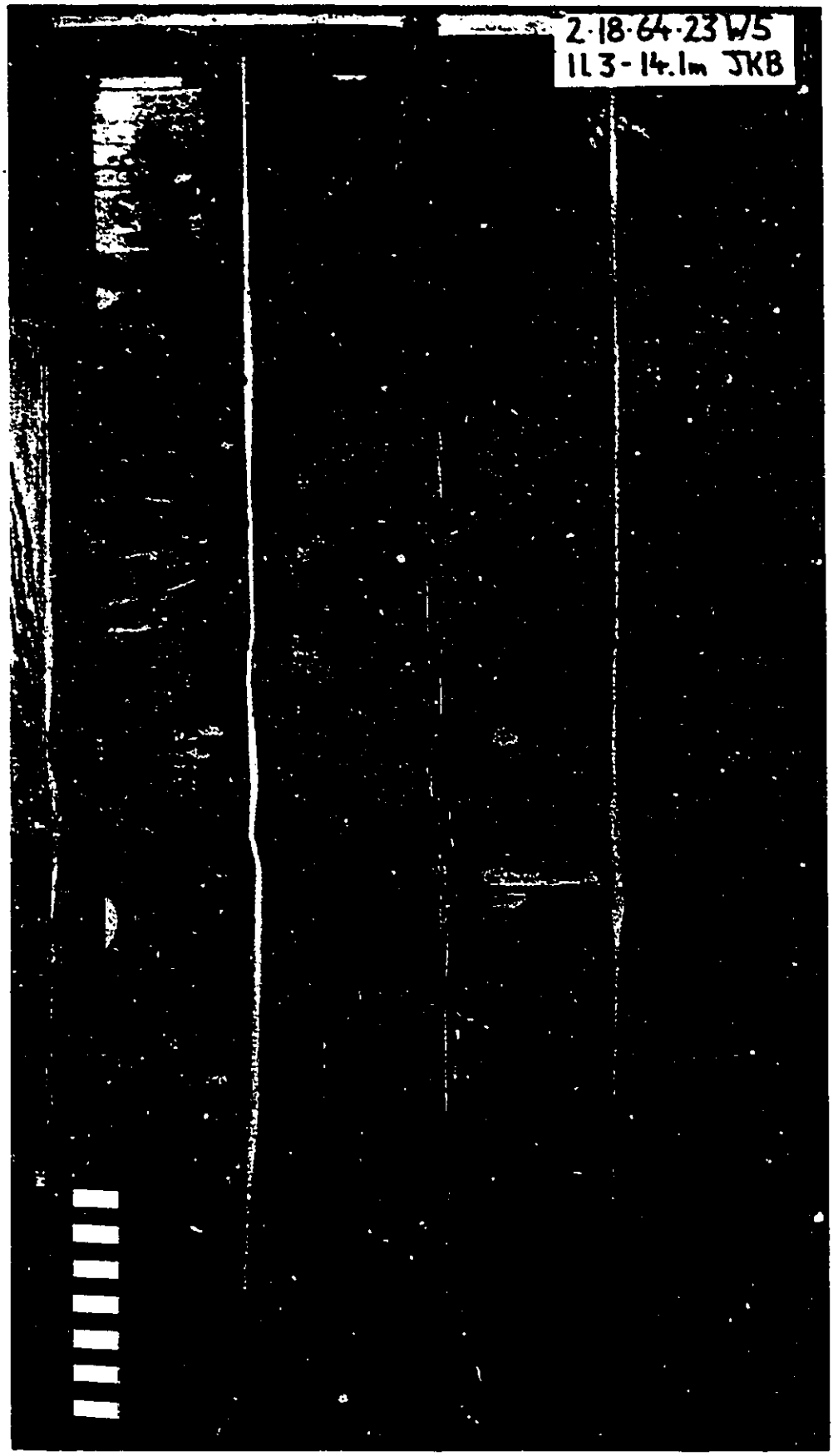
2-18-64-23 W5
1L3-14.1m JKB

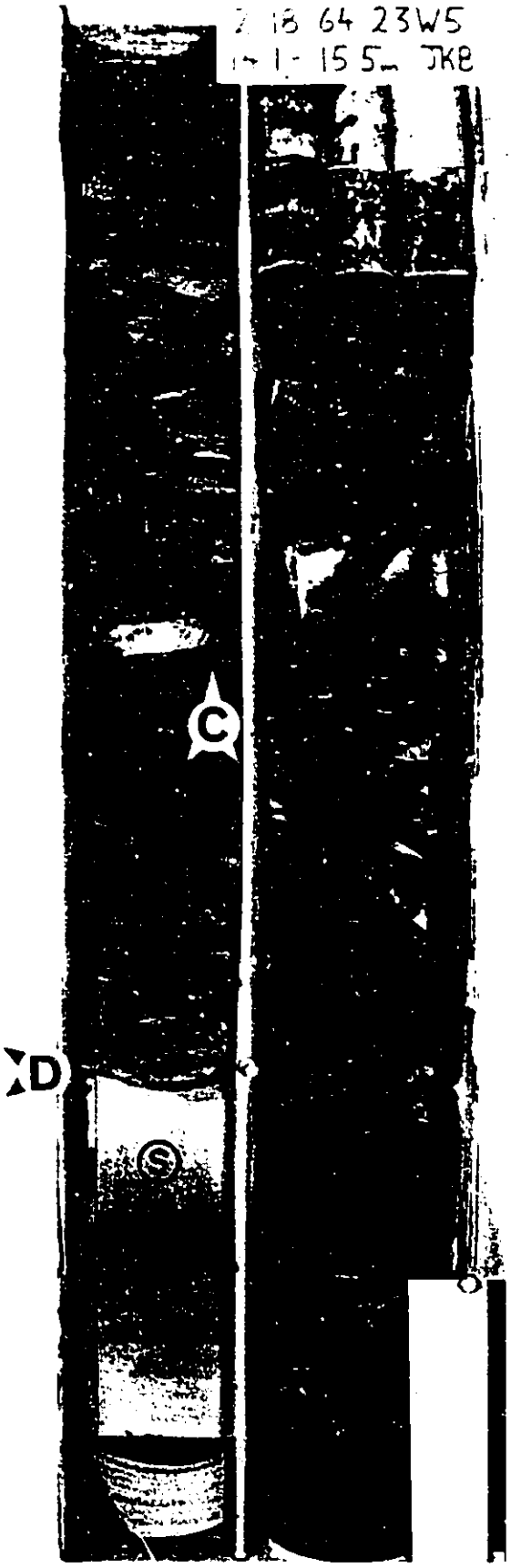
18 64 23W5
JKB
C
D

the channel may have occupied different positions or that there may have been more than one channel.

The channel clearly erodes into shingle D2 and is therefore younger. The large sandy D1 lobe to the southeast is most likely related to the Waskahigan channel. The channel is interpreted as feeding the storm- and wave-dominated shorelines of this lobe. The channel and lobe complex are therefore interpreted as representing a prograding wave and storm dominated deltaic shoreline.

The presence of tidal sigmoids and the fact that the channel is filled, in places, with burrowed marine sediments indicate that it was partly filled during transgression as an estuary. The trace fauna are typical of those found in other brackish estuarine facies in the C.W.I.S. (Beynon et al., 1988).

5-3-6. Facies, Shingles D2 and D3

The major D2 linear sand body, in the northwest, has been extensively cored. A typical core through this sandstone will be discussed followed by description of a core cross section oriented down the axis of this sand body.

Core 7-10-63-1W6 (Fig. 5-7A) represents a typical core through member D and box photos are shown in figure 5-7B. It contains two coarsening upward facies successions. The lowermost succession (boxes 10-16, Fig.5-7A,B) penetrates shingle D3 and is typical of Facies Association 1C. It begins in laminated marine mudstones (Facies 1A) and blockstones (Facies 2) containing *Inoceramus* and sandy gutter casts. These mudstones grade upwards

Figure 5-7A. Core 7-10-63-1W6, gamma log to left, logged core to right. See text for discussion and Fig.2-29 for legend. Core photos shown in figure 5-7B.

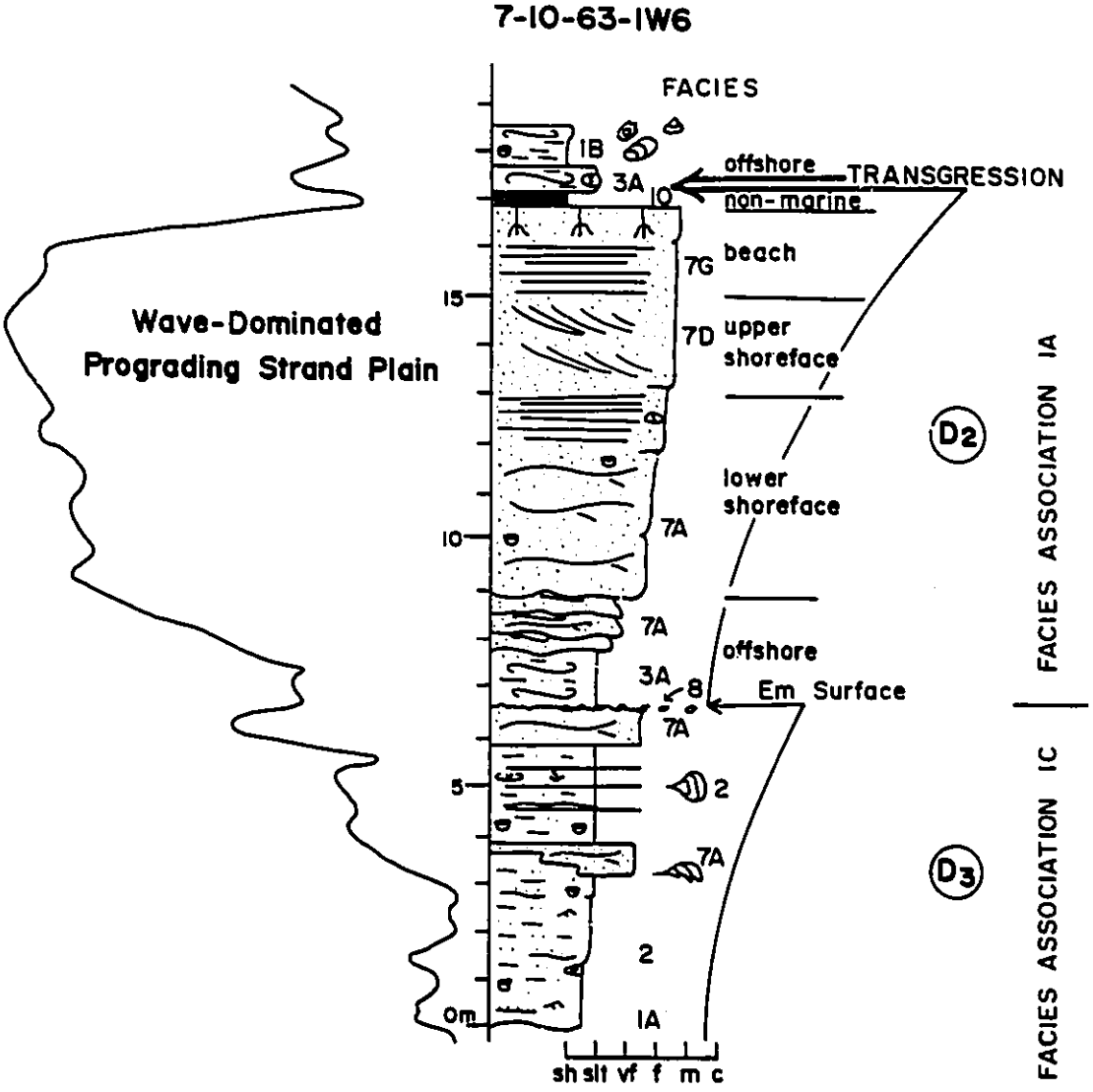
7-10-63-1W6
FACIES
1B
3A
offshore
non-marine
TRANSGRESSION
7G
beach
7D
upper shoreface
lower shoreface
7A
offshore
3A
8
Em Surface
7A
2
7A
2
1A
15
10
5
0m
sh slt vf f m c
Wave-Dominated
Prograding Strand Plain
D2
D3
FACIES ASSOCIATION IA
FACIES ASSOCIATION IC

Figure 5-7B. Core Photos from well 7-10-63-1W6. Well log and logged core section shown in figure 5-7A. Bottom of core is at lower right in box 16. Top of core is at upper left in box 1. Top of member D indicated by D2 arrow. See text for explanation and discussion.


7 10 63 1W6
16
15
14
13

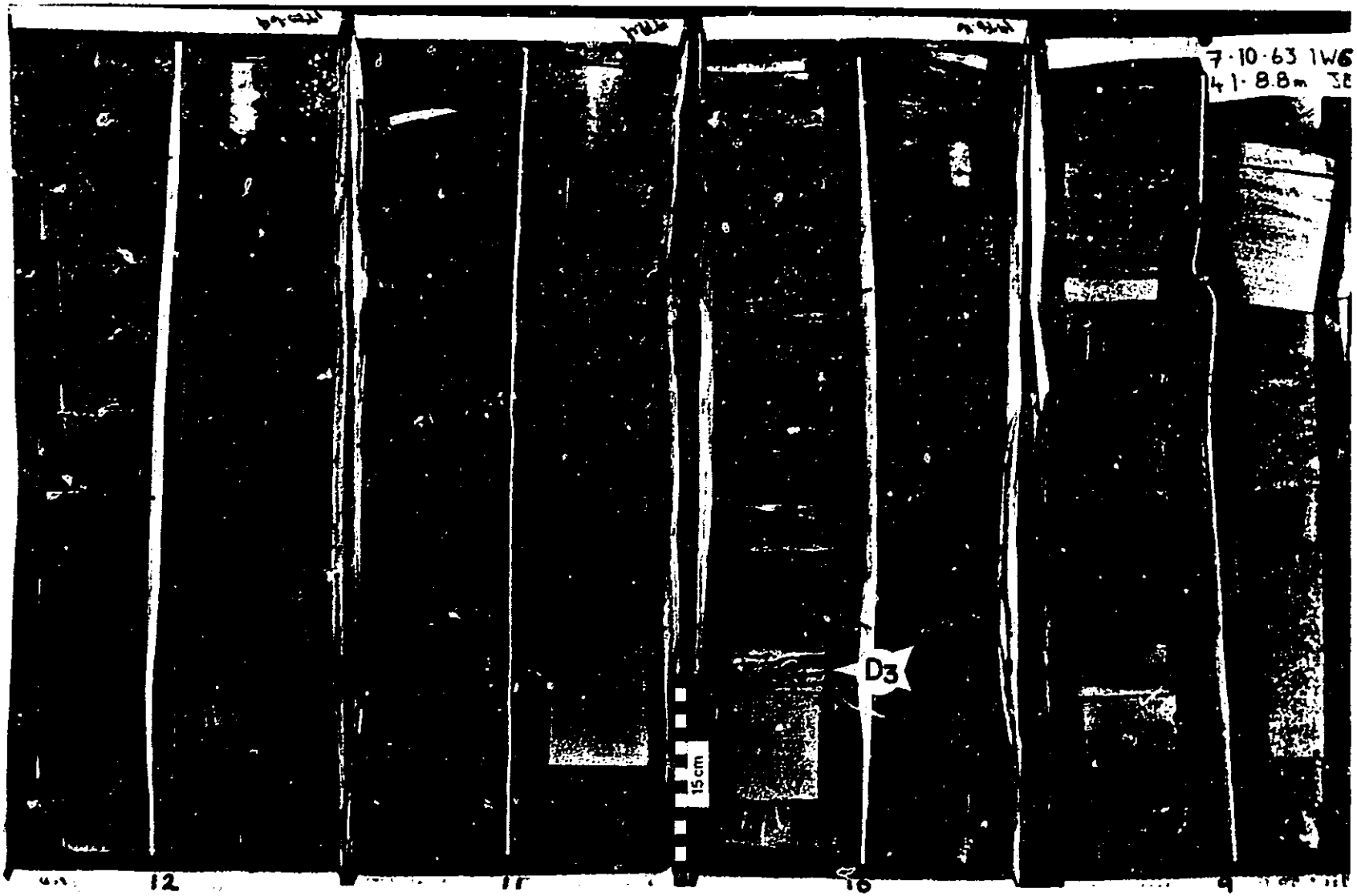
7·10·63 1W6
41·8.8m
D3
15 cm
12
11
10
9

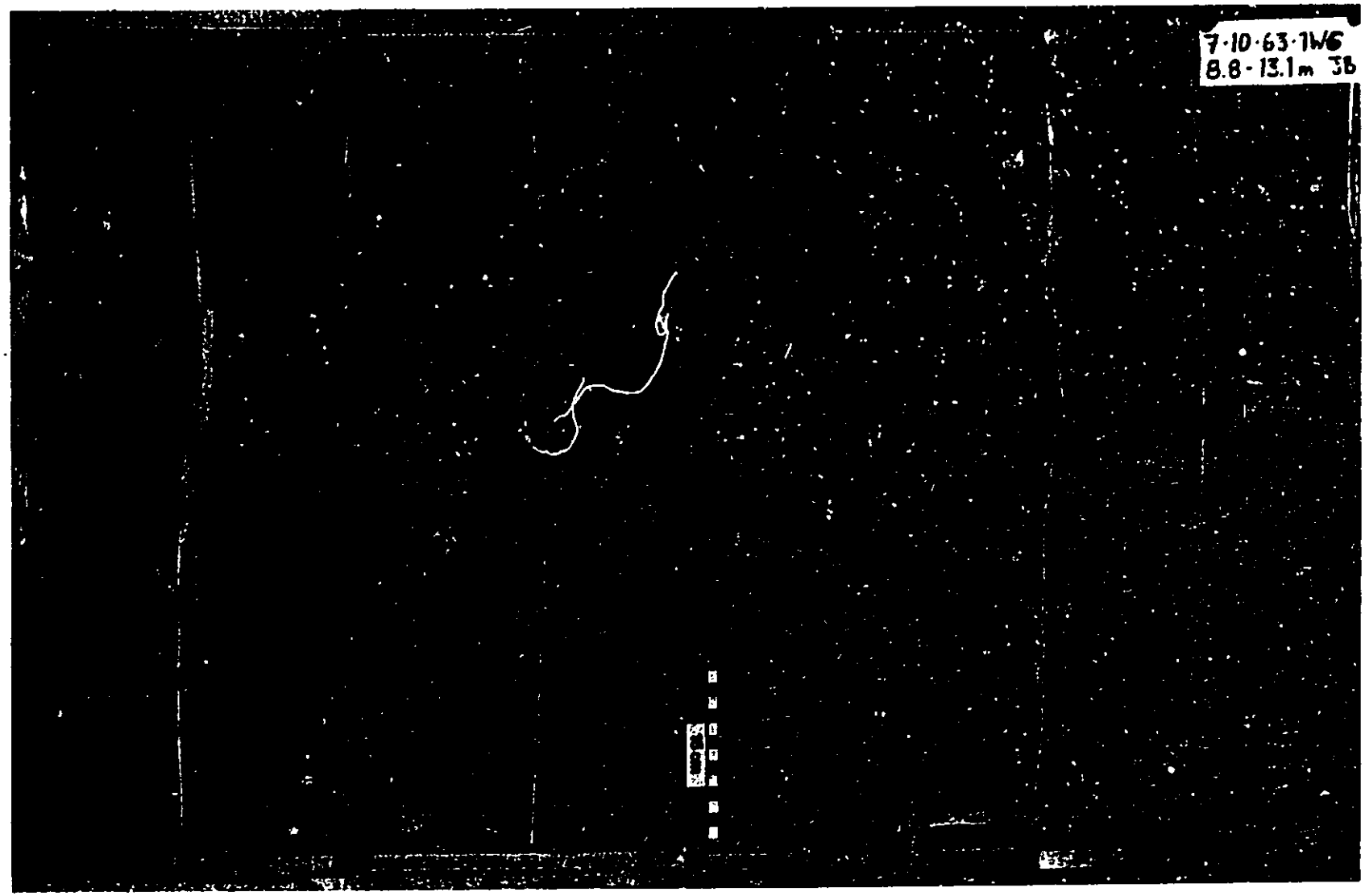
7·10·63·1W6
8.8 - 13.1 m JB

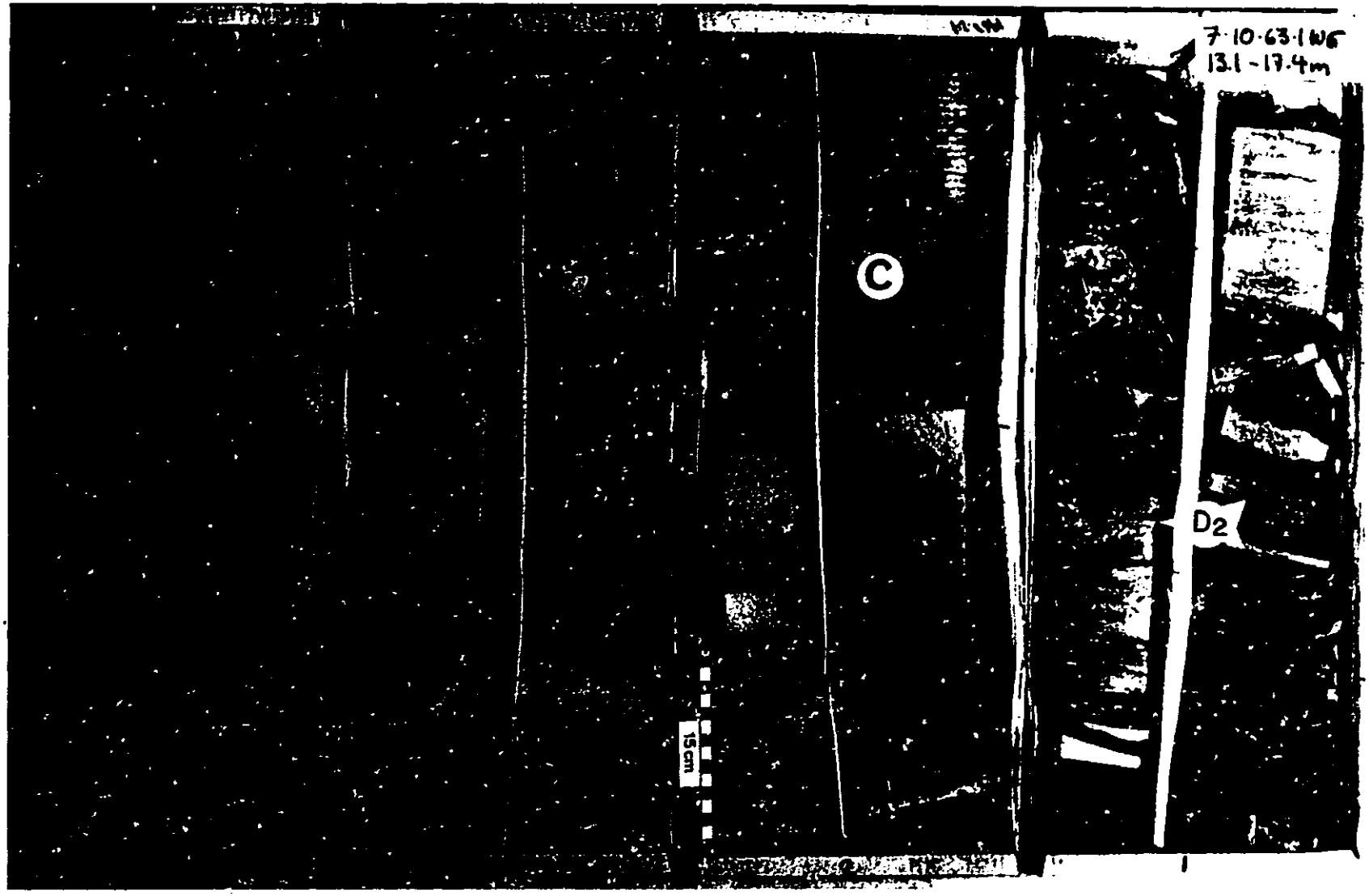
7·10·63·IWS
13.1 - 17.4m
C
D2
15cm

into HCS sandstones (Facies 7A) which are truncated at about 6.5 meters (box 10) from the base. The top of the succession is capped by a thin sandy siderite lag (Facies 8) marked by the D3 arrow in Fig.5-7B.

The upper facies succession (D2) is typical of Facies Association 1A. It is about 10 meters thick and begins with about one meter of pervasively bioturbated marine mudstones (Facies 3A). These mudstones coarsen upward into very fine-grained HCS sandstone beds with bioturbated tops (Facies 7A). The hummocky beds amalgamate upwards into coarser grained SCS sandstones. Burrowing was not observed above about 10 meters (end of box 7). Upwards, the sandstones become cross bedded (Facies 7D) and finally culminate in about 2 meters of flat laminated sandstones (Facies 7G) as shown in boxes 2 and 3 (Fig.5-7B). These parallel laminated sandstones are penetrated by *in situ* root traces at the top and are capped by a thin (20cm) coal (Facies 10) marked with a C in the photographs (Fig.5-7B). At the top of member D lies a thin bioturbated sandy horizon immediately overlain by a thick bioturbated marine shale (Facies 1B) and marked with a D arrow in figure 5-7B.

Interpretation

The presence of a lag at the top of the lower succession may suggest erosion. The presence of marine deposits on top of this lag suggests an Em surface. The facies association in the upper succession is typical of emergent, prograding, medium to high

energy strandplains as discussed in chapter 2 (section 2-3-1A). Eolian deposits, however, were not recognized. The sandy bioturbated horizon which caps D2 marks the transgressive surface at the top of member D.

5-3-7. Cross section parallel D2

The well log cross section parallel to the D2 sand body (Fig. 5-8A) is hung on the base of the Second White Specks. It is oriented approximately parallel to the D2 linear sand body (Fig.5-3B) and extends for a length of about 100km. From wells 10-33-60-5W6 to 16-8-64-23W6 the cross section trends along the crest or along the eastern (seaward) margin of the sand body. The sandstone in member D is uniformly, thick in all of these wells. From wells 11-22-64-26W5 to 6-27-67-23W5 it crosses the western and northeastern (landward) margin of the sand body. In these wells the sandstones in member D are seen to split and to becomethinner. In wells 7-13 and 6-36, on the northeast side of the cross section, gamma log traces through member D are funnel shaped. Intervening wells, especially 2-23 (Fig.5-8A), have bell shaped or blocky profiles suggesting the presence of the same erosional surface observed in the Waskahigan area (Fig.5-5A,B). The erosion surface is again asymmetrical but dips more gradually to the northeast rather than to the southwest as seen in the Waskahigan area (Fig.5-5A,B).

Sandstones thin towards the far northeast on the log cross section (Fig.5-8A) and are not present in wells 10-18-67-23W5 and 6-27-67-23W5.

The core cross section (Fig.5-8B) shows considerably more detail than the accompanying well log cross section, although it only extends for about 45 km. As shown in figure 5-8B, shingle D3 comprises a coarsening upward facies succession typical of Facies Association 1C. HCS sandstones, however, are not present in wells 7-17 and 12-24 and SCS sandstones are not present in any well. A thin sideritic pebble lag occurs at the top of D3 in well 7-10-63-1W6. In other wells (not on this particular cross section) this contact is marked by calcite cemented mudstone containing peculiar cone-in-cone structures. D3 is clearly truncated on the cross section and is seen to thin in a southwest direction.

The D2 sandstone is relatively constant in thickness along the core cross section, although it is thinnest in well 11-7-64-26W5. The coarsening upwards facies successions in wells 10-33-60-5W6, 12-24-62-3-W6 and 7-10-63-1W6 (fig.5-8B) are typical of Facies Association 1A. They begin with pervasively bioturbated mudstones and coarsen upwards into very fine-grained HCS sandstone. Wells 7-17-61-3W6 and 13-28-61-2W6 also begin with bioturbated mudstones but these mudstones, in contrast, are sharply to erosively overlain by coarser-grained cross-bedded sandstones with mud rip-ups at their bases. The facies successions in the lower

Figure 5-8A. Well log cross section parallel to D2 sandstone. Location shown in figure 5-3B. All wells represent gamma ray log traces. Thick black vertical lines represent cored intervals shown in figure 5-8B. See text for discussion.

Figure 5-8B. Core cross section parallel to D2 sandstone. Position of cored intervals indicated on figure 5-8A. Arrows indicate coarsening or fining upward facies successions. Erosively based fining upward facies successions in wells 7-17 and 13-28 interpreted as representing tidal channels in the barrier sandstone. Note thickness changes in shingle D3, interpreted as the result of marine erosion. See figure 2-29 for legend. Location of cross section shown in figure 5-3B. See text for further discussion.

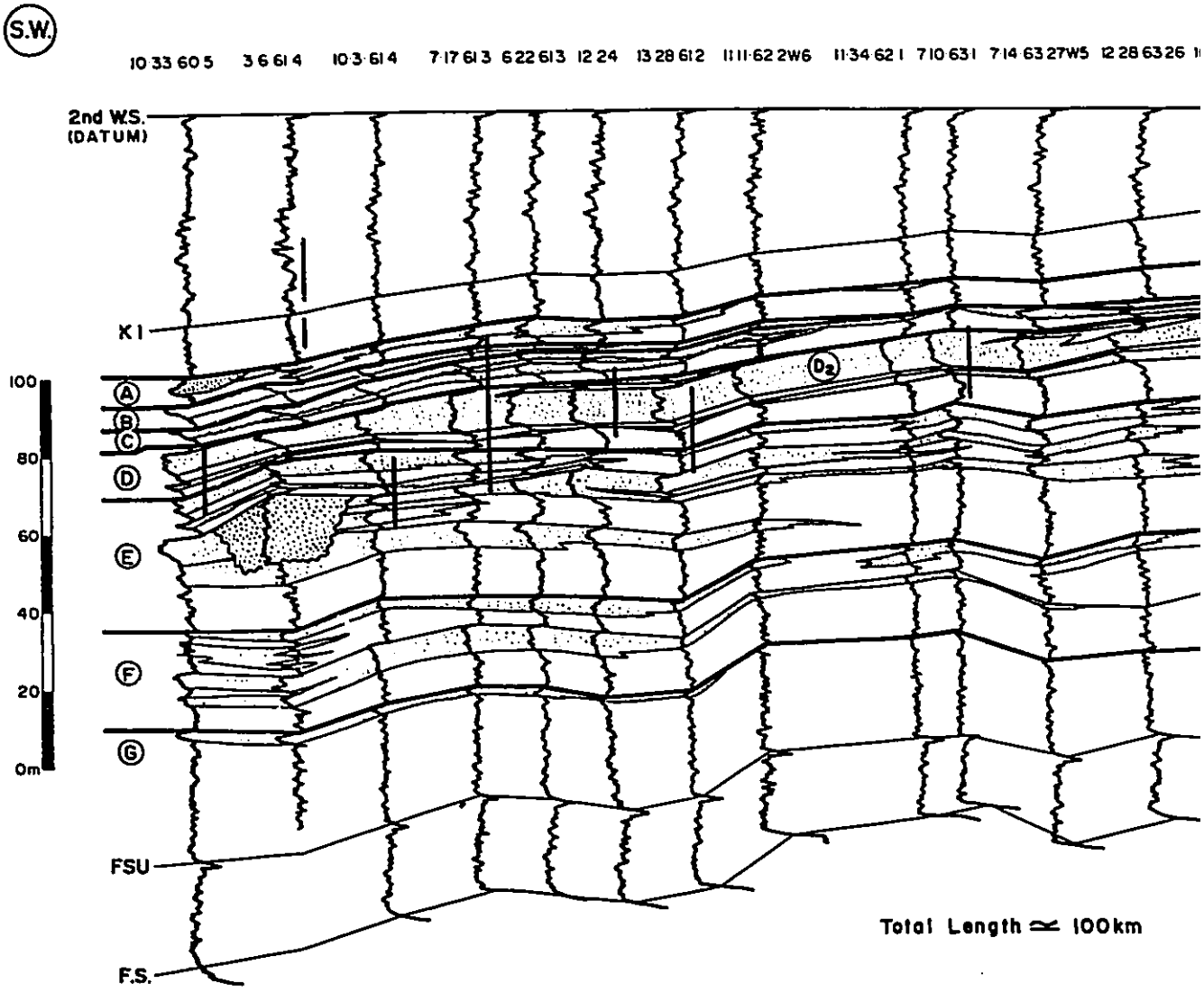
S.W.
10-33-60-5
3-6-61-4
10-3-61-4
7-17-61-3
6-22-61-3
12-24
13-28-61-2
11-11-62-2W6
11-34-62-1
7-10-63-1
7-14-63-27W5
12-28-63-26
2nd W.S.
(DATUM)
K I
A
B
C
D
E
F
G
D_2
FSU
F.S.
100
80
60
40
20
0m
Total Length ≃ 100km

N.E.

62-1 7-10-63-1 7-14-63-27W5 12-28-63-26 16-8-64-26 11-22-64-26 7-13-65-26 4-27-65-25 16-2-66-25 2-23 6-36-66-25W5 10-18-67-23 6-27-67-23W5

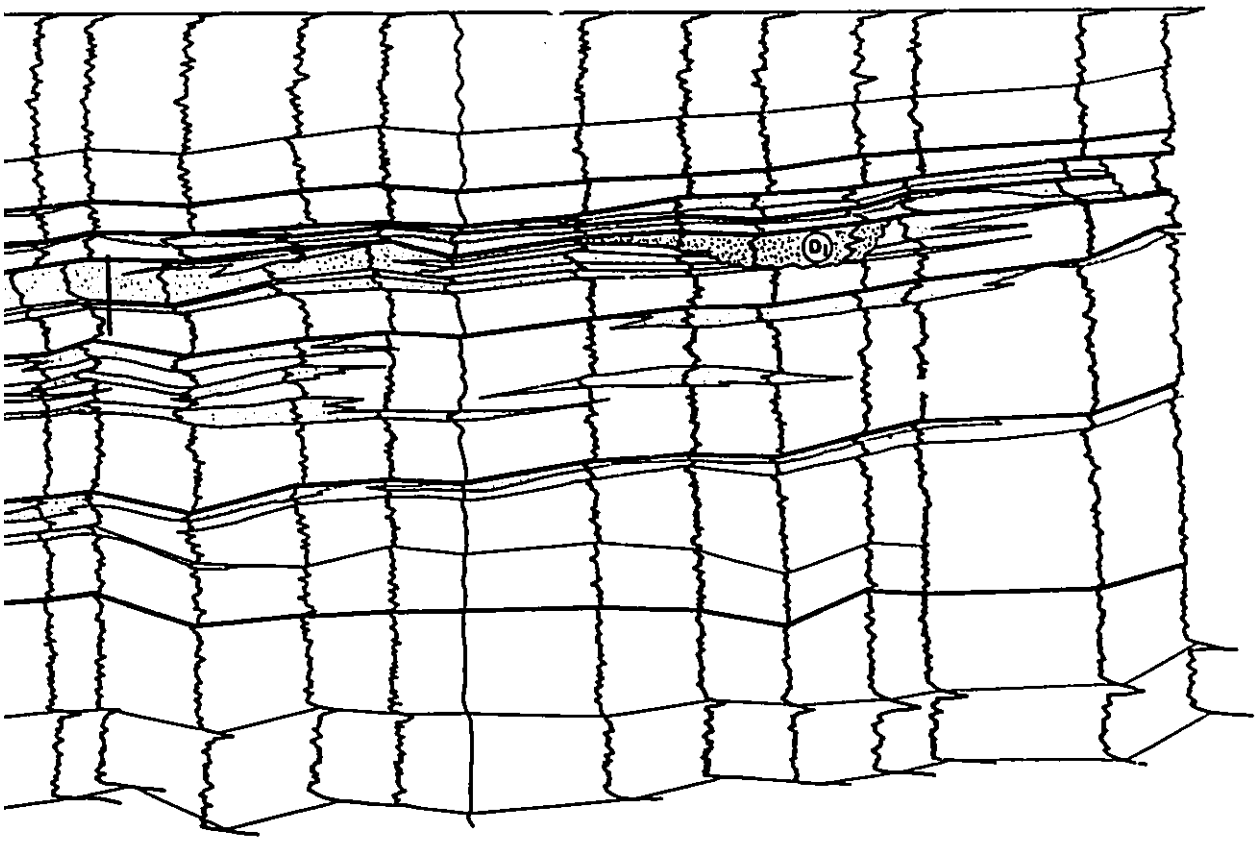

Total Length ≃ 100km

WELL LOG CROSS SECTION,
PARALLEL D_2 BARRIER

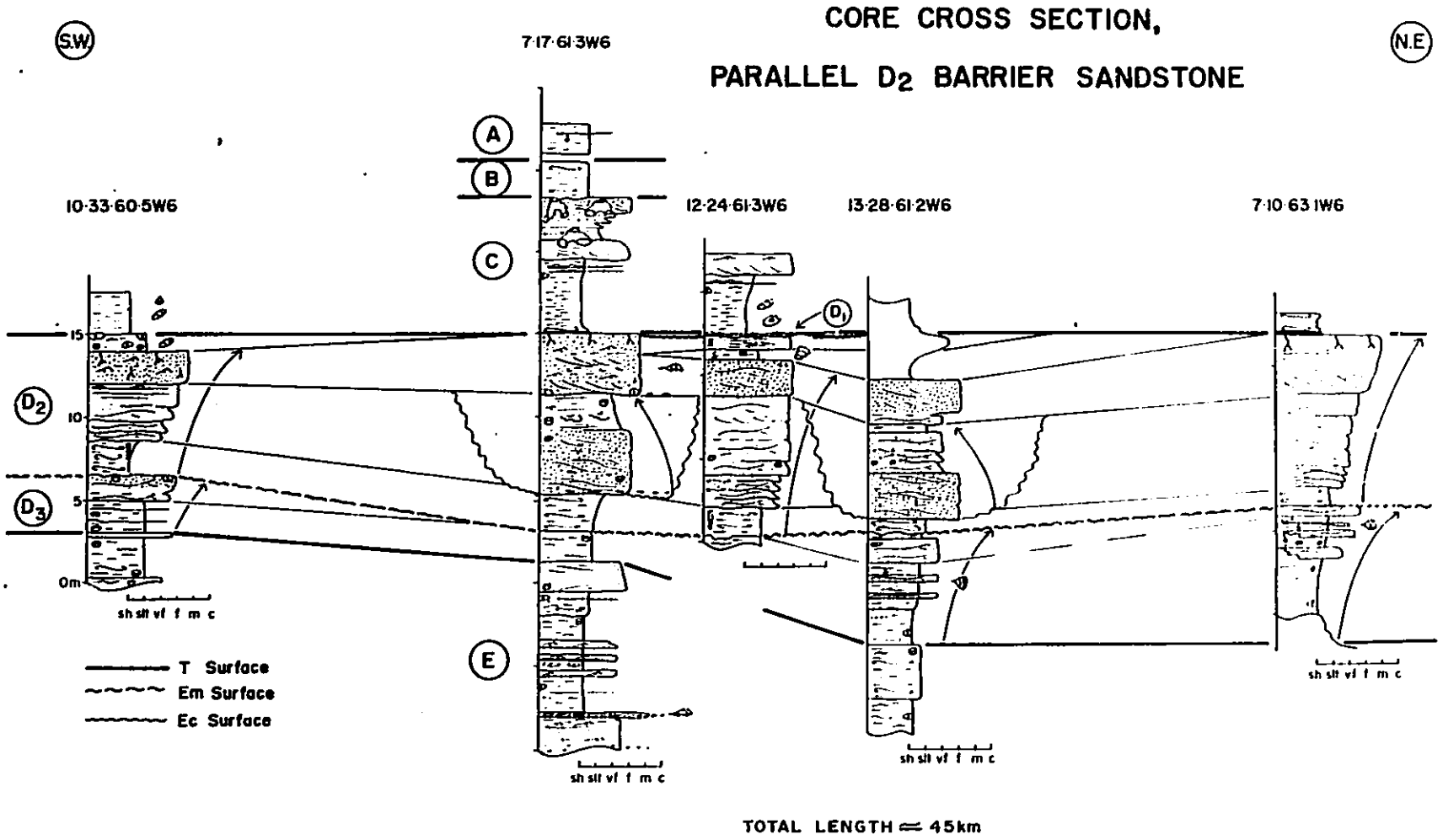
CORE CROSS SECTION,
PARALLEL D2 BARRIER SANDSTONE
S.W
N.E
7-17-61-3W6
10-33-60-5W6
12-24-61-3W6
13-28-61-2W6
7-10-63-1W6
A
B
C
D2
D3
D1
E
15
10
5
0m
sh slt vf f m c
T Surface
Em Surface
Ec Surface
TOTAL LENGTH ≈ 45km

portions of D2 in these wells, fine upwards and are descriptively similar to Facies Association 2. Some of the sandstones in these facies successions show well developed mud couplets, possibly indicating tidal cross bedding. The upper part of shingle D2 comprises fine-grained sandstone of fairly uniform thickness over the length of the cross section. Its lower contact is gradational in wells which exhibit type 1A Facies Associations (10-33, 12-24, and 7-10) but is sharp in the other wells. It is split towards the northwest by a thin, laminated mudstone tongue which dips towards the east. In well 12-24 this mudstone contains syneresis cracks and oyster shells. The sandstone is truncated at the top of member D. A thin coarse grained siderite lag occurs at the top of member D in well 12-24.

Transgressive shales at the base of member C abruptly overlie member D on the cross section (T-surface). The contact in wells 7-17 and 7-10 (Fig.5-8B) is marked by a thin pervasively bioturbated silty mudstone horizon overlying a rooted sandstone and thin coal.

5-3-8. Cross Sections Perpendicular to D2

The well log cross section perpendicular to the D2 sandstone (Fig.5-9A) is hung on the base of the Second White Specks and ties with well 7-10-63-1W6 in figure 5-8A,B. It is oriented approximately perpendicular to the D2 linear sand body (Location in Fig.5-3B) and extends for about 40 km. Sandstone in shingle D2 reaches a maximum thickness of about 10 meters in well 7-10 and

Figure 5-9A. Well log cross section perpendicular to D2 sandstone. All wells are gamma log traces except for well 10-1-63-1W6 which is a deep induction curve traced backwards. Thick black vertical lines represent cored intervals presented in figure 5-9B. Root symbols indicate non-marine facies. Location of cross section shown in figure 5-3B. See text for further discussion.

Figure 5-9B. Core cross section perpendicular to D2 sandstone interpreted as a barrier sand with lagoonal deposits northwest of well 7-10 and grading seaward into marine facies. Cored intervals on well logs indicated in cross section 5-9A. Location of cross section shown in figure 5-3B. Arrows indicate coarsening upward facies associations. Legend in figure 2-29. See text for discussion.

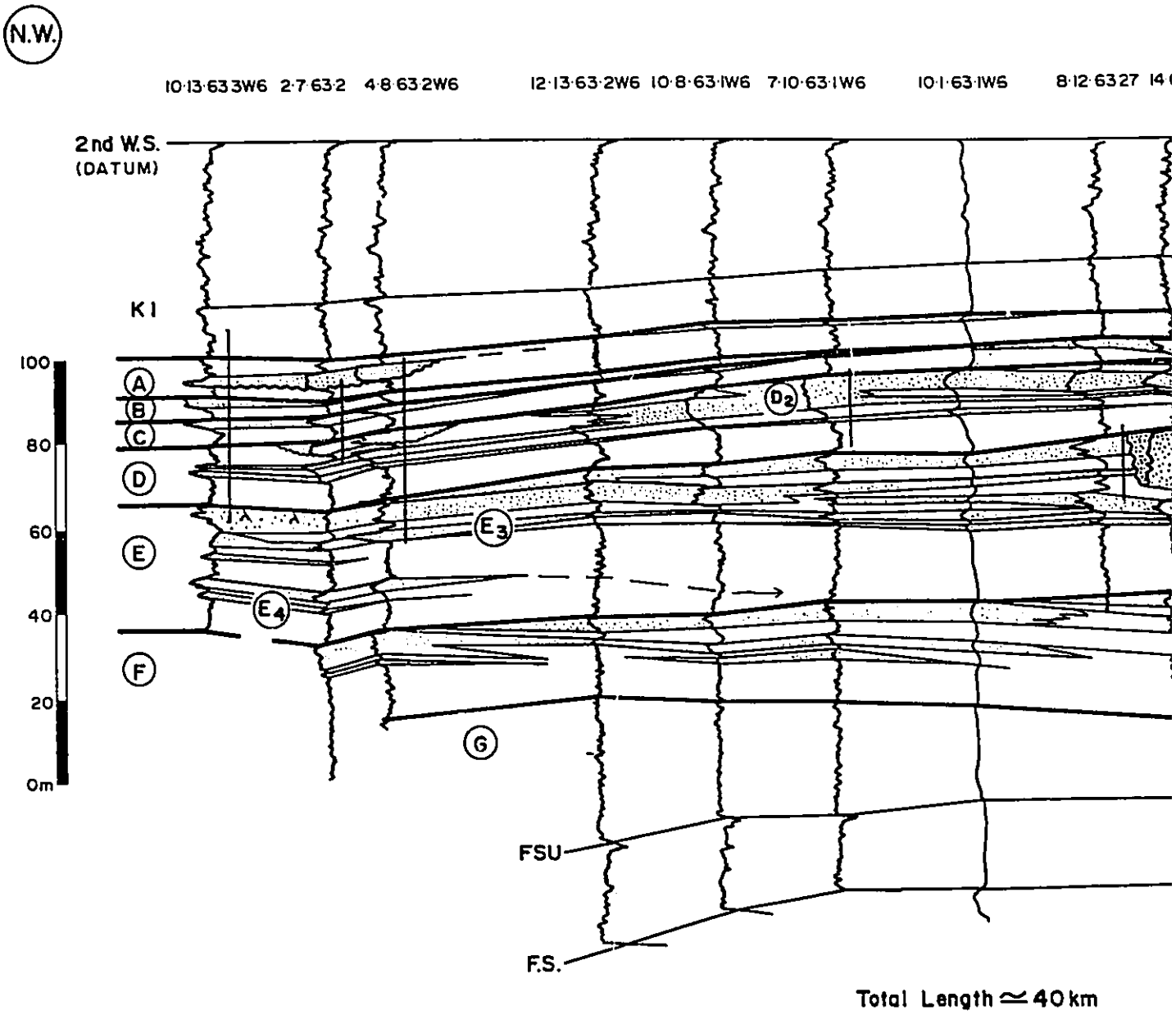
N.W.
10-13-63-3W6
2-7-63-2
4-8-63-2W6
12-13-63-2W6
10-8-63-1W6
7-10-63-1W6
10-1-63-1W6
8-12-63-27
2nd W.S.
(DATUM)
K I
100
80
60
40
20
0m
A
B
C
D
E
F
G
D2
E3
E4
FSU
F.S.
Total Length ≃ 40 km

S.E.

0·63·1W6 10·1·63·1W5 8·12·63·27 14 6 63·26 15·31 62·26W5 12 26 62 26W5 3 8 62 25W5

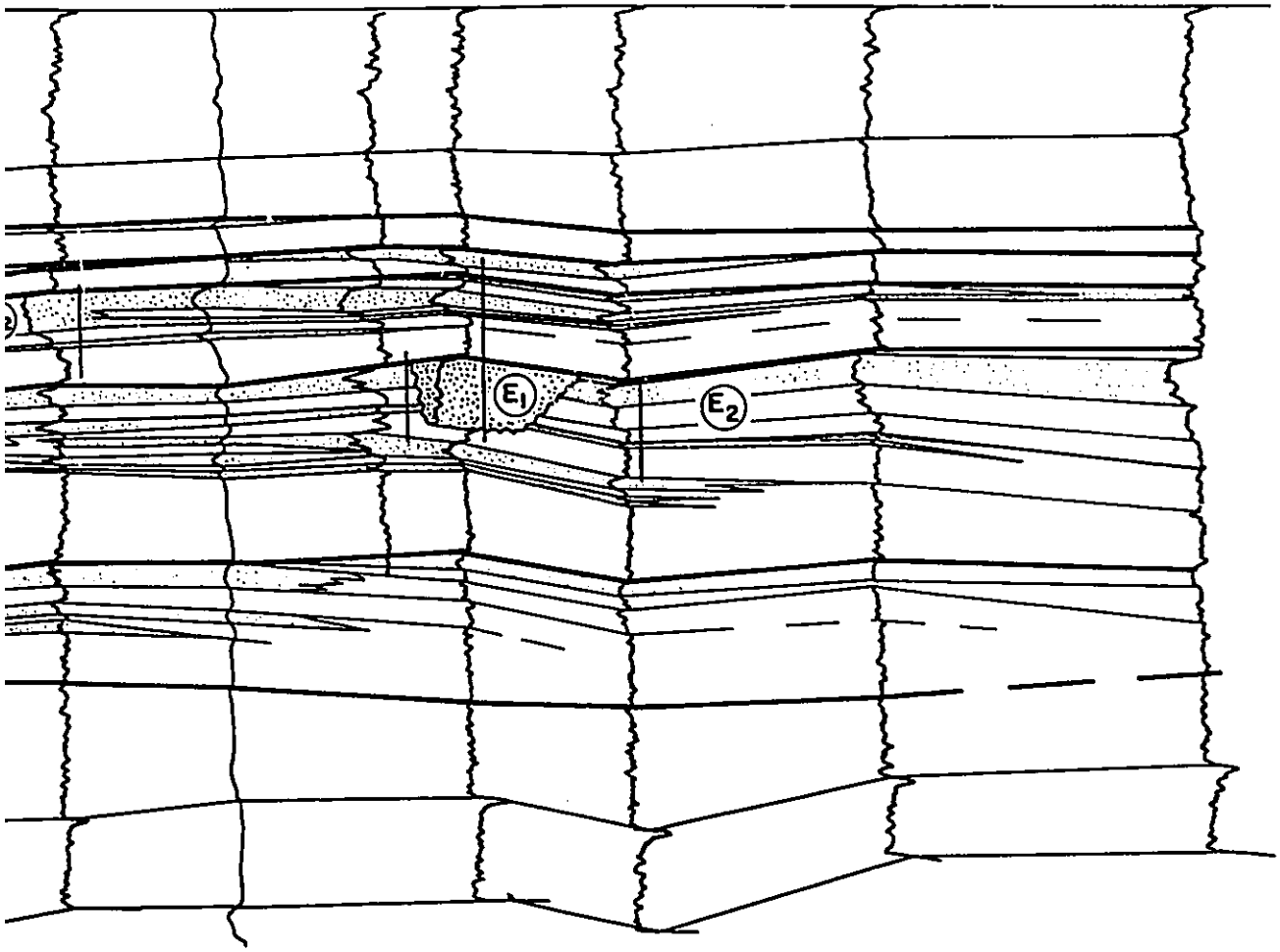

Total Length ≃ 40 km

WELL LOG CROSS SECTION
PERPENDICULAR D_2 BARRIER

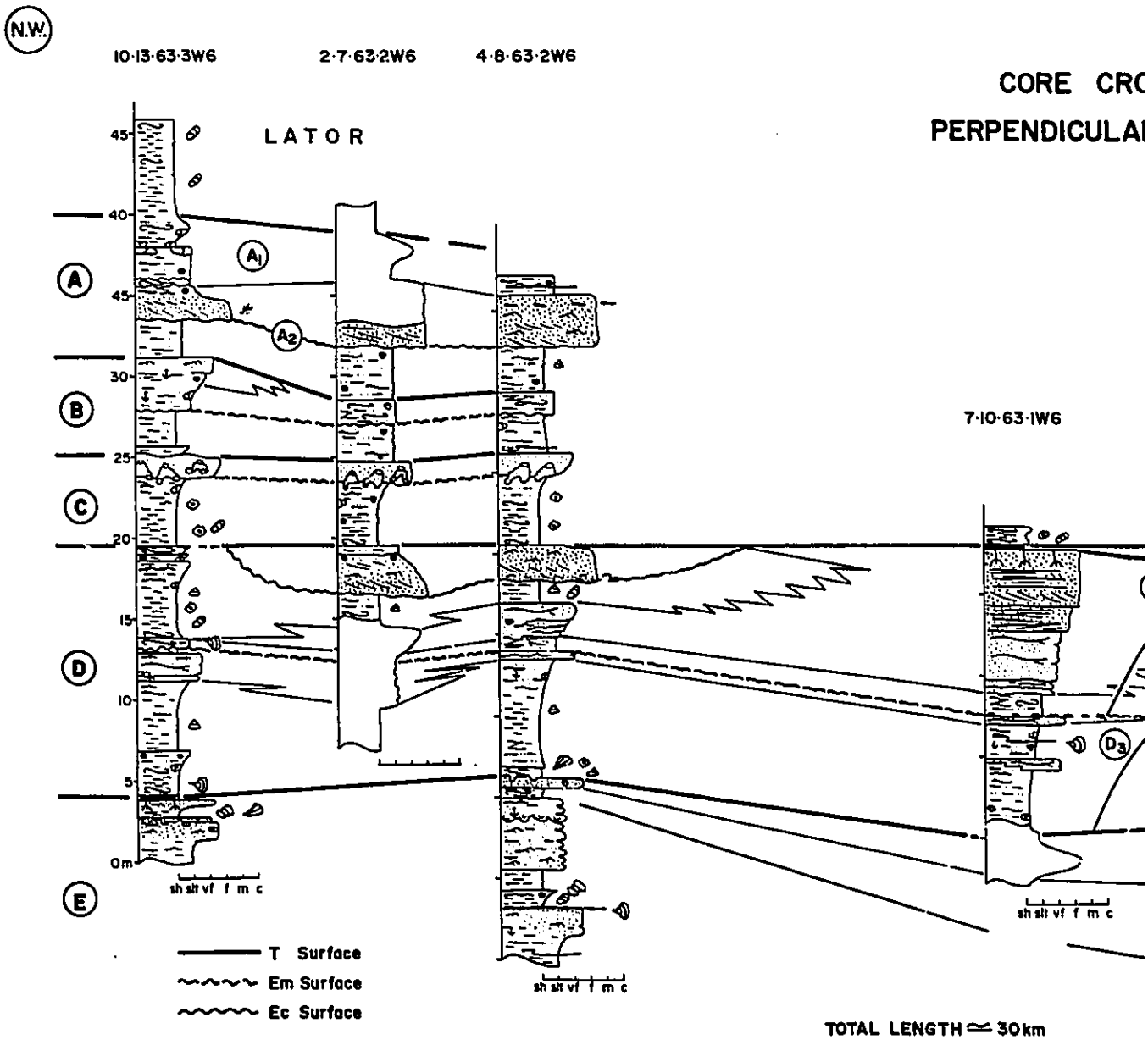
N.W.
10-13-63-3W6
2-7-63-2W6
4-8-63-2W6
7-10-63-1W6
CORE CRC
PERPENDICULAI
LATOR
45
40
45
30
25
20
15
10
5
0m
A
B
C
D
E
A1
A2
D3
sh slt vf f m c
T Surface
Em Surface
Ec Surface
TOTAL LENGTH ≃ 30km

S.E.

CORE CROSS SECTION
PERPENDICULAR D_2 BARRIER

SIMONETTE

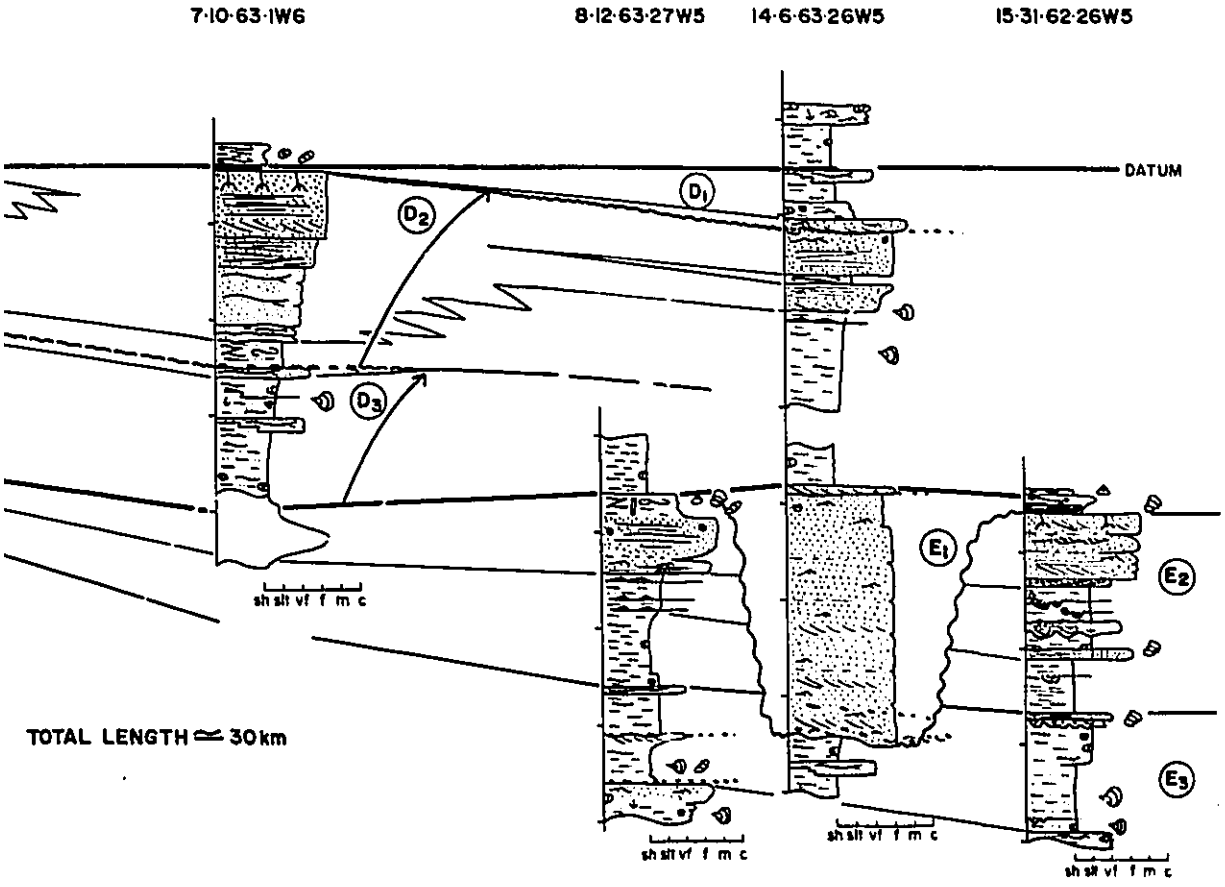

thins southeastward and northwestward. It pinches out toward the east between wells 12-26-62-26W5 and 3-8-62-25W5 and is overlain by the distal marine equivalents of D1. Sandstones in D3, which underlie D2, reach a maximum thickness of about 2 meters in well 10-13-63-3W6.

Core cross section 5-9B is hung on the top of member D. It corresponds to the log cross section (Fig.5-9A) but only extends for about 30 kilometers. From well 7-10, D2 thins in both directions. It correlates towards the northwest with about half a meter of bioturbated silty mudstone in well 10-13-63-3W6. The upper surface of shingle D2 is truncated by thin sandstones at the base of Shingle D1. In well 14-6-63-26W5, D2 is only 5 meters thick and comprises an incomplete coarsening upwards facies succession similar to Facies Association 1C. It is sharply overlain by about half a meter of cross bedded, medium-grained sandstone which grades upwards into laminated marine blockstones (Facies 2) containing gutter casts. Westward, D2 interfingers with bioturbated carbonaceous fossiliferous shales. Fauna include *Lingula*, *Corbicula*, and fish scales. Adjacert wells also contain *Brachydontes*. Thin (2 meters or less) cross-bedded to current-rippled sandstones erode into these mudstones. These sandstones contain thin basal lags and fine upwards. These fining upward facies successions are typical of Facies Association 2A as seen in wells 4-8-63-2W6 and 2-7-63-2W6.

Figure 4-14A,B, to the south, is also oriented perpendicular to the D2 sand body and shows similar relationships between the shingles in member D. Shingle D3 comprises well developed coarsening upward facies successions typical of Facies Association 1C in most of the wells in figure 4-14B. It is observed to thicken to the southeast on this cross section while it is clearly truncated to the northwest, and is only 50 cm thick in well 9-4-62-4W6. HCS sandstones (Facies 7A) are present in shingle D3 southeast of wells 2-6-62-3W6. They are thickest in well 13-28 and 6-22 (about 2 meters) and thin farther to the southeast. They are erosively truncated in the northwest.

Shingles D2 and D1 exhibit a fairly complex relationship in figure 4-14B. In many of the wells (e.g. 9-4, 7-7, 8-8, 3-9, and 2-6) coarsening upward facies successions typical of Facies Association 1A are well developed as indicated with the arrows. In other wells, such as 6-11 and 13-28, this coarsening upward facies succession is erosively truncated and overlain by a fining upward facies succession similar to Facies Association 2. In places shingle D2 is erosively truncated by shingle D1 (e.g. southeast of well 2-6). This truncation is clearly visible in wells 6-25-60-27W5 and 5-8-60-26W5 at the far right of the log cross section (Fig.4-14A). Despite this erosional truncation, sandstones of shingle D2 are seen to interfinger with and thin southeastward into marine blockstones containing *Inoceramus* (e.g. wells 5-27, 11-15, and 6-1). The D1 erosion surface in well 11-15

sits on marine blockstones and a close-up photo is shown in figure 3-3B).

The D2 sandstones also shale out and interfinger with pinstriped to banded mudstones to the northwest in wells 9-4 and 7-7. This northwest and southeast thinning is similar to that observed in figure 5-9A and B.

5-3-9. Cross Section Through D1 Finger

The fingerlike sand body in the southwestern portion of the map area represents the thickest sand in member D. The well log cross section (Fig.5-10A) which transects this sand body in a northeast-southwest direction (located on Fig.5-3B) extends for about 50km, and is hung on the base of the Second White Specks. The southwesternmost well (15-11-58-5W6) is represented by two side-by-side gamma log traces. In the original well log, these traces were continuous (connected at the arrows) and the Dunvegan Formation was observed to be anomalously thick. It was realized, based on vertical repetition of the log pattern, that about 80 meters of the Dunvegan Formation was repeated. This repetition is interpreted as due to the presence of a thrust fault, whose approximate position is indicated by the sawtooth pattern. This anomolous thickening was not observed in the adjacent wells. Correlation between the two traces indicates that the fault emplaced sediments of member E onto the Kaskapau Formation. It is not clear how much movement occurred on the fault.

Figure 5-10A. Well log cross section parallel to southwest finger in shingle D1. This cross section shows that shingle D1 comprises a major channel/valley fill. Unfortunately the top part of the channel and overlying sediments were not logged in well 11-19-59-3W6. It is assumed that the thick sands in this well correlate with other D1 channels noted on the cross section. All well traces are gamma ray logs. Thick black vertical lines represent cored intervals presented in figure 5-10B. Well 15-11 contains about 80m of repeated section resulting from a fault. This section has been restored, and the repeated sections in the same well have been drawn side-by-side. The left hand trace lies on top of the right hand trace in the original well log. All sands are stippled. The location of the cross section is shown in figure 5-3B. See text for further discussion.

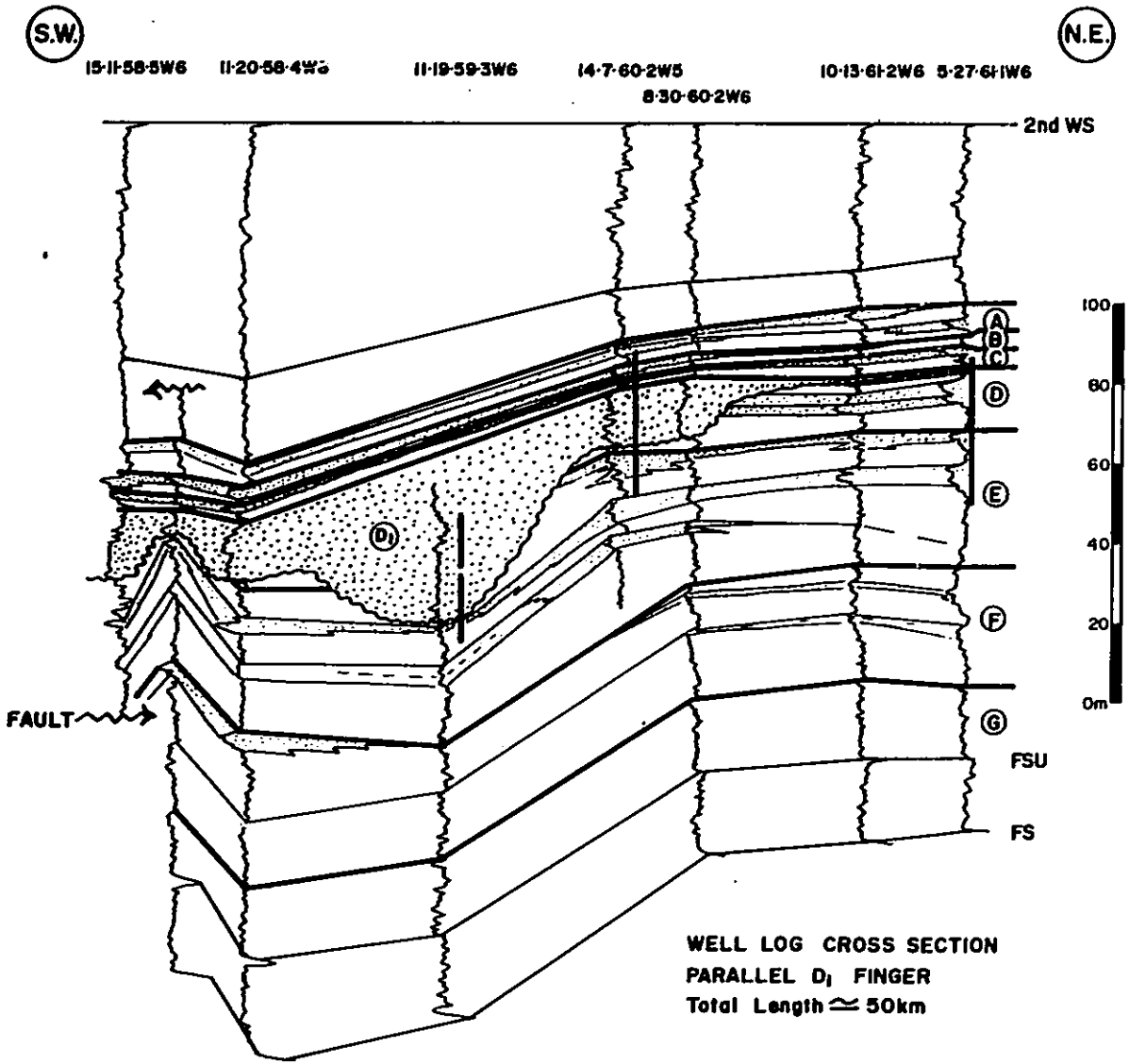
S.W.
N.E.
15-11-58-5W6
11-20-58-4W6
11-19-59-3W6
14-7-60-2W5
8-30-60-2W6
10-13-61-2W6
5-27-61-1W6
2nd WS
A
B
C
D
E
F
G
D_1
FAULT
FSU
FS
100
80
60
40
20
0m
WELL LOG CROSS SECTION
PARALLEL D_1 FINGER
Total Length ≃ 50km

Figure 5-10B. Core cross section through D1 Finger clearly illustrates erosional relationship of D1 to underlying shingles in member D. Arrows in D1 indicate fining upward facies associations and suggest channel filling. Note nearly 10m of massively bedded, structureless sandstone in well 11-19. Arrows in D3 indicate coarsening upward. Top of shingle E3 is used as a datum. See text for further discussion and figure 2-29 for legend.

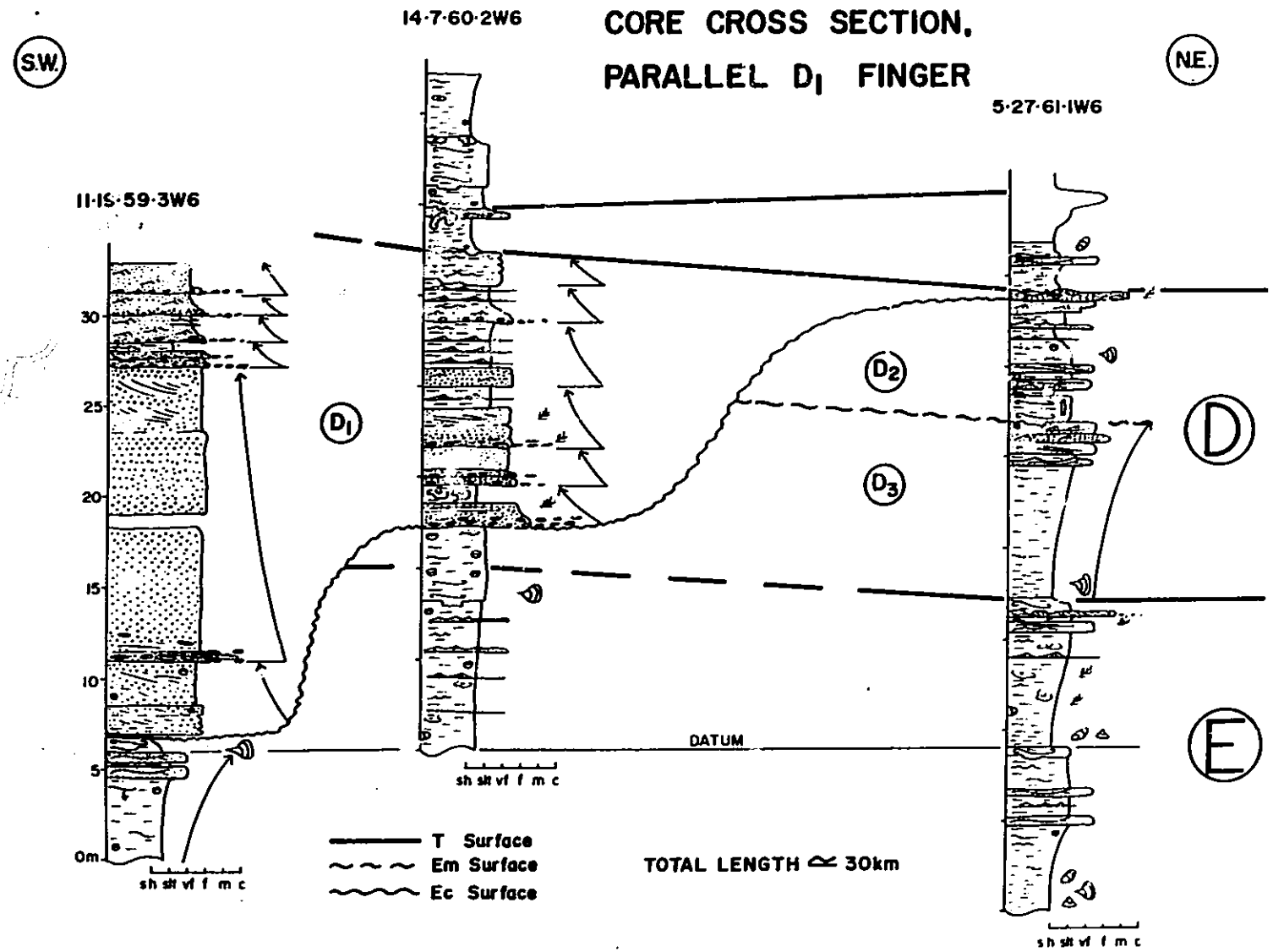
CORE CROSS SECTION,
PARALLEL D1 FINGER
S.W.
N.E.
14-7-60-2W6
5-27-61-1W6
11-15-59-3W6
30
25
20
15
10
5
0m
D1
D2
D3
D
E
DATUM
sh slt vf f m c
T Surface
Em Surface
Ec Surface
TOTAL LENGTH ≃ 30km

Gamma logs through member D in wells 5-27, 10-13, and the right hand trace of 15-11, are characterized by a series of stacked, more or less funnel-shaped, coarsening upward profiles. In contrast, gamma logs at about the same stratigraphic level in wells 8-30, 14-7, 11-19, 11-20 and in the left hand trace of 15-11 show blocky to bell-shaped profiles characteristic of channel fills. Correlation of overlying members suggests that these units belong to member D. Log markers are truncated between wells 15-11 and 10-13. In wells 15-11 (right hand trace), and 11-19 the upper portion of member E is truncated. This truncation is obviously due to erosion and is indicated on both the well log and core cross section with a wiggly correlation line (Ec Surface).

The core cross section (Fig.5-10B) extends for about 30 km and illustrates the succession of facies above and below this erosion surface. Well 11-19 penetrates two facies successions. The first 6 meters coarsens upwards and is typical of Facies Association 1C. This succession is capped by about half a meter of pervasively bioturbated mudstones (Facies 3A) containing *Inoceramus*. This passes gradationally upwards into a thin coaly shale, although there is no evidence of rooting. The second succession lies above the erosion surface and begins abruptly with 25 meters of massive, to cross-bedded to current-rippled sandstone containing abundant, large mudstone clast horizons. This fining upwards facies succession is typical of Facies Association 2A.

Superimposed are a series of smaller fining-upward cycles towards the top of the main succession.

In well 14-7, a lower coarsening upwards facies succession is abruptly overlain at about 12 m by about 15 m of interbedded fine-grained sandstones and shales showing an overall fining upwards. Superimposed are about 6 smaller fining upward successions typical of Facies Association 2A.

Core from well 5-27 contains several coarsening-upward facies successions. Member D is capped by about 40 cm of medium-grained, cross-bedded sandstone, the base of which is interpreted as correlating with the erosion surface.

Interpretation D1 Finger

The southwestern sand body represents filling of a major erosional feature. The precise geometry of this erosion surface is unclear due to a lack of close well control, although a major channel- or valley-shaped feature is suggested. Multiple fining upward cycles in wells 14-7 and 11-19 may indicate multiple channel fills in a major erosional valley. The great thickness of massive sandstones in 11-19 is problematic. The lack of noticeable breaks in deposition may indicate a single event. This erosional feature truncates shingles D2 and D3 and is clearly younger. It is therefore interpreted to be about the same age as the Waskahigan channel in shingle D1. The lack of marine fauna suggests a dominantly non-marine fill.

5-4. Interpretation of Shingles

5-4-1. Shingle D3

The coarsening upward (Type 1C) facies association in D3 (Fig.5-7A,B) may be interpreted as representing progradational storm-dominated shelf deposits possibly related to a progradational shoreline farther to the west. As indicated in Figure 5-8B, pervasively bioturbated marine mudstones (Facies 3A) at the base of shingle D2 sit erosively on shingle D3 forming an Em surface. This leads to an alternate interpretation, namely that thick sandstones may have been initially present in shingle D3 but may have been erosively removed during subsequent transgression prior to deposition of shingle D2. Given that no thick sandstones are anywhere preserved, the former interpretation is favoured. The marine erosion surface may be due to a minor transgression, perhaps due to switching of the locus of deposition between D3 and D2. The erosion is unlikely to be due to a drop in base level for two reasons; first, there is no evidence of channelling or of subaerial exposure and secondly, a drop in base level should be accompanied by an increase in sedimentation rate. This increase would result in laminated sediments, similar to those seen in the prodeltaic mudstones of member E, rather than the pervasively bioturbated mudstones which sit on top of shingle D3.

5-4-2. Shingle D2

The sand body which corresponds to D2 is interpreted as a linear, northeast-southwest (strike) oriented, shore parallel, emergent barrier island, erosively truncated at its northern end by a major distributary channel. A paleogeographic reconstruction is shown in figure 5-11. Facies associations through the axis of the sand body show coarsening upward facies successions (Facies Association 1A) typical of prograding wave- and storm-dominated shorelines (Fig.5-7A,B; Fig.5-11,A-A'). Nested within some of these coarsening upwards facies successions are fining upwards channelized facies successions (Association 2A and 2B) which contain facies interpreted as reflecting tidal processes (Fig.5-8B, Fig4-14B; Fig. 5-11, inlets in A-A'). These facies successions probably represent tidal inlet fills that cut through the barrier bar sandstones. Tidal channels commonly underlie migrating barrier islands in modern coastal settings (Reinson,1984). As shown in the dip-oriented cross sections (Fig.5-9A,B; Fig4-14A,B), and in figure 5-11, B-B', the upper surface of the barrier sandstone dips in a seaward direction (northwest) but is interpreted as interfingering westward with mudstone containing fauna typical of restricted, brackish to marine lagoonal environments, typical of Facies Association 3. These lagoonal deposits are cut by thin channelized sandstones which are probably fluvial in nature. *In situ* root traces and

Figure 5-11. Paleogeographic reconstruction of shingle D2. To make this reconstruction, sand body geometries from figure 5-3A and facies interpretations from core were used. Large arrow represents orientation of longshore drift. Arrow above cross sections points to the tie well. Shingle D2 is interpreted as a linear barrier island which probably grew from northeast to southwest by barrier spit accretion. Sediment was probably supplied by the Waskahigan channel in the northwest and carried south by longshore drift. Portions of the barrier are underlain by tidal inlet facies successions shown in cross section A-A'. In B-B', the sandy barrier grades basinward into shelf mudstones and landward into lagoonal facies.

WAVE-DOMINATED BARRIER
SHINGLE D_2

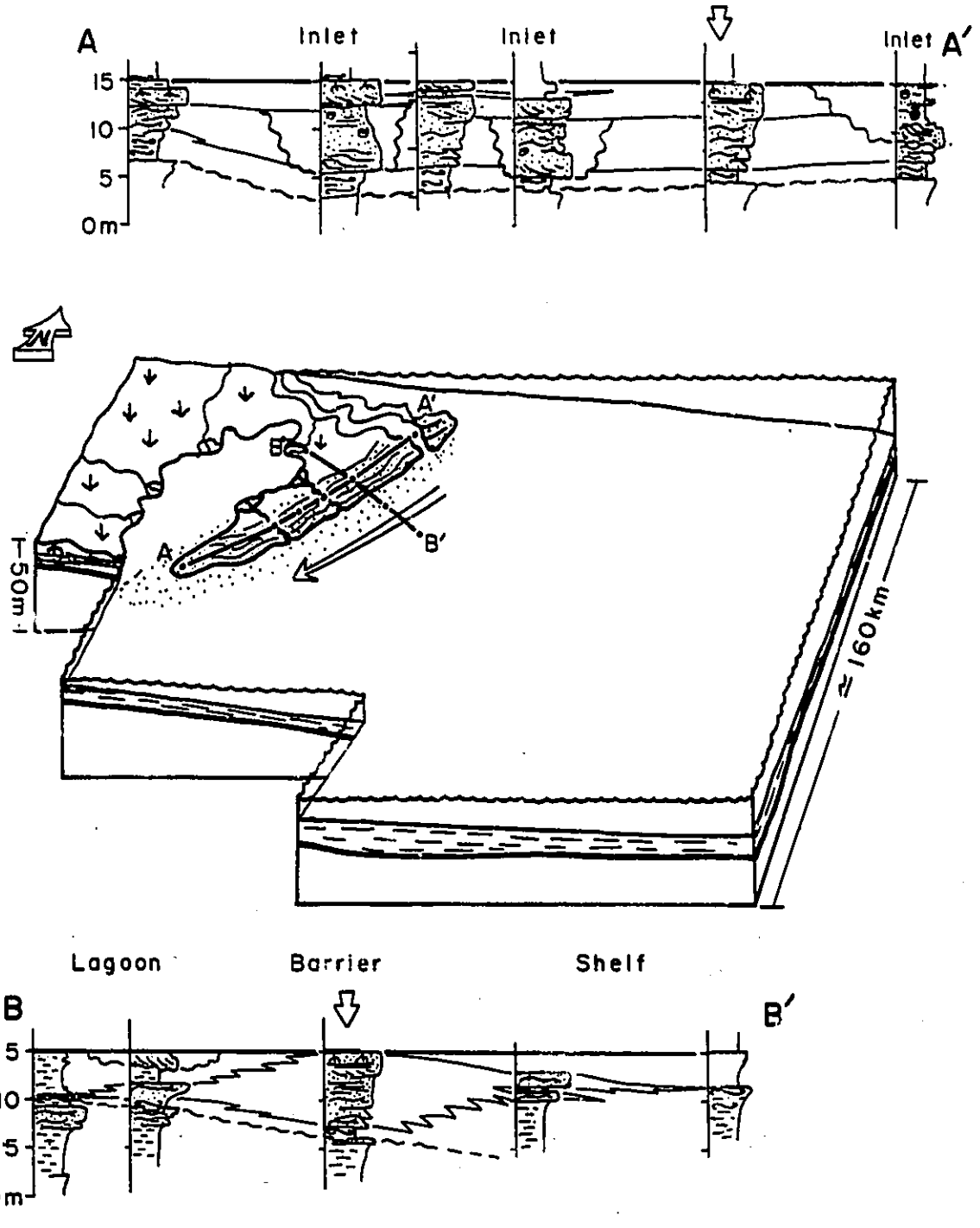

thin coals at the top of the barrier island sandstone indicate non-marine swamp and marsh environments.

The barrier probably grew from northwest to southeast, as indicated by thinning in this direction (Fig.5-3A,B). This thinning probably relates to the general direction of longshore drift (arrow in Fig.5-11). It is possible that the barrier was originally fed by a channel that lay in the same geographic position that was later occupied by the Waskahigan channel. This would suggest growth of the barrier from northeast to southwest.

Shingle D2 is also truncated in a seaward direction by shingle D1 as shown in both the cross section perpendicular to the D2 sand body (Fig.5-9B; Fig 4-14A,B) and in the regional dip cross section (Fig.5-2). It is possible that D2 was originally more extensive than is presently mapped, and that its linearity may partly be an artefact of this erosion. Figure 5-9B and Figure 4-14B both suggest, however, that sandstones in shingle D2 contain greater thicknesses of marine shales and blockstones to the southeast. This suggests that shingle D2 passes into shelf mudstones to the southeast and that the D1 erosion surface does not remove significant quantities of sandstone. The presence of lagoonal deposits in a landward direction strongly argues for interpretation as a barrier island. There is no evidence that the D2 sandstone was ever attached to the land while it was actively growing.

5-4-3. Shingle D1

D1 is interpreted as representing a storm influenced, wave-dominated delta fed by a major distributary channel, with a large southerly directed alongshore component of transport. Figure 5-12 shows a paleogeographic reconstruction of shingle D1. The lobate to cuspate geometry of D1 (Fig.5-3A,B; Fig.5-12) is similar to wave-dominated deltas described by Coleman and Wright (1975) and Weise (1979). The orientation of the sand body suggests an irregular shoreline with the sea to the east (Fig.5-3A,B; Fig.5-12). The facies succession through the middle part of the lobe (Fig.5-4; Fig.5-12, section A-A') is characteristic of Facies Association 1A which is interpreted as being produced by progradation of a wave- and storm- dominated shoreface. Progradation of this shoreface probably culminated in subaerial exposure as indicated by the presence of probable coal on well logs.

The Waskahigan bottleneck (Fig.5-3B) is interpreted as representing an updip feeder channel toward the northwest. Core and logs through this portion of the sand body clearly indicate erosion at the base (Fig.5-5A,B). The asymmetrical nature of the channel base and the presence of low angle surfaces, which dip towards the deepest portions of the channel, suggest lateral migration. The sense of asymmetry changes in the northwest where the deepest part of the channel (cutbank) lies on the northeast side (Fig.5-8A). This suggests that the channel meandered and that the northeast-southwest cross sections traverse different

Figure 5-12. Paleogeographic reconstruction of shingle D1. To make this reconstruction, sandstone body geometries from figure 5-3A were used in conjunction with cross sectional geometries and lithofacies from cores presented in the thesis. Small arrows represent shoaling waves which produce the cuspate geometry of the D1 lobe. The large arrow indicates the overall inferred direction of longshore drift. The Waskahigan channel is seen snaking through the upper northwest half of the map area. It cuts the northern end of the older D2 barrier; now abandoned and overlain by non-marine swamp and marsh environments. The Waskahigan channel feeds the D1 lobe and sands are transported up to 100 km south by longshore drift. A major erosional feature in the southwest portion of the diagram is filled with non-marine sandstones and shales. Cross section X-X' is oriented down the depositional dip of the D1 wave-dominated delta. The facies succession within the channel is typical of Facies Association 2B, and is interpreted as an estuary. The channel feeds the D1 lobe which grades seaward into bioturbated muddy shelf deposits.

WAVE-DOMINATED DELTA
SHINGLE D_1

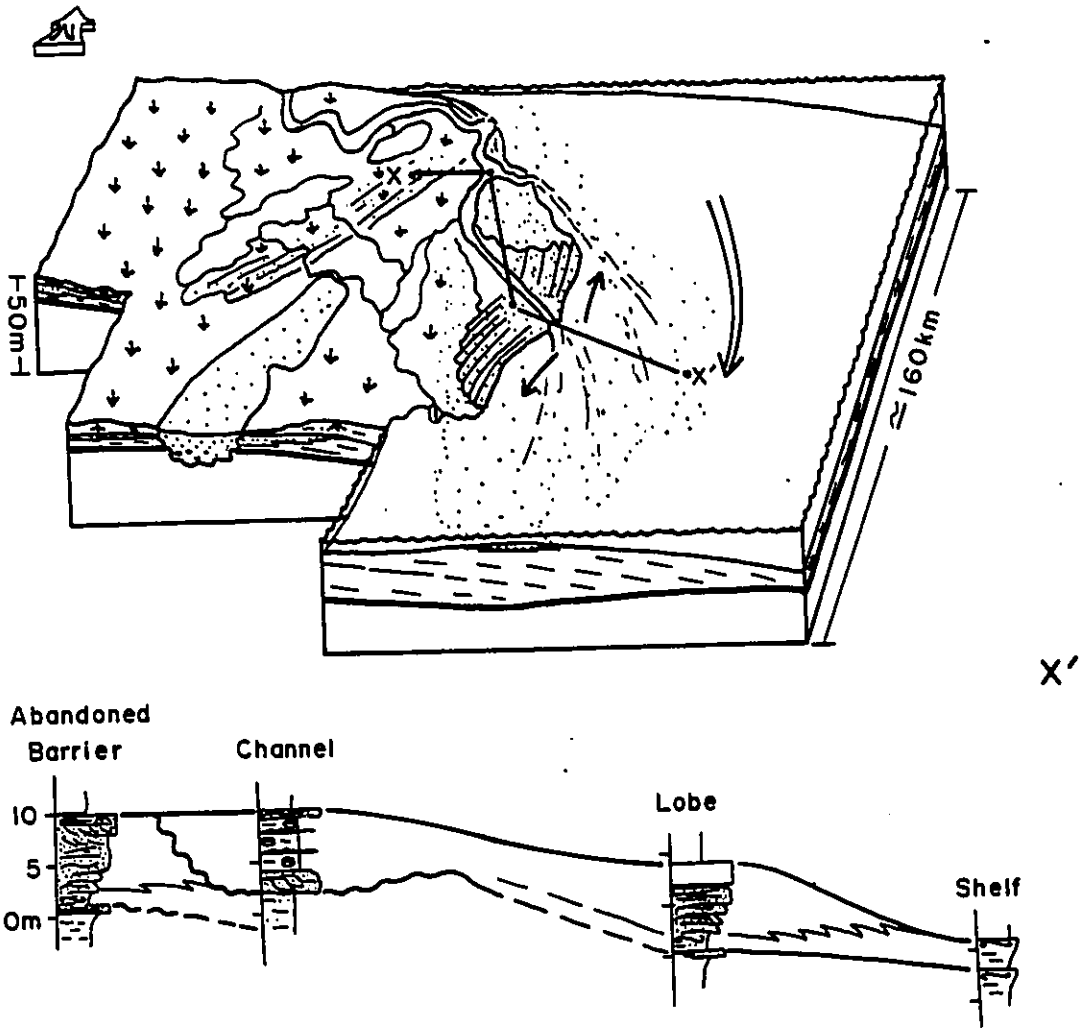

meander loops, with their cutbanks facing in different directions. The sediments that filled the channel were not necessarily deposited by the same processes that caused the erosion in the first place (except for the lags). Some of the upper portions of channel fill successions are typical of Facies Association 2B. They are partly filled with marine mudstone and contain marine trace fossils (Fiog 5-5A,B; Fig.5-6; Fig.5-12). The marine influence suggests that these channels became estuarine in their later stages and suggests that they were filled during the initial phases of transgression of member D. Sedimentation rates are interpreted to be lower than in the sand dominated channels of member E.

Most of the deltaic sands interpreted to have been supplied this channel lie to the south (Fig.5-3A; Fig.5-12) suggesting that as sand was supplied to the shoreline it was transported up to 100 kilometers south, probably by longshore drift (large arrow, Fig.5-12). This southerly directed longshore transport direction is consistent with the inferred direction in which the underlying D2 barrier also grew.

Erosion of the Waskahigan channel is also thought to correlate with erosion and deposition of a major valley fill in the southwestern portion of the area (Fig.5-10A,B; Fig.5-12). This erosional surface truncates the upper portions of shingle D2, especially towards the south, and indicates a significant drop in base level.

CHAPTER 6. MEMBER C

6-1. Introduction

There are relatively little data for member C. For this reason, separate condensed descriptive and interpretational summaries are not presented. Member C includes producing sandstones in the Giroux pool (T66 R21W5).

6-2. Description

6-2-1. Thickness and Extent

Figure 6-1 shows a total isopach map of member C. West of about range 22W5, member C varies in thickness and averages about 7 meters. Locally member C is not present and in at least one place (T61 R27W5M) member C contains a prominent bullseye indicating a local thick. It begins to thicken rather rapidly east of about range 22W5M, along a NNE/SSW oriented break in accumulation which follows the 8 meter contour. Member C reaches a maximum thickness of about 40 meters at the eastern edge of the map. Preliminary cross sections, not presented here, indicate that member C maintains this thickness for several tens of kilometers eastward.

Figure 6-1. Total Isopach Map, Member C. Dots indicate data points. Heavy black arrows indicate break in thickness of accumulation. Member C is thicker to the southeast of this line. See text for further details and explanation.

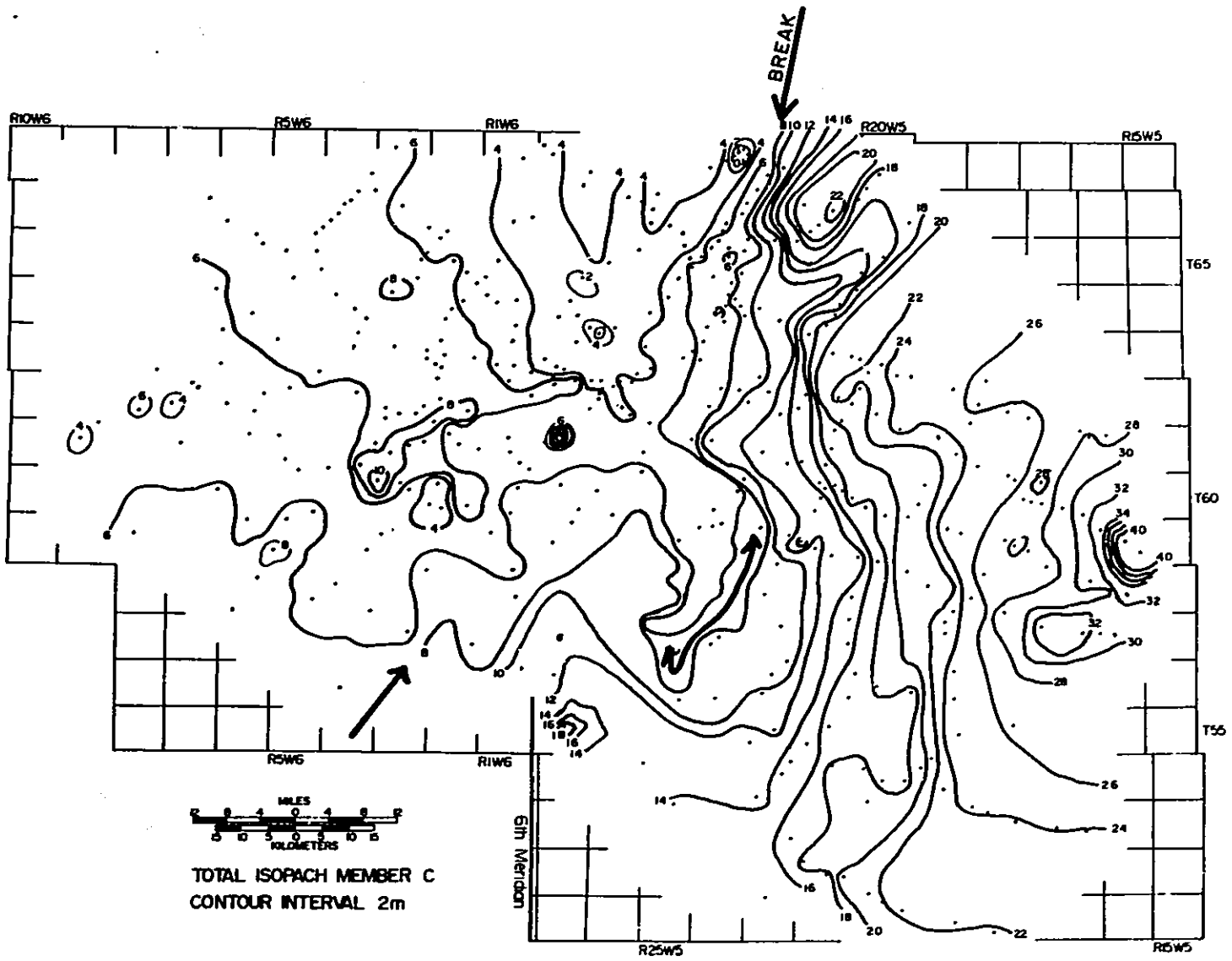
BREAK
R10W6
R5W6
R1W6
R20W5
R15W5
T65
T60
T55
R5W6
R1W6
6th Meridian
R25W5
R15W5
MILES
KILOMETERS
TOTAL ISOPACH MEMBER C
CONTOUR INTERVAL 2m

6-2-2. Regional Stratigraphy

Figure 6-2 represents a regional schematic cross section oriented parallel to depositional dip (northwest) and hung on the top of member C. The geology from the major regional dip cross section (Fig.3-9A) was plotted at twice the vertical scale and correlated on figure 6-2. Core data was used in order to determine the nature of surfaces correlated on the cross section. The depositional break, as shown on the cross section (Fig.6-2), lies between wells 3-8 and 2-26. A distinct wedge of sediment containing five thin prograding shingled sands separated by shales can be seen to the southwest of the depositional break. One of these shales was seen to be thicker than the rest and member C was divided into two major shingles. These sands dip towards the southeast and downlap onto the top of member D. Shales separating these shingled sand bodies are seen to become thinner towards the northwest and terminate up-dip against the overlying T-surface, where the sandstones are also truncated. The Em surface which truncates these sandstones can be correlated over the entire northwest half of the cross section and is overlain by a widespread sheet sandstone. Member C appears to have been planed off towards the northwest and the resulting cross sectional geometry is that of an undulating blanket or sheet. It is not clear how much sediment has been eroded. In wells 7-7, 4-8, 14-6, and 15-31 remnants of the underlying sandstones are preserved below the Em

surface. In the other wells in the northwestern half of the cross section, the Em surface sits directly on mudstones and shales.

6-2-3. Gross Sandstone Isolith Map

Figure 6-3 is a gross sandstone isolith map of all sandstones within member C. The overall geometry is that of a ragged blanket sandstone. Well developed lobes, shoestring sands, and distinct linear sand bodies are notably absent. In general, sandstone thicknesses are low, averaging between 2 to 4 meters over most of the map area. In several places, including the eastern edge of the map area, no sand is present at all, while in other places, local accumulation exceeds 15 meters. Thick sands are not associated with the thickest portion of member C in the southeast.

An anomalous 15 meter thick sandstone associated with member C occurs in well 10-26-61-27W5 but was not observed in adjacent wells. Well control around this bullseye is poor, the closest well is about 3 kilometers away and the extent of this sandstone is unknown. The well logs through this sandstone (Fig.6-5) indicates that it erodes into the underlying member D and has a distinctly blocky log shape. Other similar sandstones of local extent but greater than about 8 meters lie in township 58 R27W5 and in township 62 R22W5.

Figure 6-2. Schematic regional dip oriented cross section through member C, based on figure 3-9A. Prominent break in thickness of accumulated sediment is evident between well 3-8 and 2-26. Stipple indicates sandstone. Member C is largely eroded to the northwest and is divided into two shingles, each containing several sandstones. See text for explanation.

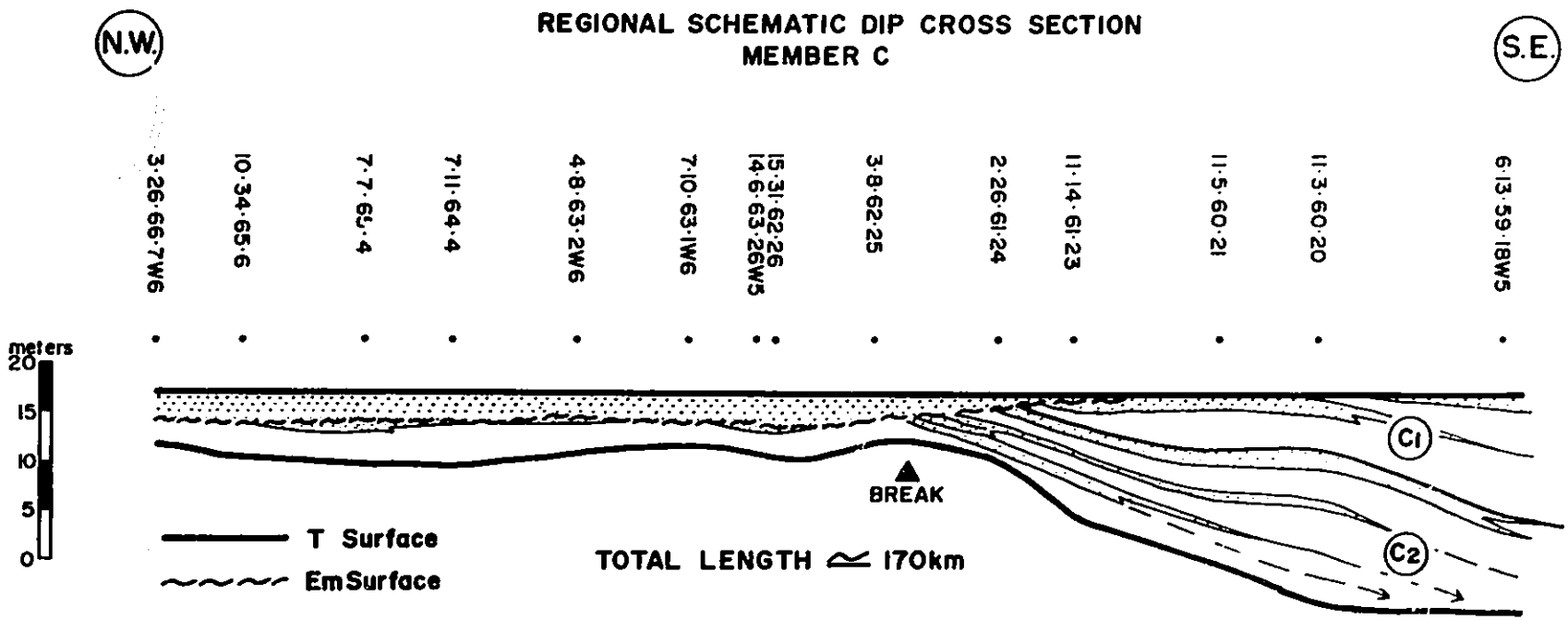
REGIONAL SCHEMATIC DIP CROSS SECTION
MEMBER C
N.W.
S.E.
3-26-66-7W6
10-34-65-6
7-7-65-4
7-11-64-4
4-8-63-2W6
7-10-63-1W6
15-31-62-26
14-6-63-26W5
3-8-62-25
2-26-61-24
11-14-61-23
11-5-60-21
11-3-60-20
6-13-59-18W5
meters
20
15
10
5
0
T Surface
Em Surface
BREAK
TOTAL LENGTH ≃ 170km
C1
C2

Figure 6-3. Gross sandstone isolith map, member C. Dots indicate data points. The geometry is that of an undulating sheet with several bullseyes. Position of cross sections 6-4 and 6-5 is also shown. See text for details and explanation.

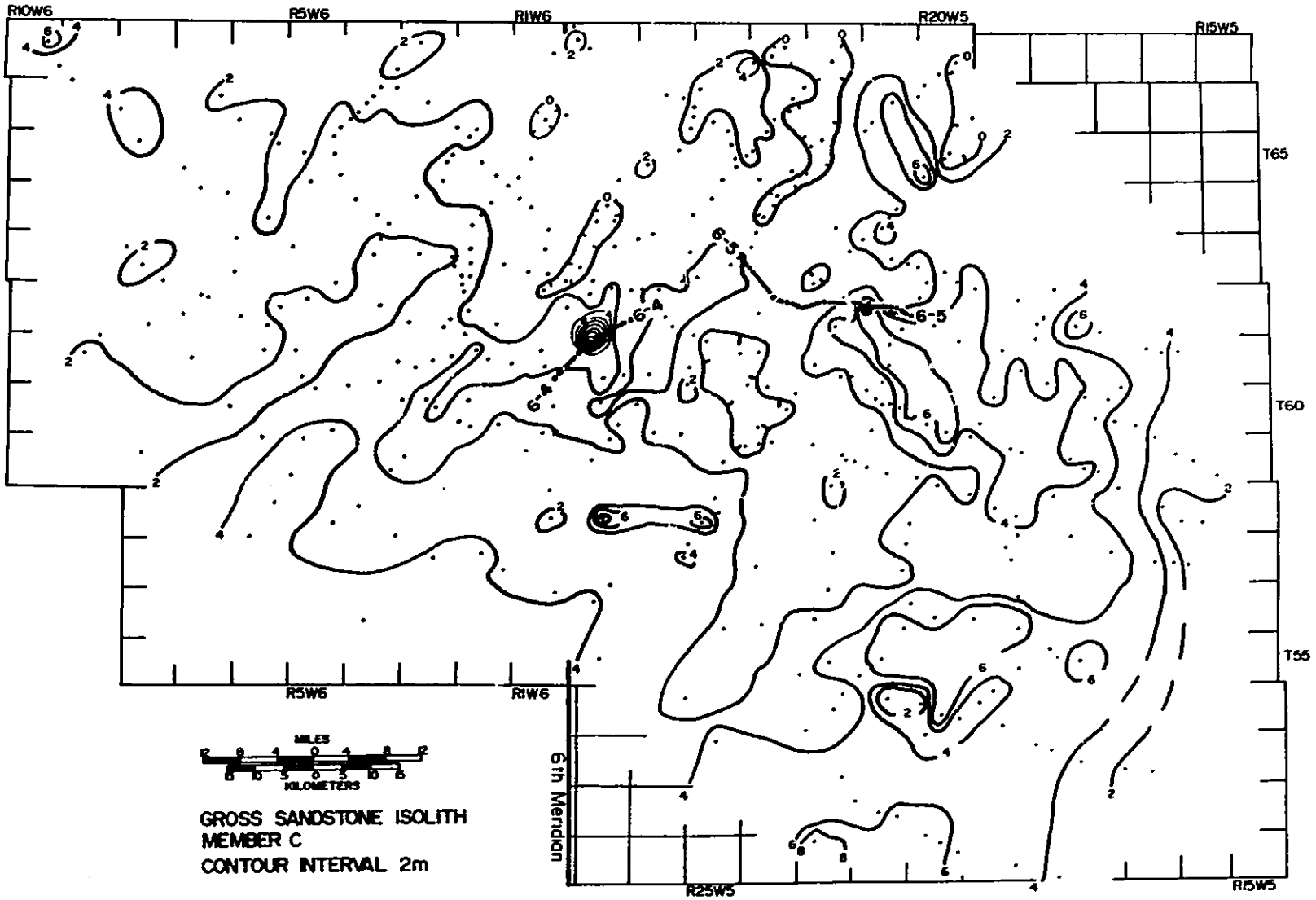
R10W6
R5W6
R1W6
R20W5
R15W5
T65
T60
T55
6-3
6-4
6-5
R5W6
R1W6
6th Meridian
R25W5
R15W5
MILES
KILOMETERS
GROSS SANDSTONE ISOLITH
MEMBER C
CONTOUR INTERVAL 2m

6-2-4. Cross Section Perpendicular to C Break

Few cores are available through member C in the eastern half of the map area. Figure 6-4A and B is a northwest/southeast cross section which includes cores in the area of the break in accumulation described above. The well log cross section is hung on the base of the Second White Specks and extends for a length of about 30 kilometers. Member C thickens from about 5 meters in the northwest to about 20 meters in the southeast. Most of the gamma logs through member C are funnel-shaped, indicating coarsening upwards. This is best developed in wells 7-25, and 3-27. The sandstone at the top of member C in well 10-22 is distinctly blocky-shaped but is not present in the adjacent wells. The well logs indicate that member C passes sharply back into shale in every well.

The accompanying core cross section extends for a length of about 23 kilometers and is hung on the top of member C. Member C is seen to thicken from about 5 meters in well 7-22 up to about 16 meters in well 3-27. Correlations suggest that depositional surfaces within the lower portion of member C dip towards the southeast. These dipping surfaces are truncated by prominent Em and Ec surfaces at the top of member C. The facies successions within member C broadly coarsen upwards in wells 7-22, 6-29 and 3-27. They begin with several meters of laminated marine shales (Facies 1A) and blockstones (Facies 2). In well 7-22 these blockstones are sharply truncated by about 1 meter of pervasively

bioturbated silty mudstones. This contact is an Em surface. Core through member C, in well 3-27, shows a rather irregular coarsening upwards facies succession which resembles Facies Association 1C. The succession begins with about 10 meters of laminated marine shales and blockstones containing a few thin wave rippled sandstone beds (Facies 7B). These blockstones grades upward into about 3 meters of interbedded, burrowed to convolute laminated sandy mudstones which are capped by about 2 meters of very fine-grained wave-rippled sandstones containing thin shaly partings. The facies succession in well 10-22, in contrast, is similar to Facies Association 2A. The log response and facies succession is similar to other bullseye sandstones within member C. The lower 6 meters, in well 10-22, are similar to the facies in well 3-27 and comprise laminated marine blockstones which become convoluted towards the top. In 10-22, these convoluted mudstones are sharply truncated by the overlying fine-grained sandstones. The contact is marked by a sideritic lag. The sandstone is about 7 meters thick and contains 7 normally graded beds. Each bed has a sharp base and begins with cross bedding (Facies 7D). The finer-grained sandy portions of some of the beds are current rippled (Facies 7C). This sandstone contains sideritic rip-up clasts at the top and is sharply capped by a few centimeters of pervasively bioturbated silty mudstone (Facies 3A).

Figure 6-4A. Well log cross section perpendicular to C break. Vertical bars indicate cored intervals presented in figure 6-4B. All wells are gamma logs. Note also bifurcating channels in shingle E1 of member E. See text for details.

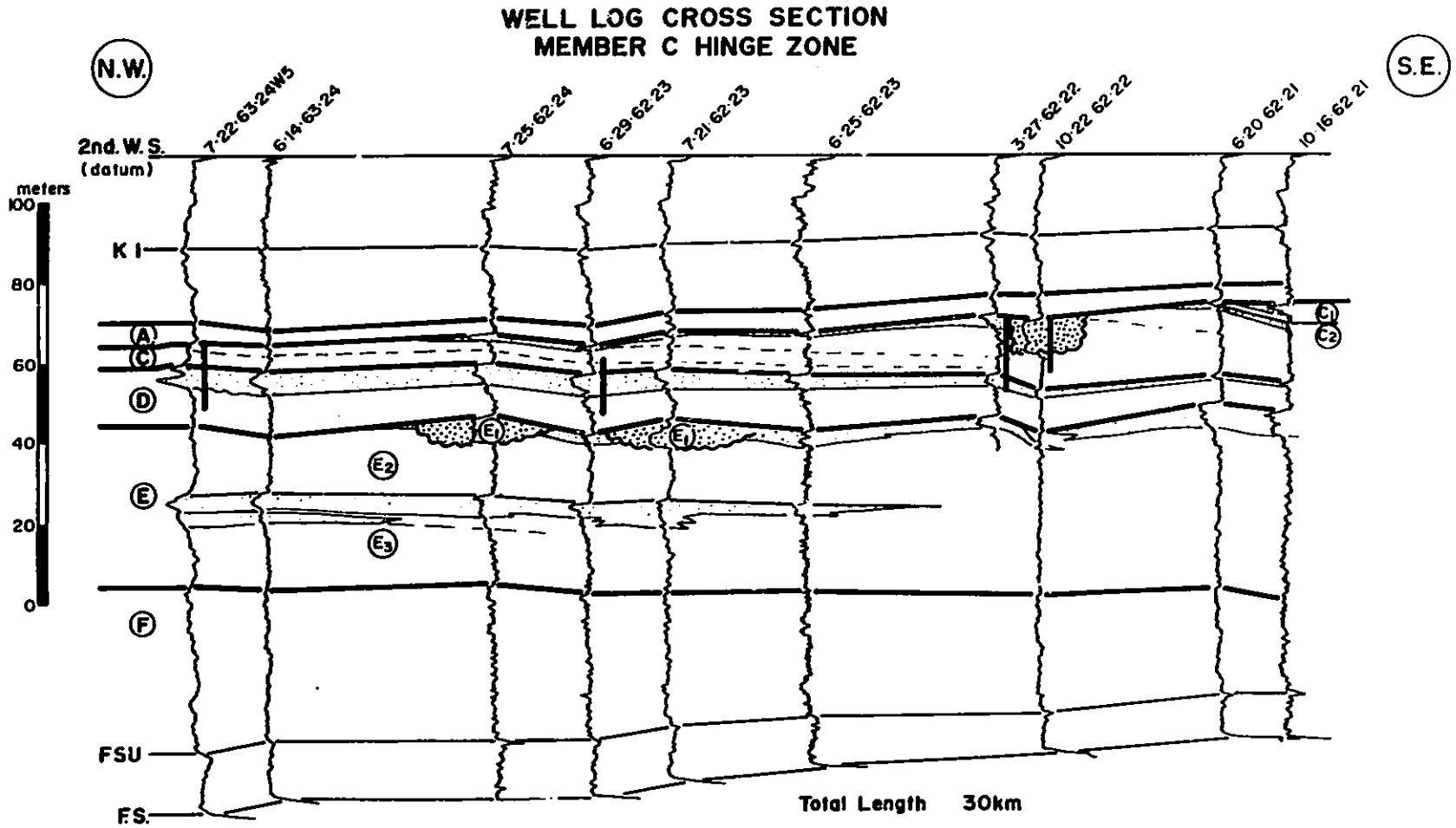
WELL LOG CROSS SECTION
MEMBER C HINGE ZONE
N.W.
S.E.
7-22-63-24W5
6-14-63-24
7-25-62-24
6-29-62-23
7-21-62-23
6-25-62-23
3-27-62-22
10-22-62-22
6-20-62-21
10-16-62-21
2nd. W. S.
(datum)
meters
100
80
60
40
20
0
K I
A
C
D
E
F
E1
E2
E3
C1
C2
FSU
F.S.
Total Length 30km

Figure 6-4B. Core cross section through C break. Note rapid thickening of member C to the southeast. Incomplete coarsening upward facies successions, indicated with the arrows, are seen in wells 7-22, 6-29, and 3-27 and are similar to the lower portion of Facies Association 1C. This coarsening upward facies succession is truncated in well 10-22 by a fining upward facies succession which is similar to Facies Association 2A. Graded beds are indicated with small arrows. See text for details and explanation and figure 2-29 for facies legend.

N.W.

CORE CROSS SECTION
MEMBER C HINGE ZONE

S.E.

7-22-63-24W5 6-29-52-23W5 3-27-62-22W5 10-22-62-22W5

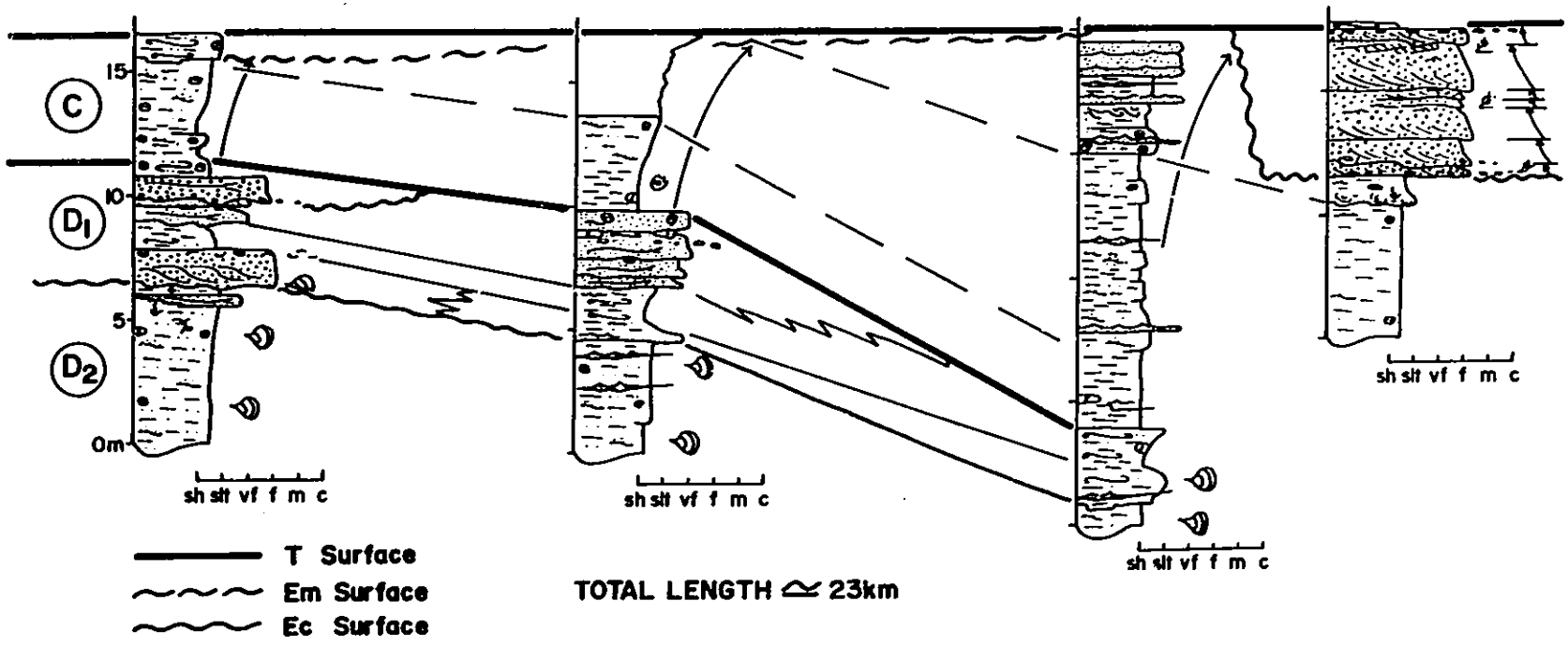

Interpretation

The overall coarsening upwards in wells 7-22, 6-29 and 3-27 indicates progradation. The facies successions are typical of Facies Association 1C which were interpreted in chapter 2 (section 2-3-1C) as indicating deposition in storm-influenced deltas. The facies succession in well 10-22 is typical of Facies Association 2A and is interpreted as a sandy channel fill. Erosion is indicated by the basal lag, the coarser nature of the sandstone fill, and the blocky response on well logs. The sedimentary structures are typical of those produced by waning unidirectional currents and contrast with the sandstones in the adjacent well (3-27) which are finer-grained and are wave rippled. The lateral changes in facies therefore indicate coarsening upwards facies successions, typical of storm influenced prograding deltas, truncated by fining upwards facies successions typical of sandy channel fills.

Member C is truncated by a widespread Em surface as indicated in well 7-22. The thinning towards the northwest is likely the result of this marine erosion.

6-2-5. Northwestern Facies Associations

Figure 5-9B represents a core cross section through the D2 barrier and has already been discussed with respect to members E and D in chapters 4 and 5 respectively. Cores through member C in wells 10-13, 2-7 and 4-8 on the core cross section (Fig.5-9B) show similar facies successions. In these wells, member C is about 5

meters thick and begins with bioturbated to laminated marine shales (Facies 1B and 1A) which coarsen upwards into sideritic pinstriped mudstones (Facies 4). In each of the three wells, this coarsening upwards facies succession is sharply overlain by bioturbated sandstone (Facies 7I) containing abundant large *Ophiomorpha* and *Thalassinoides* burrows (a close-up photo of these sandstones is shown in figure 2-19a). The contact between the overlying sandstones and underlying mudstones is invariably highly bioturbated; the fingerlike sand filled *Thalassinoides* burrows penetrate several centimeters down into the underlying mudstones (Fig.2-19b). In all three wells, this sandstone is sharply overlain by laminated marine mudstones.

Cores in several wells on the major, strike-oriented regional core cross section (Figure 3-8A) penetrate member C and indicate the lateral variability of the facies outlined above. Member C is thickest in well 7-17 and thins towards the northeast and southwest. The lower portion of member C in most of the wells shows a coarsening upwards facies succession similar to that described above in figure 5-9B. In well 7-17, however, member C is about 8 meters thick and contains a 1 meter thick sandstone bed not present in the adjacent wells on the cross section. In the core cross section parallel to the D2 sandstone (Figure 5-8B) the same core through well 7-17 is shown in more detail. This lower sandstone is cross bedded to parallel laminated and is also present in some of the adjacent wells (e.g.12-24), as indicated on

the accompanying well log cross section (Fig.5-8A). The capping, pervasively bioturbated sandstone, present in well 7-17, extends across the entire length of both cross sections for a distance of at least 100 kilometers, except in well 6-27 on figure 5-8A, where it is erosively truncated by sandstones in the overlying member B. In well 6-11 on figure 3-8A, this sandstone contains some preserved cross bedding while farther to the northeast on the same cross section (well 4-11, Fig.3-8B) this facies becomes shalier and grades into pervasively bioturbated sandy mudstone. Core photos from well 6-11 (Fig. 3-7C), show the facies succession through member C. The contact with the underlying banded mudstones of member D is razor sharp (at about 39.8m, box 1, 39.3-44.2m, Fig.3-7C). This is followed be about 4 meters of black bioturbated mudstones (Facies 1B) which grade up into pinstriped mudstones (Facies 4). At about 44.5 meters, these pinstriped mudstones are erosively overlain by pervasively bioturbated sandstones (Facies 7I), marked with am Em arrow in box 1 (44.2-49.0m). Except for a few pieces which show spectacular *Ophiomorpha* burrows, these sandstones have a dark grey colour on the photos owing to oil staining. Member C passes up into about 40 cm of banded mudstone before being overlain by the laminated shales and blockstones of member B at about 46m (box 3, 44.2-49m).

Similar lateral changes in facies are seen in Figure 4-14B. Coarsening upwards facies successions, similar to Facies Association 1B, are truncated by a widespread bioturbated marine

sandstone. Sandy erosional remnants within the upper part of member C are seen in wells 8-8, 2-6, 11-15 and 6-1. These underlying remnants show a greater proportion of wave produced sedimentary structures towards the southeast.

6-2-6. Cross Section Through C Bullseye

Figure 6-5 is a well log cross section through the anomalous bullseye in figure 6-3. The cross section is hung on the base of the Second White Specks and extends for a length of about 18 kilometers. The correlations emphasize the relatively uniform and parallel nature of the strata within members. Strata in member D and C are clearly truncated in well 10-26-61-27W5 by a prominent sandstone, 17 meters thick. This sandstone is associated with member C and is indicated by the blocky response on the gamma log. The gamma log profile is similar to other channelized sand bodies described in members D and E. This sandstone was not detected in any of the adjacent wells.

Interpretation of bullseye

The cross section (Fig. 6-5) and map (Fig. 6-3) indicate a thick erosively-based sand body of limited areal extent. This is interpreted as representing a channel. Unfortunately, well control is poor and it was not possible to accurately pinpoint or map the orientation of this channel.

Channels in members D and E averaged about 5 kilometers in width and could be traced for lengths of up to 100 kilometers. Erosional remnants of channels in member C have already been

Figure 6-5. Well Log Cross Section Through C Bullseye. All well traces are gamma logs. Note thick channelized sandstone in well 10-26 which also erodes into the underlying member D. See text for explanation and details.

CROSS SECTION THROUGH C BULLSEYE

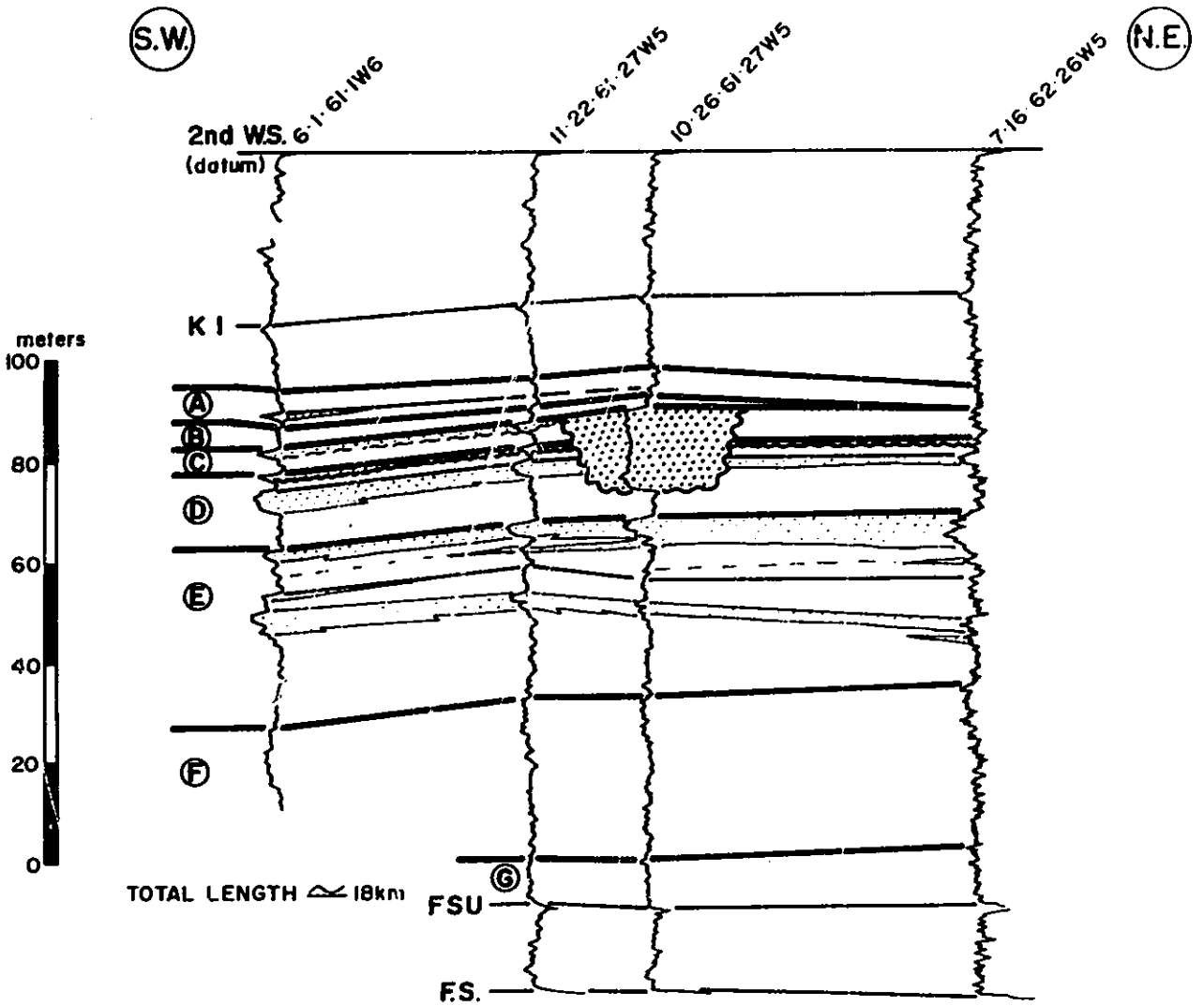

described in above (well 10-22, Fig.6-4). It is probable that the C bullseye is also a remnant of a previously more extensive channel. Given the well control and assuming an approximately northwest/southeast orientation, this remnant could be up to 5 kilometers wide and up to 20 kilometers long.

6-3. Interpretation and Discussion, Member C

Member C represents a prograding wedge of sediments whose main locus of deposition is east of about township 22W5. The factors which result in this break in deposition will be discussed in chapter 12. West of this break, sediments of member C are truncated by a widespread marine erosion surface (Em surface) overlain by a layer of bioturbated marine sandstones and mudstones, which average about 1 meter in thickness. This irregularly distributed sandstone is interpreted as representing a transgressive sand sheet derived from erosion of the underlying sediments. In places, such as in well 7-17 (figs.3-8A and 5-8B) where erosion is less and member C is thicker, remnants of shallow marine sandstone deposited during the progradational phase of member C are preserved. Portions of channels, also associated in time with the progradational phase of member C, are locally preserved, such as in well 10-22 (Fig.6-4) and in well 10-26-61-27W5 (Fig.6-5). The anomalously low sandstone values at the eastern edge of the thickest portion of member C (Figs.6-1 and 6-3) are probably due to erosional stripping of the sandy upper portions of member C during transgression in the southeast. The widespread

cannibalization of the upper portions of member C result in the deposition of a widespread ragged blanket sandstone. Well developed shoestring sandstones, sandy deltaic lobes and linear sand bodies may have been originally present but are only preserved as isolated remnants.

Sediments of member C prograde farther into the basin than in any other member. The physical geometry of sandy shingles within the southeastern half of member C suggest that they merge towards the northwest indicating an original toplapping relationship. As has been previously mentioned, distinction of toplap and erosional truncation may be difficult. It is not completely clear how much sediment has been erosionally stripped from member C towards the northwest. The preservation of portions of fluvial channels suggests that erosion has been relatively minor; but perhaps up to several meters.

6-4. Summary of the Depositional History of Member C

Member C begins with the progradation of several shingled sand bodies from northwest to southeast. These have been grouped into two main shingles. Most of the northwestern portion of the map area is probably bypassed during deposition of the upper shingle, which was deposited southeastward of a major northeast/southwest oriented depositional break. This is indicated by the preserved remnants of several channels immediately west of this break. Deposition of member C culminated with a major marine transgression. West of the depositional break, water depths were

probably shallow enough that this transgression was capable of cannibalizing the uppermost portions of member C and reworking the uppermost sandstones into a thin widespread sand sheet. Several meters of erosion are indicated during this transgression. In places, sand supply probably ran out producing areas of little or no sand. This imparts a ragged blanket geometry to sandstones in the western half of the map area.

At or near the time of maximum transgression, the basin was characterized by widespread shale deposition producing the T-surface that marks the end of deposition within member C.

CHAPTER 7. MEMBER B

7-1. Introduction

Member B is fairly limited in extent and contains no producing fields. Earlier correlations during the first phase of the study indicated that it was more widespread but were later revised to those presented here.

7-2. Description

7-2-1. Thickness, Extent and Stratigraphy

Member B is confined to the northwestern half of the map area (Fig.7-1). The total isopach map of member B (Fig.7-1) indicates that it has the shape of an undulating wedge and ranges from a maximum of about 10 meters in the northwest down to a zero depositional edge southeastward. A schematic cross section through member B (Fig.7-2) shows that it comprises two rather poorly defined sand bodies which dip towards the southeast and downlap onto the top of member C.

7-2-2. Gross Sandstone Isopach

For mapping purposes, the two sandstones within member B were not separated into shingles. The gross sandstone isolith map (Fig.7-3) indicates an irregular blanket sandstone which has an average thickness of between 2 and 4 meters and which has a highly irregular southeast (i.e. seaward) margin. The eastern (seaward)

Figure 7-1. Total Isopach Member B. Member B thins to zero in the east. Dots indicate data points. See text for details and explanation.

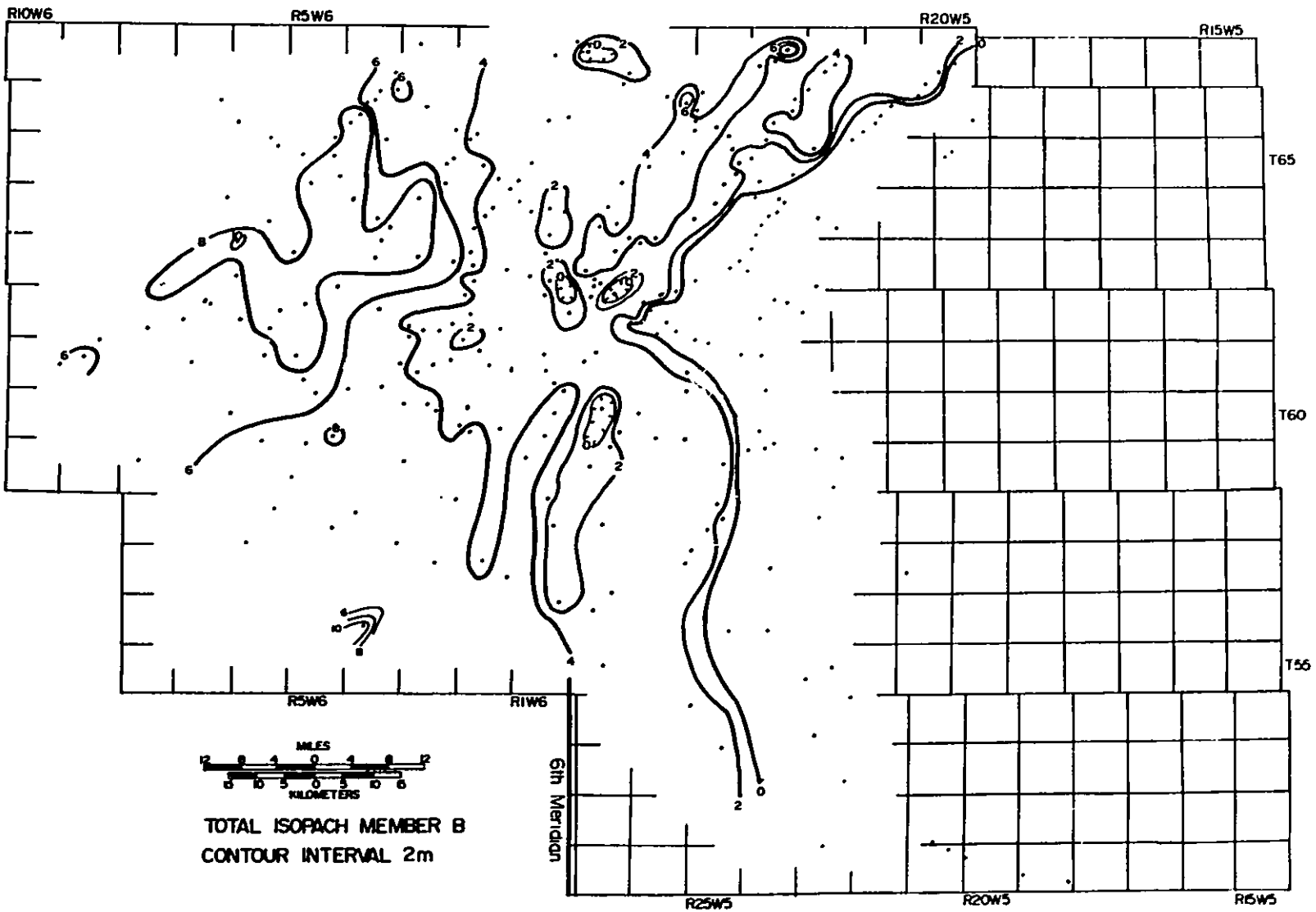
R10W6
R5W6
R20W5
R15W5
T65
T60
T55
R5W6
R1W6
R25W5
R20W5
R15W5
6th Meridian
MILES
KILOMETERS
TOTAL ISOPACH MEMBER B
CONTOUR INTERVAL 2m

Figure 7-2. Regional Schematic Dip Cross Section, Member B. Member B contains two poorly defined sand bodies which downlap to the southeast. These sandstones were not separated into shingles. This cross section is based on figure 3-9A. See text for details and explanation.

REGIONAL SCHEMATIC CROSS SECTION
MEMBER B

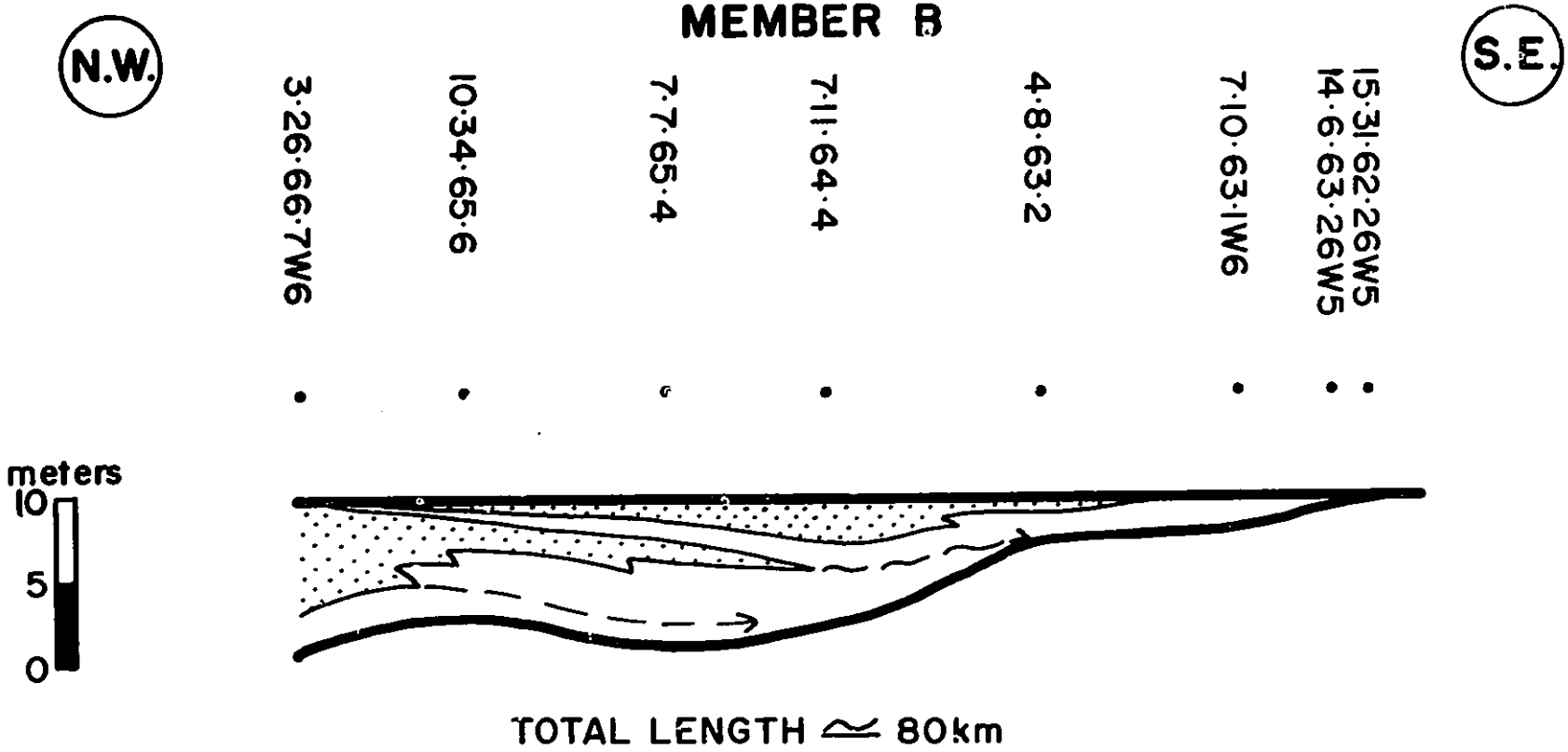

TOTAL LENGTH ≈ 80km

Figure 7-3. Gross Sandstone Isolith Map, Member B. The map indicates an irregular geometry with two protuberances to the southeast with a central embayment. Dots indicate data points. See text for explanation and details.

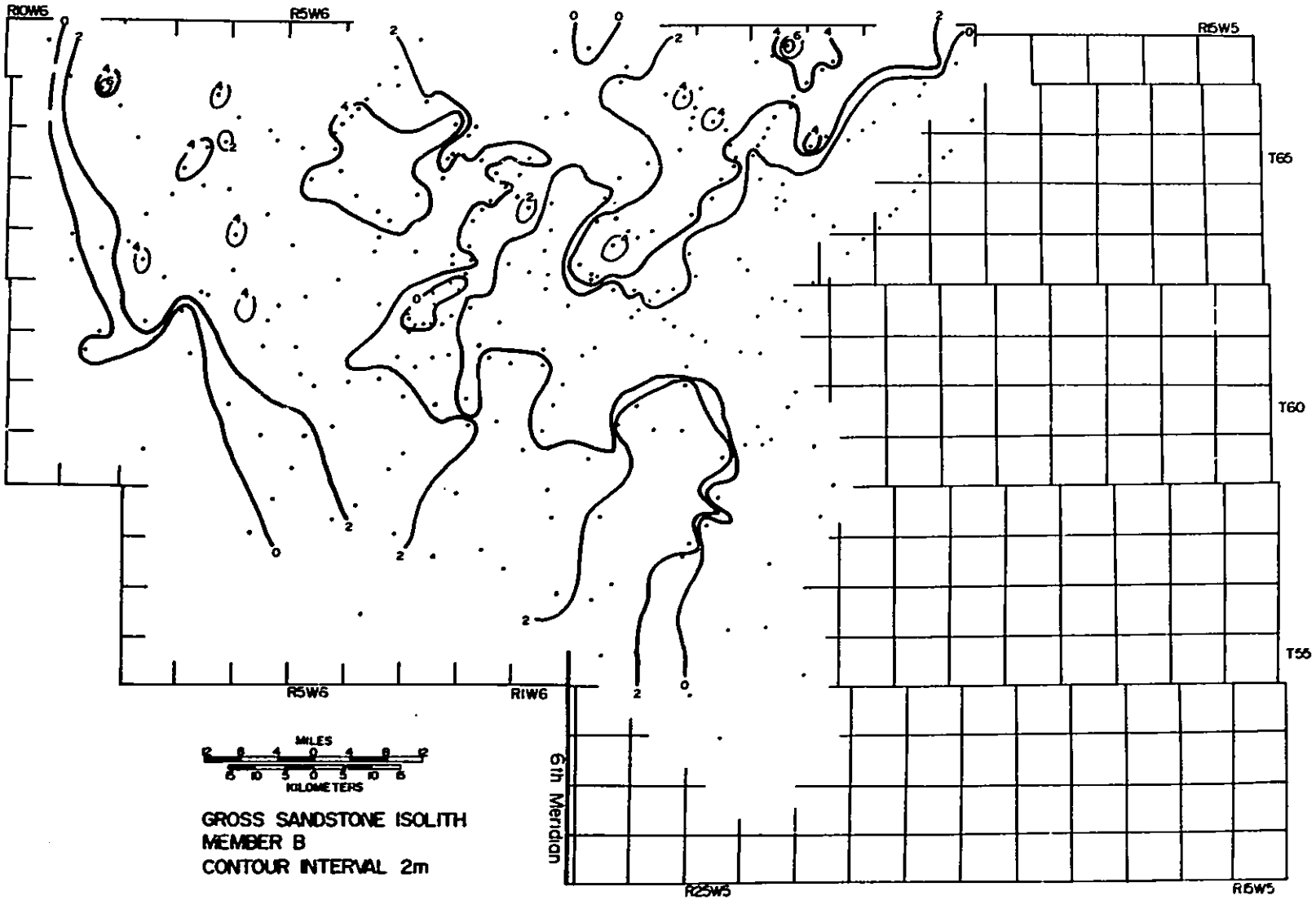
R10W6
R5W6
R5W5
T65
T60
T55
R5W6
R1W6
MILES
KILOMETERS
6th Meridian
R25W5
R15W5
GROSS SANDSTONE ISOLITH
MEMBER B
CONTOUR INTERVAL 2m

margin is oriented approximately northeast\southwest but contains a relatively large central embayment.At the western margin the sandstone thickness drops to zero. The sandstone appears to be more extensive in the north and narrower southward. Prominent shoestring sandstones were not noted.

7-2-3. Facies Associations

Separate detailed cross sections have not been constructed through member B. Information regarding typical facies successions and lateral facies changes is derived from previously constructed cross sections. Figures 4-14B and 5-8B represent dip oriented core cross sections, each of which includes sections through member B. Figure 4-14B will be discussed first. In the northwesternmost well on the cross section (well 9-4-62-4W6) member B shows two coarsening upwards facies successions. The lower succession is 2 meters thick and comprises laminated marine shales (Facies 1A) which coarsen upwards into laminated blockstones (Facies 2) containing thin wave-rippled sandy beds, although thick sandstones are not present. The upper facies succession lies sharply on top of these blockstones. It is 5 meters thick and is similar to Facies Association 1A. It begins with about 2 meters of pervasively bioturbated marine mudstones (Facies 3A) which include thin preserved wave-rippled sandstone beds upwards. This mudstone grades into about 1 meter of HCS sandstone (Facies 7A) which passes upward into about 2 meters of pervasively bioturbated sandstone. The last 20 centimeters is

cross bedded and is sharply overlain by blockstones (Facies 2). This facies pair (bioturbated mudstones sharply overlying laminated shales and mudstones) is exactly the same as that observed in member D between shingles D3 and D2. In all of the other wells in which member B is cored on Figure 4-14B, the facies succession comprises a few meters or less of laminated shales or blockstones sharply overlain by bioturbated mudstone. The underlying laminated mudstones are variable in thickness and are only a few centimeters thick in well 2-6-62-2W6. Core photographs through member B are shown in figure 3-7C. The sharp contact between laminated shales and blockstones represents an Em surface (box 3, 44.2-49.0m). Overlying this surface are a few meters of pervasively bioturbated sandy mudstones which are sharply overlain by laminated shales and blockstones belonging to member A. The contact is marked with a B arrow (Box 1, 49.0-53.1m).

The upper facies succession in the other wells in figure 4-14B contains no thick sandstones. The bioturbated sandy mudstones average about 2 meters in thickness.

Similar lateral, downdip changes in facies associations are seen in figure 5-9B. The facies succession in well 10-13-63-3W6 is similar to that seen in well 9-4-62-4W6 (Fig.4-14B). The facies succession begins with several meters of laminated marine shales (Facies 1A). These shales are sharply overlain by a coarsening upwards facies succession beginning with several meters of pervasively bioturbated mudstone (Facies 3A) which becomes sandier

and less burrowed upwards. This grades up into about one meter of current rippled sandstone (Facies 7C) which is in turn sharply overlain by laminated marine blockstones at about 31 meters. The sandstone pinches out in the adjacent wells (2-7 and 4-8) and shows a lateral change into bioturbated marine mudstones which sit sharply on top of blockstones.

Member B is also represented on the regional strike oriented cross section (Fig.3-8A). In wells 7-17, 6-11, 4-8, and 4-11 member B comprises a few meters of pervasively bioturbated sandy mudstones which sharply overlie laminated shales or blockstones. In well 7-17, this bioturbated mudstones sits directly on top of member C.

7-3. Interpretation

The coarsening upward facies successions in wells 10-13 (Fig.5-9B) and 9-4 (Fig.4-14B) are similar to Facies Association 1A. Thick sandstones, however, were not noted. These facies successions indicate progradation of shallow marine, largely wave- and storm-dominated shelf environments. The irregular distribution of laminated sediments under the bioturbated mudstone in all of the wells indicates some erosion. The contact between the overlying bioturbated sandy mudstone and the underlying blockstones is always sharp and is interpreted as an Em surface similar to that between shingles D2 and D3 in member D and probably due to a minor transgression.

The sand bodies (Fig.7-3) indicate an irregular seaward geometry comprising two protuberances with an intervening embayment. Distinct lobate geometries and associated shoestring sands were not noted and it is not clear that these irregularities in sand body geometry are directly influenced by fluvial processes. Distinct shoreline deposits (e.g. rooted beach sands) were not observed within the map area.

Member B probably represents prograding shelf deposits related to shorelines farther to the northwest. The regional stratigraphic cross section (Fig.7-2) indicates that these shelf deposits downlap onto the top of the underlying member C.

CHAPTER 8. MEMBER A

8-1. Introduction

Member A is the youngest member recognized within the Dunvegan Formation and contains two producing fields, Lator and Jayar (Fig.1-8). Core data outside of these fields is sparse and member A will not be discussed in great detail. Most of the descriptions and interpretation will concentrate on the Lator and Jayar pools. In general member A is dominated by the effects of the Kaskapau transgression.

8-2. Description

8-2-1. Thickness, Extent, and Stratigraphy

Figure 8-1 shows a total isopach of member A. It is present over the entire map area and has an overall wedge shape. It thickens to a maximum of about 22 meters westward. Over most of the southeast portion of the map area, it comprises a gently undulating blanket which averages between 5 and 10 meters in thickness.

Figure 8-2 represents a schematic regional dip-oriented cross section hung on the top of member A. The pronounced wedge shape is evident. Member A contains two shingled sand bodies (A1 and A2), each of which pinches out into shales towards the southeast. In contrast to the other members, toplap was not and both shingles thicken towards the northwest. The lower shingle

Figure 8-1. Total Isopach Map, Member A. Note that member A is fairly uniform over most of the map area and then thickens in the far northwest up to 22 meters. See text for explanation.

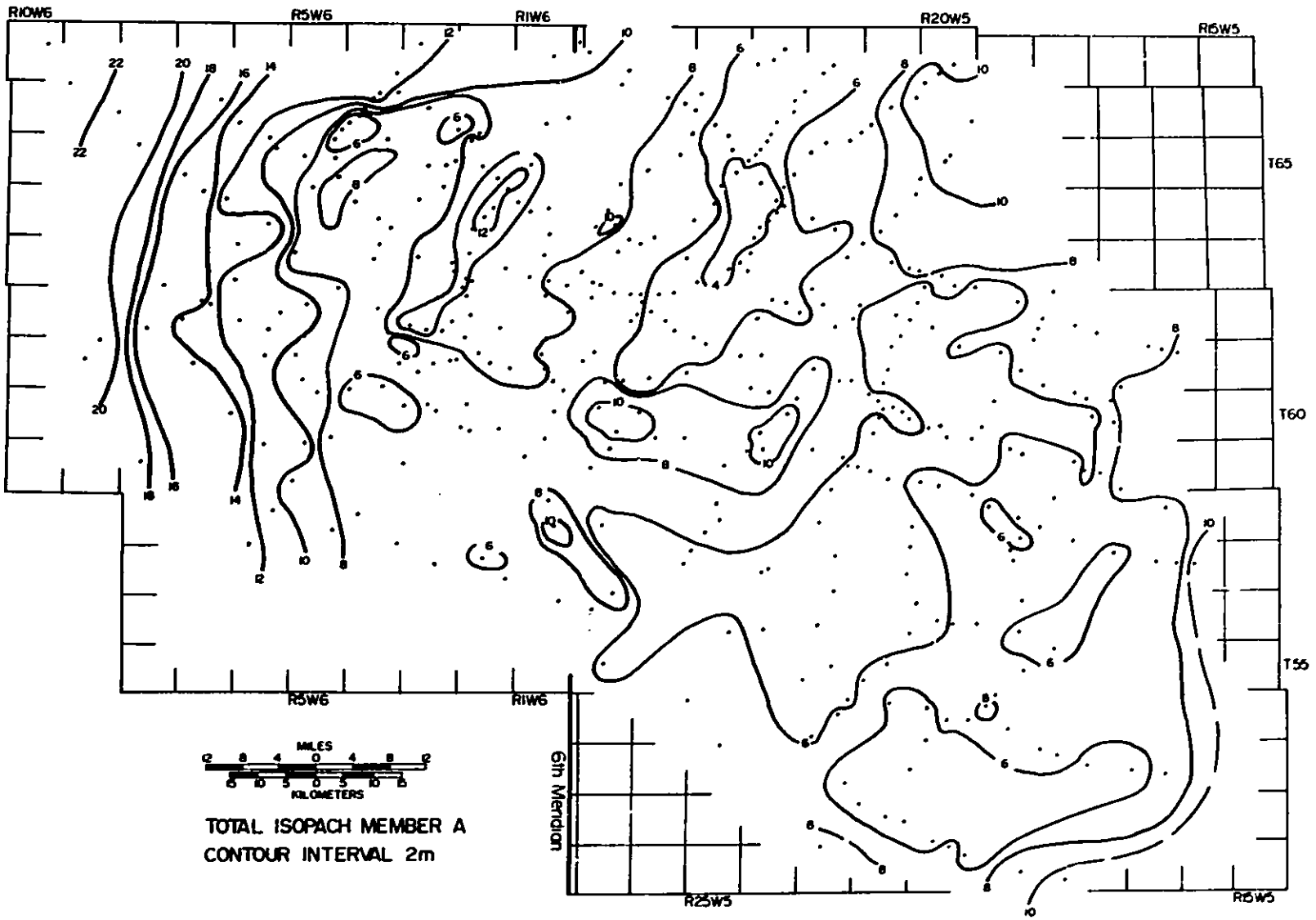
R10W6
R5W6
R1W6
R20W5
R15W5
T65
T60
T55
R5W6
R1W6
6th Meridian
R25W5
R15W5
MILES
KILOMETERS
TOTAL ISOPACH MEMBER A
CONTOUR INTERVAL 2m

Figure 8-2. Regional Schematic Dip Cross Section, Member A. This figure is based on figure 3-9A. Fine stipple indicates marine sandstone, heavy stipple indicates channelized sandstones. Note the wedge shape of member A. See text for explanation.

REGIONAL SCHEMATIC CROSS SECTION
MEMBER A

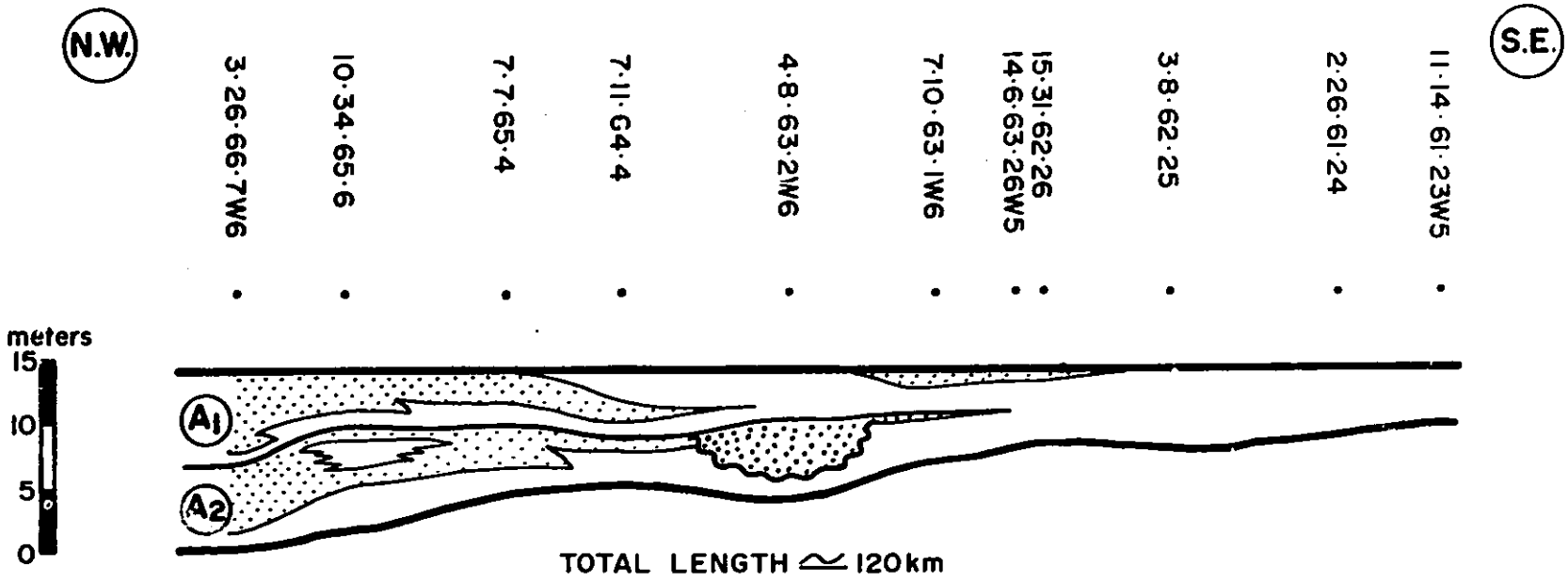

(A2) contains several channelized sand bodies, only one of which is traversed by this cross section. Channels were not noted in the upper shingle (A1).

8-2-2. Gross Sandstone Isolith Map, Shingle A2

Figure 8-3A shows a gross sandstone isolith map of sandstones within the lower shingle (A2). Sandstone thicknesses vary between zero and a maximum of about 12 meters. The eastern (seaward) edge of shingle A2 is highly irregular and includes several lobe-shaped sand bodies. There are several local areas of thick sandstones (greater than about 4 meters) as indicated by bullseyes on the map. These include producing sandstones in the Lator and Jayar fields (Fig.8-3B). Figure 8-3B shows a schematic outline of sandstones in shingle A2. Well logs through the bullseyes indicate bell-shaped profiles and probably represent channels (Fig.4-14B). If the sands are part of the same channel then connecting the bullseyes (as shown in figure 8-3B) should give an indication of the paleo-channel trend. The map also indicates thicker sandstone (4 to 6 meters) to the southwest, although the lack of well control does not allow the accurate delineation of these sand bodies. Another accumulation is indicated to the far north of the map.

8-2-3. Gross Sandstone Isolith Map, Shingle A1

Figure 8-4 shows a gross sandstone isolith map for shingle A1. The sandstone thickens irregularly towards the northwest where it reaches a maximum thickness of about 6 meters. Its

eastern margin is highly irregular and the sandstone has the geometry of an irregular, ragged sheet sandstone containing several holes (i.e. no sandstone). Well developed lobate and shoestring sandstones are not present. The main accumulation of sandstone in shingle A1 lies to the west of the underlying shingle A2.

8-2-4. Facies Associations

There are several cross sections which have already been presented which include cores and well logs through member A. Figure 3-8A and B include cores and well logs through producing sandstones in the Lator field (well 4-8-63-2W6). Member A is completely cored in wells 4-11-65-2W6 and 6-11-62-3W6. In well 4-11, member A begins with a 10 meter thick coarsening upwards facies succession which is similar to Facies Association 1C. This lower succession begins with about 8 meters of laminated shales (Facies 1A) which grade up into blockstones (Facies 2). The succession is capped with about two meters of very fine-grained HCS sandstone (Facies 7A). The succession is erosively truncated at about 50 meters (Fig.3-8A) by about 2 meters of fine-grained cross bedded sandstone (Facies 7D) containing ripped-up siderite clasts and *Inoceramus* shell fragments. About 10 centimeters of coal (Facies 10) caps this overlying sandstone. The coal is sharply overlain by about 1 meter of bioturbated, sideritic, sandy mudstones (Facies 3A) which grade upwards into bioturbated marine shales (Facies 1A) of the Kaskapau Formation.

Figure 8-3A. Gross Sandstone Isolith Map, Shingle A2. Bullseye sandstones may indicate position of channels feeding irregular shorelines to the southeast. Dots indicate data points. See text for explanation.

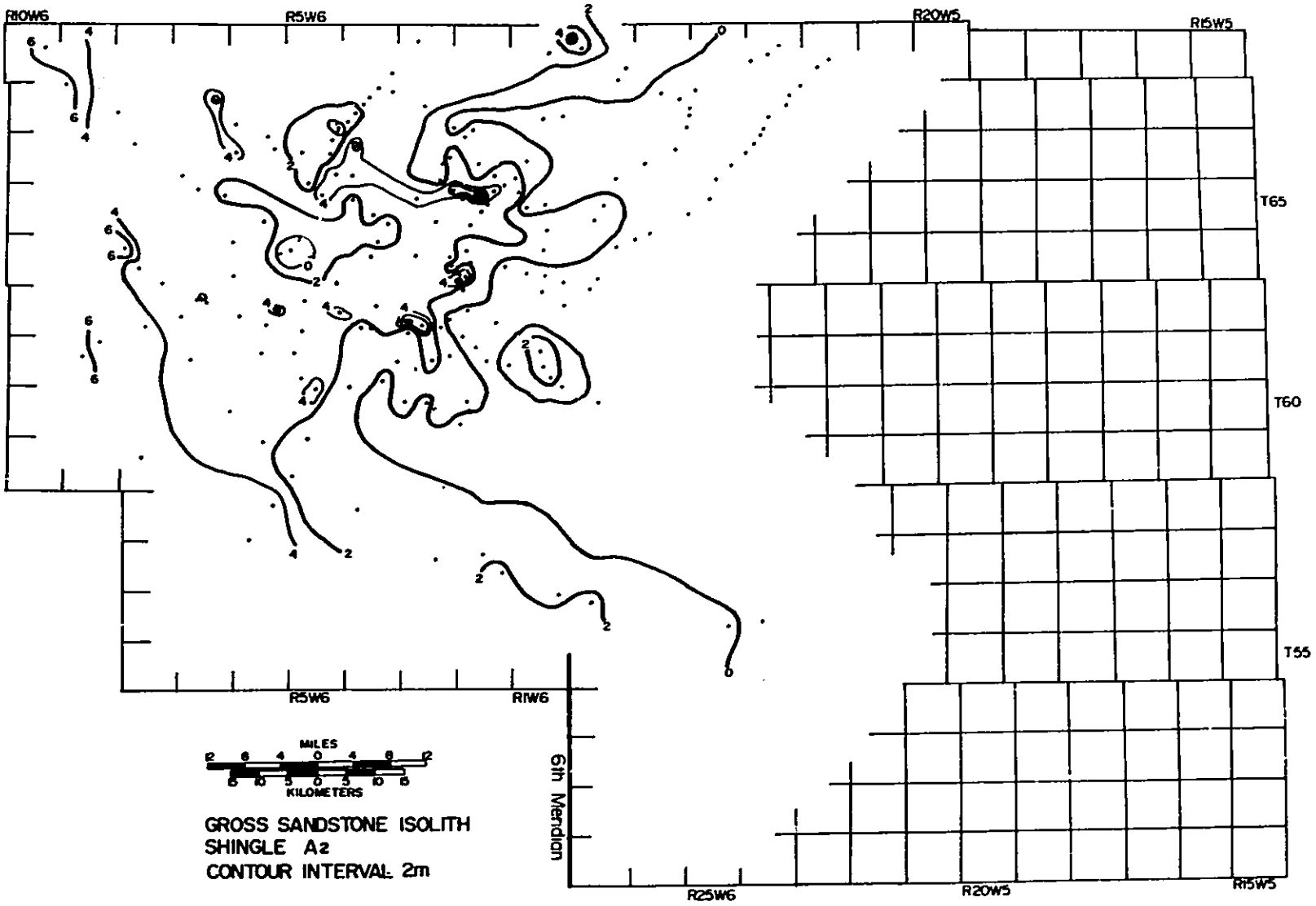
R10W6
R5W6
R20W5
R15W5
T65
T60
T55
R5W6
R1W6
R25W6
R20W5
R15W5
6th Meridian
MILES
KILOMETERS
GROSS SANDSTONE ISOLITH
SHINGLE A2
CONTOUR INTERVAL 2m

Figure 8-3B. Outline of sand bodies in shingle A2 with position of relevant cross sections shown. Bullseye sandstones from figure 8-3A have been connected to show orientation of interpreted channels. 0m and 4m contours are outlined. See text for discussion.

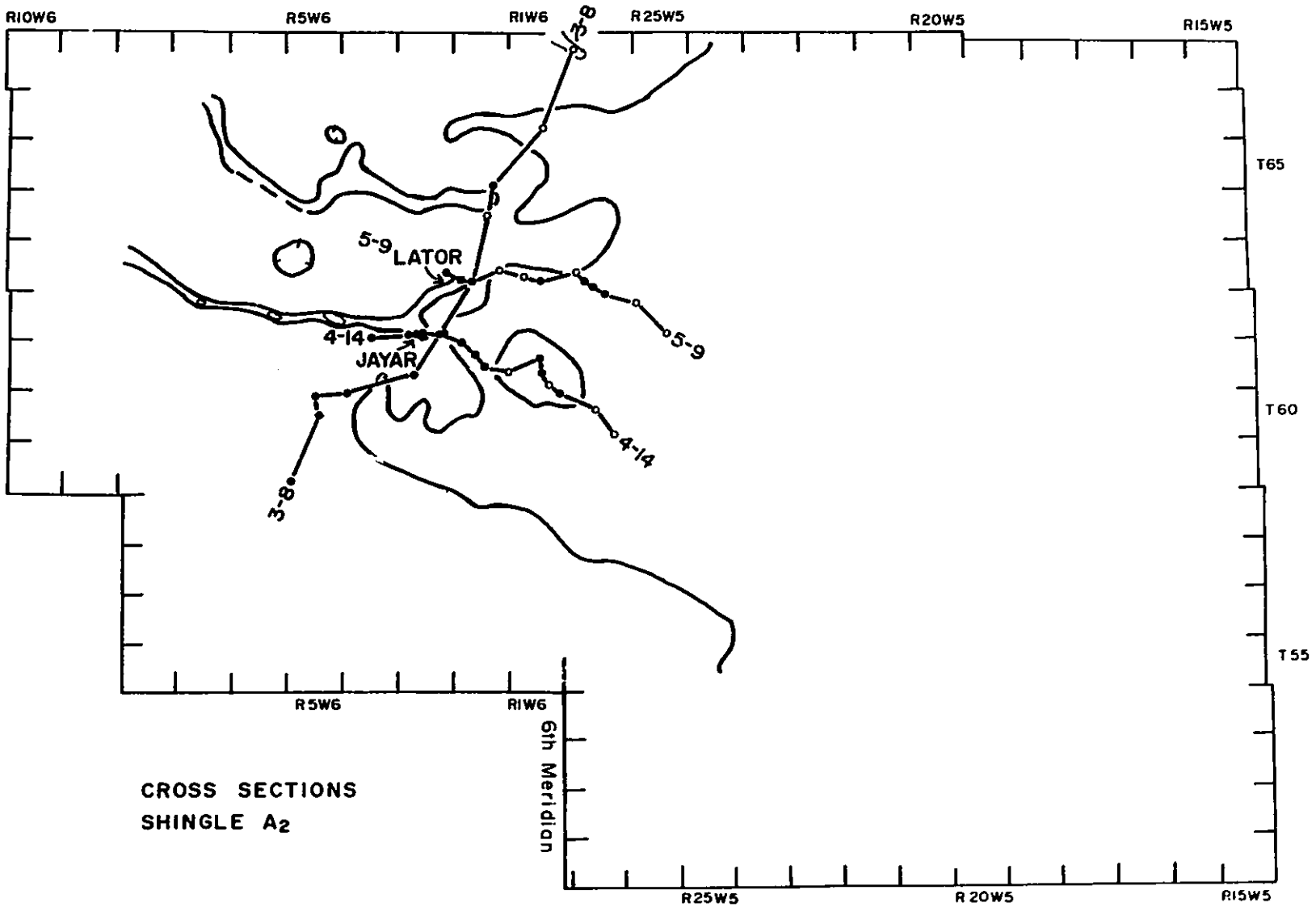
R10W6
R5W6
R1W6
R25W5
R20W5
R15W5
T65
T60
T55
6th Meridian
1-3-8
5-9 LATOR
5-9
4-14
JAYAR
4-14
3-8
CROSS SECTIONS
SHINGLE A2

Figure 8-4. Gross Sandstone Isolith Map, Shingle Al. Irregular, ragged nature of sand body probably results from Kaskapau transgression. See text for details and explanation.

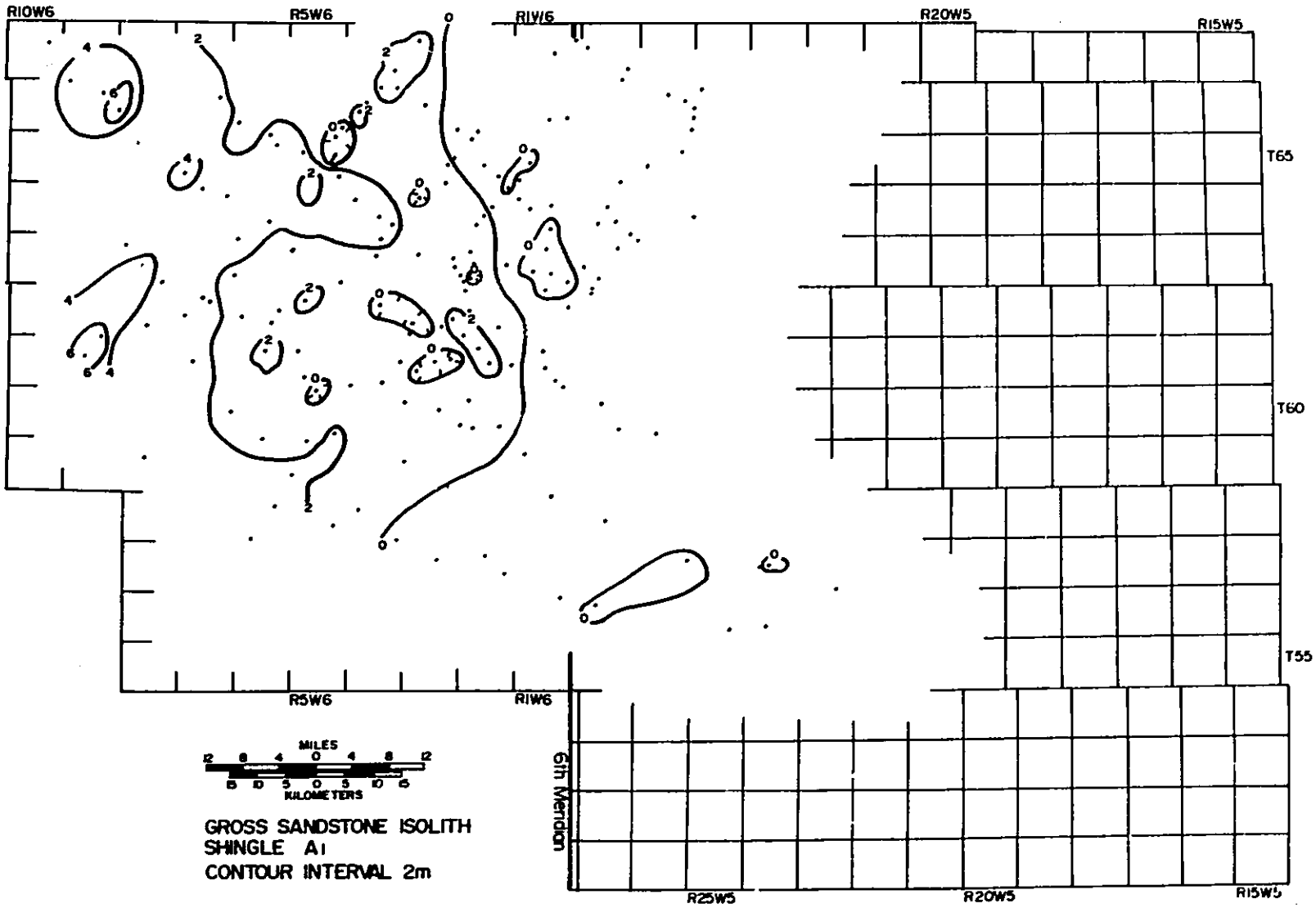
R10W6
R5W6
R1W6
R20W5
R15W5
T65
T60
T55
R5W6
R1W6
R25W5
R20W5
R15W5
6th Meridian
MILES
KILOMETERS
GROSS SANDSTONE ISOLITH
SHINGLE A1
CONTOUR INTERVAL 2m

In well 6-11-62-3W6, which is shown in more detail in figure 4-14B with photos in figure 3-7C (49.0-57.9m), member A shows a similar succession of facies. The lower succession sharply overlies member B and begins with several meters of laminated marine shales and blockstones, containing thin wave rippled sandstone beds upward, capped by about 30 cm of pinstriped mudstone. These mudstones are sharply overlain by about 3 meters of pervasively bioturbated shale and mudstone which becomes sandier upwards. The lower contact is marked by nodular siderite (A2 arrow in figure 3-7C, box 2, 53.1-57.9m). At the top of member A (Fig.3-7C), this bioturbated mudstone grades back into the overlying pervasively bioturbated shales of the basal Kaskapau Formation.

Lator

Logged core through member A from well 4-8-63-2W6 is shown in greater detail in figure 5-9B. In this well member A begins with about 3 meters of laminated blockstones (Facies 2). These blockstones are erosively overlain by about 3 meters of fine-grained sandstone. This sandstone is the producing sandstone within the Lator field. The sandstone exhibits a poorly developed fining upwards with cross bedding at the base and current ripples upward. It contains several ripped-up mudstone clasts at the top. The sandstone is sharply overlain by about one meter of laminated blockstones. This facies succession is similar to Facies Association 2A and is also seen in the adjacent wells. In well

10-13-63-3W6 (Fig.5-9B) member A is completely cored. The sandstone shows a more pronounced fining upwards and grades into about one meter of burrowed laminated blockstones. These blockstones are sharply overlain by a thin bioturbated mudstone which marks the upper boundary of shingle A2 at about 35 meters. This is followed by about 2 meters of burrowed blockstones which are sharply overlain by about 1.5 meters of pervasively bioturbated shales and mudstones. These fade back into the bioturbated marine shales of the Kaskapau Formation, producing a facies succession similar to that in well 6-11(Fig.3-7C).

Jayar

Figure 4-14B includes eight wells which include partial or complete cores through member A and which also include sandstones which produce in the Jayar field. In wells to the southeast, including 6-11, 11-15, and 6-1, coarsening upward facies successions are relatively well developed in shingles A1 and A2. In wells 11-15 and 6-1, the facies succession through A2 (lower succession) is similar to Facies Association 1A. In both wells, pervasively bioturbated marine shales (with *Inoceramus* in well 6-1) coarsen upward into HCS sandstones. These sandstones are thinner to the southeast in well 6-1. Coarsening upward is more poorly developed in wells 6-11 (described above) and 2-6.

A prominent channelized erosional surface (Ec surface) is seen to the northwest in wells 9-4, 7-7, 8-8, and 3-9. This erosion surface cuts into the underlying blockstones within shing-

le A2, and in well 7-7 is seen cutting into the top of member B. The channel fill includes producing sandstones within the Jayar field and is about 8 meters thick in wells 7-7, 8-8 and 3-9. It consists of interbedded fine-grained sandstone and shale in varying proportion. The thickest sandstones are in well 3-9, but due to oil staining, sedimentary structures are difficult to discern. Some medium to large scale cross bedding and numerous shale rip-up horizons were observed. In well 8-8, the sandstone beds are thinner and show poorly developed normal grading. The facies succession is similar to Facies Association 2A.

In well 7-7, the proportion of mudstone is much greater (about 50%). The mudstones (Banded Mudstones, Facies 5) are riddled with sand filled synæresis cracks and contain scattered oyster shells with a few burrows upwards. Some of the sandstone beds are current rippled. The channel fill succession, in well 7-7, does not show any regularity and neither fines nor coarsens upwards. It is more similar to Facies Association 2B.

The succession in well 9-4 is thinner. It begins with about a meter of banded mudstones (Facies 5) which sit sharply on top of deformed silty blockstones (Facies 2). These banded mudstones are sharply overlain by about one meter of cross bedded sandstone which are in turn sharply overlain again by banded mudstones. The succession is sharply overlain by about 1.5 meters of pervasively bioturbated sandy mudstone which passes upwards into pervasively bioturbated shales of the lower Kaskapau Formation.

In wells 9-4, 7-7, and 3-9, the overlying shingle (A1) comprises several meters or less of pervasively bioturbated sandy mudstone. Fining upwards is indicated in wells 9-4, 7-7 and 8-8. In wells 6-11 and 2-6, shingle A1 averages about 3 meters thick and coarsens upwards, although the facies are similar to the wells to the northwest (pervasively bioturbated shales and mudstones, Facies 1B and 3A). In wells 11-15 and 6-1 only the lowermost portion of shingle A1 is cored. Coarsening upward is indicated by funnel-shaped gamma log profiles, although the basal facies are blockstones (Facies 2) in both wells. *Inoceramus* is present in well 6-1.

8-3. Interpretations

8-3-1. Shingle A2

Shingle A2 begins with a well developed, but relatively thin, sandy coarsening upward facies successions as seen in wells 11-15, 6-1 (Fig.4-14B) and 4-11 (Fig.3-8A). The facies successions are similar to Facies Associations 1A and 1C and are interpreted as representing the distal deposits of a prograding shoreline farther to the northwest. Shingle A2 culminates in an erosional event resulting in channel downcutting. These channels are filled with sandstones and banded mudstones (Facies 5). The southern channel is interpreted as bifurcating between the Lator (Fig.5-9B) and Jayar (Fig.4-14B) fields. In core the channel is seen to cut into shingle A2 and in well 7-7 (Fig.4-14B) this erosion surface cuts out a portion of the underlying member B.

The presence of channels and a highly irregular southeastern (i.e. seaward) geometry suggests major distributary channels feeding rather muddy river-dominated delta lobes. The lobes are poorly developed and do not contain thick sandstones. In places, the distributary channel fill is very muddy. The presence of abundant synæresis cracks (probably due to salinity changes) and the presence of oyster shells may suggest brackish water conditions in the channel. The variable nature of the channel fill and the presence of marine (or brackish) influence suggests that these channels may have been filled as estuaries.

8-3-2. Shingle A1

The facies in shingle A1 are dominantly pervasively bioturbated mudstone or muddy sandstone. Unfortunately, there are no cores available from the thickest portion of A1 to the north and northwest. On cross section 4-14B a transition was observed from dominantly coarsening-upward facies successions in the southeast to dominantly fining-upwards facies successions in the northwest. Some of the basal mudstones were laminated in the far southeast but became more bioturbated towards the northwest. In wells 9-4, 7-7, 8-8, and 3-9, shingle A1 was interpreted as overlying an Em surface, but the degree of erosion is probably very small.

The coarsening upwards indicates progradation although the pervasive bioturbation suggests a shelf setting. Shingle A1 is everywhere overlain by the Kaskapau shale indicating a major marine transgression. Shingle A1 is therefore interpreted as the

distal edge of a prograding sedimentary system which lay to the northwest. The nature of this system has not been determined by this study. The distal edge of this system was probably thoroughly reworked by burrowing organisms during Kaskapau transgression.

CHAPTER 9.MEMBER G

9-1.Introduction and Summary of Geological History

Limited gas occurs in member G in the Kakwa area (Fig.1-8), although outside of this area there is little core data. In discussing member G, this chapter will concentrate on the geology of the Kakwa area.

9-1-1. Geological History of Member G

Member G represents the progradation of at least five sandy shingles which progressively step out (offlap) into the basin from northwest to southeast (Fig.9-2). Each of these shingles comprises one or more sandy deltaic lobes which show some reworking by storm and wave processes (a typical paleogeographic reconstruction is shown in Figure 9-6). As each lobe was abandoned it was overlain by a sandy bioturbated transgressive horizon. Deposition of member G culminates in a major marine transgression which may have marine truncation in the northwest. Detailed descriptions and interpretations of member G will follow.

9-2. Descriptions and Preliminary Interpretations

9-2-1. Thickness and Extent

Member G is confined to the northwest half of the thesis area and is distinctly wedge shaped. An isopach map (Fig.9-1) from the top of member G to the FSU marker shows regular thinning

Figure 9-1. Total Isopach Map, top member G to FSU marker. This map indicates that member G is strongly wedge-shaped and is confined to the northwest of the map area where it reaches a thickness of 90 meters. See text for explanation.

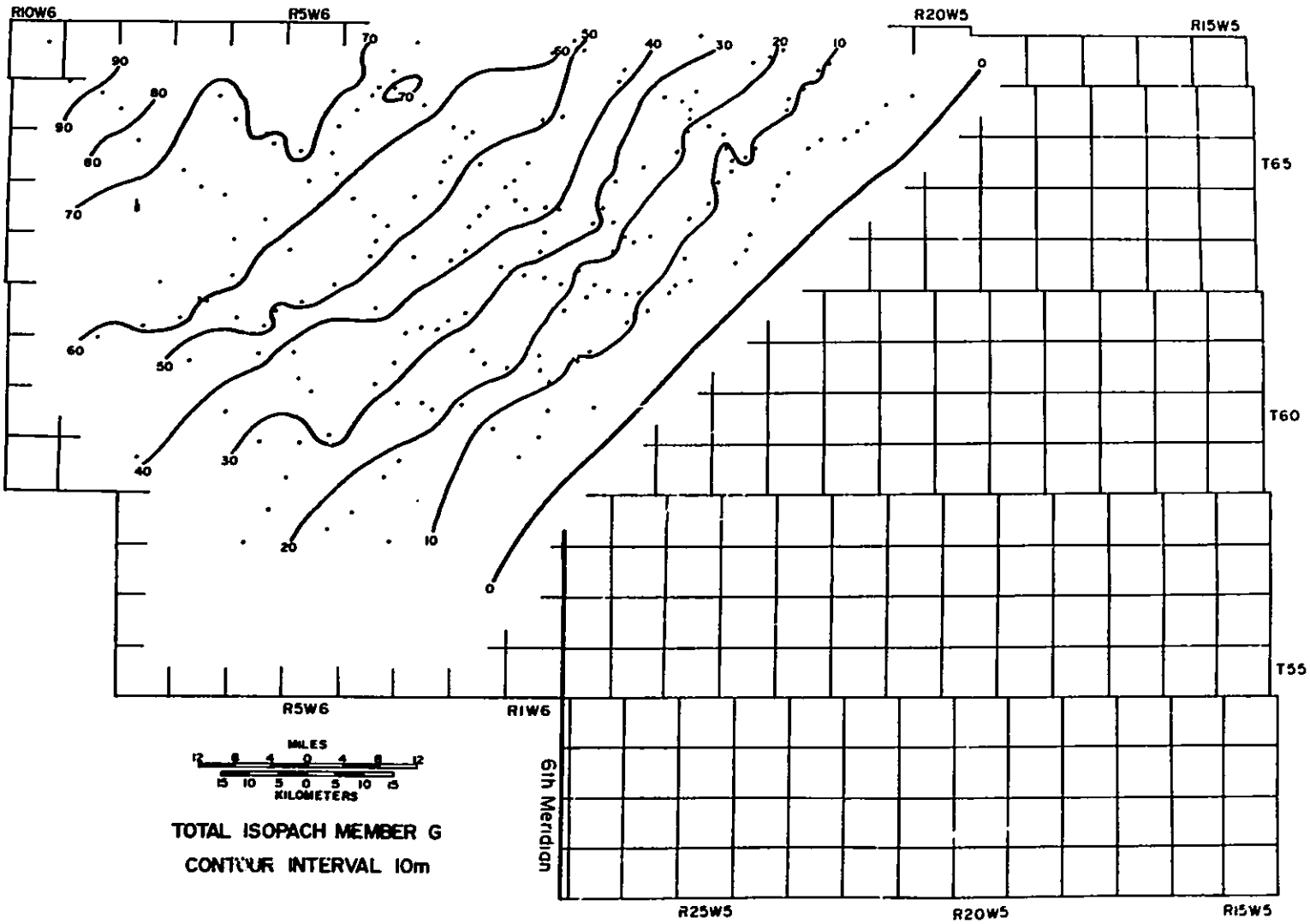
R10W6
R5W6
R20W5
R15W5
T65
T60
T55
R5W6
R1W6
6th Meridian
R25W5
R20W5
R15W5
MILES
12 8 4 0 4 8 12
15 10 5 0 5 10 15
KILOMETERS
TOTAL ISOPACH MEMBER G
CONTOUR INTERVAL 10m

Figure 9-2. Schematic Cross Section, member G. Cross section location is shown on figure 9-3B. Stipple indicates sandstones which downlap to the southeast (arrows). Notice pronounced wedge-shaped cross sectional geometry. See text for further explanation.

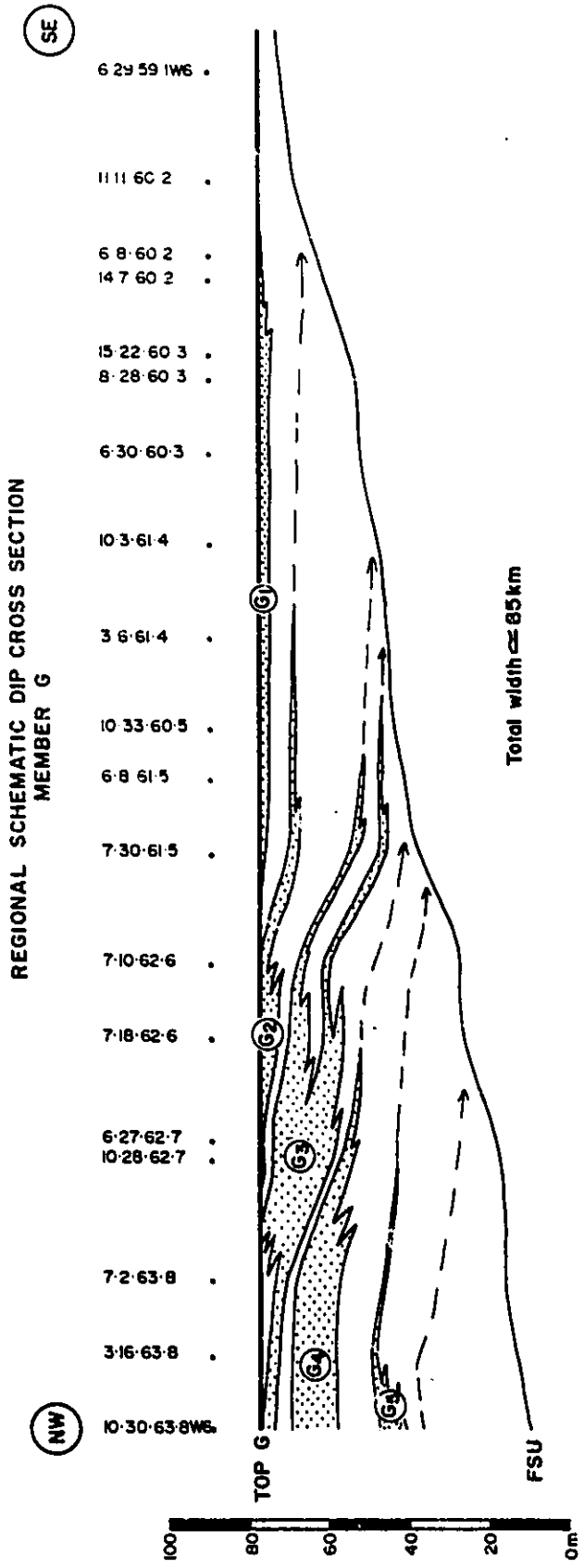
REGIONAL SCHEMATIC DIP CROSS SECTION
MEMBER G
SE
NW
6 29 59 1W6
1111 6C 2
6 8·60 2
14 7 60 2
15·22·60 3
8·28·60 3
6·30·60·3
10·3·61·4
3 6·61·4
10 33·60·5
6·8 61·5
7·30·61·5
7·10·62·6
7·18·62·6
6·27·62·7
10·28·62·7
7·2·63·8
3·16·63·8
10·30·63·8W6
G1
G2
G3
G4
G5
TOP G
FSU
Total width ≃ 85km
100
80
60
40
20
0m

towards the southeast from a maximum of about 90 meters down to zero meters.

A schematic northwest/southeast cross section (Fig.9-2) through the southern portion of member G, and hung on the top of member G, indicates at least five, stacked shingled sand bodies within this wedge. These shingles are clearly separated in places by several meters of mudstones. On other cross sections, however, these shingles erode into each other. Accurate correlation of individual shingles within member G around the basin was not successful due to complex intertonguing relationships, and they were not mapped separately. In general, these shingles (designated G1 to G5 from top to bottom) dip towards the southeast and downlap onto the FSU marker horizon (Fig.9-2). Although the successive shingles offlap to the southeast, the degree of offlap is less than in most of the other overlying members already described. This point will be discussed fully in chapter 12. The upper surfaces of these shingles terminate up-dip (northwest) against the overlying T-surface where they are truncated by a blanketing marine shale. This truncation may be erosional in nature or it may be the result of depositional toplap.

9-2-2. Gross Sandstone Isolith Map

Figure 9-3A shows a gross sandstone isolith map for all of the sandstones within the five shingles of member G. Sandstones thin from northwest to southeast and are not present east of the 6th meridian. The map indicates that the zero sand edge is

oriented northeast\southwest and is fairly smooth. Sandstone thicknesses reaches a maximum of about 24 meters although the thicker sandstones are irregularly distributed and occur in at least five distinct "pods". Well developed shoestring sandstones were not detected, although it may be harder to discern them without mapping sandstones within individual shingles. A northwest/southeast oriented linear sand body in the northwest corner of the map, may be a candidate for a channelized sandstone. The outline of the 10 meter contour (thick line) indicates an irregular geometry to the southeast probably resulting from the overlapping of several sandy lobes. The southeastern lobe includes sandstones in the Kakwa area.

Figure 9-3B shows an outline of sandstones in figure 9-3A along with the locations of relevant cross sections. Sandstones interpreted as possible feeder channels or major fluvial axes are also outlined with the dashed lines.

9-2-3. Core 3-26-66-7W6

The lower shingles in member G are cored in well, 3-26-66-7W6 as shown in figure 9-4 (also see Fig.3-9A for well log). Two coarsening upwards facies successions are penetrated in member G. About 15 meters of the lower succession is penetrated while the second is about 5 meters thick. The top of member G is marked by a thin, pervasively bioturbated sandy horizon, abruptly overlain by laminated marine shales at 20 meters from the base (Fig.9-4).

Figure 9-3A. Gross sandstone isolith map of all sandstones within member G. Data points are indicated with dots. These sandstones are outlined in figure 9-3B. The 10 meter contour shows an irregular seaward geometry perhaps suggesting a deltaic shoreline.

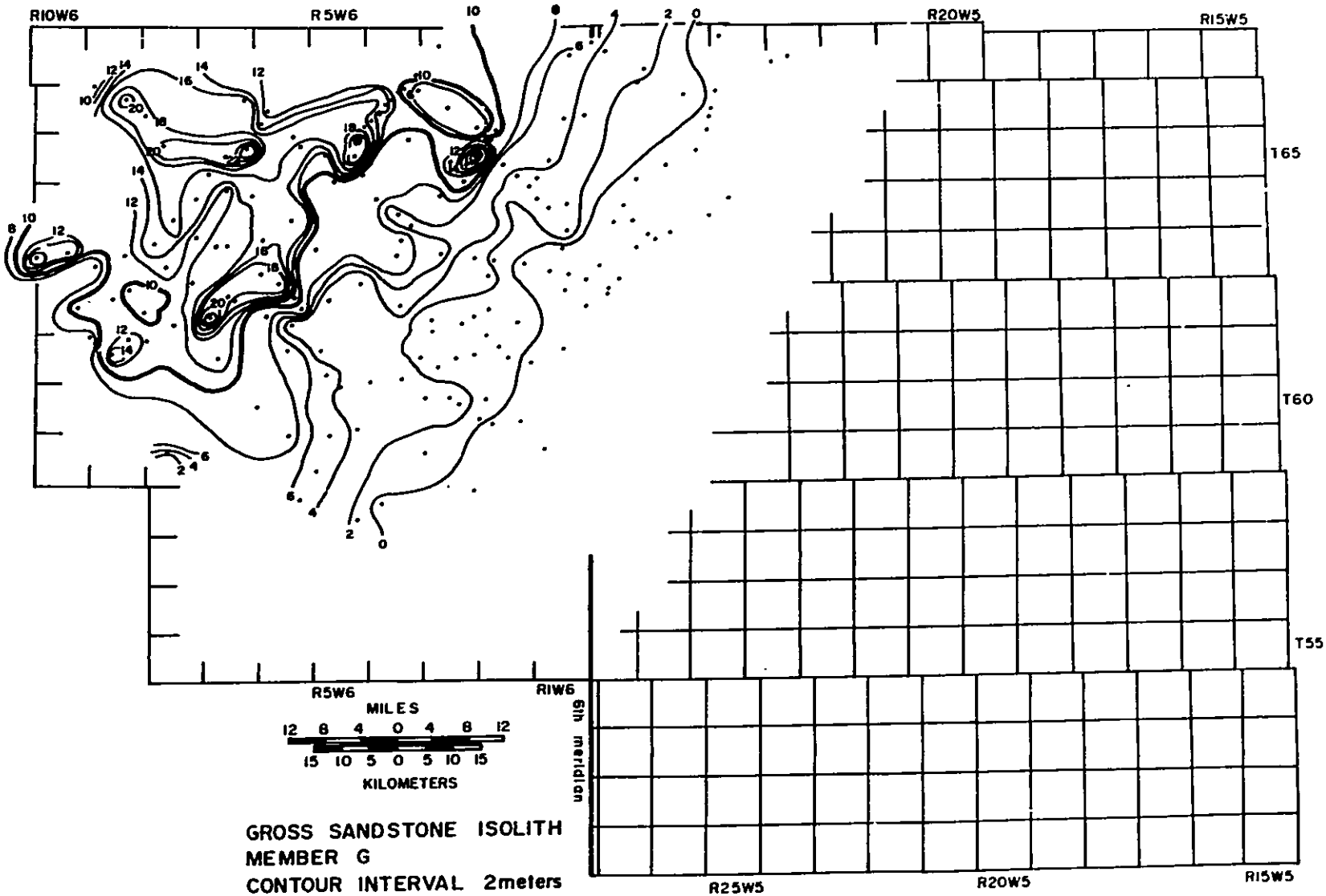

GROSS SANDSTONE ISOLITH
MEMBER G
CONTOUR INTERVAL 2meters

Figure 9-3B. Outline of sandstones shown in figure 9-3A with location of pertinent cross sections shown. Open circles represent uncored wells, black dots represent cored wells. The 0m, 4m, 10m, and 20m contours from figure 9-3A are highlighted. The dashed lines represent positions of possible distributary channels. See text for details and explanation.

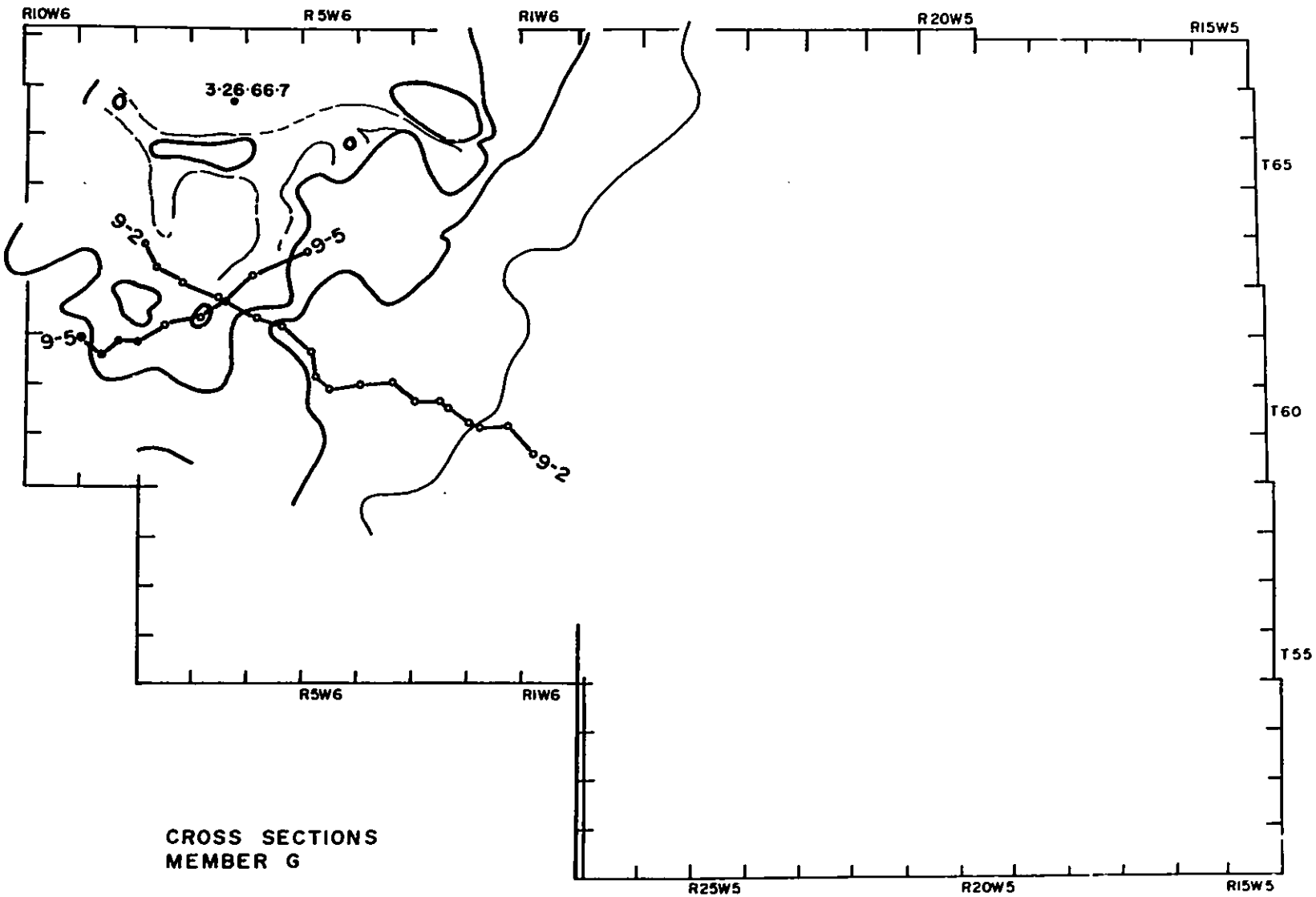

CROSS SECTIONS
MEMBER G

Figure 9-4. Core section through well 3-26-66-7W6 (see figure 3-9A, for location and well log and figure 2-29 for facies legend). Sedimentary cycles are shown with arrows. Member G comprises two coarsening upward facies successions. Both are similar to Facies Association 1B and 1C. See text for details and explanation.

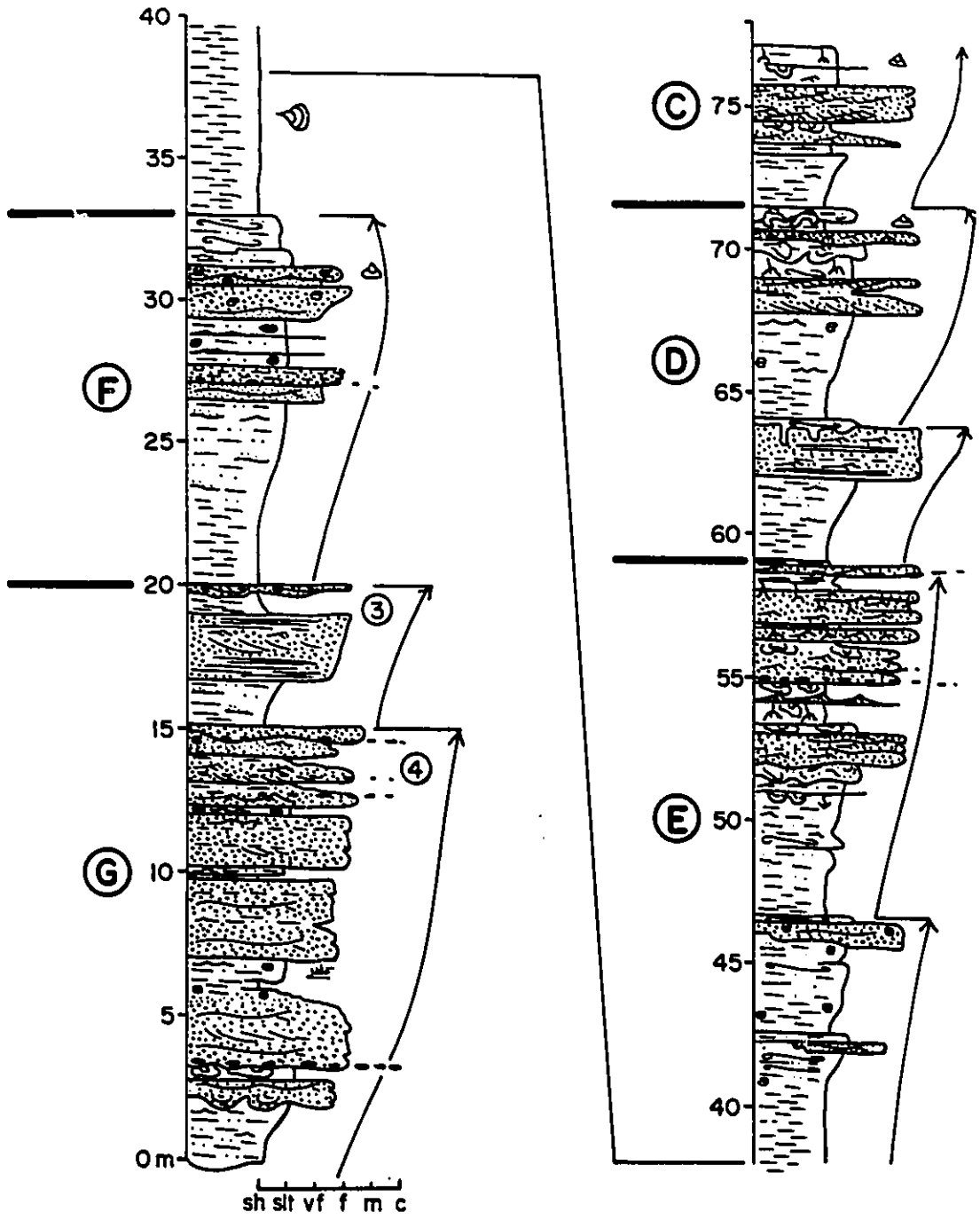
3·26·66·7W6
40
35
30
25
20
15
10
5
0 m
F
G
3
4
sh slt vf f m c
C
D
E
75
70
65
60
55
50
45
40

The lower sandy facies succession coarsens upward rather irregularly. It begins in marine blockstones and coarsens upward through convolute laminated siltstones and very fine-grained sandstones and finally into fine-grained sandstones dominated by HCS but with some cross bedding and current ripples towards the top. The succession contains interbedded mudstones throughout. It is similar to Facies Association 1B although there is a considerably greater proportion of HCS sandstone, indicating some resemblance to Facies Association 1C.

The upper thinner succession (shingle G3) is similar to Facies Association 1C.

9-2-4. Cross section through the Kakwa Lobe

Figure 9-5A,B is a northeast/southwest oriented cross section through the Kakwa area. This cross section was constructed in order to illustrate facies relationships in member G and in particular through the southern sandy pod in shingle G3 which is cored along the line of the cross section (location shown in figure 9-3B). The well log cross section (Fig.9-5A) is hung on the base of the Second White Specks and extends for a length of about 40km. In the cross section, member G averages about 60 meters. Gamma logs through member G range from funnel shaped, such as in well 12-21-61-9W6, to symmetrical, such as in wells 10-34-61-9W6 and 6-27-62-7W6. Along the cross section, gamma logs through member G indicate two such stacked funnel-shaped or coarsening upward cycles. The upper cycle (shingle G2) is about

10 meters thick in well 10-36-61-10W6 and thins towards the northeast to about 3 meters in well 6-27, which ties with figure 9-2. This cycle is designated as G2 whilst the lower cycle is designated as G3.

The core cross section (Fig.9-5B) is hung on the top of member G. The contact between member G and the overlying member F is penetrated in well 10-34 and is represented by a thin pervasively bioturbated sandy mudstone (Facies 3A) overlain by black laminated marine shales (Facies 1A).

Shingle G2 is completely cored in wells 10-36 and 10-34, and partly cored in well 6-27. G2 comprises a coarsening upwards facies succession best developed in well 10-36. In 10-36 the facies succession coarsens upwards from blockstones (Facies 2) into very fine to fine-grained HCS sandstones (Facies 7A) and is typical of Facies Association 1C. The HCS sandstones are missing in the other wells perhaps suggesting erosional truncation. G2 thins towards the northeast on the cross section (Fig.9-5B).

The top of shingle G3 is also marked by a thin pervasively bioturbated sandy mudstone. Broadly, the facies successions through shingle G3 coarsen upward and are similar to Facies Association 1B. In well 10-34 the succession begins with about 6 meters of blockstone (Facies 2). Overlying interbedded shales, siltstones and very fine-grained sandstones show evidence of soft sediment deformation (ball and pillow structures) with occasional HCS to wave rippled sandstones (Facies 7A, 7B). These are

Figure 9-5A. Well log cross section through the Kakwa Lobe, member G. Stipple indicates sandstone and vertical bars indicate cored intervals shown in figure 9-5B. All wells are gamma log traces. Main sandstone in member G (shingle G3) thins to the southwest and northeast. See text for further explanation and details. Location in figure 9-3B. Well 6-27-62-7W6 is common to both this figure and to the regional schematic cross section (Fig.9-2).

Figure 9-5B. Core cross section through the Kakwa Lobe, member G. Shingle G3 is interpreted as a major prograding deltaic lobe cut by a distributary channel in wells 12-21 and 10-34. Arrows indicate coarsening and fining upward facies successions. See text for explanation and figure 2-29 for facies legend.

STRIKE WELL LOG CROSS SECTION
MEMBER G

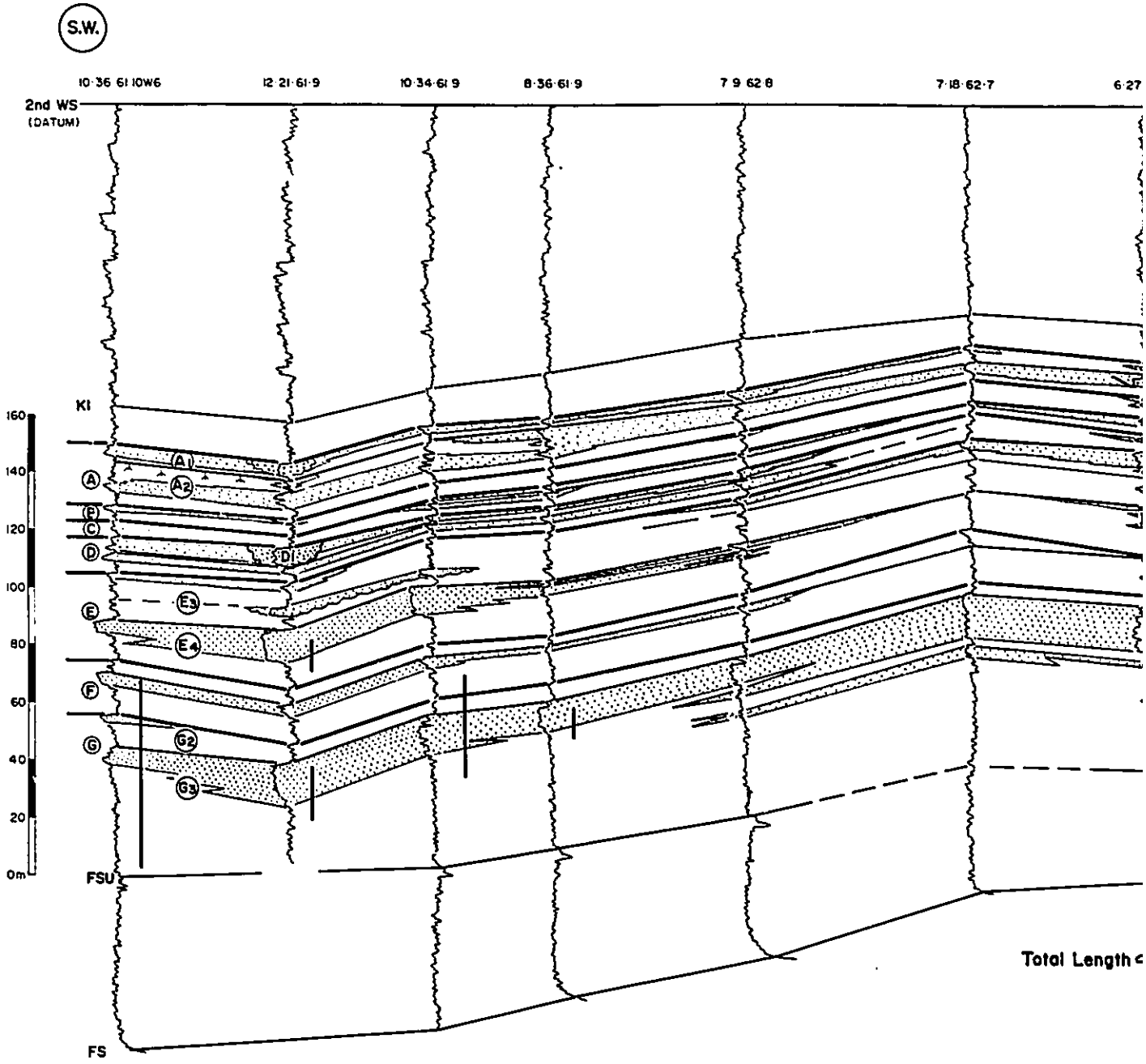

KE WELL LOG CROSS SECTION
MEMBER G

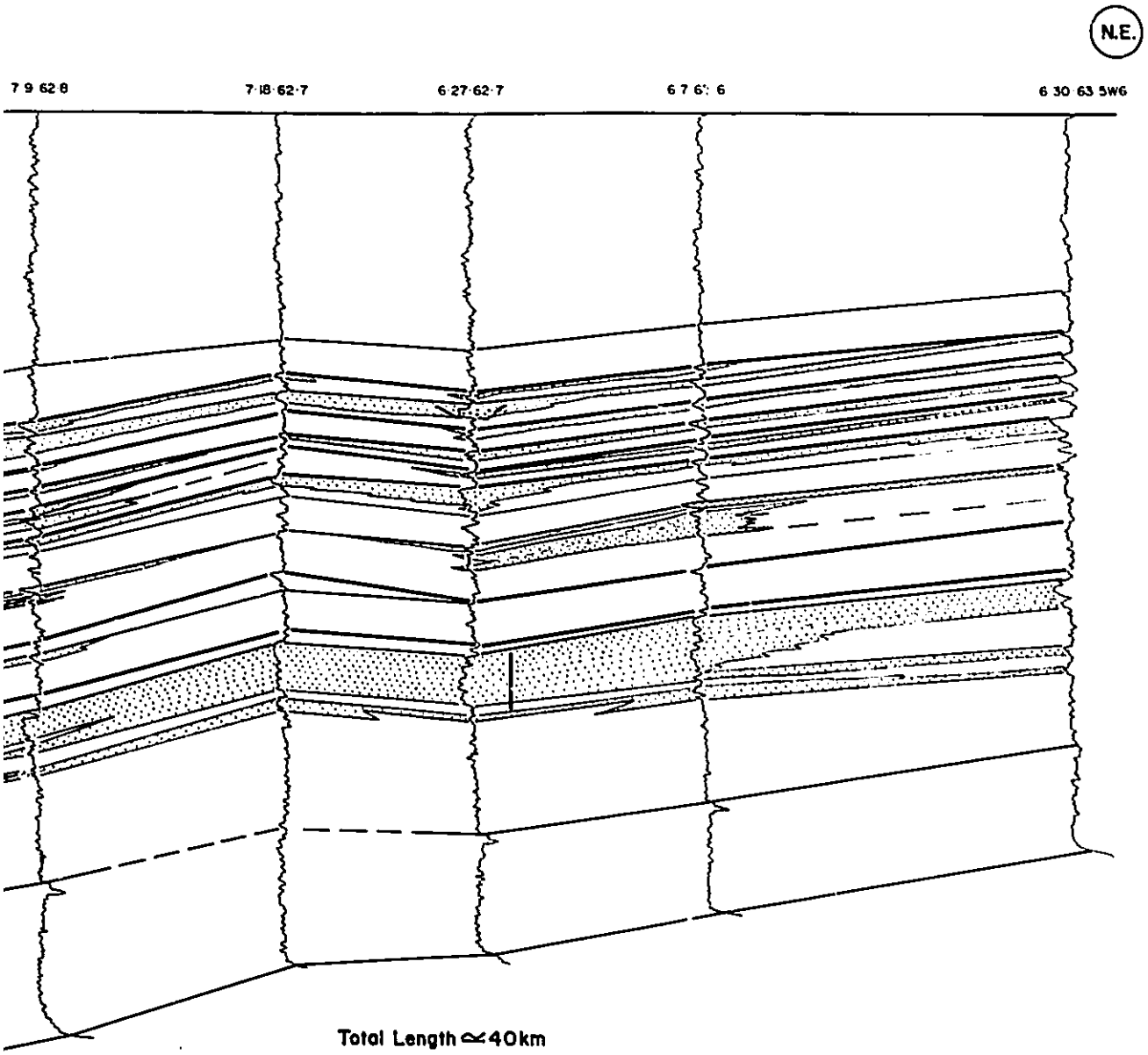

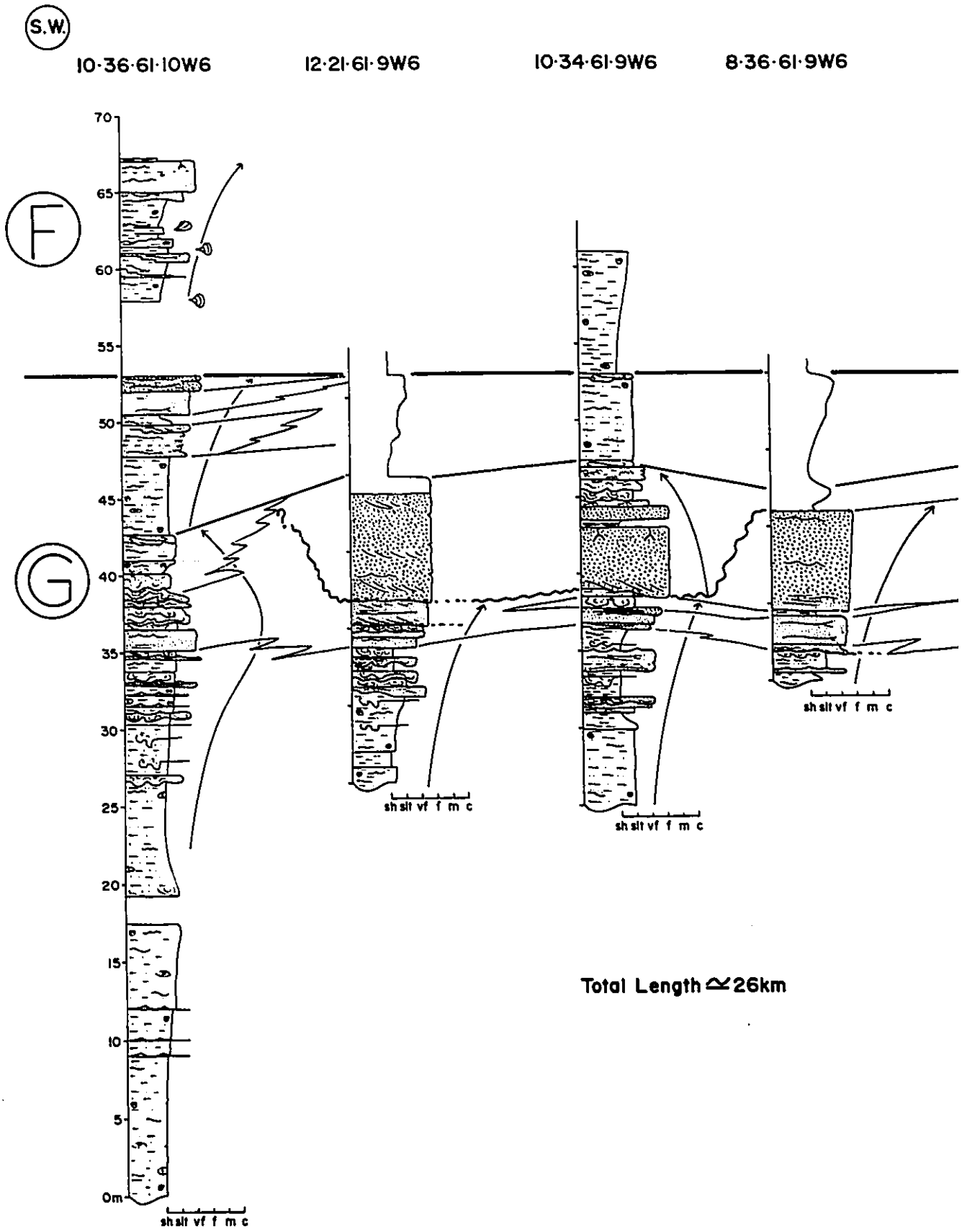
S.W.
10-36-61-10W6
12-21-61-9W6
10-34-61-9W6
8-36-61-9W6
F
G
70
65
60
55
50
45
40
35
30
25
20
15
10
5
0m
sh slt vf f m c
Total Length ≃26km

N.E.

6I·9W6 8·36·6I·9W6 6·27·62·7W6

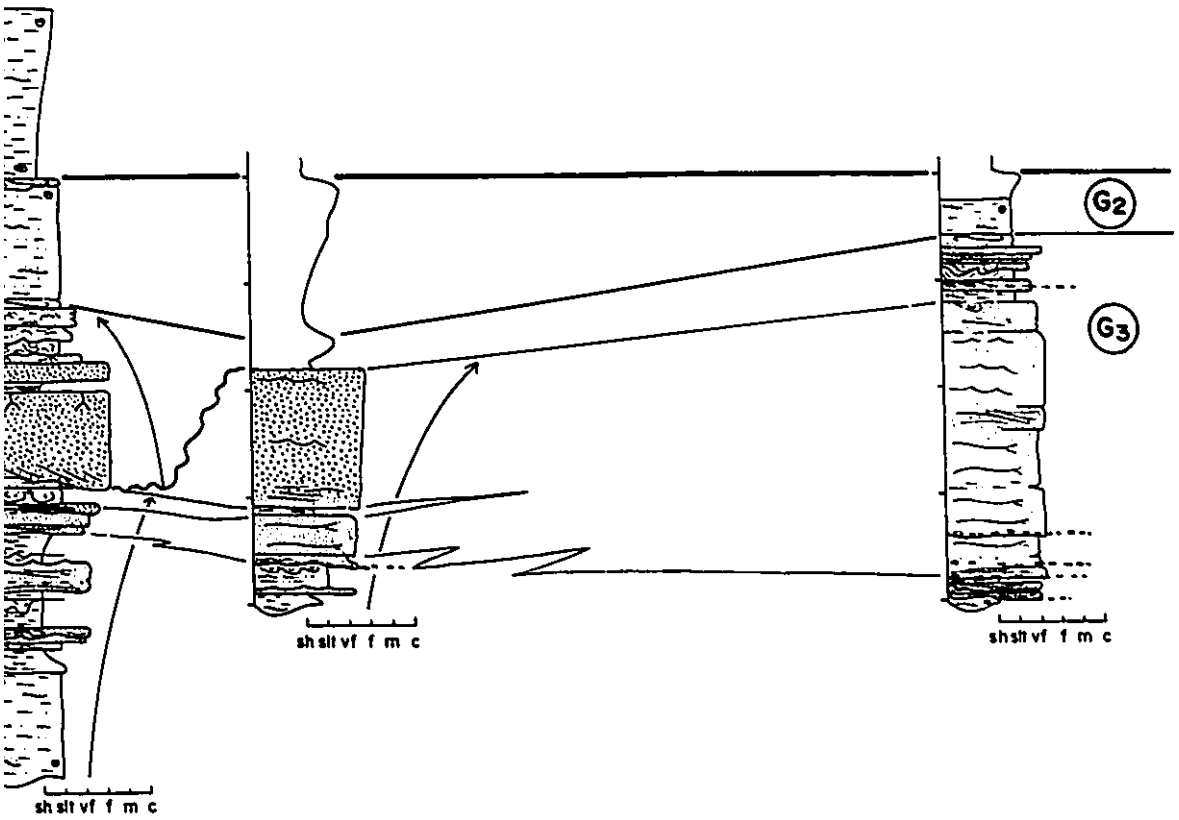

otal Length ≃26km

STRIKE CORE CROSS SECTION
MEMBER G

erosively followed by fine-grained, cross-bedded to structureless sandstone which contain *in situ* root traces at the top. These sandstones are sharply overlain by about 4 meters of interbedded carbonaceous shales (Facies 1C), structureless to convolute laminated sandstones and siltstones, and very fine-grained current-rippled sandstones. The last 4 meters is similar to Facies Association 3, although there is an indication of an overall fining upwards. This overlying fining-upwards portion of shingle G3 is well developed in wells 10-36 and 6-27 and is responsible for imparting a symmetrical shape to gamma log profiles in these wells. The coarsening upwards facies succession described in well 10-34 is similarly developed in wells 12-21 and 8-36. The thick sandstone at the top of well 8-36 gradationally overlies underlying facies and contains vague wavy lamination (Facies 7B). Thick, fine-grained sandstone is not present in well 10-36 and the facies succession fades back into convolute laminated sandstones, siltstones and eventually into blockstones. In the northeasternmost well (6-27), thick very fine-grained HCS sandstones are present and fine-grained cross-bedded sandstones were not observed.

9-3. General Interpretation

The five pods shown in figure 9-3 suggest the presence of several overlapping deltaic lobes. Some narrowing of sand to the northwest may reflect areas of fluvial input, although it is

stressed that this map is a composite of sandstones in all five shingles, so it is not clear how real these trends are.

The coarsening upward facies successions in well 3-26 (Fig.9-4) and in figure 9-5B are similar to Facies Associations 1B and 1C interpreted in chapter 2 (section 2-3-1C) as being typical of fluvial-dominated prograding deltaic systems. The abundance of wave rippled and HCS sandstones may indicate some storm and wave reworking. Relatively high sedimentation rates are indicated by the presence of soft sediment deformation features. It was difficult to precisely determine the geometry of individual deltas so it is not clear whether they have a more lobate or more birdfoot-type geometry.

The well log cross section through the Kakwa lobe (shingle G3, Fig.9-5A) indicates that the lobes are probably fairly extensive, and about 40 km wide. The core cross section (Fig.9-5B) indicates that the lobe is cut by a major distributary channel in wells 12-21 and 10-34. The delta fronts show coarsening upward facies successions typical of Facies Association 1C, while the distributary shows a fining-upward facies succession typical of Facies Association 2A. In well 10-34, the channel fill grades up into non-marine rooted coaly facies. It is emphasized, however, that in the absence of core control it may be difficult to distinguish portions of the delta front that are cut by distributary channels from those that are not. Truncated coarsening upward facies successions in the overlying shingle G2

in figure 9-5B may result from marine erosion during subsequent transgression.

Figure 9-6 is a paleogeographic summary of depositional systems within member G. It shows a large, multi-lobed delta fed by major fluvial systems to the northwest. Cross section G-G' (Fig.9-6) illustrates the facies successions through this delta complex and is based on figure 9-5B from the Kakwa area. Thick delta front sandstones grade into prodeltaic shales to the west and east and are cut by a major distributary channel.

These deltas are considered to be similar to wave-influenced shoal-water deltas from the Eocene Wilcox Group, Texas (Fisher and McGowen, 1967). These depositional systems will be discussed more rigorously in chapter 11.

Figure 9-6. Paleogeographic reconstruction of member G, based on figure 9-3 and 9-5. Fluvial systems to the northwest feed a multi-lobed, shallow water delta. Individual lobes may reach widths of several tens of kilometers. G-G' shows a core cross section through the Kakwa lobe. See text for details and explanation.

WAVE-INFLUENCED DELTA
MEMBER G

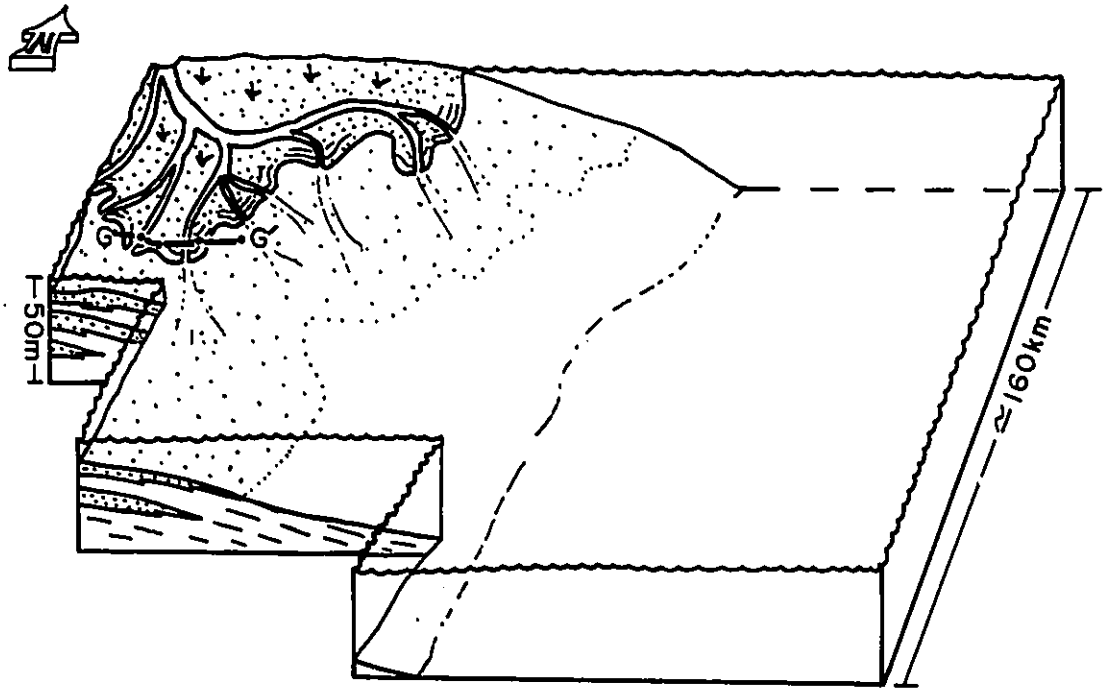

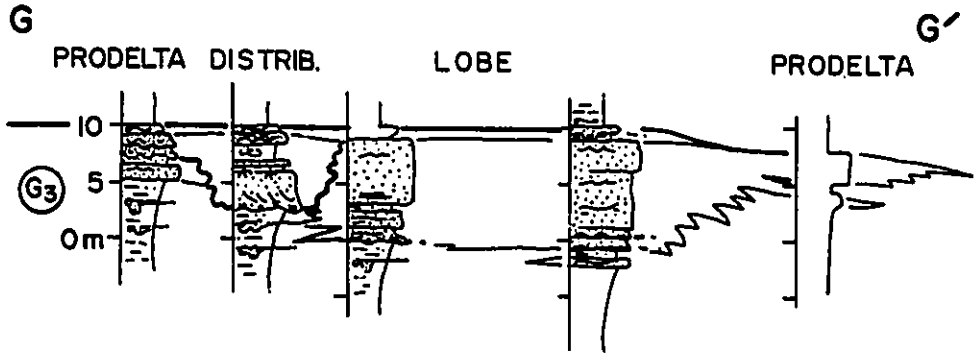

CHAPTER 10. MEMBER F

No oil or gas is produced from member F and core data is therefore sparse. It will be dealt with in a cursory manner and will conclude the detailed member descriptions presented in this thesis. Owing to the brevity of this chapter, a separate summary section is not included.

10-1 Description

10-1-1 Thickness, Distribution and Stratigraphy

Figure 10-1 shows a total isopach map of member F. It shows that member F is roughly pod-shaped reaching a maximum thickness of about 45 meters along a northeast\southeast line approximately in the middle of the map area. It thins to about 15 meters in the northwest and dies out completely in the southeast portion of the map area. This pod-shaped geometry is also seen in figure 10-2 (based on regional cross section 3-9A). Member F contains two shingles each containing several sand bodies which dip towards the southeast and which downlap onto the top of member G. Sandstone in the upper shingle are truncated towards the northwest and are overlain by relatively thick shales comprising the base of the next overlying member (member E). The strike oriented regional cross section (Fig-3-8C) indicates that member F also thickens to the southwest and northeast.

Figure 10-1. Total isopach of member F shows that member F is pod-shaped and thins both to the northwest and southeast. Dots indicate data points. See text for details and explanation.

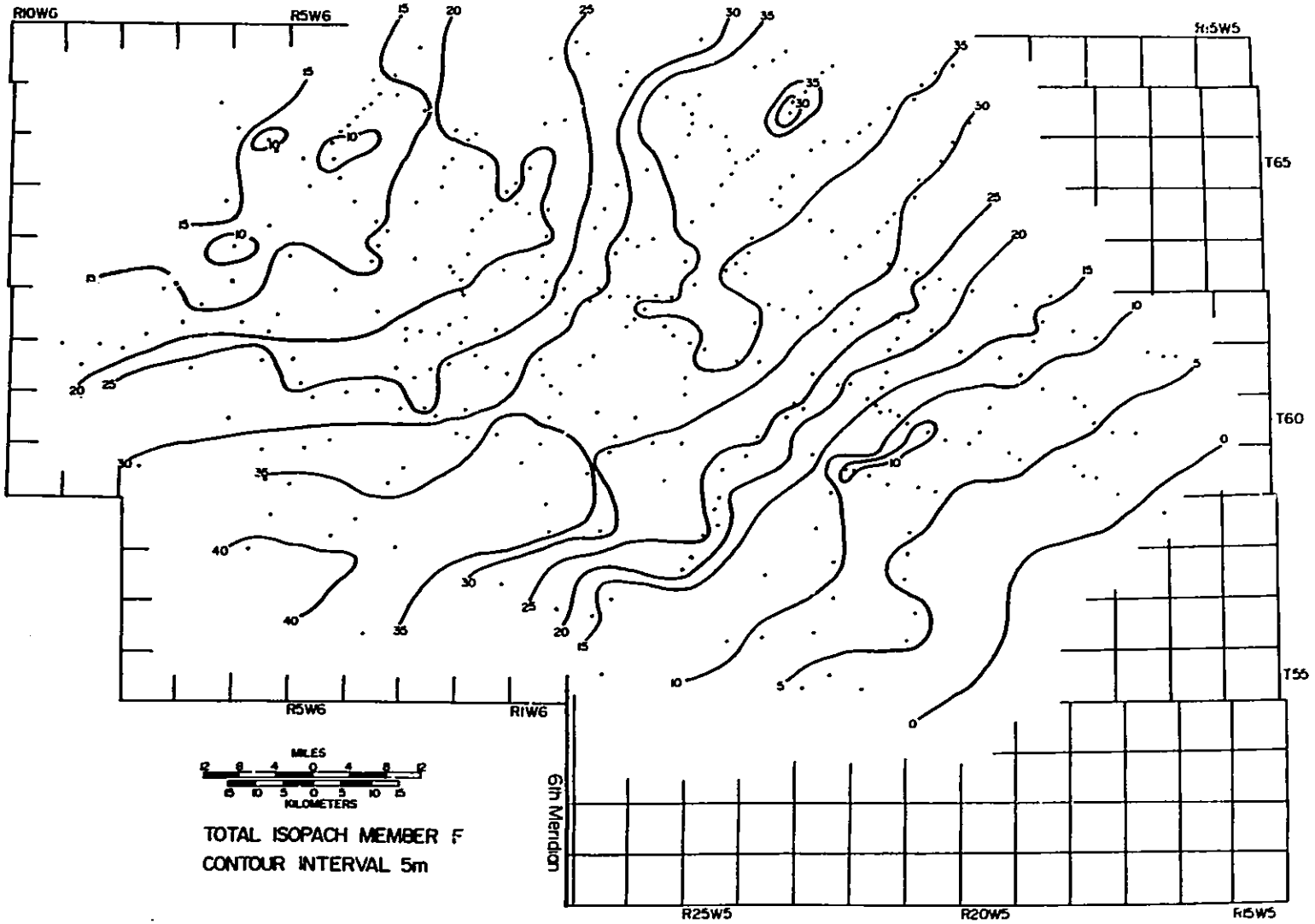
R10W6
R5W6
R5W5
T65
T60
T55
R5W6
R1W6
MILES
KILOMETERS
TOTAL ISOPACH MEMBER F
CONTOUR INTERVAL 5m
6th Meridian
R25W5
R20W5
R15W5

Figure 10-2. Schematic northwest\southeast cross section through member F, based on figure 3-9A. Shingles are truncated to the northwest. Stipple indicates sandstone. See text for explanation.

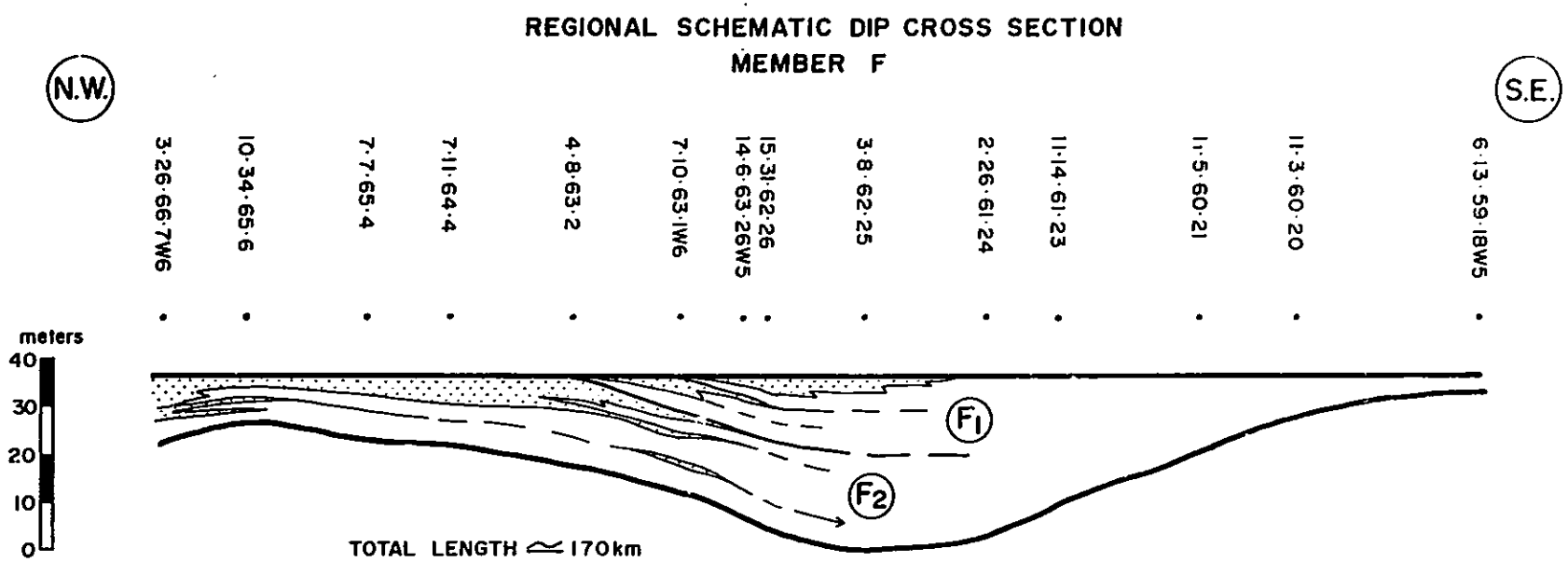
REGIONAL SCHEMATIC DIP CROSS SECTION
MEMBER F
N.W.
S.E.
3-26-66-7W6
10-34-65-6
7-7-65-4
7-11-64-4
4-8-63-2
7-10-63-1W6
15-31-62-26
14-6-63-26W5
3-8-62-25
2-26-61-24
11-14-61-23
1-5-60-21
11-3-60-20
6-13-59-18W5
meters
40
30
20
10
0
F1
F2
TOTAL LENGTH ≃ 170km

10-1-2 Isolith Maps

Shingle F2

Figure 10-3 shows a gross sandstone isolith map of shingle F2. It comprises at two rather irregularly shaped lobes. The larger southern lobe covers an area of about 2300 square kilometers and reaches a maximum thickness of about 8 meters. It has an irregular eastern margin suggesting a lobate morphology, although shoestring sands were not detected.

The northern lobe is not well delineated due to a lack of good well control. In the far south, around Township 56 Range 4W6, there is another accumulation of thick sandstone. Details of this accumulation have not been mapped owing to a lack of well control.

Shingle F1

Sandstone in shingle F1 comprises a broadly hourglass-shaped sand sheet (Fig.10-4). Each of the wider portions of the sand body covers an area of about 2500 km^2 although the northern and southern extensions of F1 have not been mapped. Shingle F1 is very silty in nature and sandstone thicknesses do not exceed about 4 meters. Its southeastern margin is fairly straight although it is not smooth and contains several irregularities. The northwestern margin is more irregular and contains a broad embayment that extends southeastward from the far northwest of the map area. This embayment produces an area of thin sands in between the northeast and southwest portions of the sand body.

Superimposition of F1 and F2 reveals that this embayment and the corresponding thin area overlies the main sandy lobe in shingle F2.

10-1-3 Facies Associations

Unfortunately, there are very few cores through member F. Well 3-26-66-7W6 penetrates member F from 20 to 33 meters (Fig.9-4). Shingle F1 is not present in this well. Shingle F2 comprises a coarsening upwards facies succession. This begins with about 6.5 meters of laminated marine shales and blockstones which pass upwards into very fine to fine-grained HCS sandstone interbedded with about 2 meters of burrowed blockstone. The last sandstone, at about 31 meters, contains a shelly lag rich in *Melania sp.* and *Corbula sp.* This is sharply overlain by about half a meter of blockstone which is in turn sharply overlain by about one meter of pervasively bioturbated mudstone. The contact is highly bioturbated. This facies succession is similar to Facies Association 1C.

The lower part of shingle F2 is cored in well 10-36-61-10W6 (Fig.9-5B). The gamma log profile (Fig.9-5A) is funnel-shaped indicating coarsening upwards. The core also shows a coarsening upward facies succession beginning with blockstones containing gutter casts filled with HCS sands (Facies 7A) which become more abundant upwards. At about 61 meters this passes back into a black bioturbated shale containing *Brachydontes sp.* This quickly coarsens back into bioturbated to laminated blockstone and upwards

Figure 10-3. Gross sandstone isolith map, shingle F2. Sandstone shows an irregular seaward edge perhaps indicative of deltaic progradation. Shoestring sands (channels) were not detected. See text for explanation and details.

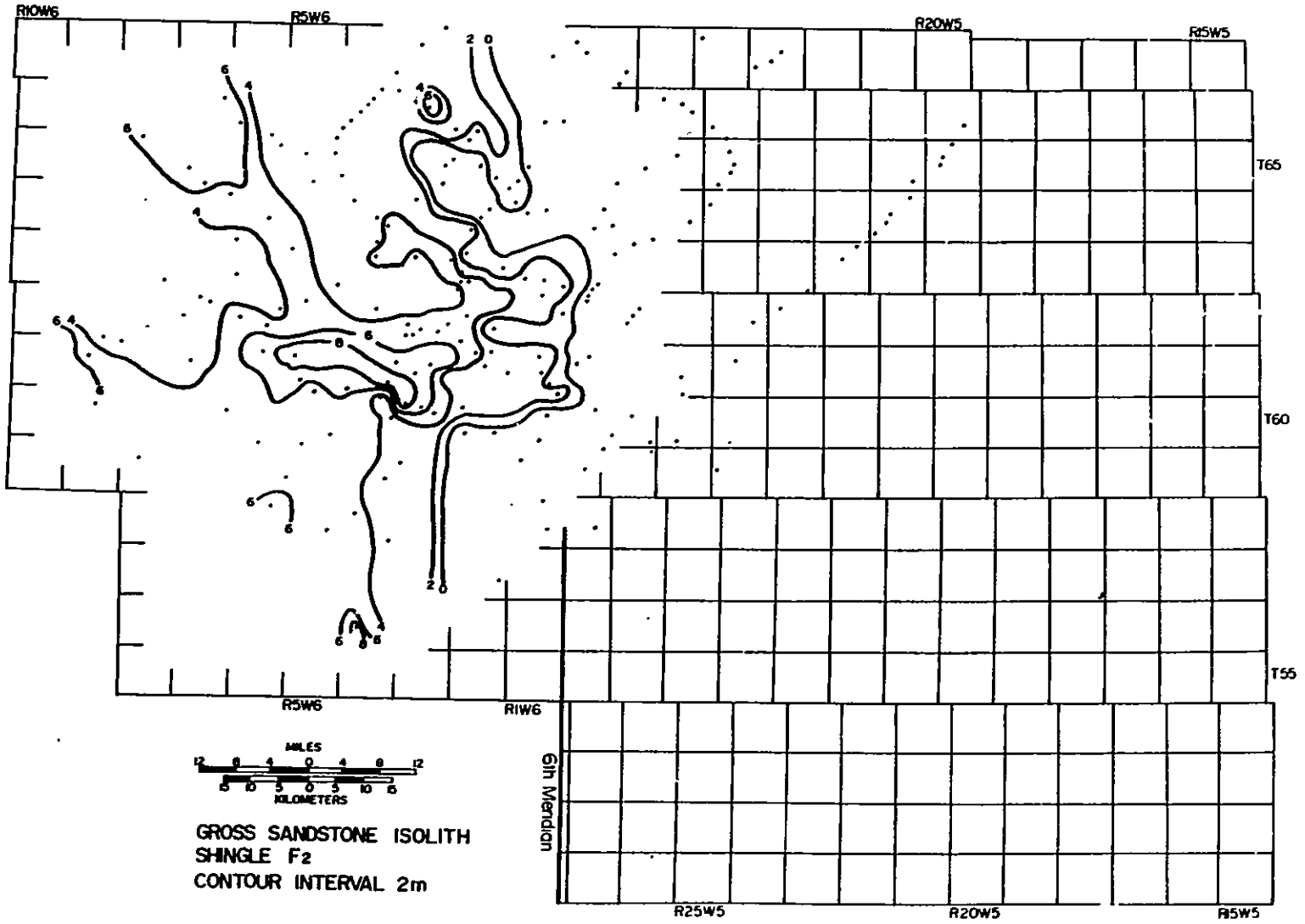
R10W6
R5W6
R20W5
R15W5
T65
T60
T55
R5W6
R1W6
6th Meridian
R25W5
R20W5
R15W5
MILES
KILOMETERS
GROSS SANDSTONE ISOLITH
SHINGLE F2
CONTOUR INTERVAL 2m

Figure 10-4. Gross sandstone isolith map, shingle F1. The seaward edge is relatively straight. Dots indicate data points. See text for explanation.

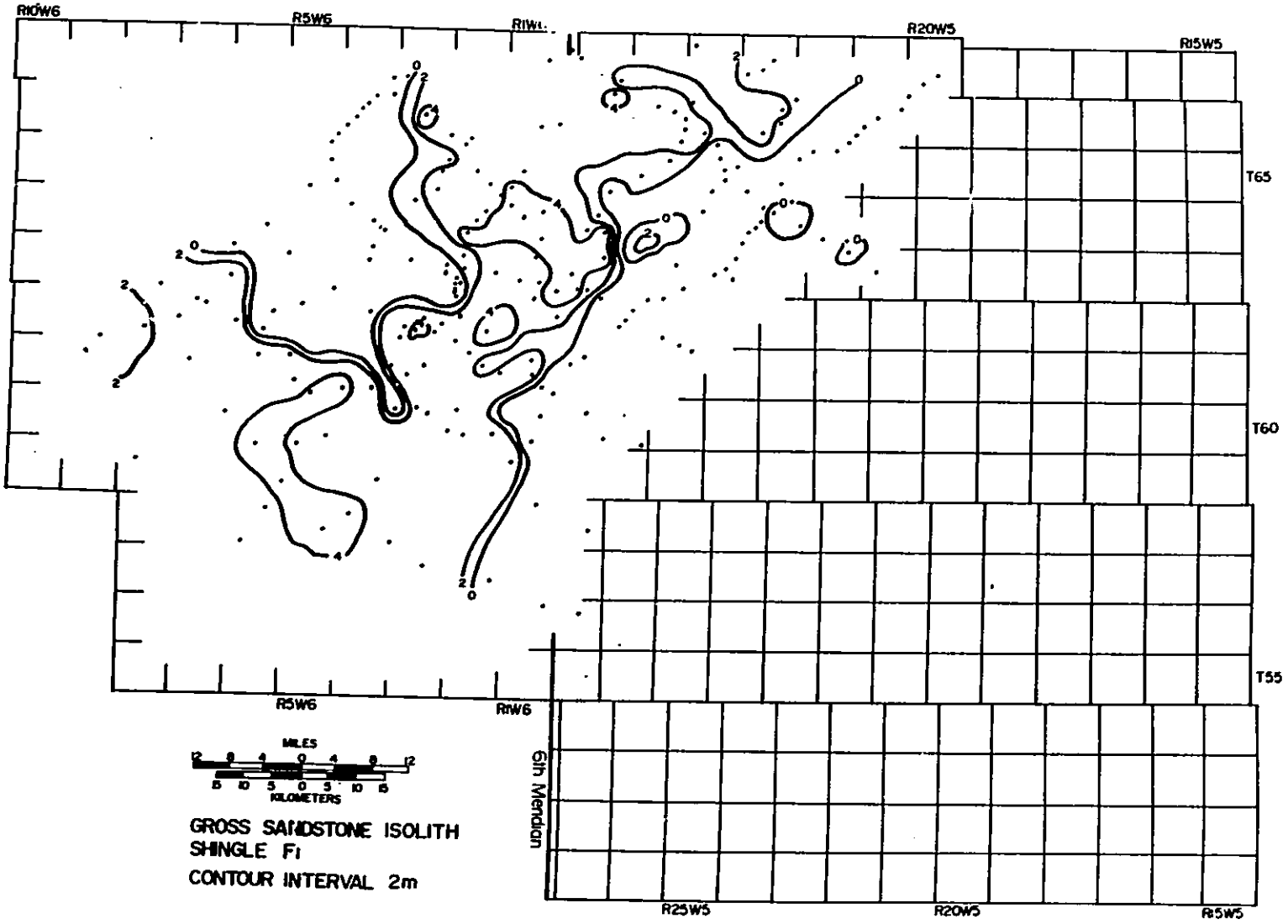
R10W6
R5W6
R1W6
R20W5
R15W5
T65
T60
T55
R5W6
R1W6
6th Meridian
R25W5
R20W5
R15W5
MILES
KILOMETERS
GROSS SANDSTONE ISOLITH
SHINGLE Fl
CONTOUR INTERVAL 2m

into very fine-grained wave rippled sandstone (Facies 7B) containing vague *in situ* root traces. Thicker sandstones are indicated on the gamma logs but unfortunately not cored.

10-2 Interpretation

The irregular nature of the eastern margin of shingle F2 may be interpreted as delta lobes. Cores and logs suggest coarsening upwards facies successions similar to Facies Association 1C which has been interpreted as representing the progradation of storm-influenced sandy shorelines. Possible emergence is indicated in well 10-36. The associated fauna are indicative of stressed brackish environments and may suggest proximity to fresh water. Occasional storm events are indicated by the presence of HCS sandstones and gutter casts. Truncation of shingle F1 suggests probable erosion at the end of member G time and may contribute to the hourglass-shaped geometry of sandstones in shingle F1. Transgressive reworking may account for the lack of thick sandstones in shingle F1.

10-3 Geological History of member F

Member F represents the progradation of at least two shingles which offlap towards the southeast. The lower shingle (F2) comprises at least two silty deltaic lobes which show a significant degree of storm and wave reworking. Sandstone in shingle F1 seems to be concentrated on the flanks of the main deltaic lobe in F2. Deposition of member F culminates in a major transgression. This transgression may have been erosive in nature

and may be responsible for planing off member F, causing truncation of shingle F1. This erosion is especially pronounced in the area previously occupied by the main lobe in F2.

CHAPTER 11. DEPOSITIONAL SYSTEMS IN THE DUNVEGAN FORMATION

11-1. Introduction

The purpose of this chapter is to show that meaningful and practical criteria exist within the sediments of the Dunvegan Formation that can used to recognize and distinguish different types of depositional systems. Depositional systems were defined by Fisher and McGowen (1967) as three-dimensional lithofacies assemblages which are genetically linked by similar processes and environments of deposition. In this study, separate depositional systems are recognized on the scale of individual shingles, although this is a smaller scale than that recognized in studies by Fisher and McGowen (1967). It is emphasized that the recognition, analysis, and mapping of depositional systems within the Dunvegan Formation would not have been possible without the regional stratigraphic framework presented in chapter 3 and elaborated in the subsequent chapters.

This chapter will emphasize a facies models approach (Walker, 1984) and will make use of published reviews of specific facies models as a guide to interpretation. Where appropriate, Dunvegan depositional systems will be compared with specific examples from modern and ancient environments. The broader implications of changes of depositional systems through time within the Dunvegan Formation will be considered in Chapter 12.

11-2. The Environmental Spectrum; Tripartite Classification of Deltaic Depositional Systems

I will use the definition of deltas proposed by Elliot (1986, p.113), namely that...

"Deltas are discrete shoreline protuberances formed where rivers enter oceans...(or other standing bodies of water)...and supply sediment more rapidly than it can be redistributed by basinal processes".

Classification of delta types is based on the relative importance of fluvial processes versus basinal processes (Coleman and Wright, 1975). The familiar triangular classification of deltas (Fig.11-1) with river-, wave- and tide-dominated end members represents a tripartite facies model based on these processes (Galloway, 1975). It satisfies some of the criteria for facies models and acts as a useful guide for interpretation (Walker, 1984). It is stressed, however, that by definition, in a delta sediment must be supplied "more rapidly than it can be redistributed by basinal processes". All deltas are therefore river-dominated to some degree.

Deltas (Elliot, 1986) comprise three main environments; the delta plain (where river processes dominate) the delta front (usually the strand plain where river and basinal processes reach some equilibrium) and the prodelta (where basinal processes may dominate).

Delta plain deposits are important in recognising deltas since these will contain the evidence that shorelines were fed by

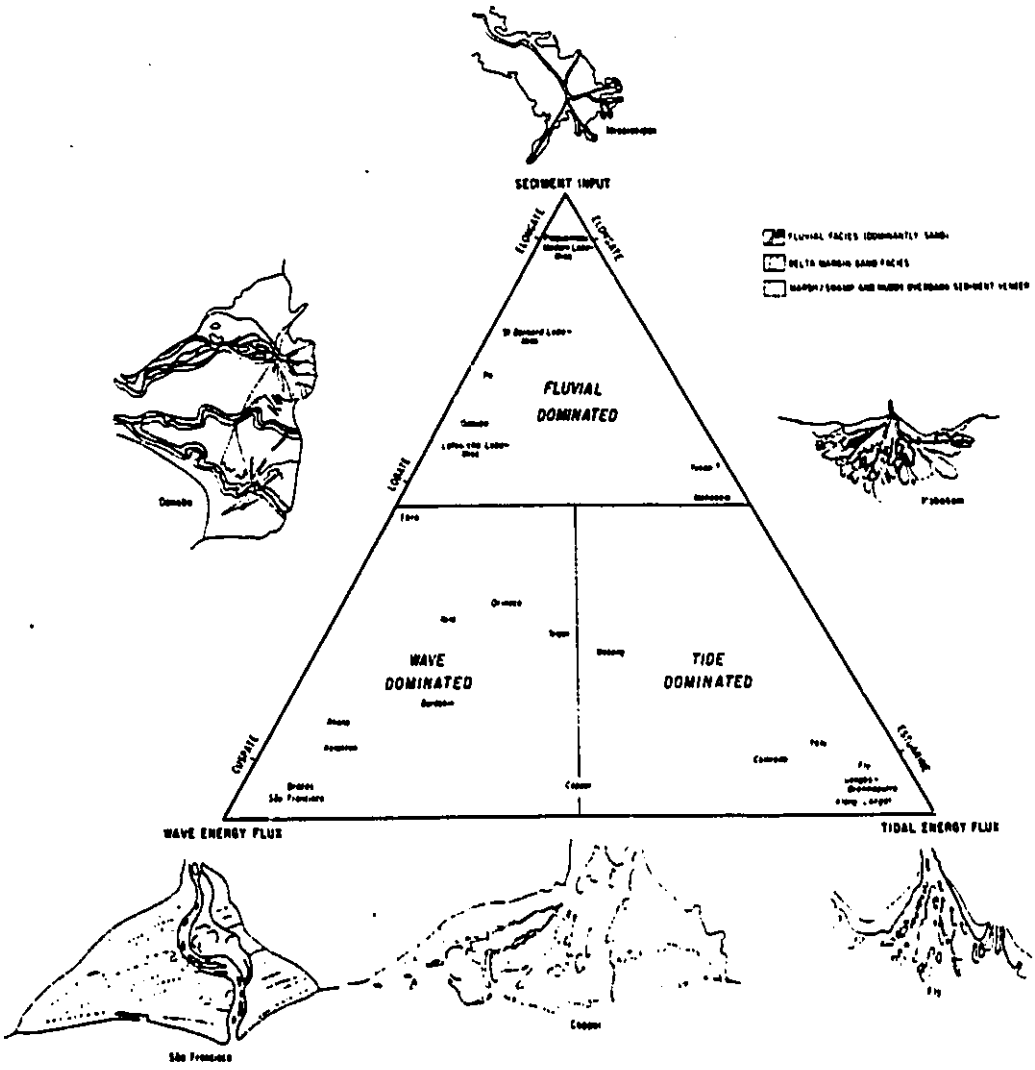

Figure 11-1. Triangular classification of Deltas (after Galloway, 1975).

rivers. Unfortunately, since they are usually above sea level, they often have a lower chance of being preserved, especially during transgressions (c.f., Weise, 1979).

The delta front, while areally and volumetrically least important, is crucial in establishing delta type (Elliot, 1986). The equilibrium morphology of the delta front will reflect the degree of reworking by marine processes. The resulting sandstone body geometry should therefore uniquely reflect the depositional environment and determine the delta type. Published reviews of deltaic facies models emphasize the importance of these geometries in recognizing and classifying ancient deltas (Fig.3, Miall, 1984a; Elliot, 1986; Coleman and Wright, 1975). Coleman and Wright (1975) developed a 6 way classification of three dimensional sandstone body geometries that would be expected in different types of deltas (i.e., river-, wave- and tide-dominated). In figure 11-2 I have re-plotted these geometries onto a similar triangular classification as that shown in figure 11-1. All of the delta geometries emphasize up-dip pinch out of sands into distributary feeder channels and contrast with linear sand bodies oriented parallel to shorelines with muddy marine facies on both landward and seaward margins, such as is common in many Upper Cretaceous sand bodies in the Cretaceous Western Interior Seaway of North America (Rice and Gautier, 1983; Plint and Walker, 1987).

Caution must be used, however, in applying these models to studies in ancient sediments. These sand body geometries are based entirely on the study of individual modern deltas, and often with a lack of good core data to accurately determine sand distribution. In addition, they do not take into account which portions of these deltas would likely be preserved in the ancient record, or how they would be preserved.

In figure 11-3 I have plotted typical sand-body geometries mapped within individual shingles of the Dunvegan Formation using a similar tripartite division, as that shown in figure 11-2. Sand-body geometries in the Dunvegan range from linear, elongate, shore-parallel sand bodies, which indicate practically no direct fluvial influence (e.g.shingle D2); to shore-normal lobate sand bodies which narrow up-dip into linear channelized shoestring sand-bodies and which indicate practically no re-working by basinal processes (e.g. shingles E2 and E1). Linear sand bodies, such as in D2, do not fit a deltaic classification and are plotted outside of the deltaic field, but included in the figure for comparative purposes.

This study shows that depositional systems within the Dunvegan Formation range from highly river-dominated deltas to wave-dominated barrier islands and transgressive sheet sands which show virtually no evidence of river influence at all. These different depositional systems are characterized not only by different sandstone body geometries (as shown in figure 11-3) but also by

Figure 11-2. Triangular Classification of Sand Body Geometries in Deltaic Depositional Systems (after Coleman and Wright, 1975).

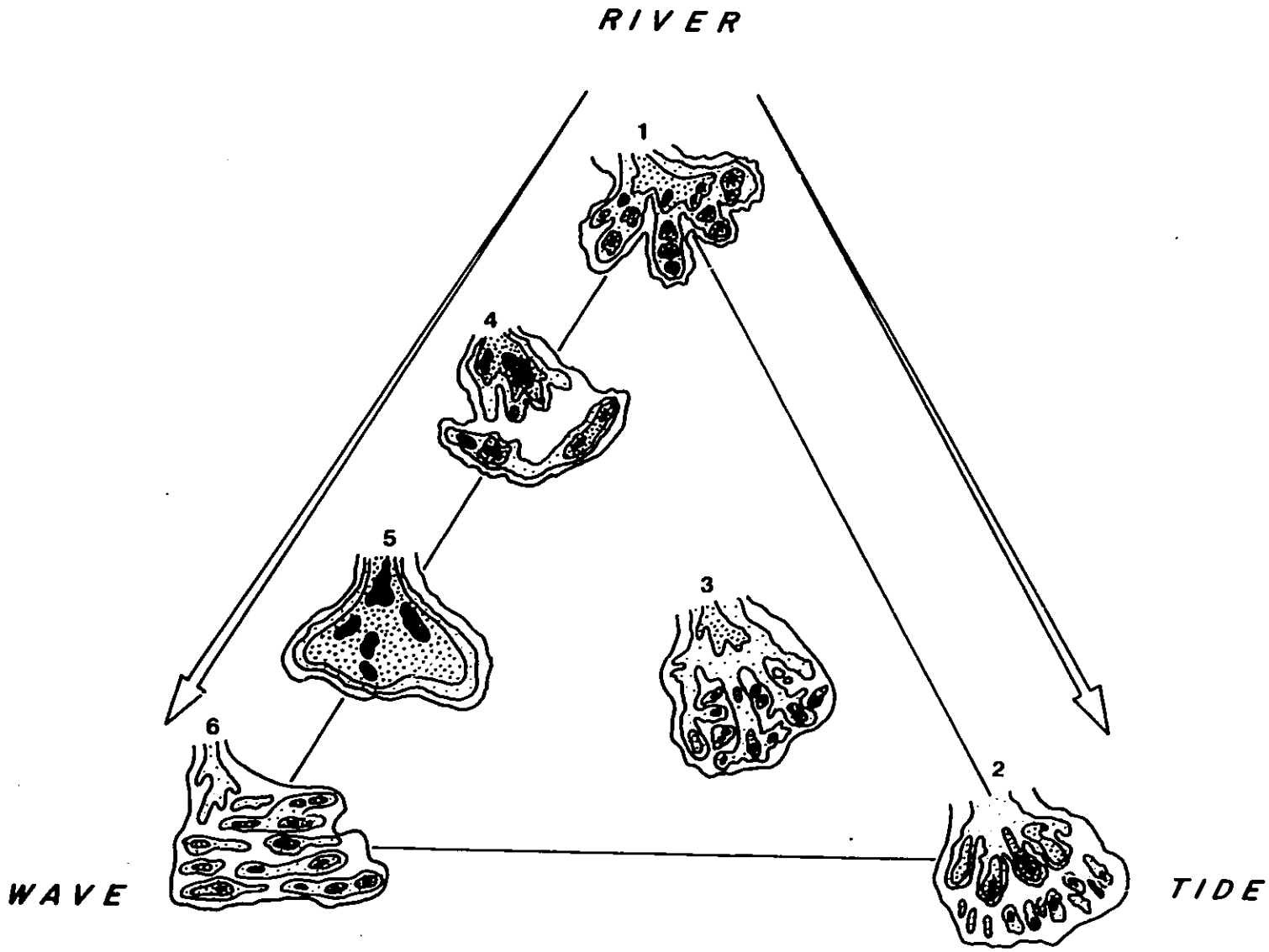
RIVER
1
4
5
3
6
2
WAVE
TIDE

different facies associations. The section below will contrast the essential characteristics of these end-member depositional systems and will then go on to discuss variations between and departures from these end-members.

11-3. River-Dominated Deltas

The best examples of highly river-dominated deltas in the Dunvegan Formation are in member E and especially in shingles E1 (Bigstone lobe) and E2 (Simonette lobe). These deltas consist of three important components,

1. channels
2. lobes
3. interlobes.

The areas that contain channels coincide with the delta plain while the depositional lobes usually indicate progradation of the delta front. Interlobe areas comprise interdistributary bay environments and grade basinward into mudstone-dominated prodelta deposits. Vertical and lateral facies associations through these elements are distinctive and are summarized in a paleogeographic reconstruction (Fig.11-4) of a typical river-dominated deltaic depositional system (Bigstone delta, Shingle E1).

11-3-1. Lobes

Depositional lobes in deep water river-dominated deltas are characteristically bird-foot shaped, while those deposited in shallower water tend to be smoother (Fisher and McGowen,1967;

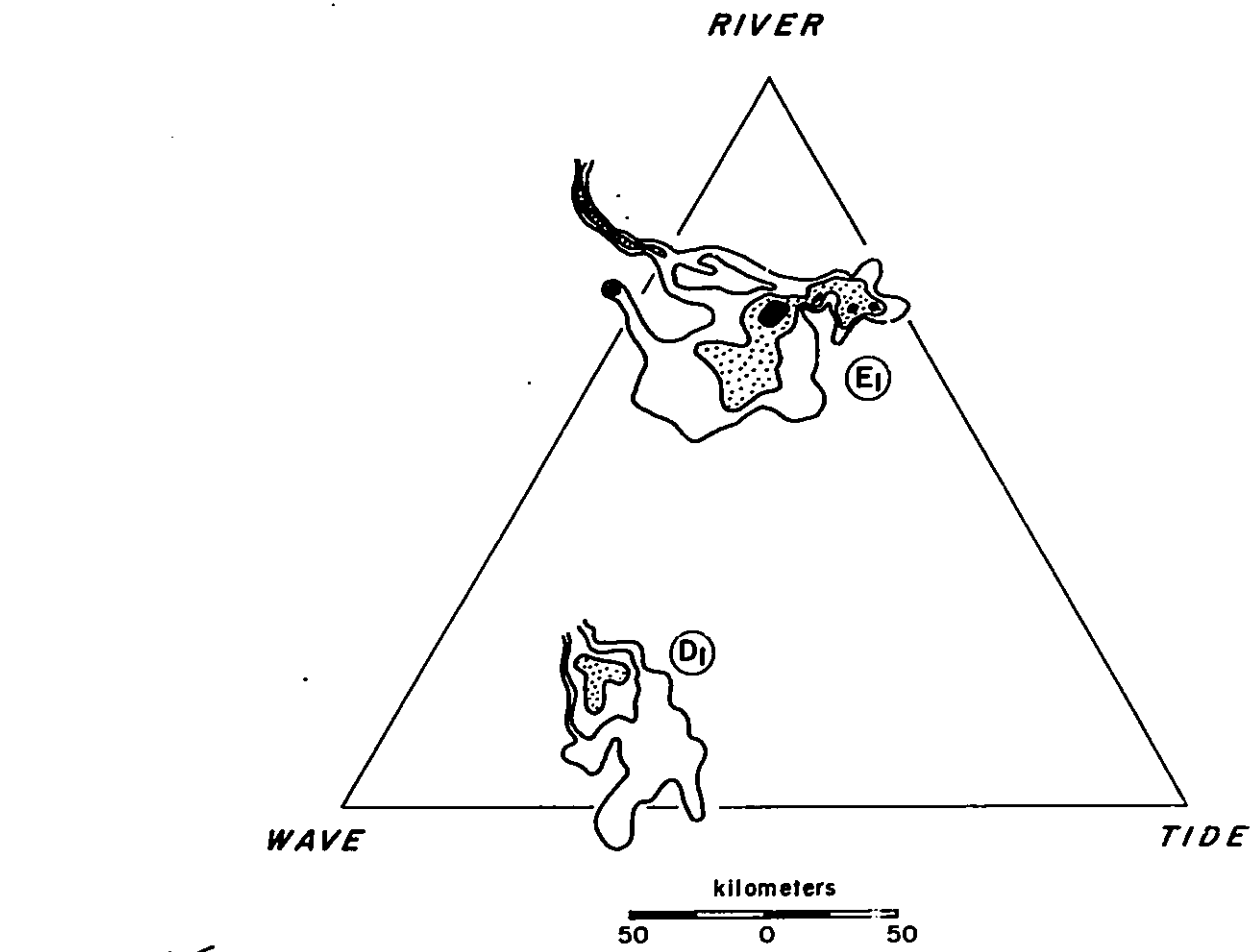

Figure 11-3. Triangular Classification of Sand Body Geometries in the Dunvegan Formation. Shingles E1, D1, and D2 are plotted. Compare these geometries with those in figure 11-2 and 1-2.

Figure 11-4. Paleogeography of River-Dominated deltas in shingle E1, member E. The Simonette channel in the northwest feeds digitate sands of the Bigstone lobe. Compare with figures 5-11, 5-12, and 9-6. See text for discussion.

RIVER-DOMINATED DELTA
SHINGLE E_1

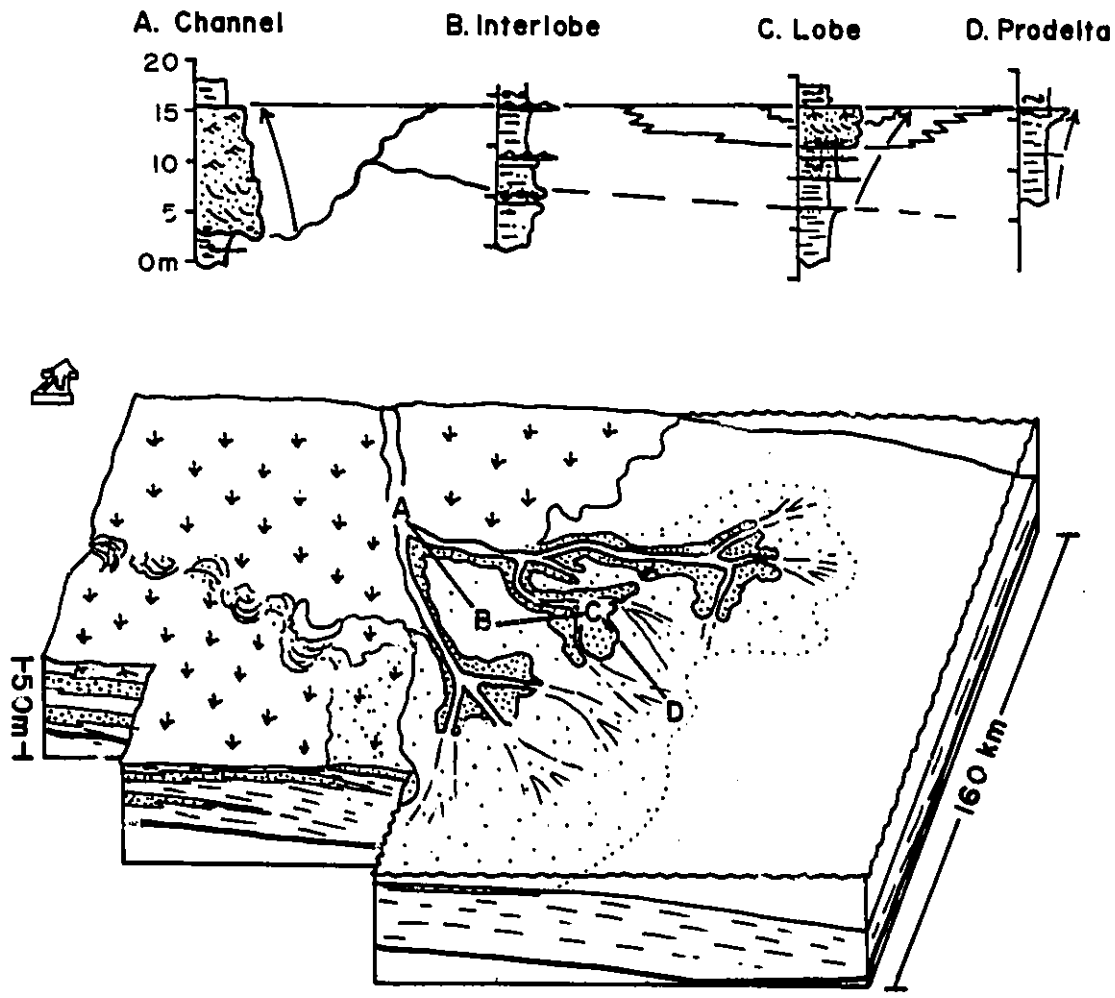

Elliot, 1986). Delta front sandstones in shingle E1 and E2 (Bigstone delta) comprise rather broad digitate patterns, compared to the scrawnier birdfoot patterns characteristic of the modern Mississippi Delta. Paleogeographic interpretation of these sand body geometries (Fig.11-4), however, suggests that these sand bodies are composite and are made up of several laterally overlapping, and rather more scrawny, distributary channel complexes and associated mouth bar sands.

Vertical facies associations through these depositional lobes are characterized by rather irregular coarsening upward facies successions beginning with mudstones and culminating with sandstones. As outlined in chapter 2 (section 2-3-1B), these types of successions define Facies Association 1B. They begin with laminated mudstones. Soft sedimentation deformation features and climbing current ripples characterize the lower portions of these facies successions and indicate high sedimentation rates. Primary sedimentary structures in the sandier upper portions are predominantly formed by unidirectional currents and include ripple drift cross lamination and angle-of-repose cross bedding. Mud rip-up horizons and shaly partings are common suggesting episodic deposition during flood stages of major distributary channels. Evidence of re-working by organisms or redistribution of sands by basinal processes (e.g. HCS, wave ripples) is lacking. This suggests relatively low basinal energy and indicates a highly river-dominated depositional system.

The delta front sandstones are interpreted as being deposited in a similar environment as bar finger sands of the modern Mississippi delta (Fisk, 1961; Coleman and Prior, 1982, figure 19,20 and 21). The width of Dunvegan mouth bar sandstones (lobes) are considerably wider than those in the Mississippi birdfoot deltas. This probably results from the much greater inferred proportion of sand in Dunvegan depositional systems. Mississippi delta front deposits comprise about 75% mud and siltstone and 25% sandstone (Fisk, 1961). The Mississippi River transports only about 19% fine- and very fine-grained sandstone (Wright, 1985). This is in direct contrast to the river-dominated deltaic deposits in the Dunvegan Formation which contain on the order of about 50% sandstone. Shifting distributary channels in the Dunvegan therefore deposit considerably more sandstone and produce more widespread sand bodies than in the Mississippi. The difference in sand body geometry is inferred to result more from a difference in the type of sediment supplied rather than a difference in the importance of fluvial processes.

11-3-2. Interlobe

Interlobe areas do not contain thick sandstones and are dominated by mudstones. As the interlobe areas progressively fill, however, the environment gets shallower. The vertical facies associations therefore record a shallowing upwards from more open marine laminated shales and blockstones into shallower and more restricted marine, sideritic, pinstriped mudstones and wave-

rippled banded mudstones. Rare parallel laminated to current rippled sandstones record episodic infilling by crevasse splays. Periods of emergence are recorded by *in situ* root and coal horizons in the upper parts of these associations.

11-3-3. Delta Plain: Channel

The most distinctive feature of the delta plain facies are major, erosively-based, channelized sandstones. The Simonette channel was observed to bifurcate downdip indicating that it was probably the trunk stream that fed the distributary channel network associated with the Bigstone delta. It is possible to get a feel for the original channel paleomorphology. Maximum probable channel depths can be estimated from the sandstone thicknesses which range up to 18 meters. Sandstone widths are more likely to relate to the width of paleo-river valleys (or meander belt width) rather than the actual channel (or thalweg) width and in the Dunvegan are usually on the order of less than about 5 kilometers. Facies successions through the channels indicate a sandy fining upwards association. Mud-filled channels, or estuarine facies, are relatively uncommon in river-dominated deltas of the Dunvegan Formation but were noted in places, particularly on the lower distributary plain.

11-3-4. Delta Plain versus Interdistributary Bay

It is often difficult to distinguish shallow marine interdistributary bay fill deposits from sediments deposited on the delta plain. Plint and Hart (1988, p.32) note marine influence in

an "apparently 'fluvial' channel 33 m above the uppermost beach deposits" in Dunvegan outcrop at Clayhurst, Alberta. The Dunvegan coastal plain was probably essentially flat and the demarcation between the marine and non-marine environment was probably extremely irregular, especially in interlobe areas. This transition zone was probably broad and consisted of shallow, vegetated salt water marshes infested with *Lingula*, *Brachydontes* and oysters, and interspersed with brackish lacustrine environments.

11-3-5. Scale and Comparison With Other Ancient and Modern River-Dominated Deltas

Figure 11-5 shows a map of the depositional lobes of the Mississippi deposited within the last 6000 years (after Frazier, 1967) superimposed over a map of the thesis area. The areal extent of delta complexes within the Mississippi is similar to the areal extent of deltas in the Dunvegan and average about 1500 square kilometers (compare with Fig.4-16). There are some similarities in the thickness of some of the older delta complexes of the Mississippi with those of the Dunvegan. The thickness of the Teche Delta Complex (including prodelta shales) averages between 10 and 15 meters (Penland et al., 1987) compared to an average of about 15 to 20 meters for sediments of the Bigstone lobe in shingle E1.

As outlined above, sediments of the Mississippi delta complex are considerably muddier than those in the Dunvegan. In addition, active progradation of the Teche delta complex took

place in a relatively short time period of about 3300 years (Penland et al. 1987). One shingle (or delta complex) in the Dunvegan Formation, in contrast, is deposited in a time period of 50,000 to 100,000 years. This greater time allows more lateral shifting of sub-environments and results in more widespread sand bodies.

Lastly, the basinal setting is also different. The Mississippi delta is deposited on an actively subsiding passive continental margin facing the open ocean while the Dunvegan was deposited into a shallow epeiric sea and onto the Alberta foreland basin. Many workers have classified deltas of the Texas Gulf Coast into shallow water (or shoal water) deltas and deep water deltas. The Bigstone delta lies farthest seaward of any delta complex in the Dunvegan. Its sand-body geometry and vertical facies associations are the most similar to bar-finger sands of the modern Mississippi (Fisk,1961) and may reflect deposition in deeper water than any other deltas in the Dunvegan Formation.

11-4. Wave-Dominated Deltas

In chapter 1 it was pointed out that very few wave- and tide- dominated deltas had been documented in the ancient record. Sediments of shingle D1 provide the best example of a wave-dominated delta in this study. Figure 5-12 summarizes the characteristics of this depositional system. Its geometry indicates a major distributary channel in the northwest feeding a rather large, smooth-lobed delta to the southeast. This contrasts

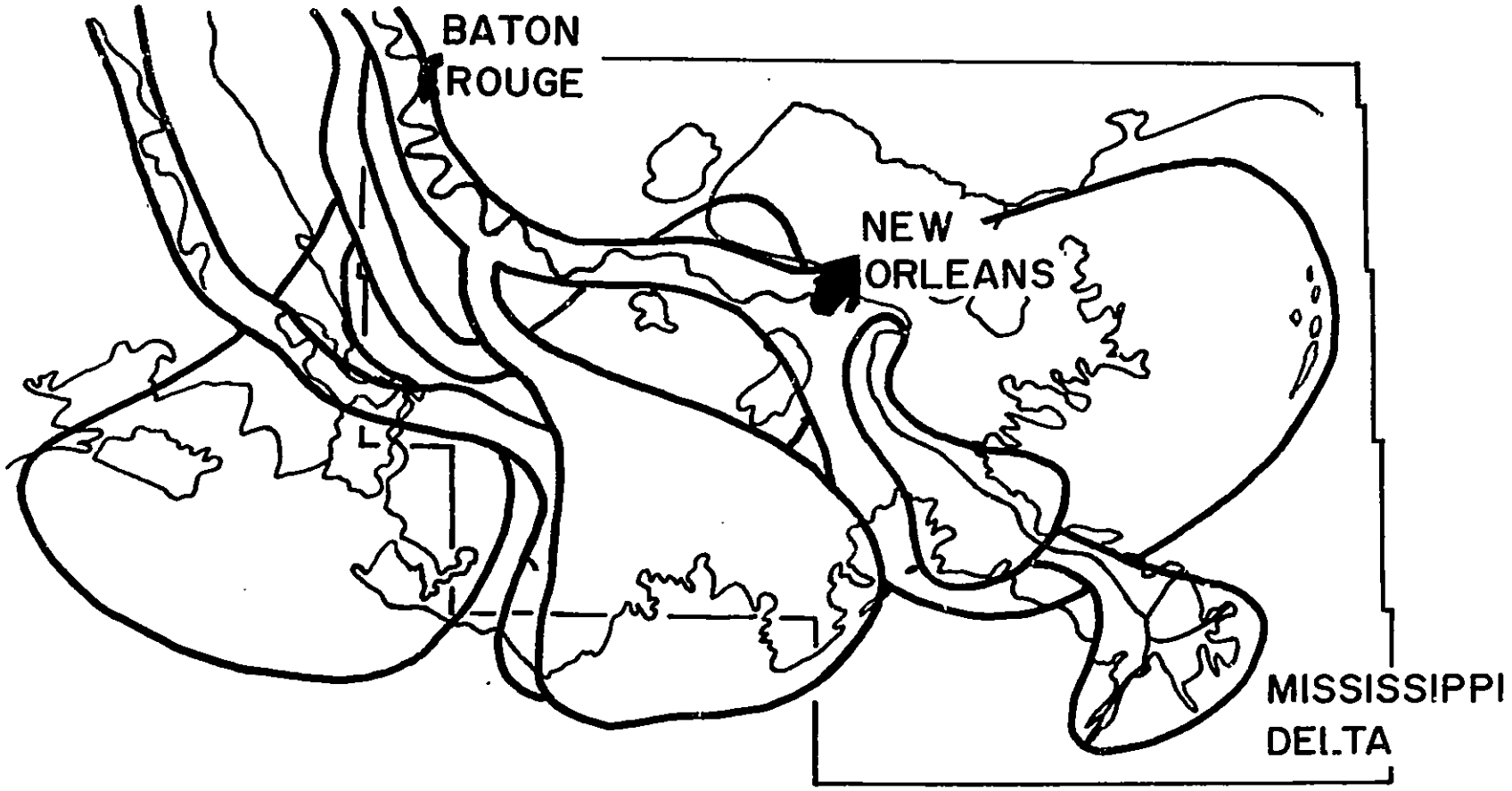

Figure 11-5. Depositional lobes of the Mississippi to scale superimposed on an outline of the thesis area. Mississippi lobes are on the same areal scale as delta lobes in the Dunvegan Formation. Compare this figure with figure 4-16. See text for further discussion.

with the rather more digitate lobes of the river-dominated deltas in the Dunvegan Formation (compare Fig.11-4 and 5-12). The geometry of the delta front is interpreted as being cuspate in shape and is similar to cuspate, wave-dominated deltas documented by Weise (1979) in the Cretaceous San Miguel Formation, Texas (Fig.1-2, E) and with end member 5 of Coleman and Wright (1975) (Fig.11-2).

The facies associations through the main portion of the lobe are also quite different from those observed in the river-dominated deltas, and indicate that delta front sandstones are characteristically reworked into wave- and storm-dominated shorefaces. A typical facies succession begins with bioturbated mudstone and shows a regular, smooth coarsening upward facies succession typical of Facies Association 1A. Wave and storm produced features (HCS and wave ripples) are the dominant sedimentary structure in the sandier facies. The delta front sands contain much less interbedded mudstone and lack the mud rip-up horizons noted in the river-dominated delta fronts. The coarsening upward indicates a prograding shoreline while the lobate geometry and association with a channelized sand body suggests that this progradation is directly influenced by a river. The distinctive facies associations and the relatively smooth nature of the delta front, however, indicates a relatively high degree of basinal reworking by storm and wave processes. This is interpreted, therefore, as a wave-dominated delta.

Distributary mouth bar sandstones are not present and the lithofacies do not directly reflect fluvial influences. Without the accompanying sandstone distribution map, this facies succession would be practically indistinguishable from sandy wave and storm dominated strand plain deposits not associated with deltaic processes.

Moslow and Pemberton (1988) distinguish facies associations in prograding shorefaces versus prograding delta fronts and note differences very similar to those discussed above for wave- versus river-dominated deltaic systems.

The D1 lobe is deflected somewhat to the southeast of the Waskahigan distributary channel (Fig.5-12). This may reflect a component of alongshore directed sand transport to the southeast due to longshore drift. The direction of longshore drift is consistent with the inferred direction interpreted from the underlying barrier island discussed below and in chapter 5. A similar southerly directed deflection of delta front sandstones and associated shelf sandstones, induced by longshore drift, was documented by Palmer and Scott (1983) in their study of wave-dominated shorelines and deltas in the La Ventana tongue of the Campanian Mesaverde Formation in the Southwestern United States. Coleman et al. (1981) studied similar sandy shelf "plumes" associated with the modern, wave-dominated Nile delta and proposed that longshore drift was resposible for sand transport. Similar

processes seem to have been operative in wave-dominated depositional systems of the Dunvegan Formation.

11-4-1. Estuarine Channel

The facies associations in the channels that are associated with this wave-dominated delta are different from those in the river-dominated deltas. The D1 delta channels (e.g. Waskahigan channel) are filled by sediments displaying a marked estuarine character (Facies Association 2B) rather than a sandy fluvial character (Facies Association 2A, e.g. Simonette channel). Estuarine facies are characterized by laminated to burrowed, restricted marine mudstones which overlie sandstones exhibiting tidal cross-bedding. Similar estuarine fills have been interpreted in the Crystal channel within the Lower Cretaceous Viking Formation, Alberta (Reinson et al., 1988), although these deposits contained abundant conglomerate phases which are lacking in the deposits of the Dunvegan within the area studied. These contrast with the dominantly sandy fills of the more fluvial channels in member E.

If, as postulated above, sedimentation rates are lower for member D than member E, then it is more likely that marine processes will affect distributary channel systems. Estuaries are usually better developed in basins with relatively low discharge especially when they undergo transgression (Nichols and Biggs, 1985). The up-channel migration of salt wedges will be favoured by channels with lower discharges, and during transgression, these

channels are more likely to be filled with sediments deposited by estuarine processes. As a result of lower sedimentation rates in member D, muddy estuaries are relatively well developed, and channel fills comprise Type 2B Facies Associations. Member E. incontrast, seems to contain sand-filled channels typical of Facies Association 2A. These differences in the types of channel fill represent the greatest difference between delta plain facies in river- versus wave-dominated deltas of the Dunvegan Formation.

1-5. River-Dominated, Wave- and Storm-Influenced Deltas

A third type of depositional system has been recognized within the spectrum of deltaic systems described above that displays characteristics of wave- and river- dominated deltas described above. The presence of these intermediate types of deltas was first indicated in chapter 2 as Facies Association 1C which displayed characteristics of wave-dominated (Facies Association 1A) and river-dominated (Facies Association 1B) depositional systems. An example from member G is illustrated in figure 9-6. Using the terminology of Fisher et al. (1969) these could also be termed high-constructional, wave-influenced deltas. Examples include deltaic systems within member G and shingle E4 within member E.

11-6. Wave-Dominated Barrier Bars

11-6-1. Criteria for Recognition

At the opposite end of the spectrum of shallow marine environments within sediments of the Dunvegan Formation are wave-dominated barrier bar sandstones. Reinson (1984) provides an up-to-date review of barrier island and associated strand-plain depositional systems. Barrier islands are characterized by,

1. the sandy barrier-island chain
2. the enclosed body of water behind it (lagoon), and
3. tidal inlets that connect the lagoon with the open sea.

Within this context Reinson (1984) presents three "end-member" facies models for barrier island stratigraphic facies successions. These are; the regressive or progradational model, characterized by a coarsening upwards facies succession; the transgressive barrier model, in which facies successions do not show fining or coarsening upward trends; and the barrier-inlet model, in which barriers consist primarily of fining-upward tidal inlet facies successions. The proportion of a barrier bar that is underlain by tidal inlet facies successions is usually a function of the tidal range, and is most common in meso-tidal environments.

Niedoroda et al. (1985) distinguish between barriers that grow by spit accretion (and which are often attached at one end to the land), which they call barrier-spits, from barriers which are completely detached and separated at both ends by tidal inlets, which they call barrier-islands. The orientation and geometry of

these sand bodies is different from those of deltaic sand bodies. Barrier bar sandstones are linear and are elongated in a roughly shore parallel direction rather than normal to shore. The seaward margin of these sand bodies is also considerably smoother than in river-, wave-, or tide-dominated delta front sandstones.

11-6-2. Examples Within the Dunvegan Formation

The best example of a wave-dominated barrier island sand body within sediments of the Dunvegan Formation is in shingle D2 (chapter 5, Fig.5-11). The main areal components of this barrier island depositional system are,

1. the sandy barrier bar,
2. a lagoon to the northwest,
3. an open shelf to the southeast.

The paleogeography of this barrier bar sandstone is shown in figure 5-11. At the seaward edge of the barrier bar is a well defined relatively smooth wave- and storm-dominated shoreface. The barrier bar is cut by a series of tidal inlets facies successions, although ebb tidal deltas were not documented. A major distributary channel probably fed this barrier bar at its northeastern end and sand was probably transported to the southwest by longshore drift. As outlined above, the overall geometry of this sand body is totally different from that for the river-dominated deltas as shown in figure 11-3. It is linear, is oriented shore-parallel, and has a relatively smooth seaward margin. The maximum sandstone thickness within this depositional

system is about 10 meters compared to a maximum of about 18 meters for delta front sands in river-dominated delta systems.

In addition to these differences in the overall geometry of sand bodies, the lateral and vertical facies associations are different. Facies succession through much of the barrier bar coarsen upwards (Facies Association 1A), and indicate that the barrier is regressive or progradational in nature. Portions of the barrier are underlain by tidal channels containing fining upwards facies successions, similar to Facies Association 2B, but with less interbedded mudstone. The coarsening upward facies successions are different from the successions observed in river-dominated delta lobes. The barrier bar successions begin with bioturbated mudstones, probably deposited on a shelf, and which are quite different from the laminated pro-deltaic shales and blockstones seen in the basal mudstones in river-dominated depositional systems. Sandstones show abundant HCS and wave ripples, and soft sediment deformation features are virtually absent. The overall coarsening upward is more regular than in river-dominated deltas and contains less interbedded mudstone. The facies reflect a much higher degree of basinal reworking by waves, storms, and organisms. The lack of convolute lamination and the thinner nature of these wave-dominated depositional systems indicate lower sedimentation rates.

The lagoonal deposits are characterized by laminated to burrowed pinstriped and banded mudstones which contain brackish

fauna. These mudstones are interbedded with wave-rippled sandstones and are cut by thin channelized sands.

Comparison with the models presented by Reinson (1984) and Niedoroda et al. (1985) suggests that this depositional system represents a microtidal to mesotidal, regressive, barrier-spit. Sediment was supplied by a major distributary at the northern end of the barrier and transported south by longshore drift. Numerous tidal channels cut the barrier to the south.

It is possible to independently verify the probable tidal range at this time. The tidal range can be estimated by the thickness of preserved foreshore (i.e. beach) deposits. In the best example (well 7-10-63-1W6, shingle D2) the preserved foreshore is about 2 meters from cross bedded sandstones in the upper shoreface to the first rooted horizon. This thickness can be used as a direct estimate of tidal range and indicates a probable tidal range of about 2 meters. This range marks the transition between micro- and meso-tidal environments.

11-6-3. Controls on Sedimentation and Comparison with Modern and Ancient Examples

It is postulated that the overall energy of the basin was low during Dunvegan time and that the controlling factor on the character of sedimentary facies is sedimentation rate. As long as sedimentation rates were fairly high, river-dominated deltaic sedimentation persisted but when it dropped below a certain level, basinal processes were capable of re-working and redistributing

much of the sediment, resulting in wave- and storm-dominated depositional systems.

The genesis of barrier islands is controversial, but three general theories of origin are accepted;

1. growth by spit elongation,
2. growth by the emergence of offshore bars, and
3. drowning of shore-attached strand-plain deposits.

The scale of the D2 barrier bar sandstone is comparable to wave-dominated, progradational barrier islands of the Texas gulf coast (e.g. Galveston Island, McCubbin, 1982, fig.3). The overall coarsening upward suggests progradation and the three dimensional geometry indicates that this progradation resulted from relatively high sediment supply from the Waskahigan channel to the north. Shingle D2 is not deposited during a transgression and the most likely mode of origin is therefore by spit elongation.

There are many examples of ancient wave- and storm-dominated strand plains and barrier sand depositional systems in the Cretaceous Western Interior Seaway, several of which are discussed in McCubbin (1983) including the Parkman Sandstone, Wyoming; and the Gallup Sandstone, New Mexico. Canadian examples include the Kakwa shoreface in the Cardium Formation (Plint and Walker, 1987). The chief difference in most of these other sandstones is that they are considerably thicker (about 20m) than observed in the Dunvegan Formation. The appearance of sandy shoreface deposits and associated back-barrier lagoonal and coastal deposits,

however, are similar to those in the Dunvegan. Plint and Walker (1987) describe non-marine facies which are nearly identical to those described in this study.

11-7. Transgressive Depositional Systems

11-7-1. Transgressive Sheet Sands

All of the depositional systems described above have one essential characteristic. They all contain coarsening upwards facies successions which indicate progradation or regression of environments. Regressive depositional systems dominate the Dunvegan Formation.

Preserved transgressive deposits, in contrast, tend to show fining-upwards facies associations, but comprise a much smaller proportion of the preserved stratigraphic record. Transgression in a foreland basin often produces a marine erosion surface (Swift et al., 1987) or a surface of non-deposition. The effect of transgression in sediments of the Dunvegan has already been discussed with respect to the formation of widespread surfaces of non-deposition, the T-surfaces. These surfaces mark the abrupt transition from coarser material into marine mudstones. It was pointed out in chapter 3, however, that marine erosional surfaces (Em surfaces) may also be produced during transgression and that the sediment preserved between Em and T-surface represent preserved transgressive deposits.

These transgressive deposits were discussed in relation to member C in chapter 6. They usually occur as a thin veneer (less

than about 2 meters) of bioturbated sandstone. When channels are transgressed, considerably thicker successions of estuarine deposits may be preserved, such as in the Waskahigan channel in member D.

The best example of a transgressive sheet sandstone is the sandstone that caps member C. The geometry and facies of this sandstone are different from any of those depositional systems described above. Well defined lobes, shoestring sands or linear shore-parallel sand bodies are absent (Fig.6-3). The geometry is that of an irregular ragged sheet. The sandstone is sharp-based and is dominated by abundant *Ophiomorpha* burrows and rarer cross-bedding in places. Similar transgressive sandstone facies were observed re-working and partially eroding the tops of sandy deltaic sequences in the San Miguel Formation, Texas (Weise, 1979). It is clear that these deposits are not primary. They are essentially sandy lags produced by erosion of the underlying substrate. Probably the best understood mechanism of marine erosion during transgression is marine shoreface retreat (Niedoroda et al., 1985, fig.8-21). This sheet sandstone was probably deposited as a series of en echelon sandy barrier bar sands as a result of erosional shoreface retreat at the end of member C time.

11-8. Conclusions; Subsurface Facies Models

In this chapter, criteria for distinguishing wave-dominated depositional systems from river-dominated shallow marine depositional systems were outlined. These criteria include the recognition of different sand body geometries as well as different lateral and vertical facies associations. These criteria are based both on observable characteristics within the Dunvegan sediments and on comparison with existing published facies models. In terms of studies of deltaic depositional systems, this study builds on the approach used by workers in the Texas Gulf Coast (Fisher & McGowen, 1967; Weise, 1979). While most of these studies are heavy on interpretations based on well log data, core data is usually relatively scarce and detailed facies analysis is usually not possible. This study combines detailed well log correlation with a much greater proportion of detailed facies information through the many cores and core cross sections presented in chapters 4 to 10. The well log data and facies information have been combined in detailed maps and block diagrams which characterize these ancient deltaic depositional systems in three dimensions (e.g. Fig.5-11, 5-12, 11-4). In contrast to many outcrop studies, the paleogeographic summary block diagrams are based on the actual three-dimensional geometries of depositional systems and are not simply artistic interpretations based solely on vertical facies successions in widely spaced outcrop sections. They represent reasonably accurate paleogeographic reconstructions

over several thousand square kilometers rather than idealized interpretations.

The precision in the resolution of the actual geometry of shorelines and other components of the depositional systems represented is a function of well control which, based on the number of wells actually correlated, averages about 1.5 wells per township. This allows the resolution of components on the order of about 50 square kilometers or about 7 kilometers. Although it is possible to delineate the overall geometry of depositional systems, the details of their components (e.g. tidal inlets, crevasse channels) may not be as clear, especially in off field areas where well control is generally not as good. Outcrop data is often more useful for interpretation and delineation at this scale of study (e.g. Miall, 1988; Duncan,1983).

I believe that interpretations based on detailed facies analysis in core are generally more convincing than studies based largely on well log facies. This study has documented similar well log patterns in rather different depositional systems, but without the supporting facies information from core it would not have been possible to delineate facies and depositional systems with the same degree of certainty as has been presented. Moslow and Pemberton (1988) document essentially similar coarsening upward funnel-shaped well log facies patterns in quite different depositional systems (deltaic versus shoreface) and point out the importance of detailed core work.

Lastly, in the absence of a detailed regional allostratigraphic framework, it would not have possible to delineate these depositional systems on a basin wide scale. Construction of such a framework is often a lot more difficult in outcrop studies, especially in older units where shales tend not to be as well exposed and where it is consequently often much more difficult to do detailed basin wide correlation (e.g. the Devonian Catskill Delta, Woodrow and Sevon, 1985). Plint and Hart (1988), in their outcrop study of the Dunvegan Formation, were able to document vertical facies associations and sedimentary cycles but did not have the control necessary to accurately correlate these cycles between exposures. Without the ability to correlate it is impossible to make paleogeographic maps except at a large (e.g. Formational) scale. Such large scale interpretations for the Dunvegan Formation have been presented by Stott (1982) and Burk (1963) but give no indication as to how individual depositional systems were deposited and give no clues as to the wide range of depositional environments, processes, and depositional systems documented within the Dunvegan Formation in this study. The Alberta subsurface is an ideal natural laboratory in which to conduct basin wide studies of depositional systems at every scale from detailed core analysis to major depositional sequences.

CHAPTER 12. EVOLUTION OF THE DUNVEGAN FORMATION

12-1. General Introduction

This chapter will consider the evolution of the Dunvegan Formation, integrating the information presented in previous chapters. It will consider changes through time in the types of facies and depositional systems up to the scale of changes in members and groups of members. The chapter will begin with a consideration of the relationships of the salient characteristics of members through time and will continue with a consideration of the mechanisms and processes by which these relationships arise. The chapter will conclude with a comparison of the Dunvegan and Cardium Formations in an attempt to determine which basin models are most appropriate in considering the evolution of the Dunvegan Formation.

12-2. Salient Descriptive Characteristics of the Dunvegan Formation

12-2-1. Evolution of Depositional Systems

Chapter 11 considered the spectrum of different depositional systems within the Dunvegan Formation but did not indicate how they changed or were related through time. This will be discussed below.

In general, the lower half of the Dunvegan Formation, including members G, F and E, are characterized by well developed deltaic depositional systems. The deltas within these lower members record a relatively modest increase in fluvial domination upwards, reaching a maximum in member E in shingles E1 and E2. The effects of basinal processes and especially storms (indicated mainly by HCS and type 1C Facies Associations) is most pronounced in members G and F. The oldest depositional system in member E (shingle E4) shows a considerably greater degree of basinal reworking (type 1A Facies Associations comprising bioturbated mudstones and HCS sandstones), although this may simply reflect the effects of the marine transgression that separates members F and E. The depositional systems within member E record a progressive increase in fluvial dominance upwards, culminating with the highly river dominated deltas in shingle E1 (Bigstone delta). During progradation of these depositional systems (i.e. shingles), sediment was supplied increasingly more rapidly than it could be re-distributed by basinal processes. The highest sedimentation rates within the Dunvegan Formation are indicated in the last shingles within member E. Diagnostic features of these high sedimentation rates include the abundance of soft sediment deformation features, climbing current ripples, and a lack of bioturbation and wave and storm produced sedimentary structures. Some of these features are also observed in member G and in

general, sedimentation rates are determined to be relatively high during deposition of all of the lower members.

This contrasts with shingles in the upper members, D, C, B, and A, which show a dramatic increase in the effects of basinal reworking. Depositional systems within member D show a progressive increase in the effects of basinal processes from storm influenced prograding shorelines in shingle D3 to storm and wave-dominated barrier islands and deltas in shingles D2 and D1 respectively. The abundant bioturbation, the predominance of wave and storm produced sedimentary structures, and the lack of soft sediment deformation features are diagnostic of lower sedimentation rates, certainly lower than in members G, F, and E. The thinner nature of these upper members also suggests that the rate of sediment accumulation was less than in members G, F, and E.

The thickness of sediment preserved between Em and T surfaces can be used as a measure of the relative energy of transgression. The greater the energy, the greater will be the likelihood of erosion and the more space will be available for the accumulation of transgressive deposits. In general, the effects of the seven transgressions that define the seven members within the Dunvegan Formation are least pronounced in the members with the highest sedimentation rates, and especially in member E. In the upper members, especially members D, C, and A, estuarine facies are more common. Transgressive sheet sands and bioturbated

sandy mudstones overlying Em surfaces are also thicker in members C, B, and A. Considerable transgressive erosional truncation is associated with the tops of members G and F, although thick transgressive deposits were not generally preserved.

In summary, the evolution of facies and depositional systems from member G through to member E records an overall decrease in the ability of basinal processes to re-work and re-distribute sediment through time. The predominance of deltaic depositional systems in the lower half of the Dunvegan Formation indicates that the effects of fluvial processes were relatively high. Members D, C, B, and A, in contrast, show a rather significant change in their facies signature and record a significant increase in the ability of basinal processes to re-work and re-distribute sediment. For the first time, barrier islands and wave-dominated deltas occur. The major transgressions show a greater influence on these upper members and result in estuarine facies within members D, C, and A, and widespread transgressive sheet sandstones in member C. The characteristics of the sediments suggests that these changes result from changes in the overall sedimentation rate. In general, the upper half of the Dunvegan Formation was characterized by lower sedimentation rates than the lower half.

12-2-2. Member Geometries; Wedges versus Pods

The overall cross sectional geometries of members within the Dunvegan Formation are illustrated in figure 12-1. This figure represents an "exploded stratigraphy" based on the regional dip-oriented well log cross section (Fig.3-9A). It combines several of the schematic dip cross sections shown for various members in chapters 4 to 10. The T-surfaces that define the top of each member have been turned into horizontal datums. The lower surfaces, which correspond to the tops of underlying members, reflect the cross sectional geometry of each member. These cross sectional geometries show some important differences and allow the classification of members according to their overall shape. Members G, B, and A show a pronounced wedge-shape while members F, E, D, and C are pod-shaped. The wedge-shaped members, and especially member G, thicken in a regular manner toward the northwest (landward). Members F, E, D, and C, in contrast, do not thicken regularly to the northwest and the area of maximum accumulation is confined within the map area. Like Brontosaurus, they are thin at one end, thicker in the middle, and thin at the other end. The thickest portions of the pods also tend to coincide with the thickest accumulations of sandstone. But how fundamental are these differences? The southeastern portions of all of the pods are wedge-shaped. If the map area did not extend as far to the northwest, many of the pods might also appear as wedges. The wedges within the map area (members G, B, and A)

Figure 12-1. Exploded Stratigraphy of the Dunvegan Formation based on the regional dip-orented cross section (Fig.3-9A,B). Member tops have been plotted as horizontal lines. The base of each member actually coincides with the top of each underlying member. See text for discussion.

EXPLODED REGIONAL DIP CROSS SECTION DUNVEGAN FORMATION

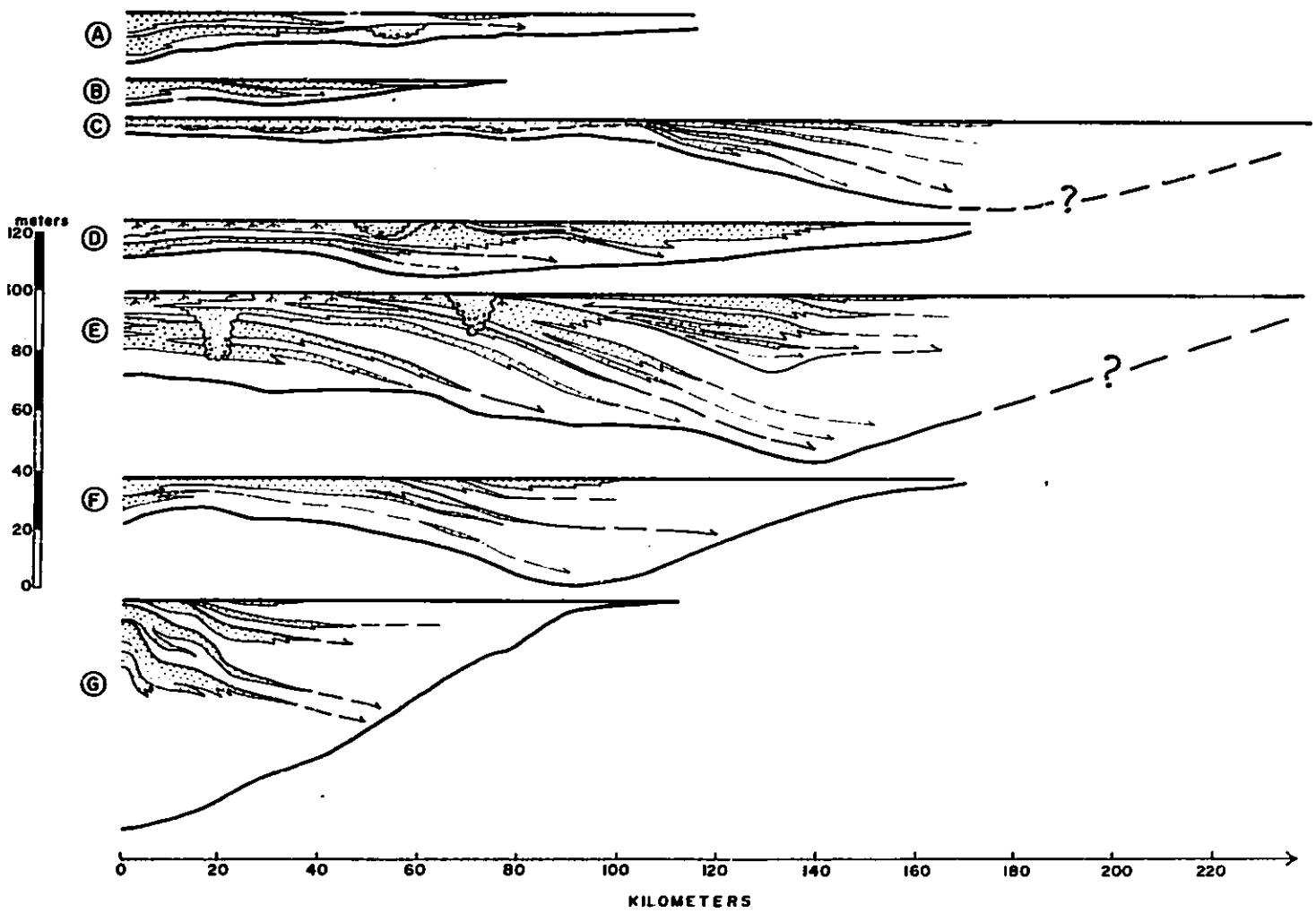

Figure 12-2. Axes of Major Accumulations of Members. Letters at the ends of the lines refer to the member, the number following refers to the contour interval (thickness in meters). Black triangles on the edges of lines A22, G40, B8, C hinge, and C30 point in the direction of thickening of a member. Dotted lines represent zero sandstone edges for members F and G. Arrows at the ends of lines indicate that the contour thickness persists past the limits of mapping. Dots at the ends of lines represent the limits of a particular contour thickness. See text for further discussion.

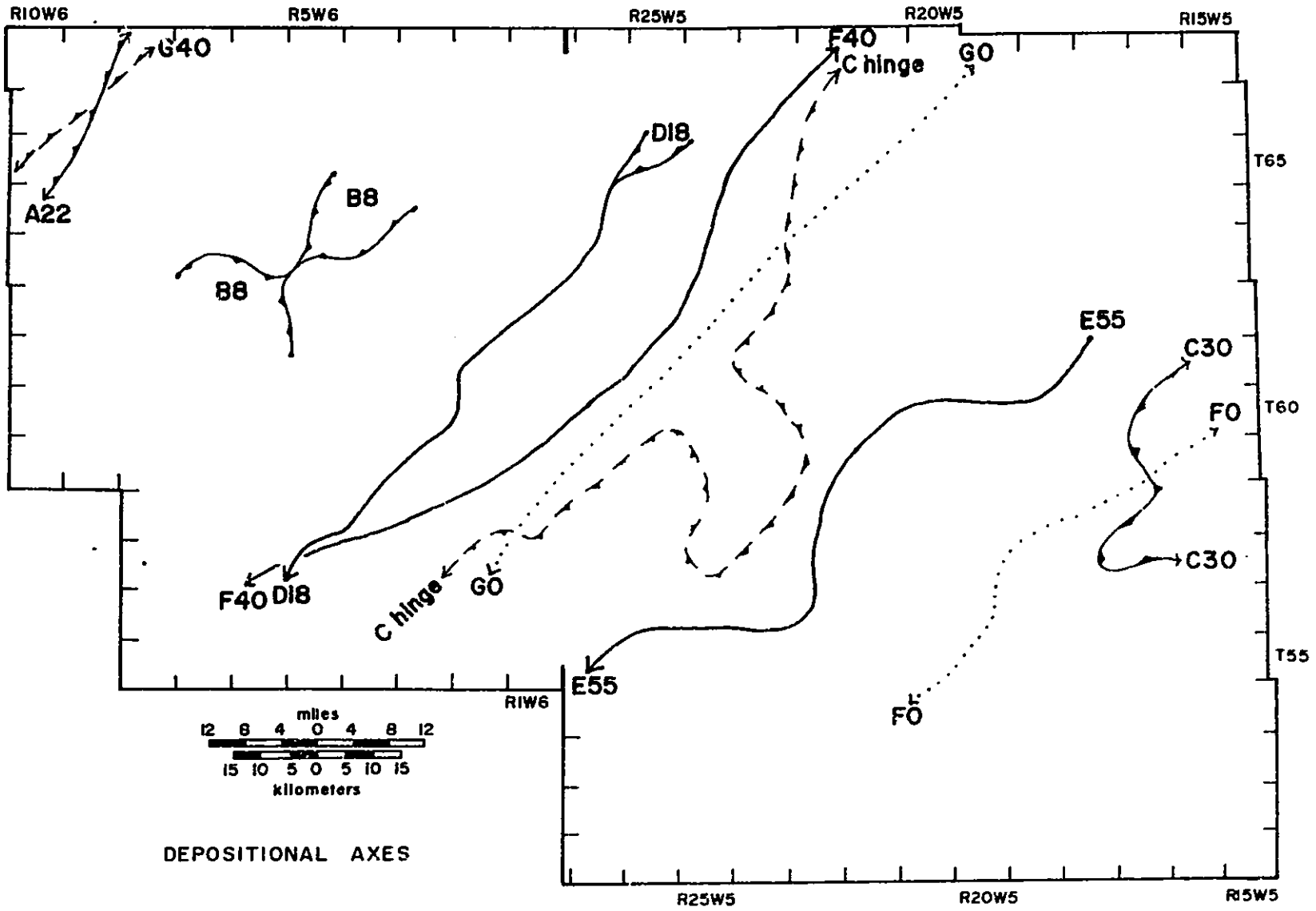

DEPOSITIONAL AXES

might represent the distal ends of larger pod-shaped accumulations which eventually thin to the northwest. The latter interpretation is considered more likely for the thinner upper members (A and B) than for member G, which is considerably thicker.

Figure 12-2, above, shows the axes of maximum accumulation of successive members within the Dunvegan Formation based on the individual member isopach maps presented in chapters 4 to 10. It shows that members, in general, are offset from each other with the position of the maximum accumulation of successive pod-shaped members appearing to coincide with areas of minimum accumulation in underlying members. This relationship is also seen on the exploded cross section (Fig.12-1), especially between the thicker members, G, F, E, and C.

12-2-3. Relationships of Shingles Within Members

The relationships between shingles varies from one member to another (Fig. 12-1). In member G, shingles show relatively modest offlap to the southeast but also show a tendency to aggrade or stack vertically. The degree of progradation of shingles within member G is therefore relatively low. This contrasts with the shingles in overlying members F, E, D, and C which show a much greater tendency to prograde. The distance between the landward and seaward limits of successive shingles within these upper members (defined by the position of toplap and downlap respectively) is greater than in member G. The shingles are more "spread out". Member A contains two shingles which, in contrast

to the underlying members, do not exhibit toplap toward the northwest. The two shingles are vertically stacked and neither thin in a landward direction. The seaward edge of sandstone in shingle A1 is interpreted as being landward of the seaward edge of the main sandstone in shingle A2. The significance of these differences will be discussed below.

12-3. Time-Stratigraphic Relationships: Wheeler Diagram of the Dunvegan Formation

The time-stratigraphic relationships of shingles and members can be shown using a Wheeler Diagram (Wheeler, 1958). This diagram (Fig.12-3) uses the physical stratigraphic relationships shown in figure 12-1 and combines these relationships with the time dimension. The purpose of this diagram is to give an indication of not only where but also when sediment was being deposited at any point in the basin along a down-dip (depositional) profile. This diagram highlights the parts of the basin where unconformities or hiatuses occur and gives an indication of their duration.

12-3-1. Estimating the Time Domain and Other Assumptions

In chapters 1 and 3, using published chronological data (paleontology and age dating, Obradovich and Cobban, 1975; Fouch et al.,1983; Haq et al., 1987), it was determined that the Dunvegan Formation was deposited over a time period of 1 to 2 million years. Given 19 shingles, a simple average suggests that each shingle was deposited in about 50,000 to 100,000 years. The

Figure 12-3. Wheeler Diagram of the Dunvegan Formation. Time is plotted on the vertical axis and the distance from the northwestern edge of the map area is plotted on the horizontal axis. There are 5 subaerial hiatuses (H) and several condensed sections (C.S.). The major transgression occurs at the end of deposition of member C.

The relative basinal downlap chart plots the relative basinward limit of sandstone with respect to time. It shows seven major regressive pulses separated by abrupt transgressions. This chart is compared with the third order eustatic sea-level curve of Haq et al. (1987). The major global transgression at 93.5Ma is correlated with the major transgression near the end of Dunvegan Deposition. The uncertainty in age dating results in several posible positions for the preceeding sea-level drop at 94Ma. The major regressive phase of the Dunvegan Formation (members C, D, and E) correspond to this global lowstand. See text for further explanation and discussion.

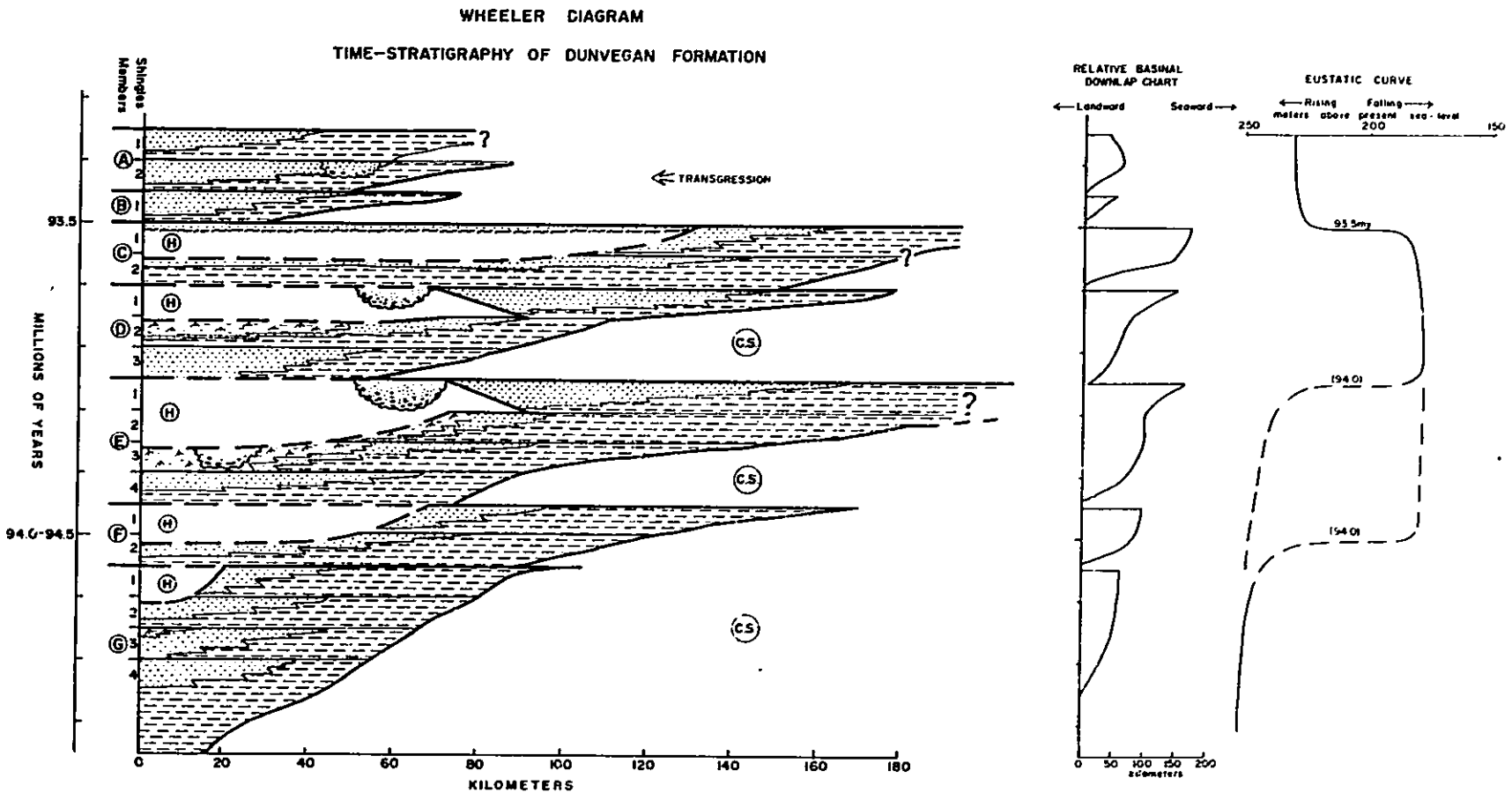
WHEELER DIAGRAM
TIME–STRATIGRAPHY OF DUNVEGAN FORMATION
Members
Shingles
MILLIONS OF YEARS
93.5
94.0-94.5
TRANSGRESSION
A
B
C
D
E
F
G
H
C.S.
0
20
40
60
80
100
120
140
160
180
KILOMETERS
RELATIVE BASINAL DOWNLAP CHART
Landward
Seaward
EUSTATIC CURVE
Rising
Falling
meters above present sea-level
250
200
150
93.5my
194.0)
194.0)
0
50
100
150
200
kilometers

upper and lower surfaces of each shingle are assumed to represent time lines and can therefore be drawn as horizontal lines on the Wheeler Diagram. It is also assumed, for the lack of any other information, that each shingle was deposited in a similar time period and these horizontal lines are therefore equally spaced. While the absolute time interval of increments may vary between 50,000 to 100,000 years, the diagram should nevertheless give an approximate indication of the relative duration of events (fig.12-3). The horizontal length of these lines corresponds to the physical limit of distribution of each shingle.

12-3-2. Wheeler Diagram

Figure 12-3 shows the time-stratigraphic relationships of the Dunvegan. Time, in millions of years, is plotted on the vertical axis while distance, measured from the northwestern or landward margin of the study area, is plotted on the horizontal axis. The stippled areas represent sandstones, the dashed areas marine shales and mudstones, and the root symbols non-marine facies. The open areas indicate the lateral extent and duration of hiatuses (H) and condensed sections (C.S.).

The members and their component shingles are labelled along the left column. Shingle boundaries are drawn with a medium line while member boundaries are drawn with a heavy black line.

Member G

The four sandstones within member G essentially stack on top of each other, resulting in an aggradational shingle stacking pattern. The related shales show a greater degree of progradation and successive shingles lie progressively farther into the basin from about 20 to 100 kilometers. A great deal of the basin (from about 20 km to the edge of the cross section) was sediment starved for a considerable time period. The time of non-deposition increased from between about 50,000 to 100,000 years in the northwest to between 300,000 to 600,000 years in the southeast. This results in a prominent condensed section (the FSU marker). The envelope enclosed by the thick dashed lines at the far right of the diagram indicates a hiatus of between about 60,000 to 120,000 years. This hiatus may have formed in two possible ways.

Firstly, sediment in shingle G1 may have been deposited there at one time and may have been removed by erosion. This erosion may have been subaerial in nature, in which case it should be associated with fluvial channels or valleys, or it may have been submarine in nature, in which case it should be related to the transgressive event which separates members G and F.

Alternately, this envelope may represent a time of subaerial exposure, rather than erosion, correlated with a depositional toplap surface produced during the progradation of shingle G1. The sandstone in shingle G1 does not show a basinward shift and is not associated with fluvial channels. The upper surface of member

G also does not show any evidence of subaerial exposure. As suggested in chapter 10, therefore, submarine erosion produced during the transgression between members G and F was probably responsible for producing this hiatus.

Member F

Widespread shale separates the top of member G from the base of member F. The transgression responsible for deposition of this shale is indicated by a 10 kilometer landward backstep in the basinward limit of shales in the lower portion of shingle F2. This shingle, however, rapidly progrades into the basin. The basinward limit of sandstone in shingle F2 indicates a basinward shift of about 30 kilometers with respect to the zero edge of sandstone in shingle G1. The equivalent shaly portion of shingle F2 shows a similar basinward shift. Sandstone within the next shingle (F1) shows a rather modest shift of 15 kilometers into the basin while the laterally equivalent shales show an additional 50 kilometers of progradation (from 120 km to 170 km). This results in a progradational set of shingles in contrast to the essentially aggradational set in member G.

A hiatal envelope of between about 60,000 to 100,000 years, similar to the one at the top of member G, occurs at the far right of the cross section. In chapter 9 it was suggested that transgressive erosional truncation of member F probably occurred in a landward direction and may account for this break.

Member E

The transgression which separates member F and E is indicated by a 90 kilometer landward backstep in the basinward position of the lowest shale in shingle E4. Sandstone in shingle E4 also experiences a landward backstep of about 30 kilometers with respect to the basinward edge of the uppermost sandstone in shingle F1. The next successive shingles in member E progressively step out into the basin forming a rapidly prograding set of shingles. The distal edge of the last sandstone in member E lies about 70 kilometers from the basinward edge of the last sandstone in the underlying member F, and about 165 kilometers from the northwestern margin of the study area. The basinward limits of shale deposition in shingles E1 and E2 have not been determined but indicate deposition over 180 kilometers from the northwestern margin for the first time in at least 500,000 years. Also for the first time, significant subaerial erosion and exposure (indicated by fluvial channels, paleosols, and other non-marine facies) occurs in the northwest, lasting for a time period of between 100,00 to 200,000 years. This subaerial hiatus corresponds to the progressive basinward deposition of shingles E4, E3, E2, and E1. Sandstones in shingle E1 show about 20 kilometers of progressive landward onlap during the last 50,000 to 100,000 years of deposition of member E.

Member D

Sandstones within the lowest shingle in member D indicate another abrupt landward backstep of nearly 100 kilometers. This represents the marine transgression which separates members D and E. Some marine reworking of the uppermost sediments in member E was noted in association with this transgression. The landward limit of this transgression, unlike those separating the other members, is within the limits of the study area and lies at about 20 kilometers from the northwestern edge.

The shingles within member D progressively step out to the southeast and indicate another prograding set. Sandstones in shingle D1 reach a maximum basinward limit of about 150 kilometers, which is about 15 kilometers less than sandstones in member E. A relatively modest subaerially produced hiatus, of between about 50,000 to 100,000 years, is once again indicated by non-marine facies to the northwest and correlates with a rather abrupt basinward shift of sandy depositional systems in shingle D1. The last stages of deposition of shingle D1 involve landward onlap of about 20 kilometers accompanied by estuarine infilling of subaerially cut channels to the northwest during the initial phases of transgression.

Member C

The transgression which separates members C and D is marked by a relatively small landward backstep of about 20 kilometers in the basinward position of the first shale in member C. Sandstones

within the two shingles in member C also comprise a prograding set and reach a maximum seaward limit of about 170 kilometers. The maximum basinward limit of shale in member C has not been determined. The northwestern hiatus is largely the result of the next marine transgression which deposits a widespread transgressive sand sheet. Part of this hiatus may result from earlier subaerial exposure and erosion, as indicated by the preserved remnants of older channel deposits associated with the progradational phase of member C.

Members B and A

Member C is abruptly followed by a major transgression of at least 120 kilometers as indicated by the abrupt landward backstep of the distal edge of the main sandstone in member B.

Finally, the two shingles within member A indicate a progressive landward shift of about 15 kilometers and comprise the only retrogradational shingle set observed within members of the Dunvegan Formation.

12-3-3. Relative Basinal Downlap Chart

It was pointed out in chapter 1 that the science of sequence stratigraphy arose from the science of seismic stratigraphy developed in the 1970's (Payton,1977). The basic approach used to interpret sedimentary sequences in the context of sequence stratigraphy is the recognition of changes in coastal onlap patterns. On passive continental margins, this approach is the most useful since the basin margin against which sediments onlap

(i.e. the landward margin) is nearly always preserved and available for study (Fig.12-4B). In a foreland basin, however, the opposite is true and studies of coastal onlap patterns are often not possible. The landward margin of a foreland basin, such as the West Alberta Basin, is nearly always destroyed, or at least highly deformed, by subsequent tectonic uplift and deformation (Fig.12-4A). In addition, even when portions of the landward margin of a foreland basin are preserved, the infilling sediments often comprise thick non-marine facies in which recognition of depositional surfaces, let alone onlap patterns, is usually impossible.

The portion of a foreland basin most easily studied is the distal end which often comprises marine lithofacies. In the absence of coastal onlap patterns, therefore, the analytic approach most easily applied is the determination of the position of relative basinal downlap based on the distal limits of sandstones into the basin (i.e. seaward). I have used the Wheeler Diagram as the basis for constructing a relative basinal downlap chart for the Dunvegan Formation (12-3).

It was shown in chapters 4 to 10, and in figure 12-1, that shingles within members downlap towards the southeast onto underlying T-surfaces. The relative points at which shingles downlap onto a T-surface can be approximated by plotting the position of the distal, zero edges of sandstones within shingles and can be taken directly from the Wheeler diagram. This chart is

also plotted on figure 12-3. Time is plotted on the vertical axis and distance from the northwestern edge of the map area is plotted on the horizontal axis. The downlap chart emphasizes the depositional history of members within the Dunvegan Formation. The seven regressive episodes are indicated, each punctuated by a major marine transgression. The landward limit of transgression is only known between member E and member D, because it is confined within the study area, and suggests a virtually instantaneous shoreline displacement of about 150 kilometers.

This chart can potentially be used to compare depositional sequences in the Dunvegan Formation with other Cenomanian units, either within the Cretaceous Western Interior Seaway or with other within Cenomanian basins described elsewhere. This relative basinal downlap chart is similar to the coastal onlap chart of Vail and Todd (1984) and it is the equivalent of the 'condensed intervals' portion of their charts (Vail and Todd, 1984 figure 2). Vail et al. (in press) point out, however, that the basinward limit of progradation (defined by the limits of basinal downlap) is a function of sediment supply and basin margin geometry implying that interpretations of relative changes in sea-level using data from this portion of the basin must be used with caution. Nevertheless, in a foreland basin, this is all that we have.

Figure 12-4. Foreland Basins versus Passive Margin Basins. S.L. - Sea Level, A. In foreland basins, rapid asymmetric subsidence produces wedge-shaped sedimentary packages (W). During times of relative tectonic quiescence, pod-shaped sedimentary packages (P) are deposited. In foreland basins the landward margin adjacent to the actively rising mountain front subsides more rapidly and the hinge zone is towards the sea. The portion of the basin closest to the actively rising mountain front is often not preserved and it is often destroyed by later tectonic events. B. In passive margin basins, the hinge zone is towards the land and the most active subsidence is in a seaward direction. The landward margin is usually preserved and onlap relationships are usually easily documented. See text for further explanation and discussion.

A. Foreland Basin

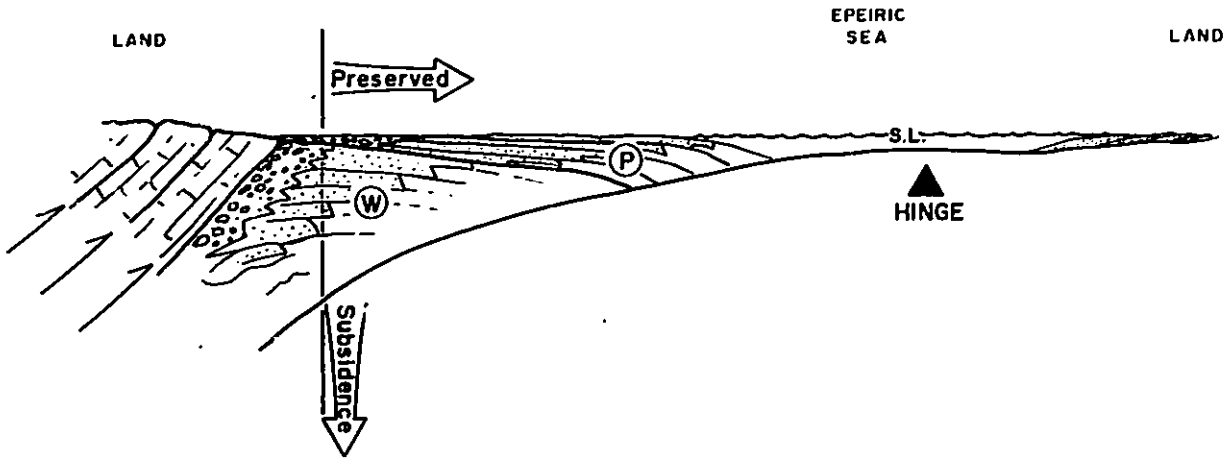

B. Passive Margin

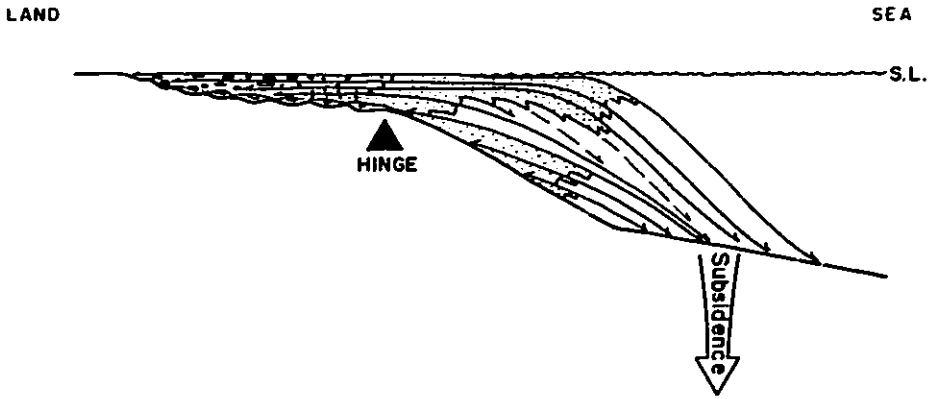

12-4. Controls on Deposition

12-4-1. Introduction, Accommodation versus Accumulation

Several important parameters may potentially affect depositional patterns and cyclicity. The main ones to consider will include changes in basin subsidence or basin uplift, changes in sea-level, changes in sedimentation rate, climatic changes, and changes in the overall basinal energy (e.g. tides, storms, waves). The terms accommodation and accumulation (Jervey, in press) are non-genetic terms that are useful in describing and interpreting the relationships of the various depositional units within the Dunvegan Formation.

Changes in basin subsidence, basin uplift, or sea-level can be lumped together into the term accommodation which is defined as the physical space available for potential sediment infilling (Jervey, in press). Accommodation may represent old space not filled by underlying depositional units or new space created after older units have been deposited.

Accumulation is defined as the sediment that actually infills the accommodation and is primarily a function of the sedimentation rate. If the sedimentation rate is less than the accommodation rate, the basin will be underfilled (Tankard, 1986a). If the sedimentation rate is greater than the accommodation rate, sediment will quickly accumulate and fill the basin. Progradation, sedimentary bypass, and erosional unconformities will be more likely. The presence of non-marine

facies (such as in members D and E) are a useful indicator that accumulation is equal to or greater than accommodation.

The Dunvegan reaches a maximum thickness of about 300 meters in outcrop indicating an average landward accumulation rate of between about 0.15 to 0.3 m/1000 years, depending on the overall time of deposition. Given the presence of non-marine facies in most of the members, this probably indicates an accommodation rate of about the same. This accommodation rate will clearly decrease into the basin (see discussion below).

12-4-2. Subsidence and Accommodation: Wedges versus Pods

It has been firmly established (Beaumont,1981) that the West Alberta Basin, into which sediments of the Dunvegan were deposited, was a foreland basin. Foreland basins are characterized by rapid subsidence due to loading of the crust by thrusting (Beaumont, 1981; Jordan,1981) (Fig.12-4). This subsidence decreases away from the zone of thrusting towards a hinge zone characterized by relatively little movement. In the West Alberta basin, this hinge zone, which is defined by the flexural wavelength of the crust, probably lay 50 to 100 kilometers away from the Cordilleran mountain front towards the Saskatchewan border (Jordan, 1981; Beaumont, 1981). The area immediately adjacent to the zone of thrusting (the western margin of the Alberta basin) is characterized by rapid subsidence which diminishes toward the east. The zone of thrusting itself will also be an area of uplift and will act as the source of the sedi-

ment which is supplied to the adjacent subsiding trough. The area of greatest accommodation will therefore lie towards the source area. This is in direct contrast to passive continental margins in which the area of greatest subsidence is usually away from the source area, or the landward margin, and toward the sea (Fig.12-4). As long as accumulation is able to keep up with accommodation then the shape of any sedimentary basin should be approximated by the shape of the sedimentary packages it contains. In a foreland basin, therefore, wedge-shaped units should indicate foreland-type subsidence. Initiation of subsidence induced by loading may be marked by an abrupt deepening of facies in the basin (Beaumont pers.comm, Jordan et al., 1988).

The overall geometry of the Dunvegan Formation is that of a large wedge and the Dunvegan as a whole therefore indicates that it filled a basin largely characterized by foreland-type subsidence. To the far northwest, outside of the thesis area, the Dunvegan reaches 300m in thickness and is dominated by non-marine, alluvial facies containing thick conglomerates (Stott, 1982). The FSU marker horizon may correlate with initiation of foreland-type subsidence followed by the deposition of member G which is also strongly wedge-shaped. Accommodation during deposition of member G was largely confined to the northwest. The presence of vertically stacked shorelines (and buried non-marine facies) within member G suggests that new accommodation was being created

while member G was being deposited and also that accumulation was able to keep up with this accommodation.

The geometry of the pod-shaped members (F,E,D, and C) is more problematic since it indicates a depositional setting where accommodation is not highest towards the mountain front, a situation more common on passive continental margins (Fig.12-4A,B). As shown in figure 12-2, the shape and position of successive pods appears to be controlled by the position of underlying members. The thinner shalier portions of members usually lie at their southeastern margins. This results both from general depositional thinning towards the southeast as well as greater compaction in the distal (pro-delta or shelf) mudstones. Most of the basinward accommodation in members F, E, D, and C is therefore thought to represent old space, unfilled during deposition of underlying members. Some of the accommodation to the northwest, especially where non-marine facies are preserved, probably represents new space and may relate to the creation of the immediately underlying T-surfaces. Accumulation rates in the pod-shaped members probably outstripped accommodation rates and accounts for the rapidly progradational style of shingles within these members. The prominent depositional break in member C (Fig.6-2) is therefore interpreted to be the result of infilling of old space, unfilled by deposition of underlying members, and perhaps related to a time of peak regression.

Members B and A, like member G, are also wedge-shaped, but are also considerably thinner. In section 12-2-2 it was suggested that these members may represent the distal end of pod-shaped units to the northwest, in which case accommodation will have been created in like manner to members E, D, and C.

The Dunvegan Formation therefore fills an initially large accommodation space of 80 meters in the far northwest (maximum thickness of member G) in a time period of probably between about 300,000 to 600,000 years. The total combined new accommodation filled by the subsequent members, in the northwest, represents filling of about 80 meters in a time period of between about 700,000 to 1,400,000 years. This represents a reduction of over 50% in the accommodation rates between the lower and upper members.

12-4-3. Sedimentation Rate

Changes in sedimentation rate may be produced by a number of processes, the main ones being changes in relative relief and climate changes. In section 12-2-1 above, it was suggested that the depositional systems in the Dunvegan Formation indicate a relatively modest increase in sedimentation rate from member G to member E followed rather abruptly by considerably lower sedimentation rates in the upper members.

Somewhat similar changes in the overall characteristics of depositional systems within thick clastic wedges have been documented by Galloway (1975), and Fisher and McGowen (1967). In

the Lower Eocene Wilcox Group of Texas, Fisher and McGowen showed a change from river-dominated depositional systems at the base to more wave-dominated systems towards the top. They interpreted such changes as being intrinsic to large-scale deltaic depositional systems. As hinterlands erode and the basin fills, sediment supply gradually decreases and the relative importance of basinal processes will increase simply as a function of decreasing sediment supply (i.e., decreasing fluvial influence). Such a simplistic interpretation does not fit observations in the Dunvegan very well. It does not account for the initial increase in sedimentation rate from member G to member E, and fails to account for the presence of the seven T-surfaces.

12-4-4. Eustasy: Comparison with Global Sea Level Curves

Haq et al. (1987) have published third order global sea-level charts for the Cretaceous. Figure 1-6 shows these sea-level curves plotted against known Cretaceous stratigraphy, including sediments of the Dunvegan Formation. During the mid-Cenomanian, at about 94Ma, the curve indicates a major rapid global drop in sea-level of about 75. This eustatic fall was followed by a lowstand of sea-level that lasted for about 500,000 years and which was followed by a geologically instantaneous sea-level rise of about 50 meters at 93.5 Ma. This rise was followed by a highstand which lasted for most of the rest of the Cenomanian. The curve therefore indicates one rapid fall and one rapid rise in sea-level during the time period in which the Dunvegan is thought

to have been deposited. Weimer (1984, Table 2, p.25), working in the Cretaceous Western Interior of the United States also indicates a drop in sea-level at about 95 my (during the end of the lower Cenomanian). His figures indicate that this drop in sea level was also followed by a lowstand which lasted for about a few hundred thousand to half a million years and was in turn followed by a rise in sea-level which lasted for the duration of the Cenomanian. According to the principles of sequence stratigraphy (Posamentier and Vail, in press), this fall in sea-level should produce an unconformity or sequence boundary within the Dunvegan. This should be followed by lowstand deposits and at least one major transgression.

The major transgression observed within the sediments of the Dunvegan Formation occurs between members C and B and is indicated by the large landward backstep of about 120 kilometers. This transgression is tentatively correlated with the major eustatic sea level rise indicated on the Haq et al. (1987) curves at 93.5 Ma. This correlation provides a tie point and allows comparison of the Cenomanian eustatic sea-level curve with the Dunvegan time-stratigraphy (Fig.12-3). Comparison of the two curves suggests some interesting possibilities and allows an estimation of the effects of the global eustatic changes. The 500,000 year lowstand of sea level correlates in timing and duration with the upper members C, D, E, and possibly also member F.

In section 12-4-2 above it was suggested that the thicker portions of pod-shaped members largely infilled old accommodation space to the southeast. The amount of new accommodation in pod shaped members, however, can be estimated from the amount of preserved sediment in the northwestern portion of the map area. In the northwest, between 20 and 65 meters of new accommodation space was infilled during the global lowstand period. If sea-level dropped by 75 meters during this time (as predicted by the curve) then it implies that the basin actually subsided between 95 to 130 meters (compaction not taken into account). This gives an overall subsidence rate of between about 0.19 to 0.26 m/1000 years but a net accommodation rate of half this amount (0.04 to 0.12 m/1000 years). In other words, the global fall in sea level attenuates the effects of basin subsidence.

Member G, and possibly member F and the lowermost shingles in member E, correlate with a general highstand of sea-level in which no change of sea-level occurs. The accommodation rate can therefore be interpreted to approximate the overall rate of basin subsidence, which (assuming sediments build up to the water surface) is approximated by the thickness. In section 12-4-2 it was shown that 80 to 120 meters of accumulation took place during the 300,000 to 600,000 years it took to deposit these members respectively. If it is assumed that the rate of sedimentary accumulation was able to keep up with the accommodation rate, and if sea-level changes and compaction terms are neglected then this

gives an overall basin subsidence rate of between about 0.20 to 0.27m/1000 years. These are practically the same as the subsidence rates calculated for the sediment deposited during the lowstand above and may indicate a relatively constant average subsidence rate for the Dunvegan of 0.19 to 0.27 m/1000 years, although as discussed below, the instantaneous subsidence rate may be quite different.

The sea-level fall at 94 my does not produce a major basin-wide subaerial unconformity. Rather, this eustatic fall in sea-level results in an overall drop in the accommodation rate resulting in widespread progradation of the upper members especially E, D, and C. It appears that the effects of the 94 Ma sea-level drop, while manifest, are somewhat diminished. Rather than producing an abrupt basinward shift in the relative position of basinal downlap, the sea-level fall is recorded by the relatively gradual migration of shallow marine depositional systems into the basin. It also appears that over the duration of deposition of the Dunvegan Formation, no overall change in the average rate of basin subsidence occurs. It would seem that the transition upwards from wedges to pods is largely controlled by the overprint of a eustatic fall in sea-level over an evenly subsiding basin. This caused a drop in the rate of accommodation towards the northwest portion of the basin resulting in a relative lowering of sea-level.

12-5. Origin of T-surfaces, Members, and Shingles

12-5-1. Autocyclic versus Allocyclic Mechanisms

In chapter 3 it was shown that the seven member-bounding T-surfaces were regional in nature and were therefore probably controlled by large scale, basin-wide or allocyclic mechanisms. Beerbower (1964) distinguished between autocyclic and allocyclic mechanisms and Miall (1984b, p.178) has succinctly outlined these differences:

> *"Autocyclic mechanisms are those which result in the natural redistribution of energy within a depositional system. Examples include the meandering of a channel in a river, tidal creek or submarine fan, subaerial flood events, subaqueous sediment gravity flows, channel switching on a subaerial or submarine fan or a delta (avulsion), storms and tidal ebb and flood. All of these potentially can produce cyclic sequences. Allocyclic mechanisms are those in which change in the sedimentary system is generated by some external cause. Tectonic control of basin subsidence, sediment supply and paleoslope tilt, eustatic sea level change and climate change are the principal types of allocyclic mechanism. These are large scale basinal sedimentary controls..."*

In a sedimentary basin, allocyclic depositional units should be regionally persistent and should correlate over the entire basin. Autocyclic depositional units, in contrast, will be regionally impersistent and will correlate over only a restricted portion of the basin under study.

Shingles are interpreted as autocyclic depositional units. In chapters 4 to 10 it was shown that shingles are regionally impersistent units. Mapping of sandstones in individual shingles shows that they comprise shallow marine, largely deltaic

depositional systems and that these deltaic depositional systems were offset from each other in both a lateral and down dip direction. Transitions between shingles were documented as representing shifts in the locus of deposition of depositional systems. The cycle of deposition represented by one single is comparable to the delta cycle of Barrell (1912) and Scruton (1960). Shingles can therefore be interpreted as autocyclic depositional units. In deltaic depositional systems (such as in member E), transitions between shingles are probably due to delta switching produced as major rivers avulsed. These shingles therefore represent relatively high frequency events produced as a function of the natural redistribution of energy within these depositional systems.

The distinction of erosional surfaces formed by autocyclic processes from those formed by allocyclic processes is a crucial one. The erosional surfaces underlying shingles E1 and D1 are interpreted tc result from the natural infilling of the foreland basin and result from sediment supply outstripping accommodation. They are not interpreted as relating to widespread sudden relative drops in sea-level. Some of the shingle bounding discontinuities resemble the unconformities and sequence boundaries of Posamentier and Vail (in press) and it might be easy to confuse them. The erosional surfaces associated with shingles are limited in extent, however, and do not have the same regional significance as Vail-type unconformities.

12-5-2. Origin of Members and Their Bounding Discontinuities (T-Surfaces)

Members, in contrast to shingles, are more regionally widespread and their bounding discontinuities (T-surfaces) can be traced for over a hundreds kilometers. This suggests that T-surfaces are controlled by allocyclic mechanisms. They approximate, in duration, the fourth order cycles of Vail et al. (1977). Several mechanisms may be responsible for producing cyclicity on the scale of a couple of hundred thousand years. These include;

1. Tectono-Eustasy,
2. Glacio-Eustasy,
3. Climatic Changes related to the Earth's Orbit (Milankovitch hypothesis),
4. Local Tectonic Effects (uplift and subsidence).

A. Tectono-Eustatic Changes

Tectono-eustatic sea-level changes are thought to be produced by changes in mid-ocean ridge volume as a result of variations in the rate of sea-floor spreading (Donovan & Jones, 1979; Pitman, 1978; Hallam,1983). These changes produce cyclicity on the scale of 10-30 million years (2nd order cycles) (Donovan & Jones,1979). These time periods are too long by several orders of magnitude to account for the fourth order cycles observed within this study.

B. Glacio-Eustatic Changes

Glacio-eustatic sea level changes, which are closely tied to changes in the earth's climate (see next section), occur on time scales of a few tens to a few hundred thousand years (Hays et al., 1976). These time scales correspond in duration to shingles and members respectively within the Dunvegan Formation. Matthews (1984a, p.429-448; 1984b) reviews the evidence for glacio-eustatic changes in the Cretaceous, including physical evidence of Cretaceous sedimentary deposits. Based both on oxygen isotope data and on the lack of documented Cretaceous glacial deposits, he concludes that the earth experienced an ice-free period during the mid-Cretaceous at about 100 million years ago (Albian) followed by progressive ice buildup at 65, 60, 50, and 38 million years ago. From his data it can be inferred that glacio-eustatic inter-regional unconformities were probably not significant until the Tertiary. Frakes and Francis (1988), in a more recent paper, discuss the presence of interpreted ice-rafted material in offshore mudstone facies within several Mesozoic basins around the world, including Cretaceous basins in Australia. These basins are all shown to have existed at very high, polar latitudes during these times. Frakes and Francis (1988) conclude that a totally ice-free world probably never existed and that there was probably always some ice in polar regions, even during the Cretaceous. Neither their data nor anyone else's, however, provides evidence for widespread ice-sheets during the Cretaceous, or evidence of

direct ice-contact deposits (e.g. tills). Scattered ice-rafted material may have been derived from winter shelf ice carrying material from adjacent shorelines. This ice may have been derived from relatively small mountain glaciers but do not imply the existence of major ice-sheets, such as existed during the Pleistocene. The volumes of ice required to affect sea-level do not appear to have existed during the Cretaceous, even if this time period was not totally ice-free.

In conclusion, while the inferred perodicities of shingle and member cyclicity are similar to those of glacio-eustatic changes, the lack of direct evidence for widespread Cretaceous glaciations makes it difficult to reasonably invoke this as a mechanism.

C. Climate Changes

Climate changes result from two main processes, large scale plate tectonic reorientations, and changes in extraterrestrial body patterns which alter the gravitational field affecting the earth and which, in turn, cause orbital variation (Milankovitch theory). As described above, changes in plate geometry probably occur at rates which are too slow to produce cyclicity on the scale of a few hundred thousand years or less. The Milankovitch theory supports an extraterrestrial origin for global climatic cycles at time scales from tens to hundreds of thousands of years. Berger et al. (1984, p.ix) have summarized the essence of the Milankovitch theory. They state that;

"...the major fluctuations in global climate associated with the ice-age cycles are caused by variations in the pattern of incoming solar radiation - variations that are, in turn, caused by slow changes in the geometry of the earth's orbit that occur in response to predictable changes in the gravitational field experienced by the Earth."

Calculations (Berger, 1984) for the Pleistocene and Recent show that Milankovitch perodicities occur at 400, 100, 41, 23 & 19 kyr, although these values are highly uncertain more than 5 million years ago. Fischer & Schwarzacher (1984) demonstrate 100,000 and 40,000 year cycles in Cenomanian limestones of the Italian Apennines and, by analogy with the modern, they suggest control by Milankovitch cycles.

Shingles and Members within the Dunvegan show cyclicity which is similar to these time scales and (given the errors and uncertainty in timing of cycles) it is tempting to suggest that Milankovitch type cyclicity may be responsible. Climate changes resulting from Milankovitch cyclicity are chiefly related to continental glaciations. Unfortunately, it is not certain how Milankovitch cycles would affect global climatic patterns in the absence of major ice-sheets. Broad changes in aridity would probably affect sedimentation rate but such changes should be indicated by evidence of alternating arid and humid environments. Not only were such changes not noted in sediments of the Dunvegan Formation, but it is not clear how these changes would create abrupt changes in the sedimentary environment (e.g. T-surfaces). Climatic changes would therefore seem an unlikely mechanism to

produce either fourth order cycles (members) or fifth order cycles (shingles) observed within the Dunvegan Formation.

D. Local Tectonics

The depositional setting of the Dunvegan Formation, in a foreland basin with an active orogenic belt to the west, suggests that local tectonic changes were the most likely mechanism that produced the member bounding discontinuities. Precise models of how cycles at the scale of several hundred thousand years or less can be produced have not been developed, although the models of Beaumont (1981) Beaumont et al. (1988) and Cloetingh (1988) are beginning to consider more explicitly relatively short term changes.

The time averaged subsidence rates calculated for the Dunvegan Formation of between 0.19 to 0.26 m/1000 years are similar to time averaged rates for various modern and ancient foreland basins around the world (Allen and Homewood, 1986; Faill,1985). It is emphasized, however, that the time averaged rate may not give an indication of the instantaneous rate of subsidence, which may be considerably higher.

Many workers (Beaumont, 1981; Jameison and Beaumont,1988; Paola, 1988; Lundberg and Dorsey, 1988; Jordan et al.,1988; Burbank and Raynolds,1988; Kominz and Bond,1986; Ricci-Lucchi,1986) have suggested that subsidence in foreland basins is not continuous. Jameison and Beaumont (1988 p.440) state that

"it is therefore entirely possible, if not likely, that important orogenic episodes proceed in relatively short pulses", at time scales of 5 million years or less. Blatt et al. (1980 p.30-32) review rates of subsidence and accumulation in various worldwide basins. They suggest that rates of 1m/1000 years are rarely exceeded but indicate that local rates of up to 11m/1000 years are known. Lundberg and Dorsey (1988) indicate that the Western Taiwan foreland basin experienced a change in accumulation rate (which can be assumed to be similar to rates of basin subsidence) during collision from 0.15m/1000 years to 3m/1000 years. Their data show that these changes can occur on time scales of a million years or less and begin to approach the time scales observed at the member scale in the Dunvegan (several hundred thousand years). It may be possible that the seven transgressions in the Dunvegan Formation record the initiation of separate foreland thrusting events. These thrusting events would produce rapid subsidence which would in turn cause the abrupt back step of depositional environments producing a T-surface. This would be followed by quiescence and later sedimentary infilling of the newly created accommodation space. Studies on the isostatic effects of crustal rebound during deglaciation indicate that the crust responds on time scales of 1000 to 10,000 years (Turcotte and Schubert, 1982, p.244-248). Based on these data, Jordan et al. (1988) suggest that the response to thrusting events on time scales of 100,000 to 1,000,000 years will be geologically instantaneous. The

allostratigraphy of the Dunvegan may therefore relate to high frequency tectonic thrusting events superimposed on a third order eustatic change in sea-level.

Cloetingh (1986, 1988) has suggested that relatively short term fluctuations in relative sea-level can be produced by relatively modest changes in intraplate stresses, on the order of a few kilobars of pressure. His calculations suggest that changes in basin uplift and subsidence, produced by this mechanism (reflected as an apparent sea level change), could cause accommodation changes on the scale of about 0.01 to 0.1m/1000 years. These changes are a little slower than those observed in the Dunvegan Formation. In the context of the Western Cordillera, these stress changes may have been produced by episodic changes in the rate of foreland thrusting or perhaps by changes in the docking patterns of accreted outboard terrains. These mechanisms are particularly useful in helping to explain differential changes in intrabasinal subsidence. Several other authors have documented similar rapid movements of the Western North American Foreland Basin.

Arnott (1988) suggests that changes in intrabasinal subsidence, related to movement of the Sweetgrass Arch, may have been responsible for five transgressive-regressive cycles in the Late Albian to Early Cenomanian Bootlegger Member in north-central Montana. The Bootlegger was deposited in a time period of about 2 million years suggesting that each sedimentary cycle was deposited

over about 400,000 years. Arnott (1988) shows that these sedimentary packages show differing thinning and thickening relationships towards the Sweetgrass Arch and concludes that these cycles are related to episodic uplift and downwarping of the Sweetgrass Arch, the crest of which lies in his study area. Arnott (1988) interprets these movements as resulting from Cordilleran tectonism. Although he does not go further in his interpretation, a Cloetingh-like mechanism seems possible.

In the Dunvegan it is possible that the geometry of pod-shaped members might be controlled by differences in intrabasinal subsidence resulting from chnges in intra-plate stresses related to Cordilleran tectonism. The relationships of pod-shaped members to underlying units, however, indicates that they are related to the infilling of old accommodation space as a result of differences in the relative degree of compaction. This suggests that a Cloetingh-like mechanism does not operate.

12-6. Comparison With Other Cretaceous Clastic Units

12-6-1. The Cardium and the Dunvegan

During many conversations with members of the McMaster Research Group, I have been asked why the Dunvegan Formation is so different from the Cardium Formation. As will be shown below, comparison of the Cardium and Dunvegan reveals important differences that may be useful in contributing to an understanding of the mechanics of sediment transport in foreland basins and in modelling the response of sedimentary infilling to changes in

tectonic style. The Cardium has been thoroughly studied and as a result is presently relatively well understood. There have been many papers which have dealt with various aspects of the Cardium Formation; the principal and most recent ones include Walker and Eyles (1988), Bergman and Walker (1986, 1988), Plint and Walker (1987), Plint et al. (1986, 1988), and Duke (1985a). The important ideas stemming from these publications are summarized below.

The Late Turonian Cardium Formation is a coarse clastic sedimentary unit which was deposited 3 to 4 million years after the Dunvegan Formation. The Cardium Formation is much more areally extensive than the Dunvegan Formation, and is relatively uniform in thickness. It rarely exceeds about 100 meters in outcrop or in the subsurface, and its overall geometry is that of a broad relatively thick sheet. It comprises six major sedimentary sequences which consist of highly wave- and storm-dominated prograding strand-plain deposits cut by several conglomeratic lowstand shoreface deposits, along with associated shelf deposits. These shorefaces comprise pod-shaped to linear chert conglomerates up to 18 m thick (e.g. Carrot Creek Member, Bergman and Walker, 1986). These conglomeratic shorefaces lie far into the basin, are encased by marine mudstones, and overlie major erosional unconformities. River-dominated deltaic sediments have not been documented in the Cardium Formation and non-marine and lagoonal facies are relatively rare. They are confined to the Western

portion of the basin in the Kakwa area, and in outcrop areas, but do not reach thicknesses greater than about 40 meters, even in outcrop (Duke, 1985a). Transgressive re-working results in the extensive modification of Cardium depositional systems, and shore parallel linear shorefaces are predominant. The only depositional systems documented in the Dunvegan Formation which resemble sandy Cardium shorefaces (such in the Kakwa area, Plint and Walker, 1987) are in shingles D1 and D2. Interestingly, these occupy a similar position in the Alberta Basin to the Cardium Kakwa shoreface.

Each of the six Cardium sequences is interpreted to have been deposited in time periods of between 167,000 to 333,000 years (Bergman and Walker, 1988); times which are similar to those of members in the Dunvegan Formation (150,000 to 300,000 years). These sequences were interpreted as being produced by tectonic processes probably involving basin uplift (Walker and Eyles, 1988; Bergman and Walker, 1988).

The overall shape of the Cardium, and the presence of lowstand shoreface chert conglomerates, contrasts with the Dunvegan. The Dunvegan Formation is strongly wedge shaped, reaches a maximum thickness of about 300 meters to the far Northwest, and contains absolutely no extraformational conglomerate towards the basin (southeast). As indicated in chapter 1 (Stott, 1982), thick extraformational conglomerates, interpreted to have been deposited in piedmont to alluvial plain

environments, are confined to the far northwestern outcrops in northern British Columbia and in the Northwest Territories. In contrast to the Cardium, none of these conglomerates ever reached the Dunvegan marine shelf.

Paola (1988) has presented mathematical models which relate subsidence and gravel transport in alluvial basins. His models may explain why conglomerates are restricted to alluvial plain sediments in the Dunvegan (Stott, 1982) but lie encased in marine shelf mudstones in the Cardium (Bergman and Walker, 1986). Paola's results show that there is an inverse relationship between the distance that gravel can be transported into a basin and the subsidence rate. Given similar rates of sediment supply, foreland basins, characterized by highly asymmetric subsidence (i.e. higher subsidence adjacent to the rising orogen, W in Fig.12-3B) will produce wedge-shaped units with most of the gravel confined close to the source (e.g. Dunvegan Formation) while foreland basins characterized by lower and less asymmetric subsidence will produce sheet gravels which lie much further into the basin, such as in the Cardium Formation.

The average maximum thickness of the Cardium Formation (about 100 meters) divided by the total time available for deposition (1-2my) suggests an average accumulation rate of between about 0.05 to 0.1m/1000 years. If this is considered as roughly equivalent to the Cardium accommodation rate, it is considerably lower than those rates calculated above for the

Dunvegan Formation (0.15 to 0.3m /1000 years). These accommodation rates seem to tally with the predictions of Paola's models.

The Cardium appears to have been deposited in a relatively slowly and uniformly subsiding basin which is may have experienced some uplift at times. Accommodation was probably less than in the Dunvegan Formation and the sediments underwent extensive reworking by basinal processes. Paola's model predicts minimal downstream fining and the deposition of widespread sheet gravels far into the basin in these types of basins. In addition, he predicts that in large basins, robust clasts (e.g. cherts, quartzites) will show relatively little downstream abrasion while softer clasts (e.g. schist, limestone) will be absent in the distal portions of the basin. Cardium conglomerates comprise essentially nothing but chert clasts.

Conglomerates of the Dunvegan, in contrast, were deposited onto a rapidly subsiding and highly asymmetric basin. In basins of this type, Paola's models predict rapid downstream fining and deposition of thick tabular to wedge shaped conglomerate bodies along the axis of greatest subsidence. His models also predict that there will be less compositional sorting in these types of basins and that conglomerates are more likely to contain clasts of differing strength. Dunvegan conglomerates, while comprising largely chert and quartzite, have an important arkosic component and also contain argillite clasts and volcanic rock fragments.

Paola's models thus provide a theoretical basis on which to make comparisons of gravel transport in different basins. He suggests that conglomerates lying in a basinward position will, contrary to popular opinion, represent times of relative tectonic quiescence, especially in foreland basin type settings.

Stott (1984), Price (1984), and Tankard (1986b) suggest that the Mesozoic was characterized by two major phases of collisional tectonics, which have been referred to as the Columbian (mid-Jurassic to Early Cretaceous) and Laramide (Late Cretaceous to Tertiary) Orogenies respectively, separated by a period of relative tectonic quiescence (anorogeny) during the mid-Late Cretaceous. As outlined in chapter 1, the Dunvegan Formation is thought to relate to the last phases of the earlier Columbian Orogeny while the Cardium is thought to have been deposited during the intervening time of relative tectonic quiescence (Stott, 1984). This would also fit with the observations of lower accommodation (and probably lower subsidence) during Cardium time and with the predictions and assumptions of Paola's models.

Several authors (Tankard, 1986a and b; Heller et al., 1988) suggest that anorogenic phases in foreland basins may be characterized by "relaxation" of the basin accompanied by uplift and erosion. Tankard (1986a) indicates that relaxation will cause relatively modest downwarping of the basin toward the mountain front (due to visco-elastic relaxation) and uplift on the peripheral bulge (hinge zone) which will also migrate in towards

the mountain front. Heller et al. (1988), in contrast, indicate that anorogeny should be accompanied by erosional denudation of the mountain front which will cause isostatic uplift of the basin toward the mountains and redistribution of sediments as sheet-like units far into the basin (seaward). These mechanisms are invoked by these authors on time scales of several millions to several tens of millions of years but are not included here in order to explain the origin of fourth order sedimentary cycles. Rather they provide a context for interpreting the overall character of the changes in the Alberta Foreland Basin through time. Evidence of basinal uplift and erosion was not observed in the sediments of the Dunvegan Formation. This is probably characteristic of active orogenic phases. The Cardium basin, in contrast, is thought to have undergone several episodes of uplift, a situation more likely to exist during the anorogenic phase interpreted to have existed during deposition of the Cardium Formation (Tankard 1986b, Stott, 1984).

12-6-2. The Mosby and the Dunvegan

As outlined in chapter 1, a possible controversy, centering on the relationship between the Mosby Formation in northern Montana and the Dunvegan Formation, was discussed. Some of the ideas discussed above may shed some light in resolving this controversy. Rice and Gautier (1983) and Rice (1984) suggested that the Mosby sandstones were derived from the so called

'Dunvegan Delta' and transported up to 1,100 km south by incremental geostrophic storm flows (Fig.1-1).

However, closer perusal of Rice's (1984) paper reveals several inconsistencies. His correlation table (figure 1, Rice,1984) shows that the Mosby Sandstone is the stratigraphic equivalent of the uppermost portion of the Dunvegan Formation and the lowermost sandy members within the overlying Kaskapau Formation. These Kaskapau members include the Doe Creek and Pouce Coupe Members (Wallace-Dudley & Leckie,1988; Stott, 1982).

Rice's paleogeographic reconstruction diagram (Fig.1-1) is highly misleading. It suggests synchronous deposition of the so called 'Dunvegan delta' and Mosby shelf sands. His text (based on Stelck and Wall, 1955), in contrast, suggests that regional tilting caused uplift and erosion of the proximal portions of the Dunvegan delta during the late Cenomanian. In the northwest this eroded sediment was subsequently transported and redeposited as the Doe Creek and Pouce Coupe Sandstones. Rice (1984) inplies that some of this sediment was transported up to 1,000 km south by long term geostrophic currents and subsequently deposited as the Mosby Formation.

In chapter 2 of this study, it was shown that the maximum grain size of extraformational material observed within the thesis area was medium-grained sandstone. Wallace-Dudley & Leckie (1988) published a study of the Doe Creek Member in northwestern Alberta. They interpret the Doe Creek sandstones to have formed as shallow

marine sand shoals deposited offshore of the Dunvegan delta during transgression of the Kaskapau sea. They show Doe Creek sandstones to thin to the southeast and also observe a maximum grain size of medium-grained sandstone. No evidence of extraformational conglomerate is observed anywhere stratigraphically between the Doe Creek and Dunvegan Formations and no conglomeratic units have been described in the Pouce Coupe Member (A.G.Plint pers.comm.; D.Dearborne, pers.comm.).

Rice (1984) notes that the Mosby Formation includes thin extraformational, chert pebble horizons which he does not discuss in his sediment transport model. He does not explain how storm processes can transport pebbles for hundreds, let alone thousands of kilometers. In addition, it is considered extremely unlikely that conglomerates could totally bypass either the Dunvegan Formation or the Doe Creek and Pouce Coupe Members. Stott (1982) notes abundant conglomerate in the Dunvegan Formation but indicates that it is all tied up to the far northwest in thick alluvial plain deposits. There is absolutely no evidence that any of this conglomerate even reached as far south as the northernmost limits of this study area, let alone Montana.

The differences in the distribution and types of conglomerate is consdered crucial in attempting to model mechanisms of sediment transport in foreland basins (Paola, 1988) as discussed above. Although thick isolated conglomerates encased in marine shales are observed in the Cardium Formation, these can

be traced landward as gravel veneers, and at least one conglomerate shoreface has been documented in outcrop (Plint and Hart, 1988). Very few pebble-free exposures of the Cardium exist. As discussed above, this contrasts with the Dunvegan which is essentially pebble-free in the subsurface and which suggests that conglomerates did not travel far into the basin (i.e. seaward). This seems incompatible with the Rice's (1984) suggestion that the Mosby Formation, which contains pebbles, was derived from the Dunvegan. There are clearly interesting problems in the Mosby Formation, however it does not appear as though sedimentation in the Mosby has any direct relationship to the sediments of the Dunvegan Formation.

12-6-3. Other Cretaceous Clastic Units

Other Cretaceous clastic units in the Alberta Foreland basin, which show similar cyclicity on similar time scales as members within the Dunvegan Formation, include the late Albian Viking Formation (Downing and Walker, 1988; Power, 1988), and the Lower Cretaceous Moosebar and Gates Formations (Leckie, 1986). The above comparison of the Cardium and Dunvegan Formations suggest an overall approach which can be applied to the analysis of all Cretaceous units within the West Alberta Basin. In the text above, I compared the Dunvegan and Cardium Formations for three reasons; both have been well studied; and they are close together in age but they are quite different in appearance. In addition, other researchers on the Dunvegan and Cardium Formations

(A.G.Plint pers. comm.) have suggested that a comparison would be useful. Comparison with yet other units, and construction of a basin analysis for the entire Cretaceous is clearly beyond the scope of this study. This comparison with the Cardium suggests the types of differences and questions that might be relevant in such a study.

CHAPTER 13. CONCLUSIONS AND FUTURE WORK

13-1. Seismic versus Well Logs, Scales of Investigation

In the first part of this study (chapter 2) the facies and facies associations observed in cores through the Dunvegan Formation were described and interpreted. In chapter 3, the scale of investigation was expanded to consider the overall allostratigraphic relationships observed within the Dunvegan Formation. Chapters 4-10 examined each allostratigraphic unit (member) in detail and considered the three dimensional geometry of depositional systems within these members. Chapter 11 integrated the results of analysis of each member in the context of,

1. large scale depositional systems, and
2. shallow marine facies models.

In chapter 12 the basin wide controls on the patterns of these depositional systems were discussed and integrated into a consideration of the evolution of the Dunvegan Formation incorporating models of the Alberta Basin.

The smallest scale of geological events considered in this study began with the description and interpretation of individual beds and facies units at the scale of tens of centimeters to a few meters in chapter 2. Next, shingles were considered with average

thicknesses of about 20 meters or less and time durations of between 50,000 and 100,000 years. Next, members were considered which reach thicknesses of several tens of meters and were probably deposited in time intervals of between about 150,000 and 300,000 years. Finally, the entire Dunvegan Formation and associated shales were considered reaching a thickness of a few hundred meters and deposited in a time period of a few million years. Time scales of a few million years or so, represent the lower limit of cyclicity normally recognized by seismic stratigraphers (Miall,1984b). The third order cycles, or "medium sequences" of Haq et al., (1987) occur in time scales of about 1.8 my, and in chapter 12 it was shown that at least one major global lowstand of sea-level, related to one of these third order cycles, was associated with Dunvegan deposition (Fig.1-6, Fig.12-3). Haq et al. (1987) also define 'minor sequences' (i.e. fourth order cycles) but suggest that they are not resolvable at the scale of seismic studies and require well log or outcrop data. This study therefore bridges this gap between the scale of events that can be resolved using seismic data and that possible using well log and core data.

Accommodation, in general, is much greater on passive continental margins than in foreland basins (Fig.12-4). This means that, given the same time interval, much more sediment is likely to accumulate on a passive margin than in a foreland basin. Using seismic data, third order cycles (equivalent in duration to

sequences of Posamentier et al., in press) are more likely to be resolvable in sediments deposited on passive continental margins than in sediments deposited in foreland basins. On average, seismic data in the Alberta basin (characterized as "railroad tracks") can resolve about 50 meters of stratigraphy. The entire Dunvegan Formation would be represented by two or three seismic reflectors. Analysis of the Cretaceous Alberta basin using well log data is probably of much more utility, therefore, than using seismic data, especially in the resolution of events shorter than a few million years.

13-2. Answering the Primary Questions

This study has answered most of the primary questions asked in chapter 1. The first set of questions were;

1. How do individual Dunvegan sandstones die into the basin?

2. Do sandstones in the Dunvegan Formation display deltaic facies patterns and morphologies and, if so, what kinds of deltas do they most resemble?

3. Was the Cretaceous Western Interior Seaway of North America wave- and storm-dominated during deposition of Dunvegan sediments and, if so, can deltas be preserved or recognized in these sediments?

The answers to these questions suggest that sandstones within the Dunvegan Formation thin gradually to the southeast and are not present south of the map area. The sand body geometries and facies associations in these sandstones indicate that they

were deposited in river-dominated deltas and wave-dominated prograding shorelines with varying degrees of storm-influence. Delta morphologies and facies associations suggest that the basinal energy during Dunvegan time was relatively low and that the primary control on facies patterns was sedimentation rate. The details of these depositional systems are discussed in chapter 11.

The second set of questions dealt with the stratigraphy of the Dunvegan Formation, specifically;

4. What are the stratigraphic relationships of sandstones within the Dunvegan Formation?

5. What kinds of sequences exist within the Dunvegan Formation and how do they compare with published stratigraphic models?

The allostratigraphic approach used in this thesis is partly based on sequence stratigraphic concepts (Posamentier et al. in press), and allows subdivision of the Dunvegan Formation into seven genetically related depositional units, or allomembers, separated by bounding discontinuities which are interpreted as regionally widespread transgressive flooding surfaces (T-surface). Each of these allomembers is made up of one or more shingles, most of which show progressive offlap (progradation) into the basin. This allostratigraphic scheme was used to carry out an analysis of the West Alberta Basin during Dunvegan time using a Wheeler Diagram (Fig.12-3). The Wheeler diagram is a two dimensional representation of the position and relative duration of events in

the basin. It emphasizes the lateral extent and approximate duration of unconformities, hiatuses, and condensed sections, and was also used to construct a Relative Basinal Downlap chart. This chart is a useful way to present the major transgressive and regressive events in the basin and may be used to compare the time-stratigraphy of the Dunvegan Formation with mid-Cenomanian sequences in other basins.

Sequence stratigraphic models are based almost entirely on passive margin depositional settings and are not readily applicable to foreland basins (Fig.12-4), in which tectonic controls are usually far more important than eustatic controls. These models must be modified considerably in order to apply the concepts of sequence stratigraphy to a foreland basin type setting such as the West Alberta basin.

The final questions considered the controls on the distribution and timing of sediments and sedimentary cycles within the Dunvegan Formation, specifically;

6. What controls the deposition of individual stratigraphic units within the Dunvegan Formation; delta progradation, storm processes, sea level changes, tides or perhaps a combination of these and other effects?

7. What other factors control the distribution of the Dunvegan Formation (e.g. tectonics, subsidence, basin structure)?

In chapter 3, two types of allostratigraphic units were defined (shingles and members) and several scales of events were

recognized. Paleontological data indicate that the Dunvegan was deposited in about 1 to 2 million years during the mid-Cenomanian. Calculations indicate that members were deposited in about 150,000 to 300,000 years while shingles were deposited in about 50,000 to 100,000 years. Shingles are interpreted to be autocyclic in nature and transitions between shingles result from processes related to river avulsion and delta switching.

Members are similar in duration to the 'minor sequences' of Haq et al. (1987), although a eustatic origin was not proposed in this study. The regional persistance of member-bounding discontinuities (T-surfaces) suggests that they are allocyclic in nature and are probably related to changes in basin subsidence caused by local tectonic effects, probably related to episodes of thrusting in the adjacent Cordill ra. Superimposed third order eustatic controls may also be important in controlling the degree of progradation and in controlling the rate of accommodation.

13-3. Answering the Secondary Questions

A series of secondary questions were posed which centered on a proposed genetic link between the Dunvegan Formation and the Mosby Formation in northern Montana (Rice, 1984), specifically;

8. What is the actual stratigraphic and paleogeographic relationship between the Mosby and Dunvegan sandstones?

9. Is deposition of the Mosby sandstones related to incremental sand transport over a distance of up to 1,100 km (as suggested by Rice,1984) or perhaps to a lowering of sea level, and

what effect, if any does this have on the sediments of the Dunvegan Formation?

In chapter 12 it was shown that deposition of the Mosby Formation was probably not related to the Dunvegan Formation. The Mosby contains interbedded chert pebble horizons which Rice (1984) does not include in his sediment transport model. It is hard to imagine how pebbles could totally bypass Dunvegan shorelines and be transported 1,100 km south by storm processes alone.

13-4. Comparison With Other Cretaceous Units

The last question stated,

10. How does the Dunvegan Formation compare to other relatively well understood Upper Cretaceous clastic formations in Western Alberta?

Some comparison was made in chapter 11 in the context of characterizing the different types of depositional systems. Detailed comparison with the Cardium Formation in chapter 12 showed that inferences about the basin history and differences in tectonic styles could be made by comparing the gross characteristics of each formation. The Cardium reflects deposition during a time of relative tectonic quiescence. Its overall geometry is tabular, and relatively low accommodation rates during Cardium time allowed conglomerate to travel far into the basin and onto the shelf. Active tectonism produced more rapid foreland-type subsidence during Dunvegan time. This caused conglomerate phases to be deposited entirely in alluvial plains to

the northwest and conglomerate was never deposited on the Dunvegan shelf. Using the models of Paola (1988) this type of analysis may have important implications for the mechanism of gravel transport in foreland basins.

13-5. Future Questions

One of the first areas of future research will be to trace the allomembers presented in this study to the north, in order to tie in to Dunvegan outcrop areas studied by A.G.Plint (Plint & Hart, 1988). It will also be necessary to continue correlations to the east and west in order to obtain a more complete determination of the geometry of allomembers. It is considered fairly crucial to determine whether members A and B, in particular, represent true wedges or the distal end of more extensive pod-shaped units. This will allow a more complete analysis of the basin history during deposition of the Dunvegan Formation.

There is some scope for more detailed analysis of the sub-components within the recognized depositional systems, especially in areas where well control is particularly good. The detailed geology and sedimentology of the estuarine channel facies and of tidal inlet channels, in particular, would add to an understanding of these types of depositional settings. Many modern reviews of deltas emphasize differences in delta front sandstones and distributary mouth bars as related to the differences in the degree of mixing and the amount of friction between outflowing sediment waters and basin waters. This type of analysis was not

attempted in this study but needs to be tested in the ancient record. Several recent studies (Galloway, 1986; Tyler and Ambrose,1986) have conducted detailed subsurface analysis of the three-dimensional facies architecture of shallow marine sandstone depositional systems. These studies emphasize recognition of architectural facies units largely on the basis of changes in well log character. They also use changes in resistivity logs to map different architectural units within individual barrier island sandstones (e.g., inlet fill, barrier core, flood tidal delta etc.). Unfortunately no core data are presented in these studies. It would be interesting to test these techniques of using resistivity logs in producing fields of the Dunvegan where detailed core information and resistivity logs are available.

There is some question as to the nature of Dunvegan "channels" mapped within this study. D.A.Leckie (pers.comm.) and Harper (pers.comm.) have suggested that some of the channels recognized within this study may, in fact, be valleys and may be filled by multiple channel fills. At the scale of deltaic depositional systems mapped within this study, major feeder systems (indicated by shoestring sandstones with erosive bases) have been designated as channels. Careful detailed mapping and correlation of facies relationships within these channels may shed light as to the actual scale and nature of channels or valleys within the Dunvegan Formation and opens up the area of fluvial

geology of Dunvegan sediments, a topic which has not been dealt with in detail in this thesis.

There is a wide range of different types of trace fossil assemblages within the different types of depositional systems of the Dunvegan Formation. These have been dealt with cursorily in this thesis. Detailed analysis of these various ichnofacies could contribute to an understanding of the relationships between sediments and organisms in a variety of different depositional environments, certainly to a greater degree than has been presented here. In particular, it would be interesting to compare in detail the different assemblages in the estuarine, lagoonal, shoreface, interlobe, prodelta, and shelf settings represented in the sediments of the Dunvegan Formation.

13-6. Numbered Conclusions

1. This study presents the first allostratigraphic subdivision of the Dunvegan Formation, based on the recognition of seven widespread transgressive flooding surfaces. The Dunvegan is subdivided into seven allomembers, designated A to G from top to bottom, each of which consists of several offlapping sandy shingles.

2. Each member represents a genetically related package of sediments related to an overall regression and is separated from other members by bounding discontinuities (T-surfaces) produced by rapid transgressive flooding events.

3. Maps of sand body geometries and facies associations show that shingles represent a wide range of prograding shallow marine to non-marine environments ranging from highly river-dominated deltas in member E, to storm- and wave-dominated prograding deltas and barriers in member D.

4. Shingles are autocyclic units and changes between shingles are related to river avulsion and delta switching.

5. Members are allocyclic units and member bounding discontinuities are thought to be related to short term thrusting events in the rising Cordillera to the northwest.

6. The Dunvegan Formation was deposited during a time of active tectonism (Columbian Orogen) which caused rapid foreland-type subsidence. Conglomerate phases were deposited entirely in alluvial plains and fluvial channels to the northwest. A global third-order eustatic lowstand of sea-level is also associated with deposition of the Dunvegan.

REFERENCES

AIGNER,T.,1982, Calcareous Tempestites: Storm-dominated Stratification in Upper Muschelkalk Limestones (Middle Trias, SW-Germany). in Einsele,G. and Seilacher,A. (eds.) Cyclic and Event Stratigraphy, Springer-Verlag, Berlin Heidelberg New York, p.180-198.

ALBERTA SOCIETY OF PETROLEUM GEOLOGISTS, 1960, Lexicon of geologic names in the Western Canada Sedimentary Basin and Arctic Archipelago, Calgary, Alberta, 380p.

ALLEN,J.R.L., 1984, Developments in Sedimentology 30; Sedimentary Structures, their character and physical basis, Vol.2, Elsevier, 663p.

ALLEN,P.A., and HOMEWOOD,P., 1986, Foreland Basins. Special Publication Number 8, International Associations of Sedimentologists, publ. Blackwell, 453p.

ARNOTT,R.W.C., 1988, Regression-transgression couplets of the Bootlegger Sandstone (Cretaceous), north-central Montana - The possible influence of the Sweetgrass Arch. in James,D.P. & Leckie,D.A. (eds.) Sequences stratigraphy, sedimentology: surface and subsurface, Canadian Society of Petroleum Geologists, Memoir 15, Calgary, Alberta, p.255-260.

BARRELL,J., 1912, Criteria for the recognition of ancient delta deposits. Geological Society of America Bulletin, v.23, p.377-446.

BEAUMONT,C., 1981, Foreland basins, Geophysical Jour. Royal Astronomical Society, v.65, p.291-329.

BEAUMONT,C., QUINLAN,G., and HAMILTON,J., 1988, Orogeny and stratigraphy: numerical models of the Paleozoic in Eastern Interior of North America. Tectonics, v.7, p.389-416.

BEERBOWER,J.R.. 1964, Cyclothems and cyclic depositional mechanisms in alluvial plain sedimentation. in Merriam,D.F. (ed.) Symposium on cyclic sedimentation, Kansas Geological Survey Bulletin, v.169, p.31-42.

BERGER,A., 1984, Accuracy and frequency stability of the Earth's orbital elements during the Quartenary, in Milankovitch & Climate, Part 1, NATO ASI Series C: Mathematical and Physical Sciences, V.126, p.3-40, D.Reidel Publishing Co.

BERGER,A., IMBRIE,J., HAYS,J., KUKLA,G., & SALTZMAN,B., 1984, Milankovitch & Climate, Part 1, NATO ASI Series C: Mathematical and Physical Sciences, V.126, 509p., D.Reidel Publishing Co.

BERGMAN,K.M., AND WALKER R.G., 1986, Cardium Formation Conglomerates at Carrot Creek Field: Offshore Linear Ridges or Shoreface Deposits? in Moslow,T.F. and Rhodes,E.G. (eds.) Modern and Ancient Shelf Clastics, A Core Workshop. SEPM Core Workshop No.9.

BERGMAN,K.M., AND WALKER,R.G., 1988, Formation of Cardium erosion surface E5, and associated deposition of conglomerate: Carrot Creek Field, Cretaceous Western Interior Seaway, Alberta. in James,D.P. & Leckie,D.A. (eds.) Sequences stratigraphy, sedimentology: surface and subsurface, Canadian Society of Petroleum Geologists, Memoir 15, Calgary, Alberta, p.15-24.

BEYNON,B.M., PEMBERTON,S.G., BELL,D.D., and LOGAN,C.A., 1988, Environmental implications of ichnofossils from the Lower Cretaceous Grand Rapids Formation, Cold Lake Oil Sands Deposit, in James,D.P. & Leckie,D.A. (eds.) Sequences stratigraphy, sedimentology: surface and subsurface, Canadian Society of Petroleum Geologists, Memoir 15, Calgary, Alberta, p.275-290.

BHATTACHARYA,J., 1985, Dunvegan Formation. Progress Report Compiling Initial Subsurface Data in Northwestern Alberta. McMaster University Tech Memo 85-4, 34p.

BHATTACHARYA,J., 1988, Autocyclic and allocyclic sequences in river- and wave-dominated deltaic sediments of the Upper Cretaceous, Dunvegan Formation, Alberta: core examples. in James,D.P. & Leckie,D.A. (eds.) Sequences stratigraphy, sedimentology: surface and subsurface, Canadian Society of Petroleum Geologists, Memoir 15, Calgary, Alberta, p.25-32.

BLATT,H., MIDDLETON,G.V., and MURRAY,R.C, 1980, Origin of Sedimentary Rocks, Prentice-Hall Inc., New Jersey, 782p.

BOUMA,A.H., 1962, Sedimentology of some flysch deposits: a graphic approach to facies interpretation. Amsterdam, Elsevier, 168p.

BURBANK,D.W. and RAYNOLDS,R.G.H., 1988, Stratigraphic keys to the timing and thrusting in terrestrial foreland basins: applications to the Northwestern Himalaya in Kleinspehn,K.L., & Paola,C. (eds.) New perspectives in basin analysis, Frontiers in sedimentary geology series, Springer-Verlag, p.331-353.

BURK,C.F.JR., 1963, Structure, Isopach, and Facies Maps of Upper Cretaceous Marine Successions, West-Central Alberta and Adjacent British Columbia. GSC Paper 62-31.

BUSCH,D.A., 1974, Stratigraphic traps in sandstones: exploration techniques. AAPG Memoir 21, Tulsa, Oklahoma, 174p.

CALDWELL,W.G.E., NORTH,B.R., STELCK,C.R., and WALL,J.H., 1978, A foraminiferal zonal scheme for the Cretaceous System in the Interior Plains of Canada. in Stelck,C.R., and Chatterton,B.D.E. (eds.) Canadian biostratigraphy. Geological Association of Canada, Special Paper 18, p.495-575.

CANT,D.J., 1984, Subsurface facies analysis. in R.G.Walker (ed.) Facies Models, Geoscience Canada Reprint Series 1, p.297-310.

CHAN,M.A. and DOTT,Jr.R.H., 1986, Depositional Facies and Progradational Sequences in Eocene Wave-dominated Deltaic Complexes, Southwestern Oregon. AAPG Bull. v.70, p.415-429.

CLIFTON,H.E. and DINGLER,J.R., 1984, Wave-formed sedimentary structures and paleoenvironmental reconstruction. Marine Geology, v.60, p.165-198.

CLOETINGH,S., 1986, Intraplate Stress: A new tectonic mechanism for fluctuations of relative sea-level. Geology, v.14, p.617-620.

CLOETINGH,S., 1988, Intraplate stresses: A new element in basin analysis. in Kleinspehn,K.L., & Paola,C. (eds.) New perspectives in basin analysis, Frontiers in sedimentary geology series, Springer-Verlag, p.205-230.

COLEMAN,J.M., and PRIOR,D.B., 1982, Deltaic Environments in Scholle,P.A., & Spearing,D.R. (eds.) Sandstone depositional environments, AAPG Memoir 31, p.139-178.

COLEMAN,J.M., ROBERTS,H.H., MURRAY,S.P., and SALAMA,M., 1981, Morphology and dynamic sedimentology of the eastern Nile delta shelf, in Nittrouer, C.A. (ed.) Sedimentary dynamics on continental shelves: Elsevier,New York, p.301-326.

COLEMAN,J.M., and WRIGHT,L.D., 1975, Modern River Deltas: Variability of Processes and Sand Bodies, in Broussard,M.L. (ed.) Deltas, Models for Exploration, publ. Houston Geological Society.

DAWSON,G.M., 1881, On the Geology of the Region Between the 54th and 56th Parallels, from the Pacific Coast to Edmonton. Geological and Natural History Survey of Canada, Report of Progress for 1879-80, p.99b-142b.

DONOVAN,D.T., & JONES,J.W., 1979, Causes of world-wide changes in sea level, Jour. Geol. Soc. Lond., V.136, p.187-192.

DOWNING,K.P., and WALKER,R.G., 1988, Viking Formation, Joffre Field, Alberta: Shoreface origin of long, narrow sand body encased in marine mudstones. AAPG. Bull., v.72, p.1212-1228.

DUKE,W.D., 1985a, Sedimentology of the Upper Cretaceous (Turonian) Cardium Formation in outcrop in southern Alberta, unpubl. Ph.D.Thesis, McMaster University, 724p.

DUKE,W.D., 1985b, Hummocky cross-stratification. tropical hurricanes, and intense winter storms. Sedimentology, v.32, p.167-194.

DUNCAN,E.A.,1983, Delineation of delta types: Norias delta system, Frio Formation, South Texas. Transactions of the Gulf Coast Association of Geological Societies, V.33, p.

EKDALE,A.A., and MASON,T.R., 1988, Characteristic trace-fossil associations in oxygen-poor sedimentary environments. Geology, v.16, p.720-723.

ELLIOT,T., 1975, The Sedimentary History of a Delta Lobe from a Yoredale (Carboniferous) Cyclothem. Proceedings of the Yorkshire Geological Society, v.40, p.505-536.

ELLIOT,T., 1986, Deltas, in H.G.Reading (ed.) Sedimentary Environments and Facies, second edition, Blackwell, Oxford, p.113-154.

EYLES,C.H. & WALKER, R.G. 1988 "Geometry" and facies characteristics of stacked shallow marine sandier-upwards sequences in the Cardium Formation at Willesden Green, Alberta. in James,D.P. & Leckie,D.A., (eds.) Sequences, Stratigraphy, Sedimentology: Surface and Subsurface. Canadian Society of Petroleum Geologists, Memoir 15, Calgary, Alberta. p.85-96.

FAILL,R.T., 1985, The Acadian Orogeny and the Catskills Delta. in Woodrow,D.L., and Sevon,W.D. (eds.) The Catskills Delta, Geological Society of America, Special Paper 201, p.15-37.

FISCHER,A.G., & SCHWARZACHER,W., 1984, Cretaceous Bedding Rhythms Under Orbital Control ? in Berger et al. (eds.) Milankovitch and Climate, Part 1, NATO ASI Series C: Mathematical & Physical Sciences, V.126, p.163-175, D.Reidel Publishing Co.

FISHER,W.L. AND McGOWEN,J.H., 1967, Depositional systems in the Wilcox Group of Texas and their relationship to the occurrence of oil and gas. Transactions of the Gulf Coast Association of the Geological Society, v.17, p.105-125.

FISK,H.N., 1961, Bar finger sands of the Mississippi delta. in Peterson,J.A., and Osmond,J.C. (eds.) Geometry of sandstone bodies - a symposium, p.29-52, AAPG., Tulsa, Oklahoma

FOUCH,T.D., LAWTON,T.F., NICHOLS,D.J., CASHION,W.B., and COBBAN,W.A.,1983, Patterns and timing of synorogenic sedimentation in Upper Cretaceous rocks of Central and Northeast Utah. in Reynolds,M.W. and Dolly,E.D. (eds.) Mesozoic Paleogeography of the West-Central United States, Rocky Mountain Paleogeography Symposium 2, SEPM, Rocky Mountain Section, Denver, Colorado, p.305-336.

FRAKES,L.A., and FRANCIS,J.E., 1988, A guide to Phanerozoic climates from high-latitude ice-rafting in the Cretaceous. Nature, v.333, p.547-549.

FRAZIER,D.E., 1967, Recent deltaic deposits of the Mississippi delta: their development and chronology, Trans. Gulf Coast Assoc. of Geological Societies, v.17, p.287-315.

FREY,R.W. and PEMBERTON,S.G., 1984, Trace Fossil Models. in Walker,R.G. (ed.) Facies Models. Geoscience Canada Reprint Series 1, Geol. Assoc. Canada.

GALLOWAY,W.E., 1986, Reservoir facies architecture of microtidal barrier systems, AAPG Bull., v.70, p.787-808.

GALLOWAY,W.E., 1975, Process Framework for Describing the Morphologic and Stratigraphic Evolution of Deltaic Depositional Systems, in M.L.Broussard (ed.) Deltas, Models for Exploration; Houston Geological Society, p.87-98.

GALLOWAY,W.E., 1968, Depositional Systems of the Lower Wilcox Group, North-Central Gulf Coast Basin. Trans. Gulf Coast Ass. Geol. Soc., v.28, p.275-289.

HALLAM,A., 1983, Pre-Quartenary Sea-Level Changes, Annual Reviews Earth Planetary Sciences, v.12, p.205-243.

HAQ,B.U., HARDENBOL,J. and VAIL,P.R., 1987, Chronology of Fluctuating Sea Levels Since the Triassic. Science, v.235, p.1156-1166.

HARMS,J.C., SOUTHARD,J.B., SPEARING,D.R. and WALKER,R.G., 1975, Depositional Environments as Interpreted from Primary Sedimentary Structures. Soc. Econ. Paleont. Mineral. Short Course 2, 161p.

HARMS,J.C., SOUTHARD,J.B., and WALKER,R.G., 1982, Structures and sequences in clastic rocks, SEPM Short Course No.9, Tulsa, Oklahoma, 249p.

HAYS,J.D., IMBRIE,J. & SHACKLETON,N.J., 1976, Variations in the Earth's Orbit: pacemaker of the ice ages, Science, v.194, p.1121-1132.

HELLER,P.L., ANGEVINE,C.L., and PAOLA,C., 1988, Two-phase model of foreland-basin sequences. Geology, v.16, p.501-504.

HORNE,J.C., FERM,J.C., CARUCCIO,F.T., AND BAGANZ,B.P., 1978, Depositional Models in Coal Exploration and Mine Planning in Appalachian Region. AAPG BULL., v.62, p.2379-2411.

HUBERT,J.F., BUTERA,J.G., AND RICE,R.F., 1972, Sedimentology of Upper Cretaceous Cody-Parkman Delta, Southwestern Powder River Basin, Wyoming. GSA Bull., v.83, p.1649-1670.

JAMEISON,R.A., and BEAUMONT,C., 1988, Orogeny and metamorphism: A model for the deformation and pressure-temperature time paths with applications to the central and southern Appalachians. Tectonics, v.7, p.417-445.

JORDAN,T.E.,1981, Thrust loads and foreland basin evolution, Cretaceous, western United States: AAPG Bull., v.65, p.2506-2520.

JORDAN,T.E., FLEMINGS,P.B., and BEER,J.A., 1988, Dating thrust-fault activity by use of foreland basin strata. in Kleinspehn,K.L., & Paola,C. (eds.) New perspectives in basin analysis, Frontiers in sedimentary geology series, Springer-Verlag, p.307-330.

KAUFMANN,E.G., 1969, Cretaceous marine cycles of the Western Interior. The Mountain Geologist, v.6, p.227-245.

KIRSCHBAUM,M.A., 1986, Depositional Environments of the Rock Springs Formation, Southwest Flank of the Rock Springs Uplift, Wyoming. The Mountain Geologist, v.23, p.63-75.

KOMINZ,M.A. and BOND,G.C., 1986, Geophysical modelling of the thermal history of foreland basins. Nature, v.320, p.252-256.

KREISA,R.D. and MOIOLA,R.J., 1986, Sigmoidal Tidal Bundles and Other Tide-generated Sedimentary Structures of the Curtis Formation, Utah. Geol. Soc. America Bull., v.97, p.381-397.

LECKIE,D.A., 1986, Rates, controls, and sand-body geometries of transgressive-regressive cycles: Cretaceous Moosebar and Gates Formations, British Columbia. AAPG Bull., v.70, p.516-535.

LECKIE,D.A., 1987, Late Albian Sea Level Fluctuations: Effects on the Viking and Boulder Creek Formations and Paddy/Cadotte Members,(Abstract) Canadian Society of Petroleum Geologists, Reservoir, v.14, No.10, p.1-2.

LUNDBERG,N. and DORSEY,R.J., 1988, Synorogenic sedimentation and subsidence in a Plio-Pleistocene collisonal basin, Eastern Taiwan. in Kleinspehn,K.L., & Paola,C. (eds.) New perspectives in basin analysis, Frontiers in sedimentary geology series, Springer-Verlag, p.265-280.

MATTHEWS,R.K., 1984a, Dynamic Stratigraphy, Prentice Hall, New Jersey, 489p.

MATTHEWS,R.K., 1984b, Oxygen-Isotope Record of Ice-Volume History: 100 Million Years of Glacio-Eustatic Sea-Level Fluctuation, in Schlee,J.S. (ed.) Interregional Unconformities and Hydrocarbon Accumulations, AAPG Memoir 36, Tulsa, Oklahama, p.97-107.

McCUBBIN,D.G., 1982, Barrier-island and strand plain facies, in Scholle,P.A., & Spearing,D.R. (eds.) Sandstone depositional environments, AAPG Memoir 31, p.247-280.

MCLEARN,F.H., 1919, Cretaceous, Lower Smoky River, Alberta. Geological Survey of Canada, Summary Report, 1918, Part C, p.1-7.

MCLEARN,F.H., 1945, The Upper Cretaceous , Dunvegan Formation of Northwestern Alberta and Northeastern British Columbia. GSC Paper 45-27.

MIALL, A.D., 1984a, Deltas, in R.G.Walker (ed.) Facies Models, Geoscience Canada Reprint Series 1, p.105-118.

MIALL, A.D., 1984b, Principles of Sedimentary Basin Analysis, Springer - Verlag, New York Berlin Heidelberg Tokyo, 490p.

MIALL,A.D., 1988, Reservoir heterogeneities in fluvial sandstones: Lessons from outcrop studies. AAPG Bull., v.72, p.682-697.

MITCHUM,R.M.Jr., VAIL,P.R., and THOMPSON,III,S., 1977, Seismic Stratigraphy and Global Changes of Sea Level, Part 2: The Depositional Sequence as a Basic Unit for Stratigraphic Analysis. in Payton,C.E., (ed.) Seismic Stratigraphy- applications to hydrocarbon exploration. AAPG Memoir 26, Tulsa, Oklahoma, p.53-62.

MOSLOW,T.F., and PEMBERTON,S.G., 1988, an integrated approach to the analysis of some Lower Cretaceous shoreface and delta front sandstone sequences. in James,D.P. & Leckie,D.A. (eds.) Sequences stratigraphy, sedimentology: surface and subsurface, Canadian Society of Petroleum Geologists, Memoir 15, Calgary, Alberta, p.373-386.

NEMEC,W., 1988, Coal correlations and intrabasinal subsidence: A new analytical approach. in Kleinspehn,K.L., & Paola,C. (eds.) New perspectives in basin analysis, Frontiers in sedimentary geology series, Springer-Verlag, p.161-188.

NICHOLS,M.M., and BIGGS,R.B., 1985, Estuaries, in Davis,R.A. (ed.) Coastal Sedimentary Environments, 2nd. edition, Springer-Verlag publ., p.77-186.

NIEDORODA,A.W., SWIFT,D.J.P., and HOPKINS,T.S., 1985, The Shoreface, in Davis, A.Jr. (ed.) Coastal Sedimentary Environments, Springer-Verlag, p.533-624.

NORTH AMERICAN COMMISSION ON STRATIGRAPHIC NOMENCLATURE, 1983, North American Stratigraphic Code, AAPG Bulletin, v.67, p.841-875.

OBRADOVICH,J.D., and COBBAN,W.A., 1975, A time-scale for the late Cretaceous of the Western Interior of North America. in Caldwell,W.G.E. (ed.) The Cretaceous System in the Western Interior of North America, Geological Society of Canada, Special Paper #13, p.31-54.

PALMER,A.R., 1983, The Decade of North American Geology 1983 Geologic Time Scale, Geology, v.11, p.503-504.

PALMER,J.J., and SCOTT,A.J., 1984, Stacked shoreline and shelf sandstones of La Ventana Tongue (Campanian), Northwestern New Mexico, AAPG Bull. v.68, p.74-91.

PAOLA,C., 1988, Subsidence and gravel transport in alluvial basins. in Kleinspehn,K.L., & Paola,C. (eds.) New perspectives in basin analysis, Frontiers in sedimentary geology series, Springer-Verlag, p.231-244.

PAYTON,C.E., 1977, Seismic Stratigraphy - applications to hydrocarbon exploration, AAPG Memoir 26, Tulsa, 516p.

PENLAND,S., SUTER,J.R., and McBRIDE,R.A., 1987, Delta plain development and sea level hidtory in the terrebonne coastal region, Louisiana in Coastal Sediments '87, WW Div./ASCE, New Orleans,LA p.1689-1705.

PITMAN,W.C., 1978, Relationship between eustasy and stratigraphic sedquences of passive margins, Geol. Soc. America Bulletin, v.89, p.1389-1403.

PLINT,A.G., and HART,B.S., 1988, Field guide to the Upper Cretaceous Dunvegan (Cenomanian) and Cardium (Turonian) Formations in the Dawson Creek-Fort St,John area, British Columbia. C.S.P.G. field guide to Sequences, Stratigraphy, Sedimentology: Subsurface and Subsurface Technical Meeting, September 14-16th, 1988, Calgary, Alberta, 51p.

PLINT,A.G., and WALKER,R.G., 1987, Cardium Formation 8. Facies and environments of the Cardium shoreline and coastal plain in the Kakwa field and adjacent areas, Northwestern Alberta. Bull.C.S.P.G., v.35, p.48-64.

PLINT,A.G., WALKER. R.G., and BERGMAN, K.M., 1986, Cardium Formation 6. Stratigraphic framework of the Cardium in subsurface. Bulletin of Canadian Petroleum Geology v.34, p.213-225.

PLINT,A.G., WALKER,R.G., and DUKE,W.L., 1988, An outcrop to subsurface correlation of the Cardium Formation in Alberta. in James,D.P. & Leckie,D.A. (eds.) Sequences stratigraphy, sedimentology: surface and subsurface, Canadian Society of Petroleum Geologists, Memoir 15, Calgary, Alberta, p.167-183.

PLUMMER,P.S. and GOSTIN,V.A., 1986, Shrinkage Cracks: Dessication or Synaeresis? Jour. Sed. Pet. v.51, p.1147-1156.

POSAMENTIER,H.W., and VAIL,P.R., in press, Eustatic controls on clastic deposition II - sequences and systems tracts. in Wilgus et al. (eds.) Sea level changes - An integratated approach, SEPM special publication 42.

POSAMENTIER,H.W, and VAIL,P.R., 1988, Sequence stratigraphy: Sequences and systems tracts development, Abstract in James,D.P. & Leckie,D.A. (eds.) Sequences stratigraphy, sedimentology: surface and subsurface, Canadian Society of Petroleum Geologists, Memoir 15, Calgary, Alberta, p.571-572.

POSAMENTIER,H.W., JERVEY,M.T., and VAIL,P.R., in press, Eustatic Controls on clastic deposition I - Conceptual framework. in Wilgus et al. (eds.) Sea level changes - An integratated approach, SEPM special publication 42.

POSTMA,D., 1981, Formation of siderite and vivianite and the pore-water composition of a recent bog sediment in Denmark. Chemical Geology, v.31, p.225-244.

POWER, B.A., 1988, Corsening-upwards shoreface and shelf sequences: examples from the Lower Cretaceous Viking Formation at Joarcam, Alberta, Canada. in James,D.P. & Leckie,D.A. (eds.) Sequences stratigraphy, sedimentology: surface and subsurface, Canadian Society of Petroleum Geologists, Memoir 15, Calgary, Alberta, p.185-194.

PRICE,R.A., 1984, Mesozoic geotectonic setting of the Western Canada Sedimentary Basin. abstract in Stott, D.F., & Glass,D.J. (eds.) The Mesozoic of North America, Canadian Society of Petroleum Geologists Memoir 9, Calgary, Alberta, p.560-561.

PYE,K., 1981, Marshrock formed by iron sulfide and siderite cementation in saltmarsh sediments. Nature, v.294, p.650-652.

REINECK, H., and WUNDERLICH,F., 1968, Classification and origin of flaser and lenticular bedding, Sedimentology, v.11, p.99-104.

REINSON,G.E., 1984, Barrier-island and associated strand-plain systems. in R.G.Walker (ed.) Facies Models, Geoscience Canada Reprint Series 1, p.119-140.

REINSON,G.E., CLARK,J.E., and FOSCOLOS,A.E., 1988, Reservoir geology of Crystal Viking Field, Lower Cretaceous estuarine tidal channel-bay complex, South-Central Alberta, AAPG Bull., v.72, p.1270-1294.

RICCI-LUCCHI,F., 1986, The Oligocene to Recent foreland basins of the northern Appenines. in Allen,P.A., and Homewood,P. (eds.) Foreland Basins, IAS Special Publ. 8, p.105-139.

RICE,D.D. and GAUTIER,D.L., 1983, Chapter 9. Shelf Sandstones in Patterns of Sedimentation, Diagenesis, and Hydrocarbon Accumulation. Cretaceous Rocks of the Rocky Mountains. SEPM., Short Course No.11, Denver, Colorado.

RICE, D.D., 1984, Widespread, Shallow-Marine, Storm-Generated Sandstone Units the Upper Cretaceous Mosby Sandstone, Central Montana, in Tillman, R.W., and Siemers, C.T. (eds.) Siliciclastic Shelf Sediments, SEPM Special Publ. No.34, p.143-161.

SCRUTON, 1960, Delta building and the deltaic sequence, in Shepard,F.P., Phleger,F.B., & van Andel,T.H. (eds.) Recent sediments, northwesten Gulf of Mexico, AAPG. p. 82-102.

SELWYN,A.R.C.,1877, Report on Exploration in British Columbia. Geological Survey of Canada, Report of Progress for 1875 - 76, p.28-86.

SHANMUGAN,G., 1988, Origin, recognition, and importance of erosional unconformities in sedimentary basins. in Kleinspehn,K.L., & Paola,C., (eds.) New perspectives in basin analysis, Frontiers in sedimentary geology series, Springer-Verlag, p.83-108.

SLOSS,L.L., 1963, Sequences in the cratonic interior of North America. Geological Society of America Bulletin, v.74., p.93-113.

STELCK,C.R., 1975, basement control of cretaceous sand sequences in western Canada, in Caldwell,W.G.E. (ed.) The Cretaceous system in the Western Interior of North America, Geological Society of Canada, Special Paper No.13, p.427-440.

STELCK,C.R., AND WALL,J.H., 1955, Foraminifera of the Cenomanian Dunveganoceras Zone from the Peace River Area of Western Canada. Research Council of Alberta Report no. 70, 81p.

STELCK,C.R., WALL,J.H. and WETTER,R.E., 1958, Lower Cenomanian Foraminifera from Peace River Area, Western Canada. Research Council of Alberta, Geological Division Bulletin 2, Part 1, 35p.

STOTT,D.F., 1982, Lower Cretaceous Fort St.John Group and Upper Cretaceous Dunvegan Formation of the Foothills and Plains of Alberta, British Columbia, District of Mackenzie and Yukon Territory. GSA Bull. No.328.

STOTT,D.F., 1984, Cretaceous sequences of the Foothills of the Canadian Rocky Mountains, in Stott, D.F., & Glass,D.J. (eds.) The Mesozoic of North America, Canadian Society of Petroleum Geologists Memoir 9, Calgary, Alberta, p.85-107.

SWIFT,D.J.P., HUDELSON,P.M., BRENNER,R.L., & THOMPSON,P., 1987, Shelf construction in a foreland basin: storm beds, shelf sandbodies, and shelf-slope deposotional sequences in the Upper Cretaceous Mesaverde Group, Book Cliffs, Utah. Sedimentology, v.34, p.423-457.

SWIFT,D.J.P., AND NIEDORODA,A.W., 1985, Fluid and Sediment Dynamics on Continental Shelves. in Tillman,R.W., Swift,D.J.P. and Walker,R.G. (eds.) Shelf sands and Sandstone Reservoirs. SEPM Short Course Notes No.13. p.47-134.

TANKARD,A.J., 1986a, Depositional response to foreland deformation in the Carboniferous of eastern Kentucky, AAPG Bulletin, v.70., p.853-868.

TANKARD,A.J., 1986b, On the depositional response to thrusting and lithosphere flexure; examples from the Appalachian and Rocky Mountain basins. in Allen,P.A., and Homewood,P. (eds.) Foreland Basins, IAS Special Publ. 8, p.369-392.

TATER,J., 1964, The Dunvegan Sandstones of the Type Area. unpubl.M.Sc.Thesis, Univ. of Alberta, 58p.

TILLMAN,R.D.,1985, A spectrum of shelf sands and sandstones, in Tillman,R.W., Swift,D.J.P., & Walker,R.G. (eds.) Shelf sands and sandstone reservoirs, Society of Economic Palaeontologists and Economic Mineralogists Short Course No.13, Tulsa, Oklahama, p.1-46.

TURCOTTE,D.L., and SCHUBERT,G., 1982, Geodynamics; applications of continuum physics to geological problems. John Wiley & sons, New York, 450p.

TYLER,N., and AMBROSE,W.A., 1986, Facies architecture and production characteristics of strand-plain reservoirs in North Markham-North Bay City Field, Frio Formation, Texas. AAPG Bull. V.70, p.809-829.

VAIL,P.R., MITCHUM,R.M.Jr. and THOMPSON,III,S., 1977, Seismic Stratigraphy and Global Changes of Sea Level, Part 4: Global Cycles of Relative Changes of Sea Level. in Payton,C.E. (ed.) Seismic Stratigraphy- applications to hydrocarbon exploration. AAPG Memoir 26, Tulsa, Oklahoma, p.83-97.

VAN WAGONER,J.C., 1988, Sequences and parasequences in siliciclastic rocks, Abstract in James,D.P. & Leckie,D.A. (eds.) Sequences stratigraphy, sedimentology: surface and subsurface, Canadian Society of Petroleum Geologists, Memoir 15, Calgary, Alberta, p.572-573.

VISSER,M.J., 1980, Neap-spring cycles reflected on Holocene subtidal large-scale bedforms deposits: a preliminary note. Geology, v.8, p.543-546.

WALL,J.H., 1987, Micropaleontology report on 16 core samples from the Upper Cretaceous of the Simonette- Smoky River district, northwestern Alberta Plains. Institute of Sedimentary and Petroleum Geology, Report No. 6-JHW-1987, Calgary, Alberta. 7p.

WALKER,R.G., 1984, General introduction: Facies, facies sequences and facies models in R.G.Walker (ed.) Facies Models, Geoscience Canada Reprint Series 1, p.1-9.

WALKER,R.G., 1986, Cardium Formation 7. Progress Report Compiling Data from Outcrop and Subsurface in Southern Alberta. McMaster University, Tech. Memo. 86-3, Hamilton, Ontario.

WALLACE-DUDLEY,K.E. & LECKIE,D.A. 1988, Preliminary observations on the sedimentology of the Doe Creek Member, Kaskapau Formation, in the Valhalla Field, northwestern Alberta. in James,D.P. & Leckie,D.A. (eds.) Sequences, Stratigraphy, Sedimentology: Surface and Subsurface, Canadian Society of Petroleum Geologists, Memoir 15, Calgary, Alberta. p.485-496.

WEIMER,R.J., 1984, Relation of unconformities, tectonics, and sea-level changes, Cretaceous of Western Interior, U.S.A. in Schlee,J.S. (Ed.) Interregional Uncomformities and Hydrocarbon Accumulation, AAPG Memoir 36, p.7-35.

WEISE,B.R., 1979, Wave-Dominated Deltaic Systems of the Upper Cretaceous San Miguel Formation, Maverick Basin, South Texas. Transactions Gulf Coast Assoc. Geol. Soc., v.29, p.202-214.

WHEELER,H.E., 1958, Time Stratigraphy, AAPG Bulletin, v.42, p.1047-1063.

WHITAKER, 1973, 'Gutter Casts', a new name for scour-and-fill structures with examples from Llandoverian of Ringerike and Malmoya, Southern Norway. Norsk. Geol. Tidsskr., v.53, p.403-407.

WRIGHT,L.D., 1985, River Deltas, in Davis,R.A. (ed.) Coastal Sedimentary Environments, 2nd. edition, Springer-Verlag publ., p.1-76.

WILLIAMS,G.D., and BURK,C.F., 1964, Upper Cretaceous. in McCrossan,R.G., and Glaister,R.P. (eds.) The Geological History of Western Canada, Chapter 12. Alberta Society of Petroleum Geologists, p.169-189.

WOODROW,D.L., and SEVON,W.D., 1985, The Catskills Delta. Geological Society of America, Special Paper 201, 240p.

APPENDIX 1. CORE LISTING

This appendix is a list of all cores that I described during this study and represents most of the available cores through the Dunvegan as of 1986. As a general rule of thumb, most cores through the Dunvegan Formation were of extremely high quality for the purposes of detailed facies analysis. They were usually highly photogenic and very well preserved. Not all cores listed below are presented in the study. I have also not listed cores which I did not describe or which were not available at the time of this study.

The cored intervals listed below are based on comparison of the interpreted core section with the accompanying well logs, and not on the actual well depths given on the core boxes or in core listings. This will allow the reader to take the well log for any core listed below and plot the cored interval accurately on the well log. The maximum discrepency between well depths given on the core boxes and the position of the cored interval as determined from correlation of the actual core with the well log is about 5m. Discrepencies of 1-2m are more common. The reader is referred to the many available sources for listings of the well depths of core based on drilling measurements (e.g. scout tickets, microfiche, computer listings).

The core length listed below is the length of core that I actually measured. This value will usually be a little less than

the length determined from the cored interval due to lost core. In some cases, the measured length may exceed the length of the cored interval. This results from the uncertainty in measuring shales and blockstones, especially when they are broken and rubbly.

In core, very precise measurements are possible on the scale of centimeters and even millimeters. Depending on the quality of core, however, it is not usually possible to accurately determine the length of the entire core with the same precision.

All lengths are given in meters. For older well logs, which use imperial units, lengths are also listed in feet (shown in brackets) so that interested readers do not have to make conversions in order to plot the cored interval on the relevant well logs. Some of the cores listed below are not presented in the thesis. They are available, upon request, from the author.

WELL LOCATION	CORE #	CORED INTERVAL WELL LOG	CORE LENGTH MEASURED
Township 51			
6-35-51-25W5	1	3367.8-3386.0m	17.24m
Township 59			
11-19-59-3W6	4,5	3022.0-3055.2m	32.8m
12-7-59-5W6	3	3038.9-3057.2m	18.3m
Township 60			
10-14-60-18W5	1	1594.0-1605.2m	11.17m
8-34-69-18W5	1	1675.5-1693.3m	18.43m
14-16-60-21W5	1,2	1963.3-1981.3m	18.09m
11-22-60-21W5	1	1931.0-1948.0m	16.73m
6-28-60-21W5	1	1932.0-1950.4m	18.39m
7-30-60-21W5	1	1953.0-1971.0m	17.00m
10-33-60-21W5	1	1915.6-1921.6m (6285-6305')	5.87m (20')
7-11-60-22W5	1	2059.0-2077.0m	18.12m
10-22-60-22W5	1	2021.0-2036.9m (6630-6680')	14.76m (49')
2-25-60-22W5	1	1959.8-1975.0m (6430-6480')	14.93m (50')
13-25-60-22W5	1	1942.0-1960.0m (6372-6430')	18.06m (60')
14-7-60-2W6	4,5	2739.0-2775.0m	36.14m
6-30-60-3W6	6	2674.0-2687.3m	13.54m
12-22-60-5W6	1,2	2929.0-2965.0m	36.71m
10-33-60-5W6	2	2822.0-2840.0	17.32m
Township 61			
16-1-61-22W5	1,2	1867.0-1904.0m	37.1m
3-28-61-24W5	1	2040.8-2052.0	10.82m
10-34-61-26W5	1	2143.0-2158.0m	14.79m
6-1-61-1W6	2,3	2443.0-2467.0m	23.73m
11-15-61-1W6	2,3	2444.8-2468.0m	23.38m
5-27-61-1W6	6,7	2405.0-2441.0	36.40m
6-22-61-2W6	1,2	2420.4-2443.2m	22.08m
13-28-61-2W6	2,3	2420.5-2441.2m	21.11m
7-17-61-3W6	4-9	2743.0-2783.0m	37.81m
12-24-61-3W6	1	2552.0-2569.0	17.37m
6-33-61-3W6	1-3	2376.6-2431.0m	55.45m
10-3-61-4W6	1	2426.0-2444.0m	17.82m
3-6-61-4W6	5-6	2680.0-2707.0m	24.0m
6-8-61-5W6	1	2794.0-2812.0m	17.68m
12-21-61-9W6	1	2897.0-2907.0m	9.26m
	2	2941.2-2959.2m	18.63m
10-34-61-9W6	1,2	2949.0-2984.0m	35.94m
8-36-61-9W6	1	2857.4-2869.4m	11.12m
10-36-61-10W6	1-4	3169.6-3234.4m	60.06m

WELL LOCATION	CORE #	CORED INTERVAL MEASURED	CORE LENGTH MEASURED
Township 62			
10-22-62-22W5	1	1653.0-1666.0m	12.77m
3-27-62-22W5	1	1653.0-1672.0m	19.39m
6-29-62-23W5	1	1750.0-1766.0m	13.52m
5-18-62-25W5	1	1915.0-1931.5m	16.43m
11-32-62-25W5	1	1831.5-1849.5m	18.76m
10-3-62-26W5	1,2	2070.0-2097.8m	27.94m
4-26-62-26W5	1	1879.0-1897.0m	17.65m
15-31-62-26W5	1	1924.0-1942.2m	18.06m
6-35-62-27W5	1,2	2027.0-2037.6m	10.2m
	3-5	2042.0-2075.5m	32.94m
14-35-62-27W5	1	2080.0-2098.2m	18.47m
10-36DU-62-26W5	1	1792.8-1810.8m	14.46m
3-20-62-2W6	3-5	2386.0-2421.5m	36.19m
12-31-62-2W6	1-4	2256.3-2311.5m	54.31m
		(7403-7584')	178'
15-31-62-2W6	1,2	2205.0-2225.0m	23.0m
2-4-62-3W6	1-3	2397.0-2450.8m	54.3m
14-5-62-3W6	1-3	2297.0-2344.0m	45.78m
2-6-62-2W6	2,3	2442.0-2478.0m	36.58m
16-6-62-3W6	1-6	2338.0-2398.4m	53.6m
7-7-62-3W6	1-4	2256.4-2315.9m	60.04m
17-7-62-3W6	1-3	2229.0-2274.2m	44.26m
8-8-62-3W6	1-3	2326.5-2374.4m	48.37m
14-8-62-3W6	1-3	2297.0-2340.2m	43.57m
3-9-62-3W6	1-5	2332.0-2402.0m	70.5m
6-11-62-3W6	4-7	2497.0-2566.2m	69.7m
6-13-62-3W6	1,2	2472.0-2506.6m	33.21m
8-35-62-3W6	2,3	2114.0-2150.0m	35.29m
9-4-62-4W6	5-7	2326.7-2370.2m	44.71m
6-27-62-7W6	1	2706.0-2724.0m	18.52m
Township 63			
11-16-63-24W5	1	1698.0-1716.2m	18.7m
		(5571-6531')	(59.5')
7-22-63-24W5	1	1646.0-1662.0m	16.27m
		(5401-5452')	(51')
10-26-63-24W5	1	1602.6-1620.0m	17.73m
		(5258-5315')	(58')
7-5-63-26W5	1	1938.8-1956.8m	17.24m
11-5-63-26W5	1	1945.0-1963.0m	17.76m
1-6-63-26W5	1	1983.0-1995.4m	11.84m
7-6-63-26W5	1	1971.0-1988.0m	17.33m
14-6-63-26W5	1,2	1942.0-1978.0m	33.78m
15-6-63-26W5	1	1935.0-1953.0m	18.14m
1-8-63-26W5	1	1888.0-1906.0m	18.31m
7-10-63-1W6	1	1967.0-1985.0m	18.15m

WELL LOCATION	CORE #	CORED INTERVAL MEASURED	CORE LENGTH MEASURED
8-12-63-27W5	1	1963.5-1981.5m	18.34m
6-27-63-1W6	1	1893.0-1899.0m	5.99m
2-6-63-2W6	2-4	2237.4-2261.2m	24.38m
		(7341-7419')	(80')
10-6-63-2W6	1	2135.0-2149.3m	13.5m
		(7005-7052')	(44')
2-7-63-2W6	1	2074.4-2092.6m	18.30m
		(6806-6866')	(60')
10-7-63-2W6	1-3	2077.0-2132.0m	55.86m
		(6815-6995')	(183')
4-8-63-2W6	1-3	2141.0-2185.3m	42.34m
		(7025-7170')	(139')
15-17-63-2W6	1	2032.9-2048.8m	15.40m
		(6672-6722')	(50')
6-29-63-2W6	1,2	2026.0-2063.2m	37.12m
7-2-63-8W6	1-4	2495.0-2532.8m	39.35m
Township 64			
14-4-64-23W5	1	1544.0-1555.0m	10.18m
15-7-64-23W5	1	1548.3-1566.6m	18.13m
		(5080-5140')	(60')
6-15-64-23W5	1	1483.0-1501.4m	18.09m
		(4866-4926')	(60')
10-16-64-23W5	1	1482.5-1494.7m	10.87m
		(4864-4904')	(36')
5-17-64-23W5	2,3	1501.0-1518.7m	7.94m
6-18-64-23W5	1	1542.0-1554.3m	18.11m
10-18-64-23W5	1	1527.0-1545.0m	16.36m
14-18-64-23W5	1	1545.0-1560.0m	15.34m
4-19-64-23W5	1	1574.0-1589.0m	14.51m
6-20-64-23W5	1	1536.1-1554.0m	17.93m
		(5040-5099')	(60')
7-21-64-23W5	1	1472.0-1487.0m	14.21m
		(4830-4879')	(47')
15-12-64-24W5	1	1557.5-1566.6m	8.84m
7-13-64-24W5	1	1580.0-1595.6m	15.78m
13-13-64-24W5	1	1592.6-1601.8m	5.88m
15-13-64-24W5	1	1574.0-1586.0m	12.39m
2-24-64-24W5	1	1578.0-1588.5m	10.43m
6-24-64-24W5	2	1595.0-1607.0m	12.05m
11-7-64-26W5	1	1754.6-1773.2m	18.67m
11-20-64-26W5	1,2	1674.6-1697.2m	24.23m
7-20-64-1W6	1	1751.0-1769.2m	19.33m
14-36-64-2W6	1	1670.2-1678.0m	7.61m
		(5480-5505.5')	(25')
	2,3	1693.1-1721.3m	26.59m
		(5555-5648')	(87')

WELL LOCATION	CORE #	CORED INTERVAL MEASURED	CORE LENGTH MEASURED
Township 65			
10-31-65-22W5	1	1240.0-1259.0m	19.05m
		(4068-4130')	(62')
10-6-65-23W5	1	1478.2-1496.2m	16.88m
		(4850-4909')	(55')
11-10-65-23W5	1,2	1351.0-1374.2m	24.32m
10-20-65-23W5	1	1353.2-1371.2m	17.38m
		(4440-4499')	(57')
6-27-65-23W5	1	1289.0-1307.0m	18.33m
2-29-65-23W5	1	1315.5-1326.5m	10.46m
11-31-65-23W5	1	1382.3-1400.1m	17.76m
		(4535-4594')	(58')
10-34-65-23W5	1	1264.6-1277.0m	12.4m
		(4149-4207')	(41')
10-1-65-24W5	1	1484.5-1502.0m	17.44m
4-22-65-24W5	1	1459.3-1478.8m	17.77m
		(4788-4852')	(58')
5-23-65-24W5	1,2	1478.0-1507.5m	29.23m
10-36-65-24W5	1	1394.0-1402.9m	8.88m
4-11-65-2W6	1-4	1709.8-1768.7m	61.48m
		(5610-5803')	(202')
Township 66			
7-6-66-23W5	1	1309.0-1327.3m	17.27m
		(4295-4355')	(57')
13-8-66-23W5	1	1374.0-1392.0m	18.24m
10-20-66-21W5	1	1104.8-1111.8m	7.02m
		(3625-3648')	(23')
10-9-66-23W5	1	1272.5-1290.8m	17.26m
		(4175-4235')	(57')
7-10-66-23W5	1	1269.7-1288.0m	18.82m
		(4166-4226')	(62')
3-26-66-7W6	6-13	1847.0-1926.2m	78.1m
		(6050-6321')	(256')
Township 67			
6-26-67-10W6	6,7	1671.7-1689.4m	18.23m
		(5485-5543')	(60')
	8	1708.9-1724.2m	14.81m
		(6507-5657')	(49')
	9	1746.0-1747.0m	1.00m
		(5727-5732')	(3.3')
	10,11	1778.0-1808.6m	27.85m
		(5834-5934')	(91')

WELL LOCATION	CORE #	CORED INTERVAL WELL LOG	CORE LENGTH MEASURED
Township 71			
10-15-71-11W6	2	1261.0-1279.0m	18.04m
	3	1348.0-1366.0m	17.97m
Township 72			
16-25-72-5W5	NA	858.0-1067.7m (2815-3503')	193.86m (636')
5-9-72-8W6	13-97	1092.0-1321.0m (3600-4351')	216.77m (711')

APPENDIX 2.

Hydrocarbon Accumulations and the Dunvegan Formation

To date, few hydrocarbon accumulations have been found in the Dunvegan Formation. The few pools which do contain commercial quantities of oil and gas are indicated in figure 1-8. Data on these pools are presented in Table 1 below. Throughout chapters 4-10, it was indicated which sandstones were productive, although this thesis did not attempt to integrate production data or reservoir studies.

Most Dunvegan oil and gas is produced from channel fill facies although not all channels within the Dunvegan Formation produce hydrocarbons. In addition, the size and extent of oil and gas pools within productive channels is considerably smaller than the size of the channels themselves. The nature of depositional systems outlined in chapter 11 is certainly not reflected in the shapes and outlines of the Dunvegan oil and gas pools. It does not appear as though there is any simple direct link between the allostratigraphy and depositional systems discussed in this thesis and the distribution of oil and gas in the Dunvegan Formation. Other factors, such as the diagenetic history of reservoirs (porosity and permeability), and the structural geology (structural traps, fracturing) of the area, may have an important

influence on the distribution of oil and gas in the Dunvegan Formation. Until these other factors are properly understood, exploration for Dunvegan oil and gas will remain a risky business. These factors clearly merit future research but are not discussed further in this thesis.

TABLE 1. OIL POOLS IN THE DUNVEGAN FORMATION

Pool	Shingle	Facies	Hydrocarbon type
Kakwa	G3	delta front	deep gas
Jayar	A2	estuary fill	oil and gas
Lator	A2	estuary fill	oil and gas
Simonette	E1	distributary	oil and gas
Waskahigan	D1	estuary fill	oil and gas
Ante Creek	D1	estuary fill	oil and gas
Bigstone	E1	distributary mouth bar	mostly gas